Physiological response and mTOR regulation to branched-chain amino acids in Atlantic salmon (*Salmo salar*).

THESIS SUBMITTED FOR THE DEGREE OF DOCTOR OF PHILOSOPHY

BY

Marie-Teresa Grobler

FEBRUARY 2025

INSTITUTE OF AQUACULTURE
UNIVERSITY OF STIRLING

UNIVERSITY of STIRLING



‘Study and in general the pursuit of truth and beauty is a sphere of activity in which we are permitted to remain children all our lives.’

(Albert Einstein, Letter to Adrianna Enriques, October 1921)

DECLARATION

This thesis has been composed in its entirety by the candidate. Except where specifically acknowledged, the work described in this thesis has been conducted independently and has not been submitted for any other degree. The candidate acknowledges the use of AI as a tool to aid in sentence structure, formatting and reducing the volume of their own work.

ACKNOWLEDGEMENTS

This PhD has been quite a journey, one which I would probably not have finished without the patience, support and guidance from my supervisor, Prof. Simon Mackenzie. Thank you for renewing my love for the unknown and giving me the courage to be curious again. Thank you for guiding me in becoming a better researcher.

Thank you to Prof. Brett Glencross for conceptualisation of the PhD and starting me on this journey, and to my second supervisor Prof. Monica Betancour.

Emma Forrest, without you none of this would have been possible. Thank you for being my reason I am here, for being by my side through everything, a part of my life and for giving me a home away from home. Thank you for postponing our wedding so many times, I promise it's not you, it's me.

Mum and dad, thanks for still being around to give me a good talking to when I needed it, and for not letting me give up. This is first and foremost for you both.

Grandma, I am so sorry I couldn't finish this in time for you to see me in a funny little hat at graduation, but I know you will be looking down at me and having a little giggle anyway.

Thank you to Dr. Chelsea Broughton, Dr. Adrian Love, Rozely De Jong and all my friends and family for your love and friendship. Dolores McCloskey-Webb, thank you for all your continued support and genuine friendship and for not letting me walk away from this.

I am sincerely grateful to all the support and guidance I have received from everyone here at the Institute of Aquaculture, Dr Ben Clockie, Dr Ahmed Elsheshtawy Ahmed, Fiona Strachan, Jacquie Ireland, Debbie Faichney, Dr Mathew Sprague and to all the staff and students who helped along the way.

I am grateful for the PhD funding I received from Dr Richard Smullen at Ridley AgriProducts Pty Ltd, and the university of Stirling match funding it. I would like to thank Rank Prize for the grant I was awarded enabling me to financially survive during COVID.

ABSTRACT

The increasing demand for sustainable aquafeed ingredients has necessitated extensive research into alternative protein sources, reducing reliance on finite marine resources in Atlantic salmon (*Salmo salar*) aquaculture. Among key dietary components, branched-chain amino acids (BCAAs)- leucine, isoleucine, and valine—play critical roles in protein synthesis, energy metabolism, and cellular signalling pathways. Despite their well-established importance in mammalian systems, research on BCAA metabolism and mechanistic/ mammalian target of rapamycin (mTOR) signalling in Atlantic salmon remains limited. This study investigates the metabolic fate of dietary BCAAs, their potential role in mTOR activation, and the physiological responses of Atlantic salmon to dietary variations and hypoxic stress.

Chapter 1 provides a comprehensive review of BCAA metabolism, dietary requirements, and regulatory factors in fish and terrestrial livestock. The role of mTOR as a central cellular hub integrating amino acid (AA) availability, energy status, and environmental cues is explored in relation to nutrient utilisation and growth regulation. Existing knowledge gaps in Atlantic salmon are highlighted, particularly regarding BCAA catabolism and mTOR-mediated metabolic control under varying physiological conditions.

Chapter 2 examines the digestibility and uptake kinetics of crystalline amino acids (cAAs) compared to intact proteins in Atlantic salmon post-smolts. Temporal BCAA absorption patterns were analysed in plasma, muscle, and liver tissue, revealing peak uptake at 4 hr post-feeding. The study confirmed that BCAAs primarily bypass first-pass hepatic metabolism, supporting the hypothesis that they serve as direct substrates for protein synthesis and signalling in muscle tissue. Despite significant temporal and tissue-specific differences in BCAA metabolism and mTOR-related gene expression, the observed mRNA abundance changes were not deemed biologically significant, emphasising the need for proteomic validation. Future investigations should assess direct protein synthesis rates and phosphorylation status of mTOR and its downstream targets.

Chapter 3 evaluates the impact of varying dietary BCAA levels and leucine enrichment on growth performance, AA homeostasis, haematological parameters, and molecular signalling in Atlantic salmon parr. A near-significant increase in growth performance was observed (p=0.052), with the highest final weight recorded in fish receiving the suboptimal BCAA diet. Stable isotope analysis revealed tissue-specific retention of δ15N-labeled leucine, with greater incorporation in muscle compared to liver, aligning with established models of BCAA metabolism. Despite no significant differences in blood biochemistry, variation between weeks were observed in haemoglobin, packed cell volume, and white blood cell counts suggested potential physiological adaptations. mRNA transcript analysis indicated temporal fluctuations in BCAA catabolism, particularly in BCKDHA mRNA abundance, reinforcing the dynamic regulation of AA metabolism in response to dietary composition and developmental stage.

Chapter 4 investigated transcriptomic and metabolic responses to hypoxia, with emphasis on mTOR modulation across liver, brain, and heart tissues of Atlantic salmon post-smolts. RNA-Seq analysis identified 372 differentially expressed genes (DEGs), with liver exhibiting the highest transcriptomic alterations. Notably, the only direct mTOR-associated DEG, E3 UBIQUITIN-PROTEIN LIGASE RNF152-LIKE, was downregulated in liver tissue, suggesting a potential suppression of mTOR activity under hypoxia. Functional enrichment analysis of the fold change (FC) results, >2FC and <-2FC, identified 37 mTOR-related mRNA transcripts interacting with external WNT and TNF-α pathways and internal ubiquitin-mediated proteolysis mechanisms. Downstream effectors of mTOR, including EIF4E2, RHOA, and SI:CH211-195B13.1, exhibited significant repression, possibly implicating translational control mechanisms in the adaptive response to oxygen deprivation. The transcriptomic data identified possible hypoxia related mTOR signalling but not through the REDD1 hypoxia pathway, but rather through both extrinsic (growth factors, inflammatory mediators) and intrinsic (ubiquitin-proteasome system, translational regulation) pathways. The identification of the same mRNA transcripts both up- and downregulated suggested possible annotation complications.

Further transcriptomic analyses on the 1FC and -1FC mRNA transcripts identified 831 mTOR associated mRNA transcripts up- and downregulated under hypoxia, suggesting alternative mechanism of regulation of the mTOR pathway. Overall, the transcriptomic data revealed oscillations within the pathways, but no distinct emergent properties were observed. This may support the hypothesis that mTOR is not transcriptionally regulated.

Collectively, this research provides critical insights into the metabolic interplay between BCAA bioavailability, mTOR regulatory pathways, and physiological adaptation in Atlantic salmon. The findings underscore the imperative of optimising dietary AA formulations to maximise growth efficiency while elucidating the intricate signaling networks governing protein metabolism under hypoxic stress. Future studies should incorporate multiomic methodologies, encompassing phosphoproteomics and metabolomics, to delineate the molecular underpinnings of mTOR-driven metabolic regulation in aquaculture species. Additionally, advancing dietary strategies to enhance nutrient assimilation while mitigating environmental stressors is pivotal for promoting sustainability in intensive salmon aquaculture.

Keywords: mTOR, Atlantic salmon, branched-chain amino acids (BCAAs), BCAA metabolism, hypoxia

TABLE OF CONTENTS

Declaration 5

Acknowledgements 7

Abstract 9

Table of Contents 13

List of Abbreviations 17

List of Figures 21

List of Tables 23

Supplementary Data 25

Chapter 1 27

General introduction 27

1.1 Introduction 28
1.1.1 Amino acid requirements, dietary considerations and growth 29
1.1.2 BCAA metabolism and physiological roles 31
1.1.3 BCAA catabolism and regulatory mechanisms 32
1.1.4 BCAA influence on feed intake and metabolism 34
1.1.5 Amino Acid Metabolism 34
1.1.6 mTOR signalling and amino acid regulation 35

Chapter 2 37

BCAA digestibility, uptake and response in Atlantic salmon post-smolts. 37

Abstract 38

2.1 Introduction 40
2.1.1 Amino acid absorption and metabolic regulation 41
2.1.2 BCAA metabolism and utilisation 42
2.1.3 The mTOR pathway 44

2.2 Materials and methods 45

2.2.1 Ethics approval 45
2.2.2 Experimental design 47
2.2.3 Analyses of feeds, ingredients, and faeces 50
2.2.4 Digestibility (diet apparent digestibility coefficient (DADC)) 59
2.2.5 Molecular biology analysis 59
2.2.6 Data analysis 70
2.3 Results 71
2.3.1 Fish 71
2.3.2 Feed 71
2.3.3 Plasma amino acids (µmol/ L) 73
2.3.4 Muscle and liver tissue 87
2.3.5 mRNA abundance 96
2.4 Discussion 108
2.4.1 Digestibility, nutrient sources and feed intake 108
2.4.2 Plasma 111
2.4.3 Tissue 118
2.4.4 Molecular studies 122
2.5 Chapter summary 133
2.5.1 Digestibility and feed intake 133
2.5.2 BCAAs and other AAs 133
2.5.3 Molecular 135
Chapter 3 137
The role of BCAAs on regulation and performance in Atlantic salmon parr/ juveniles. 137
Abstract 138
3.1 Introduction 140
3.2 Materials and methods 143
3.2.1 Fish handling, husbandry and sample collection 144
3.2.2 Feed formulation and manufacture 146
3.2.3 Calculations for growth performance, efficiency and morphometric indices 148

3.2.4 Analyses of feeds, ingredients and faeces 149
3.2.5 Digestibility 155
3.2.6 Haematology 155
3.2.7 Stable isotope analysis 155
3.2.8 Molecular 156
3.2.9 Statistical analysis 160
3.3 Results 160
3.3.1 Feed 160
3.3.2 Fish 162
3.3.3 Whole body analysis 173
3.3.4 Blood chemistry 196
3.3.5 Plasma 198
3.3.6 Stable isotope analysis 216
3.3.7 mRNA abundance 217
3.4 Discussion 220
3.4.1 Feed and performance 220
3.4.2 Physiological analyses 235
3.4.3 Amino acid interactions, metabolism and pathways 246
3.4.4 Haematology and biochemistry 251
3.4.5 $\delta^{15}N$ labelled leucine stable isotope 255
3.4.6 BCKDH mRNA abundance 256
3.5 Chapter summary 260
Chapter 4 263
TOR be or not TOR be? Regulation is the question. 263
Abstract 264
4.1 Introduction 267
4.1.1 Hypoxia in aquaculture 267
4.1.2 The mTOR pathway and its regulation under hypoxia 267
4.1.3 Transcriptomics and mtor regulation under hypoxia 268
4.2 Materials and methods 271
4.2.1 Literature search 271

4.2.2 PubMed Advanced Search Builder 272
4.2.3 Ethics 275
4.2.4 Experimental design 275
4.2.5 Data analysis 278
4.3 Results and discussion 283
4.3.1 PubMed MeSH term searches 283
4.3.2 Descriptive stats 284
4.3.3 Magnitude and intensity transcriptome landscape comparisons 284
4.3.4 Gene ontology analysis (>2 <-2 fold change) 306
4.3.5 mTOR pathway associations 323
4.3.6 Hypoxia 338
4.3.7 mTOR 1FC 344
4.4 Summary 348
4.4.1 Technical variation 348
4.4.2 Biological variation 356
Chapter 5 362
General discussion 362
5.1 Digestibility of intact proteins and cAAs 362
5.2 BCAAs and AAs 365
5.2.1 AA interactions 366
5.3 mRNA abundance 368
5.4 mTOR 372
References 377
Supplementary data 445

LIST OF ABBREVIATIONS

Abbreviation	Definition
Ø	Diameter
‰	Parts per thousand
%v/v	Volume concentration
4E-BP1	Eukaryotic translation initiation factor 4E-binding protein 1
AA	Amino acid
ADP	Adenosine diphosphate
α-KG	A-ketoglutaric acid
ALB	Albumin
ALP	Alkaline phosphatase
ALT	Alanine aminotransferase
AMPK	Adenosine 5′-monophosphate-activated protein kinase
ANFs	Anti-nutritional factors
ATP	Adenosine triphosphate
bAAs	Bound amino acid
bBCAAs	Bound Branched chain amino acid
BCAA	Branched chain amino acid
BCAT	Branched-chain aminotransferase
BCATc	Branched-chain aminotransferase cytosolic
BCATm	Mitochondrial
BCKA	Branched-chain α-keto acids
BCKDH	Branched chain α-ketoacid dehydrogenase
BCKDK	Branched chain α-ketoacid dehydrogenase kinase
BCP	1-bromo-3-chloropropane
bEAAs	Bound essential amino acid
bNEAAs	Bound non-essential amino acid
cAA	Crystalline amino acid
CAS	Casein diet
cBCAA	Crystalline branched chain amino acid
CD	Control diet
cDNA	Complementary DNA
cEAA	Crystalline essential amino acid
CEAA	Conditionally essential amino acid
cGMP	Cyclic guanosine monophosphate
CK	Creatine kinase
cNEAA	Crystalline non-essential amino acid
CO2	Carbon dioxide
CP	Crude protein
Cqs	Quantification cycle (qpcr)
CSI	Cardio somatic index
Cts	Threshold cycle (qpcr)
DADC	Diet apparent digestibility coefficient
DAVID	The Database for Annotation, Visualization, and Integrated Discovery
DEG	Differentially expressed gene
DEPTOR	DEP-domain-containing mtor-interacting protein
DNA	Deoxyribonucleic acid
e.g.	*Exempli gratia* (for example)
EAA	Essential amino acid

EIF4E	Eukaryotic translation initiation factor 4E
EPD	Ependymin
et al.	*Et alii* 'and others'
etc.	*Etcetera*
fAA	Free amino acid
fBCAAs	Free branched-chain amino acids
FC	Fold change
FCR	Feed conversion ratio
FDR	False discovery rate
FE	Fold enrichment
fEAAs	Free essential amino acids
FI	Feed intake
FM	Fish meal
fNEAAs	Free non-essential amino acids
FO	Fish oil
fzd	Frizzled
GDP	Guanosine diphosphate
GIT	Gastrointestinal tract
GLM	General linear model
GOI	Gene of interest
GPCR	G-protein-coupled receptor
GTP	Guanosine triphosphate
Hb	Haemoglobin
hba	Haemoglobin subunit alpha-4
HCL	Hydrochloric acid
HIF	Hypoxia-inducible factor
HMB	3-hydroxy-3-methylbutyrate
hpxa	Hemopexin a
hpxb	Hemopexin b
HSI	Hepatic somatic index
HSMI	Heart and skeletal muscle inflammation
i.e.	*Id est* (that is)
ICP-MS	Inductively coupled plasma atomic emission spectrophotometry
ID	Isoleucine diet
IgD	Diversity chain immunoglobulin
IGF1	Insulin-like growth factor 1
IgV	Variable chain immunoglobulin
K	Condition factor
KEGG	Kyoto Encyclopaedia of Genes and Genomes
KIC	A-ketoisocaproate, ketoleucine
KIV	A-ketoisovalerate, ketovaline
KMV	A-keto-β-methylvalerate, ketoisoleucine
Kr	Relative condition factor
L2FC	Log 2 Fold change
LATS	L-type AA transporters
LD	Leucine diet
MAPK	Mitogen-activated protein kinase
MERL	Marine environmental research laboratory
MLST8	(Mammalian) lethal with sec-13 protein 8
MM	Master mix
MOPA	Moisture, oil, protein, ash
mRNA	Messenger ribonucleic acid
MSTN	Myostatin

mTOR	Mammalian/ mechanistic target of rapamycin
mTOR1	Mechanistic target of rapamycin complex 1
mTOR2	Mechanistic target of rapamycin complex 2
MYO6	Myosin VI
MYOSTAT 1A	Myostatin 1a
n-3	Omega 3
n-6	Omega 6
NA	Sub-optimal BCAA diet
NEAAs	Non-essential amino acid
NH_3	Ammonia
NH_4	Ammonium
NL	Sub-optimal leucine diet
NO	Nitric oxide
npy	Neuropeptide Y
NTC	Non-template control
O2	Oxygen
OFN	Oxygen-free nitrogen
PCV	Packed cell volume
PepT1	Peptide transporter 1
POMC	Proopiomelanocortin
PRAS40	Proline-rich Akt substrate of 40 kDa
PTM	Post-translational modifications
PUFA	Polyunsaturated fatty acid
QC	Quality control
qPCR	Quantitative polymerase chain reaction
RAG GTPase	Ras-related GTP binding protein GTPases
Raptor	Regulatory-associated protein of mtor
Raptor	Regulatory-associated protein of mtor
RAS	Recirculating Aquaculture system
RBC	Red blood cell
RBCC	Red blood cell count
REDD1	Regulated in development and DNA damage responses 1
Rheb	GTP-binding protein Rheb-like
RNA-Seq	RNA-sequencing
RRAG	Rag GTPases
rRNA	Ribosomal ribonucleic acid
RT-	Reverse transcription negative
S.D	Standard deviation
S6	Ribosomal S6 protein
S6K	Ribosomal protein S6 kinase
scaRNA	Small Cajal body-specific rRNA
SESN	Sestrin
SLC	Solute carrier system
SLC7A5	Large neutral amino acids transporter small subunit 1
SNATs	Sodium-coupled neutral amino acid transporters)
snoRNA	Small nucleolar rRNA
snRNA	Small nuclear RNA
snRNP	Small nuclear ribonucleoproteins
SPC	Soya bean protein concentrate
SRUC	Scotland's rural college
SS	Suspended solids
STAR	Spliced Transcripts Alignment to a Reference
STD	Standard

STE20	STE20-related kinase adapter protein beta-like
TCA	Tricarboxylic acid
TFA	Transferrin-a
TSC1/TSC2	Tuberous sclerosis 1/2
ULK1	Unc-51 like autophagy activating kinase 1
VD	Valine diet
VSI	Viscerosomatic index
VST	Variance stabilised data
WB	Whole body
WBCC	White blood cell count
WHE	Whey diet
WNT	Wingless-type MMTV integration site family

LIST OF FIGURES

Figure 1.1 Structure of the BCAAs 29
Figure 1.2 The Liebig-barrel concept 30
Figure 2.1 BCAA degradation. 42
Figure 2.2 mTOR pathway 44
Figure 2.3 Block replication through time method**.** 48
Figure 2.4 BCAA diets feed intake (FI g/ fish/ day**)** 72
Figure 2.5 fBCAA percentage change (%) in post-prandial plasma 78
Figure 2.6 Plasma fEAAs change (%) from the CD diet 80
Figure 2.7 The plasma fNEAAs change (%) compared to the CD. 83
Figure 2.8 Total lipid (%) in liver and muscle tissue in LD 88
Figure 2.9 LD bBCAAs in A) liver tissue 89
Figure 2.10 bBCAAs for all the test diets A) muscle B) liver tissue 92
Figure 2.11 LD fBCAAs of A) muscle B) liver tissue 93
Figure 2.12 fBCAAs in A) muscle B) liver tissue 95
Figure 2.14 BCKDH1a within-tissue variability 98
Figure 2.15 BCKDK within-tissue variability 99
Figure 2.16 LD Plasma leucine and the BCAA mRNA transcripts 100
Figure 2.17 SESN1 within-tissue variability 102
Figure 2.18 RRAG within-tissue variability in the LD diet 103
Figure 2.19 Myostat 1a within-tissue variability 105
Figure 2.20 MYO6 within-tissue variability 106
Figure 2.21 Plasma leucine and the mTOR pathway 107
Figure 3.1 Growth parameters 166
Figure 3.2 Feed conversion ratios 167
Figure 3.3 Whole body total lipids 175
Figure 3.4 Whole body bEAAs and bNEAAs change (%) 177
Figure 3.5 Muscle individual fBCAAs 187
Figure 3.6 Muscle individual fEAAs compared to CD (%change) 188
Figure 3.7 Muscle fNEAAs compared to CD (change%) 194
Figure 3.8 Within diet fAAs in muscle tissue 195
Figure 3.9 Individual plasma fBCAA and change (%) 203

Figure 3.10 Individual plasma fEAAs change (%) compared to CD 211
Figure 3.11 Glutamate in plasma and muscle tissue over 24 hr 212
Figure 3.12 Individual plasma fNEAAs change (%) from CD**.** 214
Figure 3.13 Keto- and glucogenic fAAs 215
Figure 3.14 Labelled leucine (δ15N) 217
Figure 3.15 BCKDHA mRNA abundance in muscle 218
Figure 4.1 Example of search conducted in Nature 272
Figure 4.2 PubMed Advanced Search Builder results on mTOR 274
Figure 4.3 The nf-core/rnaseq pipeline used to process RNASeq data 278
Figure 4.4 The nf-core/differentialabundance pipeline 279
Figure 4.5 Identified and novel protein coding (PC) mRNA transcripts 284
Figure 4.6 Classification of DEGs 289
Figure 4.7 mTOR associated DEG E3 ubiquitin-protein ligase 295
Figure 4.8 Liver tissue comparison 296
Figure 4.9 Brain tissue comparisons 298
Figure 4.10 Heart tissue comparisons 300
Figure 4.11 Top 50 mRNA transcripts by variance 305
Figure 4.12 Liver mTOR pathway 325
Figure 4.13 Brain mTOR pathway 326
Figure 4.14 Heart mTOR pathway 328
Figure 4.15 The duplicated Atlantic salmon genome 330
Figure 4.16 Classifications of the top 50 mRNA transcripts by variance 335
Figure 4.17 Heatmaps for the top 50 mRNA transcripts 337
Figure 4.18 mTOR associated mRNA transcripts across all tissues 346
Figure 4.19 mTOR associated liver mRNA transcripts 347
Figure 4.20 mTOR associated brain mRNA transcripts 349
Figure 4.21 mTOR associated heart mRNA transcripts 350

LIST OF TABLES

Table 2.1 Diet formulations and compositions 46
Table 2.2 CEM Microwave digester cycle programs. 56
Table 2.3 Digestibility coefficients of crystalline and intact proteins 60
Table 2.4 Digestibility Coefficients of the BCAA test diets 61
Table 2.5 Sequencing details 68
Table 2.6 Total plasma BCAAs 74
Table 2.7 Categories of total plasma fAAs 87
Table 2.8 Proximate analysis of muscle and liver tissue 88
Table 2.9 Muscle and liver total bBCAAs and fBCAAs of the leucine diet 90
Table 3.1 Expected feed intake and growth estimations 144
Table 3.2 BCAA inclusion levels 145
Table 3.3 Diet formulation (%) and expected compositions 147
Table 3.4 qPCR program 159
Table 3.5 Proximate analysis of test feeds and ingredients. 161
Table 3.6 Ingredient composition and AA analysis of feed ingredients. 163
Table 3.7 Amino acid analysis of test feeds (g/100g or %). 164
Table 3.8 Digestibility Coefficients of the test diets 165
Table 3.9 Individual variation in total weights and lengths 169
Table 3.10 Individual morphometric indices 170
Table 3.11 Length weight relationships between week-3 and week-7. 171
Table 3.12 Somatic indices 172
Table 3.13 Proximate analysis of whole bodies (%wet matter). 174
Table 3.14 Whole body total bAAs of the test diets 178
Table 3.15 Total fAAs in muscle tissue 183
Table 3.16 Muscle fAAs 189
Table 3.17 Blood chemistry analysis between diets and weeks 197
Table 3.18 Total plasma fAAs of the test diets 200
Table 3.19 Week-7 total plasma fBCAAs 206
Table 3.20 Stable isotope analyses of $\delta^{15}N$ leucine 216
Table 4.1 Search terms and difficulties encountered 271
Table 4.2 mTOR PubMed MeSH search terms 273

Table 4.3 Diet formulation and composition 276
Table 4.4 Performance 277
Table 4.5 mTOR MeSh results by year from 2019 to 2024**.** 282
Table 4.6 Summary of the RNA-seq data 283
Table 4.7 Total mRNA transcripts 324
Table 4.8 Duplicated mTOR associated mRNA transcripts 329
Table 4.9 Identified mRNA transcripts of interest 331
Table 4.10 mTOR associated mRNA transcripts of interest 344
Table 4.11 Additional pathways 345
Table 4.12 Variation between webtools using FDR (BH). 354

SUPPLEMENTARY DATA

Chapter 4 electronic supplementary data files available at:

https://github.com/mtg-25/PhD_supplementary_data_2025.git

S 2.1 Proximate analysis of feeds, ingredients and faeces (MOPA) 445
S 2.2 Mineral content in ingredients 446
S 2.3 Mineral content in feeds 446
S 2.4 Minerals Faeces 447
S 2.5 Amino acid analysis of test ingredients (g/100 g) 447
S 2.6 Amino acid analysis of test feeds (g/100 g) 448
S 2.7 Faeces bAAs BCAAs and Intact protein diets (g/100 g) 449
S 2.8 bAA analysis of faeces from the BCAA diets (g/100 g) 450
S 2.9 AccQ-Tag method conditions 450
S 2.10 Primers 451
S 2.11 Primer co-efficient of determination 452
S 2.12 RNA quality control gel with both muscle and liver tissue 454
S 2.13 High-capacity cDNA Reverse Transcription mastermix 454
S 2.14 cDNA synthesis Thermocycler program 455
S 2.15 Mastermix preparation / reaction for MyTaq (PCR) 455
S 2.16 PCR conditions for primer efficiencies 455
S 2.17 Primer optimisation 456
S 2.18 Serial dilutions of cDNA superpools 458
S 2.19 qPCR program 458
S 2.20 Primer efficiencies for BCAA catabolism 459
S 2.21 Primer efficiencies for mTOR pathway 460
S 2.22 PCR product gel preparation for cloning 461
S 2.23 MYO6 plasmid PCR dilutions 461
S 2.24 Sequences: Myosin 6 (myo6) 210bp 462
S 2.25 Sequences: RRAG A 231bp 462
S 2.26 Sequences: BCKDK 233bp 463
S 2.27 Sequences: BCKDHA E1 143bp 464

S 2.28 Sequences: Sestrin 1 91bp 465
S 2.29 Sequences: BCAT, cytosolic-like bp 181 466
S 2.30 Sequences: BCAT 1b..... 466
S 2.31 Sequences: Myostat 1a..... 467
S 2.32 bAAs Muscle 4hr post feeding (umol/ g) 469
S 2.33 bAAs Liver 4hr post feeding (umol/ g)..... 470
S 2.34 Total bAAs liver and muscle tissue LD g/100g..... 471
S 2.35 fAAs Muscle LD diet all timepoints umol/g 472
S 3.1 Water quality parameters..... 473
S 3.2 Average water quality parameters 474
S 3.3 Mineral content in feeds and faeces 475
S 3.4 Faeces bAAs g/100g (week 3)..... 476
S 3.5 Thermo and Qiagen cDNA troubleshooting 477
S 3.6 Thermo qPCR melt curves.. 478
S 3.7 Qiagen qPCR melt curves..... 478
S 3.8 PCR BCKDHA gel with Thermo and Qiagen..... 478
S 3.9 qPCR melt curves for BCKDHA standards 479
S 4.1 RNA-seq summary.. 480
S 4.2 Statistically different transcripts..... 481
S 4.3 Protein coding transcripts identified within heatmaps. 491
S 5.1 Plasma uptake in Trial 1 compared to CD (change %) 493
S 5.2 Plasma uptake in Trial 2 compared to the CD (change %) 494
S 5.3 Trial 2 fBCAAs and fNEAAs in muscle..... 494

Chapter 1

GENERAL INTRODUCTION

1.1 Introduction

The aquaculture feed manufacturing sector is integral to sustainable fish farming, supplying nutritionally balanced feeds to optimise growth, health, and productivity (FAO, 2022). The industry formulates feeds with precise nutrient compositions, including marine and plant proteins, vitamins, and minerals, to meet species-specific dietary requirements across developmental stages (Li et al., 2009). Manufacturing techniques such as extrusion and pelleting enhance feed digestibility and stability while minimising nutrient loss (Csapó et al., 2008). Moreover, the industry increasingly prioritises sustainability by incorporating alternative protein sources and feed additives to reduce dependence on fishmeal and fish oil, thereby mitigating environmental impacts (Gatlin et al., 2007).

Sustainability in aquaculture hinges on defining resource efficiency, particularly regarding fishmeal and fish oil use (Zlaugotne et al., 2022). The Fish In-Fish Out (FIFO) ratio measures wild fish utilisation, yet variations in calculation methods can misrepresent aquaculture's dependency on wild stocks (Kok et al., 2020). Industry-driven research aims to develop cost-effective and environmentally sustainable alternatives, particularly for high-value species such as salmonids and shrimp species, which require protein-dense diets (Hardy, 2010). The introduction of functional feed additives, including prebiotics, probiotics, and enzymes, has demonstrated metabolic and physiological benefits, further advancing sustainability efforts (Boyd et al., 2020). The nutritional value of aquafeeds is dictated by ingredient composition, nutrient bioavailability, and digestibility (Nunes et al., 2014). Animal feeds formulated purely on protein content, may have adverse effects on growth (Langi et al., 2024). Fish do not have direct protein requirements *per se*, but rather specific amino acids (AA) that may vary across life stages and between species (Wilson, 1986). For example, AA requirements vary in shrimp species between the different moult stages such as increased requirements for arginine, histidine, leucine and threonine and less phenylalanine (Lemos & Weissman, 2021). In fish and crustacean larvae culture, rotifers and *Artemia* are often commonly enriched with vitamins, AAs and fatty acids (Gálvez et al., 2024). Juvenile fish require higher levels of AAs in order for growth/ protein synthesis while adult fish/ broodstock require less protein but

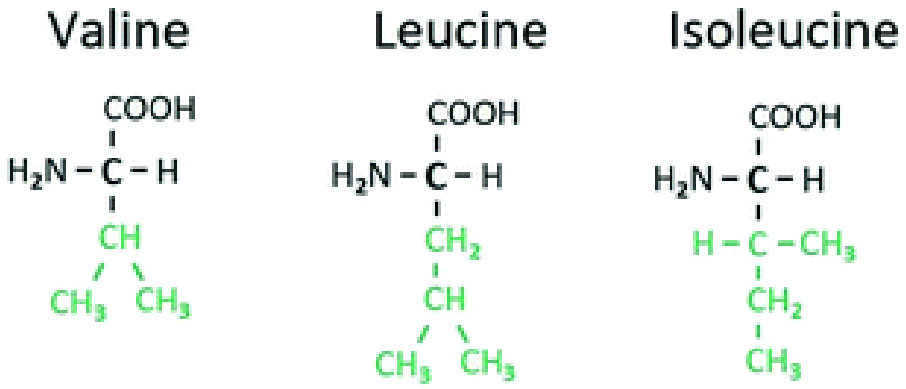


Figure 1.1 Structure of the BCAAs displaying the branched side chains from Isakov et al. (2020).

higher incorporation of fats and carbohydrates in their feed (Ahmed & Ahmad, 2020).

AAs are fundamental organic compounds characterised by a central carbon atom bonded to an amino (-NH2) and carboxyl (-COOH) functional group, along with a variable R-group that confers distinct chemical properties (Sowers, 2009). Branched-chain amino acids (BCAAs) are distinguished by their aliphatic side-chain branching, which has implications for metabolic pathways and dietary optimisation in aquaculture (Nie et al., 2018; Reifenberg & Zimmer, 2024).

1.1.1 Amino acid requirements, dietary considerations and growth

The dietary requirements of AAs in fish are influenced by both intrinsic metabolic factors and extrinsic conditions such as feed formulation and environmental parameters (Lall & Tibbetts, 2009; Sugiura, 2025). Crystalline amino acids (cAAs) are frequently incorporated into aquafeeds, though their bioavailability and metabolic efficiency in comparison to protein-bound AAs remain a subject of ongoing discourse (Lall & Anderson, 2005). Plant proteins do not contain whole AA profiles suitable for fish and are often limiting in AAs, requiring dietary supplementation with cAAs such as lysine, methionine, taurine, and threonine (Li et al., 2009).

Imbalances in AA profiles have been demonstrated to impede optimal growth and feed conversion efficiency (Xing et al., 2024). The optimal dietary BCAA levels for Atlantic salmon are approximately 2.5-3.0% of the diet for leucine, 1.5-2.0%

for isoleucine, and 1.5-2.0% for valine or 4.9, 3.3 and 3.8 % of crude protein (Xing et al., 2024).

Essential amino acids (EAAs), particularly lysine and methionine, are frequently first-limiting in formulated aquafeeds (Craig & Helfrich, 2009). Strategic dietary formulation to optimise AA balance is imperative for maximising growth efficiency and minimising feed costs, which can constitute up to 50-60% of aquaculture operational expenses (Dani, 2017).

The increasing reliance on plant-derived protein sources necessitates the supplementation of EAAs to avert suboptimal feed conversion and growth performance (Zehra & Khan, 2017). Proteins deficient in EAAs are categorised as nutritionally imbalanced, leading to diminished feed efficiency and elevated nitrogen excretion (Miles & Chapman, 2006; Wecke & Liebert, 2013). The Liebig-Sprengel's barrel concept, more commonly referred to as the Liebig-barrel model (Figure 1.2), is based on Carl Sprengel's 'Law of the Minimum'. The visual metaphor effectively illustrates the constraints imposed by a limiting AA on overall protein synthesis, whereby if the first limiting AA (such as methionine in Figure 1.2) is increased, then protein synthesis should increase (Einarsson et al., 2019).

Empirical studies in various vertebrate models indicate that cAA supplementation can enhance growth while simultaneously reducing reliance on high-crude-protein diets, thereby lowering costs and mitigating nitrogen waste (Li et al., 2017; Nguyen et al., 2020; Wang et al., 2022).

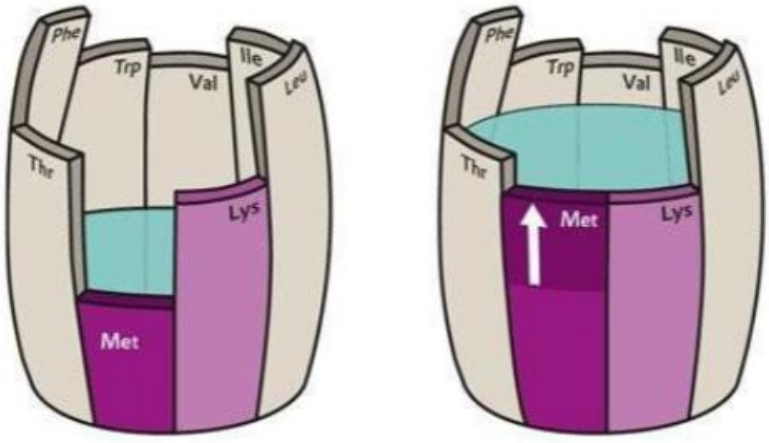


Figure 1.2 The Liebig-barrel concept based on Carl Sprengel's law of the minimum from Einarsson et al. (2019).

1.1.2 BCAA metabolism and physiological roles

BCAA catabolism is initiated by transamination via branched-chain amino acid aminotransferase (BCAT), followed by irreversible oxidation mediated by branched-chain keto acid dehydrogenase (BCKDH) (Langer et al., 2000). BCAA metabolism in mammalian models are uniquely characterised by minimal hepatic BCAT expression, leading to preferential oxidation within skeletal muscle (Dimou et al., 2022) (1.1.3).

Fish exhibit superior feed conversion efficiencies compared to terrestrial organisms (Brown et al., 2025). The preferential utilisation of protein as an energy source over carbohydrates and lipids is attributed to the lower energetic costs associated with ammonia excretion (Ip & Chew, 2010). Computational modelling estimates the basal maintenance requirements for leucine (9.1 ± 13.7 g/100g), valine (9.3 ± 26.6 g/100g), and isoleucine (6.4 ± 24.8 g/100g) mg/kg Body weight/ day (BW/day), though standard errors remain substantial, indicating interspecific variability (Hua, 2013).

The comparative efficacy of cAAs versus protein-bound AAs remains a contentious issue. While some investigations report equivalent absorption and metabolic efficiency, others suggest that the asynchronous absorption kinetics of crystalline AAs may result in increased oxidation rather than protein incorporation (Dabrowski et al., 2003). Plant-based diets typically necessitate methionine supplementation, whereas microbial-derived protein sources require additional lysine fortification (Aragão et al., 2022; Hu et al., 2008).

Elevated leucine intake does not invariably correlate with increased protein accretion. Choo et al. (1991) demonstrated that dietary leucine levels above 6.5% negatively impacted protein deposition in rainbow trout, with excessive inclusion (≥13.4%) inducing physiological abnormalities. Leucine is integral to protein biosynthesis and metabolic homeostasis, exerting anti-catabolic effects on muscle tissue while promoting lipid oxidation (Wilson et al., 2011).

Isoleucine, a structural isomer of leucine, plays a multifaceted role in muscle repair, endocrine regulation, and immune function (Zhang et al., 2017). It modulates glucose transport and enhances muscle integrity, as evidenced in

grass carp, where dietary isoleucine supplementation has been linked to improved flesh quality (muscle protein and fat deposition) via antioxidant pathways such as NF-E2-related factor 2 (NRF2)/ mTOR/ ribosomal S6 protein kinase 1 (S6K) and casein kinase 2 (CK2) pathway (Gan et al., 2014).

Valine, a glucogenic BCAA, is vital for muscle maintenance and energy balance. However, supra-optimal dietary valine concentrations may disrupt protein metabolism and impair hepatic function, adversely affecting growth performance of golden pompano (*Trachinotus ovatus)* (Huang et al., 2018). Studies on red drum (*Sciaenops ocellatus*) identified optimal dietary BCAA levels- leucine (15.7 g/kg), isoleucine (11.1 g/kg), and valine (12.4 g/kg)- which collectively enhanced weight gain, feed efficiency, and protein retention (Castillo & Gatlin, 2018).

Alanine serves as a pivotal gluconeogenic substrate, facilitating glucose homeostasis via glycolytic and gluconeogenic pathways, which are evolutionarily conserved among piscine species (Marandel et al., 2015). The availability of metabolic energy exerts a profound influence on protein utilisation, with AAs serving as principal substrates for ATP generation (Molina-Poveda, 2016).

Additionally, proteolytic activity during reproductive cycles supplies requisite AAs for metabolic processes, while surplus AAs undergo deamination, with their carbon skeletons subsequently utilised for energy production or lipogenesis (Bera et al., 2025).

1.1.3 BCAA catabolism and regulatory mechanisms

This metabolic pathway primarily occurs in skeletal muscle, with limited hepatic involvement during first-pass metabolism (Wiltafsky et al., 2010). BCAT facilitates the conversion of BCAAs into branched-chain keto acids (BCKAs), while BCKDH enzymatically regulates their oxidative degradation (Conway & Hutson, 2016). BCKAs are further metabolised into tricarboxylic acid (TCA) cycle intermediates, serving as substrates for cellular respiration (Holeček, 2020).

Leucine functions as a ketogenic AA, valine as a glucogenic substrate, and isoleucine exhibits dual functionality (Szabo et al., 2024). BCKDH expression is predominantly hepatic, with regulatory control over energy metabolism and protein turnover (Wessels et al., 2016). Excess leucine intake can modulate

BCKDH activity in pigs, with potential repercussions on serotonin biosynthesis and appetite regulation. (Wessels et al., 2016)

BCAAs are integral to proteostasis and metabolic adaptation and Zheng et al. (2016) demonstrated that BCAA supplementation enhanced anabolic signalling and mitigated proteolytic degradation through the ubiquitin-proteasome pathway. However, excessive leucine intake may dysregulate AA transporter expression, thereby reducing the bioavailability of isoleucine and valine and perturbing nitrogen homeostasis (Cervantes et al., 2015).

The BCAAs are hydrophobic AAs primarily embedded within globular proteins, contributing to structural stability and protein accretion (Castillo & Gatlin, 2018). In mammalian models, BCAAs undergo initial catabolism in extrahepatic tissues, predominantly muscle, where they are transaminated into BCKA before subsequent hepatic oxidation (Espe, 2016). These AAs constitute approximately 18–20% of total AAs in plant and animal proteins, though literature reports a wider range of up to 35% (Neinast et al., 2019). Metabolically, valine is glucogenic, leucine is ketogenic, and isoleucine exhibits both glucogenic and ketogenic properties, underscoring their diverse physiological roles (Adeva-Andany et al., 2017).

Ontogenetic shifts in nutritional needs are characterised by an increased demand for AAs during early developmental stages to support rapid somatic growth and energy demands, followed by a decline in requirements during later life (Li et al., 2013). AAs in aquafeeds are provided in protein-bound, free amino acid (fAA), or peptide forms, with absorption mechanisms mirroring those in mammals.

Optimal protein levels in aquaculture diets are dictated by dietary energy content and AA balance, while competitive interactions- such as those between leucine and isoleucine, or arginine and lysine- can induce metabolic imbalances (Block & Harper, 1991). While BCAA antagonism has been extensively characterised in mammalian systems, its implications in fish remain incompletely understood (Dimou et al., 2022; Wei et al., 2022).

1.1.4 BCAA influence on feed intake and metabolism

Dietary leucine excess has been implicated in feed intake suppression across multiple taxa due to its competitive inhibition of isoleucine and valine metabolism (Wiltafsky et al., 2010). This phenomenon is mechanistically linked to the activation of BCKDH, which accelerates isoleucine and valine catabolism, leading to deficiency states. Observations in mammalian studies have demonstrated that increased leucine intake correlates with diminished growth hormone-insulin-like growth factor-1 (GH-IGF-1) expression, a critical regulator of somatic growth (Laager et al., 1993). Similarly, nutrient-sensing pathways, including mechanistic target of rapamycin (mTOR) activation and AMP-activated protein kinase (AMPK) suppression, are influenced by BCAA availability, impacting metabolic homeostasis (Conde-Sieira & Soengas, 2017).

While substantial research has elucidated BCAA interactions in terrestrial species, their regulatory roles in piscine feed intake remain largely unexplored (Ahmad et al., 2021). In various vertebrate models, deficiencies in arginine, leucine, lysine, and methionine are known to negatively impact voluntary feed consumption while tryptophan exerts pronounced regulatory effects on feeding behaviour suggesting a broader interplay between AAs and appetite modulation (Hou & Wu, 2018). Investigations in rats have demonstrated that leucine administration elicits hypothalamic mTOR signalling, thereby suppressing appetite and body mass (Cota et al., 2006). However, research in rainbow trout found no significant impact of dietary leucine excess on plasma valine or isoleucine levels, contradicting findings from mammalian models (Choo et al., 1991; Wiltafsky et al., 2010).

1.1.5 Amino Acid Metabolism

AA oxidation contributes significantly to the energetic demands of fish, accounting for up to 90% of ATP generation but discrepancies exist regarding AA utilisation rates across species and environmental conditions (Palma et al., 2019). In terrestrial vertebrates, high-protein diets promote satiety and enhance thermogenic energy expenditure. In contrast, fish exhibit inherently higher protein requirements, with AA composition in formulated diets directly modulating plasma AA levels. Thermal conditions also critically influence metabolic rates; increased

temperatures augment protein oxidation rates, while low-temperature adaptations may involve enhanced lipogenesis or the expression of alternative enzyme isoforms. Osmoregulatory challenges in euryhaline fish elevate AA catabolism, particularly leucine oxidation, to sustain cellular ATP production for ion transport (Tseng & Hwang, 2008). Hypoxic stress exacerbates AA catabolism, culminating in elevated ammonia excretion.

Diurnal oscillations exert a significant influence on the plasma AA profile, with peak concentrations typically manifesting during the nocturnal phase. The precise mechanistic drivers of these fluctuations, however, remain a subject of inquiry, specifically whether they are primarily governed by feeding rhythms or by the influence of photoperiod (Carrillo et al., 1980; Zhang et al., 2024).

Hormonal regulation further modulates AA metabolism with studies suggesting cortisol elevates circulating AA levels, predominantly BCAAs, by enhancing hepatic proteolysis (Bifari & Nisoli, 2017). Additionally, insulin and glucagon reciprocally regulate AA transport, with leucine acting as a potent insulin secretagogue (Yang et al., 2012). The liver serves as the principal site of AA degradation, orchestrating gluconeogenesis and lipid biosynthesis. Notably, excessive leucine intake may amplify ammonia production, with glutamine synthesis an ammonia detoxification strategy, necessitating further investigation into its physiological ramifications in fish.

1.1.6 mTOR signalling and amino acid regulation

The mTOR pathway governs cell growth, metabolism, and proteostasis in response to nutrient availability, energy status, and growth factor signalling (Hall, 2008). Leucine serves as a pivotal mTOR activator, stimulating protein synthesis while concurrently inhibiting proteolysis (Rehman et al., 2023) The mTOR cascade consists of two primary complexes: mTORC1, which controls anabolic processes, and mTORC2, which influences cytoskeletal remodelling and cellular survival (Laplante & Sabatini, 2009).

mTORC1 facilitates cap-dependent translation via phosphorylation of ribosomal protein S6 kinase (S6K1) and eukaryotic initiation factor 4E-binding protein (4E-BP1), thereby enhancing protein biosynthesis (Wullschleger et al., 2006). mTOR

activation is dictated by growth factors, intracellular ATP concentrations, oxygen tension, and AA availability and leucine-mediated mTOR stimulation is mediated via RAG GTPase-dependent translocation to RHEB-enriched subcellular compartments, underscoring its critical role in nutrient sensing (Ma & Blenis, 2009).

In other vertebrates, leucine enhances mRNA translation by promoting the formation of the eukaryotic initiation factor 4F complex (EIF4F), activating ribosomal protein S6, and through other mechanisms not yet fully understood (Cao et al., 2021; Suryawan et al., 2008). Similar studies revealed that flooding doses of single EAAs (*e.g.,* leucine, phenylalanine, threonine, or valine) doubled skeletal muscle protein synthesis rates. In contrast, flooding doses of NEAAs (*e.g*. arginine, glycine, and serine) had no effect on muscle protein synthesis. These findings highlight the unique role of EAAs, particularly leucine, in regulating muscle protein synthesis (Anthony et al., 2000).

By integrating molecular analyses, nutrient utilisation studies, and growth trials, this research seeks to refine AA requirements in aquaculture, optimising feed formulations to enhance sustainability. Future investigations may also explore the role of isoleucine in modulating AA transporter expression (Zhang et al., 2017), leucine's influence on tryptophan metabolism (Wessels et al., 2016), and the broader metabolic ramifications of BCAA antagonism (Castillo & Gatlin, 2018).

Thus, this thesis had 3 main categories of research questions:

1) were there digestibility differences between intact and cAAs, were there digestibility differences with a 21% cAA feed inclusion, did varying levels of the BCAAs affect growth?

2) could we identify the AA uptake in plasma, muscle and liver tissues and identify peak uptake times?

3) was there an effect of the BCAAs on the BCAA catabolism and mTOR pathway mRNA transcripts, and from a transcriptomics perspective, did hypoxia affect mTOR associated mRNA transcripts?

Chapter 2

BCAA DIGESTIBILITY, UPTAKE AND RESPONSE IN ATLANTIC SALMON POST-SMOLTS.

Abstract

This study explored the digestibility and metabolic assimilation of branched-chain amino acids (BCAAs) in post-smolt *Salmo salar* (Atlantic salmon), emphasising the physiological impact of dietary supplementation. Comparative analyses of digestibility suggested that there were differences in each nutrient, with no distinguishable separation between intact proteins and BCAA supplemented diets. Feed intake (FI) exhibited statistically significant differences, wherein the whey diet elicited the highest FI, whereas isoleucine diet demonstrated the lowest intake. Temporal fluctuations across sampling intervals possibly suggest adaptive physiological responses to environmental stimuli rather than variations in palatability.

Plasma biochemical profiling indicated effective absorption of supplemented BCAAs, with temporal heterogeneity in peak uptake kinetics. Notably, leucine concentrations in the valine diet were significantly reduced compared to the control diet 8 hr postprandial, suggesting a competitive interaction between valine and leucine for cellular uptake. Corroborating prior studies, leucine exhibited preferential absorption, potentially inhibiting valine and isoleucine uptake via competitive inhibition of shared transport mechanisms. These dynamic plasma BCAA fluctuations underscore the intricate interplay between dietary amino acid (AA) availability and transport efficiency, aligning with established findings in teleost and mammalian models.

Quantitative analysis in muscle tissue revealed decreased leucine and isoleucine concentrations at 24 hr postprandial, indicative of sustained oxidative catabolism. Hepatic tissue exhibited differential modulation of arginine and taurine concentrations, while plasma AA profiles aligned with competitive transport phenomena. Discrepancies in peak plasma values further delineate the multifactorial influence of intact dietary proteins, environmental temperature fluctuations, and metabolic stressors on AA homeostasis

Transcriptomic analyses revealed that the primary enzyme in BCAA catabolism, branched-chain aminotransferase, mRNA abundance was predominantly upregulated in muscle tissue, reinforcing the hypothesis that primary BCAA

transamination occurs within myocytes rather than hepatocytes. The expression of branched chain α-ketoacid dehydrogenase, a pivotal enzyme in BCAA catabolism and the second step in this pathway, peaked at 4–8 hr postprandial, with muscle tissue exhibiting markedly higher mRNA abundance relative to hepatic tissue. Upstream of the mTOR pathway, the nutrient sensor Sestrin and Ras-related GTP-binding protein A mRNA abundance patterns followed tissue-specific trends, suggesting differential activation of nutrient-sensing pathways. Notably downstream of mTOR, variations in MYOSTATIN 1a and MYOSIN 6 mRNA abundance imply a regulatory role for BCAAs in modulating skeletal muscle hypertrophy and protein turnover.

The preliminary objective was to assess the metabolic response of Atlantic salmon to dietary BCAAs and evaluate whether these responses aligned with patterns reported in monogastric vertebrates. Specifically, the digestibility of experimental diets was compared between intact protein sources and cAA diets, as well as within the BCAA-enriched diets themselves. Additionally, postprandial responses of BCAAs within the BCAA diets, were tracked over a 24 hr period. The findings provide important insights for aquaculture, indicating that cBCAAs can be utilised effectively without compromising digestibility, offering flexibility in diet formulation and the potential to reduce reliance on conventional protein sources. The secondary objective was to identify whether BCAA added to a diet bypass the liver and provide a direct stimulation of the mTOR pathways of protein synthesis regulation. This study elucidates the intricate interdependencies between dietary BCAA supplementation, systemic absorption, tissue-specific metabolic processing, and molecular regulation in Atlantic salmon. The findings substantiate preferential leucine uptake, competitive transport interactions among BCAAs, and the pivotal role of BCAA metabolism-associated gene networks in nutrient utilisation. These insights contribute to optimising aquaculture nutritional strategies aimed at enhancing metabolic efficiency and growth performance in farmed salmonids.

Keywords: Atlantic salmon, digestibility, crystalline amino acids, mTOR, BCAA metabolism, amino acids, branched chain amino acids

2.1 Introduction

The shift towards plant-based aquafeeds presents formulation challenges, including suboptimal amino acid (AA) profiles and the presence of anti-nutritional factors (ANFs) that hinder digestibility (Glencross, 2020). ANFs can be mitigated through processing methods such as heat treatment, fermentation, and enzyme supplementation (Krogdahl et al., 2010). The use of microbial, yeast, and insect-based proteins has gained attention, though nutritional variability and production costs remain limiting factors (Belghit et al., 2018).

Aquaculture feeds are classified as either complete or supplemental, with complete feeds providing all essential nutrients for intensive farming systems (Naylor et al., 2000). Nutrient-based formulation methods are preferred over ingredient-based approaches, as they ensure balanced AA profiles without excessive crude protein inclusion (Nunes et al., 2014). Poorly formulated feeds contribute to nitrogenous waste and eutrophication, underscoring the need for precision in diet formulation (Azevedo et al., 2002). Processing methods, including extrusion and pelletisation, impact nutrient digestibility. High-temperature extrusion may degrade heat-sensitive nutrients, while ingredient particle size affects digestibility (Glencross et al., 2021). Feed hardness and water stability influence feeding behaviour and nutrient retention (Jacobsen et al., 2018).

Crystalline AAs (cAAs) are synthetic AAs and supplement plant-based diets by compensating for deficiencies in first-limiting AAs such as lysine and methionine (Nunes et al., 2014). Their efficacy remains debated, as cAAs are said to be absorbed more rapidly than intact proteins, potentially leading to imbalances and increased oxidation rather than protein synthesis (Schuhmacher et al., 1997). This discrepancy necessitates precise feed formulation to optimise AA bioavailability and minimise nitrogen waste.

Achieving optimal growth performance requires a balanced energy-to-protein ratio, ensuring that energy for maintenance is met before allocating protein for growth (Taj et al., 2023). Imbalanced energy intake can lead to protein catabolism, increasing nitrogen excretion and reducing feed efficiency (Yadata et

al., 2020). Deaminated AA carbon skeletons contribute to metabolic fuel or fatty acid synthesis, with 10–20% utilised for energy (Molina-Poveda, 2016).

Of the 20 proteogenic AAs, essential amino acids (EAAs) such as lysine and methionine must be sourced from feed, as fish cannot synthesise (Craig & Helfrich, 2009). EAAs are critical for protein synthesis, and deficiencies in first-limiting AAs stall growth due to peptide chain elongation constraints, as described by Liebig's-barrel analogy. Liebig's-barrel concept highlights the importance of the most deficient or limiting nutrient, such as methionine (Figure 1.2) on growth and is used to optimise nutrient management in animal feeds. Non-essential AAs (NEAAs) can be synthesised endogenously, while conditionally essential AAs (CEAAs) vary in dietary dependence based on developmental stage or physiological stress.

AAs supply 14-85% of fish energy needs, serving as substrates for ATP production that supports muscle contraction, biosynthesis, and cellular transport (Falco et al., 2020). This metabolic preference is species-dependent; for instance, 35-40% of leucine is oxidised for energy in rainbow trout, compared to 10-40% in sturgeon (Li et al., 2021). Fish display superior feed conversion ratios (FCRs) in protein-to-muscle conversion than terrestrial livestock (Besson et al., 2020).

2.1.1 Amino acid absorption and metabolic regulation

AA absorption occurs primarily in the intestine via active transport and facilitated diffusion, with substrate competition influencing uptake efficiency (Conceição et al., 2003). Microbiome composition plays a role in nutrient assimilation, with diet-induced shifts affecting gut health and digestion (Navarrete et al., 2013).

Fish rely on digestive enzymes, including proteases, lipases, and carbohydrases, to break down dietary components (Burton & Burton, 2017). Enzymatic activity is modulated by diet composition, with variations observed across species (Krogdahl et al., 2015). Peptide absorption via Peptide Transporter 1 (PEPT1) is a primary protein utilisation route, highlighting the importance of dietary protein structure (Wang et al., 2017).

Free amino acids (fAAs) constitute a dynamic pool in fish, continuously exchanging between dietary intake, protein synthesis, and energy production (Yu et al., 2025). Dietary AAs enter circulation following digestion, while others are mobilised for metabolic functions (Yimam et al., 2025).

2.1.2 BCAA metabolism and utilisation

Branched-chain amino acids (BCAAs), leucine, isoleucine and valine, constitute 18–35% of total AAs in plant and animal proteins and play structural and metabolic roles (Sowers, 2009). Unlike most AAs, which undergo first-pass hepatic metabolism, BCAAs are predominantly metabolised in muscle tissues, generating glutamate and branched-chain α-keto acids (BCKAs) (Espe, 2016). Their metabolism differs, with valine being glucogenic, leucine ketogenic, and isoleucine exhibiting both pathways (Brosnan & Brosnan, 2006). The first step of BCAA metabolism occurs primarily in muscle tissue, where branched-chain aminotransferases (BCATs) convert BCAAs into their respective BCKAs (Figure 2.1), with glutamate production occurring via amino group transfer to α-ketoglutarate (α-KG) (Holeček, 2020; Neinast et al., 2019).

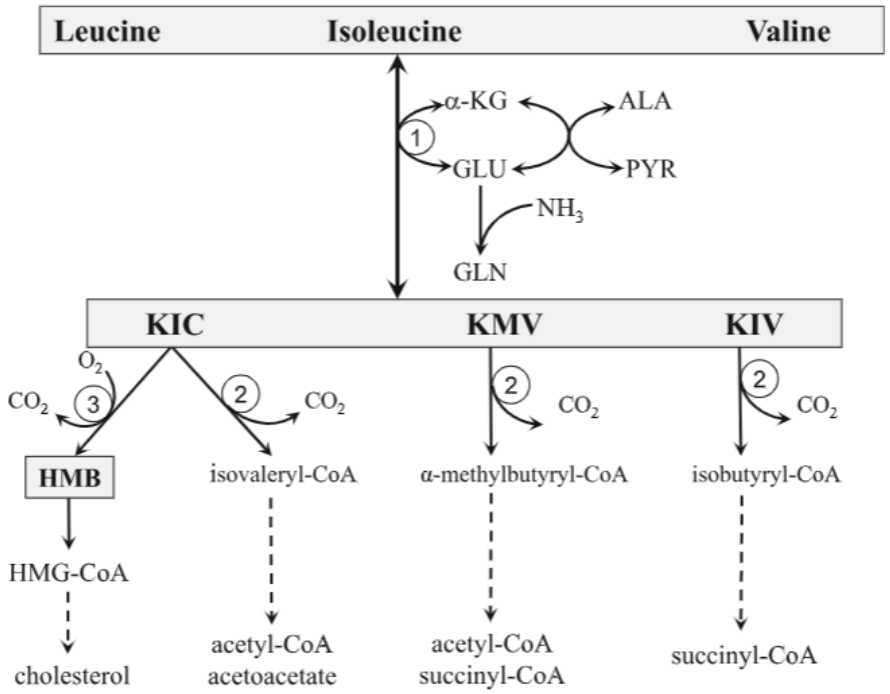


Figure 2.1 BCAA degradation. Image obtained from Holecek (2018). ALA=alanine, GLU= glutamate, GLN= glutamine, HMB= β-hydroxy-β-methylbutyrate, HMG-CoA= 3-hydroxy-3-methyl-glutaryl-CoA, KIC= α-ketoisocaproate, KIV= α-ketoisovalerate, KMV= α-keto-β-methylvalerate, α-KG= α-ketoglutarate. 1) branched-chain-amino-acid aminotransferase (BCAT), 2) branched-chain α-keto acid dehydrogenase (BCKD), 3) KIC dioxygenase.

Glutamate subsequently contributes to alanine synthesis via transamination or serves as a precursor for glutamine, facilitating ammonia detoxification (Holeček, 2018). Cole (2015) has suggested that there is an order to the substrate preference of the BCAT enzymes- firstly isoleucine, leucine and lastly valine.

The second catabolic step, catalysed by branched-chain α-ketoacid dehydrogenase (BCKDH), occurs in the mitochondrial inner membrane and is subject to phosphorylation-mediated regulation by branched chain ketoacid dehydrogenase kinase (BCKDK) and activation by protein phosphatase 2Cm (PP2Cm) (Dimou et al., 2022). In mammals, BCKDH activity is low in skeletal muscle but elevated in hepatic mitochondria (Holeček, 2017). Langer et al. (2000) demonstrated that excess BCAAs increase BCKDH activity in liver and muscle tissue, with BCKDK exhibiting a strong affinity for α-ketoisocaproic acid (KIC), metabolic intermediate of leucine catabolism, indicating its role as a primary regulator. Additional studies such as Ding et al. (2016) isolated different liver cells in mice and found that hepatocytes expressed all the enzymes required for BCAA metabolism apart from BCAT, reinforcing the theory of tissue-specific enzyme roles.

The final step of BCAA catabolism diverges into distinct metabolic fates: KIC is converted into acetyl-CoA and acetoacetate (ketogenic), α-ketoisovalerate (KIV) the valine metabolic intermediate, into succinyl-CoA (glucogenic), and α-keto-β-methylvalerate (KMV) the isoleucine metabolic intermediate into both succinyl-CoA and acetyl-CoA (dual ketogenic and glucogenic) (Mann et al., 2021). Additionally, leucine undergoes an alternative catabolic route via oxidation of KIC to 3-hydroxy-3-methylbutyrate (HMB) by KIC dioxygenase (Van Koevering & Nissen, 1992). In mammals, HMB conversion rates range between 5–18% while in muscle tissue, 20% of leucine is catabolised into KIC and HMB, with the remainder allocated to protein synthesis (Duan et al., 2016; Holeček, 2017). HMB supplementation has demonstrated anabolic and immunostimulatory effects in fish, mitigating intensive farming stressors and enhancing growth performance (Siwicki et al., 2000). Given that fish skeletal muscle accounts for over 50% of body weight, it serves as the largest reservoir of both bound and fAAs (Coppes Petricorena, 2015) . This proportion varies with ontogenetic stage, as smaller fish

exhibit lower muscle fAA levels. Fish larvae utilise AAs for energy, suggesting a higher catabolism of AAs than mature fish (Rønnestad et al., 1999) while somatic growth is affected by the cost of reproduction (Brosset et al., 2016). Similarly to mammals, BCAA oxidation is predominantly localised in muscle tissue (Nemova et al., 2016).

2.1.3 The mTOR pathway

The mechanistic target of rapamycin (mTOR) acts as a central regulator of cell growth, integrating energy availability, AA influx, and growth factor signalling (Saxton & Sabatini, 2017) (Figure 2.2). mTOR exists in two distinct complexes: mTORC1, which governs protein synthesis, and mTORC2, involved in cytoskeletal organisation(Wang & Holst, 2015). Activation of mTORC1 requires insulin receptor substrate 1 (IRS-1), phosphatidylinositol-3 kinase (PI3K), and protein kinase B (AKT), in conjunction with BCAA-mediated Sestrin/GATOR/RAG signalling (Ainslie et al., 2016; Mann et al., 2021).

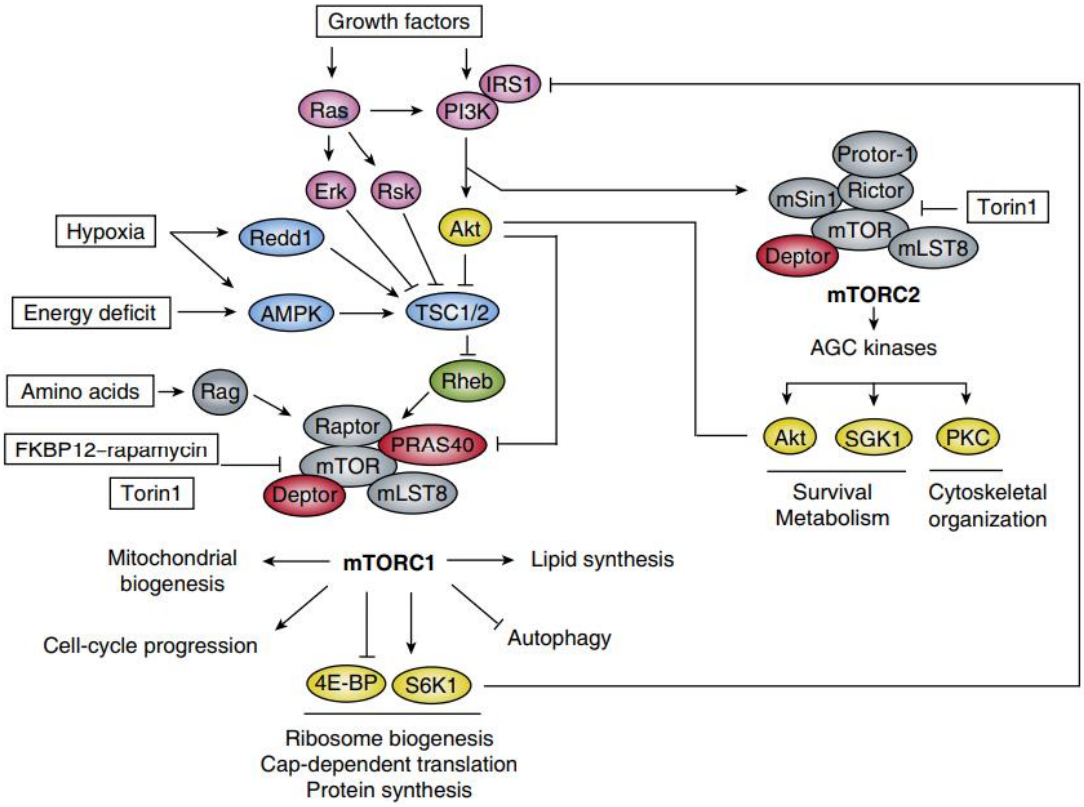


Figure 2.2 mTOR pathway. Image obtained from Laplante & Sabatini (2009). mTOR1 is composed of the mTOR catalytic subunit, RAPTOR, mLST8, PRAS40, and DEPTOR. mTOR2 consists of six proteins: mTOR, RICTOR, MSIN1, PROTOR-1, MLST8, and DEPTOR.

Leucine inhibits Sestrin 2 (SESN2), a negative mTOR regulator, thereby facilitating mTORC1 activation (Wolfson & Sabatini, 2017). RAS-related GTPases (RAGs) recruit RAPTOR to the mTORC1 complex, ensuring activation under AA abundance (Rehman et al., 2023). Downstream targets include myostatin (MSTN), a negative regulator of muscle growth, which impairs mTORC1-mediated protein synthesis (Churova et al., 2017). Studies in salmonids have identified multiple MSTN paralogs, with IGF1-regulated MSTN inhibition promoting muscle hypertrophy (Seiliez et al., 2013).

The mTOR signalling pathway regulates protein synthesis in response to AA availability, energy status, and hormonal signals. Leucine serves as a key activator of mTOR, influencing growth and feed intake. Elevated valine levels have also been shown to modulate feeding behaviour through mTOR-related pathways in rainbow trout (Comesaña et al., 2018).

The preliminary aim of this experiment was to examine the response of Atlantic salmon (*Salmo salar*) to a supply of BCAAs and assess whether the responses were similar to other vertebrates. This first section examined the digestibility of the experimental diets compared to intact protein diets, and within the BCAA experimental diets.

The secondary aim of this experiment was to examine the post-prandial physiological response of Atlantic salmon to a supply of BCAAs and assess whether the uptake and molecular responses were comparable to other vertebrates. This second section examined the plasma and tissue fAAs as well as the mRNA transcript response of targets within the BCAA diets.

2.2 Materials and methods

2.2.1 Ethics approval

The experiment was approved by the University of Stirling Animal Welfare and Ethical Review Body (reference AWERB/1718/176) in accordance with the UK Home Office under the Animals (Scientific Procedures) Act 1986. The trial was conducted at Marine Environmental Research Laboratory (MERL, Machrihanish, UK) and ran from 24 September 2018 to 10 October 2018.

Table 2.1 Diet formulations and compositions of the seven extruded experimental diets in Trial 1 digestibility analyses. Test ingredients were included at 30% for intact proteins and 2% for the cBCAA experimental feeds. BCAA diets were isonitrogenous and isocalorific.

	BCAA diets				Whole protein diets		
	CD	LD	VD	ID	WHE	CAS	SPC
Formulation (g/ Kg)							
Fishmeal (Anchoveta) [a]	200.0	196.0	196.0	196.0	140.0	140.0	140.0
Fishoil (Anchoveta) [a]	75.0	74.0	74.0	74.0	52.5	52.5	52.5
Soy Protein Concentrate [a]	250.0	245.0	245.0	245.0	175.0	175.0	**475.0**
Wheat Flour [a]	168.0	165.0	165.0	165.0	117.6	117.6	117.6
Wheat Gluten [b]	150.0	147.0	147.0	147.0	105.0	105.0	105.0
Corn Gluten [b]	150.0	147.0	147.0	147.0	105.0	105.0	105.0
Choline Chloride [a]	1.0	0.98	0.98	0.98	0.7	0.7	0.7
Yttrium Oxide [c]	2.0	1.96	1.96	1.96	1.4	1.4	1.4
OVN Premix [d]	4.0	3.92	3.92	3.92	2.8	2.8	2.8
Leucine [e]		**20**					
Valine [e]			**20**				
Isoleucine [e]				**20**			
Whey					**300**		
Casein						**300**	
Analysed composition (DM%)							
Crude protein	53.1	54.8	54.6	54.6	60.4	61.5	56.9
Lipid	13.9	14.2	13.9	14.2	12.8	9.4	9.1
Energy (MJ/kg)	22.6	22.8	22.7	22.8	23.0	22.1	21.7
Sum of AA	50.6	51.9	55.9	52.0	60.8	63.3	57.4
Alanine	2.7	2.7	2.8	2.6	3.1	2.7	2.9
Arginine	2.7	2.4	2.9	2.7	2.7	2.9	3.5
Asparagine	4.1	4.2	4.3	4.0	5.2	4.8	5.3
Cysteine	0.4	0.4	0.5	0.4	0.6	0.5	0.5
Glutamate	12.4	12.3	12.7	11.8	12.5	14.2	12.7
Glycine	2.3	2.2	2.4	2.2	2.2	2.2	2.6
Histidine	1.3	1.0	1.4	1.3	1.5	1.7	1.4
Isoleucine	2.4	2.1	2.5	**4.0**	3.1	2.7	2.3
Leucine	4.7	**6.7**	5.0	4.7	6.1	5.9	5.2
Lysine	2.5	2.5	2.6	2.4	3.8	3.6	2.9
Methionine	1.0	1.0	1.1	1.0	1.3	1.5	1.1
Phenylalanine	2.6	2.5	2.8	2.6	2.9	3.3	3.0
Proline	4.0	4.0	4.2	4.0	4.4	5.8	4.2
Serine	1.7	2.0	2.4	2.5	3.1	3.3	3.2
Threonine	1.5	1.8	1.8	1.8	3.0	2.5	2.2
Tyrosine	1.8	1.8	1.9	1.9	2.2	2.7	2.2
Valine	2.6	2.4	**4.7**	2.3	3.2	3.1	2.5

All formulation values are g/kg and analysed composition values are dry matter (DM%) unless otherwise indicated. CD= Control diet, LD= Leucine diet, VD= Valine diet, ID= Isoleucine diet, WHE= Whey diet, CAS= Casein diet and SPC= Soya Protein Concentrate diet. [a] Supplied by BioMar Ltd, Grangemouth, Scotland. [b] Supplied by Roquette Ltd, Hull, England. [c] Supplied by Stanford Materials, Aliso Viejo, California, United States. [d] Supplied by DSM, Basel, Switzerland as OVN vitamin and mineral premix for salmonids (dose per kilogram of diet: Vitamin A: 2400 UI/kg; Vitamin D3:1200 IU/kg; Vitamin K3: 8 mg/kg; Vitamin B1: 12 mg/kg; Vitamin B2: 20 mg/kg; Niacin: 120 mg/kg; Vitamin (Pantothenate) B5: 32 mg/kg; Vitamin (Pyridoxine) B6: 16 mg/kg; Vitamin (Folate) B9: 8 mg/kg; Biotin: 0.8 mg/kg; Vitamin (Cyanocobalamine) B12: 0.04 mg/kg; Vitamin C: 120 mg/kg; Vitamin E: 160 UI/kg; Manganese: 16 mg/kg; Iodine: 1.6 mg/kg; Copper: 4 mg/kg; Cobalt: 4 mg/kg; Magnesium: 80 mg/kg; Zinc: 80 mg/kg; Iron: 24 mg/kg; Selenium: 0.16 mg/kg) [e] Supplied by Bulk powders. *Carbohydrate content determined based on dry matter minus protein, ash and lipids.

2.2.2 Experimental design

Raw ingredients were obtained from feed manufacturers and cAAs were sourced from Bulk sport supplement powders (Sports Supplements Limited t/a Bulk™, Colchester, UK). A diet substitution strategy was used to formulate and prepare the diets, whereby either cAAs (2%) or ingredients (30%) were added to the basal mash. The basal mash was designed to form the base for all the test diets and was produced using pre-weighed hammer-milled ingredients with an 800 µm mesh to ensure homogenised particle size.

A total of 10 kg of each diet was made by adding a subsample of the basal mash and adding either the crystalline BCAAs at a 2% (200 g) inclusion rate or a 30% (3000 g) ingredient inclusion level. Experimental feeds were extruded via cooking expansion extrusion technology at University of Nottingham using a ThermoMix twin-screw extruder and a 4mm Ø die (ThermoFisher Scientific, Karlsruhe, Germany). The extruded pellets were dried at 60 °C for 24 hr before being allowed to cool and then bagged and labelled.

Atlantic salmon were obtained from a commercial supplier and acclimated for several months at the Marine Environmental Research Laboratory (MERL, Machrihanish, UK) in holding tanks before transferral to 500 L experimental tanks. The system used a flow-through process of filtered marine water (salinity ~34 PSU) with a temperature of 12.3 ±0.6 °C (mean ± S.D.), dissolved oxygen of 8.1 ± 0.28 mg/L (mean ± S.D.) and a flow rate of around 5 L/min. A photoperiod of 16:8 (L:D) was maintained, and environmental parameters were monitored and recorded by an OxyGuard monitoring system (OxyGuard International A/S, Farum, Denmark).

The experimental design consisted of a replication through time method, achieved by replicating tanks over a three-week period (Figure 2.3). Tanks were stocked with 35 post-smolts with a mean weight of 263 ±25g and mean length of 293 ±10 mm. A commercial diet was fed for two weeks during the acclimation period before exchanging to the test diets. Treatments were randomly assigned each week, and the fish were evenly redistributed amongst the tanks.

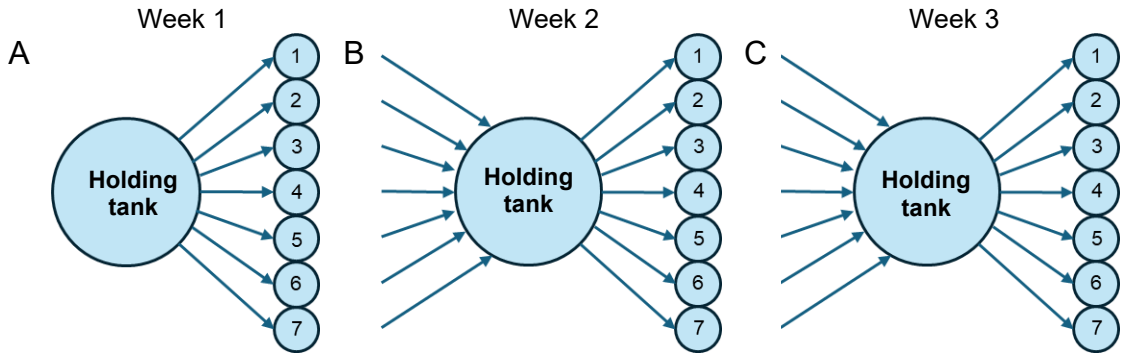


Figure 2.3 Block replication through time method**.** Allowing biological replicates to be collected in triplicate using time when tanks are limited (3 fish/ tank/ timepoint/ diet/ week) A) at the start of the experiment, 35 post-smolts fish were weighed, counted and distributed from a holding tank into each experimental tank and fed on a commercial diet for 2 weeks to acclimatise before Week 1 trial start. B) At the end of Week 1 sample collection, all fish were put into the central holding tank and redistributed to the experimental tanks for the start of Week 2. C) At the end of Week 2 fish were again, all placed into a holding tank before final redistribution amongst experimental tanks. Over the entire experimental period, 1 experimental tank represented 1 experimental diet and to minimise tank effect, the experimental diets were randomly assigned to tanks for each weekly period.

Fish were fed their respective diets over a 3 hr period (0600–0900) using automated drum feeders (Arvo-tec Oy, Arvo-Tec T Drum 2000 Feeder, Huutokoski, Finland) followed by hand feeding to apparent satiety. The test diets were fed for a minimum of a week before faecal stripping commenced. Waste feed was collected by sieving the outflow water, weighing the collection of uneaten pellets on an analytical scale (Mettler Toledo, PE24, Greifensee, Switzerland) and recording the data to be corrected to dry weight at a later stage.

On sampling days, fish were fed in a staggered basis (30 min between each treatment tank). Three fish (n=3) from each of the treatment tanks were schedule-1 killed and sampled at each time point as follows: -2 (0), 2, 4, 8 and 24 hr post-feeding. The 8 hr time-point started with the faecal stripping sample collection and at this point all remaining fish (except the three for the 24 hr sampling) were removed to a holding tank.

Fish were allowed to acclimatise to their diets for 7 days before faecal collection commenced 8 hr post-prandial, consistent with studies by Huyben et al. (2021). Fish were netted, transferred into a smaller aerated tank, and sedated with Tricaine methanesulfonate/ MS-222 (Syndel, Syncaine®, Ferndale, USA) at 0.1 g/L until they lost consciousness. Faecal stripping was completed by utilising the technique of Glencross et al. (2005) where faeces were removed by gentle

application of pressure on the abdominal region and placed into labelled plastic vials and immediately stored at -20 °C. The schedule-1 euthanised fish (anaesthetic followed by either destruction of the brain, neck or exsanguination) were wiped down, with the weights recorded to 0.5 g and fork length was taken from the tip of the nose to the fork in the tail.

Approximately 3 mL of blood was removed from the caudal vein of each fish using a heparinised 5 mL syringe with a 19G needle. The Eppendorfs were centrifuged at 6000 rpm for 2 min (Eppendorf AG, MiniSpin® centrifuge, Hamburg, Germany), plasma separated from the precipitated material and stored at -70 ºC until required for further analysis.

Tissue collections were taken at each sampling time and stored in 1.8 mL cryotubes (Thermo Scientific, Nunc™ Cryotube™ Vials 1.8 mL, Roskilde, Denmark) on dry ice and stored at -70 °C for future analysis.

Feed intake was determined by collecting and weighing the uneaten waste feeds, drying them and reweighing when dried. Applying the waste feed correction factor and deducting this from the known amount of feed fed per day. This was then worked out on a weekly basis to determine the feed intake (FI) in g/fish/day as below:

$$\text{Feed intake} = \frac{\text{(feed fed-(WF÷CF)}}{\text{total fish/ tank}}$$

where WF is the total weight of the collected waste feed in each tank, CF is the correction factor of the wet feed to dry feed.

To determine the correction factor (CF), dry feed from each experimental diet was weighed in groups of 20 pellets to determine dry weight of each individual pellet. These groups were then left in water for either 1 to 2 hr, and removed by shaking the sieve three times before weighing. Each wet weight of 20 pellets was then divided by the original number of dry pellets (20) producing a correction factor back to dry weight. The total uneaten wet waste weight/ tank was divided by the CF, resulting in total waste feed (dry matter).

$$\text{Waste feed (DM)} = \frac{\text{wet waste feed}}{\text{correction factor}}$$

2.2.3 Analyses of feeds, ingredients, and faeces

2.2.3.1 MOPA

Experimental ingredients, feeds and faeces were analysed for protein, moisture, ash, total lipids and energy (S 2.1).

2.2.3.1.1 Determination of moisture content of whole fish, tissue, feed and faeces.

Samples such as feeds, ingredients, tissues and whole body (WB) samples were homogenised using either a pestle and mortar or a Fosstech water cooled grinder (Foss, KN 295 Knifetec™, Runcorn, United Kingdom). Samples were weighed (Ohaus Pioneer, PX224, Nänikon, Switzerland) to 3 decimal places into pre-weighed plastic Polypropylene fixing pots (Thermo Fisher Scientific Inc., Gosselin™ Straight Containers 15478814, Loughborough, UK). These were then frozen for approximately 2 hr (depending on sample size) before being put into the freeze-dryer (SciQuip, ALPHA 1-4 LSC, Rotherham, United Kingdom). The lids were slightly loosened and allowed to freeze dry for 24 to 48 hr. When dry, samples were removed, placed into a desiccator and weighed.

Oven drying consisted of weighing numbered crucibles, with weights recorded on a 4 decimal place balance (Mettler Toledo, AC 100, Greifensee, Switzerland). When possible, 1-2 g of homogenised wet or freeze-dried samples were added to the crucibles, weighed, and weights were recorded. This was not always feasible with smaller quantities of original sample. Care was taken to avoid static when working with feeds, ingredients, freeze-dried tissues or any other dried material. These were then carefully put into a drying oven (Gallenkamp, Hot Box Oven, Cambridge, United Kingdom) at 110 °c for a minimum of 4 hr, but preferably overnight. These were then cooled in a desiccator before reweighing.

$$\% \text{ Moisture} = \frac{\text{Sample Weight (g)} - \text{Dried Sample Weight (g)}}{\text{Sample Weight (g)}} \times 100$$

2.2.3.1.2 Ash content of whole fish, tissue, feed and faeces

A muffle furnace set at 600 °C (Carbolite, AAF 1100 Ashing Furnace, Derbyshire, United Kingdom) was used to determine the ash content of experimental

samples. If very little of the experimental sample was available to complete all the analytical analysis, the pre-weighed crucibles used for moisture analysis were then put into the muffle furnace overnight. For removal, the furnace door was left ajar for an hour to allow the crucibles to cool to a more handleable temperature before being cooled in the desiccators; the crucibles were then reweighed to determine ash content. If enough of the original sample was available (*e.g.* feed, ingredients, WB), clean crucibles were weighed (Ohaus Pioneer, PX224) recorded and 1-2 g of sample was added before enclosing in the furnace overnight. The same procedure as mentioned above was repeated on removal from the muffle furnace.

$$\% \text{ ash} = \frac{\text{ash weight (g)}}{\text{sample weight (g)}} \times 100$$

or:

$$\% \text{ ash} = \frac{\text{ash weight (g)}}{\text{Original moisture sample weight (g)}} \times 100$$

2.2.3.1.3 Folch-Lee method for the extraction of lipids from tissue and feeds

The method used is based on the Folch-Lee method (Folch et al., 1957) with a slight deviation in the method to allow for the analysis of smaller quantities of tissue. Liver and muscle tissues were individually homogenised, weighed, and pooled (3 fish/ tank/ pool) before freeze-drying. All treatments were analysed at the 4 hr post-prandial timepoint, which was identified as the peak plasma fAA uptake in this experiment, and thereby possibly identifying trends between fAAs and lipids. In addition, the LD muscle and liver samples were analysed over all 5 time points (3 fish/tank/pool/ timepoint). Approximately 20 mg of homogenised freeze-dried tissue (liver and muscle) were weighed to 5 decimal places on (Ohaus Pioneer, PX224) and added into pre-weighed and labelled tubes.

HPLC grade Chloroform/methanol (C:M) (2:1, v/v) (Merck KGaA, Chloroform 366927, Methanol 34885-M, Darmstadt, Germany) was added at 6 mL per sample to the tubes under the fumehood, and volumes were recorded. Samples were kept on ice during this process and then homogenised using a mini Ultra Turrax™ (IKA, Ultra Turrax™ homogeniser, Staufen im Breisgau, Germany). Care was taken to rinse the probe in C:M (2:1) between sample tubes. When

using the mini Turrax^{TM} correct PPE was used (safety glasses and thick protective gloves). Lids /stoppers were added to the tubes, and these were stored at -20 °C for 1 hr.

Analytical reagent grade potassium chloride (KCl) (Merck KGaA, P3911, Darmstadt, Germany) was added at 0.25 volumes of 0.88% (w/v) to the homogenised samples (1.5 mL /sample) and left on ice for a minimum of 5 min. Tubes were then centrifuged at 1000rpm (400g) for 5 min, and the top layer was removed by aspiration.

Labelled 15 mL quickfit tubes were weighed to 4 decimal places and recorded before transferring the bottom layer of the centrifuged samples to prewashed (C:M 2:1) Whatman no.1 filter papers. The tubes were then transferred to either a nitrogen evaporator or TurboVap® (Biotage GB Ltd., TurboVap® Classic, Hengoed, UK) whereby the solvent was evaporated with oxygen-free nitrogen (OFN). Once this had occurred the tubes were left overnight in a vacuumed desiccater.

The tubes were then re-weighed, and weights were recorded before the lipids were redissolved in C:M (2:1) + 0.01% (w/v) Butylated hydroxytoluene (BHT) (Merck KGaA, W218405, Darmstadt, Germany) at a concentration of 10 mg/ mL. OFN was then added before sealing the tubes to protect the lipids for potential further analysis. These were then stored at -18 °C.

$$\% \text{ lipid} = \frac{\text{weight lipid (g)}}{\text{weight sample (g)}} \times 100$$

2.2.3.1.4 Kjeldahl crude protein using the OPSIS LiquidLINE system

The industry standard method, the Kjeldahl method was used for the determination of nitrogen as explained by Sprague et al. (2020). The crude protein concentration was calculated using a correction factor of 6.25 (0.16 g Nitrogen/ g of protein). The manufacturers of OPSIS LiquidLINE adapted the method specifications, and was used for fish feed, ingredients, tissue, and WB. The method had 3 phases: digestion, neutralisation/distillation and titration.

Depending on test sample quantities, 80-200 mg was weighed onto 42.5 mm filter paper discs, recorded, and added to the 250 mL Kjeldahl tubes. Reagent blanks were added to each batch. Copper Kjeltabs tabs (Thermo Fisher Scientific Inc., Kjeldahl Copper Catalyst Tablets 10020220, Loughborough, UK) and 12 mL concentrated sulphuric acid (Merck KGaA, 258105, Darmstadt, Germany) was added to each tube before transferral to the digestion block (420 °C) for 1 hr. Once the Kjeldahl tubes had cooled for at least 40 min, they were moved to the OPSIS LiquidLINE KjelROC Analyser and OPSIS LiquidLINE KjelROC Sampler KD-525 (OPSIS AB, Furulund, Sweden) for the start of the distillation/titration stage. All weights of test samples were manually added to the analyser to allow the OPSIS LiquidLINE system to calculate crude protein percentages.

The calculation used by the OPSIS LiquidLINE system is as follows:

$$\% N = \frac{(T - B) \times M \times 14.007}{\text{Weight sample (mg)}} \times 100$$

$$\% \text{ Protein} = N \times F$$

Where T = titration volume for sample (mL)
B = titration volume for blank (mL)
M = molarity of acid (to 4 decimal places)
F = conversion factor for nitrogen to protein (6.25)
14.007= Atomic mass of Nitrogen

'F factors are 5.70 for wheat, 6.38 for dairy products, and 6.25 for other feed materials.'

2.2.3.1.5 Energy determination using a bomb calorimeter

A Parr 6200 bomb calorimeter was used to determine gross energy (Parr Instrument Company, 6200, Moline, USA). In short, once all the set-up was completed (heater, pumps on, oxygen on, machine stabilisation, *etc.*) a 1 g benzoic acid pellet (Parr Instrument Company, 3415 Benzoic acid pellets, Moline, USA) was weighed in a crucible and recorded to 4 decimal places to be used as a standard (Mettler-Toledo GmbH, AC 100, Greifensee, Switzerland). Dried sample weights were required between 500-600 mg.

A firing wire was then attached to both electrodes in the assembly holder, with a loop formed above the pellet. Precaution was taken to ensure that the loop did

not touch itself otherwise this would lead to misfires. The electrode assembly unit was then placed into the bomb, and the lid was tightened. Care was taken to ensure that the lid was not too tight, to allow for expansion. This was then connected to the O_2 and filled to the pre-set requirements on screen.

The bucket for the bomb calorimeter was filled with water and weighed to 2812.8 g (Mettler-Toledo GmbH, PM6000, Greifensee, Switzerland) before insertion into the calorimeter. The bomb unit was then inserted into the bucket of water using specific tongs to avoid disturbing the weight of the water before the electrodes were connected. Onscreen data required was sample name and weight. Once completed, the results appeared onscreen and were recorded manually. The standard was accepted if it fell within the range of 26.50 ± 0.10 Kj/ g, otherwise the above steps were repeated.

2.2.3.1.6 Mineral analysis

Total minerals, trace elements and yttrium concentration in ingredients (S 2.2**),** feeds (S 2.3) and faeces (S 2.4) were determined using inductively coupled plasma atomic emission spectrophotometry (ICP-MS) with collision cell technology (Thermo Scientific, XSeries 2 ICP-MS, Cheshire, United Kingdom). Analytes were chromium, calcium, cobalt, copper, iron, manganese, magnesium, nickel, phosphorus, potassium, sodium, vanadium, yttrium, and zinc.

Test samples were weighed (20-50 mg) into Mars Xpress Teflon tubes (CEM Microwave Technology Ltd., 907576, Buckingham, UK) and 5 mL of 69% Nitric acid (Aristar® analytical grade; VWR Chemicals, Poole, UK) was individually added. To achieve digestion, a Mars Xpress microwave digester (CEM Microwave Technology Ltd., Mars Xpress, Buckingham, UK) was used in three stages. The ramping first stage was set at 21 to 190 °C for 15 min at 800 W, the second stage, the holding phase, was set at 190 °C for 20 min at 800 W and the final stage was a 30 min cooling down period.

Each of the digested samples was transferred into 10 mL volumetric flasks and ultra-pure water (Merck KGaA Millipore, Milli-Q ultrapure water system, Darmstadt, Germany) was used to make up the volume. This step was repeated but using 0.4 mL of the dilute into 10 mL centrifuge tubes to achieve a total dilution

factor of x25. Digests were processed by the Stirling university water quality lab (Stirling, UK). Kinetic energy discrimination (KED) mode used 100% helium as collision gas to correct for any interference and Argon was used as plasma gas. A control reference material was used to monitor integrity (Fish Muscle ERM-BB42; Institute for Reference Materials and Measurements (IRMM, Geel, Belgium).

2.2.3.2 Amino acid hydrolysis and derivitisation of feeds, ingredients, and tissues (bAAs)

2.2.3.2.1 Amino acid hydrolysis

For bound amino acids (bAAs), ingredients, feeds, faeces, and tissues were freeze-dried, and homogenised using a pestle and mortar or electric blender (Ingredients S 2.5, feeds S 2.6, faeces S 2.7, faeces S 2.8). A 100-250 mg of test sample was weighed, recorded, and transferred into Mars Xpress Teflon vessels (CEM Microwave Technology Ltd., 907576, Buckingham, UK) before adding 10 mL of phenolic (6M HCl) to each tube (Merck KGaA, Phenol detached crystals 99+% A15760-22, Darmstadt, Germany). Teflon tubes were allowed to stand for 15 min before 20 s of OFN was added. Teflon caps were screwed on tightly using the CEM Torque Tool (CEM Microwave Technology Ltd., 185245, Buckingham, UK) before being hydrolysed using a Mars 6 CEM Microwave digester (CEM Microwave Technology Ltd., Mars 6, Buckingham, UK). Phenolic 6M HCl was prepared fresh daily by dissolving 1 g of phenol crystals (Merck KGaA, Phenol detached crystals 99+% A15760-22, Darmstadt, Germany) in 500 mL of deionised water and then slowly adding 500 mL of HCL (37%) (Merck KGaA, HCl (37%) M2612-13, Darmstadt, Germany).

As a cross-validation method, the controls used were a standard fishmeal (Nutreco MasterLab, Standard Fishmeal Ring Test, Boxmeer, Netherlands) and a standard fish feed (Nutreco MasterLab, Fish Feed Ring Test, Boxmeer, Netherlands) and these were interchanged randomly as controls. These controls were chosen as the values were known and validated through the accredited international aquaculture ring test (ISO /IEC 17043 accredited (RvA R022)).

Table 2.2 CEM Microwave digester cycle programs.

Method	Stage	Ramp (min)	Hold (min)	Temp (°C)	Power (watts)
190°C	1	12	1	185	800
	2	5	20	190	800
	3	Cool down			
150°C	1	12	1	145	800
	2	5	20	150	800
	3	Cool down			

The optimal microwave settings used were 190 °C for the recovery of most of the AAs but for the more sensitive sulphur based AAs (methionine and cysteine), a setting of 150 °C was used. Tryptophan was destroyed in this process (Table 2.2).

Hydrolysed samples were transferred to 250 mL volumetric flasks. Teflon tubes were rinsed twice with ultrapure water and added to the flasks before the volume was made up to 250 mL. Flasks were mixed by inverting and 4 to 5 mL was removed using a sterile 5 mL plastic syringe. Contents were then filtered using a 0.45 µm hydrophilic syringe filter (Millipore Merck KGaA, Millex™ PVDF 0.45 µm syringe filter, SLHVX13, Darmstadt, Germany) into pre-labelled Eppendorfs and stored at 4 °C for derivitisation.

2.2.3.3 Amino acid method for plasma and tissue fAAs

The method used for plasma fAAs analysis was described by (Gray et al., 2019, 2017) for use in human plasma and rat urine. Ice cold isopropanol (Merck KGaA, 2-Propanol 34863, Darmstadt, Germany) 0.1% formic acid (v/v) (Thermo Scientific Chemicals- Acros Organics, Formic Acid 98+%, 270480250, Loughborough, UK) was added to plasma at a 1:4 ratio (10 µL plasma: 40 µL isopropanol), vortexed to precipitate proteins (SciQuip Ltd, Vortex VariMix, Rotherham, UK) and allowed to stand for 20 min in -20 °C freezer. Samples were then centrifuged for 10 min at 10 000g (Baxter Scientific, Heraeus Biofuge 13 model 3637, Hanau, Germany), supernatant removed and stored at 4 °C for future derivitisation. Deproteinised supernatant was directly derivitised as discussed by Gałęzowska et al. (2021).

Tissue fAAs used the same method as plasma fAAs although adapted, whereby 100 mg of tissue was combined with 400 µL of ice-cold isopropanol (0.1% v/v formic acid) and briefly homogenised using a mini Turrex™ (IKA, Ultra Turrax™ homogeniser, Staufen im Breisgau, Germany). Samples were vortexed and allowed to stand for 20 min at -20 °C. On removal, samples were centrifuged for 10 min (10 000g), and the supernatant was removed (Baxter Scientific, Heraeus Biofuge 13 model 3637). A vacuum manifold (Merck KGaA Supelco, Visiprep™ DL 24 Port, Darmstadt, Germany) was set up using Oasis® PRiME HLB (Waters Corporation, 1cc columns (30 mg), Milford, USA) vac cartridges for clean-up to remove matrix interferences such as salts, proteins, fats, and phospholipids. The resulting samples were stored at 4 °C for future analysis.

2.2.3.3.1 Amino acid derivitisation

All AA analysis (AAA) used the pre-column derivatization Waters AccQ•Tag Method and was run on Waters AQUITY Class Ultraperformance® Liquid Chromatography (UPLC) using AccQ·Tag Ultra Derivitisation Kit (Waters Corp., P/N 186003836, Milford, USA) and Waters Food & Feed Standard Kit as the standard (Waters Corp., P/N WAT088122, Milford, USA). Standards were prepared by adding 100 µL of Water's standard to 900 µL of ultrapure water. Taurine (Merck KGaA Supelco, Taurine PHR1109, Darmstadt, Germany) or tryptophan (Merck KGaA Supelco, Tryptophan PHR1176, Darmstadt, Germany) were additionally included into the standards by adding 50 µL of a 5 mM/L stock solution for a final concentration of 25 pmol/µL. Stock solutions were determined by the following equation:

Mass (mg) = Concentration (mM/L) x Volume (mL) x Molecular Weight (g/mol)
(#g=M x V x MW)

Waters AAA method for derivitisation of samples was adhered to according to the manufacturer's specifications. Briefly, 70 µL of AccQ•Tag Ultra borate buffer (Waters, Corp., Reagent 1 186009283, Milford, USA) was added via pipette to UPLC grade total recovery vials (Waters, Corp., P/N 186000384C, Milford, USA) and vortexed briefly (Baxter Scientific, Heraeus Biofuge 13 model 3637). Either 10 µL of sample or standard was added to the buffer, briefly vortexed, before

adding 20 µL of reconstituted AccQ-tag Ultra reagent (vials 2A and 2B) (Waters, Corp., AccQ•Tag Ultra Derivatization Kit, 186003836, Milford, USA) and vortexing for a further 20 s. The AccQ-tag Ultra reagent powder (6-aminoquinolyl-N-hydroxysuccinimidyl carbamate (AQC)) was reconstituted by adding 1 mL of AccQ•Tag Ultra Reagent Diluent 2B (acetonitrile) to the powder (2A), (Waters, Corp., 186003836, Milford, USA) vortexing for 10 s and then heating at 55 °C for a maximum of 10 min or until the powder had dissolved.

Samples were then added to a preheated hot block (55 °C) for 10 min (Bibby Scientific Techne, Dri-Block DB100/2, Stone, UK), allowed to cool, vortexed for a further 20 s. These were then transferred to UPLC for analysis. Reagent and gradient control samples were included as quality control measures. The reagent control was prepared by adding 20 µL of reagent to 80 µL of buffer, while the gradient control contained all the mobile phases as a 20 µL sample. All controls and standards were prepared during sample preparation. A control sample was included in every run and within each run every 10^{th} sample was repeated.

Reversed phase separation was accomplished using a Waters AccQ-Tag Ultra, BEH (ethylene-bridge hybrid) C_{18} 1.7 µm, 2.1 x 100 mm with Aquity TUV detection at 260nm, at a 1 µL injection volume and a run time of 10.2 min (S 2.9). Empower 3 software was used for processing and data analysis.

2.2.3.3.2 Preparation of mobile phases and UPLC priming

All solvents used for the mobile phase were LC–MS or HPLC grade and eluents A and B were Waters AccQ•Tag™ Ultra Eluents (Waters, Corp., 186003838 186003839, Milford, USA). Waters AccQ•Tag™ Ultra Eluent A consisted of 80–90% water, 5–10% acetonitrile, 3–7% formic acid, and 1–5% ammonium formate and eluent B consisted of water, acetonitrile, and approximately 3% formic acid.

Preparation of mobile phases was conducted according to Water's specifications, whereby 250 mL of AccQ-Tag Ultra Eluent A (Waters, Corp., 186003838) was added to a 500 mL reagent bottle A. 225 mL of MilliQ ultrapure water (Merck KGaA Millipore, Milli-Q ultrapure water system, Darmstadt, Germany) and 25 mL (90:10) of AccQ-Tag Ultra Eluent B (Waters, Corp., 186003839) were mixed thoroughly on a magnetic stirring plate for 5 min before transferring to a 500 mL

reagent bottle B. Mobile phase C consisted of 500 mL of ultrapure water (Merck KGaA Millipore, Milli-Q) in a 500 mL reagent bottle C. Mobile phase D consisted of 250 mL of pure AccQ-Tag Ultra Eluent B (Waters, Corp., 186003839) in a 500 mL reagent bottle D. Needle wash was prepared by mixing 250 mL of acetonitrile (Merck KGaA, 34851, Darmstadt, Germany) and 250 mL of ultrapure water (Merck KGaA Millipore, Milli-Q) by magnetic stirrer for 5 min before transferral to a 1 L reagent bottle. UPLC priming was conducted before UPLC analysis by priming the seal wash in the quaternary solvent manager for a minimum of 5 min or until lines had no bubbles. The sample manager was primed, and needle wash was conducted 3-5 times depending on usage. Solvents were primed for 5 min/line, and the flowrate was changed to 0.1 µL /min when idle.

2.2.4 Digestibility (diet apparent digestibility coefficient (DADC))

To determine the diet apparent digestibility coefficient (DADC) of various nutrients, ratios of those nutrients to yttrium were examined for each test diet using the following formula as described in Sugiura et al. (1998):

$$AD_{diet} = \left(1 - \left(\frac{Y_{diet} \times Parameter_{faeces}}{Y_{faeces} \times Parameter_{diet}} \right) \right) \times 100$$

where Y_{diet} and Y_{faeces} represent the yttrium content of the diet and faeces, and $Parameter_{diet}$ and $Parameter_{faeces}$ represent the parameter of interest *e.g.* protein, AAs, *etc*.

DADC values were compared between the intact protein diets and the BCAA diets (Table 2.3) and separately between the BCAA diets (Table 2.4).

2.2.5 Molecular biology analysis

2.2.5.1 Primer design

Primers were designed for both mTOR and the BCAA pathways by initially searching humans, other vertebrate and finally Atlantic salmon sequences for targets of interest. For the mTOR pathway, both upstream and downstream targets were of interest, while for the BCAA pathway, the first two shared catabolic steps were areas to be investigated.

Table 2.3 Digestibility coefficients of crystalline and intact proteins test diets (DADC). Yttrium was added at 0.2% and used as an inert marker to establish DADCs. Crude protein, lipid and energy results were obtained from proximate analysis and individual AAs from hydrolysis.

	CD	WHE	CAS	SPC	LD	ID	VD	P-value
		Whole proteins			Crystalline			
Crude protein	0.85±0.03 ^{cd}	0.89±0.01 ^{b}	0.92±0.00 ^{a}	0.83±0.03 ^{d}	0.85±0.02 ^{cd}	0.87±0.01 ^{bc}	0.84±0.01 ^{cd}	**0.000**
Lipid	0.89±0.01	0.85±0.01	0.84±0.04	0.82±0.01	0.85±0.05	0.84±0.03	0.83±0.01	0.161
Energy	0.72±0.03 ^{bcd}	0.76±0.01 ^{ab}	0.80±0.01 ^{a}	0.65±0.02 ^{e}	0.72±0.04 ^{cd}	0.74±0.03 ^{bc}	0.69±0.01 ^{de}	**0.000**
Sum of AA	0.92±0.02 ^{bc}	0.93±0.01 ^{ab}	0.95±0.01 ^{a}	0.90±0.01 ^{c}	0.90±0.02 ^{c}	0.92±0.02 ^{bc}	0.90±0.01 ^{c}	**0.004**
Alanine	0.78±0.13	0.88±0.01	0.91±0.02	0.84±0.02	0.85±0.01	0.86±0.02	0.84±0.03	0.206
Arginine	0.96±0.02 ^{ab}	0.96±0.00 ^{ab}	0.97±0.01 ^{a}	0.95±0.01 ^{abc}	0.93±0.01 ^{c}	0.95±0.01 ^{bc}	0.94±0.01 ^{bc}	**0.028**
Asparagine	0.93±0.02 ^{abc}	0.94±0.00 ^{ab}	0.95±0.01 ^{a}	0.91±0.01 ^{d}	0.92±0.02 ^{bcd}	0.93±0.02 ^{bc}	0.92±0.01 ^{bc}	**0.023**
Cysteine	0.75±0.09	0.83±0.07	0.83±0.04	0.65±0.10	0.45±0.44	0.53±0.30	0.65±0.08	0.274
Glutamate	0.96±0.01 ^{b}	0.96±0.00 ^{bc}	0.98±0.00 ^{a}	0.95±0.01 ^{c}	0.96±0.01 ^{bc}	0.96±0.01 ^{b}	0.96±0.00 ^{bc}	**0.008**
Glycine	0.82±0.07	0.83±0.02	0.87±0.02	0.78±0.01	0.78±0.02	0.80±0.02	0.77±0.06	0.072
Histidine	0.95±0.01 ^{b}	0.98±0.00 ^{a}	0.98±0.01 ^{a}	0.92±0.02 ^{bc}	0.90±0.03 ^{c}	0.93±0.01 ^{bc}	0.93±0.01 ^{bc}	**0.000**
Isoleucine	0.91±0.04 ^{ab}	0.95±0.02 ^{a}	0.94±0.01 ^{a}	0.90±0.01 ^{b}	0.89±0.02 ^{b}	0.95±0.01 ^{a}	0.90±0.03 ^{b}	**0.028**
Leucine	0.88±0.07 ^{abc}	0.90±0.00 ^{ab}	0.93±0.02 ^{a}	0.85±0.02 ^{bc}	0.89±0.01 ^{abc}	0.86±0.01 ^{bc}	0.84±0.03 ^{c}	**0.031**
Lysine	0.91±0.03	0.92±0.00	0.93±0.00	0.91±0.02	0.90±0.01	0.91±0.01	0.91±0.02	0.298
Methionine	0.86±0.03	0.90±0.04	0.93±0.02	0.83±0.06	0.85±0.07	0.85±0.08	0.88±0.01	0.291
Phenylalanine	0.95±0.03	0.96±0.00	0.97±0.01	0.95±0.01	0.94±0.01	0.95±0.01	0.95±0.01	0.141
Proline	0.93±0.04 ^{ab}	0.92±0.00 ^{bc}	0.95±0.01 ^{a}	0.89±0.02 ^{c}	0.90±0.01 ^{bc}	0.91±0.01 ^{bc}	0.90±0.01 ^{bc}	**0.023**
Serine	0.90±0.03	0.92±0.01	0.95±0.02	0.91±0.04	0.88±0.03	0.92±0.03	0.91±0.02	0.215
Threonine	0.89±0.04 ^{b}	0.91±0.01 ^{ab}	0.94±0.02 ^{a}	0.88±0.03 ^{b}	0.87±0.02 ^{b}	0.89±0.02 ^{b}	0.88±0.01 ^{b}	**0.050**
Tyrosine	0.93±0.04	0.93±0.01	0.95±0.00	0.90±0.03	0.91±0.02	0.93±0.03	0.85±0.09	0.151
Valine	0.90±0.04	0.91±0.04	0.91±0.01	0.82±0.00	0.87±0.06	0.88±0.06	0.84±0.01	0.076

Values are means ± standard deviation (days between sampling in week-1 *n*=7, week-2 *n*=6 and week-3 *n*=5). Analysis was performed using one-way ANOVA, with Fisher LSD method used for *post-hoc* examination. Values represent means of three pools (*n*=3) with different subscripts denote significant difference among diets ($p<0.05$). CD= Control diet, WHE= Whey diet, CAS= Casein diet, SPC= Soya protein concentrate diet, LD= Leucine diet, VD= Valine diet, ID= Isoleucine diet.

Table 2.4 Digestibility Coefficients of the BCAA test diets (DADC values).

	CD	LD	ID	VD	P-value
Crude protein	0.85±0.03	0.85±0.02	0.87±0.01	0.84±0.01	0.298
Lipid	0.89±0.01	0.85±0.05	0.84±0.03	0.83±0.01	0.172
Energy	0.72±0.03	0.72±0.04	0.74±0.03	0.69±0.01	0.334
Sum of AA	0.92±0.02	0.90±0.02	0.92±0.02	0.90±0.01	0.648
Alanine	0.78±0.13	0.85±0.01	0.86±0.02	0.84±0.03	0.712
Arginine	0.96±0.02	0.93±0.01	0.95±0.01	0.94±0.01	0.399
Asparagine	0.93±0.02	0.92±0.02	0.93±0.02	0.92±0.01	0.458
Cysteine	0.75±0.09	0.45±0.44	0.53±0.30	0.65±0.08	0.509
Glutamate	0.96±0.01	0.96±0.01	0.96±0.01	0.96±0.00	0.636
Glycine	0.82±0.07	0.78±0.02	0.80±0.02	0.77±0.06	0.573
Histidine	0.95±0.01	0.90±0.03	0.93±0.01	0.93±0.01	0.103
Isoleucine	0.91±0.04	0.89±0.02	0.95±0.01	0.90±0.03	0.152
Leucine	0.88±0.07	0.89±0.01	0.86±0.01	0.84±0.03	0.408
Lysine	0.91±0.03	0.90±0.01	0.91±0.01	0.91±0.02	0.820
Methionine	0.86±0.03	0.85±0.07	0.85±0.08	0.88±0.01	0.890
Phenylalanine	0.95±0.03	0.94±0.01	0.95±0.01	0.95±0.01	0.876
Proline	0.93±0.04	0.90±0.01	0.91±0.01	0.90±0.01	0.441
Serine	0.90±0.03	0.88±0.03	0.92±0.03	0.91±0.02	0.512
Threonine	0.89±0.04	0.87±0.02	0.89±0.02	0.88±0.01	0.776
Tyrosine	0.93±0.04	0.91±0.02	0.93±0.03	0.85±0.09	0.526
Valine	0.90±0.04	0.87±0.06	0.88±0.06	0.84±0.01	0.444

Data are expressed as mean ± standard deviation and different superscripts indicate significant differences (p<0.05). Analysis was performed using one-way ANOVA, with Fisher LSD method used for *post-hoc* examination. Values represent means of three pools (Total n=102). Analysis performed in triplicate (n=3). CD= Control diet, LD= Leucine diet, VD= Valine diet, ID= Isoleucine diet.

Targets of interest from varying vertebrate models, were blasted against the Atlantic salmon genome using NCBI to identify and confirm the targets. Primers were designed using NCBI Primer design tool (primer-BLAST) with primer pairs spanning the last exon-exon junctions to try and minimise gDNA amplification. Primer sequences were ordered through Eurofins Genomics (Eurofins Genomics GmbH, Ebersberg bei München, Germany) (S 2.10, 11).

2.2.5.2 RNA extraction

LD liver (n=180 (3/tank/diet/time/week)) and muscle (n=180) tissue samples were removed from -70 °C and thawed slowly on ice. Approximately 50-100mg of tissue was removed and 1 mL of TRI Reagent (Merck KGaA, TRI Reagent® T9424, Darmstadt, Germany) was added. Samples were then homogenised using a BioSpec Mini-Beadbeater (BioSpec Products, Mini-Beadbeater 24,

Bartlesville, USA) for two cycles of 45 s each, with a 45 s rest period in between cycles before centrifugation at 12 000g for 10 min at 4 °C.

The supernatant was removed and added to Eppendorfs containing 100 µL of BCP (1-bromo-3-chloropropane, Merck KGaA, B9673, Darmstadt, Germany) mixed by hand thoroughly, incubated at room temperature for 15 min and then centrifuged at 20 000g for 15 min at 4 °C. Approximately 300-400 µL of the aqueous upper phase was carefully transferred into new Eppendorfs before the RNA precipitation solution and isopropanol (Merck KGaA, 2-Propanol 34863, Darmstadt, Germany) were added at half the volume of the RNA aqueous phase each (*i.e.* 200 µL RNA precipitation solution and 200 µL of isopropanol). The RNA solution was precipitated using a solution of sodium chloride (Merck KGaA, S9888, Darmstadt, Germany), sodium citrate sesquihydrate (Merck KGaA, 359084, Darmstadt, Germany) and isopropanol (Merck KGaA, 2-Propanol 34863, Darmstadt, Germany).

Samples were gently inverted 4-6 times before incubating at -20 °C for 10-30 min, and again centrifuged at 20 000g for 10 min at 4 °C. The remaining solution was removed leaving an RNA pellet which was then washed with 1 mL of 75% ice cold ethanol for 15 min at room temperature, with the tubes flicked and inverted to lift the pellet from the bottom. This was then centrifuged at 7 000 g for 5 min at room temperature. This step was repeated to remove glycogen. After the second repetition of RNA washing, all the supernatant was carefully removed, ensuring no pipette tips touch the pellet, and allowed to air dry in a fumehood until all visible traces of ethanol were gone.

The RNA pellet was then resuspended using 30-100 µL of RNase-free water depending on the visible pellet size for 30-60 min at room temperature. Samples were gently flicked every 10 min to aid in the resuspension before finally determining concentration and quality of RNA on the Nanodrop (Thermo Fisher Scientific, Nanodrop ND-1000 Spectrophotometer, Loughborough, UK).

RNA samples were analysed by Nanodrop (Thermo Fisher Scientific, Nanodrop ND-1000 Spectrophotometer) to determine quality and concentration. Nuclease-free dH_2O (Merck KGaA Millipore, Milli-Q) was used as a blank and as a control

after every 10 samples. Samples were loaded at 1.5 µL using 10 µL nuclease-free, aerosol resistant filter tips (Corning Life Sciences Axygen,TF-300-L-R-S,Tewksbury, USA) and a P2 Gilson pipette. Lint-free precision were used to clean the pedestal before and after every use.

An RNA concentration of 1000-2000 ng/µL was aimed for, if a higher concentration was reported, this was then diluted to within the 1000-2000 ng/µL range. The 260/280nm and 260/230nm ratios were used to assess the quality of the samples and highlight the possibility of contamination. 260/280nm Ratios of 2.0 are considered 'pure' RNA while ratios of 1.8 are considered 'pure' DNA (Matlock, 2015). RNA acceptable ranges for 260/280 ratios were between 2 and >2.2 while for DNA ranges between 1.8-2.0 were acceptable. Acceptable ranges for 260/230nm ratios were between 2 and >2.2. Samples were repeated if they fell outside of the acceptable ranges.

Agarose (1%) gels were used to determine quality and integrity of RNA and PCR products. Briefly, agarose gels were made by adding 1 g of agarose (Merck KGaA (Sigma-Aldrich), Agarose, Darmstadt, Germany) into 100 mL 0.5X TAE buffer (Merck KGaA (Sigma-Aldrich), Tris Acetate-EDTA (TAE) buffer T9650, Darmstadt, Germany) and heating until the agarose melted. Once slightly cooler, 2.5 µL of ethidium bromide (Merck KGaA (Sigma-Aldrich), ethidium bromide E7637, Darmstadt, Germany) was mixed into the warm gel before pouring into the gel tray and allowed to set for 30-60 min. The running buffer used was 0.5X TAE. Quality of the products was assessed by identifying the bands on a Syngene InGenius transilluminator (Synoptics (Syngene), InGenius, Cambridge, UK). Gels were examined for smearing, thickness of the bands and location in relation to the ladders. Pure and intact RNA gave two bands (28S and 18S) with DNA and PCR products a single band (S 2.12).

2.2.5.3 cDNA synthesis

As described in Huyben et al. (2021), Applied Biosystems™ High-Capacity cDNA Reverse Transcription Kits (Thermo Fisher Scientific, Loughborough, UK) were used to prepare complementary DNA (cDNA) synthesis master mixes for LD

muscle (*n*=30) and liver (*n*=30). A two-step RT-PCR approach was used to allow for more cDNA flexibility between experiments and to reduce RNA degradation.

Prior to reverse transcription, each sample was diluted to 200ng/ µL, allowing for a total of 2000ng/10 µL and then denatured at 75 °C for 5 min on a thermal cycler (Analytic Jena GmbH, Biometra Tadvanced, Jena, Germany). A mastermix (MM) was prepared (S 2.13) with 10 µL micropipetted to each tube on completion of the denaturing step. Quality control non-template controls (NTCs) and reverse transcription negatives (RT-s) were included, with NTCs assessing quality of the MM (no RNA added) and RT-s assessing genomic DNA contamination (no enzyme added) (IF contaminated= melt curve in qPCR) Samples were then returned to the thermal cycler to complete the program with 25 °C for 10 min, 37 °C for 120 min and 85 °C for 5 min (S 2.14**)** The reaction was terminated by incubating at 85 °C for 5 min. Each sample was diluted 1:20 (10 µL cDNA:190 µL H_2O) with nuclease free water.

2.2.5.4 Primer optimisation and efficiencies

Two cDNA 'superpools' were prepared by removing 2 µL of cDNA from all liver and muscle samples and combining into a muscle or liver superpool. Primers were diluted to 10pmol/ µL. A MM consisting of MyTaq™ DNA Polymerase (Meridian Bioscience, London, UK) water, and primers were prepared, with 1 µL of the cDNA superpool added (S 2.15). Thermal cycler temperatures were adjusted, and cycles ranged from 30-35 (S 2.16). The cDNA superpools were used to test the primers by running each set of primers at 4 different temperatures and assessing the PCR product by gel electrophoresis (S 2.17). To visually confirm PCR products by electrophoresis, a 1% agarose gel was run for 10 min at 75W and then reduced to 50W for 30 min. Gels were loaded with 3 µL of nuclease free water, 2 µL loading dye (2x) and 1 µL of PCR product. A 100 bp ladder was used for measurement.

Once individual optimum annealing temperatures were identified, dilution series ranging from 1/5 to 1/500 were made from each superpool (S 2.18) and run on qTower3 G real-time PCR Thermal Cycler (Analytic Jena GmbH, Jena, Germany) (S 2.19). MM was loaded into each well at 7.5 µL with 2.5 µL of cDNA added

afterwards. Each dilution of each gene of interest (GOI) was performed in duplicate, with every 8th well an NTC to confirm the integrity of the Luminaris HiGreen qPCR MM (Thermo Fisher Scientific, Loughborough, UK).

As discussed by Ginzinger (2002), primer efficiencies (R^2 values) were determined by plotting scatterplots using mean Cts and log dilutions, with a fitted regression equation (S 2. 20, 21).

$$\text{PCR efficiency \%} = (10^{(1/-s)} - 1) * 100$$

2.2.5.4.1 PCR product preparation

Nucleospin PCR clean-up and Gel extraction kit (Macherey-Nagel, Germany) was used to clean PCR products in preparation for cloning (S 2.22). NTI buffer (100 µL) was added to 50 µL of PCR product, run through a PCR clean-up column, centrifuged at 11 000 g (30 s) and the flow-through was discarded.

NT3 buffer (700 µL) was added to the column, centrifuged (11 000 g for 30 s) and the flow-through discarded. Column was again centrifuged (11 000 g for 1 min) ensuring removal of all NT3 buffer. PCR clean-up column was flushed through with 15 µL of NE buffer (incubated at 72 °C), incubated for 1 min and then centrifuged (11 000 g for 1 min). Remaining PCR product and buffer was then nanodropped with 30- 40 ng/µL DNA expected.

2.2.5.4.2 Ligation

Purified PCR product (3 µL) was added to pGEM®-T Easy Vector Systems ligation mixture (Promega, pGEM®-T Easy Vector Systems, Madison, USA). The standard reaction contained 5 µL of 2x rapid ligation buffer, 1 µL (50 ng) of pGEM-T easy vector, 1 µL of T4 DNA ligase enzyme and 3 µL of PCR product. For every PCR product, a positive (with control insert) and a negative (no PCR product or insert) controls were used. Samples were then incubated at 4 °C for 18 to 24 hr.

2.2.5.4.3 Transformation

In preparation for transformation, 4 Luria-Bertani (LB) agar plates (15 g/ L) were prepared for each product (2x product, 1x positive control (+ve) and 1x negative control (-ve)). Once gel was cooled 100 µg/ mL of ampicillin was added and plates were poured.

E. coli XL1-Blue Competent Cells (Agilent Technologies Inc., XL1-Blue Competent Cells, Santa Clara, USA) were removed from -80 °C and allowed to thaw gently on ice. Micro centrifuge tubes were labelled, 50 µL of XL1-Blue Competent Cells were added to each tube before the addition of 0.85 µL 1.42M β-mercaptoethanol (Merck KGaA, β-Mercaptoethanol (BME), Darmstadt, Germany), incubated on ice for 10 min, with gentle swirling every 2 min. Ligated DNA (10 µL) was added to the competent cells, while 1 µL of pUC18 control DNA added to the +ve control aliquot before incubating on ice for 30 min.

The cells were shocked for 45 s in a water bath maintained at 42 °C before resting in ice for 2 min to allow for the plasmid to enter the bacteria cell. Warmed LB medium (300 µL/ aliquot broth (25 g/ L)) was added to transformation aliquots and then incubated at 37 °C on a shaking incubator (250 revs/ min) for 1 hr (Thermo MaxQ 2000, Thermo Fisher Scientific, Loughborough, United Kingdom).

For white and blue colony screening, a MM consisting of 80 µL Thermo Scientific™ X-Gal Solution (Thermo Fisher Scientific, Loughborough, UK) and 40 µL Thermo Scientific™ IPTG Solution (Thermo Fisher Scientific, Loughborough, UK) was prepared for each plate including the +ve and -ve controls and carefully spread on each agar plate until dry. Each transformation aliquot was spread on its corresponding agar plate (150 µL/plate) and incubated overnight at 37 °C.

Agar plates were transferred to a fridge at 4 °C for 5-10 min and observed for bacterial growth. Three individual white colonies were selected per transformation. Bacterial Falcon tubes (12 mL) were prepared with 5 µL of ampicillin and 5 mL of LB broth. Selected colonies were transferred to their corresponding tubes and incubated overnight at 37 °C in the shaker incubator. Tubes were identified as having bacterial growth if the growth medium was cloudy. For the preservation of the bacterial cells at -20 °C, 5 Eppendorf tubes (1.5 ml) per target were prepared with 100 µL glycerol-LB into which 100 µL of cell medium was added.

2.2.5.4.4 Plasmid DNA purification

NucleoSpin® Plasmid QuickPure (Macherey-Nagel, Germany) was used to isolate plasmid DNA from *E. coli*. On removal from incubator, bacterial 12 mL

tubes were vortexed, 4.5 mL of the transformed bacteria removed, and then centrifuged at 11 000 g for 30 s. Supernatant was discarded. A1 buffer (250 µL) was added and vortexed to resuspend the pellet. A2 buffer (250 µL) added, inverted 6-8 times and incubated for 2 min at room temperature (to lyse the cells). A3 buffer (300 µL) added, inverted until the lysate was colourless, and then centrifuged at 11 000g for 5 min. A NucleoSpin® Plasmid QuickPure Column was placed in a collection tube (2 mL) and 800 µL of clear supernatant was added, centrifuged for 1 min at 11 000g and flow-through was discarded.

AQ buffer (450 µL) was added to the column, centrifuged for 3 min at 11 000g twice, and tube was discarded. Spin column was inserted into a new Eppendorf (1.5 mL), pre-heated AE buffer added, incubated at 72 °C for 1 min before centrifuging for 1 min at 11 000g. Column was discarded, and plasmid DNA (100 µL per aliquot) was added to 100 µL glycerol, 100 µL LB (Lysogeny Broth) broth and transferred to storage at -80 °C. Plasmid DNA concentration and quality was measured using Nanodrop Spectrophotometer (Thermo Fisher Scientific, Nanodrop ND-1000 Spectrophotometer, Loughborough, UK). PCR was used to confirm target insertions into the plasmid samples with the target specific primers used. All plasmid DNA were confirmed by PCR (S 2.23) with dilutions from 1:10, 1:100 and 1:1000 and visually confirmed by gel electrophoresis.

2.2.5.4.5 Plasmid sequencing

Plasmid targets were prepared for sequencing using Eurofins Mix2Seq Kits (Eurofins Genomics GmbH, Mix2Seq Kit, Ebersberg, Germany) and were sequenced using LIGHTrun sequencing. Briefly, Eppendorf tubes were prepared with 2.5 µL of T7 (10 pmol) (ATTATGCTGAGTGATATCCC) primer and 7.5 µL of plasmid DNA (80-100 ng/µL). For targets that failed the initial sequencing, T7 primer was added at 20pmol (1.25 µL T7 and 8.75 µL plasmid sample) and successfully rerun.

Targets were blasted (BLAST, NCBI) against plasmid sequencing FASTA file results from Eurofins. The sequence and primers were added into OMEGA Clustal W for multiple sequence alignment (Clustal W v. O (1.2.4) Sievers & Higgins, 2021).

Table 2.5 Sequencing details (Oligonucleotide primers designed to assay mRNA abundance by rt-qPCR).

Targets	Forward (5'-3')	Reverse (5'-3')	Accession numbers	Product size (bp)	Annealing temp. (°c)	E (%)	R^2
BCAT1a	CTGGCCAAGAGGTTCCACAAA	CCTATCAGAAGGAGTGCATTAAAGG	XM_045719461 NM_001140839.1	181	60.6	89.7	0.9982
BCKDHA E1	CGTTCACTACGGCAGCAAAG	CGCCCTCTCCGAAGTAACAG	XM_014215532	143	60.4	95.7	0.9967
RRAG	AATGGGCAAGAGTGGGTCTG	ATCAGCACCTCCACATTCCG	NM_001141190	231	59.4	96.6	0.9981
Myostat 1a*	CACAACGCCTGTTGGACTTG	TGGACGGAGCGTGTAACATT	NM_001123549.1 (1b) JN990746.1	91bp designed 99bp (run 1) 106bp (run 2)	58.4	113.7	0.9912
SESN1	TTTGTGGTTGGGTGGTGGTT	ACAGTGCGATGATTGACTGGA	XM_045709492	91	57.6	82.2	0.9975
Myo6	GTACGAGCTCAGCAAGTGGA	GGTGCGAGATCATAGTCGGT	BT072664 XM_014204928.2	210	59.4	95.0	0.9997
BCKDK	CCCTCGCATGAACAACCTCT	CAGGGCTAAGCAGCAAGTGA	XM_014197166	233	59.4	86.4	0.9932
BCAT1b	GTAATGCTGTGAAACAGCCGC	GCACGGACAACCCTATAGACG	XM_045715268.1 (100%) NM_001140839.1 (89%)	188	60.8		
BCKDH1b	CCATCTTGCCTTGGGACACT	GGAAGCACTCCTCTTGCACT			59.4		
BCAT1b	GCGGCTGTTTCACAGCATTAC	GCACGGACAACCCTATAGACG	XM_045715268.1 (100%) NM_001140839.1 (89%)	188			

*Myostat 1a sequencing was repeated twice as the primers were not identified in the sequences. To identify and ensure the correct product was inserted into the vector, the vector primers (F-GGAATTCGAT and R- ATCACTAGTG) were used to identify the insertion of Myostat 1a. The product was then blasted in NCBI blastn to achieve 89.4% (DZX237) similarity in the first run and 78.5% (DXZ241) similarity in the second run to Myostat 1a. *DNA – TCAG RNA= UCAG.

The Sequence Manipulation Suite, Reverse Complement section was used to reverse primers for the alignment (Stothard, 2000). The area between the two primers was selected and reinserted into BLAST (NCBI) for confirmation of targets and aligned against *S. salar* (8030) (Table 2.5). Products were additionally identified and confirmed by searching FASTA file results for pGEM-T easy vector start of insertion sequences (GGAATTCGAT) and end of insertion sequences (ATCACTAGTG). Products were identifiable between the start and end insertion sequences. These were verified on NCBI BLAST (S 2.24 - 31).

2.2.5.4.6 Plasmid DNA standards for absolute quantification

Plasmid target DNA was estimated (ng/µL) by using a Qubit® 2.0 Fluorometer (Qubit® 2.0 Fluorometer, Invitrogen Thermo Fisher Scientific Inc., Paisley, United Kingdom) and Qubit™ dsDNA high sensitivity (HS) Quantification Assay Kits (Invitrogen Thermo Fisher Scientific Inc., Qubit™ dsDNA Quantification Assay Kit (HS), Eugene, USA) according to manufacturer's specifications. This was then used to work out the DNA g/µL and the DNA copies/µL.

Molecular weight (1 mol) = (insert bp + vector bp) x 660
DNA g/µL= DNA ng/µL $*10^{-9}$
DNA copies/µL= (DNA g/µL / (total plasmid vector bp x 660)) x 6.02 x 10^^{23}

Where 660 is the average molecular weight of each base pair (bp) of plasmid nucleotides and 6.023 x 10^{23} is Avogadro's number (the number of molecules in 1 mol).

Similarly to RT-qPCR primer efficiencies (2.2.5.4), absolute quantification of GOI mRNA transcripts was accomplished by creating a standard curve (10^7 to 10^1 molecules/µL) from known plasmid copy numbers and comparing test samples against this curve (standard-curve method). These plasmid dilutions were used as controls and were run in duplicate on every 96-well plate.

Log copy number= (observed Ct − y intercept)/slope
Copy number/ µL= 10^ Log copy number

^= Exponentiation (to the power of)

2.2.5.5 RT-qPCR

LD muscle and liver tissue mRNA transcripts of BCAA catabolism (BCAT1a, BCKDHA, BCKDK) and mTOR (SESN1, RRAG, MYOSTAT 1A, MYO6) pathway targets were quantified using Thermo Scientific™ Luminaris HiGreen qPCR Master Mix (Thermo Fisher Scientific, Luminaris HiGreen qPCR Master Mix, Loughborough, UK).

Briefly, 1 µL of cDNA (1:20) was added to 9 µL of qPCR MM, with each sample run in triplicate. All 96-well plates contained NTCs and RT-, and to avoid potential contamination, only 1 GOI was run on each plate. STDs, NTCs, liver and muscle tissues were identified into groups, labelled on the internal qTower^3/G template and run on the same plates. qPCRs were done using a qTower^3/G real-time PCR Thermal Cycler (Analytic Jena GmbH, Jena, Germany) with template setup and analysis using qPCRsoft program. The annealing temperatures (step 4) were adjusted for each GOI and the runtime protocol, melt curves, STDs and NTCs for each run were examined for QC purposes.

qTower^3/G qPCRsoft qPCR results of mRNA transcripts were analysed in Microsoft Excel (Microsoft Corp., Excel v.2307, Redmond, USA) by comparing the Cts/ Cqs (threshold cycle/ quantification cycle) to the standard curve created from the STDs in each run.

2.2.6 Data analysis

2.2.6.1 Statistical analysis

All values were means ± St. dev. (standard deviation) unless specified differently. Significance was set at p=<0.05, with normality assessed on data using an Anderson-Darling test, and Grubbs' test to check for outliers (p=<0.05). One-way ANOVA was used to determine differences with Fishers LSD *post-hoc* test used to distinguish the differences among the comparisons. GLMs (general linear model) were used to identify significance and interactions, with Fishers LSD *post-hoc* test classifying the differences. All statistical analysis was undertaken using Minitab v18.1 (Minitab Ltd., Coventry, UK).

2.3 Results

2.3.1 Fish

2.3.1.1 All diets feed intake

Feed intake (FI) in g/fish/day was explored by GLM to examine the FI between the seven diets relating to differences in diet, week and an interaction between diet and week (D*W). Differences were noted in both diet and week (p=0.001, p=*0*), with an observed interaction between Diet*Week (p=*0*). Fishers' LSD *post-hoc* analysis highlighted the differences in diets, with the highest overall FI for WHE (3.26 ±1.15 g/day) and the lowest in ID (2.53 ±0.48 g/day). WHE was different to all diets apart from SPC, which was only different to ID.

Although not different, variability in FI between the intact proteins and the crystalline diets was noted in SPC, LD, CAS, VD and CD diets. As expected, differences were observed in overall weekly FIs, with week-3 being different to week-2 and week-1. In week-1, LD diet had the highest FI (2.31 ±0.17 g/day) and SPC the lowest (1.87 ±0.24 g/day). WHE diet had the highest intake for both week-2 and 3 (3.44 ±0.35 g/day and 4.36 ±0.25 g/day), with ID the lowest in week-2 and CD the lowest in week-3 (2.56 ±0.26 g/day and 2.76 ±0.36 g/day).

2.3.1.2 BCAA diets feed intake

A GLM with Fisher's LSD *post-hoc* analysis was run on the BCAA diet means to examine the effect of week and diet on FI (Figure 2.4). There were no differences between diets (p=0.348) but there were differences between weeks (p=*0*) while no interaction (D*T) between week and diet was observed (p=0.324). In week-1, LD diet had the highest mean FI at 2.31 ±0.17 g/day, with the VD diet having the highest in week-2 and 3 (3.04 ±0.20 and 3.10 ±0.62 g/day).

2.3.2 Feed

2.3.2.1 Crystalline and intact protein digestibility coefficients (DADC).

Overall, there were variability in DADCs between ingredients regardless of whether their source was from cAAs or intact proteins (Table 2.3).

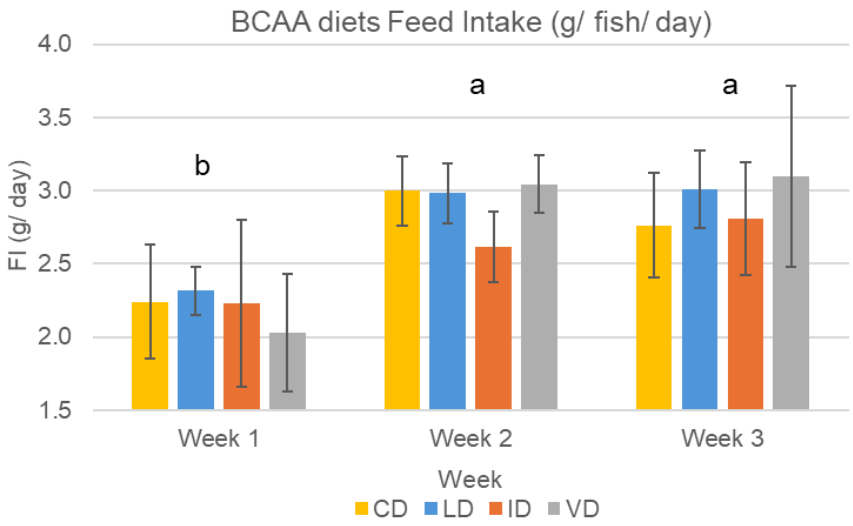


Figure 2.4 BCAA diets feed intake (FI g/ fish/ day**)** replicated by week. Values are means with standard deviations of the mean (week-1 *n*=7, week-2 *n*= 6 and week-3 *n*=5 days). Different lettering denote significant differences between combined weekly FI ($p<0.05$). CD= Control diet, LD= Leucine diet, VD= Valine diet, ID= Isoleucine diet.

Within the BCAAs, there were differences across the diets for isoleucine and leucine (p=0.028, 0.031) with near significance ($p\leq 0.10$) noted between the diets for valine (p=0.076). Differences in isoleucine were between the WHE, CAS, ID diets versus SPC, LD and VD diets. Additional EAA differences were observed in arginine (p=0.028), histidine (p=*0*), and threonine (p=0.050), while in the NEAA differences were seen in glutamate and proline (p=0.008, p=0.023). Diet digestibilities displayed no differences for lipids (p=0.161). Glycine had near significance ($p\leq 0.10$) across the seven diets (p=0.072).

Crude protein DADC was significantly different (p=*0*), and it ranged from SPC 0.83 to CAS 0.92. CAS had the highest DADC for crude protein, energy, and the sum of AAs (p=*0*, p=*0*, p=0.004). The largest DADC variability was apparent for energy, between CAS and SPC (0.80 ±0.01, 0.65 ±0.02). CAS diet had the highest DADC for sum of AAs (0.95 ±0.01), with LD (0.90 ±0.02) VD (0.90 ±0.01) and SPC (0.90 ±0.01) having the lowest DADCs of the eight diets. Of the 21 DADC nutrients measured, CAS had the highest values in 19 of them, with three of them shared with WHE.

2.3.2.2 Digestibility of amino acids, protein, and lipids within BCAA diets

A one-way ANOVA was used to determine any significant differences in the DADCs of the BCAA test diets (DADC values); not observing any differences

(Table 2.4), however the CD tended to be higher in lipid and histidine DADC although not significant (*p*=0.172, *p*=0.103). In addition, ID seemed to have the highest DADC of isoleucine although not significant (*p*=0.152). DADC of crude protein seemed highest, although not significant, in the ID diet with the sum of AAs highest in CD and ID diets. DADC of glutamate was the highest of all the AAs equally across all diets, with arginine equalling glutamate DADC levels but only in the CD diet (0.96 ±0.02).The largest variability seemed to be in the sulphur-based AAs, cysteine and methionine. Overall, although not different, the CD and ID diets appeared to have the highest DADCs whereas the LD and VD diets had the lowest ranges across all AAs.

2.3.3 Plasma amino acids (µmol/ L)

One-way ANOVA was used to determine differences in the levels of circulating fAAs among fish fed the different dietary treatments (LD, ID, VD, CD) over the five timepoints (0 (-2), 2, 4, 8 and 24 hr). Fisher's LSD *post-hoc* analysis was used to differentiate the differences (Table 2.6).

2.3.3.1 Plasma BCAAs

2.3.3.1.1 Each timepoint across diets

Significant differences (*p*=<0.05) between the diets at the -2 hr pre-feeding point (-2 hr) were observed for isoleucine (p=0) and valine (p=0). *Post-hoc* analysis displayed differences in isoleucine between the ID diet and the other three diets and similarly for valine in the VD diet (*p*=<0.05) (Table 2.6 horizontal *zyx* subscripts). No differences across the diets for leucine (*p*=0.971). At 2 hr post-feeding, differences were in all the BCAAs between the 4 diets, with *post-hoc* analysis displaying the differences in isoleucine in ID and valine in the VD diet (*p=0*). Although leucine was significant (*p*=0.039), *post-hoc* analysis indicated that leucine in the LD diet was significantly higher than the CD and VD diets, but similar to the ID diet. Similarly, at the 4 hr timepoint, all BCAAs were different across the four diets, with *post-hoc* analysis exhibiting that leucine in the LD diet, isoleucine in the ID diet and valine in the VD diet were all significantly higher in their own diets when compared across the other diets (e.g. leucine LD>ID, CD, VD).

Table 2.6 Total plasma BCAAs of the test diets at 5 different timepoints. Data are expressed as mean ± standard deviation in µmol/ L and different superscripts indicate significant differences (p <0.05) with *abc* displaying vertical and *zyx* horizontal differences.

Time		CD	LD	ID	VD	One-way ANOVA	Two-way ANOVA P-value		
						P-value	Diet	Time	D*T
Isoleucine	-2hr	185.2±41.5 ^{bcy}	148.8±57.2 ^{bcy}	313.2+63.2 ^{cz}	191.7+48.0 ^{by}	**0.000** (f 3, 32= 16.32)	**0.000**	**0.000**	**0.000**
	2hr	223.4±55.0 ^{aby}	175.7±44.7 ^{aby}	681.4+257.3 ^{abz}	244.4+64.3 ^{ay}	**0.000** (f 3, 32= 26.43)			
	4hr	208.8±41.2 ^{aby}	185.5±39.6 ^{aby}	779.2+261.9 ^{az}	243.3+64.8 ^{ay}	**0.000** (f 3, 32= 32.28)			
	8hr	274.1±116.6 ^{ay}	197.3±61.7 ^{ay}	514.5+212.1 ^{bz}	231.2+57.1 ^{aby}	**0.000** (f 3, 31= 11.01)			
	24hr	144.5±43.4 ^{czy}	109.9±21.1 ^{cy}	236.6+87.0 ^{cz}	116.2±19.3 ^{cy}	**0.000** (f 3, 32= 12.00)			
	P-value	**0.003** (f 4, 40= 4.69)	**0.002** (f 4, 40= 4.94)	**0.000** (f 4, 39= 12.71)	**0.000** (f 4, 40= 9.28)				
Leucine	-2hr	542.2±129.6 ^{a}	512.5±174.6 ^{b}	537.5+122.7 ^{a}	526.6+128.9 ^{a}	0.971 (f 3, 32= 0.08)	**0.000**	**0.000**	**0.021**
	2hr	547.0±122.7 ^{ay}	804.2±248.6 ^{az}	662.4±208.9 ^{azy}	594.6+151.3 ^{ay}	**0.039** (f 3, 32= 3.15)			
	4hr	499.7±98.7 ^{ay}	840.6±231.8 ^{az}	638.6+127.9 ^{ay}	550.1+133.9 ^{ay}	**0.000** (f 3, 32= 8.32)			
	8hr	628.6±254.2 ^{a}	720.2±238.8 ^{a}	618.6+155.8 ^{a}	552.6+115.6 ^{a}	0.380 (f 3, 31= 1.06)			
	24hr	322.6±104.7 ^{bzy}	273.9±42.8 ^{cy}	351.8+84.7 ^{bz}	260.1+41.0 ^{by}	**0.044** (f 3, 32= 3.03)			
	P-value	**0.002** (f 4, 40= 4.95)	**0.000** (f 4, 40= 12.27)	**0.000** (f 4, 39= 6.74)	**0.000** (f 4, 40= 11.24)				
Valine	-2hr	412.5±94.9 ^{aby}	343.3±108.1 ^{aby}	418.6+66.9 ^{bcy}	812.5±160.1 ^{bz}	**0.000** (f 3, 32= 32.25)	**0.000**	**0.000**	**0.000**
	2hr	478.2±101.0 ^{ay}	414.1±82.8 ^{ay}	502.9±124.7 ^{aby}	1178.2±328.3 ^{az}	**0.000** (f 3, 31= 32.32)			
	4hr	440.6±79.7 ^{ay}	415.4±78.2 ^{ay}	510.7±85.8 ^{aby}	1327.7±507.8 ^{az}	**0.000** (f 3, 32= 24.86)			
	8hr	511.9±177.9 ^{ay}	400.2±106.7 ^{ay}	573.0±261.6 ^{ay}	956.2±240.2 ^{bz}	**0.000** (f 3, 32= 12.41)			
	24hr	339.9±84.5 ^{by}	267.4±53.0 ^{bx}	342.9±81.5 ^{cy}	464.8±63.6 ^{cz}	**0.000** (f 3, 32= 11.70)			
	P-value	**0.028** (f 4, 40= 3.04)	**0.003** (f 4, 40= 4.68)	**0.015** (f 4, 40= 3.53)	**0.000** (f 4, 40= 10.50)				
Arginine	-2hr	379.2±149.5 ^{c}	336.6±125.4 ^{b}	356.2±96.2 ^{b}	322.1±67.1 ^{b}	0.736 (f 3, 32= 0.43)	0.107	**0.000**	0.976
	2hr	726.8±297.3 ^{a}	634.4±145.7 ^{a}	803.6±347.0 ^{a}	655.0±193.7 ^{a}	0.507 (f 3, 32= 0.79)			
	4hr	637.8±196.1 ^{a}	644.8±339.6 ^{a}	846.3±209.3 ^{a}	683.1±239.3 ^{a}	0.277 (f 3,32= 1.34)			
	8hr	617.7±273.1 ^{ab}	616.5±289.0 ^{a}	646.9±347.3 ^{a}	572.7±212.1 ^{a}	0.957 (f 3, 31= 0.10)			
	24hr	427.5±130.6 ^{bc}	354.0±150.7 ^{b}	443.0±137.3 ^{b}	378.1±86.4 ^{b}	0.431 (f 3, 32= 0.94)			
	P-value	**0.007 (f 4, 39= 4.12)**	**0.005** (f 4, 40= 4.31)	**0.000** (f 4, 40= 6.71)	**0.000** (f 4, 40= 7.92)				
Histidine	-2hr	52.1±18.7	54.9±24.9	58.3±16.7	53.6±18.0	0.923 (f 3, 32= 0.16)	0.106	**0.026**	0.636
	2hr	78.9±26.3	63.8±14.1	64.9±18.1	71.6±19.1	0.358 (f 3, 32= 1.11)			
	4hr	60.1±18.7	70.2±27.5	83.9±27.7	73.3±22.6	0.247 (f 3, 32= 1.45)			
	8hr	69.8±43.7	67.9±31.6	85.6±38.9	60.7±27.6	0.813 (f 3, 31= 0.32)			
	24hr	70.8±20.4	57.6±19.8	81.3±23.8	61.0±20.4	0.107 (f 3, 31= 2.20)			
	P-value	0.285 (f 4, 40= 1.30)	0.643 (f 4, 39= 0.63)	0.116 (f 4, 40= 1.98)	0.284 (f 4, 39= 1.31)				
Lysine	-2hr	55.4±32.3 ^{c}	53.0±25.0 ^{b}	59.4±31.3 ^{b}	53.2±18.8 ^{c}	0.955 (f 3, 32= 0.11)	0.725	**0.000**	0.996
	2hr	117.2±49.7 ^{ab}	110.2±42.3 ^{a}	115.3±40.5 ^{a}	111.9±61.3 ^{ab}	0.990 (f 3, 32= 0.04)			

	4hr	114.1±37.0 ^{ab}	121.0±41.1 ^{a}	117.9±29.1 ^{a}	123.4±27.1 ^{a}	0.944 (f 3, 32= 0.13)			
	8hr	144.4±65.3 ^{a}	124.6±49.3 ^{a}	123.4±61.8 ^{a}	121.8±45.6 ^{a}	0.809 (f 3, 31= 0.32)			
	24hr	95.2±29.7 ^{bc}	70.3±24.6 ^{b}	92.0±74.3 ^{ab}	77.0±19.9 ^{bc}	0.565 (f 3, 32= 0.65)			
	P-value	**0.003 (f 4, 40= 4.86)**	**0.000** (f 4, 40= 6.56)	0.063 (f 4, 39= 2.44)	**0.001** (f 4, 40= 5.91)				
Methionine	-2hr	60.3±23.0	48.8±12.3 ^{b}	47.7±9.2 ^{b}	51.7±11.2 ^{c}	0.282 (f 3, 32= 1.33)	0.195	**0.000**	0.829
	2hr	73.5±26.5	75.3±19.0 ^{a}	81.4±25.2 ^{a}	69.7±17.6 ^{ab}	0.735 (f 3, 32= 0.43)			
	4hr	78.9±24.2	79.6±21.8 ^{a}	85.6±24.6 ^{a}	78.9±17.9 ^{a}	0.902 (f 3, 32= 0.19)			
	8hr	87.6±40.5	87.3±32.9 ^{a}	85.2±45.4 ^{a}	65.6±18.4 ^{a}	0.500 (f 3, 31= 0.81)			
	24hr	55.4±12.5 ^{z}	39.2±7.1 $^{b\,y}$	46.7±13.5 $^{b\,zy}$	41.3±6.0 $^{bc\,y}$	**0.013** (f 3, 31= 4.23)			
	P-value	0.087 (f 4, 40= 2.19)	**0.000** (f 4, 39= 8.64)	**0.002** (f 4, 39= 5.36)	**0.000** (f 4, 40= 8.88)				
Phenylalanine	-2hr	147.0±38.7 ^{bc}	133.1±33.8 ^{c}	122.0±29.2 ^{c}	143.0±18.8 ^{b}	0.339 (f 3, 32= 1.16)	0.208	**0.000**	0.569
	2hr	185.4±65.9 ^{ab}	171.5±33.2 ^{b}	196.3±49.3 ^{ab}	178.4±30.9 ^{a}	0.714 (f 3, 32= 0.45)			
	4hr	180.2±48.2 ^{ab}	202.7±53.6 ^{ab}	207.1±39.5 ^{a}	186.9±44.1 ^{a}	0.575 (f 3, 32= 0.67)			
	8hr	197.0±54.6 ^{a}	208.8±73.2 ^{a}	209.4±81.3 ^{a}	167.7±37.0 ^{ab}	0.462 (f 3, 31= 0.88)			
	24hr	125.6±17.9 ^{c}	108.4±16.7 ^{c}	148.2±68.7 ^{bc}	103.8±13.8 ^{c}	0.066 (f 3, 32= 2.65)			
	P-value	**0.013** (f 4, 39= 3.64)	**0.000** (f 4, 40= 7.95)	**0.006** (f 4, 40= 4.29)	**0.000** (f 4, 40= 10.50)				
Threonine	-2hr	159.5±66.6	136.8±25.8 ^{b}	155.8±53.8 ^{c}	133.5±31.7 ^{c}	0.565 (f 3, 32= 0.69)	**0.007**	**0.000**	0.210
	2hr	206.6±68.1	215.6±43.2 ^{a}	223.6±55.3 ^{bc}	186.9±50.5 ^{ab}	0.536 (f 3, 32= 0.74)			
	4hr	210.0±78.6	219.3±47.6 ^{a}	256.7±78.2 ^{ab}	195.8±31.6 ^{ab}	0.216 (f 3, 32= 1.57)			
	8hr	209.0±96.1	232.0±86.3 ^{a}	312.9±137.0 ^{a}	200.6±29.9 ^{a}	0.080 (f 3, 31= 2.48)			
	24hr	213.5±39.5	163.2±47.5 ^{b}	168.5±51.9 ^{c}	163.4±33.6 ^{bc}	0.056 (f 3, 32= 2.80)			
	P-value	0.482 (f 4, 40= 0.89)	**0.002** (f 4, 40= 5.25)	**0.001** (f 4, 40= 5.60)	**0.002** (f 4, 39= 5.11)				
Tryptophan	-2hr	18.1±1.1	20.8±4.3	18.1±1.6 ^{b}	20.8±4.3	0.433 (f 3, 12= 0.98)	0.310	0.240	0.834
	2hr	20.9±5.1	19.3±3.7	21.9±3.2 ^{b}	20.1±2.9	0.711 (f 3, 27= 0.46)			
	4hr	20.8±4.1	20.4±2.4	21.9±3.2 ^{b}	19.7±2.5	0.583 (f 3, 26= 0.66)			
	8hr	22.8±4.6 ^{zy}	22.9±3.5 ^{zy}	26.5±4.0 $^{a\,z}$	20.3±2.3 ^{y}	**0.021** (f 3, 26= 3.83)			
	24hr	20.8±1.7	19.3±1.0	20.6±2.7 ^{b}	20.3±1.4	0.404 (f 3, 26= 1.01)			
	P-value	0.345 (f 4, 28= 1.17)	0.160 (f 4, 29= 1.78)	**0.024** (f 4, 28= 3.30)	0.971 (f 4, 32= 0.13)				
Alanine	-2hr	456.1±124.0	347.5±77.4 ^{b}	419.3±112.0 ^{c}	351.9±90.5 ^{c}	0.086 (f 3, 32= 2.40)	**0.003**	**0.000**	0.144
	2hr	532.0±153.7	544.0±171.3 ^{a}	621.1±147.6 ^{b}	573.5±122.7 ^{ab}	0.600 (f 3, 32= 0.63)			
	4hr	444.2±135.9 ^{y}	590.5±154.7 $^{a\,z}$	614.4±122.4 $^{b\,z}$	524.9±121.8 $^{b\,zy}$	**0.050** (f 3, 32= 2.90)			
	8hr	512.4±158.5 ^{y}	603.5±176.9 $^{a\,y}$	816.2±243.7 $^{a\,z}$	705.3±204.6 $^{a\,zy}$	**0.022** (f 3, 31= 3.68)			
	24hr	588.5±184.1	545.2±119.5 ^{a}	648.8±249.8 ^{ab}	545.5±137.2 ^{b}	0.578 (f 3, 32= 0.67)			
	P-value	0.273 (f 4, 39= 1.34)	**0.004** (f 4, 40= 4.58)	**0.002** (f 4, 40= 5.23)	**0.000** (f 4, 40= 7.30)				
Glycine	-2hr	320.1±53.5	267.1±53.8 ^{b}	295.9±68.4 ^{b}	284.0±54.6 ^{c}	0.275 (f 3, 32= 1.35)	0.478	**0.000**	0.960
	2hr	403.6±62.7	371.1±116.6 ^{a}	376.7±53.9 ^{a}	386.6±64.6 ^{ab}	0.826 (f 3, 32= 0.30)			
	4hr	338.1±92.8	367.8±84.6 ^{a}	396.1±63.5 ^{a}	335.8±79.3 ^{bc}	0.357 (f 3, 32= 1.12)			
	8hr	426.8±138.3	408.5±107.9 ^{a}	438.5±60.6 ^{a}	423.6±64.3 ^{a}	0.934 (f 3, 32= 0.14)			

	24hr	399.3±100.2	395.5±101.8 [a]	414.2±96.5 [a]	380.9±59.3 [ab]	0.893 (f 3, 32= 0.20)			
	P-value	0.097 (f 4, 40= 2.12)	**0.027** (f 4, 40= 3.06)	**0.001** (f 4, 40= 5.42)	**0.001** (f 4, 40= 6.15)				
Glutamate	-2hr	75.1±27.6	133.5±65.0 [a]	127.4±56.2 [a]	107.3±49.8 [a]	0.091 (f 3, 32= 2.35)	0.120	**0.000**	**0.040**
	2hr	96.0±16.9	76.9±16.0 [bc]	79.7±19.1 [c]	101.8±38.7 [a]	0.104 (f 3, 32= 2.32)			
	4hr	84.6±33.0	84.3±21.5 [b]	87.5±26.2 [bc]	88.2±22.9 [ab]	0.984 (f 3, 32 = 0.05)			
	8hr	87.8±23.9	93.5±34.9 [b]	105.6±25.5 [ab]	122.0±49.1 [a]	0.186 (f 3, 32= 1.70)			
	24hr	62.2±17.2	50.0±11.6 [c]	67.4±13.0 [c]	64.1±15.0 [b]	0.075 (f 3, 32= 2.53)			
	P-value	0.057 (f 4, 40= 2.51)	**0.000** (f 4, 40= 6.58)	**0.003** (f 4, 40= 4.93)	**0.029** (f 4, 40= 3.02)				
Proline	-2hr	420.7±195.5	223.1±142.2 [b]	271.0±226.8 [b]	247.8±186.0	0.139 (f 3, 32= 1.97)	0.267	**0.000**	0.696
	2hr	524.2±332.1	454.1±269.4 [ab]	517.7±320.7 [ab]	397.0±181.1	0.750 (f 3, 32= 0.41)			
	4hr	485.8±397.7	722.2±488.5 [a]	611.4±238.8 [a]	431.1±276.2	0.346 (f 3, 31= 1.15)			
	8hr	494.0±307.4	519.5±316.6 [a]	689.4±419.4 [a]	368.8±236.0	0.241 (f 3, 32= 1.47)			
	24hr	203.5±209.7	220.4±136.6 [b]	259.3±209.7 [b]	318.2±265.6	0.678 (f 3, 31= 0.51)			
	P-value	0.164 (f 4, 39= 1.73)	**0.006** (f 4, 39= 4.30)	**0.008** (f 4, 40= 4.03)	0.498 (f 4, 40= 0.86)				
Serine	-2hr	98.3±51.3 [bc]	72.3±25.4 [b]	81.0±17.9 [b]	79.1±15.5 [c]	0.344 (f 3, 32= 1.15)	**0.016**	**0.000**	0.179
	2hr	155.7±71.1 [a]	134.7±37.9 [a]	166.1±71.2 [a]	129.3±33.1 [ab]	0.472 (f 3, 32= 0.86)			
	4hr	143.3±59.6 [ab]	160.6±51.9 [a]	171.1±61.6 [a]	150.9±44.2 [a]	0.730 (f 3, 32= 0.43)			
	8hr	128.0±48.0 [abc y]	170.9±69.0 [a zy]	209.4±95.7 [a z]	116.4±28.7 [b y]	**0.022** (f 3, 31= 3.70)			
	24hr	87.3±16.1 [c]	79.4±22.3 [b]	89.2±20.1 [b]	75.9±28.0 [c]	0.540 (f 3, 32= 0.73)			
	P-value	**0.041** (f 4, 39= 2.76)	**0.000** (f 4, 40= 9.33)	**0.000** (f 4, 40= 7.49)	**0.000** (f 4, 40= 9.66)				
Tyrosine	-2hr	80.6±24.1 [bc]	77.1±24.9 [cd]	70.3±25.9 [b]	77.3±22.0 [b]	0.836 (f 3, 32= 0.29)	0.087	**0.000**	0.568
	2hr	112.4±48.8 [ab]	89.1±23.2 [bc]	119.5±39.4 [a]	98.8±21.9 [ab]	0.278 (f 3, 32= 1.34)			
	4hr	123.2±57.6 [a]	109.7±32.7 [b]	132.6±44.3 [a]	108.3±28.5 [a]	0.575 (f 3, 32= 0.67)			
	8hr	123.0±39.8 [a]	142.7±55.6 [a]	135.5±66.7 [a]	96.5±33.1 [ab]	0.251 (f 3, 31= 1.43)			
	24hr	70.5±20.8 [c]	55.0±10.4 [d]	64.8±16.4 [b]	53.1±7.3 [c]	0.054 (f 3, 32= 2.83)			
	P-value	**0.022** (f 4, 39= 3.24)	**0.000** (f 4, 40= 9.23)	**0.001** (f 4, 40= 5.95)	**0.000** (f 4, 40= 7.39)				

Values represent means of 3 samples at each week at each time (Total *n*=9/ treatment/ time). All values are means (*n*=9) ± standard deviation. Different superscripts indicate significant differences (p <0.05). CD= Control diet, LD= Leucine diet, VD= Valine diet, ID= Isoleucine diet. Analysis was performed using one-way ANOVA, with Fisher's LSD method used for *post-hoc* examination. A GLM was used to determine significance in diet, time and the interaction between diet and time (D*T) with Fisher's LSD method used for *post-hoc* examination.

At the 8 hr sampling timepoint, a similar trend occurred with isoleucine and valine, whereby both the ID and VD were significantly higher compared to the other diets (*p*=<0.05).

Whereas interestingly, no differences between diets were noted for leucine (*p*=0.380). All the BCAAs were different across the 4 diets at the 24 hr timepoint. *Post-hoc* analysis identified valine as different in the VD diet (*p*=0) when compared to CD and ID diets, with LD diet having the lowest detectable valine amongst the four diets. Isoleucine in the ID diet was different (*p*=0) between all the diets. Intriguingly, leucine in the ID was higher than the LD and VD diets, but not to the CD diet. No differences were noticed for leucine across the diets at -2 and 8 hr.

2.3.3.1.2 Overall timepoint analysis within each diet

Overall, there were differences within each diet between the five timepoints for all plasma BCAA analysed (Table 2.6 vertical *abc* subscripts). All diets displayed both significant and highly significant differences (*p*=0.05 and *p*=0) over the 5 timepoints for the plasma BCAAs.

Return to baseline concentrations were seen over 24 hr across the CD, LD and ID diets for isoleucine and valine, with the -2 hr and 24 hr timepoints showing similar values. VD diet was the exception to this trend, with higher values at the -2 hr compared to the 24 hr timepoint. Plasma leucine portrayed a slightly different uptake entirely across the CD, ID and VD diets, whereby the 24 hr sampling point was the lowest dissimilar value in comparison to the other times. LD leucine concentrations were similar at -2 hr and 24 hr. Variations in plasma peaks were viewed across the diets. Valine had the highest concentrations at the 2 and 4 hr points, followed by -2 hr and 8 hr, with the lowest concentration at the 24 hr mark.

A similar observation was seen for Isoleucine, with the peaks at 2 hr and 4 hr being different to -2 hr, and the lowest different concentration at 24 hr. A GLM was used to explore differences in diet, time and the interaction between diet and time (D*T) in the plasma BCAAs. Differences were observed for all the BCAAs in diet, time and the interaction between diet and time (D*T) (*p*=<0.05).

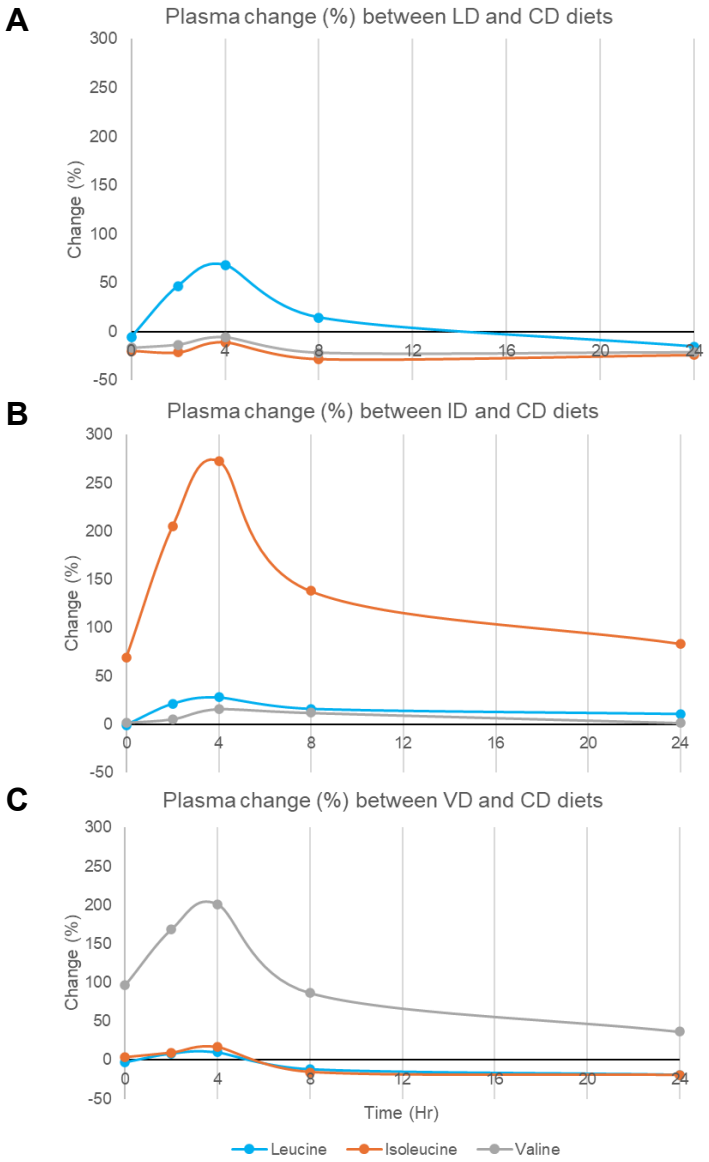


Figure 2.5 fBCAA percentage change (%) in post-prandial plasma for A) LD B) ID C) VD diets in comparison to the CD diet over five timepoints (-2 (0), 2, 4, 8, 24 hr). Values represent means (%) (n=9/ timepoint). Analysis was performed in triplicate (n=9). CD= Control diet, LD= Leucine diet, VD= Valine diet, ID= Isoleucine diet.

2.3.3.1.3 Differences in plasma BCAAs between test diets and the CD

To recognise the variations in the plasma BCAAs in comparison the CD diet, percentage (%) from baseline CD was measured (Figure 2.5). The graphs depicted the percentage (%) variation/change between the BCAAs in each diet and the BCAAs in the CD diet. Although each BCAA was added to the CD at a 2% inclusion rate, hypothesising that the plasma uptake would be similar, the graphs displayed different preferential uptake between the diets, with preferential uptake observed with leucine (A)→ valine (C)→ isoleucine (B).

2.3.3.2 Plasma EAAs

2.3.3.2.1 All diets at each timepoint

For the EAAs, all the diets across the 5 timepoints showed minor variation (Table 2.6 *zyx* subscripts). A few exceptions were methionine which had differences between the diets at the 24 hr timepoint, and tryptophan at the 8 hr point (p=0.013 and p=0.021). *Post-hoc* analysis highlighted differences in methionine, with the CD diet significantly higher than LD and VD diets (p=0.013), whereas 8 hr tryptophan displayed observable differences between ID and VD (p=0.021) with ID significantly higher than VD. Near significance (p≤ 0.10) was detected at the 24 hr timepoint across diets for phenylalanine (p=0.066) and at 8 hr and 24 hr for threonine (p=0.080 and p=0.056).

2.3.3.2.2 Plasma EAAs within each diet over time

Unlike the overall EAA observations made previously between diets across each timepoint, variation within each diet between timepoints was observed. Arginine and phenylalanine had differences in the four diets over the 5 timepoints (Table 2.6 *abc* subscripts). Threonine and methionine were different in all the test diets, but not in the CD diet (p=0.482, p=0.087). In the ID diet, lysine was not different in uptake (p=0.063) whereas tryptophan inversely had differences between timepoints (p=0.024). Near significance (p≤ 0.10) was seen in the CD diet for histidine (p=0.098) and in the ID diet histidine and lysine (p=0.092, p=0.063).

Peak uptake observations across the five (5) timepoints of the EAAs between diets were similar to previously observed trends. Peak uptake times were between 2 to 8 hr post-prandial, with baseline levels viewed at -2 and 24 hr post feeding. Baseline levels across the EAA -2 and 24 hr points were similar although for threonine were lower across diets at -2 hr compared to 24 hr levels.

GLMs (two-way ANOVA) were used to determine if there were differences in diet means, time and interactions between diet and time (D*T) in all fAAs. No differences in fEAAs between diets means were identified but near significance (p≤ 0.10) was noticed in arginine (p=0.058) and histidine (p=0.088), Highly significant differences were detected for time (p=*0*) across all fAAs apart from

tryptophan (p=>0.05) and a slight variation to histidine (p=0.021). No interactions were seen in the EAAs between diet and time.

2.3.3.2.3 The EAAs change (%) between the BCAA diets and CD

The change (%) in arginine between the BCAA diets and the CD diet had peak increases at the 4 hr point, with ID having the highest peak increase at 33% (Figure 2.6). All diets had decreases at 8 hr, with VD having the greatest decrease at -23%. At 24 hr, both LD and VD were still below CD levels, but ID had a 4% increase above CD levels.

All diets at -2 hr were above CD histidine levels (3-12%) but decreased at 2 hr (-9% to -19%) with both the LD and ID having the lowest decrease. An increase in uptake was observed at 4 hr, with ID diet having the highest increase above CD levels at 40% followed by VD and LD (22% and 17%). All diets decreased at the8 hr mark, with both VD and LD decreasing below CD levels at 24 hr (-14% and -19%) and ID staying 18% above the CD levels.

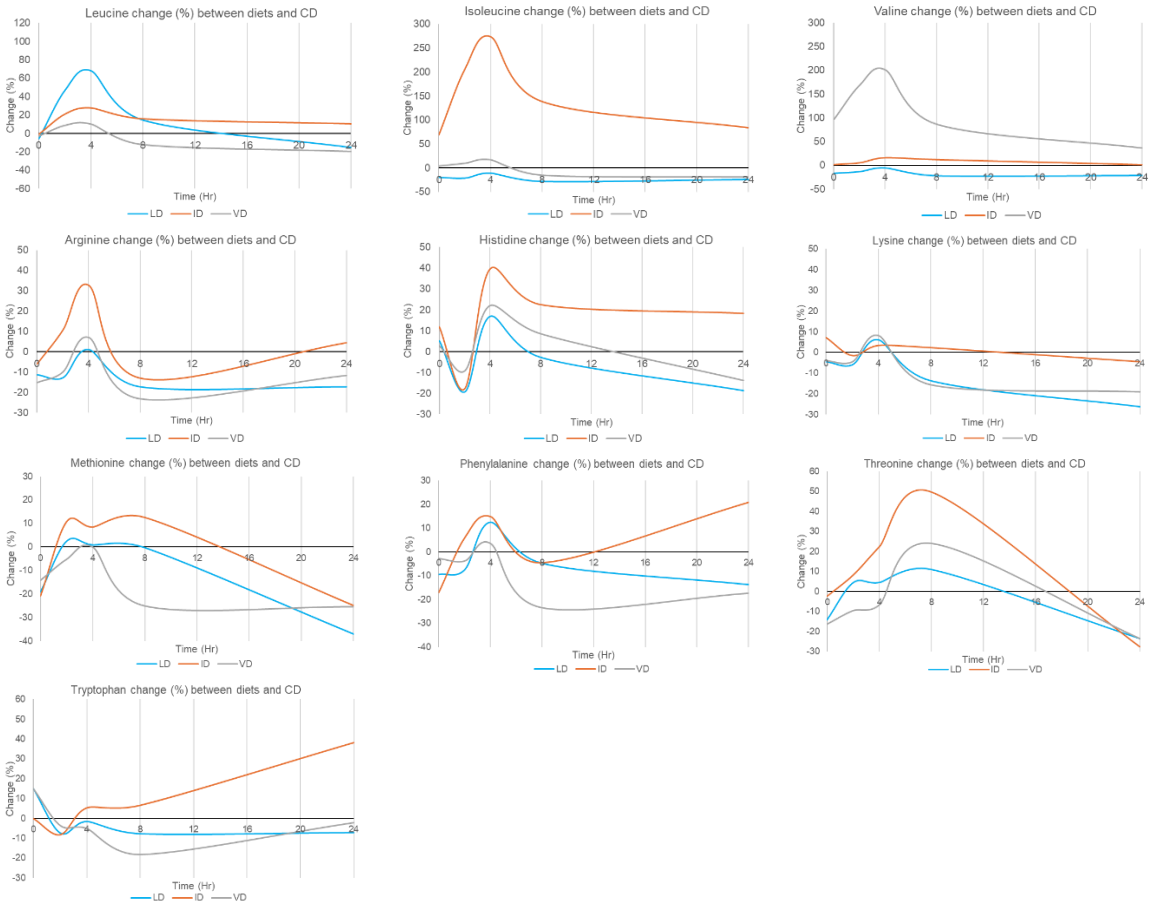


Figure 2.6 Plasma fEAAs change (%) from the CD diet over 5 timepoints.

Interestingly, in the ID diet, lysine at -2 hr was 7% higher than CD levels compared to LD and VD who were both 4% lower than CD. All diets further decreased at 2 hr all dropping below CD levels, before rising above CD at the 4 hr point. VD and LD had slightly greater increases than ID (8%, 6% and 3%) but both fell again below the CD levels at 8 hr, whereas ID stayed 2% above the CD level. At 24 hr all diets were below the CD level with the largest decrease seen in LD and VD (26% and 19%) compared to a 5% decrease for ID.

Methionine levels at -2 hr were all well below the CD diet, with the greatest % decrease seen for ID and LD followed by VD (21%,19%, 14%). At 2 hr all diets increased, with only ID and LD levels reaching above CD values (11%, 2%) and VD diet still below at 5% less than CD. At 4 hr, methionine levels in the VD diet were the same as CD with 0% change, whereas although both ID and LD levels were above CD they both experienced a % decrease (1% and 8%). Interestingly, at 8 hr, ID had the highest change (%) over the 24 hr period with a 13% increase over CD base levels. VD experienced a 25% decrease compared to CD and LD stayed at CD base levels. At 24 hr, all diets were well below the CD diet, with the biggest negative change seen in LD at 37% followed by both ID and VD at a 25% decrease compared to CD levels.

All diets at -2 hr were below CD levels for phenylalanine, with the biggest negative change (%) seen in ID (17%), although at 2 hr, ID had a 6% increase above the CD levels while both LD and VD were below (4%, 7%). At the 4 hr peak, ID and LD had similar positive change (%) (15%,12%) whereas VD only had a 4% increase. 8 hr saw a drop below CD levels in all diets, with the greatest decrease witnessed in VD (24%) and a similar decrease for LD and ID (4%, 5%). ID at 24 hr experienced the highest peak, with a 21% change observed above CD levels whereas both LD and VD levels were below CD (14%, 17%).

Threonine saw similar negative change (%) for LD and VD at -2 hr (14%, 16%) whereas ID was similar to CD with only a slight 2% decrease. ID and LD at 2 hr, 4 hr and 8 hr had positive increases above CD baseline levels, with LD displaying the least amount of change (%) at 2 hr and 4 hr and a slightly higher increase at

8 hr (4%, 4%, 11%) compared to ID which had a 50% increase at 8 hr (8%, 22%, 50%).

VD diet displayed a slightly delayed trend for the first three time points, with negative change (%) witnessed (16%, 10%, 7%) but at 8 hr a 24% increase above CD was seen. This spike in threonine in VD was higher than LD which only had an 11% increase above CD. At 24 hr, all diets fell to similar levels below CD with ranges from 28% in ID to 23% in VD. LD and VD Tryptophan levels at -2 hr were both 15% higher than CD levels whereas ID experienced no change.

Although fluctuations were witnessed, both LD and VD levels were below CD for the next 4 timepoints. The greatest negative difference was seen at 8 hr in the VD diet (-18%). ID showed an opposing trend, with an increase above CD levels at the 4 hr, 8 hr and 24 hr points (5%, 6%, 38%).

2.3.3.3 Plasma fNEAAs

2.3.3.3.1 Each timepoint between diets

Differences in plasma were observed between diets at 4 hr and 8 hr for alanine (p=0.050, p=0.022) and at 8 hr for serine (p=0.022). *Post-hoc* analysis indicated that for alanine at 4 hr, the LD and ID were different to CD but not to VD diets, and at 8 hr ID was different to LD and CD (Table 2.6 *zyx* subscripts). Similarly, for serine at 8 hr ID was different to CD and VD (p=<0.05). Near significance (p≤ 0.10) was detected for alanine -2 hr (p=0.086), tyrosine at 24 hr (p=0.054), and glutamate had near significance at -2 hr, and 24 hr (p=0.091, p=0.075).

2.3.3.3.2 fNEAAs within each diet over the 5 timepoints

Within each BCAA diet, across the 5 times, differences were noted for all NEAAs apart from proline in the VD diet. In the CD diet the only differences noted were in serine and tyrosine (p=0.041, p=0.022) with near significance (p≤ 0.10) observed in glycine and glutamate (p=0.097, p=0.057) (Table 2.6 *abc* subscripts).

Alanine, glutamate, and glycine in the BCAA diets appeared to have the lowest significant levels at -2 hr followed by non-significant high-level peaks from 2 to 24 hr post-prandial, with no return to -2 hr baseline values at 24 hr. Proline, serine, tyrosine had similar peak expression noted in the EAAs, whereby majority uptake

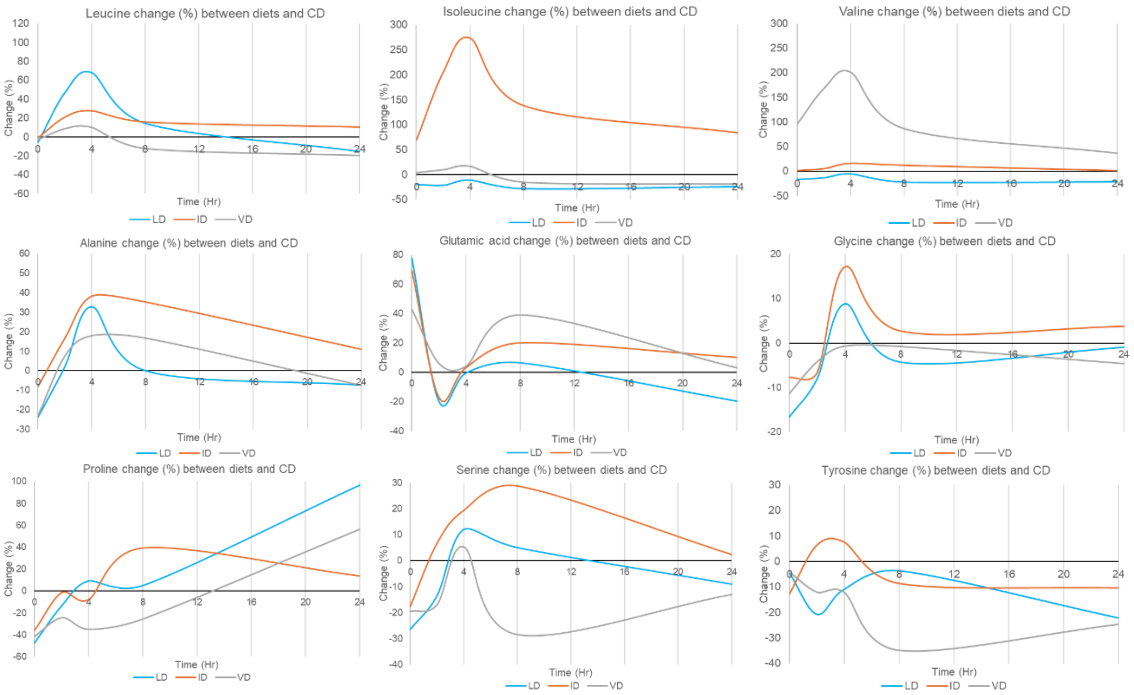


Figure 2.7 The plasma fNEAAs change (%) compared to the CD.

occurred between 2 to 8 hr post feeding with a baseline at -2 hr and a return to baseline at 24 hr.

GLMs displayed differences between diets in serine (p=0.036) and alanine (p=0.015) with near significance (p≤ 0.10) noticed in tyrosine (p=0.061). Highly significant differences were observed in time (p=*0*) across all NEAAs and an interaction in glutamate was seen between diet X time (p=0.040).

2.3.3.3.3 The fNEAAs and change (%) between the BCAA diets and CD

LD and VD diets had the lowest negative change (%) for alanine at -2 hr (24% and 23%) with ID having an 8% negative change (%) (Figure 2.7). All diets had increased change (%) at both the 2 hr and 4 hr points, with ID having the largest change (%) at 2 hr and 4 hr (17%, 38%). 8 hr saw little variation in change (%) for both ID and VD (35%, 17%) but LD had no change (%) compared to the CD level. Both LD and VD decreased at 24 hr and had negative change (%) (7%) whereas ID had an 11% positive change (%).

Glutamate change (%) at -2 hr was the highest in LD and ID 78% and 70% respectively, compared to a 43% change in VD. All diets decreased at 2 hr, but both LD and ID fell below CD levels (20%, 17%) whereas VD stayed slightly

above CD levels registering a 6% change. VD and ID saw increases above CD at 4 hr, 8 hr and 24 hr with the highest post-prandial peak being at 8 hr. VD had a 39% change followed by ID with a 20% positive change.

LD showed little change compared to CD, with only a slight increase at 8 hr (6%) before dropping down to a 20% decrease below CD at 24 hr. Glycine had similar trends over the 5 timepoints for LD and VD compared to ID. All diets were below the CD at -2 hr, with both LD and VD increasing slightly at 2 hr (8% and 4%) but remaining below CD levels. ID at -2 hr and 2 hr remained constant below CD (8%, 7%) before rising to 17% change at 4 hr and remaining slightly above CD levels for 8 hr and 24 hr points (3%, 4%). LD also increased above CD levels at 4 hr, observing a 9% change before dropping slightly below CD levels at 8 hr and 24 hr. VD levels at 4 hr and 8 hr were very similar to the CD with only a constant 1% negative change.

Proline -2 hr starting levels saw all BCAA diets below CD levels, with LD having the biggest negative change (%), followed by VD and ID (47%, 41%, 36%). Although there was a reduction in change (%) at 2 hr, all levels were still below the CD diet. LD diet at 4 hr was the only diet with a positive change (%) above CD levels (9%), while conversely both ID and VD levels dropped again to greater negative change (%) (7%, 35%), with VD having a 35% negative change (%). ID had a 40% change at 8 hr before dropping down to a 14% positive change at 24 hr. At 8 hr LD had a 9% positive change, while VD was 25% below CD. Interestingly, at 24 hr both LD and VD rose to a 97% and 56% positive change (%) compared to CD levels.

Serine had negative change (%) levels across the diets at -2 hr with LD diet having the lowest at 26% below CD and ID and VD similar values (18% and 19%). ID had positive %changes compared to CD from the 2 hr to 24 hr point (7%,19%, 29%, 2%) with the highest peak change at 8 hr. VD had a positive change above CD levels at 4 hr of 5%, before dropping to the lowest value at 8 hr, a 28% decrease compared to CD. LD had its highest peak above CD levels at 4 hr (12%), dropping down to 5% at 8 hr and a negative change (%) below CD levels at 24 hr (9%).

Tyrosine underwent temporal variability between diets compared to CD diet. LD and VD levels never rose above CD levels over the 24 hr period. At -2 hr, ID diet had a 13% negative change (%) compared to both LD and VD which were both 4% below CD. ID rose above CD levels at 2 hr and 4 hr (6%, 8%) before dropping below CD at 8 hr and 24 hr (9% and 10%). LD dropped to 21% below CD levels at 2 hr before rising slightly at 4 hr and 8 hr (11%, 4%) and then dropping again at 24 hr to 22% below CD levels. VD followed a similar trend to LD up until the 8 hr mark, where VD dropped to the lowest change (%) (35%) compared to a slight rise in LD levels. At 24 hr, LD change (%) decreased to 22% with VD levels increasing to 25% below CD levels.

2.3.3.4 Total plasma fAA categories mg/100 mL

The total sum of fAAs between each diet at each timepoint had no observable differences (p=>0.05). Total fEAAs (including the fBCAAs) between diets had differences at the 4 hr and 24 hr timepoints (p=0.016 and p=0.027). ID total fEAAs at 4 hr were significantly higher than LD and CD (5050 ±1074, 3998 ±931, 3510 ±823 mg/100 mL) while CD and ID were significantly higher than LD at 24 hr (2587 ±463, 2778 ±681, 2072 ±414 mg/100 mL). fEAAs (excluding the fBCAAs) only had differences at the 24 hr point (p=0.047), with ID and CD significantly higher than LD (1605 ±432, 1576 ±385, 1255 ±312 mg/100 mL).

The fBCAAs had differences at every time apart from the 8 hr point (p=0.008, p=0.002, p=*0*, p=0.022), near significance (p≤ 0.10) was observed at the 8 hr point (p=0.066). At -2 hr, the VD was significantly higher than CD and LD (1894 ±417, 1437 ±306 and 1270 ±430 mg/100 mL). At 2 hr post-prandial, VD and ID were significantly higher than LD and CD (2607 ±781, 2352 ±701, 1770 ±462, 1571±339 mg/100 mL). A similar trend to the 4 hr concentrations was seen at 8 hr, with VD and ID significantly higher than LD and CD (2596 ±842, 2458 ±580, 1833 ±435, 1445 ±274 mg/100 mL). At 24 hr, ID and VD were significantly higher than LD (1173 ±302, 1038 ±147, 817± 139 mg/ 100 mL).

fNEAAs had no differences between diets at every time point (p=>0.05).

Within each diet over the five timepoints showed significance at every timepoint for every category (p=<0.05) except for fNEAAs in the CD diet. In the CD, total

fAAs had the significantly highest concentration at 2 hr and the lowest at 24 hr (*p*=0.017, 5715 ±1502, 3957 ±851 mg/100 mL). Total fEAAs had significantly higher volumes at 2 and 8 hr compared to -2 and 24 hr (*p*=0.011, 3826 ±1099, 3632 ±1007, 2803 ±625, 2587 ±463 mg/100 mL). fEAAs excluding the fBCAAs were significantly higher at 2 hr compared to -2 and 24 hr (*p*=0.010, 2255 ±805, 1366 ±385, 1576 ±385 mg/100 mL). Total fBCAAs over time in the CD had significantly lower concentrations at 24 hr compared to the other times (*p*=0.003, 1011 ±281 mg/100 mL).

LD, ID and VD had statistically different trends for total fAAs, total EAAs and EAAs excluding the BCAAs, with statistically the highest concentrations between 2, 4 and 8 hr, and the lowest at -2 and 24 hr baseline levels (*p=0*).

In the LD, total fBCAAs were significantly higher at 2, 4 and 8 hr and the lowest significantly different total was at 24 hr (*p=0*, 1770 ±462, 1833 ±435, 1672 ±512, 817 ±139 mg/100 mL). Total fNEAAs had significantly higher peak uptake at 4 hr, with the lowest uptake at -2 hr (*p*=0.005, 2125 ±687, 1179 ±303 mg/100 mL). In ID, total fBCAA uptake was significantly the highest at 2 hr and 4 hr, with lowest uptake at 24 hr (*p=0*, 2352 ±701, 2458 ±580, 1173 ±302 mg/100 mL). fNEAAs had the highest significant uptake at 8 hr with the lowest uptake at -2 hr (*p=0*, 2471 ±728, 1308 ±402 mg/100 mL).

VD fBCAA had the highest significant peak uptake at 2 hr and 4 hr with the lowest uptake at 24 hr (*p=0*, 2607 ±781, 2596 ±842, 1038 ±147 mg/100 mL). fNEAA uptake was significantly higher at 8 hr, with the lowest uptake at -2 hr (*p*=0.003, 1848 ±285, 1193 ±304 mg/100 mL).

GLMs were used to determine differences between diet means and time as well as the interactions between diet and time (D*T) (Table 2.7). Differences in diet were seen for total AAs, total EAAs, and total BCAAs (*p*=0.006, *p=0*, *p=0*), with near significance (p≤ 0.10) recorded for EAAs (excluding BCAAs) and NEAAs (*p*=0.084, *p*=0.091). All categories displayed differences in time (*p=0*) and a near significance was noted in the interaction (D*T) for BCAAs (*p*=0.066).

Table 2.7 Categories of total plasma fAAs p-values between the diets (mg/100 mL). Anova with Fishers LSD *post-hoc* analyses.

	Diet	Time	D*T
Sum of AA	**0.006** (f 3, 157= 4.25)	**0.000** (f 4, 157= 33.81)	0.683 (f12, 157= 0.77)
Tot. EAAs	**0.000** (f 3, 157= 7.46)	**0.000** (f 4, 157= 36.36)	0.394 (f12, 157= 1.06)
EAAs ex. BCAAs	0.084 (f 3, 158= 2.25)	**0.000** (f 4, 158= 29.80)	0.882 (f12, 158= 0.55)
BCAAs	**0.000** (f 3, 158= 20.85)	**0.000** (f 4, 158= 30.50)	0.066 (f12, 158= 1.73)
NEAAs	0.091 (f 3, 160= 2.19)	**0.000** (f 4, 160= 14.31)	0.811 (f12, 160= 0.63)

Fishers' LSD pairwise *post-hoc* analysis was used to recognise trends in time and diet. Diet means for total AAs showed distinct mean differences, with the ID diet having higher overall mean in comparison to the CD and LD diets.

Total AA differences in overall combined means for time had the 2, 4 and 8 hr with higher means in comparison to -2 and 24 hr, indicating that overall total AA uptake occurred between 2 to 8 hr post-prandial.

Total EAAs (inc. BCAAs) showed a similar trend for time, but a slightly different outcome for diet, whereby both ID and VD were different to CD and LD (*p=0*). Total BCAAs mirrored the uptake mean differences in diets as Total EAAs (inc. BCAAs) but a slightly different time uptake with the 2 to 8 hr point having the highest concentrations followed by -2 hr and finally the lowest values at the 24 hr sampling point.

No differences between diets in plasma EAAs (exc. BCAAs) uptake was observed, but a difference in mean uptake over time was seen (*p=0*) with a similar observable trend to Total AAs and Total EAAs (exc. BCAAs). NEAAs showed differences in mean uptake over time, with the highest different observable mean uptake at 8 hr, then 2 hr followed by 24 hr and finally the -2 hr point having the lowest overall mean values.

2.3.4 Muscle and liver tissue

2.3.4.1 Proximate analysis of tissues

All experimental diets lipids, moisture, ash and protein (MOPA) were examined with one-way ANOVA at the 4 hr post-prandial timepoint within liver and muscle tissues. Three pools were made for each tissue per timepoint consisting of three fish (*n*=3) per pool. No significance was identified within diets across all tissue

Table 2.8 Proximate analysis of muscle and liver tissue of all diets at the 4 hr post-prandial (WM%).

	CD	LD	VD	ID	
Muscle composition (WM%)					
Moisture	75.0±0.6	74.4±0.2	74.8±0.5	74.7±0.7	0.722 (f 3,8= 0.45)
Ash	1.8±0.8	1.8±0.6	1.7±0.8	1.9±0.3	0.876 (f 3,8= 0.23)
Protein	21.5±1.7	21.2±2.4	21.4±0.5	21.4±1.4	0.211 (f 3,8= 1.88)
Lipid	1.1±0.1	1.4±0.3	1.2±0.2	1.4±0.2	0.520 (f 3,8= 0.82)
Liver composition (WM%)					
Moisture	72.6±0.2	73.2±0.4	73.0±0.5	72.8±0.2	0.557 (f 3,8= 0.74)
Ash	1.2±1.3	1.5±0.7	1.3±1.8	0.9±1.2	0.260 (f 3,8= 1.62)
Protein	18.0±3.5	17.2±5.0	17.3±2.4	18.1±1.6	0.696 (f 3,8= 0.49)
Lipid	2.6±0.2	2.3±0.3	2.3±0.2	2.5±0.1	0.606 (f 3,8= 0.65)

Data are expressed as mean total percentage (%) ± standard deviation, and different superscripts indicate significant differences (p=<0.05). Analysis was performed using one-way ANOVA, with Fisher's LSD method used for *post-hoc* examination. Values represent means of three pools consisting of three fish per pool (n=3 pools).

parameters (p=>0.05) (Table 2.8). Although not significant, muscle overall had higher observed results compared to liver for moisture (%), ash (%) and protein, with higher lipid (%) seen across liver. The LD liver and muscle MOPA was additionally explored with one-way ANOVA over the 5 timepoints to determine any temporal differences (p=<0.05). Although no different occurred over time for any of the parameters, an interesting trend was observed in lipid (WM %) between the tissues (Figure 2.8).

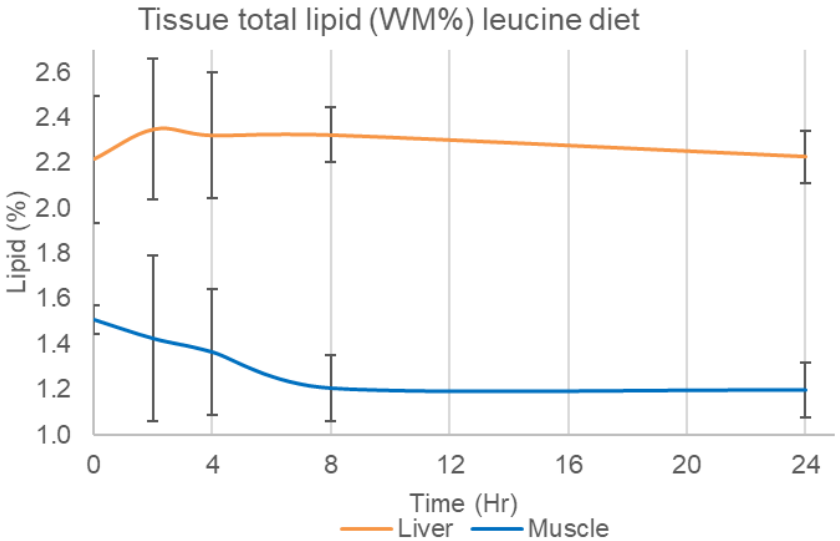


Figure 2.8 Total lipid (%) in liver and muscle tissue in LD over 5 timepoints (-2hr (0hr), 2hr, 4hr, 8hr, 24hr), Analysis was performed using one-way ANOVA. Values represent means of three pools (Total n=9) per timepoint. Analysis was undertaken in triplicate and reported in wet matter basis (WM%) means ±standard deviation.

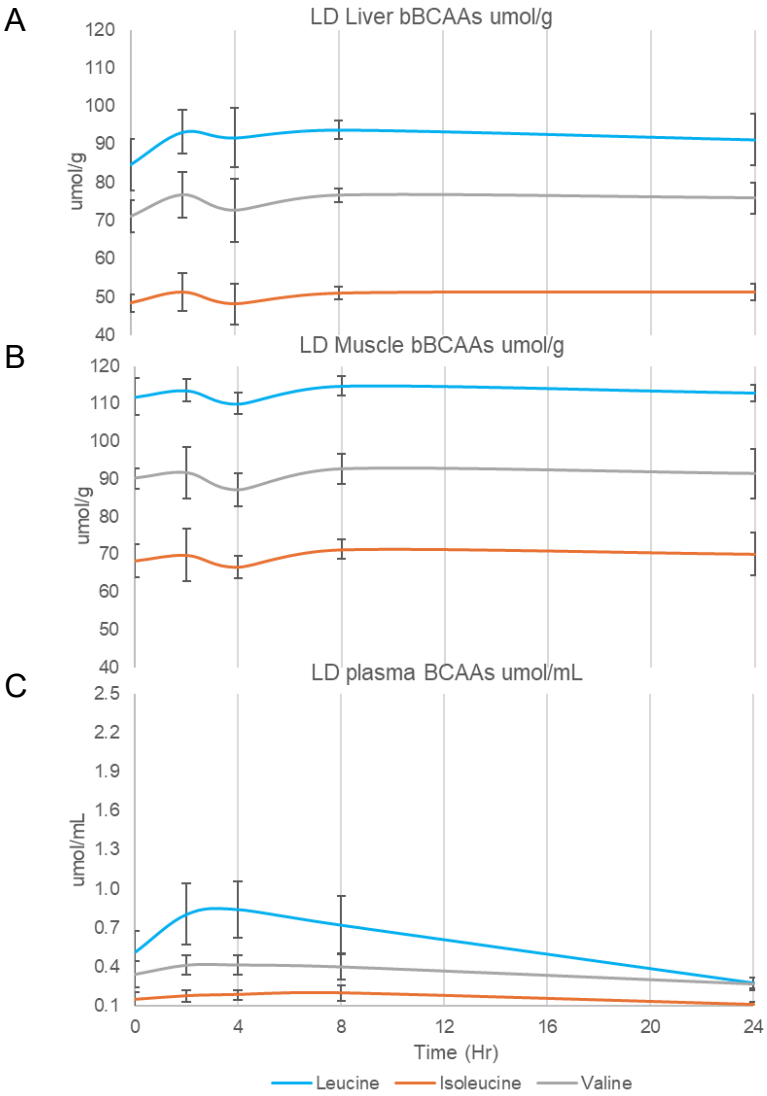


Figure 2.9 LD bBCAAs in A) liver tissue B) muscle tissue C) Plasma fBCAAs at 5 timepoints over 24 hr (-2 hr (0 hr), 2 hr, 4 hr, 8 hr and 24 hr). Analysis was performed using one-way ANOVA, with Fisher LSD method used for *post-hoc* examination. Values represent means in µmol/ g of three pools (Total *n*=9) with error bars indicating standard deviation with analysis completed in triplicate (*n*=3). LD plasma graph included for graphical representation and displayed in µmol/ mL.

In the liver tissue, the CD diet had the highest lipid (WM%) (2.6 ±0.2 %) and the LD had the lowest (2.3 ±0.3%) but there were no differences (p= 0.637). Although no differences were found in the muscle tissue (p=0.526), the reverse observation was noted to liver, with the LD and ID diets having the highest values (1.4 ±0.3, 1.4 ±0.2 %) and the CD the lowest lipid (WM%) (1.1 ±0.1%).

Table 2.9 Muscle and liver total bBCAAs and fBCAAs of the leucine diet **(**LD) 5 different time points (-2 hr, 2 hr, 4 hr, 8 hr and 24 hr).

bAAs	-2hr	2hr	4hr	8hr	24hr	One-way ANOVA P-value
Muscle µmol/ g						
Isoleucine	68.3±4.4	69.8±6.9	66.6±2.9	71.3±2.6	70.1±5.7	0.786 (f 4, 10= 0.43)
Leucine	111.9±4.9	113.5±2.9	110.0±2.8	114.7±2.6	112.9±2.2	0.502 (f 4, 10= 0.90)
Valine	90.2±2.7	91.6±6.8	87.1±4.4	92.6±4.1	91.4±6.6	0.726 (f 4, 10= 0.52)
Liver µmol/ g						
Isoleucine	48.4±2.2	51.3±4.9	48.2±5.3	50.98±1.62	51.4±2.1	0.671 (f 4, 10= 0.60)
Leucine	84.6±6.7	93.2±5.7	91.7±7.9	93.84±2.34	91.2±6.7	0.415 (f 4, 10= 1.08)
Valine	71.1±4.2	76.7±6.0	72.7±8.2	76.62±1.74	75.9±4.0	0.609 (f 4, 10= 0.70)
FAAs						
Muscle µmol/ g						
Isoleucine	0.2±0.0 [a]	0.2±0.0 [a]	0.2±0.0 [a]	0.2±0.0 [a]	0.1±0.0 [b]	**0.026** (f 4, 9= 4.67)
Leucine	0.6±0.1 [a]	0.7±0.1 [a]	0.6±0.2 [a]	0.6±0.0 [a]	0.3±0.0 [b]	**0.008** (f 4, 10= 6.42)
Valine	0.4±0.0	0.4±0.1	0.4±0.0	0.3±0.0	0.3±0.0	0.134 (f 4, 9= 2.33)
Liver µmol/ g						
Isoleucine	0.7±0.1	0.6±0.1	0.8±0.1	0.7±0.1	0.8±0.2	0.623 (f 4, 10= 0.68)
Leucine	1.9±0.2	2.1±0.4	2.0±0.3	2.0±0.3	2.2±0.6	0.933 (f 4, 10= 0.20)
Valine	1.3±0.2	1.3±0.2	1.5±0.4	1.2±0.2	1.6±0.4	0.554 (f 4, 10= 0.80)

Data are expressed as mean ± standard deviation in µmol/g. Different superscripts indicate significant differences (p<0.05). Analysis was performed using one-way ANOVA, with Fisher LSD method used for *post-hoc* examination. Values represent means of 3 samples at 3 sampling points (Total n=9).

2.3.4.2 Bound amino acid analysis (µmol/ g) wet weight

2.3.4.2.1 bBCAAs in LD diet over time

A one-way ANOVA was used to determine if bBCAAs in muscle and liver were different over the five different timepoints in the LD diet (Table 2.9). In muscle tissue, there were no significant differences for leucine (p= 0.502), isoleucine (p= 0.786) and valine (p=0.726) (Figure 2.9 B). Significant differences were detected in lysine, with highest concentration at 8 hr and the lowest at 4 hr (p=0.020). In tyrosine, highest peak concentrations were at 2 hr and 8 hr, with the lowest concentrations at 4 hr (p=0.029). No other differences were observed for the other bAAs (p=>0.05).

A similar trend was determined in the liver tissue, with no significant differences in leucine (p= 0.415), isoleucine (p= 0.671) and valine (p= 0.609) (Figure 2.9 A). No other significant differences were identified for the other bAAs (p=>0.05).

The percentage difference in bBCAAs between the two tissues revealed that in the muscle tissue, leucine had on average 24% higher leucine concentration than in liver tissue. Valine and isoleucine had averages of 21% and 38.4% higher concentration in muscle compared to liver tissue across the five timepoints.

2.3.4.2.2 Differences in bBCAAs between diets at 4 hr postprandial

Muscle tissue pools (n=3) were used in the analysis to determine differences in each bBCAA between the test diets at the 4 hr post-feeding point (Figure 2.10 A). One-way ANOVA determined no significant differences for leucine (p= 0.247), isoleucine (p= 0.520) and valine (p= 0.403). No other significant differences were detected in any of the other bAAs (p=>0.05).

The same analysis was conducted for liver tissue (Figure 2.10 B), with no significant differences for leucine (p= 0.680), isoleucine (p= 0.106) and valine (p= 0.224), although significance was detected for histidine (p=0.035) and serine (p=0.004). For histidine, the CD diet had the highest different concentration, whereas with serine, CD had the lowest different concentration compared to the other three test diets. No other differences were noted in the other AAs between the diets (p=>0.05), although it should be mentioned that near significance ($p \leq 0.10$) was observed in threonine (p= 0.061) (S 2. 32, 33).

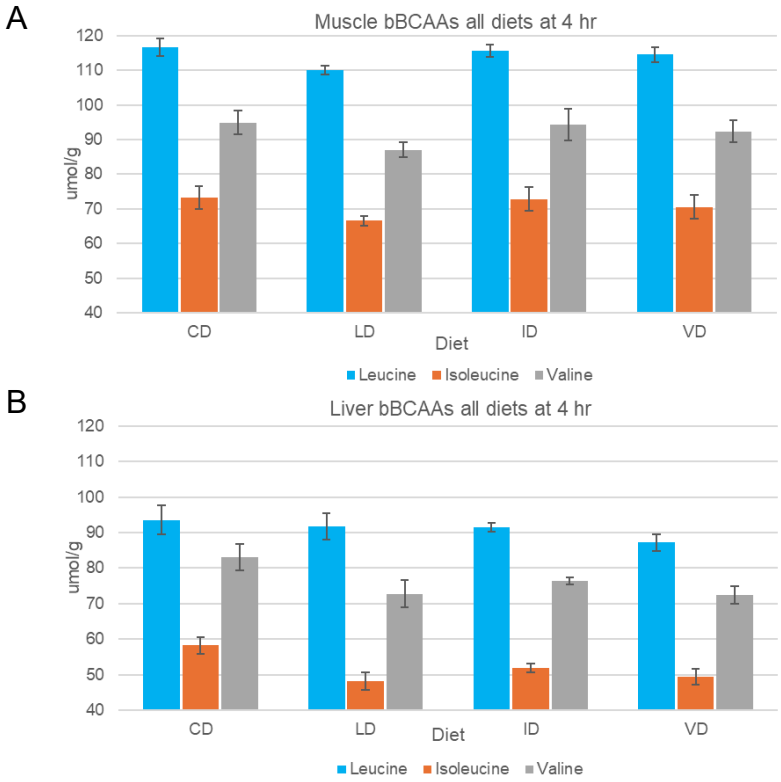


Figure 2.10 bBCAAs for all the test diets A) muscle B) liver tissue at 4 hr post-prandial. Analysis was accomplished using one-way ANOVA. Values represent means in total µmol/ g (wet weight) standard deviation of 3pools (Total n=9) and analysis was completed in triplicate (n=3). CD= Control diet, LD= Leucine diet, VD= Valine diet, ID= Isoleucine diet.

A comparison in change (%) between the 3 BCAA diets and the CD for each tissue at the 4 hr timepoint showed that for leucine, muscle concentrations were between 1.8-5.6% lower than in the CD diet. A similar effect was spotted for isoleucine (3.7-9.0%) and valine (2.7-8.3%). Liver tissue when compared to the CD liver tissue had similar change (%) results, with 2.0-6.8% for leucine, 10.9-17.3% for isoleucine and 8.1-12.8% for valine. BCAAs total change (%) for each diet compared to the CD diet in muscle, showed that LD was 22.9% lower than the CD diet, ID 13.7% and VD 8.2% respectively. A similar observation was made for liver tissue, although the highest % change was observed in the VD diet at 34.8%, followed by LD 31.8% and finally ID 21.2%.

2.3.4.2.3 Total bAA categories g/ 100g

The totals of the bAA categories were analysed by one-way ANOVA with Fisher's LSD *post-hoc* identifying locations of differences in the LD over the 5 timepoints for liver and muscle tissue. Statistical differences occurred in muscle sum of the

bAAs across the time points, with the statistically higher peaks at 2 and 8 hr and the lowest peaks at -2 and 4 hr (p=0.045, 17.49 ±0.24, 17.60 ±0.13, 16.90 ±0.42, 16.92 ±0.37 g/100g). Near significance (p≤ 0.10) was observed for muscle bEAAs excluding bBCAAs (p=0.069) and no observable differences occurred in liver tissue (p=>0.05) (S 2.34). The same categorical analyses were conducted across the diets at 4 hr in liver and muscle tissues, no statistical differences noted (p=>0.05).

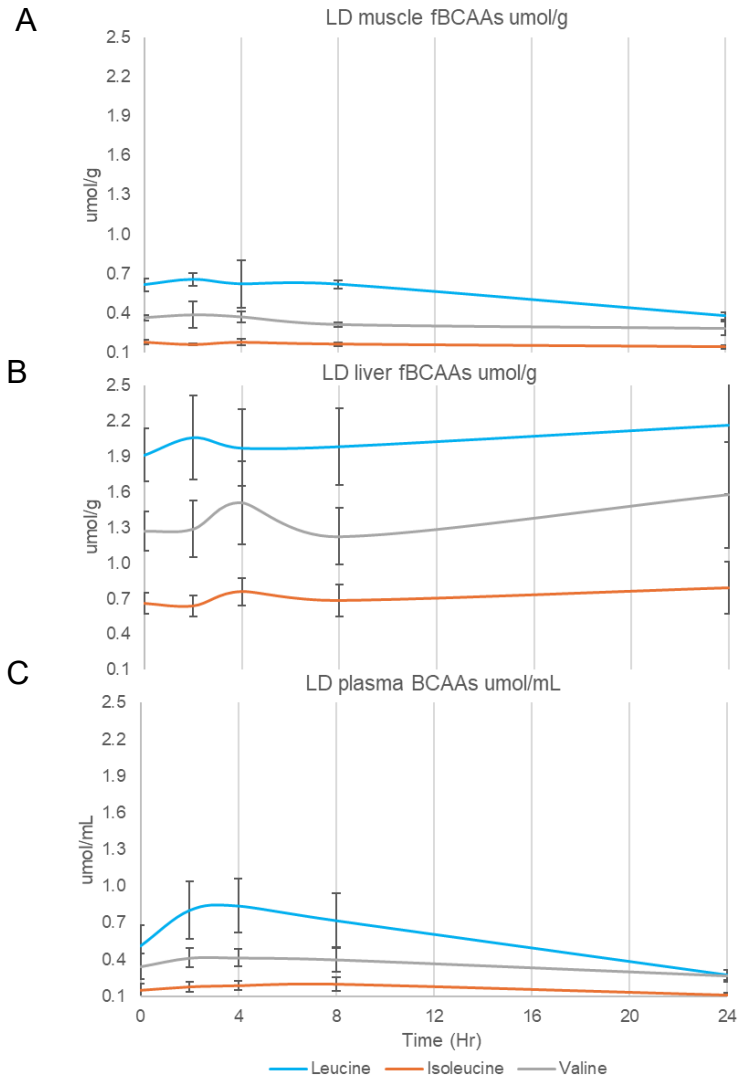


Figure 2.11 LD fBCAAs of A) muscle B) liver tissue C) plasma at 5 timepoints over 24 hr timepoints (-2 (0 hr), 2, 4, 8, and 24 hr). Analysis was conducted using one-way ANOVA. Values represent means in µmol/g with standard deviation of 3 pools (Total n=9) and analysis was completed in triplicate (n=3). Plasma amino acids values presented in µmol/mL and included for trend comparison. Subscripts with different values indicate significance. CD= Control diet, LD= Leucine diet, VD= Valine diet, ID= Isoleucine diet.

2.3.4.3 Free amino acid analysis (µmol/g)

2.3.4.3.1 fBCAAs in LD over time

One-way ANOVA was used to determine the statistical differences in the LD diet over 5 different timepoints between fBCAAs found in muscle and liver tissue (Figure 2.11). Three pools from the LD diet were prepared using 3 fish (*n*=3) per pool for each timepoint. In LD muscle tissue (Figure 2.11 A), a difference in leucine and isoleucine was noted (*p*=0.008, p=0.026) with further *post-hoc* analysis using Fisher's LSD indicating that the differences were at the 24 hr timepoint means, which were significantly lower in comparison to the other 4 timepoints. No differences were noted for valine (*p*=0.134). The change (%) when compared to the -2 hr baseline concentrations for leucine, had a high of 7% at 2 hr and the largest decrease of -44% at 24 hr. Valine followed a similar trend, with a 6% increase at 2 hr and a -27% decrease at 24 hr. Isoleucine had a decrease from the -2 hr baseline across the other 4 timepoints, with the lowest decrease of -1% at 4 hr and the greatest decrease of -28% at 24 hr post-prandial.

Temporal differences were noted in lysine and glutamate (*p*=0.033, *p*=0.011) with *post-hoc* analysis showing that concentrations of lysine were significantly higher at 2 hr and lower at 4 hr (S 2.35). Glutamate followed a similar trend although the 4 and 24 hr were significantly lower than the other timepoints. When examining the change (%) from -2 hr for lysine, 2 hr saw an 11% increase while 4 hr had a 50% decrease below -2 hr. Similarly to lysine, glutamate saw a 10% increase at 2 hr, but a -54% decrease at 24 hr.

In the liver tissue (Figure 2.11 B), no statistical differences were noted in leucine (*p*=0.933), isoleucine (*p*=0.623) or valine (*p*=0.834) but a significant difference was observed in arginine (*p*=0.027). Arginine concentrations were significantly lower at -2 hr compared to 4 to 24 hr timepoints. No other significances were seen in any other of the tested fAAs (*p*=>0.05).

Interestingly, when looking at the change (%) from -2 hr, valine had a -3% decrease below -2 hr levels at 8 hr, followed by a 24% increase at 24 hr. Although of varying significance, isoleucine similarly followed this undulating trend, with a -3% decrease at 2 hr followed by the highest increase at 24 hr of 20%.

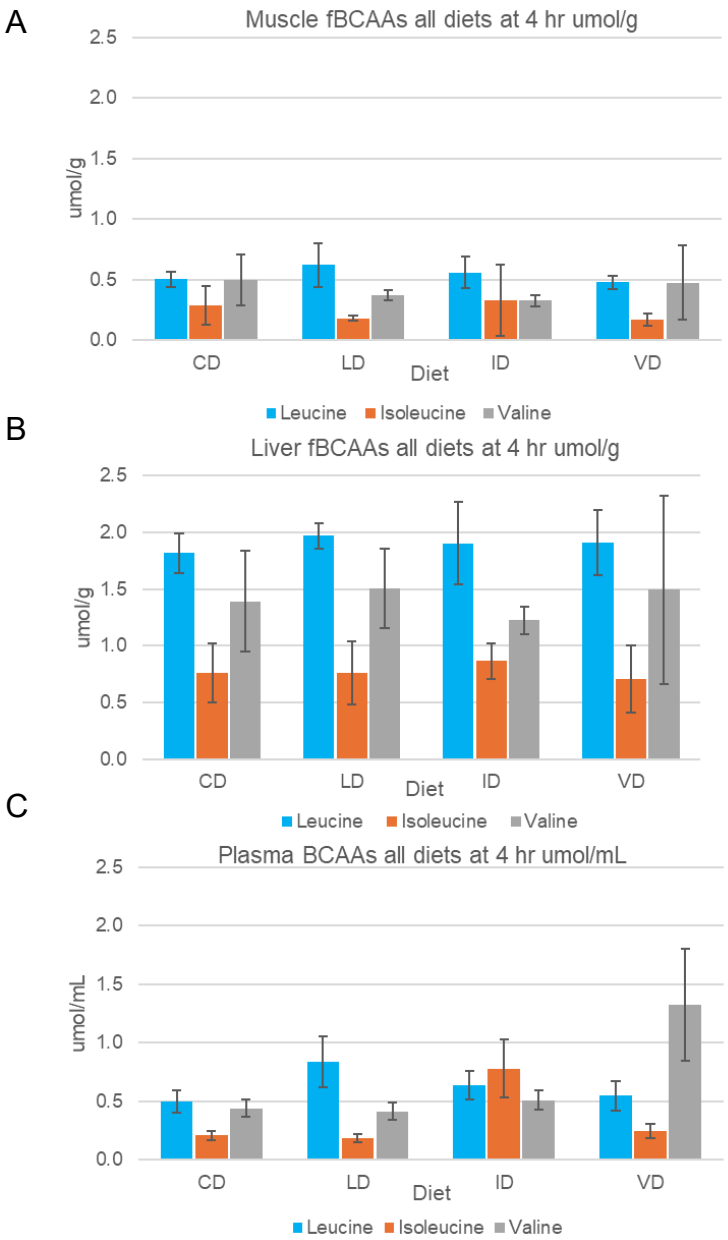


Figure 2.12 fBCAAs in A) muscle B) liver tissue C) plasma at the 4 hr timepoint for all diets. One-way ANOVA was used for statistical testing of the individual AAs across diets and GLM was used to determine an interaction between diets and AAs. Values are represented µmol/g with standard deviation, with plasma as µmol/mL. 3 pools/diet (Total *n*=9) were used. Analysis was conducted in triplicate (*n*=3). CD= Control diet, LD= Leucine diet, VD= Valine diet, ID= Isoleucine diet.

Leucine had less change over time although the lowest difference from -2 hr was seen at 4 hr (3%) and the highest at 24 hr (13%).

fAA categories in the LD across time for muscle and liver tissues were investigated using one-way ANOVA and Fisher's LSD *post-hoc* examinations. Muscle had significance over time for total fEAAs (*p=0*) with the highest quantity (mg/100 g) seen at 4 hr and the lowest different value at 24 hr. For fEAAs

excluding the fBCAAs, -2, 2 and 8 hr were significantly higher than 24 hr (p=0.038). Total fBCAAs were significantly higher at 4 hr, followed by -2, 2, and 8 hr, with the lowest significant quantity at 24 hr.

2.3.4.3.2 Differences in fAAs between diets at 4 hr post-feeding

A One-way ANOVA was conducted to determine if individual fBCAAs in either muscle or liver tissue were different between the test diets at 4 hr (Figure 2.12). Samples were classified into the four diet groups with three pools per diet and each pool consisting of three fish (n=3). No differences between diets were observed in muscle tissue for the BCAAs at the 4 hr point and neither in liver tissue (p=>0.05). Total fAAs (mg/100 g) across the diets at 4 hr, had no differences in muscle or liver tissue (p=>0.05).

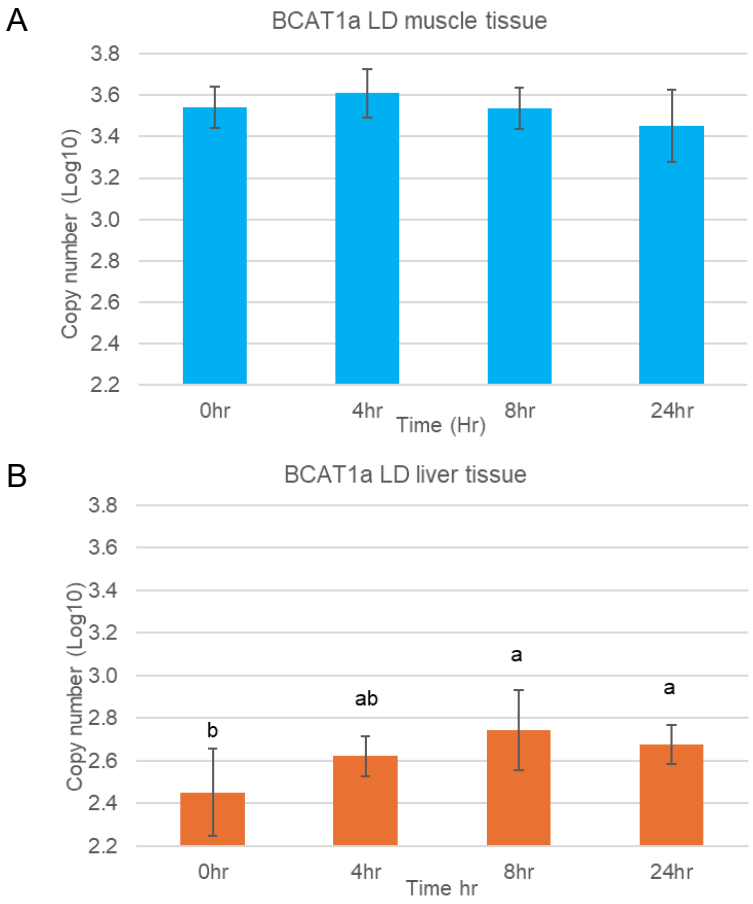
2.3.5 mRNA abundance

2.3.5.1 BCAA metabolism (BCAT1a, BCKDH1a, BCKDK)

A one-way ANOVA was conducted to determine if abundance of the transcript (BCAT1a) in muscle and liver tissue differed over a 24 hr period after being fed the LD diet. Six fish (n=6) from each timepoint were analysed in triplicate and 4 timepoints were looked at -2 hr pre-feeding, 4, 8 and 24 hr post-feeding.

No statistical differences were noted in the muscle tissue between timepoints (p=0.303), but differences were noticed in liver tissue (p=0.042) with Fishers LSD *post-hoc* analysis identifying the differences between the -2 hr and the 8 and 24 hr points (Figure 2.13). A larger transcript abundance was seen at 8 and 24 hr compared to -2 hr.

Between tissue mRNA abundance of copy numbers indicated an overall higher abundance in muscle tissues. Copy numbers varied from a low of 3093 ±1523 /uL at 24 hr to 4213 ±1158 /uL at 4 hr post-prandial. The percentage change in copy numbers when compared to the baseline at -2 hr was highest at 4 hr with an 18% increase. Liver tissue in comparison had lower copy numbers from a low of 315 ±158/uL at -2 hr to 609 ±284 /uL at 8 hr. The percentage change displayed a 93% increase in abundance at 8 hr compared to baseline levels. In liver tissue, the highest increase in abundance was 41% which occurred between 4 and 8 hr.



in A) muscle B) liver in the Leucine diet (LD) at 0 hr (-2 hr), 4 hr, 8 hr and 24 hr. Statistical analysis was performed using one-way ANOVA. Values are reported as means (Copy number (Log_{10})/uL, ± standard deviation of the mean (*n*=6) with analysis conducted in triplicate (*n*=18). LD= leucine diet, 0hr= -2hr.

Fold changes (FC) in mRNA abundance in muscle when compared to the -2 hr control timepoint were 1.01 (0.6%) in the 4 hr, 0.99 (-1.4%) in the 8 hr and 0.96 (-3.9%) at the 24 hr timepoint. A 1.01 (0.6%) FC was noted between the -2 to 4 hr, 0.98 (-1.9%) in the 4 to 8 hr, and 0.97 (-2.5%) in the 8 to 24 hr timepoints. FC in liver mRNA abundance against the -2 hr control had a positive trend with 1.07 (6.9%) in the 4 hr, 1.12 (11.8%) in the 8 hr and 1.09 (9.4%) at the 24 hr timepoint. Between timepoint FC indicated 1.07 (6.9%) FC was noted between the -2 to 4 hr, 1.05 (4.6%) in the 4 to 8 hr, and 0.98 (-2.2%) in the 8 to 24 hr timepoints. In muscle tissue, the peak FC was detected at 4 hr whereas in liver tissue, the apparent trend indicated that the peak FC was identified at the 8 hr sampling point.

In determining absolute copy numbers of BCKDH1a in both muscle and liver tissue, samples were analysed at four timepoints over a 24 hr period. In muscle tissue, significance was observed (p=0.004) and with Fisher's *post-hoc* analysis displaying the differences at the 4 hr and 8 hr between -2 hr and 24 hr (Figure 2.14 A). A similar statistical trend was noticed for liver tissue (p=*0*) with Fisher's *post-hoc* displaying higher abundance at 4 hr and 8 hr compared to -2 hr and 24 hr (Figure 2.14 B).

When looking at the absolute copy numbers of the transcript, in muscle tissue, BCKDH1a ranged from a high of 9724 ± 2665/ µL at 4 hr to a low of 5640 ± 1863/ µL at -2 hr. The highest change (%) compared to -2 hr was 72% at 4 hr, followed by 57% at 8 hr. The largest increase between timepoints was 72% between the -2 hr to 4 hr points.

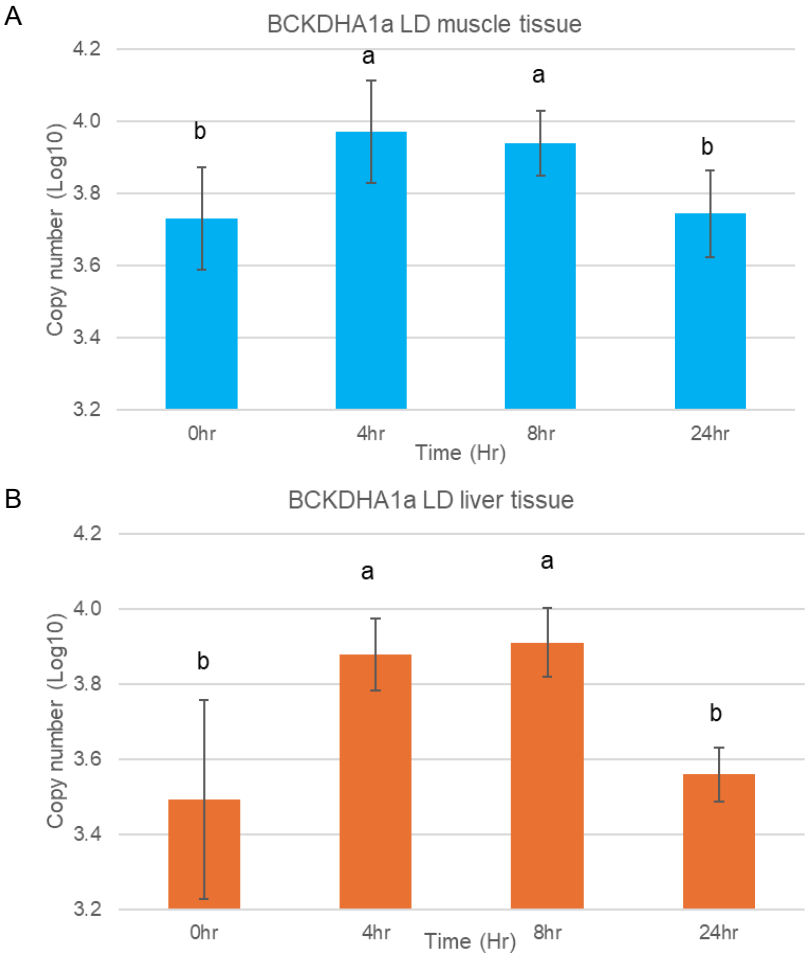


Figure 2.13 BCKDH1a within-tissue variability in A) muscle B) liver in the LD diet at 4 timepoints. Statistical analysis was performed using one-way ANOVA. Values are reported as means (copy number (Log_{10})//uL) ± standard deviation of the mean (n=6) with analysis conducted in triplicate (n=18). LD= leucine diet, 0hr= -2hr.

In liver tissue, absolute mRNA abundance ranged from a high of 8306 ±1602/ µL at 8 hr to a low of 3565 ±1779/ µL at -2 hr. The highest change (%) compared to baseline was 133% at 8 hr, with the greatest change (%) of 117% between -2 hr and 4 hr post-prandial. Differences in muscle FCs between the timepoints and the -2 hr control timepoint were 1.06 at the 4 hr (6.4%), 1.06 at the 8 hr (5.6%) and 1.00 at the 24 hr timepoint 0.3%). FCs between the timepoints were 1.06 -2 to 4 hr (6.4%), 0.99 4 to 8 hr (-0.8%) and 0.95 at the 8 to 24 hr timepoints (-5.1%).

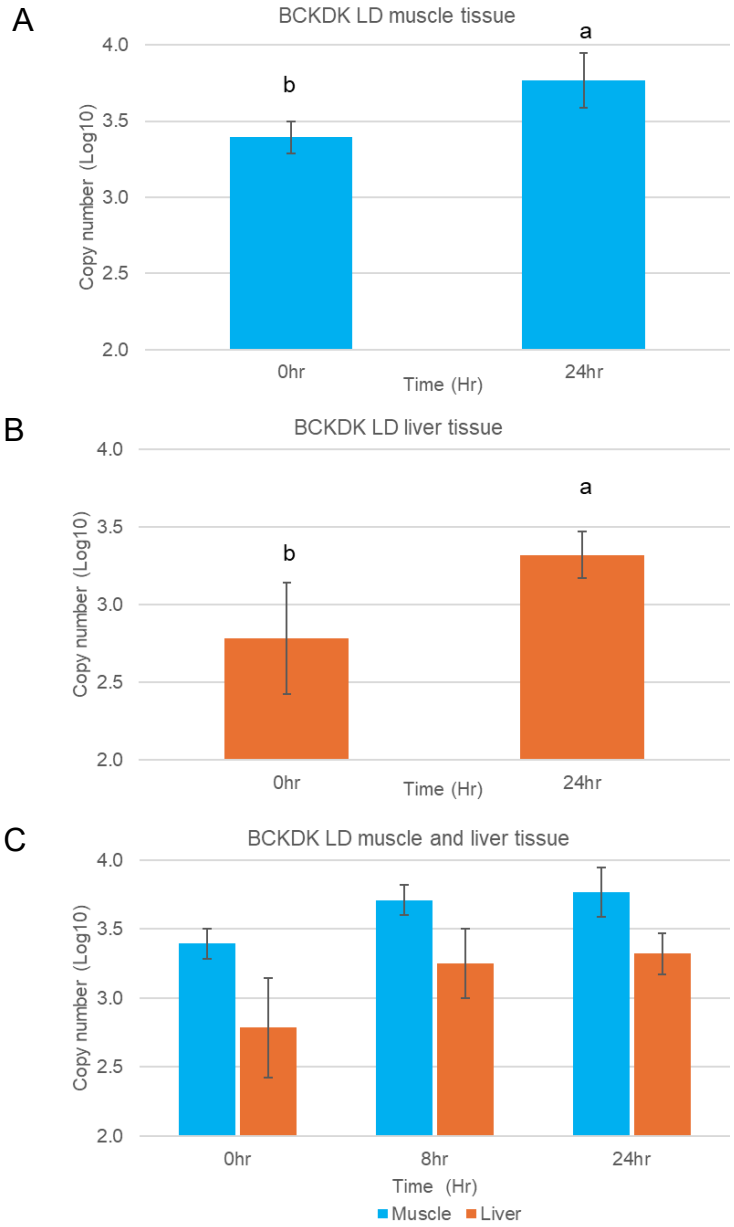


Figure 2.14 BCKDK within-tissue variability in the LD diet A) muscle B) liver at 2 timepoints C) muscle and liver at 3 timepoints (8 hr for exploratory analysis). Statistical analysis was performed using one-way ANOVA. Values are reported as means (copy number (Log_{10})/uL) ± standard deviation of the mean (*n*=6) with analysis conducted in triplicate. LD= leucine diet, 0hr= -2hr.

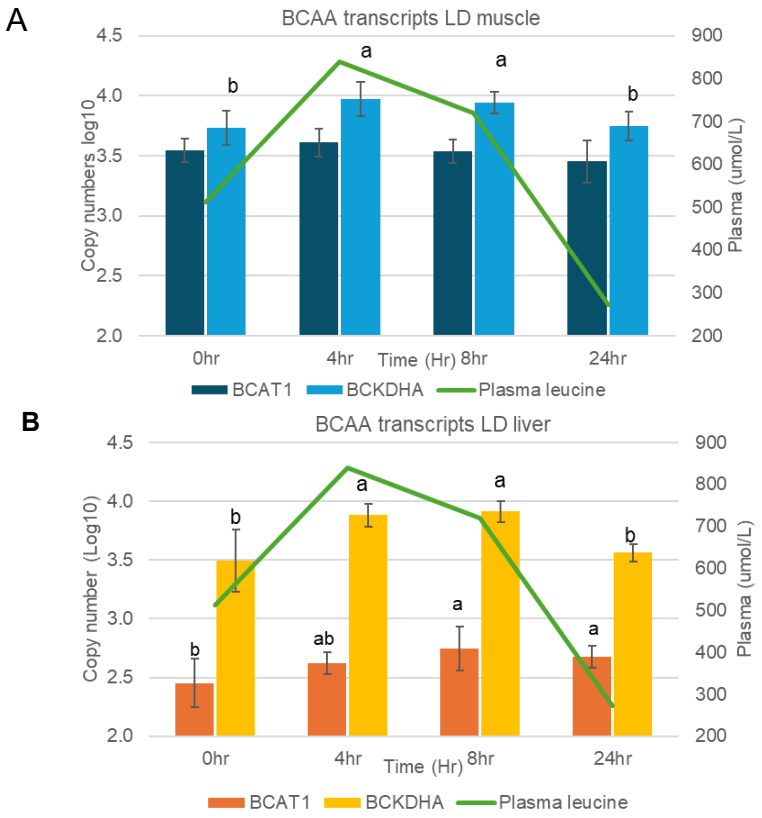


Figure 2.15 LD Plasma leucine and the BCAA mRNA transcripts in A) muscle B) liver tissues. Statistical analysis was performed using one-way ANOVA. Values are reported as means (copy number(Log_{10})/uL) ±standard deviation of the mean (*n*=6) with analysis conducted in triplicate (*n*=18). LD= leucine diet, 0hr= -2hr.

The FCs noted between timepoints in liver tissue when compared to the -2 hr control were 1.11 4 hr (11.2%), 1.12 8 hr (12.1%) and 1.02 (2%) at the 24 hr sampling point. Between timepoint FCs were 1.11 (11.2%) -2 to 4 hr, 1.01 (0.8%) 4 to 8 hr and 0.91 (-9%) for the 8 to 24 hr point. Between tissue FC comparisons displayed similar trends, with both tissues increasing 4 hr after feeding, before falling at 8 hr and 24 hr.

BCKDK mRNA abundance in muscle tissue was significantly different between -2 hr and 24 hr (*p*=0.001) with the 24 hr point higher than the initial baseline at -2 hr (Figure 2.15 A). Absolute abundance displayed mRNA levels at 6267 ± 2579/ µL at 24 hr compared to 2537 ± 603/ µL at -2 hr. Similarly in liver tissue, significantly higher mRNA abundance was observed between -2 hr and 24 hr (*p*=0.007) (Figure 2.15 B). mRNA copy numbers varied from 2202 ±800/ µL at 24 hr to 764 ±463/ µL at -2 hr. Additional 8 hr samples (*n*=3 /tissue) were analysed

as an exploratory method to determine if it was feasible to pursue BCKDK further. In muscle tissue, the average mRNA abundance was 5229 ±1279/ µL compared to liver tissue with a yield of 1974 ±965/ µL (Figure 2.15 C).

In Figure 2.16, in an effort to identify trends relating to LD plasma leucine concentration and the BCAA mRNA abundance response, plasma leucine temporal data was superimposed on the BCAA mRNA abundance results for muscle (2.16 A) and liver tissue (2.16 B). LD plasma leucine concentration was significantly higher at 4 hr and 8 hr peaks, followed by -2 hr pre-feeding baseline (p=<0.05). The 24 hr timepoint had the lowest concentration over the 24 hr postprandial period.

In muscle tissue, BCKDHA mRNA abundance and LD plasma leucine significantly peaked at 4 hr and 8 hr (p=<0.05), while -2 hr and 24 hr were similar in mRNA abundance. Muscle BCAT1 mRNA abundance remained stable over time and did not follow the plasma leucine temporal trend.

In liver tissue, BCAT1 mRNA abundance was significantly higher at 8 hr and 24 hr compared to the lowest at -2 hr (pre-feeding levels). Liver BCKDHA mRNA abundance displayed a similar trend as muscle tissue, by imitating the LD plasma leucine peaks and troughs. The exception to this trend was that the 24 hr BCKDHA mRNA abundance for both tissues were comparable to the -2 hr BCKDHA mRNA abundance, whereas LD plasma concentrations at 24 hr were significantly lower than at -2 hr.

2.3.5.2 mTOR pathway (SESN1, RRAG, MYO6, Myostat 1a)

No statistical differences of mRNA abundance over the 4 timepoints in liver or muscle tissues were observed for SESN1 (p=0.330, p=0.405) (Figure 2.17 A, B). Although no significance in transcript abundance of tissues was observed, this similarly undulating trend, by which each tissue acted in opposition to the other, was mirrored across both tissues, including the 4 hr and 8 hr sampling points.

In muscle tissue, the highest abundance (640 ±254 /µL) of mRNA was seen at 24 hr, with the lowest (392 ±143 /µL) at -2 hr. The highest change (%) compared to -2 hr was 63% at 24 hr and the highest change between timepoints was 50%

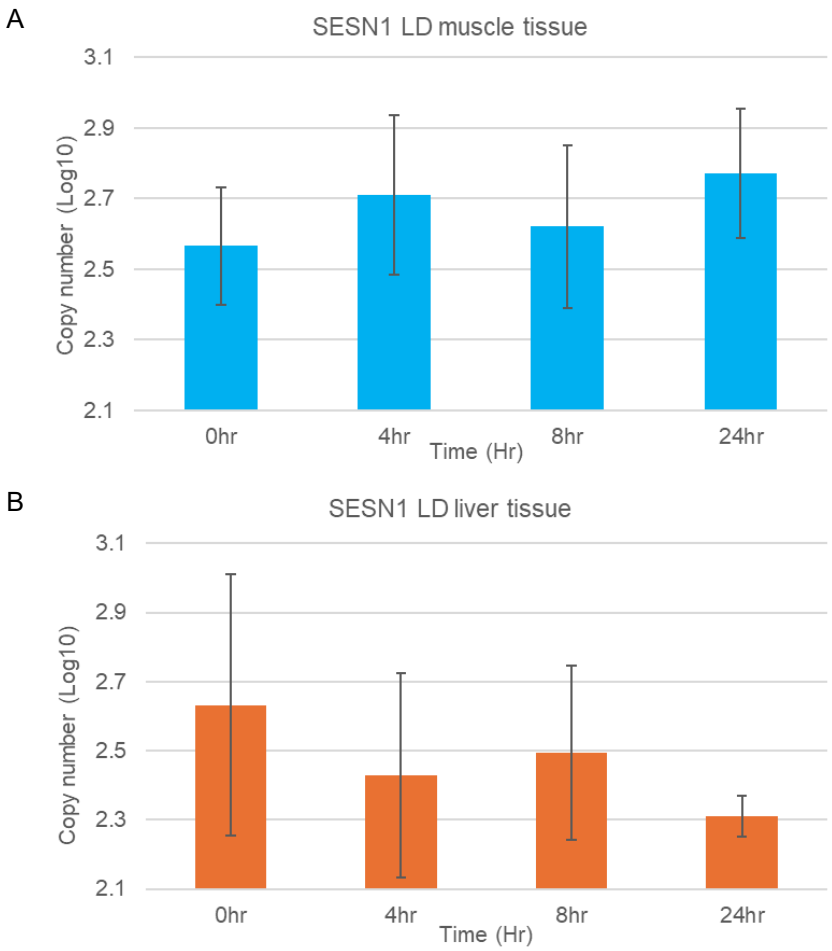


Figure 2.16 SESN1 within-tissue variability in A) muscle B) liver tissue in the LD diet at 4 timepoints. Statistical analysis was performed using one-way ANOVA. Values are reported as means (copy number(Log_{10})/uL) ± standard deviation of the mean (*n*=6) with analysis conducted in triplicate (*n*=18). LD= leucine diet, 0hr= -2hr.

between -2 hr and 4 hr. FCs compared to the -2 hr control in muscle samples were 1.05 (5.4%) at 4 hr, 1.02 (1.9%) at 8 hr and 1.08 (7.8%) at the 24 hr timepoint. FCs between the timepoints were 1.05 (5.4%) between -2 to 4 hr, 0.97 (-3.3%) between 4 to 8 hr and 1.06 (5.7%) between the 8 to 24 hr timepoints.

In liver tissue, the exact opposite trend was witnessed, with the highest abundance (609 ±511/ µL) at -2 hr and the lowest (206 ±31 /µL) at 24 hr. The change (%) in liver tissue compared to -2 hr were negative across timepoints, but a 9% increase was seen between 4 hr and 8 hr. In liver tissue, FCs compared to the -2 hr control were 0.92 (-7.6%) at 4 hr, 0.95 (-5.3%) at 8 hr and 0.88 (-12.2%) at the 24 hr timepoint. FCs between timepoints were 0.92 (-7.6%) between -2 to

4h, 1.02 (2.5%) between 4 to 8 hr and 0.93 (-7.2%) between the 8 to 24 hr timepoints.

In analysis of the mRNA abundance of RRAG, significant differences were determined through one-way ANOVA. Muscle tissue significance was observed (*p*=0.028) with further *post-hoc* analysis identifying the differences at the -2 hr point in comparison to the 4 hr and 8 hr, and the 4 hr different to the 24 hr (Figure 2.18 A). A similar trend seemed to occur in the liver tissue with significance detected between all times, apart from the 4 hr and 8 hr timepoints (*p=0*) (Figure 2.18 B). The highest abundance was detected at the 4 hr and 8 hr timepoints, 24 hr was lower, and the lowest different abundance was at -2 hr

Absolute copy numbers in muscle tissue ranged from a low of 2279 ±534/ µL at -2 hr to a high of 3684 ±882/ µL at 4 hr post-prandial, while in liver tissue a low of 980 ±564/ µL was observed at -2 hr and a high of 2841 ±809/ µL were seen at 8 hr post-prandial. In muscle tissue, the highest change (%) when compared to

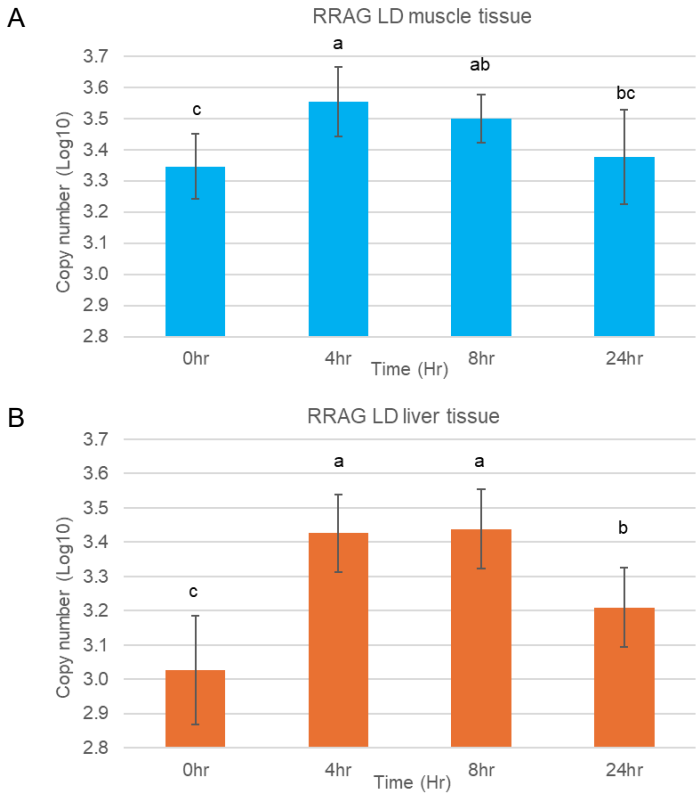


Figure 2.17 RRAG within-tissue variability in the LD diet at 4 timepoints. Statistical analysis was performed using one-way ANOVA. Values are reported as means (copy number(Log_{10})/uL) ± standard deviation of the mean (*n*=6) with analysis conducted in triplicate (*n*=18). LD= leucine diet, 0hr= -2hr.

baseline values was 62% at 4 hr, compared to liver tissue, where a 190% increase above baseline was seen at 8 hr. When comparing increases between timepoints, a 183% change was seen between -2 hr and 4 hr post-prandial but only a 3% increase from 4 hr to 8 hr.

Fold differences in mRNA abundance in muscle tissue when compared to the -2 hr control were 1.06 (6%) at 4 hr, 1.04 (4.5%) at 8 hr and 1.01 (0.9%) at the 24 hr sampling point. Further exploration of fold differences between the time points were 1.06 (6%) -2 to 4 hr, 0.99 (-1.4%) at 4 to 8 hr and 0.97 (-3.4%) for the 8 to 24 hr point. FCs in liver versus the control -2 hr point were 1.13 (13.2%) at 4 hr, 1.14 (13.5%) at 8 hr and 1.06 (5.9%) at the 24 hr sampling point. FCs between the timepoints were 1.13 (13.2%) between -2 to 4 hr, 1.00 (0.3%) between 4 to 8 hr and 0.93 (-6.7%) between the 8 to 24 hr times.

Between tissue trends appeared to be similar, with both tissue mRNA abundance increasing after feeding. In muscle tissue, the peak abundance appeared to be at 4 hr before gradually returning close to -2 hr levels at 24 hr. Comparatively in liver tissue, peak abundance seemed to be at 8 hr, before returning closely back to 24 hr. It is worth noting that the 24 hr point had significantly higher abundance (5.9%) than the -2 hr point.

In Myostat 1a, differences were observed in the muscle tissue (p=0.002) using one-way ANOVA, with Fisher's *post-hoc* analysis identifying that the 4 hr and 8 hr timepoints were significantly higher than the -2 hr and 24 hr (Figure 2.19 A). In liver tissue, very low mRNA copy numbers were obtained but significance was noted (p=0.004) with *post-hoc* analysis indicating the difference at the 24 hr timepoint (Figure 2.19 B).

Abundance of mRNA copy numbers in liver tissue was lower than in muscle tissue, with the highest concentration of 19 ±10/ µL at 4 hr and the lowest observable concentration of 4 ±3/ µL at 24 hr post-prandial. The highest change (%) compared to -2 hr was a 46% increase at 4 hr. Muscle appeared to follow a similar trend, with peak abundance of 845 ±354/ µL at 8 hr and the lowest abundance of 349 ±174/ µL at 24 hr post-prandial. The highest change (%) when

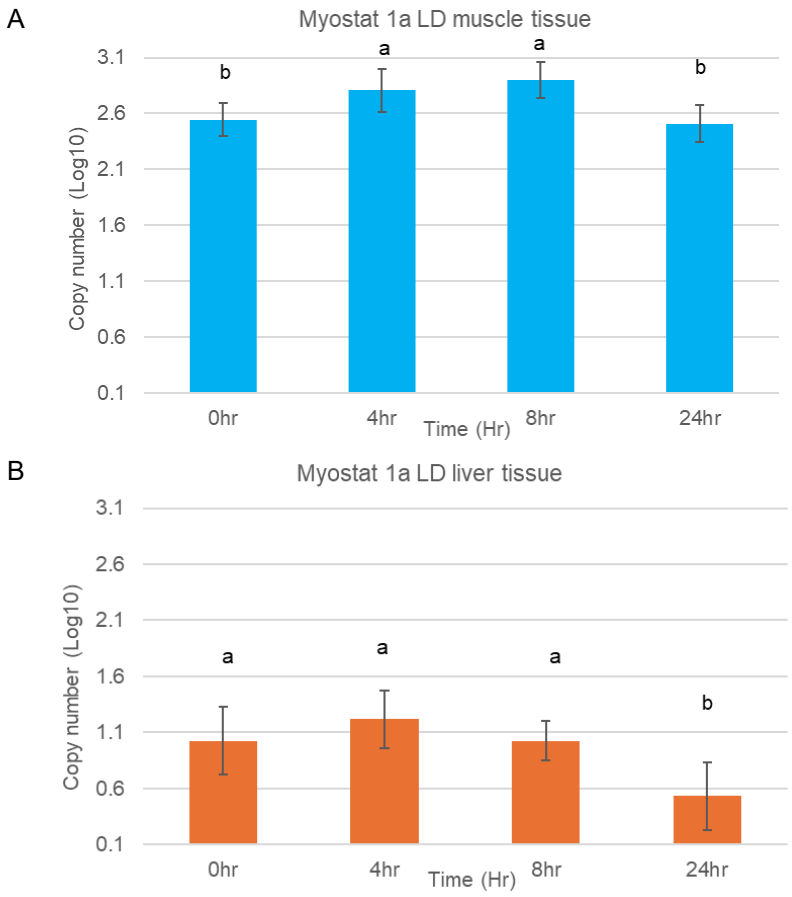


Figure 2.18 Myostat 1a within-tissue variability in A) muscle B) liver in the LD diet at 4 timepoints. Statistical analysis was performed using one-way ANOVA. Values are reported as means (copy number(Log_{10})/uL) ± standard deviation of the mean (*n*=6) with analysis conducted in triplicate (*n*=18). LD= leucine diet, 0hr= -2hr.

compared to -2 hr abundance was 128% at 8 hr, whilst the highest increase between times was an 88% increase from -2 hr to 4 hr.

FCs in comparison to the -2 hr control were 1.10 (10.2%) at 4 hr, 1.14 (13.7%) at 8 hr and 0.98 (-1.6%) for the 24 hr point. FCs between timepoints were 1.10 (10.2%) between -2 to 4 hr, 1.03 (3.2%) between 4 to 8 hr and 0.87 (-13.4%) between the 8 to 24 hr points. FCs in liver tissue in comparison to the -2 hr control were 1.18 (18.4%) at 4 hr, 1.00 (0%) at 8 hr and 0.51 (-48.5%) at the 24 hr point. Between timepoint FCs were 1.18 (18.4%) between -2 to 4 hr, 0.84 (-15.6%) between 4 to 8 hr and 0.51 (-48.5%) between the 8 to 24 hr sampling points.

MYO 6 (Myosin 6) initial sample analysis consisted of -2 hr and 24 hr points in both liver and muscle tissues (Figure 2.20 A, B). No differences were observed in muscle tissue (*p*=0.860), but a difference was noted in liver tissue (*p*=0.005), with Fisher's *post-hoc* analysis identifying the 24 hr point as being significantly

higher than the -2 hr point. mRNA abundance in the muscle tissue was lower than in the liver tissue, with the muscle -2 hr point having an abundance of 55 ±18/ µL and a similar result for 24 hr at 57 ±39/ µL. Abundance in liver tissue was noticeably higher, with a high of 886 ±212/ µL at 24 hr and 440 ±156/ µL at -2 hr.

Similarly to BCKDK, a small number of samples from 8 hr were analysed (Figure 2.20 C). In muscle tissue, the 8 hr mRNA yield was 40 ±32/ µL whereas in liver tissue, the yield was considerably higher at 512 ±80/ µL.

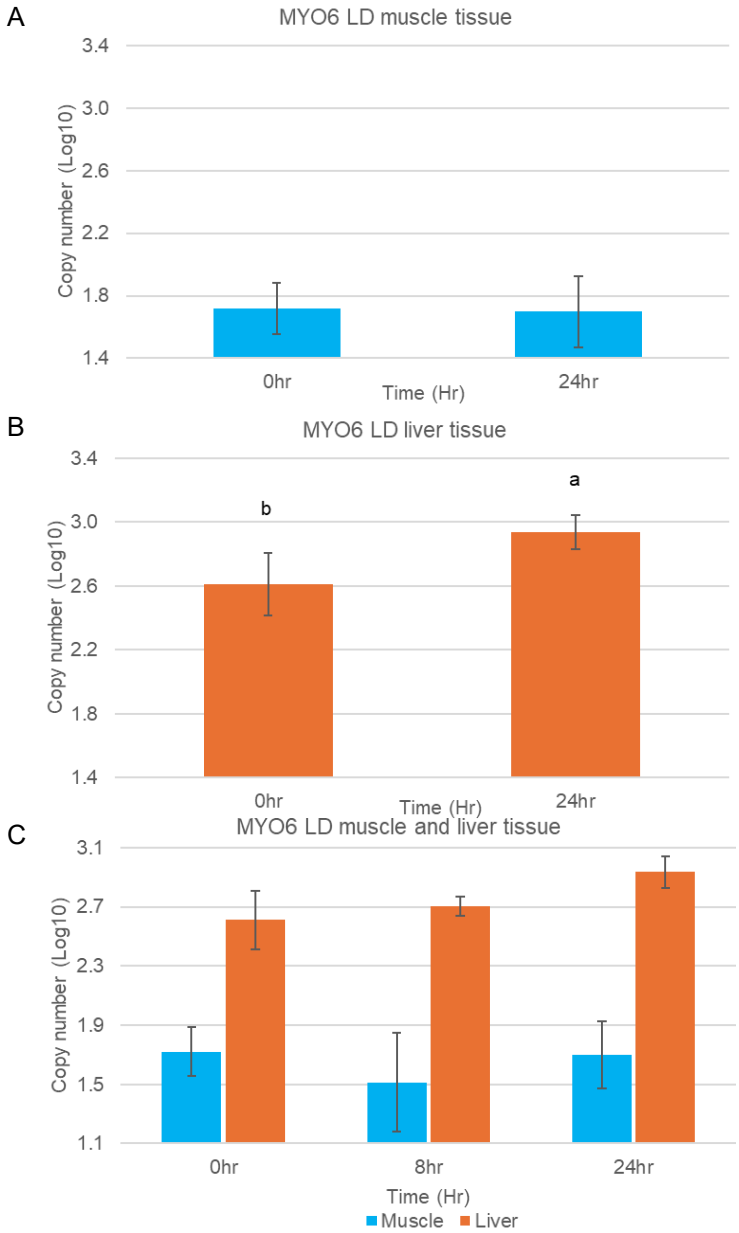


Figure 2.19 MYO6 within-tissue variability in A) muscle B) liver tissue in the LD diet at 2 timepoints C) Combined tissues including the 8 hr timepoint. Statistical analysis was performed using one-way ANOVA. Values are reported as means (copy number/(Log_{10})/uL) ± standard deviation of the mean (*n*=6) with analysis conducted in triplicate. LD= leucine diet, 0hr= -2hr.

In Figure 2.21 (A, B) to visually identify trends in relation to plasma leucine uptake, LD plasma leucine was superimposed on the temporal mTOR mRNA abundance of muscle (A) and liver (B) tissues.

No temporal differences within each tissue were observed for SESN1 but opposing mRNA abundance trends were observed between tissues. In muscle tissue, peak mRNA abundance occurred at 24 hr (640 ±254 /µL) with the lowest mRNA abundance observed at -2 hr (392 ±143 /µL) whereas in liver tissue peak abundance occurred at -2 hr (609 ±511/ µL) and the lowest mRNA abundance was at 24 hr (206 ±31 /µL). This opposing trend may signal a tissue-specific mRNA response to plasma leucine.

Temporal RRAG A within tissue mRNA abundance trends were comparable to plasma leucine, with the muscle 4 hr timepoint significantly higher (p=<0.05) than the -2 and 24 hr timepoints. Liver tissue had a similar trend although 4 and 8 hr were significantly higher (p=<0.05) than 24 hr, while the -2 hr timepoint was significantly lower than all the other timepoints.

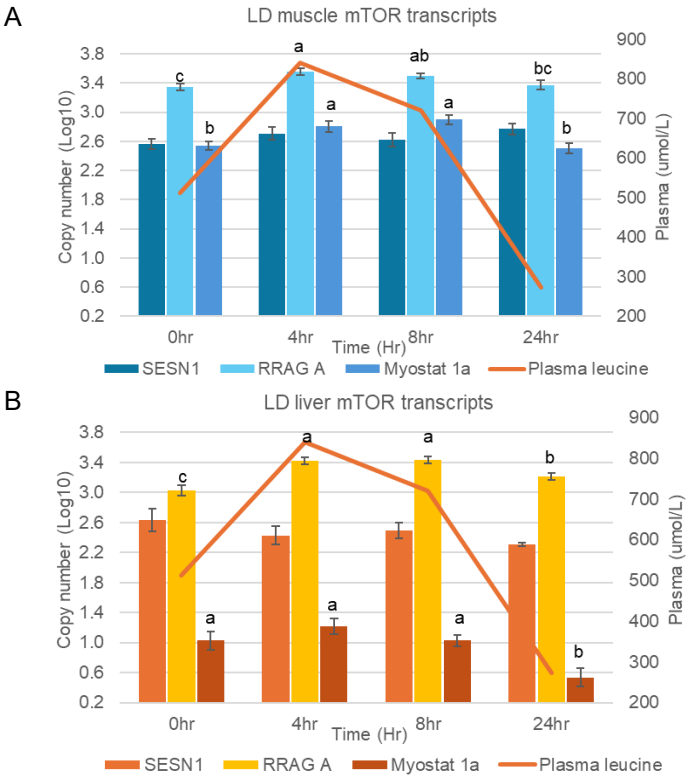


Figure 2.20 Plasma leucine and the mTOR pathway mRNA transcripts in A) muscle B) liver tissues. Statistical analysis was performed using one-way ANOVA. Values are reported as means (copy number(Log_{10})/uL) ± standard deviation of the mean (n=6) with analysis conducted in triplicate (n=18). LD= leucine diet, 0 hr= -2 hr.

Between tissue differences occurred with the lowest significant mRNA abundance (p=<0.05) at -2 hr for both muscle (2279 ±534/ µL) and liver tissue (980 ±564/ µL) while peak mRNA abundance occurred at 4 hr in muscle (3684 ±882/ µL) and 8 hr in liver (2841 ±809/ µL). This suggested a non-tissue specific response to plasma leucine. Both tissues had the lowest response at -2 hr, suggesting it responded to leucine, but did not reduce at 24 hr as much as plasma, but stayed higher than -2 hr.

Myostat 1a within-tissue temporal mRNA abundance occurred, although trends were similar to plasma leucine, with the 4 and 8 hr timepoints significantly higher (p=<0.05) than the -2 and 24 hr timepoints in muscle tissue, whereas the 24 hr timepoint was significantly lower (p=<0.05) than the other 3 timepoints in liver. mRNA abundance between the tissues pinpointed peaks at 8 hr in muscle (845 ±354/ µL) and 4 hr in liver (19 ±10/ µL), with the lowest mRNA abundance at 24 hr in muscle (349 ±174/ µL) as well as liver (4 ±3/ µL). This suggested a tissue specific response to plasma leucine, with a higher mRNA abundance in muscle than liver tissue.

2.4 Discussion

The hypothesis for the first section of this trial was that the actual dietary source of the BCAAs would not affect their uptake in salmon. The primary focus was on the digestibility of intact proteins in comparison to substitution with cAAs and secondly, digestibility differences between the cBCAA diets.

2.4.1 Digestibility, nutrient sources and feed intake

Digestibility is a useful tool to determine the proportion of nutrients an animal can absorb from the feed, and the more digestible a feed is, the more accessible nutrients are for absorption, but some factors can affect the digestibility of feeds and need to be considered (Chojnacka et al., 2021).

The ever-increasing pressure to relieve the demands on fishmeal production, and produce feeds that are sustainable and cost effective, has increased the requirement for use of alternative protein sources in feed production across board

(Xing et al., 2024). Although mostly cheaper than fishmeal, this has inadvertently led to other obstacles such as ANFs, incomplete AA profiles, ethical conflicts *etc*. (Hussain et al., 2024). There have been many studies using alternative protein sources to determine the required profiles needed for fish, and formulating feeds has led to supplementation with fAAs.

There are divided opinions as to whether the inclusion of intact proteins and peptides are different to fAA supplementation and the effect of these, with some studies such as Espe & Lied (1994), showing that replacement of 20-30% of intact proteins with cAAs resulted in high protein synthesis.

Intestinal microbial activity may also impact digestion, especially when fed new feeds, as research has outlined the importance of the microbiome on digestion and overall fish health (Gómez & Balcázar, 2008). Navarrete et al. (2013) studying the impacts of soybean meal on Atlantic salmon, concluded that diet affected bacterial groups and similarly Green et al. (2013) looking at soybean protein concentrate (SPC) found that SPC caused intestinal disorders by changing the microbiome.

Fish in this trial were fed the experimental feeds for a minimum of a week. Studies have indicated that microbiome changes can occur within 24 hr in southern catfish (*Silurus meridionalis*) to months in Atlantic salmon (Zarkasi et al., 2016; Zhang et al., 2017). Although no distinct differences in digestibility between the intact and cAAs diets was seen, perhaps with a longer period on the feeds this result may be different.

Apparent Digestibility Coefficients (DADCs) were used to identify the nutrient availability across the test diets and determine if there were any differences between the intact proteins and the BCAA supplemented diets. Although overall, CAS diet had the highest digestibility values, ranging from 98% to 80% (histidine, glutamate, and energy), there were differences in each parameter, with no distinguishable separation between intact proteins and BCAA supplemented diets. CAS as an ingredient, is known as a slow digestible protein in comparison to whey and has revealed to have 95-100% digestibility in various species such as salmonids and Penaid shrimp (*Penaeus vannamei*) (Jobling, 2012).

Li et al. (2021) suggested that in fish, dietary fAAs were up to 100% digestible, animal proteins up to 93% and plant proteins up to 85%. The digestibility of the AAs varied between the intact protein and BCAA feeds, with differences observed in leucine, isoleucine, arginine, histidine, threonine, glutamate, proline and near significance ($p \leq 0.10$) in digestibility for glycine and valine.

Literature has varying views on the efficiency of cAAs compared to intact/whole protein diets. Ambardekar et al. (2009) inferred that peak absorption rates varied between intact proteins and purified AAs in their study of channel catfish (*Ictalurus punctatus*). Nunes et al. (2014) suggested that cAAs may be absorbed too quickly resulting in lower growth rates in various species, whereas other studies showed that peptides absorption rates were quicker compared to cAAs. Zhang et al. (2006) fed juvenile carp AAs as fAA, peptides or whole protein diets, concluded that fAAs and peptide diets resulted in reduced WB fAAs, and could not meet the requirements for growth. Conversely, Lin et al. (2024) found no difference in carp muscle growth between coated AAs or cAAs dietary supplementation.

In summary, digestibility of cAAs and intact proteins across literature had varying results, with some suggestions of species-specific results. In the current study, DADCs suggested variability between parameters regardless of source.

Significant differences in FI were observed between intact and cBCAA diets, with WHE the overall highest FI and ID the lowest across the diets. Variability in FI was observed in week-1, LD had the highest FI while SPC the lowest, whereas in week-2 and 3, WHE had the highest intake while ID had the lowest in week-2 and CD the lowest in week-3. FI across the cBCAA diets was similarly variable, with week-1 highest FI in the LD while for week-2 and 3 VD had the highest FI between the cBCAA diets. Initially, the concept of palatability was explored, with WHE overall FI higher than all other diets and the ID lowest.

This suggested that ID diet was possibly less palatable than the WHE diet. But when compared to the other cBCAA diets, variability also occurred over the 3 sampling points between the highest FI diets. This variability in intake may have been due to individual biological reactions to stressors, as fish were pooled and

assigned new tanks after every weekly sampling point rather than potential palatability issues.

2.4.2 Plasma

2.4.2.1 BCAAs

Plasma BCAA concentrations indicated that the additional cBCAAs were effectively absorbed into the plasma in fish fed the BCAA diets, and within each diet including the CD, peak uptake was different over time. All the diets had temporal differences within each diet over time, and between each diet at each time point, apart from leucine at -2 and 8 hr.

Across the diets at each timepoint displayed differences for both isoleucine and valine, with leucine having no differences at -2 and 8 hr between diets. The leucine change (%) when compared to the CD at -2 hr pre-feeding had very little change between the BCAA diets and the CD diet, although a slightly negative change was observed ranging from 1% to 5% lower than CD. Although not significantly different, at the 8 hr point leucine in the VD diet was 12% lower than CD compared to both ID and LD having a 15-16% change above CD levels. This may indicate an effect of valine on leucine uptake. Rolland et al. (2016) studying methionine postprandial EAA levels in rainbow trout, demonstrated the effect of the individual BCAAs on their plasma concentrations suggested that isoleucine and valine may affect leucine. This may be due to the BCAAs sharing enzymes for the initial two steps of catabolism and sharing membrane transport systems. Their model supported the theories that the BCAA influence kinetics and requirements of each other. Additionally, their findings also indicated a linear relationship between the BCAAs and that manipulation of one AA, in their case methionine, especially in the crystalline form, may impact other plasma AA profiles.

For leucine, all diets had significantly higher -2 hr concentrations than 24 hr, this trend was also seen for valine in VD diet. Other studies have shown that AAs differences at the 24 hr peak may be due to a slower absorption and digestion either due to protein break down or absorption competition such as Tantikitti & March, (1995) in rainbow trout had post-prandial peaks for some AAs between 3

to 12 hr followed by further peaks at 36 hr for the same AAs. In the current trial, higher leucine concentrations were observed at the pre-feeding stages compared to 24 hr postprandial, which may have been an effect of starvation or slow absorption as suggested by Tantikitti & March, (1995). Rønnestad et al. (2000) in a study using post-larval Senegalese Sole (*Solea senegalensis*), found that fAAs were absorbed 3.5 times faster from gut to tissues than intact proteins. Cowey & Walton (1988) studying the differences in absorption of intact proteins and fAAs in rainbow trout (*Oncorhynchus mykiss*) feeds, found that with intact proteins peak uptake was seen at 16 hr postprandial.

LD diet had reduced levels of isoleucine and valine, with ranges for isoleucine 11-28% and valine 6-22% lower than CD over the five timepoints. Morales et al. (2012) suggested that excess leucine limited valine availability in pigs whereas Mai et al. (2022) stated a negative effect of leucine on both valine and isoleucine. Wang et al. (2023) in their study of imbalanced inclusion levels of each BCAA in feeds on turbot (*Scophthalmus maximus*), had differences in each diet, where individual BCAAs were included at excess levels when compared to their control diet. But within each diet, there did not appear to be an effect of the excess BCAA on the other two in plasma, muscle, and liver concentrations. In contrast, plasma in the current trial did appear to be affected by the individual BCAAs on post-smolt Atlantic salmon.

The preferential uptake of leucine and subsequent lower uptake of isoleucine and valine in the LD may be due to the BCAAs sharing a common transporter at the initial intestinal absorption site (Mai et al., 2022). In a study observing interactions of BCAAs in pigs, Langer et al. (2000) had opposing opinions in that the lower observed values of valine and isoleucine in plasma did not imply leucine inhibition or an effect of absorption or transport.

Abumrad et al. (1985) exploring the effects of BCAAs and BCKAs in humans, administered IV infusions of leucine into human forearms resulting in similar lower responses of valine and isoleucine. It is worth pointing out that the study used whole blood rather than plasma, and although blood consists of an average 55% plasma, AA concentrations are generally higher across board in blood than

plasma, although trends are similar. Langer et al. (2000) suggested that if there were tissue uptake conflictions, then the circulating plasma levels of valine and isoleucine should increase and not decrease. In the current study, the LD when compared to the CD did have lower concentrations and a decreased change (%) for isoleucine and valine over the five timepoints. Interestingly, inverse trends were seen in the ID diet, with leucine and valine concentrations and change (%) higher than the CD diet. VD followed a different trend, whereby leucine and isoleucine levels dropped below CD between 8 to 24 hr.

The ID had higher plasma concentrations compared to the CD for the fBCAAs over time. The change (%) over time compared to the CD showed increased levels of isoleucine of 273% at 4 hr post-prandial and maintained an increase above CD over all timepoints, indicating an increase over and above the CD levels. At -2 hr, isoleucine was 69% above CD levels and 84% at 24 hr indicating it did not return to base levels as expected. Leucine and valine ranged from 11 to 28% in leucine and 1 to 16% in valine, with valine peaking at 4 hr before returning to base levels at 24 hr. Leucine had a similar trend although it did not return to base levels at 24 hr. These trends were comparable to Tantikitti & March (1995) who found that in rainbow trout (*Oncorhynchus mykiss*) additional dietary supplementation of free isoleucine also increased leucine and valine plasma concentrations. They theorised that the elevated levels over time could have been due to enzymatic competition. The current results indicating elevated isoleucine and the incomplete return of leucine to CD baseline levels suggested a possible metabolic interaction among the BCAAs.

When looking at the digestibility of isoleucine between the crystalline and intact protein diets, the ID diet was significant (p=0.028). Although not different to the CD diet, it did have a higher digestibility compared to the CD (0.95 ±0.01, 0.91 ±0.04). In addition to enzymatic competition/ metabolic interactions, the increased digestibility may have contributed to the increase (%) above CD levels.

Valine in the VD had an increase of 97% at -2 hr, when compared to CD diet. Highest change (%) of 201% was at 4 hr, with the lowest increase above CD, of 37% seen at 24 hr. When looking at the digestibility of valine in VD, it was lower

than CD (0.84 ±0.01, 0.90 ±0.04) although no differences between intact and crystalline diets were seen (p=0.076). Observing the change (%) of leucine in the VD diet, valine appeared to influence leucine and isoleucine uptake, with a 12 to 19% decrease below CD levels for leucine and 16 to 20% decrease for isoleucine between 8 and 24 hr. This could indicate uptake of leucine and isoleucine between these times. The elevated concentrations of valine at 8 hr and 24 hr may be indicative of flooding, competition at the carrier sites or the possible effect of a slowed rate of intact protein absorption as discussed previously by. This is less likely due to the formulation of the CD including intact proteins compared to the addition of cAAs in the BCAA diets. Valine and isoleucine levels in the LD diet were continuously below the CD baseline over all the timepoints, with leucine dropping below CD levels at -2 and 24 hr. Wiltafsky et al. (2010) suggested that in pig serum, high leucine diets reduced valine serum concentrations and to mitigate this, additional supplementation of valine was required.

In Figure 2.5, the graphs depicted the plasma fBCAA change (%) from the CD, suggesting a preferential uptake amongst the plasma BCAAs. When formulating the feeds, each BCAA was included at 2% above the CD basal levels, with formulated cBCAA dietary contributions previously. Analysed feed bAAs for the CD returned results for leucine at 4.9 g/100g (49 g/kg), isoleucine 2.5 g/100g (25 g/kg) and valine 2.7 g/100g (27 g/kg). Leucine in the LD diet was 42% higher than CD at 7.0g/100g (70g/kg), isoleucine in the ID diet was 69% higher than CD at 4.2g/100g (42 g/kg) and valine in the VD diet was 67% higher than CD levels at 4.5 g/100g (45 g/kg).

The increases/decreases (%) seen in plasma BCAA uptake in the LD at the 4 hr peak was comparable to bAA feed results for leucine possibly a reflection of the differences between the formulated AA and bAAs in the feeds. Isoleucine in the ID at the 4 hr peak was >250% higher than CD levels, and remained elevated over 24 hr. If the isoleucine bAAs in the ID were only 69% higher than the CD then the plasma >250 change (%) compared to the CD may indicate the rapid cAA uptake compared to the intact proteins in the CD. Similarly for valine in the VD, the 4 hr peak was ±200% higher than CD, and remained above CD levels at 24 hr.

The elevated levels of isoleucine and valine in the ID and VD diets over the 24 hr compared to CD may be combination of multiple factors. Factors such as a continual uptake of cAAs/ intact proteins in the GIT, possible transporter preferences/ competition, differential uptake times between cAAs/ intact proteins due to digestion, possible inter-tissue flux with isoleucine and valine being transported between tissues and metabolic processes.

In summary, temporal plasma BCAA variations occurred within each diet and between diets at each timepoint. Although formulated dietary BCAAs were included at an additional 2% /diet, the overall contributions were different. The extent of the effects of the contributions to the plasma BCAA uptake differences compared to the CD are estimated but may required more research. These findings reveal the complexity of BCAA metabolism and the necessity to understand these dynamics in Atlantic salmon with regards to feed optimisation.

2.4.2.2 All AAs

Temporal differences occurred within each diet for EAAs and NEAAs whereas comparative uptake between diets at each time was relatively stable. Differences in plasma peak values have been reported suggesting an effect of intact proteins as well as temperature on uptake times. Vikeså et al. (2015) had peak total plasma concentrations in Atlantic salmon at 8 hr post-prandial at 13 °C whereas at 19 °C the peak was 4 to 8 hr post-prandial. Schuhmacher et al. (1997) have shown peak plasma concentrations in salmonids at 6 hr post-prandial while Walton & Wilson (1986) in a study containing casein, witnessed plasma uptake starting 2 hr post-prandial with a peak at 12 hr. Interestingly their study showed that NEAA plasma concentrations returned to baseline at 24 hr and EAA at 48 hr. Glycine and alanine were the only two NEAAs in the current study who may follow this trend as their 24 hr concentrations where higher than their starting concentration before feeding (alanine, aspartate, and glutamate metabolism pathway).These studies provided insights into the variability of post-prandial fAA dynamics and the factors influencing them, highlighting the difficulties in trying to understand AA metabolism.

While in this study, most plasma fAAs had peaks at 4 hr, with some exceptions at 2 hr and 8 hr. Some studies have suggested an increased starvation period of 48 hr pre-feeding to eliminate possibility of lag phase or late plasma peaks. Tantikitti & March (1995) had post-prandial peaks for AAs between 3 to 12 hr followed by further peaks at 36 hr for the same AAs in rainbow trout. The difficulties with an increased starvation period is that results may be influenced by factors such as starvation or stress, with possible metabolic adaptions such as proteolysis or other mechanisms employed to maintain cellular homeostasis (Holeček, 2020).

In the current study, fAAs that displayed differences at the 24 hr peak may have additionally been due to slower absorption and digestion either due to protein break down or absorption competition. Sveier et al. (1999) studying gastric evacuation times in Atlantic salmon, estimated that at 7.1 ±0.3 °C times varied from 10.8 to 14.8 hr to evacuate 50% of the faeces. This suggested a possibility of continuous absorption after 14.8 hr, although their times may have been influenced by the water temperature.

Studying the effects of low methionine availability in juvenile Atlantic salmon, Espe et al. (2016) suggested an effect on plasma, with levels of lysine, leucine, isoleucine, valine, and proline elevated in the low methionine diet. This disruption could possibly be due to competition for transport via the L-system or BCKDH competition (Babu et al., 2003). Langer et al. (2000) found that excess leucine did not affect methionine in pigs, but it did reduce the plasma concentration of isoleucine and valine significantly. This effect of leucine on plasma isoleucine and valine was comparable to the current findings.

Abumrad et al. (1985) found that humans after 3 hr of being administered with IV doses of KIC (α-Ketoisocaproic acid) had significantly lower whole blood results for threonine, glycine, glutamine, alanine, tyrosine, valine and isoleucine. Although in the current study leucine was analysed rather than KIC, as a leucine metabolite involved in synthesis and degradation, a comparative assumption was made in that it would be present. In this sense, an estimated 20% of leucine is converted to KIC and β-hydroxy-β-methylbutyrate (HMB) (Duan et al., 2016). In

addition, Lee et al. (2015) looking at ^{14}C-leucine metabolism in rats, found that ^{14}C-KIC first appeared in plasma 1hr post dosing. Their study also showed that in plasma 2 to 24 hr post dosing, the ^{14}C found was already in plasma protein form. An additional noteworthy result of their study was that they discovered two new leucine products, inferring additional metabolism pathways.

All BCAA diets had significantly higher plasma -2 hr glutamate levels compared to the post-prandial concentrations. This may have been an effect of synthesis/degradation, with the liver involved in glutamate synthesis as discussed by Holecek (2013), although this study did not detect any glutamate differences in fAA or bAA liver tissue in the LD diet. Abumrad & Miller (1983) suggested that 70% of the AAs released by muscle tissue are alanine and glutamine, even though they form 15% of muscle tissue. White et al. (2020) stated that inhibiting BCAT enzymes reduced plasma alanine and increased glycine levels in rats. In the current study, at -2 hr, LD plasma alanine concentrations were 24% lower than CD, glycine levels were 17% lower than CD levels, but inversely glutamate was 78% higher than CD levels.

Plasma temporal differences were noted across all diets for arginine, and similarly for lysine apart from near significance ($p \leq 0.10$) in the ID diet. Temporal differences in arginine followed similar trends for all diets, with peak concentrations from 2 to 8 hr postprandial, and similarly different lower baseline levels at -2 hr and 24 hr. Similarly, lysine in the LD and ID diets had peak uptake concentrations 2 to 8 hr postprandial, although ID had near significance. CD and VD diets had slightly delayed uptake with peaks in CD at 8 hr and VD 4 to 8 hr. Lysine and arginine share transport systems and therefore possible competition for cellular uptake between the two EAAs exist (Cynober, 2002). Although in this study that was not noticeable, Berge et al. (1999) did suggest, in Atlantic salmon that the effects of lysine either to inhibit or to stimulate arginine, depended on concentration, adversely, arginine inhibited lysine regardless of concentration.

Variation in plasma concentrations may also have been an effect of stress, due to sampling, handling, noise, movement *etc*. over the 24 hr period (Fazio et al., 2015). Cortisol may impact metabolic effects in nutrients in fish as discussed by

Van Der Boon et al. (1991). Elevated levels of individual plasma AAs over time could be an indication of enzymes flooded with substrate, slowing down the catabolic processes and thereby resulting in high concentrations for longer periods (Barroso et al., 1999).

When comparing the 2% inclusion levels in the feed of each BCAA, to plasma change (%) compared to CD levels, it is worth taking note that although each BCAA was include at 2% above CD levels, the increase (%) above CD levels of the 2% inclusion was different for each of the BCAAs (leucine 42%, isoleucine 69%, valine 67%). This may explain some of the plasma variations of the BCAAs when compared to the CD, with 4 hr peak change (%) compared to CD for leucine 68%, isoleucine 273%, and valine 201%. If plasma proteins were made 2 to 24 hr after feeding as suggested by Lee et al. (2015), then this effect should be unanimous between diets or potentially reduced as one would expect the CD diet to have similar results.

In summary, plasma EAAs and NEAAs across the diets at each timepoint were stable for the majority of the EAAs, but differences in uptake were observed within each diet over the 5 timepoints. These findings have agreed with studies and have demonstrated the difficulties of influencing factors such as dietary composition, metabolic interactions, and physiological factors when studying AA metabolism in aquaculture species.

2.4.3 Tissue

2.4.3.1 BCAAs

Muscle tissue from the LD diet had differences in fAAs for leucine, isoleucine, glutamate and lysine over time (p=<0.05). The lowest different concentrations in leucine and isoleucine were identified at the 24 hr post-prandial sampling point compared to the other 4 timepoints. This trend was similar to observations in plasma, with the -2 hr concentrations higher than the 24 hr points. Interestingly, the pre-feeding sampling point was higher than the 24 hr point even though fish were starved for 24 hr before feeding.

The reduced concentrations of leucine and isoleucine at 24 hr may indicate oxidation as muscle tissue is the main site of BCAA catabolism/ oxidation

(Milligan, 1997). Although there are naturally occurring tissue variations of fAAs, experimental design consisting of varying temporal testing timepoints should identify baseline levels.

Chabot et al. (2016) stated that depending on meal size and water temperature, metabolism in fish may be elevated up to 48 hr post-prandial. Perhaps a similar study to Lee et al. (2015) using ^{14}C-L-leucine is required to study temporal effects over a 48 hr period, although this may highlight possible mechanisms in the postabsorptive state rather than post-prandial.

In the current study, levels of free leucine were statistically higher in all the timepoints assessed apart from the 24 hr postprandial timepoint which was significantly lower (p=<0.05). Espe et al. (2021) found that free leucine in the liver and muscle of Atlantic salmon was not affected by dietary leucine 24 hr postprandial. It would be interesting if in future, the study conducted by Espe et al. (2021) was repeated with additional timepoints up to 24 hr and potential continuing to 48 hr. Interestingly, when stressing the fish, muscle concentrations of free valine and isoleucine were higher than in the unstressed fish 24 hr postprandial (Espe et al., 2021).

Vikeså et al. (2015) fed a commercial diet, found that at 13 °C, both leucine and isoleucine had peaks in Atlantic salmon post-smolt muscle fAAs at 12 hr (BW 101 ± 2.1 g). Additionally, in the same study using larger fish (3.68 ±0.19 kg) and sampling from 4 hr pre-feeding to 6 hr post-feeding, they found that pre-feeding leucine levels were similar to post feeding levels apart from a significant drop at 4 hr post-feeding. Their study highlighted the importance of temperature on uptake, but unfortunately, the study did not sample 24 hr postprandial in the larger fish. If it had, it would support the trends witnessed in this trial, and neither did it sample the pre-feeding to 2 hr postprandial stages in the smaller fish.

In the LD liver tissue, no differences were seen across the fBCAAs, but differences were seen in arginine and taurine. Arginine saw the lowest different concentration at -2 hr compared to 4, 8 and 24 hr whereas taurine had the largest concentration at -2 hr, followed by 2 hr, with the lowest concentrations between 4 to 24 hr. Mente et al. (2003) in a study of muscle fAAs in Atlantic salmon fed

various levels of maize gluten, found that arginine in the control group had the highest concentrations in muscle followed by glycine (15.87 ±0.50 μmol/ g, 10.54 ±0.76 μmol/ g). In this current study, the LD liver arginine ranged from 0.37-0.79 μmol/g compared to muscle tissue, which ranged from 0.32 to 0.59 μmol/ g. When comparing the AA composition of their feeds to this study, the difference (%) of inclusion levels was 116% in arginine and 100% different in glycine. This may explain the differences in concentrations between the two studies.

Teodósio et al. (2022) in a study on metabolic fate in gilthead seabream using a ^{14}C-methionine tracer found that methionine was preferentially deposited in muscle tissue and potentially used for growth. In LD muscle tissue, near significance ($p \leq 0.10$) was seen in valine, tyrosine and methionine, with valine and methionine trends different to the seabream study of Mente et al. (2021). The highest peak for valine was at 2 hr, although -2 to 4 hr concentrations ranged from 0.36 to 0.39 μmol/ g before dropping down to the lowest concentration at 24 hr. Methionine had a similar trend to leucine and isoleucine, with little variation between times, apart from a noticeably lower concentration at 24 hr. Carter et al. (2000) in a study observing the fAA changes in Atlantic salmon after a reduced feed ration, had higher concentrations of methionine in muscle tissue than isoleucine, leucine, lysine, phenylalanine, and tryptophan. In the current study this was not the case in the LD, all fAAs had higher concentrations than methionine apart from lysine.

Unlike plasma and the molecular studies, all fAA analysis on tissue was performed on pools and not individual fish. An example of individual variation is nicely demonstrated by Řehulka & Minařík (2016) in a long-term study (86 days) looking at plasma AAs and BCAA temporal dynamics in rainbow trout at 0, 22, 56 and 86 days. They had a plasma variation from 131-855 μmol/L for leucine, 31-393 μmol/ L in isoleucine and 187 to 1209 μmol/ L in valine. Their study demonstrated some of the difficulties encountered in the current study, with large individual variation possibly masking biological effects.

In summary, fAA concentrations in muscle and liver tissues exhibited post-prandial temporal dynamics not in agreement with other studies. These may have

been influenced by factors such as feeding status and diet. Observed variations in the fBCAAs and other AAs underscore the complexity of AA metabolism in fish and the importance of time-course studies. Inter-individual variability in AA levels should also be considered in future studies.

2.4.3.2 All AAs

Glutamate and lysine had similar trends, whereby concentrations were lowest at 4 hr, a slight increase at 8 hr, and a decrease again at 24 hr. Mente et al. (2021) in a study on seabream, showed significant peak lysine concentrations at 8 hr, while the 24 hr concentrations were higher than the pre-feeding point. This may be due to leucine and lysine sharing sodium carriers, both dependant and independent, as suggested by Munck and Munck (1992) in a study on rabbit intestine. Ling et al. (2023) supported the theory that BCAAs share L-type amino acid transporter (LATs), and in cells glutamine can be exchanged for extracellular leucine via LAT1 transporters.

Cleveland and Radler (2019) concluded that excess leucine and phenylalanine added to media did lower rates of proteolysis in rainbow trout myocytes, while excess valine and lysine in comparison to other EAAs, increased protein degradation. Cleveland & Radler (2019) did suggest that formulating diets with the correct AA profile using intact proteins and supplementing with BCAAs and lysine may provide an optimal AA profile over a longer period post-prandial. This may be an area to be studied further.

Total bAA in LD liver tissue did not have any significant temporal differences. bAAs in LD diet muscle tissue showed significant differences over time for lysine and tyrosine. Lysine peak concentrations were at 8 hr, while tyrosine had two peaks, one at 2 hr and one at 8 hr. Both had the lowest different concentration at 4 hr.

Feeds were formulated to lysine requirements as it is widely accepted as being the first limiting AA as well as an important part of protein (Hua, 2013). fAA lysine muscle concentrations in LD diet had highest concentrations at 2 hr and lowest at 4 hr, whereas bAA Lysine peak concentrations were at 8 hr and the lowest at 4 hr suggesting a possible regulation/ activation continuation/ link.

In summary, several findings and key insights into post-prandial AA dynamics, their implications and the factors influencing their uptake such as dietary composition, AA interactions, AA imbalances, oxidation of the excess AAs and time were explored.

2.4.4 Molecular studies

In this study, BCAA metabolism and mTOR pathway mRNA transcripts were explored by RT-qPCR. In mammals, leucine availability has been shown to be involved in regulation (feed intake and energy) through sensing mechanisms such as BCAA metabolism, glutamine metabolism, mTOR and the general control non-depressible 2 (GCN2) kinase nutrient sensing pathway (Comesaña et al., 2021; Heeley et al., 2018; Morrison et al., 2007).

2.4.4.1 BCAA metabolism

It is widely accepted that in mammals BCAAs are primarily catabolised in the muscle, followed by secondary catabolism in the liver (Dimou et al., 2022). Past studies have shown that BCAT exists in mammals in two forms, BCAT1 (cytosolic) or BCAT2 (mitochondrial) (Go et al., 2022). When developing the primers for this study, the BCAT2 transcript could not be identified for Atlantic salmon. Databases do not seem to have it for other species either, although there is one instance of where it has been listed as found in Arctic charr (*Salvelinus alpinus*), although with further investigation it is BCAT1 cytosolic. To verify this, it was blasted against Atlantic salmon, and it came back as BCAT1.

In humans, the BCAT2 enzyme is mostly observed in muscle tissue, whereas BCAT1 is expressed in brain and immune cells (Hall et al., 1993). The BCATs act on the three BCAAs in a reversible first step of BCAA metabolism (Dimou et al., 2022). BCATs transfer nitrogen to a-KG producing glutamine and the branched chain keto acids (BCKA) and in reverse, with the BCAT enzymes transferring nitrogen from glutamate and the BCKAs to regenerate the BCAAs and a-KG (Sivanand & Vander Heiden, 2020).

In this study, BCAT1a had the highest mRNA abundance in LD muscle tissue when compared to LD liver tissue. Although no statistical temporal differences

were seen in muscle, mRNA differences did occur in liver (p=0.042), with -2 hr having a lower abundance of mRNA than 8 hr and 24 hr. Observation of trends in the FCs of BCAT1a mRNA transcripts compared to the -2 hr sampling control point, showed that peak change in muscle were at 4 hr postprandial with a gradual decline from 8 hr to 24 hr. The highest change in liver tissue was seen at 8 hr before decreasing at 24 hr.

Peak plasma leucine levels were observed at 2, 4 and 8 hr post-prandial with the 24 hr concentration significantly lower than the -2 hr pre-feeding level (p=<0.05). Temporal variation in mRNA abundance of BCAT1a in muscle tissue was seen. Although no differences were observed in abundance, this trend was comparable to plasma and muscle fAA concentrations, with the lowest leucine concentrations at 24 hr and the highest at 4 hr post-prandial.

In liver tissue, mRNA abundance was a fold lower than in muscle tissue and this observation was dissimilar to plasma and liver fAA trends. The observable high variation may be an indication of biological variation. White et al. (2016) explained that the transamination step activated by BCAT in rat muscle, transformed a-KG (a-ketoglutarate) into glutamate, then pyruvate and then alanine, with glycine converted to pyruvate.

In the current study, alanine plasma concentrations were significantly higher in LD and ID diets at 4 hr, and in ID diet at 8 hr compared to CD diet. Glycine had no differences across times between diets, but plasma glutamic acid had near significance ($p \leq 0.10$) for all diets across all the timepoints apart from 4 hr. Holeček (2020) suggested that alanine and glutamine although synthesised in muscle, are released back into circulation. In the current study, LD muscle glutamic acid was statistically different over time, with the highest peak at 2 hr and the lowest concentrations at 4 hr and 24 hr while glycine and alanine had no differences over time.

In LD liver tissue no temporal differences were observed for glutamic acid, glycine, and alanine. Holeček (2001) suggested that in the initial stages of starvation in humans, BCAA synthesis from BCKAs may be activated by glutamine or alanine.

Another theory from Holecek et al. (2001) was that during starvation in rats, inhibition of BCKDHA in the liver may also activate BCAA synthesis. In the current study, fish were starved for 24 hr before feeding, the elevated levels of the plasma BCAAs across all diets at -2 hr compared to 24 hr may have been to do an effect of starving. This effect was also mirrored in LD muscle tissue fAA, with leucine and isoleucine both exhibiting significantly lower 24 hr concentrations than -2 hr levels.

Sweatt et al. (2004) exploring pathway enzymes in mammalian organ tissues, found that BCATm protein located in muscle myofibrils but not liver. It was also suggested that BCATc protein occurred in cells that did not express BCKDH. On the assumption that mRNA abundance may lead to protein synthesis, albeit smaller volumes, their findings were in opposition to the study data, whereby BCAT1a and BCKDHA1a mRNA transcripts were quantified in both liver and muscle tissue. The results suggested that although BCAT1 mRNA was active in both tissues, the higher mRNA abundance in muscle tissue may indicate that first step BCAA catabolism took place in the muscle rather than the liver as discussed by (Walton & Cowey, 1982).

In mammals, branched-chain α-keto-acids (BCKA) are broken down in the second irreversible step of BCAA catabolism by mitochondrial branched-chain α-keto acid dehydrogenase (BCKDH) complex (Wiltafsky et al., 2010). The BCKDHA enzyme is the rate limiting enzyme involved in BCAA catabolism (Mann et al., 2021). Differences in BCKDH mRNA abundance were seen between and within the two tissues. Both tissues followed a similar trend, with the highest tissue specific abundance seen at 4 hr and 8 hr, and the 24 hr point returning to similar -2 hr baseline levels. Interestingly, muscle had the higher absolute abundance when compared to liver at -2 hr and 24 hr. The difference (%) in copy numbers between the tissues at -2 hr and 24 hr were 45% and 44%, while the lowest was at 8 hr (6%).

In a study on pigs, observing the interactions of BCAAs and their effects on methionine, Langer et al. (2000) found that BCKDH enzyme activity in both liver and muscle were significantly increased (p=<0.05) by either excess leucine or

BCAAs. From their findings, they theorised that excess leucine and therefore increased levels of BCKA especially KIC, led to subsequent lower concentrations of isoleucine and valine in plasma. By inhibiting BCKDK (BCKDH kinase) this increased BCKDHA activity by reducing phosphorylation. This theory may explain the reduced plasma levels of isoleucine and valine in LD diet. As well as BCKDHA, they also suggested interactions between the metabolism of methionine and the BCAAs through sharing transport via the L-system.

Aftring et al. (1986) looking at BCAA activation of BCKDHA in muscle tissue of rats, stated that BCKDHA enzymes were rapidly activated with excess leucine supply. The BCKDHA enzyme activity was initially activated 10 min after IV administration with 0.25 mmol/kg of leucine but had started decreasing by 20 min. This trend was observed in their plasma results, where elevated leucine concentrations decreased both valine and isoleucine concentrations.

Holeček (2001) looked at starvation effects on BCKDH in rat tissues, and they determined that an effect of long-term starvation (6 days) led to elevated BCKDH activity in muscle tissue. In the current study, fish were only starved for 24 hr but absolute copy numbers of mRNA BCKDH1a mRNA transcripts were higher in muscle tissue than in liver, but mRNA abundance is not a predictor of enzymic activity but rather a biomarker of regulation (Hoppe, 2012; Vogel & Marcotte, 2012).

Wang et al. (2023) documenting the effects of imbalanced BCAAs on Turbot (*Scophthalmus maximus*), found that the mRNA levels of BCAT2 in muscle and BCKDHA in liver, were up regulated when fed excessive dietary BCAAs. Although only the LD in the current study was analysed, tissue specific transcript differences were noted for BCAT1 and BCKDHA.

In this trial, the highest overall mRNA abundance of BCKDHA was seen in the muscle tissue compared to the liver tissue, but England et al. (1995) suggested that abundance of mRNA does not necessarily predict the translation levels of BCKDH protein. BCKDK is involved in regulating BCKDHA activity, and BCKDK protein has been shown in mice tissue to be increased by starvation or decrease due to elevated levels of BCAAs (Zhou et al., 2012).

Absolute quantification of BCKDK in exploratory samples at -2 hr and 24 hr were initially examined, while a further few samples at 8 hr were also examined. The highest mRNA abundance was seen in muscle tissue, with -2 hr lower than 8 to 24 hr. Although overall lower mRNA abundance was observed in liver tissue, it followed a similar trend to muscle. Similar results were obtained by Doering et al. (1998) with rat muscle tissue mRNA higher than liver. Interestingly, the authors did suggest that although the BCKDK mRNA was detectible in liver tissue, they could not identify the antigenic protein.

Overall muscle tissue had higher mRNA abundance than liver, but both tissues had lower transcript numbers at -2 hr. This could be due to the elevated circulating levels of plasma BCAAs at -2 hr, while inversely the increase of BCKDK mRNA transcripts at 24 hr may be due to the reduction in plasma BCAAs at 24 hr. Low BCKDK transcript numbers and little temporal variation, necessitated the decision to not continue further with BCKDK.

In order to visually identify mRNA abundance trends within the BCAA catabolism pathway, LD plasma leucine concentrations were superimposed on the muscle and liver mRNA transcripts (Figure 2.15 A, B).

In mammalian models, muscle is considered as the main catabolic tissue in the 1st step BCAA catabolism (BCAT) yielding BCKAs. Liver tissue is not thought to catabolise BCAAs, with studies demonstrating limited expression of BCAT in liver tissue (Bo & Fujii, 2024). The current results agreed, demonstrated by the overall temporally elevated muscle mRNA abundance comparative to liver, and the discrepancy between the peak mRNA copy numbers for muscle (4213 ±1158 /uL at 4 hr) and liver tissue (609 ±284 /uL at 8 hr). This may reinforce current mammalian model theories, such as the BCAAs (leucine) bypass the liver for initial catabolism in muscle tissue and in turn require the BCAT enzyme in muscle tissue. The BCAAs are additionally associated with muscle synthesis and when required are used as substrate. The catabolism of the BCAAs into the BCKAs by BCAT is said to be reversible, to regulate and maintain proteostasis, one can propose that muscle BCAT levels would need to maintain stability for this step to be reversible.

In this study, within liver tissue there did appear to be a temporal effect of plasma leucine BCAT mRNA transcript abundance. BCAT1 temporal mRNA abundance in liver tissue had significantly elevated mRNA transcripts at 8 and 24 hr compared to -2 hr ($p=<0.05$), suggesting a possible delayed response to plasma leucine. In mammalian studies, liver is said to rather catabolise the BCKAs in the irreversible 2nd step through BCKDH although Shin et al. (2014) suggested that in addition to liver, adipose tissue may catabolise BCKAs, although no comparative studies could verify this. This may suggest a possible alternative BCAA catabolism tissue-specificity in Atlantic salmon and further research is required to verify these trends.

A few factors may explain the temporal stability of BCAT transcript abundance in muscle tissue. The BCAAs share the first 2 catabolic enzymes, and this could possibly explain the stability seen in muscle tissue of BCAT transcript abundance in relation to plasma leucine. BCAT catabolism is reversible, possible suggesting continuously elevated levels of BCAT to maintain protein homeostasis. Or alternatively, muscle BCAT is less responsive to leucine in Atlantic salmon.

BCKDHA mRNA abundance for both muscle and liver, did appear to correspond to LD plasma leucine peak concentrations, with the 4 and 8 hr timepoints significantly higher than -2 and 24 hr ($p=<0.05$). This may suggest a possible non-tissue specific irreversible 2nd step catabolism, universal BCKDHA mRNA transcript responsiveness to plasma leucine concentrations. This non-tissue specificity of BCKDHA mRNA abundance may be due to the toxicity of excess AAs, and by converting the BCKAs to Krebs cycle for energy, glucose or fatty acids, this toxicity is reduced (Lim et al., 2001; Nurdalila et al., 2020).

In summary, temporal differences in mRNA abundance for BCAT and BCKDH were observed between tissues and within tissues, possibly indicating an effect of plasma leucine. Corresponding with other mammalian studies, Atlantic salmon muscle tissue is possibly the primary site for the first step of BCAA catabolism, with similar responses to BCKDH for liver and muscle tissue. Plasma leucine appeared to influence tissue-specific mRNA abundance of BCAT and BCKDH, with potential implications for BCAA homeostasis and energy metabolism.

Further research is needed to understand BCAA catabolism and to explore the regulatory mechanisms underlying these processes in Atlantic salmon.

2.4.4.2 mTOR pathway

mTOR1 regulates cell growth and metabolism by depending on four main signals- AAs, oxygen, energy status and growth factors (Laplante & Sabatini, 2009). mTOR and AAR (AA response) are two main AA signalling pathways involved in protein synthesis, with mTOR sensing AA abundance and AAR sensing AA deficiency (Hardy & Kaushik, 2021). When mTOR is inactive, it is found in the cytoplasm but when it senses AAs, leucine or arginine, it relocates to the lysosome and is activated by Rheb (Betz & Hall, 2013). Arginine activates mTOR through Castor1/2 by inactivating GATOR1 whereas leucine activates mTOR via SESN and GATOR1 (Bröer & Bröer, 2017). In this exploratory first trial, Atlantic salmon upstream (SESN and RRAG) and downstream (MYOSTATIN 1A and MYOSIN VI) targets of mTOR were examined in the LD to try and identify leucine activation of mTOR.

No differences were seen in SESN1 within the tissues. This may have been due to biological responses and the relatively low transcript numbers, but overall, muscle mRNA abundance was higher than in liver. The highest peak in muscle was seen at 24 hr, which was 103% different to liver abundance at 24 hr. Whereas in liver tissue, the highest abundance was -2 hr which was 43% different to muscle -2 hr abundance.

Chantranupong et al. (2014) identified SESNs in human cell lines as proteins that regulate AA sensing in the upstream branch of MTORC1. Their results also showed that Sestrins require GATOR1 and the RAGS to inhibit MTOR signalling. In mammals, intracellular leucine has been shown to bind and inactivate SESN, which is a negative regulator of mTOR (Sivanand & Van der Heiden, 2020). Leucine has been shown to inactivate SESN, and liver tissue has the highest expression of SESN1 (Rehman et al., 2023). Kousoulaki et al. (2015) looking at transcriptomic changes in Atlantic salmon fed varying diets, stated that SESN1, when down-regulated, controlled growth in response to stressors, and thereby inhibiting growth.

Although no differences were observed, an interesting temporal trend was seen between the tissues, with muscle mRNA abundance increasing whenever liver abundance decreased. This opposing trend was observed across all timepoints.

When overlaying plasma leucine concentrations and mRNA abundance, there did not seem to be any similar trends. When comparing tissue leucine fAA concentrations and SESN1 mRNA abundance, although muscle tissue fAA concentrations were lower than liver, the trend in muscle tissue was relatively constant with a noticeably significant drop in concentration below -2 hr baseline levels at 24 hr. Comparatively, liver tissue fAA concentration of leucine were higher than muscle, and the concentrations were relatively stable apart from the 24 hr point whereby the liver leucine concentrations were at its highest (2.2 ±0.6 μmol/ g) and muscle tissue at its lowest (0.3 ±0.0 μmol/ g). Unlike the muscle tissue, liver tissue did not have any significantly different temporal concentrations.

Wolfson et al. (2016) discussed that in mammalian cell culture, SESN2 interacts with leucine with a dissociation constant of ~20 μM, whereas half maximal effective concentration (EC50) of 20-40 μM on the SESN2- GATOR2 interaction and mTOR activation was observed. In the current study, concentrations of leucine were lower than 20-40 μM, possibly indicating either leucine concentrations were too low to identify an effect, or alternatively Atlantic salmon respond differently to mammalian cell culture studies.

Comesaña et al. (2021) exploring the effects of varying leucine concentrations (control, 1mM, 5mM and 25mM) on rainbow trout hypothalamus cells, found that relative mRNA abundance of BCKDE2, BCKDK and SESN2 varied between concentrations indicating a dose-dependent relationship. Relative mRNA abundance of BCKDE2 was increased at 1mM and 5mM but lower in the control and 25mM, BCKDK had lower mRNA abundance at 1mM and 5mM whereas *sesn2* had increased abundance at 5mM compared to the control. Similarly to Comesaña et al. (2021), mRNA abundance values in the current study, although in different tissues, may indicate that leucine is involved in AA sensing through the activation of BCAA metabolism and the GCN2 kinase signalling pathway (SESN).

Differences were seen within the tissues for RRAG A mRNA abundance, with the highest peak in muscle at 4 hr and the lowest peaks at -2 hr and 24 hr. In liver tissue, the highest peak mRNA abundance was seen at 4 hr and 8 hr, followed by 24 hr and the lowest mRNA abundance was seen at -2 hr. Overall RRAG A mRNA abundance was the highest in muscle tissue, with ranges from a low of 2279 ±534/ µL at -2 hr to a high of 3684 ±882/ µL at 4 hr, compared to liver ranges from a low of 980 ±564 /µL at -2 hr and a high of 2841 ±809/ µL at 8 hr.

RRAG A is one of four RAG proteins that are sensitive to AAs, and their expression activates MTOR by binding to RAPTOR (Sancak et al., 2010). Using leucine-stimulated cell culture, Sancak et al., (2008) found that low expression of RRAG led to reduced downstream phosphorylation of S6K1 indicating the effect of AA signalling on MTOR.

When looking at the RRAG A mRNA abundance of the baseline at -2 hr, there was an 80% difference in abundance between both tissues. Although the -2 hr point had the lowest abundance overall, the higher abundance in muscle baseline compared to liver may indicate that RRAG A may be more active in muscle tissue than liver tissue. Gollwitzer et al. (2022) in a study using human cell lines, discussed that although RAG A/ RAG B were not tissue specific, the more numerous RAG A would inactivate mTOR when sensing AA depletion.

RRAG A mRNA abundance when compared to plasma and fAA leucine concentrations, displayed interesting trends that may be indicative of an effect. With higher observed plasma and muscle fAA concentrations of leucine at -2 hr when compared to 24 hr, RRAGA mRNA abundance was similar, but did not mirror this trend as the -2 hr and 24 hr transcript abundance was statistically alike. Although liver mRNA was significantly lower at -2 hr, it did not mirror the plasma leucine nor the fAA liver leucine trend.

The lowest RRAG A mRNA abundance in both tissues was seen at -2 hr, followed by 24 hr in liver tissue. In muscle tissue -2 hr was similar to 24 hr. Peak mRNA abundance at 4 hr for both tissues may indicate an effect of feeding. Liver mRNA abundance at 24 hr was higher than -2 hr but less than 4 to 8 hr, whereas fAA leucine in liver was highest at 24 hr. With plasma levels the lowest at 24 hr, and

fAA leucine highest at 24 hr in liver, it may indicate that excess leucine has been catabolised *i.e*. energy *etc*. But if looking at BCKDHA, liver mRNA abundance at 24 hr was lower than muscle tissue abundance.

Differences within each tissue were observed, with muscle tissue displaying overall higher RRAG A mRNA abundance than liver tissue. In muscle tissue, the highest mRNA abundance was observed at 4 hr and 8 hr, with -2 hr and 24 hr having similar lower mRNA abundance. In liver tissue, the highest peak mRNA abundance was seen at 4 hr, although the only different mRNA abundance timepoint was 24 hr. Interestingly the -2 hr transcript abundance was higher than the 24 hr point, indicating it did not return to baseline, but rather decreased by 69% below -2 hr.

McPherron et al. (1997) identified MYOSTATIN and suggested that it played a role in negatively regulating muscle growth. In their study using mice, by disrupting MYOSTATIN the animals had an increase in skeletal muscle by both hypertrophy and hyperplasia. Myostatin negatively regulates muscle growth and if activated, may affect MTOR pathway via IGF-1 (Seiliez et al., 2013). Liu et al., (2020) used muscle cells of Japanese Flounder (*Paralichthys olivaceus*) to demonstrate that MYOSTATIN 1 (MSTN1) inhibited cell proliferation via inhibition of mTOR/p70S6K signalling pathway.

mTOR activation has been shown to reduce MSTN1 expression and thereby elevating muscle growth (Gao et al., 2016). When looking at transcript numbers, muscle tissue had a larger abundance of mRNA than liver tissue, with difference (%) between tissues ranging from 186% at -2 hr to 195% at 24 hr.

Liver mRNA abundance did seem to follow a similar trend to plasma leucine concentrations, with a drop at 24 hr and no differences between -2, 4 and 8 hr. There did not seem to be a trend when comparing leucine fAAs in liver tissue with liver mRNA abundance.

MYOSIN VI (MYO 6) is a light chain motor protein and has been shown to be involved in cellular transport and muscle contraction (Magistrati & Polo, 2021). It is important for maintaining normal cellular function and tissue repair (Valenzuela-Muñoz et al., 2023). No statistical differences were observed

between times in muscle tissue, but a difference was seen in liver with the 24 hr point having a larger transcript abundance. Between tissues, MYO 6 had higher difference (%) in mRNA abundance at the -2 hr point (155%) and 176% at 24 hr. Within muscle tissue there was a 4% increase in abundance at 24 hr, whereas in liver tissue there was a 50% increase at 24 hr. Similarly to BCKDK, low copy number yield and little variation within tissue influenced the decision to not continue further with MYO 6.

In Figure 2.21, LD plasma leucine temporal uptake was superimposed on the mTOR pathway muscle (A) and liver (B) mRNA transcripts to visually identify trends in relation to plasma leucine uptake. Although temporal and tissue variability was observed in SESN1 it did not seem to be influenced by plasma leucine concentration, possibly suggesting an alternative signalling mechanism in place.

In *Drosophila* models and mammalian cell culture studies, mTOR activation by AAs or stress, may be suppressed by the family of stress-inducible metabolic regulators, the Sestrins (Kim et al., 2021).The low mRNA abundance in both muscle and liver tissues may signify a limited response to plasma leucine, possibly indicative of mTOR activation and anabolic processes. Alternatively, in Atlantic salmon, the Sestrins may be less responsive to AAs or other unknown mechanistic factors.

RRAG A abundance in both liver and muscle appeared to follow plasma leucine concentrations, with peak abundance and leucine concentration at 4 hr post-prandial. Similarly, muscle Myostat 1a followed the same trends as RRAG A, while liver abundance was relatively stable apart from a significant reduction at 24 hr (p=<0.05). RRAG A and Myostat 1a transcript abundance did appear to be affected by plasma leucine concentrations, suggesting the possibility of leucine in signalling. More studies are required to verify these trends in Atlantic salmon.

In summary, while this study examined several components of the mTOR pathway in relation to dietary leucine, no clear direct changes of significant magnitude were observed but dietary leucine appeared to influence mTOR signalling seen by RRAG A and MSTN1A mRNA abundance in relation to plasma

leucine concentrations. Muscle tissue had higher mRNA abundance of mTOR-related targets compared to liver although SESN1 may not be the leucine-sensing mechanism in Atlantic salmon. The complex interplay between leucine, mTOR signalling, and its downstream targets in Atlantic salmon require further investigation, while further research is needed to clarify these pathways and their implications for growth and metabolism in aquaculture species. The observed differences in mRNA abundance suggest potential tissue-specific regulatory mechanisms that may need further studies to determine the biological significance of these results.

2.5 Chapter summary

2.5.1 Digestibility and feed intake

The preliminary aim of this trial was to determine if there were distinct significant digestibility differences between intact protein and cAAs across the diets. Intact protein diets contained 30% inclusion of experimental ingredients (Whey, casein and soya protein concentrate, (WHE, CAS, SPC)) into a basal mash whereas the cAA diets had a 2% inclusion of each of the cBCAAs into a basal mash (leucine, valine and isoleucine, (LD, VD, ID)) in addition to a control diet CD.

While no distinct differences were found between intact proteins and cBCAAs, nutrient-specific variations were observed ($p \leq 0.05$) (Table 2.3). For example, isoleucine digestibility was highest in ID, WHE, and CAS, while leucine digestibility was highest in CAS, followed by WHE and LD ($p \leq 0.05$). The second aim of the digestibility section was to evaluate digestibility differences between cBCAA diets (LD, VD, ID), but no significant differences were detected ($p > 0.05$).

2.5.2 BCAAs and other AAs

Plasma leucine was significantly different across diets at 2, 4 and 24 hr, with the LD highest at 2 and 4 hr while ID was highest at 24 hr (p=<0.05). At each timepoint across diets, plasma **i**soleucine in the ID was significantly higher at each timepoint across all diets (p=<0.05) and similarly valine was significantly higher in the VD at each timepoint compared to other diets *(*p=<0.05).

Within each diet over time for plasma isoleucine had similar peak trends for all diets whereby peak uptake occurred between 2 to 8 hr and the lowest concentrations were -2 and 24 hr (p=<0.05). Similarly for valine, ID and VD followed a similar trend to isoleucine uptake but CD and LD had constant uptake over time with the 24 hr having significantly lower uptake than the other times (p=<0.05). All diets apart from LD were relatively constant and had no differences over time for leucine uptake apart from lower concentrations at 24 hr (p=<0.05).

At each timepoint, plasma isoleucine was significantly higher in the ID compared to other diets ($p \leq 0.05$), while valine was significantly higher in the VD ($p \leq 0.05$). Leucine showed significant differences across diets at 2, 4, and 24 hours, with the LD highest at 2 and 4 hours and the ID highest at 24 hours ($p \leq 0.05$).

Total fAA in plasma had differences within each diet over time for all categories (p=<0.05), apart from no differences for fNEAAs in the CD (p=>0.05). Across the diets at each time had differences between the diets in fBCAAs at -2, 2, 4 and 24 hr times (p=<0.05). Total fEAAs had differences in concentrations between the diets at 4 and 24 hr, while fEAAs (excluding fBCAAs) had differences at 24 hr (p=<0.05).

Within each diet over time had significantly higher overall peak uptake of the plasma EAAs between 2 to 8 hr post prandial (p=<0.05). Similarly, -2 and 24 hr concentration were overall significantly lower than the peaks (p=<0.05). Exceptions to both did occur. Within each diet over time displayed statistically significant variable temporal peak uptake for the plasma NEAAs (p=<0.05). Compared to the BCAA diets, CD was the most stable over time, with significance observed in only 2 of the 6 NEAAs (p=<0.05). The NEAAs in the BCAA diets had variable and opposing uptake trends across the diets.

Total fAAs in plasma showed differences within each diet over time for all categories ($p \leq 0.05$), except for fNEAAs in the CD, which had no differences ($p > 0.05$). Across diets at each timepoint, differences were observed in fBCAAs at -2, 2, 4, and 24 hours ($p \leq 0.05$). Total fEAAs differed between diets at 4 and 24 hours, while fEAAs (excluding fBCAAs) showed differences at 24 hours ($p \leq 0.05$).

LD muscle fBCAAs had significant differences over time for leucine and isoleucine with the 24 hr concentration significantly lower than the other times (p=<0.05). No differences in BCAA concentrations across time were observed in liver tissue (p=>0.05). Total fAA categories in muscle tissue had differences in total fEAAs, fEAAs (excluding fBCAAs) and fBCAAs over time (p=<0.05). Total fEAA and fBCAAs concentrations were significantly higher at 4 hr than 24 hr, fEAAs (excluding fBCAAs) were significantly higher at -2, 2 and 8 hr compared to 24 hr (p=<0.05). No differences were observed for liver tissue (p=>0.05).

2.5.3 Molecular

mRNA abundance related to BCAA metabolism and mTOR signalling exhibited tissue-specific and time-dependent variations in Atlantic salmon. BCAT1a mRNA abundance peaked at 8 and 24 hr in liver, but at 4 hr in muscle, with overall higher mRNA abundance in muscle. BCKDH showed similar trends, peaking at 4 and 8 hr in both tissues, though mRNA transcripts were generally higher in muscle. BCKDK mRNA abundance was significantly elevated at 24 hr in both tissues. Regarding the mTOR pathway, RRAG mRNA abundance peaked at 4 hr in muscle and at 4 and 8 hr in liver. Myostatin 1a mRNA abundance peaked at 4 and 8 hr in muscle, while liver levels were stable except for a decrease at 24 hr. Myosin VI mRNA abundance was significantly higher at 24 hr in liver, but not in muscle. SESN1 mRNA abundance was highest at 24 hr in muscle, but conversely, highest at -2 hr in liver. These results demonstrate distinct temporal effects on the mRNA transcripts involved in BCAA metabolism and mTOR signalling, suggesting complex regulatory mechanisms operating in a tissue-specific manner, although the magnitude of the changes may not be considered biologically significant.

Overall this study compared cBCAA diets in Atlantic salmon and focused on bAAs, plasma AAs, muscle and liver fAAs and mRNA expression of the BCAA catabolic pathway and the mTOR pathway. Plasma profiles revealed strong diet- and time-dependent uptake patterns, with each cBCAA diet elevating its respective amino acid and total/fEAAs peaking 2–8 h postprandially. mRNA abundance linked to BCAA metabolism and mTOR signalling displayed distinct,

tissue-specific temporal patterns, with higher transcript abundance in muscle, though changes were modest in biological magnitude. Overall, the cBCAA diets elicited subtle but significant metabolic and molecular differences, governed by amino acid type, time, and tissue.

The findings are relevant to aquaculture as they demonstrate that the cBCAA diets elicit distinct AA absorption patterns and tissue-specific metabolic responses that may influence growth and feed efficiency. The strong temporal dynamics in plasma and muscle AA availability highlight the importance of synchronising nutrient delivery with metabolic demand, a key factor for optimising protein utilisation in Atlantic salmon production. Furthermore, the differential regulation of BCAA metabolism and mTOR signalling pathways suggests that diet formulation can modulate molecular mechanisms underpinning muscle growth, with implications for enhancing feed performance and reducing reliance on costly protein sources. These results therefore provide a mechanistic basis for refining dietary protein strategies in aquaculture to improve growth efficiency, sustainability, and economic viability.

Chapter 3

THE ROLE OF BCAAS ON REGULATION AND PERFORMANCE IN ATLANTIC SALMON PARR/ JUVENILES.

Abstract

This study evaluated the influence of dietary branched-chain amino acids (BCAAs) on the growth performance, morphometric indices, and physiological adaptations of juvenile Atlantic salmon (*Salmo salar*). A 7-week trial was conducted, with sampling at weeks 0, 3, and 7, wherein biometric parameters, including individual length, weight, and somatic indices, were systematically recorded. Notably, significant variations in viscera weight and hepatosomatic index (HSI%) were observed across dietary treatments, suggesting differential impacts on energy allocation and metabolic activity. Statistical modelling using generalised linear models (GLMs) further revealed significant dietary effects on viscera development, potentially attributable to gonadal maturation or methodological inconsistencies in sampling.

Growth performance metrics, encompassing weight gain and feed conversion ratio (FCR), deviated from expected trends. The negative all BCAA diet (NA) exhibited the most substantial increase in body mass (77%), whereas the supra-optimal leucine diet (PL) yielded the lowest growth response (64%). These findings challenge conventional industry benchmarks, particularly as the NA diet surpassed projected outcomes. Whole-body (WB) compositional analysis at week-3 demonstrated a significant reduction in protein content in NA-fed fish (p=0.002), potentially due to elevated lipid deposition. However, lipid accumulation across dietary treatments at week-7 remained statistically indistinct. Amino acid (AA) profiling suggested that leucine and isoleucine exert modulatory effects on lipid metabolism, with the sub-optimal leucine diet (NL) facilitating more consistent morphological outcomes relative to other dietary groups.

Plasma and muscle free amino acid (fAA) dynamics exhibited temporal variability, underscoring potential interdependencies between BCAAs and essential amino acids (EAAs). Elevated isoleucine and valine concentrations in the NL diet indicated potential competitive absorption mechanisms modulated by leucine availability. Moreover, temporal shifts in muscle leucine concentrations appeared to influence the bioavailability of arginine and other EAAs, further substantiating the hypothesis of competitive uptake interactions.

Haematological and biochemical assays detected significant temporal fluctuations in haemoglobin (Hb), packed cell volume (PCV), and white blood cell counts (WBCC), although dietary influence on these parameters was not statistically significant. Hepatic enzyme markers, including alkaline phosphatase (ALP) and creatine kinase (CK), remained stable across dietary regimens, implying that BCAA manipulation did not exert adverse effects on liver function.

Stable isotope tracing using δ15N-labelled leucine elucidated tissue-specific retention dynamics, with elevated whole-body leucine incorporation at week-3 relative to week-7. Furthermore, transcriptional analysis of branched chain α-ketoacid dehydrogenase 1a (BCKDH1A) mRNA abundance revealed tissue- and time-dependent regulatory patterns, indicative of adaptive metabolic responses to BCAA supplementation.

This study offers novel insights into the mechanistic role of dietary BCAAs in shaping metabolic trajectories, protein accretion, and lipid utilisation in juvenile Atlantic salmon. The findings underscore the necessity of further longitudinal research to elucidate the long-term ramifications of BCAA interactions in aquaculture nutrition. Optimising dietary BCAA composition may enhance growth performance and metabolic efficiency, with potential implications for sustainable aquafeed development.

Keywords: Atlantic salmon, crystalline amino acids, mTOR, BCAA metabolism, amino acids, branched chain amino acids, growth

3.1 Introduction

Industry-driven feed formulation is critical for cost control, pollution reduction, and maintaining fish health (Cooney et al., 2021; Zhang et al., 2020). While modern feeds focus on nutrients rather than specific ingredients, fishmeal (FM) and fish oil (FO) remain essential in marine diets (Majluf et al., 2024). Substituting fish-based ingredients with plant-based alternatives has been shown to alter Omega-3/Omega-6 (n-3/n-6) polyunsaturated fatty acid (PUFA) ratios, gut function, microbiota diversity, and transporter gene expression (Hu et al., 2016). Protein, the most expensive component of fish diets, must be carefully balanced to avoid waste and health issues (Teles et al., 2020). Poorly formulated feeds can lead to reduced growth, skeletal defects, and increased disease susceptibility due to nutrient imbalances or environmental factors like water quality (Sørensen et al., 2021).

Amino acids (AAs) are fundamental to fish growth, serving as building blocks for protein synthesis, energy metabolism, and various physiological processes (Mai et al., 2022). Among AAs, branched-chain amino acids (BCAAs)- leucine, isoleucine, and valine- play a particularly critical role in growth, immune function, and metabolic regulation in fish, including Atlantic salmon (*Salmo salar*) and other teleosts (Ahmad et al., 2021).

Substituting fishmeal with plant-based proteins can alter AA profiles, necessitating supplementation with synthetic AAs to meet BCAA requirements (Gatlin et al., 2007). Optimising BCAA and AA levels in fish feeds is essential for maximising growth and feed efficiency and in Atlantic salmon and other vertebrates, dietary BCAA levels should be tailored to specific life stages and environmental conditions to support growth and health (Espe, 2016). The optimal dietary BCAA levels for Atlantic salmon are approximately 2.5-3.0% of the diet for leucine, 1.5-2.0% for isoleucine, and 1.5-2.0% for valine (Rolland et al., 2016).

Gómez-Requeni et al. (2004) evaluated the impact of replacing fishmeal with plant protein in gilthead seabream (*Sparus aurata*) diets with a 100% replacement resulting in a 30% reduction in growth, potentially due to palatability issues. Although crystalline AAs (cAAs) were added to meet essential amino acid (EAA)

requirements, the ratio between EAA and non-essential amino acid (NEAA) was maintained at 1:1.

Choo et al. (1991) examined the effects of excessive leucine in rainbow trout (*Oncorhynchus mykiss*) diets. Diets containing up to 6.5% leucine did not impair weight gain or feed intake, though body protein concentrations declined with increasing leucine levels. In a subsequent trial, diets with 13.4% leucine led to health issues, including lesions and deformities in over 20% of fish, suggesting leucine toxicity. Despite these findings, polyamine analysis, used as a metabolic growth marker, showed no significant variations across dietary treatments.

Protein synthesis is the primary driver of growth in fish, and AAs are essential substrates for this process (Falco et al., 2020). BCAAs, particularly leucine, are known to stimulate muscle protein synthesis by activating the mechanistic target of rapamycin (mTOR) pathway, a central regulator of cell growth and metabolism (Drummond & Rasmussen, 2008). In Atlantic salmon, dietary leucine has been shown to enhance growth performance by promoting muscle hypertrophy and reducing protein degradation (Ahmad et al., 2021).

BCAAs are not only substrates for protein synthesis but also act as signalling molecules that regulate metabolic pathways (Hinkle et al., 2022). In salmonids and other vertebrates, BCAAs influence nutrient sensing pathways, such as mTOR and AMP-activated protein kinase (AMPK), which balance anabolic and catabolic processes (Morin et al., 2020). While leucine is the most potent activator of mTOR, isoleucine and valine also contribute to protein synthesis and energy production (Duan et al., 2016). Isoleucine is involved in glucose uptake and utilisation, while valine supports muscle metabolism and nitrogen balance (Li et al., 2009).

Leucine activates mTOR signalling, which upregulates ribosomal protein S6 kinase (S6K1) and eukaryotic initiation factor 4E-binding protein 1 (4E-BP1), key regulators of protein synthesis (Lansard et al., 2010). In Atlantic salmon, optimal dietary leucine levels are critical for maximising growth, as both deficiency and excess can impair protein synthesis and growth performance (Rolland et al., 2016).

BCAAs play a vital role in maintaining immune function and mitigating stress responses in fish. In Atlantic salmon, dietary BCAAs have been shown to enhance immune cell proliferation and reduce inflammation, supporting overall health and growth (Rolland et al., 2016). Leucine supports the proliferation of lymphocytes and macrophages, which are critical for immune defence in fish (Mokhtar et al., 2023). In teleosts, BCAA supplementation has been linked to improved resistance to bacterial infections and reduced mortality rates (Li et al., 2009) and help mitigate stress responses by reducing cortisol levels and oxidative stress. In rainbow trout (*Oncorhynchus mykiss*), BCAA supplementation has been shown to improve growth performance under stressful conditions, such as high stocking densities (Yamamoto et al., 2020).

The growth-promoting effects of BCAAs are influenced by their interactions with other AAs. Imbalances in AA profiles can lead to antagonistic effects, reducing growth performance, such as excess lysine may increase the requirement for arginine, leading to reduced growth in fish (Mai et al., 2022). In Atlantic salmon, balanced lysine and arginine levels are essential for optimal growth and feed efficiency (Rolland et al., 2016). Sulphur-containing AAs, such as methionine and cysteine, are critical for protein synthesis and antioxidant defence, while in teleosts, methionine deficiency can impair growth and increase susceptibility to oxidative stress (Li & Gatlin III, 2007).

The growth-promoting effects of AAs, in particular the BCAAs, may be influenced by environmental factors and life stages. For example, in Atlantic salmon during smoltification, (the biological process consisting of physiological, morphological, and behavioural changes juvenile salmonids endure allowing for the adaption from fresh to saltwater), demand for BCAAs increase due to the high energy requirements for osmoregulation and morphological changes (Glover et al., 2013; Hoar, 2024). During this transition from freshwater to seawater, BCAAs support energy production and protein synthesis, ensuring successful adaptation (Mommsen, 2004). Smoltification and gonadal development can divert nutrients from somatic growth, leading to smaller fish and increased aggression (Mobley et al., 2021).

Haematological parameters, such as red blood cell count (RBCC), haemoglobin (Hb), and white blood cell count (WBCC), may be affected by nutritional status, particularly BCAA levels. Enzymes like alkaline phosphatase (ALP) and alanine aminotransferase (ALT) serve as biomarkers for liver and muscle function, reflecting overall health (Rozas-Serri et al., 2022).

The preliminary aim of the second experiment was to examine the response of Atlantic salmon (*Salmo salar*) parr to varying inclusion levels and ratios of the BCAAs and assess whether the responses were similar to other vertebrate studies. This first section examined performance parameters such as growth, feed intake and health. The potential effects of variable BCAAs on health, blood chemistry including enzyme activity were investigated between week-3 and week-7. Weight gain, morphometric and somatic indices were assessed in addition to the various AA analyses in plasma, whole body (WB) and muscle tissue.

The secondary aim of this experiment was to examine the post-prandial physiological responses to the BCAAs and assess whether the uptake and molecular responses were comparable to other vertebrates. This second section examined the plasma and tissue fAAs as well as metabolic biomarkers such as 15N labelled leucine stable isotope incorporation and branched chain α-ketoacid dehydrogenase (BCKDH) mRNA abundance.

3.2 Materials and methods

The experiment was approved by the University of Stirling Animal Welfare and Ethical Review Body (AWERB 2019/20/021) in accordance with the UK Home Office under the Animals (Scientific Procedures) Act 1986. This trial was performed at the Niall Brommage Freshwater Research Unit (Buckieburn, UK) and ran from 5 November 2019 to 17 December 2019.

3.2.1 Fish handling, husbandry and sample collection

3.2.1.1 Experimental design

In this trial, Atlantic salmon (*Salmo salar*) eggs were obtained from a commercial supplier and reared for several months at the Niall Brommage Freshwater Research Unit (Buckieburn, UK).

The mixed sex parr were fed a commercial diet until they had reached a suitable start weight in the holding tanks. They were sedated using MS-222 (0.1 g/L), weighed, and stocked into 700 L experimental tanks at 120 fish /tank with an initial average weight of 19.4g ±0.39. Tank selection was randomly allocated, with three tanks per treatment and a one-way ANOVA was used to determine that there were no differences in tank weights at the initial start-up (p=0.294).

A freshwater Recirculating Aquaculture System (RAS) was used containing mature biofilters, ozone cones, UV, drum filters and trickle towers. Over the 7-week trial, a temperature of 13.0 ±0.7 °C, dissolved oxygen of 10.9 ±0.59 mg/L and a commercial light regime of 24:0 (L:D) was maintained. The environmental factors were monitored in the tanks as well as in the biofilter and recorded by an OxyGuard monitoring system (OxyGuard International A/S, Farum, Denmark). An increase in water turbidity (suspended solids) total ammonia nitrogen (TAN), ammonia (NH_3), ammonium (NH_4) and carbon dioxide (CO_2) were identified starting at the week-3 sampling date (25/11/2019). Increased water changes were performed and the Chloride: Nitrite–N Ratios were monitored and maintained at >20:1 to minimise the toxicity of nitrites (S 3.1, 2).

Table 3.1 Expected feed intake and growth estimations for the control diet x360 fish.

Time (day)	**Fish** (g)	**Ration** (%BW/d)	**Feed** (g/fish/d)	**Total** (kg/d)	**Cuml.** (kg)	**FCR** (feed/gain)
0	15	2.8%	0.4	0.15	0.00	0.68
4	18	2.6%	0.5	0.16	0.61	0.69
8	20	2.4%	0.5	0.18	1.28	0.70
12	23	2.3%	0.5	0.19	2.00	0.72
16	26	2.2%	0.6	0.21	2.78	0.73
20	29	2.1%	0.6	0.22	3.62	0.74
25	33	2.0%	0.7	0.24	4.52	0.75
29	36	1.9%	0.7	0.25	5.48	0.76
33	40	1.8%	0.7	0.26	6.50	0.77
37	44	1.8%	0.8	0.28	7.58	0.78
41	48	1.7%	0.8	0.29	8.72	0.80
45	52	1.7%	0.9	0.31	9.92	0.81
49	56	1.6%	0.9	0.32	11.18	0.81

Fish were fed to apparent satiety for 7-weeks using Arvotec automatic feeders (Arvo-tec Oy, Arvo-Tec T Drum 2000 Feeder, Huutokoski, Finland). Feeders were stocked with an estimated industry start ration of 2.8% BW/d and then reduced to an anticipated 1.8% BW/d at the end of the 7-week trial (Table 3.1).

Feeding observations throughout the 7-week trial were accomplished by approaching tanks with minimal disturbance to the fish. Health and welfare of the fish were routinely checked for visible physical abnormalities such as fin damage, abrasions and overall condition, and behaviours such as feed response, feed intake, placement in the water column, aggression *etc*. were monitored daily.

At week-3, 8 fish (*n*=8/ tank) were schedule 1 euthanised 4 hr post-feeding for whole-body (WB) composition analysis (*n*=4/ tank) and tissue sampling (*n*=4/ tank). Blood was removed, centrifuged and plasma stored at -70 °C, while the tissues were removed, weighed and stored at -70 °C for further downstream

somatic index and other analyses. In addition to sample collection at 4 hr, all remaining fish at the 8 hr post-prandial timepoint were netted, sedated, bulk weighed, stripped of faeces using the method of Glencross et al. (2005) and returned to their respective tanks.

At week-7, 4 fish (*n*=4) from each tank were schedule 1 euthanised at -2 (0 hr timepoint), 2, 4, 8, and 24 hr post-feeding and biological samples were removed. Blood was centrifuged, with the plasma and biological samples stored at -70 °C. Similarly to week-3, an additional 4 fish (*n*=4 /tank) were schedule 1 euthanised 4 hr post-feeding for whole-body (WB) composition analysis. All individual schedule 1 euthanised fish at both week-3 and week-7 were individually weighed, and fork lengths were taken.

Table 3.2 BCAA inclusion levels and expected outcomes (1.5 and 2mm pellet formulation)

Treatment	Protein	Lipid	LYS	LEU	ILE	VAL		Outcome Exp. (%)
NA	50%	20%	3.0%	2.0%	1.0%	1.0%	All BCAAs low	50%
NL	50%	20%	3.0%	2.0%	1.5%	1.8%	LEU low	70%
PL	50%	20%	3.0%	5.0%	1.5%	1.8%	LEU fortified	90%
CD	50%	20%	3.0%	2.7%	1.5%	1.8%	Control	100%

CD= Control diet, NA=Negative BCAAs, NL= Negative Leucine, PL= Positive Leucine. LYS= lysine, LEU-leucine, ILE= isoleucine, VAL= valine.

Due to the size of the fish, blood from 4 fish /tank (*n*=4 /tank) at each timepoint were pooled, spun, and plasma was collected using the method described by Huyben et al. (2023). At the 4 hr timepoint, plasma and whole blood from 8 fish/tank (*n*=8 /tank) were separated into 2 Nunc™ CryoTube™ tubes (Thermo Scientific, Nunc™ Cryotube™ Vials 1.8 mL, Roskilde, Denmark) and stored on dry ice for transport to Scotland's Rural College (SRUC) for haematology analysis (Central Analytical Laboratory at SAC Consulting Veterinary Services, Edinburgh, UK) and at -70 °C future plasma analysis. Similarly, to the first trial, all tissue samples were stored immediately on dry ice before being transferred to -70 °C freezers for later analysis.

3.2.2 Feed formulation and manufacture

The test feeds were formulated to examine whether leucine or the BCAAs, affected growth responses in salmon after a 7-week trial (Table 3.2). The 4 diets consisted of NA, which contained sub-optimal levels of BCAAs, NL sub-optimal levels of leucine (2%), PL supra-optimal leucine levels (5%) and a reference/control diet, CD. The Atlantic salmon juveniles required higher protein and lipid content and were formulated to be isoproteic (50%) and isolipidic (20%). A diet substitution formulation strategy was used to allow for the BCAA variability between the diets without sacrificing protein or EAAs. Alanine, glycine and serine volumes were altered, enabling all diets to have the same levels of protein and EAAs, but varying NEAAs (alanine, glycine and serine).

Raw ingredients were milled (800 µm) and a basal mash containing all ingredients apart from the AAs was prepared (Table 3.3). Mineral premix was ground using a pestle and mortar, weighed, added to the basal mix and thoroughly mixed on a generic cement mixer. The allocated amount of fish oil was added and mixed for 5 min before the homogenised basal mash was separated into equal quantities for each test diet. cAAs were ground, weighed into labelled test diet bags, which were then added to the individual pre-weighed basal mixes. Water was added at around 5-10% and mixed on a Hobart mixer (Hobart, Planetary Mixer M802, Peterborough, United Kingdom) for a further 5 min or until the mixture formed the correct consistency.

Table 3.3 Diet formulation (%) and expected compositions (g/ kg).

Formulation:	**Diet 1**	**Diet 2**	**Diet 3**	**Diet 4**
Name:	**NA**	**NL**	**PL**	**CD**
Anchovy-SP [a]	10.0%	10.0%	10.0%	10.0%
HP1 [b]	1.0%	1.0%	1.0%	1.0%
WGluten [a]	8.0%	8.0%	8.0%	8.0%
SPC [a]	8.1%	8.1%	8.1%	8.1%
SPI	10.0%	10.0%	10.0%	10.0%
Pregel/Dextrose	10.8%	10.8%	10.8%	10.8%
Cellulose	8.3%	8.3%	8.3%	8.3%
ARG	0.6%	0.6%	0.6%	0.6%
HIS	0.3%	0.3%	0.3%	0.3%
ILE [e]	**0.0%**	**0.5%**	**0.5%**	**0.5%**
LEU [e]	**0.0%**	**0.0%**	**3.2%**	**0.6%**
LYS	1.7%	1.7%	1.7%	1.7%
MET	0.6%	0.6%	0.6%	0.6%
VAL [e]	**0.0%**	**0.6%**	**0.6%**	**0.6%**
TAU	0.4%	0.4%	0.4%	0.4%
ALA	**5.6%**	**5.2%**	**4.1%**	**5.0%**
GLY	**5.7%**	**5.4%**	**4.4%**	**5.2%**
SER	**5.6%**	**5.2%**	**4.1%**	**5.0%**
THR	0.5%	0.5%	0.5%	0.5%
Premix [c d]	1.1%	1.1%	1.1%	1.1%
Calcium phosphate [a]	3.0%	3.0%	3.0%	3.0%
Fish oil [a]	18.7%	18.7%	18.7%	18.7%
Diet Compositions as Formulated				
Dry matter	943	943	943	943
Crude protein	478	478	478	478
DPro	500	500	500	500
Lipid	200	200	200	200
CHO	194	194	194	194
Starch	100	100	100	100
Energy (MJ/kg)	22.2	22.2	22.2	22.2
DE	19.8	19.8	19.8	19.8
Alanine	63	59	49	57
Arginine	23	23	23	23
Aspartic acid	26	26	26	26
Cysteine	5	5	5	5
Glutamic acid	62	62	62	62
Glycine	63	61	52	59
Histidine	9	9	9	9
Isoleucine	11	16	16	16
Leucine	21	21	50	27
Lysine	30	30	30	30
Methionine	11	11	11	11
Phenylalanine	14	14	14	14
Proline	21	21	21	21
Serine	65	61	51	59
Taurine	4	4	4	4
Threonine	15	15	15	15
Tyrosine	10	10	10	10
Valine	12	18	18	18
Tryptophan	3	3	3	3

All values are g/kg as used unless otherwise indicated. CD=Control diet, NA=Negative all, NL=Negative leucine, PL= Positive leucine. [a] Supplied by BioMar Ltd, Grangemouth, Scotland. [b] Supplied as HP1 by Diana Aqua, Elven, France. [c] Yttrium Supplied by Stanford Materials, Aliso Viejo, California, United States. [d] Supplied by DSM, Basel, Switzerland as OVN vitamin and mineral premix for salmonids (dose per kilogram of diet: Vitamin A: 2400 UI/kg; Vitamin D3:1200 IU/kg; Vitamin K3: 8 mg/kg; Vitamin B1: 12 mg/kg; Vitamin B2: 20 mg/kg; Niacin: 120 mg/kg; Vitamin (Pantothenate) B5: 32 mg/kg; Vitamin (Pyridoxine) B6: 16 mg/kg; Vitamin (Folate) B9: 8 mg/kg; Biotin: 0.8 mg/kg; Vitamin (Cyanocobalamine) B12: 0.04 mg/kg; Vitamin C: 120 mg/kg; Vitamin E: 160 UI/kg; Manganese: 16 mg/kg; Iodine: 1.6 mg/kg; Copper: 4 mg/kg; Cobalt: 4 mg/kg; Magnesium: 80 mg/kg; Zinc: 80 mg/kg; Iron: 24 mg/kg; Selenium: 0.16 mg/kg) [e] Supplied by Bulk powders
*Carbohydrate content determined based on dry matter minus protein, ash and lipids.

The reference (CD) had 12g of 15N labelled leucine added for further traceability analysis (Cambridge Isotope laboratories, Inc.,15N L-Leucine 98%, Tewksbury, USA). The pellets were then manufactured at the University of Stirling, using a Dolly™ cold-extrusion screw-press (La Molliferina, Dolly™, Rome, Italy) to produce 1.5 mm and a 2 mm pellets and dried at 60 °C for 24 hr.

3.2.3 Calculations for growth performance, efficiency and morphometric indices

Performance was determined using the following equations:

Weight gain (g/ fish) = final weight – initial weight.
FCR 1 = Feed fed/weight gain
FCR 2= (Feed fed-waste feed)/weight gain
bFCR= (Biomass gain/ feed fed)

Feed intake (FI) g /fish /day utilised the measured feed fed, minus the feed waste to which a correction factor was applied using the method discussed in Section 2.2.2. but with a 24 hr pellet soak time as the waste feed was collected once a day.

$$\text{Feed intake} = \frac{\text{(feed fed-(WF÷CF)}}{\text{total fish/ tank}}$$

where *WF* is the total weight of the collected waste feed in each tank, *CF* is the correction factor of the wet feed to dry feed.

Weight (W) can be predicted from length (L) by Length-Weight Relationships (LWR). These were determined by the following equation of Le Cren (1951) and as described in Froese et al. (2014).

$$W = aLb$$

The parameters *a* and *b* were calculated from the linear regression of log(W) and log(L), where *a* represents the intercept and *b* represents the slope.

$$\text{Log } W = \text{Log } a + b$$

Log L was computed using Microsoft Excel (Microsoft Corp., Excel v.2307, Redmond, USA) to estimate the "*a*" and "*b*" values.

L*W '*b*' was used as an indication of growth (Isometric growth = 3, Positive allometric growth = > 3 (heavier fish with increasing length); and negative allometric = < 3 (slimmer fish with increasing length).

L*W '*a*' was used as an indication of body shape *(a* = 0.01 fusiform fish, *a* = 0.001 in eel-like fish and *a* = 0.1 spherical fish) (Froese, 2006).

Le Cren's relative condition factor, Kr, was calculated by the following:

$$Kr = (W/w)$$

Where W is the mass of the fish, and w is the expected mass of a fish of the same length as calculated from the LWRs. Kr is used as a comparison to the study population 'the deviation of an individual from the average weight for length Kr>1 = good, <1 = bad.

$$Kr=W/aLb$$

Fulton's Condition factor (K) was the ratio of body mass, and the cube of length as described in Richter et al. (2000). It was used as an indication of leanness/ fattiness of a fish.

$$K = \text{wet mass (g)}/\text{standard length (mm)}^3 \times 100$$
$$(K = 100 \times \text{weight/length\^3})$$

$$K = W^* 100/ L^3$$

Somatic indices were calculated according to the following formulae:

$$HSI (\%) = (\text{liver weight/final weight}) \times 100$$
$$VSI (\%) = (\text{viscera weight/final weight}) \times 100$$
$$VFSI (\%) = (\text{viscera fat/final weight}) \times 100$$
$$CSI\% = (\text{heart weight/ body weight}) \times 100$$
$$Change (\%) = 100x ((\text{final} - \text{initial})/\text{initial})$$

3.2.4 Analyses of feeds, ingredients and faeces

3.2.4.1 MOPA

3.2.4.1.1 Moisture

Samples with high moisture content such as faeces and tissue samples were initially freeze dried before analyses. Fixing pots (Thermo Fisher Scientific Inc., Gosselin™ Straight Containers 15478814, Loughborough, UK) containing wet homogenised samples were weighed (Ohaus Pioneer PX224, Nänikon, Switzerland), frozen at -18 °C for approximately 2 hr and then freeze dried (SciQuip ALPHA 1-4 LSC, Rotherham, United Kingdom) for approximately 24-48 hr depending on sample size. When dried, these were stored in a desiccator and reweighed to determine freeze dried moisture content.

For total moisture (dry matter), samples were weighed (Ohaus Pioneer, PX224), oven dried at 110 °C for a minimum of 4 hr (Gallenkamp Hot Box Oven, Cambridge, United Kingdom), reweighed for moisture content and stored in a desiccator.

$$\% \text{ Moisture} = \frac{\text{Sample Weight (g) - Dried Sample Weight (g) x 100}}{\text{Sample Weight (g)}}$$

3.2.4.1.2 Ash

Samples of interest were weighed into pre-weighed crucibles (Ohaus Pioneer, PX224) and transferred to a muffle furnace overnight at 600 °C (Carbolite AAF 1100 Ashing Furnace, Derbyshire, United Kingdom). These were then removed and allowed to cool in a desiccator before weighing.

$$\text{Ash (\%)} = \frac{\text{ash weight (g)}}{\text{sample weight (g)}} \times 100$$

3.2.4.1.3 Lipids

The Folch-Lee method (Folch et al., 1957) was used to determine lipid content of WB. In brief, 20 mg of homogenised tissue was weighed to 4 decimal places (Ohaus Pioneer, PX224) and added to pre-weighed tubes. HPLC grade Chloroform/methanol (C:M) (2:1, v/v) (Merck KGaA, Chloroform 366927, Methanol 34885-M, Darmstadt, Germany) was added (6 mL), homogenised, and stored at -20°c for 1 hr. On removal, 1.5 mL of analytical reagent grade potassium chloride (KCL) (Merck KGaA, P3911, Darmstadt, Germany) was added and then centrifuged at 1000rpm (400g) for 5 min. The top layer was then aspirated. This was then filtered through prewashed Chloroform/methanol (C:M) (2:1, v/v) Whatman no. 1 filter papers into 15 mL pre-weighed quickfit tubes and then transferred to a TurboVap® (Biotage GB Ltd., TurboVap® Classic, Hengoed, UK) until the solvent had evaporated. Quickfit tubes were then weighed and recorded, and lipids were redissolved in C:M (2:1) ± 0.01% (w/v) Butylated hydroxytoluene (BHT) (Merck KGaA, W218405, Darmstadt, Germany) at a concentration of 10 mg/ mL at -18 °C.

$$\text{Lipid (\%)} = \frac{\text{weight lipid (g)}}{\text{weight sample (g)}} \times 100$$

3.2.4.1.3.1 Acid hydrolysis and Soxhlet extraction

Feeds and faeces were weighed (800 mg) and recorded to 4 decimal places (Ohaus Pioneer, PX224) into FOSS hydrocaps. The same weight of Kieselguhr/ celite (Thermo Fisher Scientific, Kieselguhr 10763991, Loughborough, UK) was added to the sample and the weight was re-recorded. These were then placed in the hydrolysing unit (Foss, Hydrotec™ 8000, Runcorn, UK) containing 2 L of 3M HCl. The Hydrotec program consisted of a 5 min heating stage, 1 hr boiling, a cooling stage followed by 15 rinse cycles. These were then dried overnight in a drying oven (100-105 °C) in preparation for solvent extraction.

Glass balls (5-10) were added to each cup and placed into the prewarmed (135 °C) Soxtec unit. Petroleum ether (80 mL, Merck KGaA, 184519, Darmstadt, Germany) was added, and the programme initiated with pre-set boiling and rinsing times. Cups were dried for 1-2 hr in a drying oven (100-105°C) and then cooled in a desiccator before final weighing. Final lipid (%) was worked out using the equation listed in the Folch method.

3.2.4.1.4 Protein

Feeds, ingredients, and tissues were analysed for crude protein using the OPSIS LiquidLINE system based on the Kjeldahl method as explained by Sprague et al. (2020). Samples were weighed between 80-200 mg (Ohaus Pioneer PX224, Nänikon, Switzerland) onto 42.5 mm filter paper disks, weights recorded and added to 250 mL Kjeldahl tubes. Reagent blank controls were added at every 10^{th} sample. Copper Kjeltabs tabs and 12 mL concentrated sulphuric acid (Merck KGaA, 258105, Darmstadt, Germany) were added to every tube, and transferred to the OPSIS LiquidLINE KjelROC digestion block (OPSIS AB, Furulund, Sweden) for 1 hr at 420 °C. Once cooled, these were then transferred to the OPSIS LiquidLINE KjelROC Analyser and OPSIS LiquidLINE KjelROC Sampler KD-525 (OPSIS AB, Furulund, Sweden) for the distillation/titration stage. Sample weights were manually added to the OPSIS LiquidLINE system to allow for the analysis of crude protein percentages. Glycine was used as a standard control, with values of 115% ±1%.

3.2.4.1.5 Energy

A Parr 6200 bomb calorimeter was used to determine gross energy (Parr Instrument Company, 6200, Moline, USA) by weighing and recording samples between 500-600 mg (Mettler-Toledo GmbH, AC 100, Greifensee, Switzerland). A firing wire was attached between the electrodes in the assembly unit, with a loop formed above the pellet/ sample, and placed inside the bomb. The lid was tightened and the O_2 attached. The calorimeter bucket was filled with water, weighed to 2812.8 g (Mettler-Toledo GmbH, PM6000, Greifensee, Switzerland) and carefully placed inside the calorimeter. The bomb was carefully then placed into the water, avoiding any water displacement and electrodes connected. Sample names and weights were manually added onscreen before analysis, with onscreen results displayed and recorded. Benzoic acid pellet (1 g) was used as a standard (Parr Instrument Company, 3415 Benzoic acid pellets, Moline, USA).

3.2.4.1.6 Crude fibre (CF)

Crude fibre was determined using the FOSS FibreCap™ 2021/2023 system (FOSS application note ASN3801, Foss Analytical, Hillerød, Denmark) as mentioned in Devic et al. (2017).

Feed samples were weighed to 4 decimal places (0.5-1 g, Ohaus Pioneer PX224, Nänikon, Switzerland) into pre-weighed FOSS FibreCap™ capsules and defatted in 120 mL of petroleum ether (Merck KGaA, 184519, Darmstadt, Germany) by 3 cycles of 30 s agitation. This step was repeated twice, each time with new petroleum ether. Samples were placed in 350 mL boiling sulphuric acid solution (1.25% H_2SO_4, Merck KGaA, 258105, Darmstadt, Germany) for 30 min, followed by boiling in 350 mL of deionised water for 1 min. This was repeated twice with fresh boiling water.

Samples were placed in 350 mL boiling sodium hydroxide solution (1.25% NaOH, Merck KGaA, 567530, Darmstadt, Germany) for 30 min, followed by 3 cycles of 30 s in fresh acetone (Merck KGaA, 179124, Darmstadt, Germany). Capsules were dried for 5 hr at 105 °C and then cooled in a desiccator before weighing. Capsules were placed into pre-weighed crucibles and then ashed in the muffle furnace for 4 hr at 600 °C, allowed to cool and reweighed.

Fibre (%) = {("Capsule + sample dry weight" x 1.0011) – Capsule weight" – ((Crucible + ashed sample weight) – 0.0025)}/Sample weight x 100

Where 1.0011 = correction factor to account for loss of mass of the capsule itself during solvent and acid washing. 0.0025 = mean ash residue of a washed, empty capsule.

3.2.4.1.7 Nitrogen-free extract (NFE)

NFE supposedly represents the soluble carbohydrates of the feed, such as starch and sugar, and is the difference between the original sample weight and the sum of the weights of moisture (water), ether extract, crude protein, crude fibre, and ash.

NFE (%) = (DM (%) − (ether extract (%) + protein (%) + ash (%) + crude fibre (%))

3.2.4.2 Mineral analysis

Feeds, ingredients and faeces were processed by the University of Stirling water quality lab (Stirling, UK) for total minerals, trace elements and yttrium concentrations using plasma atomic emission spectrophotometry (ICP-MS) with collision cell technology (Thermo Scientific, XSeries 2 ICP-MS, Cheshire, United Kingdom) as described by Sprague et al. (2020). Samples (20-50 mg) were digested using 5 mL of 69% Nitric acid (Aristar® analytical grade; VWR Chemicals, Poole, UK) and run on a Mars Xpress microwave digester (CEM Microwave Technology Ltd., Mars Xpress, Buckingham, UK). Digests were then diluted (x25) and stored at 4 °C before analysis on the ICP-MS (Thermo Scientific, XSeries 2 ICP-MS) (S 3.3 - 4).

3.2.4.3 Amino acid hydrolysis and derivitisation of feeds, ingredients, and tissues (bAAs)

3.2.4.3.1 Amino acid hydrolysis (bAAs)

Total bound AAs (bAAs), such as proteins and peptides, are AAs joined through peptide bonds. Hydrolysis is the method used to break these bonds and provide about 90% of the protein-bound AA profile (Teo et al., 2024). bAA analysis was conducted on dried feed, faeces, ingredients and tissue samples, whereby 10 mL

of phenolic (6M HCl) (Merck KGaA, Phenol detached crystals 99+% A15760-22, Darmstadt, Germany, Merck KGaA, M2612-13, Darmstadt, Germany) was added to 100-250mg of sample, with 20 s of oxygen-free nitrogen (OFN) added before sealing and run on a Mars 6 CEM Microwave digester (CEM Microwave Technology Ltd., Mars 6, Buckingham, UK). Every 10th sample was duplicated, and controls were used in every run. Every sample had to be run at both 190 °C and 150 °C to ensure sulphur-based AA recovery which occurred at 150 °C.

Hydrolysed samples were added to 250 mL volumetric flasks and filled up to 250mL with MilliQ ultrapure water (Merck KGaA Millipore, Milli-Q ultrapure water system, Darmstadt, Germany). Contents were mixed, and a volume up to 5 mL was extracted via syringe and filtered through a 0.45 µm syringe filter (Millipore Merck KGaA, Millex™ PVDF 0.45 µm syringe filter, SLHVX13, Darmstadt, Germany) into pre-labelled Eppendorfs and stored at 4 °C for further analysis.

3.2.4.4 Plasma and tissue fAAs

Briefly, ice cold isopropanol (Merck KGaA, 2-Propanol 34863, Darmstadt, Germany) 0.1% formic acid (v/v) (Thermo Scientific Chemicals- Acros Organics, Formic Acid 98+%, 270480250, Loughborough, UK) was added at a 1:4 ratio to either plasma or tissue samples. This was vortexed, allowed to settle for 20 min at -20 °C and then centrifuged at 10000g for 10 min. Supernatant was removed and passed through vac cartridges (Waters Corporation, Oasis® PRiME HLB (1cc columns (30 mg), Milford, MA, USA). Resulting samples were stored at 4 °C for further analysis. Waters AccQ•Tag AA pre-column derivitisation method was utilised and run on Waters AQUITY Class Ultraperformance® Liquid Chromatography (UPLC), using AccQ·Tag Ultra Derivitisation Kit (Waters Corporation, P/N 186003836, Milford, MA, USA) and Waters Food & Feed Standard Kit as the standard (Waters Corporation, P/N WAT088122, Milford, MA, USA).

Preparation of mobile phases and UPLC priming methods were mentioned in Chapter 2 method section 2.2.3.3.2.

3.2.5 Digestibility

(See Chapter 2 section 2.2.4)

Diet apparent digestibility coefficients (DADC) were determined for crude protein, lipid, energy and AAs for each diet as discussed in Glencross et al. (2024):

$$AD_{diet} = \left(1 - \left(\frac{Y_{diet} \times Parameter_{faeces}}{Y_{faeces} \times Parameter_{diet}} \right) \right) \times 100$$

where Y_{diet} and Y_{faeces} represent the yttrium content of the diet and faeces respectively, and $Parameter_{diet}$ and $Parameter_{faeces}$ represent the nutritional parameter of interest (protein, lipid, energy, or AAs) content of the diet and faeces respectively.

All diets were prepared using a basal mix to which varying levels of AAs were added totalling 21% of overall contribution to each diet. In animal feeds, digestibility is a measure of digestion and absorption of an ingredient through an animal's system. Glencross et al. (2007) explained that by including an inert marker to the feed, the ratio of this marker in the feeds and faeces determined apparent digestibility. In the current trial, a basal mash was prepared with yttrium as the marker and 21% of varied AAs between the diets.

3.2.6 Haematology

Heparinised blood and plasma were analysed by SRUC (Scottish Agricultural College Veterinary Services, Penicuik, Scotland). Blood was removed from euthanised fish, centrifuged for 2 min, with plasma removed from the blood pellet and stored in cryotubes on dry ice for transport to SRUC. Full haematology and blood chemistry was conducted and analysed as discussed in Glencross et al. (2024) using standard assay kits on an auto-analyser and an automated chemistry analyser (Olympus Optical Co. Ltd., AU400, Tokyo, Japan).

3.2.7 Stable isotope analysis

To determine leucine incorporation, distribution and retention, 12g of ^{15}N labelled L-leucine (Cambridge Isotope laboratories, Inc.,^{15}N L-Leucine 98%, Tewksbury, USA) was added to the CD feed for the first 3 weeks of the trial only. This was

done to track and quantify ^{15}N labelled L-leucine over time and identify tissue specific retention. Liver, muscle, WB, and feed from the CD tanks were taken at week-3 and week-7, while faeces were only taken at week-3. Liver and muscle tissue were taken from 4 individual fish (*n*=12/ tank/ week) while WB were taken from homogenised pools containing 4 fish /pool (*n*=3 pools /week). Due to the low quantities required for these analyses, the feed was homogenised and separated into 4 pools of feed /week, with each pool contributing individually.

All samples were freeze-dried and additionally homogenised using a cleaned pestle and mortar. Less than 1 mg (0.5 mg) of sample was weighed into tin capsules, crushed, and placed into 96-well plates. This was then analysed at Scottish Universities Environmental Research Centre (SUERC, Glasgow, UK) for ^{15}N labelled l-leucine using continuous flow isotope ratio mass spectroscopy using a vario Pyrocube (Elementar Analysensysteme GmbH, Hanau, Germany) coupled to a Delta XP Plus IRMS (Thermo Fisher Scientific, Bremen, Germany) as discussed in Sabadel et al. (2025). International standards used were USGS40 (L-glutamic acid), IAEA305B (ammonium sulphate), and IAEA311 (ammonium sulphate enriched in 15N). Protein retention ratios:

$$\text{Ratio} = \frac{\delta^{15}\text{N Week-7}}{\delta^{15}\text{N Week-3}}$$

3.2.8 Molecular

3.2.8.1 RNA extraction and cDNA synthesis

RNA was extracted from muscle and liver tissues from each diet at week-3 (4 hr) and week-7 (-2 (0), 2, 4, 24 hr) as discussed in Huyben et al. (2021) Chapter 2 section 2.2.5.2. Briefly, 50-100 mg of muscle and liver tissue from two fish per tank per timepoint (*n*=6/ diet) were homogenised with 1 mL of TRI Reagent (Merck KGaA, TRI Reagent® T9424, Darmstadt, Germany) centrifuged at 12 000 g for 10 min, the supernatant added to 100 µl of BCP (1-bromo-3-chloropropane, Merck KGaA, B9673, Darmstadt, Germany), hand mixed for 15 s and incubated at room temperature for 15 min. After centrifuging at 20 000 g for 15 min (4 °C), 300-400 µL of aqueous upper phase was removed into new Eppendorfs, and approximately 200 µL RNA precipitation solution and 200 µL of isopropanol was

added, incubated at -20 °C for 10-30 min followed by centrifuging as before. The solution was discarded, and the RNA pellet was washed twice with 1 mL of 75% ice cold ethanol, rested for 15 min at room temperature and allowed to air dry before resuspension with 30-100 µL of RNase free water.

Quality and concentration were investigated using a Nanodrop ND-1000 spectrophotometer (Thermo Fisher Scientific, ND-1000, Loughborough, UK) ensuring all samples were within expected guidelines for 260/230 nm 260/280 ratios (above 2.0 and 1.8). In addition, all extracted RNA were run on 1% agarose gels (Merck KGaA (Sigma-Aldrich), Agarose, Darmstadt, Germany) with ethidium bromide (Merck KGaA (Sigma-Aldrich), ethidium bromide E7637, Darmstadt, Germany) to verify the two RNA bands.

Individual samples were prepared for cDNA synthesis by diluting with RNase free water to 200 ng/ µL (2 µg). Samples were denatured on a thermal cycler (Analytic Jena GmbH, Biometra Tadvanced, Jena, Germany) at 75 °C for 5 min, and 10 µL of Applied Biosystems™ High-Capacity cDNA Reverse Transcription (Thermo Fisher Scientific, Loughborough, UK) mastermix (MM) was added to 10 µL of sample RNA. Additionally, NTCs and RT-s were prepared and included. The thermal cycler conditions were 25 °C for 10 min, 37 °C for 120 min and 85 °C for 5 min. On completion, cDNA was diluted to 1:20 with RNase free water and stored at -20 °C.

Random cDNA samples and BCKDK primers were run on PCR to determine quality (contamination) with gels run using the product. Potential double bands were visible, and cDNA synthesis was then repeated using QuantiTect Reverse Transcription Kit (Qiagen Ltd., QuantiTect Reverse Transcription Kit, Manchester, UK) as the kit included integrated genomic DNA (gDNA) removal by including a gDNA Wipeout Buffer (S 3.5 -3.9).

Briefly, in preparation of the gDNA removal reaction, 2 µL of gDNA Wipeout Buffer (7x) was added to 2 µL of sample RNA (500 ng/µL), 10 µL RNase free water and incubated at 42 °C for 2 min. samples were then immediately stored on ice.

Qiagen Reverse-transcription MM was prepared according to protocol with 14 µL of RNA from the gDNA elimination step added to 1 µL Quantiscript Reverse

Transcriptase, 4 µL Quantiscript RT Buffer, (5x), and 1 µL RT Primer Mix. This was followed by incubation at 42 °C for 30 min and a final incubation of 3 min at 95 °C.

PCR was performed on random liver and muscle Qiagen cDNA (1:20), using a MM of MyTaq™ DNA Polymerase (Meridian Bioscience, London, UK) with BCKDHA and RRAG primers and run on a 1% agarose gel (S 3.5). Double bands were visible in liver tissue, implying unintended amplicons. Thermo cDNA and Qiagen cDNA were run on qPCR using the method and parameters in Chapter 2 and melt curves were examined (S 3.6 - 3.9). As most double bands in the gels appeared in liver cDNA samples, previous Thermo liver cDNA samples were used to examine qPCR melt curves for BCKDHA and BCKDK, with only BCKDHA melt curves successful. Whereas for Qiagen, a range of varying cDNA samples (4 liver and 1 muscle for each target) were run for BCKDHA, RRAG and BCKDK, with only the muscle sample in BCKDHA and RRAG having a successful melt curve using the Qiagen cDNA synthesis kit.

To try and identify whether there was an issue with the samples or whether it was the cDNA synthesis kits, additional PCRs were run. Liver samples consisted of 3 (*n*=3) Trial 1 Thermo cDNA liver samples, 3 (*n*=3) current (Trial 2) Thermo cDNA samples and 3 (*n*=3) Trial 2 Qiagen method cDNA samples. The first set of primer aliquots were used as well as new BCKDHA primer aliquots which were prepared to see if there was an issue with the primers. This was achieved by running the 9 Thermo and Qiagen samples (*n*=9) using the freshly diluted primer aliquots of BCKDHA primers and 6 Thermo and Qiagen samples (*n*=6) using the older set of primers. It appeared that regardless of the primers, Qiagen cDNA liver samples did not work. Going forward, all further analyses were conducted on Thermo cDNA synthesised samples.

3.2.8.2 Standard preparation

Standards were prepared as discussed Chapter 2.2.5, briefly, serial dilutions of plasmid BCKDHA ranging from 10^9 to 10^1 molecules/µL were prepared and run on qPCR. A qPCR MM consisting of 5 µl Luminaris HiGreen qPCR Master Mix (Thermo Fisher Scientific, Loughborough, UK) 0.5 µl of each primer and 1.5 µl

Table 3.4 qPCR program for BCKDHA (qTower3/G real-time PCR Thermal Cycler, Analytic Jena GmbH, Jena, Germany).

Step	Temperature (°C)	Time (m:s)	Go to	Loops
1	50	02:00	0	0
2	95	10:00	0	0
3	95	00:15	0	0
4	58	00:30	0	0
5	72	00:30	3	34
6	60	00:06	6	35

Nuclease free water was prepared with 2.5 µL pooled muscle and liver cDNA subsequently added. NTCs were included at every 10th sample and qPCR was run on qTower^3/G real-time PCR Thermal Cycler (Analytic Jena GmbH, Jena, Germany) using the qPCRsoft program (Table 3.4).

Melt curves were examined for quality and to identify the best dilutions to run the standards, in this case 10^7 to 10^1 molecules/µL. BCKDHA plasmid dilution 10^8 was quantified using a Qubit® 2.0 Fluorometer (Qubit® 2.0 Fluorometer, Invitrogen, Paisley, United Kingdom) and Qubit™ dsDNA high sensitivity (HS) Quantification Assay Kits (Invitrogen Thermo Fisher Scientific Inc., Eugene, USA). This result (ng/ µL) was then used to determine the DNA copy number/ µL as previously discussed in Chapter 2.2.5.

3.2.8.3 Absolute RT-qPCR

Muscle and liver tissue mRNA transcripts of BCKDHA were quantified using Luminaris HiGreen qPCR Master Mix (Thermo Fisher Scientific, Loughborough, UK), as described previously. cDNA from NA, NL, PL and CD diets at week-3 (4 hr post-prandial) and week-7 (-2 (0), 4, 24 hr post-prandial) were run in triplicate on 96-well plates, in addition to STDs, NTCs and RT-s with each tissue run on its own individual plate. A qPCR MM was prepared as discussed in section 2.2.5, with 1 µL of cDNA (1:20) added to 9 µL of MM (3 µL Nuclease free water). Templates were prepared using the qTower^3/G real-time PCR Thermal Cycler (Analytic Jena GmbH, Jena, Germany) qPCRsoft software program with samples (*n*=72) identified as a separate group to the STDs. qTower^3/G results of the Cts were analysed and transformed into copy number estimates as described previously. Relative qPCR data is based on a ratio/ fold change relative to

housekeeping genes (controls) whereas absolute qPCR provided precise absolute direct quantification of the samples in known units. In addition to the data, relative qPCR was avoided due to possible fluctuations in reliability and stability of reference genes (Kuhlmann et al., 2021).

3.2.9 Statistical analysis

All data values represent means and were expressed as mean ±standard deviation (SD) unless otherwise stated. Significance thresholds were set at p=<0.05 with recognition of near significance at p=<0.10. Data were subjected to normality tests (Anderson-Darling) and Grubbs' test for outliers (p=<0.05). One-way ANOVA was used to determine differences within data sets, 2-sample t tests were used to determine differences in means between 2 groups and General linear models (GLM) were used to determine relationships between factors and the response, and interactions between them. Fisher's LSD *post-hoc* tests were used to identify the location of the differences for the statistical analyses. All statistical analysis was undertaken using Minitab (Minitab Ltd., Minitab v18.1, Coventry, UK).

3.3 Results

3.3.1 Feed

3.3.1.1 Formulation, composition and amino acid analysis of feeds and ingredients

Feeds were formulated to try and determine whether leucine had an impact on growth. All diets were isocalorific, with an additional 18.7% fish oil included to equate to a total dietary lipid content of 20%. Diets were also formulated to be isoproteic to contain 50% protein (Table 3.3). Only 6 AAs were formulated and included at different levels in each of the diets, the three BCAAs and three NEAAs, all other ingredients and AAs were included in each diet at the same rate. cAAs were included at a total of 21% across all diets and added to a basal diet mix. The CD was formulated according to commercial feeds, with total formulated

BCAAs were isoleucine 1.6%, leucine 2.7% and valine 1.8%. When comparing the BCAAs in formulated feeds to the CD formulation, NA had 31% less isoleucine, 22% less leucine and 33% less valine. NL had 22% less leucine, and the PL had 85% more leucine than the CD. bAA analysis of the feeds displayed similar change (%) from the CD. NA had 28% less isoleucine, 22% less leucine and 29% less valine. NL had 21% less leucine, 8% more valine while PL had 1% less isoleucine, 4% more valine and 83% more leucine than the CD.

The BCAA results when compared to the formulations had an increase of 0.2 g/100g isoleucine (13-20%), 0.2-05 g/100g increase in leucine (9-12%) and 0.3-0.4 g/100g increase in valine (14-23%).

NEAAs were used to increase protein levels (nitrogen) so that all diets contained similar formulations (Table 3.3). Serine, alanine and glycine were used to bulk up the shortfalls. The CD diet had inclusion levels of 5.7g for alanine and 5.9 g/100g for both glycine and serine. In the NA, alanine and glycine were included at 6.3g/100g and serine at 6.5 g/100g. NL had inclusion levels of alanine at 5.9 g/100g, glycine and serine at 6.1 g/100g. PL diet had the lowest inclusion levels of the three NEAAs with alanine included at 4.9 g/100g, glycine at 5.2 g/100g and serine at 5.1 g/100g.

Table 3.5 Proximate analysis of test feeds and ingredients.

Dry matter basis %	Moisture %	Ash %	Protein %	Lipid %	CF %	Energy MJ/kg	NFE %
Diet composition							
NA	9.40	6.11	53.24	19.12	1.39	23.48	21.66
NL	9.35	6.39	53.28	19.22	1.49	23.68	20.86
PL	9.38	6.13	52.53	20.36	1.97	23.95	20.40
CD	9.45	6.28	54.39	20.41	0.68	23.64	19.01
Ingredient composition							
Fishmeal (Anchovy-SP)	8.61	16.29	72.27	12.52		20.50	
Wheat gluten (Biomar)	4.37	0.86	79.54	7.35		23.19	11.41
SPC	8.14	6.90	64.22	1.41		19.95	23.65
SPI	8.89	4.93	89.43	2.91		22.26	
Pregel/dextrose	8.87	0.02	2.96	*		*	
Cellulose	4.72	*	2.52	*		16.88	
ALA	0.02	0.08	96.55	*		17.86	
GLY	0.02	*	114.95	*		12.75	
SER	0.01	*	82.51	*		13.36	

All values are percentages (%) dry matter basis (DM%) unless otherwise stated. CD= Control diet, NA=Negative BCAAs, NL= Negative Leucine and PL= Positive Leucine. CF= crude fibre, NFE= Nitrogen-free extract.

As a comparison, the change (%) in each diet formulation compared to the CD formulation showed that the NA had an increase in alanine, glycine and serine above the CD levels of 11%, 7% and 10%.

NL had an increase above CD formulation levels of 4%, 3% and 3% for alanine, glycine and serine. While PL diet formulation had a decrease below CD formulated levels in alanine, glycine and serine (14%, 12% and 14%).

Analysis of the feeds showed similar values as the formulated bNEAAs although across all the diets glycine values appeared to be higher than expected (Table 3.5, 6, 7). When examining the change (%) in each analysed diet compared to the formulated diets, glycine results were between 15-28% higher than the glycine in the formulated feeds. This equated to 0.8-1.7 g/100g difference.

3.3.1.2 Digestibility of amino acids, protein and lipids

Diets were prepared using a basal mix to which varying levels of AAs were added totalling 21% of overall contribution to each diet. PL and NL diets had higher digestibilities than CD and NA for lysine, methionine and valine (Table 3.8). PL and CD diet had the highest different digestibility for lipids, with CD the lowest for tyrosine. PL had the highest different digestibility for isoleucine and leucine. All DADCs were above 90% across board apart from tyrosine in the CD with 87% digestibility, compared to 90% for the other diets. The highest digestibility across all diets was seen for alanine 98-99%. Near significance ($p \leq 0.10$) was observed for proline ($p=0.057$).

3.3.2 Fish

3.3.2.1 Water quality, feed intake and growth

Monitored water quality parameters were 13.0 ±0.7 °C, pH 7.3 ±0.1, dissolved oxygen 109.8 ±6.0 %, ammonia: N (TAN) 0.2 ±0.2 mg /L, ammonia (NH_3) 0.3 ±0.2 mg /L, ammonium (NH_4^+) 0.3 ±0.2 mg /L, nitrite (NO_2^-–N) 0.3 ±0.1 mg/ L N, nitrate (NO_3^-–N) 6.4 ±1.3 mg/ L N (S 3.1). Chloride: Nitrite–N ratios were maintained above >20:1 and ranged from 260:1 to 440:1, with the lowest ratio on the 19NOV19. Alkalinity ranged from 30–300 mg/L $CaCO_3$, with a possibility of

Table 3.6 Ingredient composition and AA analysis of feed ingredients.

Dry matter basis %	Anchovy-SP	WG	SPC	SPI	Pregel/Dextrose	Cellulose	b-ALA	GLY	SER
Ingredient composition									
Moisture %	8.61	7.26	7.98	8.89	8.87	4.72	0.02	0.02	0.01
Ash %	16.29	0.86	6.90	4.93	0.02	*	0.08	*	*
Protein %	72.27	79.54	64.22	89.43	2.96	2.52	96.55	114.95	82.51
Energy (MJ/kg)	20.50	23.19	19.95	22.26	*	16.88	17.86	12.75	13.36
Ingredient AA composition (dry matter basis) %									
Sum of AA	75.53	75.24	67.02	94.78	1.50	1.52	82.85	110.33	111.47
Alanine	5.03	1.74	2.80	3.88	*	*	*	*	*
b-Alanine	0.13	0.39	0.07	0.04	*	*	81.80	*	0.10
Arginine	4.71	2.97	5.40	7.65	0.00	0.00	0.00	0.00	0.00
Asparagine	7.54	2.08	7.13	9.87	0.00	0.00	0.00	0.00	0.00
Cysteine	0.54	1.62	0.89	1.04	0.00	0.00	0.00	0.00	0.00
Glutamate	10.64	25.17	11.78	17.09	0.24	0.00	0.00	0.32	0.36
Glycine	4.66	2.66	3.06	4.10	0.04	0.04	0.03	108.79	0.10
Histidine	2.42	1.73	1.85	2.56	0.00	0.00	0.00	0.00	0.00
Isoleucine	3.69	3.13	3.67	5.16	0.41	0.36	0.31	0.36	0.33
Leucine	7.38	6.53	6.64	9.50	0.06	0.05	0.04	0.06	0.05
Lysine	6.69	1.31	4.13	6.01	0.23	0.23	0.20	0.21	0.27
Methionine	2.47	1.45	1.12	1.54	0.12	0.36	0.08	0.10	0.21
Phenylalanine	2.27	3.04	2.69	3.63	0.10	0.12	0.07	0.08	0.08
Proline	3.27	9.25	3.52	4.96	0.00	0.00	0.06	0.00	0.22
Serine	2.99	3.99	3.47	5.07	0.00	0.00	0.00	0.00	109.38
Taurine	0.70	0.00	0.00	0.00	0.00	0.00	0.00	0.00	0.00
Threonine	3.29	1.81	2.26	3.28	0.00	0.00	0.00	0.00	0.00
Tyrosine	2.70	3.15	2.85	4.09	0.23	0.28	0.21	0.33	0.27
Valine	4.40	3.24	3.70	5.31	0.08	0.09	0.05	0.08	0.08

All values are percentages (%) unless otherwise stated. CD= Control diet, NA=Negative BCAAs, NL= Negative Leucine and PL= Positive Leucine

Table 3.7 Amino acid analysis of test feeds (g/100g or %).

	CD	NL	NA	PL	P-value	Two-way ANOVA P -value		
						Diet	Batch	D*B
Dry matter basis (%)								
Protein	54.39±0.65	53.28±0.59	53.24±0.11	52.53±0.26				
Sum of AA	49.11±0.02	49.62±0.02	49.07±0.05	48.01±0.07				
Alanine	1.27±0.04	1.28±0.02	1.27±0.02	1.24±0.04	0.307 (f 3, 12= 1.34)	0.386 (f 3, 8= 1.15)	0.944 (f 1, 8= 0.01)	0.548 (f 3, 8= 0.76)
b-Alanine	4.97±0.26 [b]	5.00±0.26 [b]	5.30±0.05 [a]	3.79±0.12 [c]	**0.000** (f 3, 12= 46.34)	**0.000** (f 3, 8= 262.08)	0.977 (f 1, 8= 0.00)	**0.000** (f 3, 8= 19.95)
Arginine	2.48±0.03	2.51±0.03	2.45±0.07	2.38±0.13	0.158 (f 3, 12= 2.07)	0.251 (f 3, 8= 1.66)	0.691 (f 1, 8= 0.17)	0.698 (f 3, 8= 0.49)
Asparagine	2.71±0.02	2.77±0.04	2.72±0.04	2.70±0.09	0.240 (f 3, 11= 1.63)	0.244 (f 3, 8= 1.70)	0.758 (f 1, 8= 0.10)	0.848 (f 3, 8= 0.27)
Cysteine	0.13±0.01	0.21±0.04	0.19±0.06	0.18±0.05		0.218 (f 3, 8= 1.84)	0.951 (f 1, 8= 0.00)	0.779 (f 3, 8= 0.37)
Glutamate	6.44±0.03	6.51±0.05	6.43±0.10	6.30±0.24	0.410 (f 3, 12= 1.04)	0.517 (f 3, 8= 0.82)	0.474 (f 1, 8= 0.56)	0.820 (f 3, 8= 0.31)
Glycine	7.27±0.18 [a]	7.78±0.47 [a]	7.64±0.27 [a]	5.96±0.49 [b]	**0.000** (f 3, 12= 14.78)	**0.000** (f 3, 8= 25.76)	0.975 (f 1, 8= 0.00)	**0.044** (f 3, 8= 4.30)
Histidine	0.90±0.04	1.00±0.10	1.03±0.13	0.95±0.09	0.344 (f 3, 12= 1.22)	0.225 (f 3, 8= 1.80)	**0.023** (f 1, 8= 7.90)	0.643 (f 3, 8= 0.58)
Isoleucine	1.84±0.11 [a]	1.84±0.13 [a]	1.32±0.19 [b]	1.82±0.16 [a]	**0.001** (f 3, 12= 11.56)	**0.007** (f 3, 8= 8.65)	0.911 (f 1, 8= 0.01)	0.810 (f 3, 8= 0.32)
Leucine	2.99±0.02 [b]	2.35±0.04 [c]	2.32±0.05 [c]	5.46±0.25 [a]	**0.000** (f 3, 12= 971.56)	**0.000** (f 3, 8= 483.73)	0.475 (f 1, 8= 0.56)	0.535 (f 3, 8= 0.79)
Lysine	2.80±0.12	2.94±0.04	2.86±0.08	2.75±0.12	0.074 (f 3, 12= 2.98)	0.161 (f 3, 8= 2.24)	0.823 (f 1, 8= 0.05)	0.812 (f 3, 8= 0.32)
Methionine	1.27±0.11	1.33±0.07	1.27±0.09	1.33±0.09	0.649 (f 3, 12= 0.56)	0.735 (f 3, 8= 0.43)	0.703 (f 1, 8= 0.16)	0.789 (f 3, 8= 0.35)
Phenylalanine	1.52±0.02	1.55±0.02	1.53±0.05	1.52±0.07	0.663 (f 3, 12= 0.54)	0.765 (f 3, 8= 0.39)	0.963 (f 1, 8= 0.00)	0.892 (f 3, 8= 0.20)
Proline	1.33±0.02	1.37±0.02	1.36±0.02	1.32±0.05	0.119 (f 3, 11= 2.44)	0.153 (f 3, 8= 2.41)	0.259 (f 1, 8= 1.51)	0.620 (f 3, 8= 0.63)
Serine	6.07±0.59 [ab]	5.73±0.23 [bc]	6.76±0.59 [a]	5.15±0.54 [c]	**0.006** (f 3, 12= 6.89)	**0.020** (f 3, 8= 5.92)	0.240 (f 1, 8= 1.61)	0.870 (f 3, 8= 0.23)
Taurine	0.53±0.01	0.54±0.02	0.52±0.02	0.50±0.03	0.097 (f 3, 12= 2.64)	0.062 (f 3, 8= 3.70)	0.693 (f 1, 8= 0.17)	0.104 (f 3, 8= 2.87)
Threonine	1.48±0.09 [bc]	1.59±0.05 [a]	1.52±0.07 [ab]	1.39±0.07 [c]	**0.005** (f 3, 12= 7.24)	**0.002** (f 3, 8= 13.13)	0.251 (f 1, 8= 1.53)	**0.050** (f 3, 8= 4.07)
Tyrosine	1.08±0.01 [b]	1.11±0.01 [ab]	1.15±0.03 [a]	1.11±0.04 [ab]	**0.026** (f 3, 12= 4.40)	0.097 (f 3, 8= 2.97)	0.868 (f 1, 8= 0.03)	0.995 (f 3, 8= 0.02)
Valine	2.05±0.18 [a]	2.21±0.07 [a]	1.45±0.15 [b]	2.13±0.27 [a]	**0.000** (f 3, 12= 14.18)	**0.004** (f 3, 8= 10.21)	0.839 (f 1, 8= 0.04)	0.894 (f 3, 8= 0.20)
Alanine ±b-Ala	6.19±0.23 [b]	6.28±0.27 [ab]	6.56±0.07 [a]	5.03±0.16 [c]	**0.000** (f 3, 12= 46.17)	**0.000** (f 3, 8= 148.50)	0.645 (f 1, 8= 0.23)	**0.004** (f 3, 8= 10.12)

All values are percentages (%) unless otherwise stated. Values are means ±standard deviation. Different subscripts denote significant difference among diets (*abc*) (p<0.05). CD= Control diet, NA=Negative BCAAs, NL= Negative Leucine and PL= Positive Leucine

Table 3.8 Digestibility Coefficients of the test diets (DADC values) week-3 at 8 hr.

	CD	NL	NA	PL	P-value
Crude protein	0.93±0.01	0.94±0.01	0.94±0.00	0.94±0.01	0.776 (f 3, 7= 0.37)
Lipid	0.95±0.00 [a]	0.92±0.01 [bc]	0.91±0.00 [c]	0.94±0.02 [ab]	**0.010 (f 3, 8= 7.56)**
Alanine	0.92±0.01	0.94±0.01	0.93±0.01	0.94±0.01	0.120 (f 3, 8= 2.65)
Arginine	0.96±0.01	0.97±0.00	0.97±0.01	0.98±0.01	0.145 (f 3, 8= 2.38)
Asparagine	0.92±0.02	0.95±0.00	0.93±0.01	0.95±0.02	0.189 (f 3, 8= 2.02)
b-Ala	0.95±0.01	0.97±0.00	0.96±0.00	0.97±0.01	0.113 (f 3, 8= 2.75)
Glutamate	0.97±0.01	0.98±0.00	0.97±0.00	0.98±0.01	0.145 (f 3, 8= 2.38)
Glycine	0.96±0.01	0.97±0.00	0.97±0.00	0.97±0.01	0.348 (f 3, 8= 1.27)
Isoleucine	0.94±0.01 [bc]	0.95±0.01 [ab]	0.92±0.00 [c]	0.96±0.01 [a]	**0.017 (f 3, 8= 6.30)**
Leucine	0.94±0.01 [b]	0.95±0.01 [b]	0.94±0.00 [b]	0.98±0.01 [a]	**0.001 (f 3, 8= 16.31)**
Lysine	0.92±0.02 [b]	0.95±0.00 [a]	0.94±0.01 [ab]	0.95±0.01 [a]	**0.049 (f 3, 8= 4.09)**
Methionine	0.92±0.01 [b]	0.94±0.01 [a]	0.94±0.00 [ab]	0.95±0.01 [a]	**0.022 (f 3, 8= 5.66)**
Phenylalanine	0.93±0.02	0.93±0.01	0.93±0.00	0.95±0.02	0.221 (f 3, 8= 1.82)
Proline	0.91±0.02	0.94±0.01	0.93±0.00	0.94±0.01	0.057 (f 3, 8= 3.83)
Serine	0.97±0.01	0.98±0.00	0.98±0.01	0.97±0.01	0.404 (f 3, 8= 1.10)
Threonine	0.91±0.02	0.94±0.01	0.93±0.01	0.94±0.02	0.176 (f 3, 8= 2.12)
Tyrosine	0.87±0.02 [b]	0.90±0.02 [a]	0.90±0.00 [a]	0.90±0.01 [a]	**0.047 (f 3, 8= 4.19)**
Valine	0.92±0.01 [b]	0.94±0.00 [a]	0.91±0.01 [b]	0.95±0.01 [a]	**0.005 (f 3, 8= 9.55)**

*Cysteine, histidine and taurine were not analysed. Data are expressed as mean ±standard deviation and different superscripts indicate significant differences (p=<0.05). Analysis was performed using one-way ANOVA, with Fisher LSD method used for *post-hoc* examination. Values represent means ±standard deviations.

reduced resilience to acidification on the 14NOV19 when alkalinity was at its lowest at 30 mg/ L. In addition to system monitoring, visual monitoring identified elevated turbidity (cloudy) and suspended solids (SS) onwards from week-3 sampling point. Increased system-wide water changes were conducted.

3.3.2.1.1 Weight gain

On start-up (week-0), a one-way ANOVA was used to determine that there were no differences in salmon parr biomass (live bulk weight) between the tanks (p=0.294). Similarly at trial end, biomass was compared with no differences noted between the diets (p=0.723). A GLM was used to determine any differences in total biomass between week-0 and week-7, and an interaction between diet and week (D*W). No differences were seen across diet (p=0.779) or the interaction D*W (p=0.573), but a difference of week was observed (p=0). A one-way ANOVA determined differences between the diets for mean total live weight gain/ fish (bulk weights). No differences were noted between start weights (week-0) and week-3 (p=0.514), although the largest observed weight gain was seen in PL and the lowest in NL (9.6 ±0.3 g and 7.9 ±0.8 g).

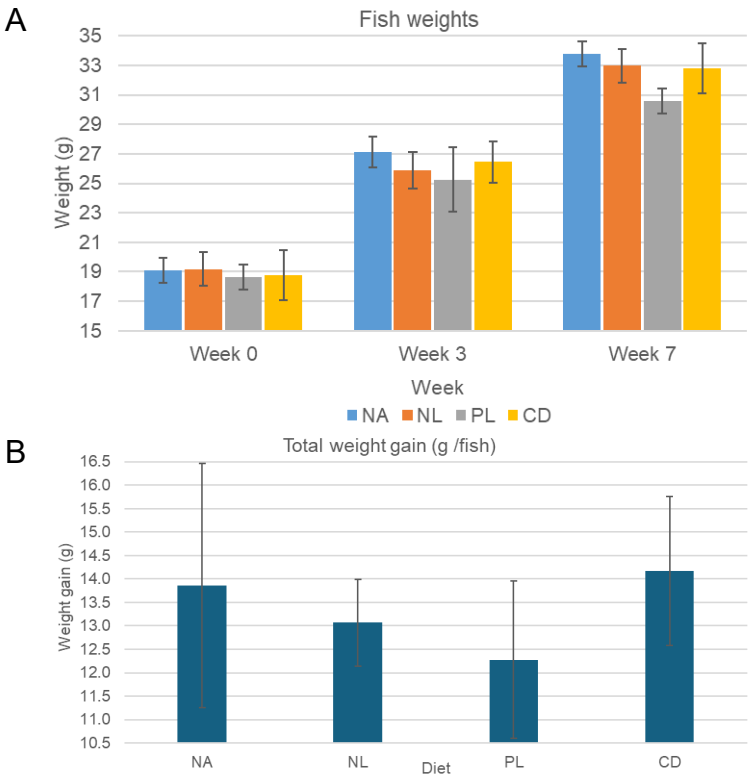


Figure 3.1 Growth parameters based on bulk weighing A) mean individual weight at week-0, week-3 and week-7 B) total weight gain (g/ fish) between diets over the 7-week period. All values are means ±standard deviation. Analysis was performed using one-way ANOVA, with Fisher's LSD method used for *post-hoc* examination. CD= Control diet, NL= Negative leucine, NA= Negative All, PL= Positive leucine.

Weight gain between week-3 and week-7 similarly displayed no differences (p=0.243) with the largest gains in CD and the lowest in PL (5.2 ±1.0 g and 2.6±1.6 g) (Figure 3.1 A). Total weight gain over the whole 7-week period had no differences between diets (p=0.595), but the largest overall weight gain was seen in CD and the lowest in PL (14.2 ±1.6 g, 12.3 ±1.7 g) (Figure 3.1 B). The live weight gain (g /fish) took into consideration the number of fish removed at each sampling point. No differences were noted for final live bulk weights between diets (p=0.437).

The heaviest fish were in NA and CD (33.0 ±2.3 g and 33.0 ±1.5 g) with the lightest fish in the PL diet (30.9 ±1.6 g). Initial stocking density for 120 fish/tank was an average of 3.2kg ±0.07/m^3 with a final stocking density average for 112 fish/tank at 5.2 ±0.24 kg/m^3.

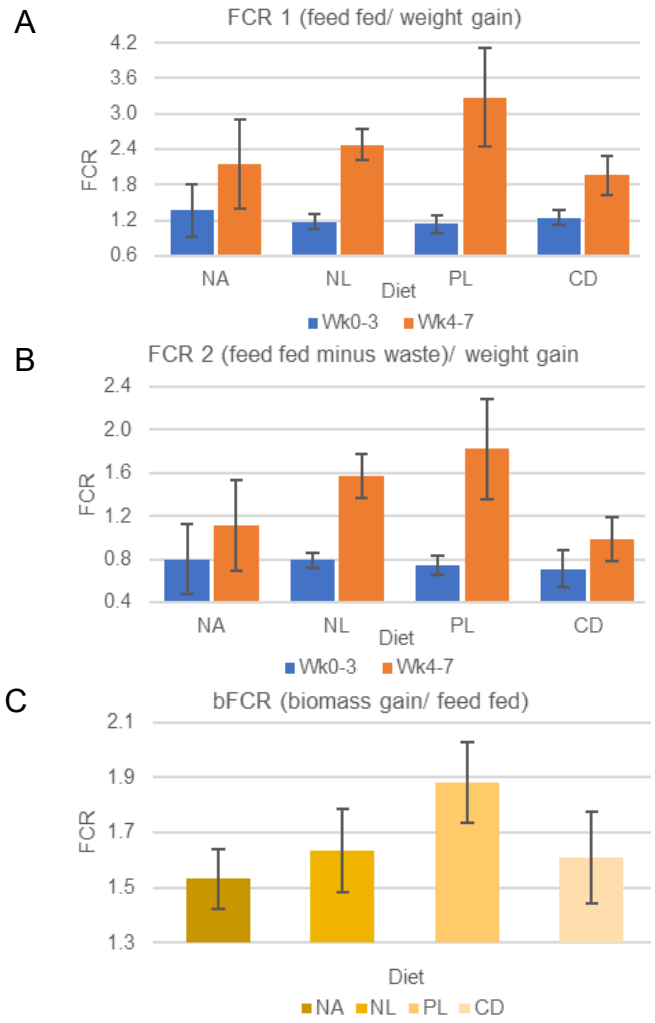


Figure 3.2 Feed conversion ratios (FCR) A) FCR 1 Feed fed/ weight gain B) FCR 2 (feed fed-waste feed)/weight gain C) biological FCR (total biomass/ feed fed). CD= Control diet, NL= Negative leucine, NA= Negative All, PL= Positive leucine

3.3.2.1.2 FCR

Feed Conversion Rate (FCR) was determined via three different methods (Figure 3.2). FCR 1 was feed fed/ weight gain (Figure 3.2 A), FCR 2 was (feed fed-waste)/ weight gain (Figure 3.2 B) and bFCR (biological FCR) was (biomass 2 – biomass 1)/feed fed (Figure 3.2 C). All FCRs followed a similar trend, with overall better FCRs in the first half of the trial (week-0 to week-3) in comparison to the second half (week-4 to week-7), with the PL diet having the worst overall FCR and the highest variability. Over the first 3 weeks, FCR 1 ranged from 1.4 ±0.4 in the NA to a low of 1.1 ±0.2. FCR 2 ranged from 0.8 ±0.1 in NL to 0.7 ±0.1 in PL. When looking at the FCRs for week 4-7, FCR 1 had a high of 3.3 ±0.8 in PL and

a low of 2.0 ±0.3 in the CD diet. FCR 2 had a high of 1.8 ±0.5 in PL and a low of 1.0 ±0.2 in the CD diet. bFCRs over the whole period had a similar trend to weeks 4-7, with a high of 1.9 ±0.1 in PL and a low of 1.5 ±0.1 for NA. The poor FCR over the second stage of the trial (week-4 to week-7) may have been a result of the reduced growth experienced over this period (Figure 3.2).

3.3.2.2 Morphometric and somatic indices

3.3.2.2.1 Bulk weights, individual lengths and weights

At week-3, fish were starved for 24 hr and then fed their respective diets before sampling 4 hr post-prandial. Each tank was bulk weighed, 8 fish from each tank euthanised, individually weighed and fork length was taken. Of the 8 fish euthanised, 4 fish were randomly selected for further sample selection. There were no differences in bulk weights between diets (p=0.515), but the NA diet had the highest average weight (27.1 ±1.0 g) and the PL diet the lowest (25.2 ±2.2 g).

No differences were observed for individual weights and lengths (p=0.308, p=0.544) but NL diet had the highest mean individual weights and PL the lowest (25.6 ±3.3 g, 23.5 ±4.3 g). Individual lengths had a similar trend, with the NL diet having the highest mean lengths, both PL and CD the lowest (12.9 ±0.6 cm, 12.6 ±0.7 cm). There was a large range of variability in the individual fish across treatments, with ranges in weight from 12.6 to 34.1 g and in length from 11.1 to 14.4 cm.

At week-7, a similar sampling procedure was carried out as week-3, although a total of 24 individuals per tank were euthanised over the 5 timepoints. Four individual samples were taken at all timepoints apart from the 4 hr timepoint whereby 8 individuals were sampled. Similarly to week-3, no differences between diets for individual weights and lengths were observed (p=0.147, p=0.293) but CD diet had the highest individual mean weights and PL the lowest (34.2 ±5.4 g, 30.8 ±5.6 g).

A GLM was used to determine differences in individual weights and lengths between diets, time and the interaction between them (D*T). A difference was observed for weight means between diets with Fisher's LSD post-hoc analysis

Table 3.9 Individual variation in total weights and lengths across the sampled fish 4 hr post-prandial.

Week	Fish	Weight	Variation	Length	Variation
	(#)	(g)	(%)	(cm)	(%)
Week 0	36	18.9 ±3.0	15.8	12.1 ±2.7	22.2
Week 3	96	24.8 ±4.1	16.3	12.7 ±0.7	5.4
Week 7	96	32.5 ±5.2	16.1	14.4 ±7.2	50.0

indicating that the NA diet was different to the other three diets (p=0.002). The NA diet had a mean weight of 34.2 ±5.2 g and the PL diet had the lowest with 30.9 ±4.6 g. In all 4 diets, there was large individual variability amongst fish, with maximum ranges between 41.8 g in NL to 45.4 g in NA and CD diets. The minimum ranges across treatments were from 19.9 g for NL and CD to 21.1 g for NA and PL. When comparing the combined treatment weekly individual lengths and weights across all treatments, variation in weight was stable (15.8-16.3%) whereas a large variation in lengths occurred (5.4-50%) (Table 3.9). Similarly, near significance (p≤ 0.10) was observed between diets when comparing lengths (*p*=0.096) with *post-hoc* analysis suggesting differences between NA and PL diets.

The means of the two diets were similar with NA means of 14.1 ±0.8 cm and PL 13.8 ±0.7 cm. Maximum lengths ranged from 15.3 cm in PL to 16.0 cm in NL and minimum lengths had a low of 11.5 cm in both NL and CD to 12.2 cm in PL. Near significance was observed using one-way ANOVA for the week-7 mean bulk weights (*p*=0.052) with NA having the largest mean weights and PL the lowest (33.8 ±0.9 g, 30.6 ±0.9 g).

3.3.2.2.2 Length weight relationships

Length weight relationships were used to try and decipher the overall type of growth and shape of fish. The *a*-values were used to determine the type of body shape between the two sampling times. In Table 3.10 and 3.11, *a*-values in week-3 across the diets were indicative of fusiform fish (*a-value*= 0.01) compared to the fish in week-7 that appeared to with eel-like bodies (*a-value*= 0.001).

Table 3.10 Individual morphometric indices between week-3 and week-7 fish at 4 hr post-prandial (*n*=8 /diet).

	CD	NL	NA	PL	One-way ANOVA P-value	Two-way ANOVA P-value		
						Diet	Week	D*W
Weight (g)								
Week 3	25.0±4.0	25.6±3.3	25.2±4.5	24.0±3.7	0.541 (f 3, 91= 0.72)			
Week 7	34.2±5.4	32.5±4.9	33.6±5.8	30.8±5.6	0.147 (f 3, 92= 1.83)			
Length (cm)								
Week 3	12.6±0.7	12.9±0.6	12.7±0.8	12.7±0.7	0.561 (f 3, 91= 0.69)			
Week 7	14.2±0.7	13.9±0.7	14.0±0.7	13.8±0.8	0.293 (f 3, 92= 1.26)			
L*W 'b'								
Week 3	2.7	2.6	2.9	2.6				
Week 7	3.2	3.0	3.1	3.1				
Total	2.8	2.9	3.0	2.9				
L*W 'a'								
Week 3	0.025	0.031	0.017	0.032				
Week 7	0.006	0.011	0.009	0.009				
Total	0.020	0.014	0.012	0.017				
K								
Week 3	1.23±0.05 ^{z}	1.19±0.05 ^{yx}	1.21±0.06 ^{zy}	1.18±0.06 ^{x}	**0.010** (f 3, 91= 4.03)	**0.000**	0.195	0.111
Week 7	1.19±0.05 ^{y}	1.19±0.05 ^{zy}	1.22±0.08 ^{z}	1.16±0.05 ^{y}	**0.005** (f 3, 92= 4.51)			
Kr								
Week 3	1.02±0.04 ^{z}	0.99±0.04 ^{yx}	1.01±0.05 ^{zy}	0.98±0.05 ^{x}	**0.008** (f 3, 91= 4.20)	**0.000**	0.961	0.143
Week 7	1.00±0.04 ^{y}	1.01±0.04 ^{zy}	1.03±0.07 ^{z}	0.98±0.04 ^{y}	**0.007** (f 3, 92= 4.35)			
Total	1.01±0.05 ^{zy}	1.00±0.04 ^{yx}	1.02±0.06 ^{z}	0.98±0.05 ^{x}				

K<1 = thin/ undernourished, K>1 related to fattiness (species dependant) (lipid content/energy reserves in salmonids) Kr relative condition compared to the study population 'the deviation of an individual from the average weight for length Kr>1 = good, <1 = bad, L/W a=0.01 fusiform, a= 0.001 eel-like, a=0.1 spherical, b=3 isometric growth, b=>3 positive allometric, b=<3 negative allometric

Table 3.11 Length weight relationships between week-3 and week-7.

Diet		Length and weight equations	R2 Value
Week 3			
	Combined	$W=0.0255 \times L^{2.7037}$	0.910
	CD	$W=0.0251 \times L^{2.7185}$	0.934
	NL	$W=0.0303 \times L^{2.6203}$	0.901
	NA	$W=0.0174 \times L^{2.8582}$	0.931
	PL	$W=0.0317 \times L^{2.6086}$	0.910
Week 7			
	Combined	$W=0.008 \times L^{3.1493}$	0.908
	CD	$W=0.0062 \times L^{3.243}$	0.927
	NL	$W=0.0106 \times L^{3.0441}$	0.942
	NA	$W=0.0089 \times L^{3.1197}$	0.858
	PL	$W=0.0086 \times L^{3.1158}$	0.942

Week-3 n=8, week-7 n=24/ diet. a-value 0.01 fusiform fish, a-value 0.001 eel-like fish, a-value 0.1 spherical shaped fish. b-value ±3 isometric growth, b-value >3 positive allometric growth, b-value<3 negative allometric growth. Combined = total population. CD= Control diet, NL= Negative leucine, NA= Negative All, PL= Positive leucine

NL was the exception, with a more fusiform body shape (*a-value*=0.0106). The *b*-values were used to determine growth type, with all diets at week-3 having negative allometric growth (*b*-value=<3) whereas in week-7 all diets had positive allometric growth (*b*-value=>3). NL diet in week-7 had the closest *b*-value to isometric growth, 3.0441, compared to the CD with the highest allometric growth, 3.2430. Le Cren's relative condition factor (*Kr*) was used to measure any individual differences from the average weight for that length. Differences in diets for week-3 and week-7 were seen (p=0.008, p=0.007). Fisher' s *post-hoc* indicated that the difference in diet means at week-3 had the highest *Kr*-value in CD which was different to NL and PL. At week-7, NA had the highest different mean *Kr*-value compared to CD and PL. A GLM was used looking at the differences in means between diet, week and the interaction (D*W). A significant difference in diet was observed, with *post-hoc* analysis distinguishing differences between the highest Kr-values in NA to the lowest in NL and PL.

Fulton's Condition factor (*K*-factor) was used as an indicator for weight or fattiness, assuming that the lower the value from 1, the lower the individual body weight of the fish or condition. *K*-factor worked on the assumptions of cube law, whereby weight may vary as the cube of length. The diets were compared to each other at week-3 and week-7 and were statistically different (p=0.010, p=0.005).

Table 3.12 Somatic indices compared between diets and sampling points.

	CD	NL	NA	PL	One-way Anova P-Value	Two-way ANOVA P-Value		
Week 3						Diet	Week	D*W
Weight (g)	25.0±4.0	25.6±3.3	25.2±4.5	23.5±4.3	0.308 (f 3, 92= 1.22)	**0.050** (f 3, 184= 2.36)	**0.000** (f 1, 184= 131.91)	0.632 (f 3, 184= 0.57)
Length (cm)	12.6±0.7	12.9±0.6	12.7±0.8	12.6±0.7	0.544 (f 3, 92= 0.72)	0.480 (f 3, 184= 0.83)	**0.000** (f 1, 184= 150.44)	0.325 (f 3, 184= 1.16)
Liver (g)	0.3±0.1	0.3±0.1	0.3±0.1	0.2±0.1	0.101 (f 3, 44= 2.20)	**0.009** (f 3, 86= 4.09)	**0.002** (f 1, 86= 10.62)	0.924 (f 3, 86= 0.16)
Viscera (g)	2.8±0.5 ^{z}	2.4±0.4 ^{y}	2.7±0.3 ^{z}	2.2±0.3 ^{y}	**0.002** (f 3, 44= 5.96)	**0.004** (f 3, 88= 4.09)	**0.000** (f 1, 88= 38.42)	0.933 (f 3, 88= 0.14)
Viscera fat (g)	0.4±0.2	0.4±0.1	0.4±0.1	0.4±0.1	0.208 (f 3, 44= 1.58)	0.087 (f 3, 86= 2.26)	**0.000** (f 1, 86= 23.02)	0.824 (f 3, 86= 0.30)
Heart (g)	0.03±0.01	0.03±0.01	0.04±0.01	0.03±0.01	0.831 (f 3, 44= 0.29)	0.356 (f 3, 87= 1.09)	0.063 (f 1, 87= 3.54)	0.286 (f 3, 87= 1.28)
VSI (%)	10.2±1.1	9.5±1.4	9.9±0.9	8.8±1.4	0.051 (f 3, 44= 2.80)	0.083 (f 3, 88= 2.30)	**0.018** (f 1, 88= 5.77)	0.405 (f 3, 88= 0.98)
HSI (%)	1.1±0.2	1.1±0.2	1.1±0.2	1.0±0.2	0.430 (f 3, 44= 0.94)	0.052 (f 3, 86= 2.68)	**0.000** (f 1, 86= 16.99)	0.660 (f 3, 86= 0.53)
CSI (%)	0.1±0.0	0.1±0.0	0.1±0.0	0.1±0.0	0.636 (f 3, 44= 0.57)	0.553 (f 3, 87= 0.70)	**0.000** (f 1, 87= 398.13)	0.631 (f 3, 87= 0.58)
VFSI (%)	1.6±0.7	1.4±0.3	1.6±0.3	1.4±0.3	0.586 (f 3, 44= 0.65)	0.630 (f 3, 87= 0.58)	**0.000** (f 1, 87= 166.13)	0.590 (f 3, 87= 0.64)
Week 7								
Weight (g)	34.2±5.4	32.5±4.9	33.6±5.8	30.8±5.6	0.147 (f 3, 92= 1.83)			
Length (cm)	14.2±0.7	13.9±0.7	14.0±0.7	13.8±0.8	0.293 (f 3, 92= 1.26)			
Liver (g)	0.3±0.1	0.3±0.0	0.4±0.1	0.3±0.1	0.120 (f 3, 42= 2.06)			
Viscera (g)	3.4±0.7	3.1±0.4	3.4±0.8	3.0±0.7	0.284 (f 3, 44= 1.31)			
Viscera fat (g)	0.7±0.3	0.6±0.3	0.7±0.3	0.5±0.3	0.328 (f 3, 42= 1.18)			
Heart (g)	0.04±0.02	0.04±0.01	0.04±0.01	0.03±0.01	0.151 (f 3, 43= 1.86)			
VSI (%)	8.9±1.3	8.5±1.1	9.5±1.9	8.8±1.8	0.431 (f 3, 44= 0.94)			
HSI (%)	0.9±0.2	0.8±0.1	1.0±0.2	0.8±0.1	0.055 (f 3, 42= 2.74)			
CSI (%)	0.1±0.0	0.1±0.0	0.1±0.0	0.1±0.0	0.104 (f 3, 43= 2.18)			
VFSI (%)	1.8±0.8	1.6±0.9	1.9±1.0	1.5±0.7	0.430 (f 3, 44= 0.94)			

Values represent means ±standard deviation (SD) of 12 samples/test diet at the 4 hr sampling points at week-3 and week-7 (Total *n*=12). All values are means (*n*=12) ±standard deviation. Different superscripts indicate significant differences (*p*=<0.05). CD= Control diet, NA=Negative BCAAs, NL= Negative Leucine and PL= Positive Leucine. VSI= Viscera Somatic Index, HSI= Hepatic Somatic Index, CSI= Cardio Somatic Index, VFSI= Viscera Fat Somatic Index. Analysis was performed using one-way ANOVA, with Fisher LSD method used for *post-hoc* examination. A GLM was used to determine significance in diet, week and the interaction between diet and week.

Week-3 had the highest different *K*-value for CD, which was different to NL and PL. Week-7 had the highest different K-value in the NA diet compared to the CD and PL.

CD diet was significantly different within the diet between weeks (p=0.008). The week-3 mean of 1.23 was higher than the mean of 1.19 in week-7. No other differences were seen in the other diets between weeks. A GLM was used to see if there were any mean differences in diet, week and the interaction (D*W). A difference in diet means was seen with further Fisher's *post-hoc* analysis indicating that the differences in diets were between NA with the highest mean, NL and then followed by PL with the lowest different mean.

Different somatic measurements were taken at the 4 hr sampling time, on 4 fish/ tank (12 fish/test diet) at week-3 and week-7 as an estimate of growth, condition and other health parameters. These two sampling points were then compared to each other as well as within each week (Table 3.12).

In week-3, there were differences between the CD and NA diets compared to the NL and PL diets for total visceral weight (p=0.002). Near significance (p≤ 0.10) was noted in liver (p=0.101) and VSI (%) (p=0.051). The CD diet had the highest values for Viscera and VSI (%) and the PL diet the lowest values for those two parameters. In week-7, no differences were noted across the different parameters although near significance (p≤ 0.10) was observed in CSI (p=0.104) and HSI (%) (p=0.055).

When comparing the two weeks using a GLM, there were differences in all 9 parameters for weekly means apart from heart, which was near significant (p=<0.10). Whereas between diets, mean differences were noted in weight (p=0.050), liver (p=0.009), and viscera (p=0.004) and near significance (p≤ 0.10) in viscera fat and HSI (%).

3.3.3 Whole body analysis

WB analysis for moisture, ash, protein and oil (total lipids) was conducted on pools consisting of 4 fish /tank (n=12). Results were analysed using one-way ANOVAs, within each week and between the weeks (Table 3.13).

Table 3.13 Proximate analysis of whole bodies (%wet matter).

	CD	NL	NA	PL	P-Value	Two-way ANOVA		
%WM						P value		
						Diet	Week	D*W
Moisture								
Week 3	68.7±0.3	67.8±0.4	68.7±1.2	67.6±0.3^{b}	0.152 (f 3, 8= 2.32)	0.205 (f 3, 16= 0.171)	**0.000 (f 1, 16= 29.56)**	0.654 (f 3, 16= 0.55)
Week 7	70.0±1.0	69.9±0.1	69.9±1.0	69.7±0.2^{a}	0.909 (f 3, 8= 0.18)			
P-value	0.113	**0.002**	0.270	**0.001**				
Ash								
Week 3	2.3±0.1	2.4±0.2	2.3±0.0^{b}	2.5±0.1	0.221 (f 3, 8= 1.82)	0.062 (f 3, 16= 2.99)	0.766 (f 1, 16= 0.09)	0.302 (f 3, 16= 1.32)
Week 7	2.3±0.1	2.4±0.1	2.4±0.0^{a}	2.4±0.0	0.126 (f 3, 8= 2.32)			
P-value	0.867	0.819	**0.005**	0.331				
Protein								
Week 3	17.1±0.4$^{a\ z}$	17.0±0.2^{z}	15.1±0.3^{y}	16.9±0.5$^{a\ z}$	**0.002 (f 3, 7= 13.86)**	**0.011 (f 3, 15= 5.23)**	**0.046 (f 1, 15= 4.73)**	**0.005 (f 3, 15= 6.56)**
Week 7	15.9±0.5^{b}	16.5±0.4	16.2±0.8	15.8±0.3^{b}	0.451 (f 3, 8= 0.97)			
P-value	**0.035**	0.123	0.085	**0.026**				
Lipid								
Week 3	8.9±0.5	10.2±0.7	8.7±0.9	9.2±0.7	0.143 (f 3, 8= 2.41)	0.251 (f 3, 16= 1.51)	0.516 (f 1, 16= 0.44)	0.284 (f 3, 16= 1.38)
Week 7	9.1±0.8	9.1±0.1	9.0±0.4	9.2±0.7	0.989 (f 3, 8= 0.04)			
P-value	0.817	0.052	0.681	0.989				

Values represent means of three pooled samples in duplicate per test diet at the 4hr sampling points for week-3 and week-7 (Total *n*=12). All values are means (*n*=12) ±standard deviation. Different superscripts indicate significant differences (p=<0.05). CD= Control diet, NA=Negative BCAAs, NL= Negative Leucine, PL= Positive Leucine. Analysis was performed using one-way ANOVA, with Fisher's LSD method used for *post-hoc* examination. A GLM was used to determine significance in diet, week and the interaction between diet and week (D*W).

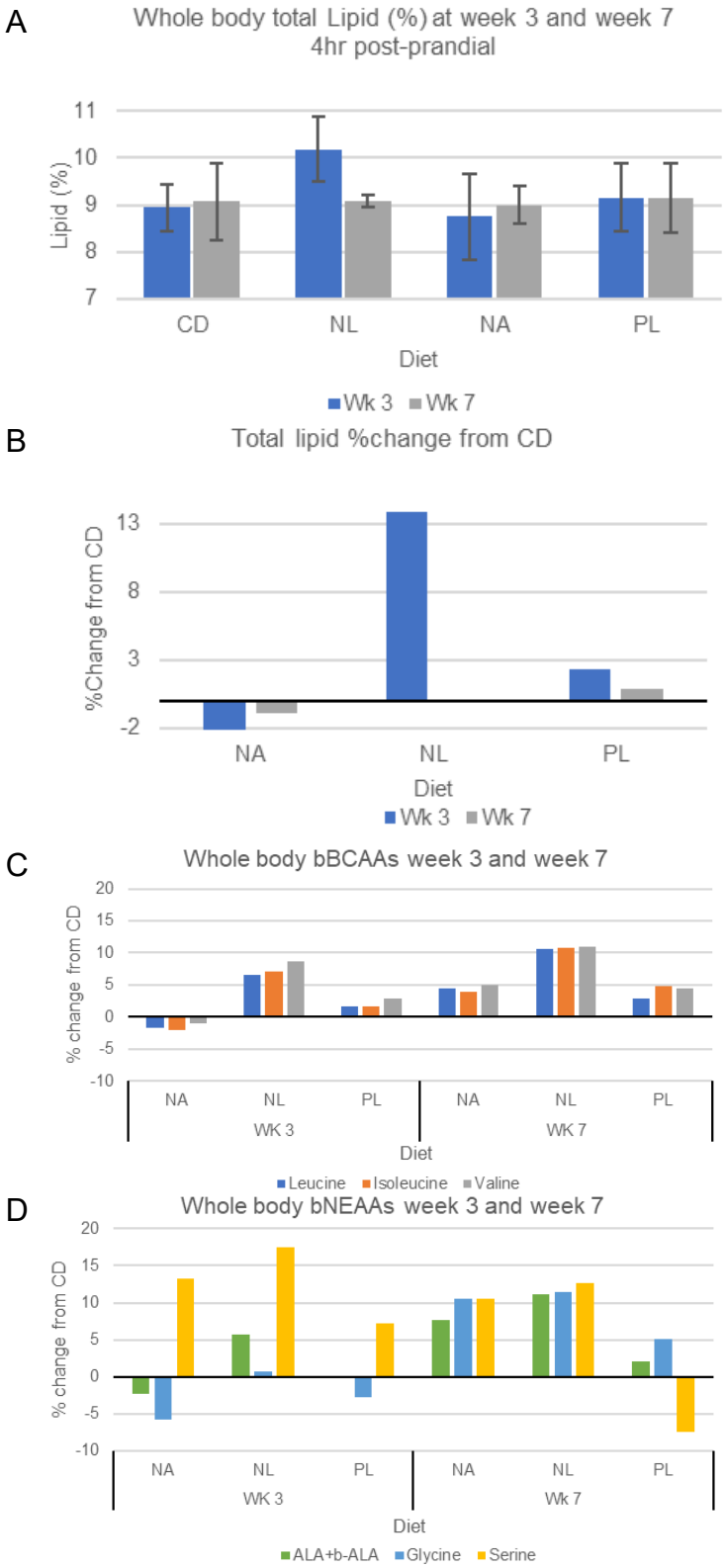


Figure 3.3 Whole body total lipids (Wet matter %) for A) each diet at week-3 and week-7 B) Total lipid (%) change from the CD diet C) Whole body bBCAAs compared to control diet (CD %change) D) Whole body bNEAAs between week-3 and week-7. CD= Control diet, NA=Negative BCAAs, NL= Negative Leucine, PL= Positive Leucine.

In week-3, there was a difference in protein between the diets (p=0.002). Fisher's *post-hoc* analysis indicated that the NA diet was significantly lower than the other 3 diets. No differences were noted in any of the other parameters in week-3 and week-7. GLMs were conducted between diets, weeks and the interaction between diet and week (D*W). Protein had differences in diet, week and D*W (p=0.011, p=0.046, p=0.005). Differences were also seen between weeks in moisture content (p=*0*) with Fisher's *post-hoc* analysis indicating that the means of week-7 were higher than the means of week-3.

3.3.3.1 Whole body lipids

No differences were observed in WB lipids (wet matter%) between week-3 and week-7. The largest difference in diets between weeks occurred in the NL diet, with a near significance observed (p=0.052) indicating a higher lipid (%) at week-3 compared to week-7 (Figure 3.3 A, B).

3.3.3.2 Bound amino acids in whole bodies at 4 hr in week-3 and week-7

3.3.3.2.1 The bBCAAs

WB bBCAA analysis displayed no differences in concentrations in diets across week-3 or week-7 (p=>0.05) (Table 3.14). Similarly, within each diet over time, no differences were observed between the two sampling points (p=>0.05). GLMs did not display any significance in diet, week or the interactions (p=>0.05), but near significance was seen in valine means across the BCAA diets (p=<0.10). In Figure 3.3 C, D, WB bBCAA comparisons between the BCAA diets and the CD at week-3 and week-7 visually portrayed an interesting phenomenon, whereby week-7 bBCAAs had a greater change (%) from the CD than week-3. NA bBCAAs in week-3 were up to 3% lower than CD but by week-7 were 5% higher than CD. All diets at week-7 had increased bBCAA deposition than at week-3 when compared to CD (change %). A similar trend was observed for alanine, glycine and serine.

3.3.3.2.2 The bEAAs

WB bEAA analysis across the different diets at each week, had differences in week-3 for phenylalanine, and histidine in week-7 (p=0.032, p=0.041) (Table 3.14).

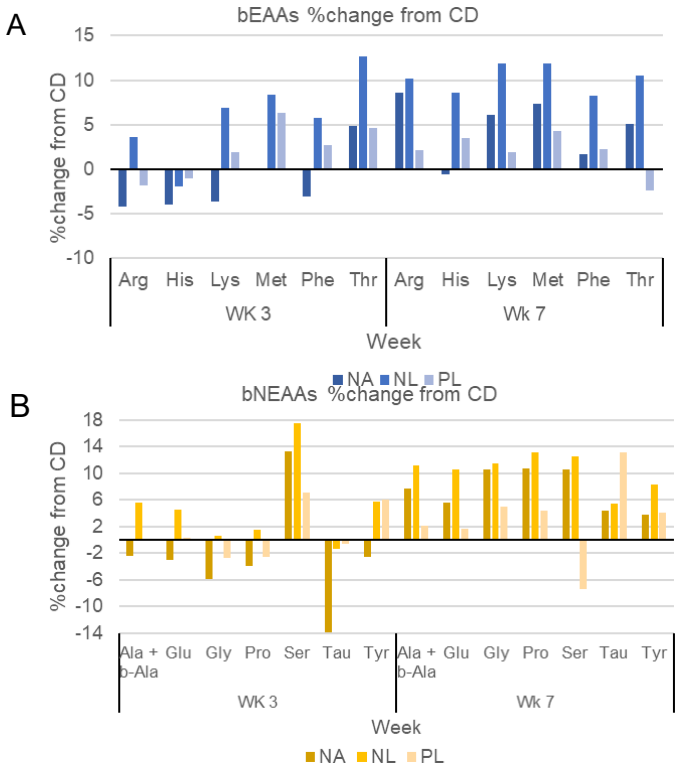


Figure 3.4 Whole body bEAAs and bNEAAs change (%) from control diet (CD) A) bEAAs B) bNEAAs between week-3 and week-7. CD= Control diet, NA=Negative BCAAs, NL= Negative Leucine, PL= Positive Leucine.

Post-hoc analysis identified the differences between diets having significantly higher concentrations of histidine in NL than CD and NA. Similarly, phenylalanine in the NL diet was different to CD and NA. PL diet was similar to NL diet for both histidine and phenylalanine. Near significance ($p \leq 0.10$) was seen across diets at week-7 for arginine, lysine and phenylalanine.

Within each diet over time, differences were seen for WB histidine in the CD diet (p=0.023) while near significance was seen in the NA for arginine, histidine, lysine and methionine. Additionally, phenylalanine in the PL diet was near significance, with week-3 having higher concentrations than week-7.

WB GLMs looking at diet, week and the interaction (D*W) had differences in diet means for methionine and phenylalanine (p=0.047, p=0.003). *Post-hoc* analysis revealed that in methionine, the concentration means between NL and CD were different, with NL having higher concentrations than CD. Similarly, methionine mean concentrations were higher in NL than both CD and NA.

Table 3.14 Whole body total bAAs of the test diets at week-3 and week-7, 4hr post-prandial. Data are expressed as mean ±standard deviation in µmol/g wet weight and different superscripts indicate significant differences (*p*=<0.05) with *abc* displaying vertical and *zyx* horizontal differences.

					One-way ANOVA	2-way ANOVA		
Time 4hr	CD	NL	NA	PL	P-value	Diet	Week	D*W
Isoleucine								
Week 3	49.50±4.42	53.04±4.43	48.45±3.02	50.31±4.66	0.599 (f 3, 8= 0.66)	0.154	0.715	0.903
Week 7	47.48±3.77	52.64±2.11	49.37±1.11	49.74±1.38	0.134 (f 3, 8= 2.50)			
P-value	0.581 (f 1, 4= 0.36)	0.896 (f 1, 4= 0.02)	0.645 (f 1, 4= 0.25)	0.850 (f 1, 4= 0.04)				
Leucine								
Week 3	79.40±5.10	84.65±7.07	78.10±3.68	80.77±9.63	0.666 (f 3, 8= 0.54)	0.192	0.890	0.872
Week 7	76.98±6.38	85.10±1.66	80.44±3.75	79.15±1.29	0.145 (f 3, 8= 2.39)			
P-value	0.635 (f 1, 4= 0.26)	0.921 (f 1, 4= 0.01)	0.482 (f 1, 4= 0.60)	0.781 (f 1, 4= 0.09)				
Valine								
Week 3	63.22±4.76	68.66±5.21	62.54±3.25	65.03±5.66	0.451 (f 3, 8= 0.97)	0.095	0.453	0.872
Week 7	62.92±5.55	69.83±2.61	66.09±1.66	65.77±1.60	0.161 (f 3, 8= 2.24)			
P-value	0.948 (f 1, 4= 0.00)	0.745 (f 1, 4= 0.12)	0.168 (f 1, 4= 2.83)	0.839 (f 1, 4= 0.05)				
Arginine								
Week 3	54.36±0.62	56.30±3.36	52.08±1.48	53.38±4.47	0.408 (f 3, 8= 1.09)	0.127	0.152	0.244
Week 7	52.99±3.37	58.41±2.01	57.52±3.63	54.14±0.70	0.108 (f 3, 8= 2.81)			
P-value	0.526 (f 1, 4= 0.48)	0.403 (f 1, 4= 0.87)	0.074 (f 1, 4= 5.78)	0.791 (f 1, 4= 0.08)				
Histidine								
Week 3	23.38±0.53 [a]	22.82±1.76	22.36±0.72	23.03±1.51	0.829 (f 3, 8= 0.29)	0.262	0.060	0.313
Week 7	21.42±0.72 [b y]	23.25±0.67 [z]	21.28±0.86 [y]	22.16±0.69 [zy]	**0.041 (f 3, 8= 4.43)**			
P-value	**0.023 (f 1, 4= 13.03)**	0.717 (f 1, 4= 0.15)	0.172 (f 1, 4= 2.76)	0.414 (f 1, 4= 0.83)				
Lysine								
Week 3	66.20±6.42	70.73±11.21	63.79±4.92	67.49±11.92	0.823 (f 3, 8= 0.30)	0.418	0.275	0.818
Week 7	66.91±5.97	74.83±1.96	70.99±2.29	68.18±1.01	0.082 (f 3, 8= 3.24)			
P-value	0.895 (f 1, 4= 0.02)	0.567 (f 1, 4= 0.39)	0.083 (f 1, 4= 5.28)	0.926 (f 1, 4= 0.01)				
Methionine								
Week 3	29.94±0.90	32.45±1.77	29.98±1.09	31.82±1.82	0.151 (f 3, 8= 2.33)	**0.047**	0.144	0.524
Week 7	30.32±3.13	33.94±0.86	32.57±1.45	31.63±1.51	0.212 (f 3, 8= 1.88)			
P-value	0.847 (f 1, 4= 0.04)	0.258 (f 1, 4= 1.74)	0.069 (f 1, 4= 6.10)	0.897 (f 1, 4= 0.02)				
Phenylalanine								
Week 3	38.44±0.50 [yx]	40.63±1.68 [z]	37.28±1.03 [x]	39.49±0.93 [zy]	**0.032 (f 3, 8= 4.93**)	**0.003**	0.059	0.455
Week 7	36.86±1.76	39.90±0.05	37.49±1.41	37.67±1.01	0.072 (f 3, 8= 3.44)			

P-value	0.209 (f 1, 4= 2.24)	0.491 (f 1, 4= 0.57)	0.841 (f 1, 4= 0.05)	0.084 (f 1, 4= 5.23)				
Threonine								
Week 3	46.37±6.88	52.28±2.22	48.62±0.90	48.51±9.48	0.690 (f 3, 8= 0.50)	0.263	0.976	0.927
Week 7	47.45±4.87	52.43±1.17	49.85±4.94	46.30±2.70	0.272 (f 3, 8= 1.56)			
P-value	0.835 (f 1, 4= 0.05)	0.920 (f 1, 4= 0.01)	0.692 (f 1, 4= 0.18)	0.717 (f 1, 4= 0.15)				
Alanine								
Week 3	87.66±5.50	91.62±12.90	84.88±4.88	88.05±13.85	0.878 (f 3, 8= 0.22)	0.462	0.281	0.742
Week 7	87.09±6.44	96.95±4.41	93.45±4.32	89.06±1.94	0.107 (f 3, 8= 2.82)			
P-value	0.912 (f 1, 4= 0.01)	0.536 (f 1, 4= 0.46)	0.085 (f 1, 4= 5.19)	0.906 (f 1, 4= 0.02)				
***b*-Alanine**								
Week 3	6.66±0.68	8.02±1.03	7.21±0.76	6.36±0.91	0.172 (f 3, 8= 2.15)	**0.024**	0.155	0.532
Week 7	7.10±0.40	7.74±0.37	7.95±0.53	7.08±0.17	0.055 (f 3, 8= 3.90)			
P-value	0.383 (f 1, 4= 0.96)	0.684 (f 1, 4= 0.19)	0.242 (f 1, 4= 1.88)	0.252 (f 1, 4= 1.79)				
Glycine								
Week 3	148.49±3.05	149.43±15.90	139.82±3.84	144.46±16.45	0.742 (f 3, 8= 0.42)	0.656	0.753	0.439
Week 7	137.82±9.77	153.60±17.44	152.33±13.88	144.76±5.27	0.426 (f 3, 8= 1.04)			
P-value	0.145 (f 1, 4= 3.27)	0.755 (f 1, 4= 0.09)	0.207 (f 1, 4= 2.27)	0.977 (f 1, 4= 0.00)				
Glut. acid								
Week 3	122.08±7.65	127.58±17.28	118.34±6.15 ^{b}	122.44±16.26	0.850 (f 3, 8= 0.26)	0.348	0.129	0.748
Week 7	123.35±6.28 ^{y}	136.32±2.95 ^{z}	130.22±2.76 $^{a\ zy}$	125.36±2.53 ^{y}	**0.016 (f 3, 8= 6.45)**			
P-value	0.836 (f 1, 4= 0.05)	0.437 (f 1, 4= 0.74)	**0.038 (f 1, 4= 9.33**)	0.774 (f 1, 4= 0.09)				
Proline								
Week 3	52.28±2.19	53.04±6.97	50.21±2.50	50.96±7.54	0.915 (f 3, 8= 0.17)	0.556	0.729	0.574
Week 7	48.84±3.78	55.29±4.55	54.08±4.55	50.96±1.80	0.233 (f 3, 8= 1.76)			
P-value	0.245 (f 1, 4= 1.85)	0.664 (f 1, 4= 0.22)	0.266 (f 1, 4= 1.67)	0.999 (f 1, 4= 0.00)				
Serine								
Week 3	46.71±14.62	54.89±2.04	52.93±4.27	50.05±15.27	0.808 (f 3, 8= 0.32)	0.399	0.769	0.915
Week 7	0.48±0.07	0.54±0.03	0.53±0.09	0.45±0.06	0.329 (f 3, 8= 1.34)			
P-value	0.885 (f 1, 4= 0.02)	0.781 (f 1, 4= 0.09)	0.960 (f 1, 4= 0.00)	0.596 (f 1, 4= 0.33)				
Taurine								
Week 3	6.19±0.25 $^{a\ z}$	6.10±0.49 ^{z}	5.33±0.11 ^{y}	6.15±0.35 ^{z}	**0.036 (f 3, 8= 4.69)**	**0.018**	0.531	**0.043**
Week 7	5.54±0.12^{b}	5.84±0.38	5.78±0.44	6.27±0.10	0.092 (f 3, 8= 3.05)			
P-value	**0.015 (f 1, 4= 16.43)**	0.511 (f 1, 4= 0.52)	0.157 (f 1, 4= 3.02)	0.596 (f 1, 4= 0.33)				
Tyrosine								
Week 3	28.59±0.46 ^{yx}	30.24±1.26 ^{zy}	27.85±0.86 ^{x}	30.34±0.77 ^{z}	**0.021 (f 3, 8= 5.84)**	**0.021**	0.835	0.333

Week 7	28.02±2.24	30.34±0.32	29.09±1.22	29.16±0.91	0.297 (f 3, 8= 1.46)
P-value	0.688 (f 1, 4= 0.19)	0.898 (f 1, 4= 0.02)	0.221 (f 1, 4= 2.10)	0.162 (f 1, 4= 2.93)	

Values represent means of three pooled samples per test diet (Total *n*=12) at the 4 hr sampling points for week-3 and week-7. All values are means (*n*=12) ±standard deviation. Different superscripts indicate significant differences (*p*=<0.05). CD= Control diet, NA=Negative BCAAs, NL= Negative Leucine and PL= Positive Leucine. Analysis was performed using one-way ANOVA, with Fisher's LSD method used for *post-hoc* examination. A GLM was used to determine significance in diet, time and the interaction between diet and time. Glut. Acid= glutamate

3.3.3.2.3 The WB bNEAAs

WB bNEAAs across diets at each week had differences in week-3 for taurine and tyrosine, and in week-7 for glutamate (p=0.036, p=0.021, p=0.016) (Table 3.14, Figure 3.4). Near significance was seen in week-7 for alanine, b-alanine and taurine. Within each diet over time, had differences in weeks, with higher concentrations in week-7 for glutamate in NA and higher concentrations in week-3 for taurine in the CD (p=0.038, p=0.015). Near significance was seen between weeks in NA for alanine and taurine, glycine in CD and tyrosine in PL.

WB GLMs using diet, week, and the interaction (D*W), differences in diet were highlighted for b-alanine, taurine, and tyrosine. *Post-hoc* analysis showed that NL had higher overall mean concentrations in b-alanine compared to PL, and different mean concentrations of tyrosine to PL and CD. Both PL and NL had the highest mean concentrations for taurine compared to NA.

3.3.3.3 Free amino acids in muscle tissue at week-3 and week-7 (4 hr post-prandial)

3.3.3.3.1 The muscle fBCAAs

Peak fAA uptake in Chapter 2, commonly occurred 4 hr post-prandial. With this in mind, week-3 tissue samples were only taken at 4 hr, while week-7 samples were taken over 24 hr. This was done at week-7 to observe whether there was similar uptake between parr and post-smolts over 24 hr. Pooled muscle fAAs showed variations in fBCAAs across the diets at each week (Table 3.15).

Isoleucine and valine concentrations were significantly higher in NL across the diets at week-3 (p=*0*, p=*0*). A similar trend was seen in week-7 for isoleucine and valine, but a difference was seen for leucine, with PL having the highest different concentration across diets (p=0.020). This trend was seen again in the GLMs, whereby the concentration means of isoleucine and valine were highest in NL, with leucine concentrations higher in PL. The lack of significance across diets at week-3 may be due to variability within each diet mean. PL had a concentration of 0.25 ±0.06 µmol/g compared to the lowest in CD (0.17 ±0.03 µmol/g). When working with such small concentrations, this variability may be due to compounded errors.

3.3.3.3.2 The muscle fEAAs

Muscle fEAA differences between diets across time, had week-3 differences for arginine, lysine, and methionine (p=0.027, p=*0*, p=0.021) (Table 3.15). CD had higher arginine concentrations than NL and PL, while lysine was higher in NL, and methionine the highest in NL and NA. No differences were seen in week-7 although near significance (p≤ 0.10) was seen in histidine and lysine. GLMs distinguished differences in diets for lysine and methionine, with differences in week seen for arginine and lysine (p=0.007, p=0.001). An interaction between diet and week was seen in lysine (p=0.011) and a near difference in interaction for arginine. Within diets over time saw differences in arginine for both CD and NA, with week-3 concentrations higher than week-7 (p=0.006, p=0.038). NL had differences in lysine concentrations between the weeks with week-3 having higher concentrations than week-7 (p=0.012). Near significance (p≤ 0.10) was seen in CD for histidine, lysine in NA, and threonine in NL.

3.3.3.3.3 The muscle fNEAAs

Muscle fNEAAs across the diets at each week had differences in week-3 for alanine, b-alanine and glutamate (p=0.020,p=0.025, p=0.047) (Table 3.15). Fisher's *post-hoc* analysis identified NA and PL alanine concentrations to be higher than CD, b-alanine concentrations were significantly lower in PL. While in glutamate, NA concentrations were higher than CD and PL. Week-7 had differences between diets for proline, With NL and NA having higher concentrations than CD and PL (p=0.011).

Within each diet between weeks, had differences in glutamate for NA, with week-3 having higher concentrations than week-7, with a similar trend seen in tyrosine in the CD (p=0.039, p=0.029). Near significance (p≤ 0.10) between weeks was seen in NA for alanine, PL for proline and NL for tyrosine. GLMs had differences in the diet means for alanine and b-alanine, with PL overall means higher than CD for alanine, while inversely, PL had the lowest overall means in b-alanine (p=0.021, p=0.002). Near significance was noted in diet means for glutamate and proline and between the week total means for glutamate and tyrosine.

Table 3.15 Total fAAs in muscle tissue at week-3 and week-7, 4hr post-prandial. Data are expressed as mean ±standard deviation in µmol/g wet tissue and different superscripts indicate significant differences (p=<0.05) with abc displaying vertical and zyx horizontal differences.

					One-way ANOVA	Two-way ANOVA P-value		
Time 4hr	CD	NL	NA	PL	P-value	Diet	Week	D*W
Isoleucine								
Week 3	0.10±0.01 ^{y}	0.20±0.02 ^{z}	0.10±0.00 $^{y\,b}$	0.09±0.03 ^{y}	**0.000** (f 3, 8= 24.31)	**0.000**	0.408	0.215
Week 7	0.11±0.01 ^{yx}	0.18±0.02 ^{z}	0.12±0.01 $^{y\,a}$	0.09±0.02 ^{x}	**0.001** (f 3, 8= 14.49)			
P-value	0.412 (f1, 4= 0.84)	0.378 (f1, 4= 0.98)	**0.025 (f1, 4= 12.10)**	0.834 (f1, 4= 0.05)				
Leucine								
Week 3	0.17±0.03	0.21±0.02	0.19±0.01	0.25±0.06	0.112 (f 3, 8= 2.75)	**0.002**	0.132	0.723
Week 7	0.19±0.01 ^{y}	0.21±0.04 ^{y}	0.21±0.04 ^{y}	0.29±0.04 ^{z}	**0.020** (f 3, 8= 5.91)			
P-value	0.698 (f1, 4= 0.17)	0.100 (f1, 4= 4.56)	0.283 (f1, 4= 1.54)	0.313 (f1, 4= 1.33)				
Valine								
Week 3	0.20±0.03 ^{y}	0.41±0.05 ^{z}	0.18±0.02 $^{y\,b}$	0.18±0.04 ^{y}	**0.000** (f 3, 8= 28.99)	**0.000**	0.420	0.207
Week 7	0.23±0.02 ^{y}	0.37±0.06 ^{z}	0.23±0.01 $^{y\,a}$	0.19±0.03 ^{y}	**0.001** (f 3, 8= 18.15)			
P-value	0.661 (f1, 4= 0.22)	0.356 (f1, 4= 1.09)	**0.021 (f1, 4= 13.65)**	0.861 (f1, 4= 0.03)				
Arginine								
Week 3	0.09±0.01 $^{a\,z}$	0.05±0.01 ^{x}	0.09±0.01 $^{a\,zy}$	0.05±0.03 ^{yx}	**0.027** (f 3, 7= 5.74)	0.100	**0.007**	0.051
Week 7	0.04±0.01 ^{b}	0.04±0.01	0.06±0.02 ^{b}	0.06±0.04	0.656 (f 3, 8= 0.56)			
P-value	**0.006 (f1, 3= 47.99)**	0.501 (f1, 4= 0.54)	**0.038 (f1, 4= 9.37)**	0.966 (f1, 4= 0.00)				
Histidine								
Week 3	0.04±0.01	0.05±0.02	0.04±0.01	0.03±0.01	0.497 (f 3, 8= 0.87)	0.166	0.051	0.854
Week 7	0.03±0.01	0.04±0.01	0.04±0.01	0.03±0.00	0.177 (f 3, 8= 2.12)			
P-value	0.179 (f1, 4= 2.66)	0.361 (f1, 4= 1.06)	0.544 (f1, 4= 0.44)	0.213 (f1, 4= 2.19)				
Lysine								
Week 3	0.12±0.03 ^{y}	0.26±0.03 $^{a\,z}$	0.30±0.01 ^{z}	0.08±0.02 ^{y}	**0.000 (f 3, 8= 53.99**)	**0.000**	**0.001**	**0.011**
Week 7	0.12±0.03	0.14±0.03 ^{b}	0.18±0.04	0.07±0.03	0.107 (f 3, 8= 2.82)			
P-value	0.865 (f1, 4= 0.03)	**0.012 (f1, 4= 19.47)**	0.061 (f1, 4= 6.70)	0.870 (f1, 4= 0.03)				
Methionine								
Week 3	0.09±0.02 ^{y}	0.14±0.02 ^{z}	0.10±0.01 ^{y}	0.08±0.02 ^{y}	**0.021 (f 3, 8= 5.77)**	**0.010**	0.972	0.487
Week 7	0.09±0.01	0.12±0.00	0.12±0.04	0.09±0.02	0.253 (f 3, 8= 1.65)			
P-value	0.696 (f1, 4= 0.18)	0.213 (f1, 4= 2.19)	0.505 (f1, 4= 0.54)	0.762 (f1, 4= 0.11)				
Phenylalanine								
Week 3	0.07±0.01	0.09±0.01	0.08±0.01	0.08±0.02	0.226 (f 3, 8= 1.79)	0.120	0.617	0.744
Week 7	0.06±0.01	0.08±0.00	0.08±0.02	0.08±0.02	0.421 (f 3, 8= 1.05)			

P-value	0.666 (f1, 4= 0.22)	0.250 (f1, 4= 1.81)	0.640 (f1, 4= 0.26)	0.924 (f1, 4= 0.01)				
Threonine								
Week 3	0.30±0.05	0.38±0.05	0.37±0.03	0.28±0.09	0.180 (f 3, 8= 2.09)	0.104	0.095	0.828
Week 7	0.27±0.04	0.30±0.04	0.33±0.10	0.26±0.04	0.580 (f 3, 8= 0.70)			
P-value	0.479 (f1, 4= 0.61)	0.078 (f1, 4= 5.53)	0.548 (f1, 4= 0.43)	0.726 (f1, 4= 0.14)				
Tryptophan								
Week 3	0.01±0.00	0.01±0.00	0.01±0.00	0.02±0.01	0.259 (f 3, 8= 1.62)	0.102	0.923	0.630
Week 7	0.01±0.00	0.01±0.00	0.01±0.00	0.01±0.00	0.420 (f 3, 8= 1.05)			
P-value	0.180 (f1, 4= 2.63)	0.831 (f1, 4= 0.05)	0.716 (f1, 4= 0.15)	0.570 (f1, 4= 0.38)				
Alanine								
Week 3	1.25±0.15 ^{y}	1.58±0.30 $^{z\,y}$	1.85±0.21 ^{z}	2.01±0.27 ^{z}	**0.020 (f 3, 8= 5.87)**	**0.021**	0.676	0.337
Week 7	1.43±0.26	1.71±0.51	1.48±0.26	1.87±0.20	0.389 (f 3, 8= 1.14)			
P-value	0.339 (f1, 4= 1.18)	0.722 (f1, 4= 0.15)	0.123 (f1, 4= 3.81)	0.502 (f1, 4= 0.54)				
***b*-Alanine**								
Week 3	2.07±0.35 ^{z}	2.56±0.73 ^{z}	2.51±0.47 ^{z}	1.03±0.48 ^{y}	**0.025 (f 3, 8= 5.45)**	**0.002**	0.430	0.410
Week 7	1.66±0.49	2.04±0.37	2.38±0.67	1.42±0.10	0.128 (f 3, 8= 2.56)			
P-value	0.312 (f1, 4= 1.34)	0.339 (f1, 4= 1.18)	0.800 (f1, 4= 0.07)	0.235 (f1, 4= 1.95)				
Glycine								
Week 3	7.20±1.20	7.74±0.75	8.17±1.09	8.25±2.45	0.822 (f 3, 8= 0.30)	0.714	0.608	0.869
Week 7	7.14±1.12	8.08±0.74	7.36±1.42	7.65±0.82	0.731 (f 3, 8= 0.44)			
P-value	0.957 (f1, 4= 0.00)	0.606 (f1, 4= 0.31)	0.479 (f1, 4= 0.61)	0.710 (f1, 4= 0.16)				
Glu. acid								
Week 3	0.16±0.01 ^{y}	0.21±0.04 ^{zy}	0.23±0.02 $^{a\,z}$	0.16±0.04 ^{y}	**0.047 (f 3, 8= 4.19)**	0.096	0.147	0.284
Week 7	0.16±0.04	0.18±0.05	0.17±0.03 ^{b}	0.17±0.02	0.918 (f 3, 8= 0.16)			
P-value	0.861 (f1, 4= 0.03)	0.428 (f1, 4= 0.78)	**0.039 (f1, 4= 9.11)**	0.847 (f1, 4= 0.04)				
Proline								
Week 3	0.11±0.03	0.16±0.05	0.15±0.06	0.16±0.04	0.578 (f 3, 8= 0.70)	0.080	0.781	0.640
Week 7	0.11±0.01 ^{y}	0.17±0.02 ^{z}	0.16±0.03 ^{z}	0.12±0.01 ^{y}	**0.011 (f 3, 8= 7.24)**			
P-value	0.847 (f1, 4= 0.04)	0.826 (f1, 4= 0.05)	0.704 (f1, 4= 0.17)	0.187 (f1, 4= 2.53)				
Serine								
Week 3	1.95±1.68	1.00±0.13	2.06±1.59	1.60±2.02	0.850 (f 3,7= 0.26)	0.619	0.267	0.922
Week 7	1.37±1.48	0.86±0.34	1.45±1.40	0.44±0.01	0.614 (f 3, 8= 0.63)			
P-value	0.678 (f1, 4= 0.20)	0.534 (f1, 4= 0.46)	0.677 (f1, 3= 0.21)	0.375 (f1, 4= 1.00)				
Taurine								
Week 3	0.25±0.32	0.08±0.06	0.46±0.35	0.36±0.43	0.550 (f 3, 8= 0.75)	0.636	0.393	0.613

	Week 7	0.33±0.52	0.11±0.08	0.14±0.15	0.15±0.02	0.762 (f 3, 8= 0.39)		
	P-value	0.835 (f1, 4= 0.05)	0.658 (f1, 4= 0.23)	0.215 (f1, 4= 2.16)	0.440 (f1, 4= 0.73)			
Tyrosine								
	Week 3	0.06±0.00 [a]	0.07±0.01	0.06±0.01	0.07±0.02	0.756 (f 3, 8= 0.40)	0.463	0.058	0.853
	Week 7	0.04±0.01 [b]	0.05±0.00	0.06±0.02	0.05±0.02	0.538 (f 3, 8= 0.78)			
	P-value	**0.029 (f1, 4= 11.24)**	0.137 (f1, 4= 3.45)	0.765 (f1, 4= 0.10)	0.523 (f1, 4= 0.49)			

Values represent means of four samples at three sampling points (Total *n*=12). All values are means (*n*=12) ±standard deviation. Different superscripts indicate significant differences (*p*=<0.05). CD= Control diet, NA=Negative BCAAs, NL= Negative Leucine, PL= Positive Leucine. Analysis was performed using one-way ANOVA, with Fisher LSD method used for *post-hoc* examination. A GLM was used to determine significance in diet, time and the interaction between diet and time. Glut. Acid= glutamate.

3.3.3.4 Free amino acids in week-7 muscle across each timepoint and between timepoints.

3.3.3.4.1 The muscle fBCAAs

Muscle fBCAAs at week-7 across the diets for each timepoint, showed a similar trend, with statistically differential uptake occurring between the 2 hr, 4 hr and 8 hr timepoints (p=<0.05) (Table 3.16). Leucine was the exception with only near significance observed at the 2 hr point (p=0.076). PL had the highest leucine concentrations at 4 hr compared to the other diets, while at the 8 hr, CD had the lowest different concentration across diets (p=0.020, p=0.025).

Muscle isoleucine at 2 hr had the highest different concentrations for NL and CD compared to NA and PL (p=0.021), with NL the highest at 4 hr, and NL and NA at 8 hr (p=0.001, p=0.002). A similar trend was seen in valine, with NL having higher concentrations at 2 hr than NA and PL, 4 hr and at 8 hr compared to CD and PL (p=0.025, p=0.001, p=0.030). Within each diet overtime, for the CD diet had differences for all fBCAAs.

In isoleucine, the 2 hr sampling point was higher than the 8 and 24 hr concentrations, while in valine the lowest concentration was at the 8 hr point (p=*0*, p=0.001). In CD leucine, the highest difference in concentration was seen at 2 hr compared to -2, 8 and 24 hr.

In NL, differences in time were seen for isoleucine and valine (p=0.002, p=0.009) with near significance in leucine (p=>0.05 but p=<0.10). In isoleucine, the highest different timepoint was at 4 hr, while similarly the highest concentration in valine was at 4 hr although it was not different to 2 hr. In PL, differences were seen in leucine and valine (p=0.002, p=0.024). Leucine had the highest concentration at 4 hr compared to -2, 8 and 24 hr. Interestingly for valine, the 8 hr concentration was the lowest over the 5 timepoints. GLMs for diet, time and the interaction of D*T had differences across all parameters (p=<0.05).

Within the NA diet over time, no significantly different uptake concentrations were observed for any of the muscle fBCAAs. Peak uptake did occur at 4 hr for all fBCAAs, but this was not significant (p=>0.05) (Figure 3.5).

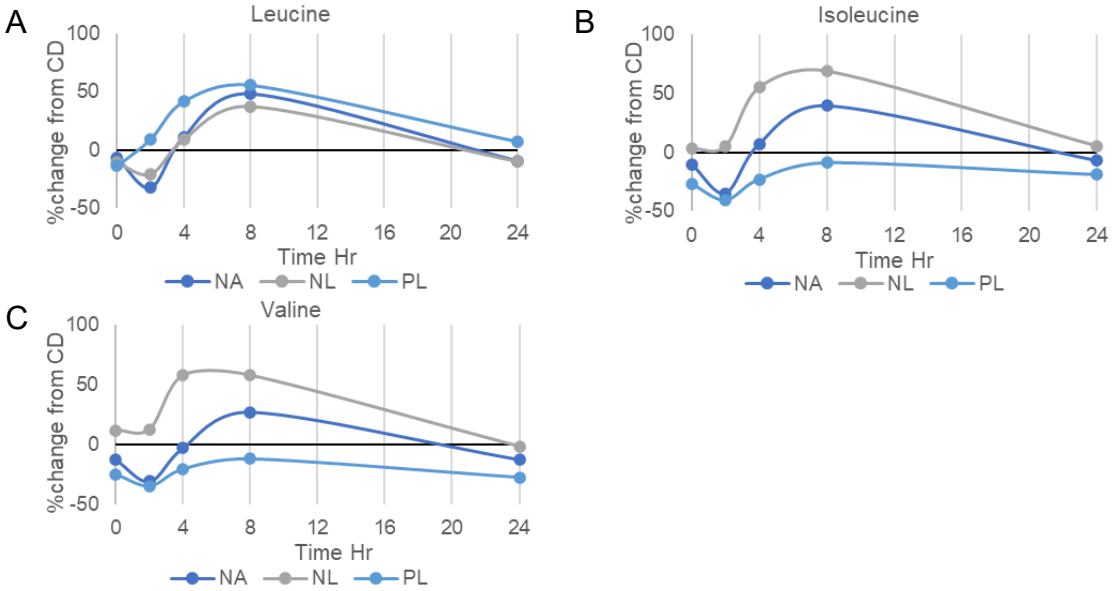


Figure 3.5 Muscle individual fBCAAs between diets change from CD (change (%)) A) leucine B) isoleucine C) valine between diets at week-7. CD= Control diet, NA=Negative BCAAs, NL= Negative Leucine and PL= Positive Leucine.

3.3.3.4.2 The fEAAs in muscle tissue at week-7

In Table 3.16 and Figure 3.6 each diet across time, had the most variances over time in lysine, with differences across diets at -2, 2 and 8 hr (p=0.039, p=0.023, p=0.021). PL was different to the other 3 diets at -2 hr and 2 hr with the lowest concentration of the diets. At 8 hr, NA had the highest different concentration across the diets. Muscle histidine had a difference across the diets at 8 hr, with the highest concentration being in NL and NA compared to the other two diets (p=0.010). Similarly for phenylalanine, NA and NL were significantly higher in concentration than CD but not PL (p=0.046). Threonine at 8 hr was significantly higher in NA than CD and PL but not different to NL (p=0.046). Near significance was seen for lysine at 8 hr, methionine at 8 hr and 24 hr, phenylalanine at -2 hr and threonine at 2 hr (p=<0.10).

Within each diet over time had a difference in arginine in NA, with 4 hr being significantly higher than 8 hr and 24 hr (p=0.033). Histidine in the PL had the highest different concentration at 24 hr, lower at -2 hr and 4 hr, and 8 hr significantly lower than all times (p=0.012). Lysine in the CD had highest peak concentrations at 4 hr compared to -2 hr, and 24 hr, with the lowest different concentration at 8 hr.

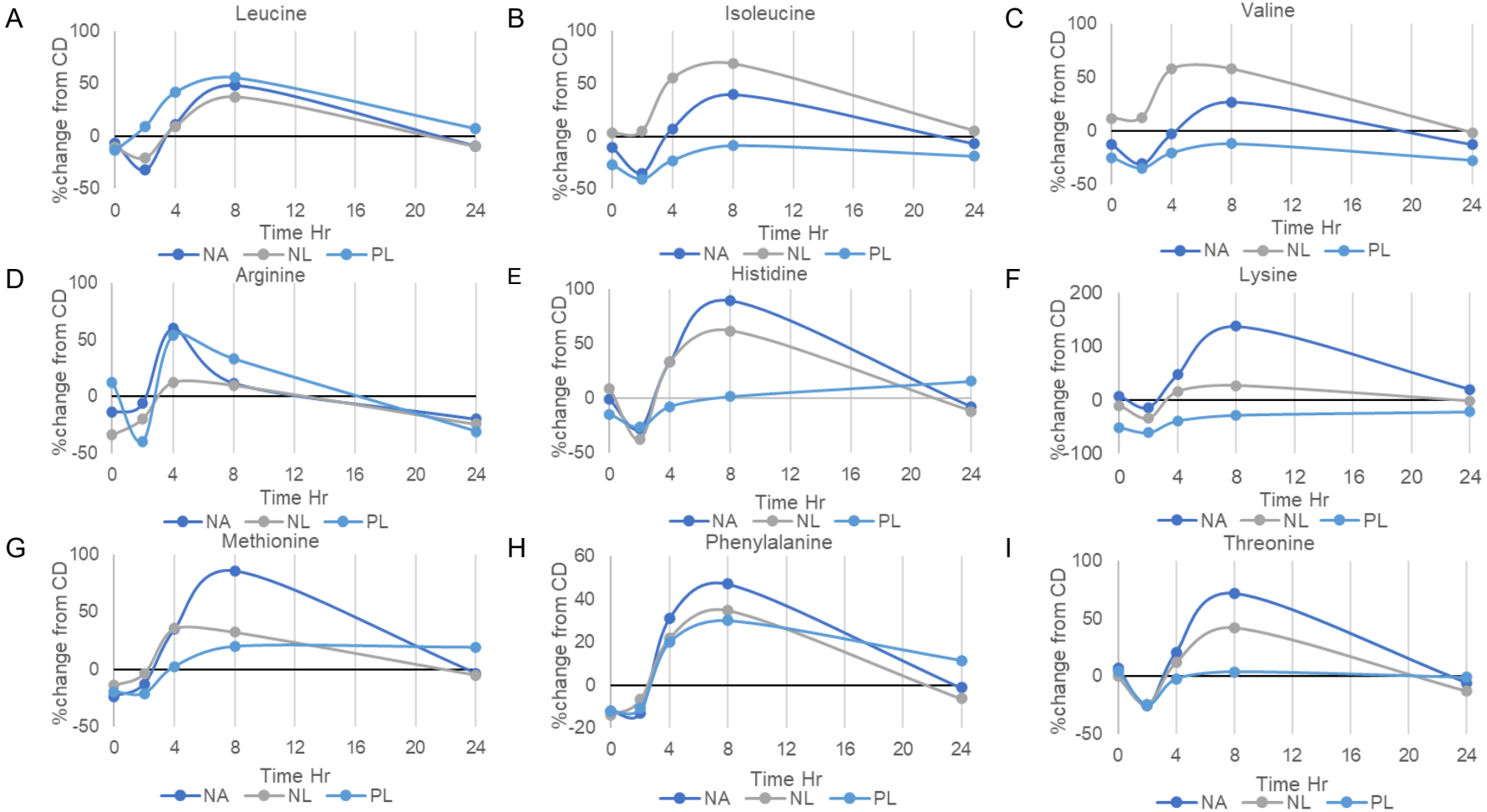


Figure 3.6 Muscle individual fEAAs compared to CD (%change) A) leucine B) isoleucine C) valine D) arginine E) histidine F) lysine G) methionine H) phenylalanine I) threonine between diets at week-7. CD= Control diet, NA=Negative BCAAs, NL= Negative Leucine, PL= Positive Leucine.

Table 3.16 Muscle fAAs between and within diets over time at week-7. Data are expressed as mean ±standard deviation in µmol/ g and different superscripts indicate significant differences (p=<0.05), with *abc* displaying vertical and *zyx* horizontal differences.

						One-way ANOVA	Two-way ANOVA P-value		
Time		CD	NL	NA	PL	P-value	Diet	Time	D*T
Isoleucine	-2hr	0.10±0.01 ^{ab}	0.11±0.01 ^{bc}	0.09±0.02	0.08±0.01	0.066 (f 3, 8 = 3.59)	**0.000**	**0.000**	**0.005**
	2hr	0.13±0.02 $^{a\,z}$	0.14±0.02 $^{b\,z}$	0.08±0.03 ^{y}	0.08±0.00 ^{y}	**0.021 (f 3, 8 = 5.79)**			
	4hr	0.11±0.01 $^{ab\,yx}$	0.18±0.02 $^{a\,z}$	0.12±0.01 ^{y}	0.09±0.02 ^{x}	**0.001 (f 3, 8 = 14.49)**			
	8hr	0.06±0.00 $^{c\,y}$	0.10±0.02 $^{c\,z}$	0.08±0.00 ^{z}	0.05±0.01 ^{y}	**0.002 (f 3, 8 = 12.11)**			
	24hr	0.10±0.00 ^{b}	0.10±0.02 ^{c}	0.09±0.02	0.08±0.02	0.310 (f 3, 8 = 1.41)			
	P-value	**0.000 (f 4, 10= 17.26)**	**0.002 (f 4, 10= 9.55)**	0.117 (f 4, 10= 2.42)	0.121 (f 4, 10= 2.38)				
Leucine	-2hr	0.17±0.01 ^{b}	0.15±0.02	0.16±0.03	0.15±0.03 ^{c}	0.618 (f 3, 8 = 0.63)	**0.006**	**0.000**	**0.022**
	2hr	0.21±0.03 ^{a}	0.17±0.04	0.14±0.05	0.23±0.04 ^{ab}	0.076 (f 3, 8 = 3.36			
	4hr	0.19±0.01 $^{ab\,y}$	0.21±0.04 ^{y}	0.21±0.03 ^{y}	0.29±0.04 $^{a\,z}$	**0.020 (f 3, 8= 5.91)**			
	8hr	0.09±0.00 $^{c\,y}$	0.13±0.02 ^{z}	0.14±0.01 ^{z}	0.15±0.03 $^{c\,z}$	**0.025 (f 3, 8 = 5.45)**			
	24hr	0.16±0.01 ^{b}	0.14±0.04	0.14±0.00	0.17±0.03 ^{bc}	0.530 (f 3, 8 = 0.80)			
	P-value	**0.000 (f 4, 10= 27.46)**	0.065 (f 4, 10= 3.13)	0.067 (f 4, 10= 3.09)	**0.002 (f 4, 10= 9.99)**				
Valine	-2hr	0.20±0.03 ^{a}	0.23±0.05 ^{b}	0.18±0.03	0.15±0.02 ^{a}	0.130 (f 3, 8 = 2.54)	**0.000**	**0.000**	**0.027**
	2hr	0.25±0.04 $^{a\,zy}$	0.29±0.04 $^{ab\,z}$	0.18±0.07 ^{yx}	0.17±0.02 $^{a\,x}$	**0.025 (f 3, 8 = 5.43)**			
	4hr	0.23±0.02 $^{a\,y}$	0.37±0.06 $^{a\,z}$	0.23±0.01 ^{y}	0.19±0.03 $^{a\,y}$	**0.001 (f 3, 8= 18.15)**			
	8hr	0.12±0.02 $^{b\,y}$	0.20±0.05 $^{b\,z}$	0.16±0.01 ^{zy}	0.11±0.03 $^{b\,y}$	**0.030 (f 3, 8 = 5.06)**			
	24hr	0.21±0.02 ^{a}	0.21±0.04 ^{b}	0.19±0.01	0.15±0.02 ^{a}	0.088 (f 3, 8 = 3.12)			
	P-value	**0.001 (f 4, 10= 11.87**)	**0.009 (f 4, 10= 6.11)**	0.210 (f 4, 10= 1.78)	**0.024 (f 4, 10= 4.52)**				
Arginine	-2hr	0.05±0.02	0.03±0.01	0.04±0.01 ^{ab}	0.05±0.03	0.586 (f 3, 8 = 0.68)	0.639	**0.004**	0.932
	2hr	0.04±0.01	0.04±0.01	0.04±0.02 ^{ab}	0.03±0.00	0.424 (f 3, 8 = 1.05)			
	4hr	0.04±0.01	0.04±0.01	0.06±0.02 ^{a}	0.06±0.04	0.656 (f 3,8= 0.56)			
	8hr	0.02±0.01	0.02±0.01	0.02±0.00 ^{b}	0.03±0.02	0.913 (f 3, 8 = 0.17)			
	24hr	0.03±0.01	0.03±0.02	0.03±0.00 ^{b}	0.02±0.01	0.692 (f 3, 8 = 0.50)			
	P-value	0.333 (f 4, 10= 1.30)	0.388 (f4, 10= 1.15)	**0.033 (f4, 10= 4.07)**	0.409 (f4, 10= 1.10)				
Histidine	-2hr	0.03±0.01	0.03±0.01	0.03±0.01	0.03±0.01 ^{bc}	0.706 (f 3, 8 = 0.48)	0.370	**0.046**	**0.030**
	2hr	0.05±0.02	0.03±0.00	0.03±0.00	0.03±0.00 ^{ab}	0.185 (f 3, 8 = 2.05)			
	4hr	0.03±0.01	0.04±0.01	0.04±0.01	0.03±0.00 ^{bc}	0.177 (f 3, 8= 2.12)			

	8hr	0.02±0.01 ^{y}	0.03±0.00 ^{z}	0.04±0.01 ^{z}	0.02±0.00 $^{c\ y}$	**0.010 (f 3, 8 = 7.71**)			
	24hr	0.03±0.01	0.03±0.01	0.03±0.01	0.04±0.01 ^{a}	0.556 (f 3, 8 = 0.74)			
	P-value	0.097 (f 4, 10= 2.65)	0.421 (f4, 10= 1.07)	0.613 (f4, 10= 0.69)	**0.012 (f4, 10= 5.60)**				
Lysine	-2hr	0.07±0.00 $^{bc\ z}$	0.06±0.03 $^{b\ z}$	0.08±0.02 ^{z}	0.03±0.00 $^{bc\ y}$	**0.039 (f 3, 8 = 4.53)**	**0.000**	**0.000**	0.150
	2hr	0.10±0.03 $^{ab\ z}$	0.07±0.01 $^{b\ zy}$	0.09±0.03 ^{z}	0.04±0.01 $^{bc\ y}$	**0.023 (f 3, 8 = 5.55)**			
	4hr	0.12±0.03 ^{a}	0.14±0.03 ^{a}	0.18±0.08	0.07±0.03 ^{a}	0.110 (f 3, 8= 2.78)			
	8hr	0.04±0.01 $^{c\ y}$	0.05±0.01 $^{b\ y}$	0.10±0.04 ^{z}	0.03±0.00 $^{c\ y}$	**0.021 (f 3, 8 = 5.83)**			
	24hr	0.07±0.01 ^{bc}	0.07±0.04 ^{b}	0.08±0.02	0.05±0.01 ^{ab}	0.420 (f 3, 8 = 1.06)			
	P-value	**0.002 (f 4, 10= 9.86)**	**0.010 (f 4, 10= 5.93)**	0.068 (f 4, 10= 3.07)	**0.010 (f 4, 10= 6.01)**				
Methionine	-2hr	0.08±0.01 ^{a}	0.07±0.03 ^{b}	0.06±0.00 ^{b}	0.06±0.02	0.542 (f 3, 8 = 0.77)	0.271	**0.000**	**0.045**
	2hr	0.08±0.01 ^{a}	0.08±0.02 ^{b}	0.07±0.01 ^{b}	0.07±0.01	0.404 (f 3, 8 = 1.10)			
	4hr	0.09±0.01 ^{a}	0.12±0.00 ^{a}	0.12±0.04 ^{a}	0.09±0.02	0.253 (f 3, 8 = 1.65)			
	8hr	0.05±0.00 ^{b}	0.07±0.01 ^{b}	0.09±0.03 ^{ab}	0.06±0.01	0.053 (f 3, 8 = 3.97)			
	24hr	0.06±0.01 ^{b}	0.06±0.01 ^{b}	0.06±0.01 ^{b}	0.08±0.01	0.128 (f 3, 8 = 2.56)			
	P-value	**0.001 (f 4, 10= 12.11)**	**0.011 (f 4, 10= 5.82)**	**0.050 (f 4, 10= 3.48)**	0.199 (f 4, 10= 1.83)				
Phenylalanine	-2hr	0.08±0.01 ^{a}	0.07±0.00	0.07±0.01	0.07±0.00	0.088 (f 3, 8= 3.12)	0.657	**0.000**	0.073
	2hr	0.08±0.01 ^{a}	0.08±0.01	0.07±0.01	0.07±0.01	0.585 (f 3, 8 = 0.69)			
	4hr	0.06±0.01 ^{b}	0.08±0.00	0.08±0.02	0.08±0.02	0.421 (f 3, 8 = 1.05)			
	8hr	0.05±0.01 $^{c\ y}$	0.06±0.01 ^{z}	0.07±0.01 ^{z}	0.06±0.01 ^{zy}	**0.036 (f 3, 8 = 4.67)**			
	24hr	0.06±0.01 ^{b}	0.06±0.01	0.06±0.01	0.07±0.00	0.393 (f 3, 8 = 1.13)			
	P-value	**0.001 (f 4, 10= 11.81)**	0.097 (f 4, 10= 2.64)	0.186 (f 4, 10= 1.90)	0.554 (f 4, 10= 0.80)				
Threonine	-2hr	0.20±0.03 ^{b}	0.20±0.09	0.22±0.02	0.21±0.05 ^{a}	0.981 (f 3, 8 = 0.06)	0.422	**0.000**	0.311
	2hr	0.29±0.03 ^{a}	0.22±0.04	0.21±0.06	0.22±0.02 ^{a}	0.152 (f 3, 8 = 2.31)			
	4hr	0.27±0.04 ^{a}	0.30±0.04	0.27±0.02	0.26±0.04 ^{a}	0.580 (f 3, 8 = 0.70)			
	8hr	0.13±0.01 $^{c\ y}$	0.18±0.04 ^{zy}	0.22±0.06 ^{z}	0.13±0.02 $^{b\ y}$	**0.046 (f 3, 8 = 4.20)**			
	24hr	0.23±0.02 ^{ab}	0.20±0.06	0.22±0.01	0.23±0.02 ^{a}	0.393 (f 3, 8 = 1.13)			
	P-value	**0.001 (f 4, 10= 11.84)**	0.155 (f 4, 10= 2.10)	0.458 (f 4, 10= 0.99)	**0.007 (f 4, 10= 6.66)**				
Alanine	-2hr	1.29±0.25 ^{b}	1.15±0.16	1.47±0.18	1.34±0.22 ^{bc}	0.365 (f 3, 8 = 1.21)	0.331	**0.000**	0.135
	2hr	1.88±0.38 ^{a}	1.30±0.24	1.34±0.36	1.41±0.20 ^{b}	0.154 (f 3, 8 = 2.30)			
	4hr	1.43±0.26 ^{ab}	1.71±0.51	1.48±0.26	1.87±0.20 ^{a}	0.389 (f 3, 8 = 1.14)			

	8hr	0.79±0.06 ^{c}	1.00±0.05	1.02±0.18	0.94±0.20 ^{c}	0.276 (f 3, 8 = 1.55)			
	24hr	1.54±0.18 ^{ab}	1.23±0.51	1.31±0.24	1.71±0.32 ^{ab}	0.340 (f 3, 8 = 1.30)			
	P-value	**0.004 (f 4, 10= 7.68)**	0.217 (f 4, 10= 1.74)	0.248 (f 4, 10= 1.60)	**0.005 (f 4, 10= 7.29)**				
b-Alanine	-2hr	1.24±0.24 ^{bc}	1.47±0.48	1.77±0.33	1.00±0.25 ^{bc}	0.113 (f 3, 8 = 2.75)	**0.002**	0.430	0.410
	2hr	2.05±0.18 $^{a\ z}$	1.14±0.20 ^{yx}	1.62±0.45 ^{zy}	1.06±0.26 $^{abc\ x}$	**0.010 (f 3, 8 = 7.48)**			
	4hr	1.66±0.49 ^{ab}	2.04±0.37	2.38±0.67	1.42±0.10 ^{a}	0.128 (f 3, 8 = 2.56)			
	8hr	0.71±0.08 $^{c\ y}$	1.28±0.18 ^{x}	1.70±0.28 ^{z}	0.75±0.20 $^{c\ y}$	**0.001 (f 3, 8 = 16.88)**			
	24hr	1.24±0.30 ^{bc}	1.30±0.51	1.40±0.35	1.22±0.23 ^{ab}	0.922 (f 3, 8 = 0.16)			
	P-value	**0.003 (f 4, 10= 8.86)**	0.098 (f 4, 10= 2.62)	0.153 (f 4, 10= 2.12)	**0.033 (f 4, 10= 4.08)**				
Glycine	-2hr	5.90±0.84 ^{b}	6.94±2.23	6.92±1.12	7.04±0.91	0.730 (f 3, 8 = 0.44)	0.674	**0.003**	0.387
	2hr	8.03±0.28 ^{a}	6.26±0.71	6.77±1.03	7.45±1.73	0.275 (f 3, 8 = 1.55)			
	4hr	7.14±1.12 ^{ab}	8.08±0.74	7.36±1.42	7.65±0.82	0.731 (f 3, 8 = 0.44)			
	8hr	4.07±0.85 ^{c}	6.01±1.72	6.75±1.42	5.27±1.77	0.197 (f 3, 8 = 1.97)			
	24hr	7.47±0.41 ^{a}	6.66±2.26	7.32±0.74	7.52±0.26	0.809 (f 3, 8 = 0.32)			
	P-value	**0.001 (f 4, 10= 12.77)**	0.614 (f 4, 10= 0.69)	0.921 (f 4, 10= 0.22)	0.190 (f 4, 10= 1.89)				
Glut. acid	-2hr	0.10±0.03 ^{bc}	0.10±0.04	0.11±0.01	0.09±0.01 ^{c}	0.764 (f 3, 8 = 0.39)	0.430	**0.000**	0.584
	2hr	0.13±0.01 ^{ab}	0.11±0.03	0.13±0.05	0.09±0.01 ^{c}	0.354 (f 3, 8 = 1.25)			
	4hr	0.16±0.04 ^{a}	0.18±0.05	0.17±0.03	0.17±0.02 ^{a}	0.918 (f 3, 8 = 0.16)			
	8hr	0.08±0.01 ^{c}	0.11±0.02	0.11±0.03	0.07±0.02 ^{c}	0.115 (f 3, 8 = 2.71)			
	24hr	0.13±0.03 ^{ab}	0.11±0.03	0.11±0.00	0.14±0.01 ^{b}	0.359 (f 3, 8 = 1.23)			
	P-value	**0.023 (f 4, 10= 4.61)**	0.103 (f 4, 10= 2.57)	0.117 (f 4, 10= 2.42)	**0.000 (f 4, 10= 15.24)**				
Proline	-2hr	0.10±0.00	0.10±0.02 ^{b}	0.09±0.03 ^{b}	0.09±0.02	0.930 (f 3, 8 = 0.14)	0.080	0.781	0.640
	2hr	0.13±0.05	0.09±0.02 ^{b}	0.08±0.01 ^{b}	0.10±0.01	0.229 (f 3, 8 = 1.78)			
	4hr	0.11±0.01 ^{y}	0.17±0.02 $^{a\ z}$	0.16±0.03 $^{a\ z}$	0.12±0.01 ^{y}	**0.011 (f 3, 8 = 7.24)**			
	8hr	0.07±0.02	0.09±0.00 ^{b}	0.11±0.02 ^{b}	0.10±0.01	0.060 (f 3, 8 = 3.76)			
	24hr	0.09±0.02	0.08±0.02 ^{b}	0.07±0.02 ^{b}	0.12±0.01	0.089 (f 3, 8 = 3.10)			
	P-value	0.093 (f 4, 10= 2.70)	**0.001 (f 4, 10=10.93)**	**0.007 (f 4, 10= 6.58)**	0.107 (f 4, 10= 2.52)				
Serine	-2hr	0.72±0.77	0.49±0.33	0.94±0.92	0.49±0.32	0.799 (f 3, 8 = 0.34)	0.272	**0.029**	0.966
	2hr	0.55±0.10	0.67±0.31	0.86±0.65	0.53±0.37	0.745 (f 3, 8= 0.42)			
	4hr	1.37±1.48	0.86±0.34	1.45±1.40	0.44±0.01	0.614 (f 3, 8= 0.63)			

	8hr	0.21±0.07 ^{y}	0.30±0.10 ^{zy}	0.37±0.06 ^{z}	0.20±0.04 ^{y}	**0.048 (f 3, 8= 4.12)**			
	24hr	0.64±0.65	0.30±0.10	0.28±0.05	0.26±0.02	0.490 (f 3, 8= 0.88)			
	P-value	0.533 (f 4, 10= 0.83)	0.101 (f 4, 10= 2.60)	0.434 (f 4, 10= 1.04)	0.327 (f 4, 10= 1.32)				
Taurine	-2hr	0.36±0.39	0.23±0.33	0.34±0.39	0.44±0.56	0.941 (f 3, 7= 0.13)	0.742	0.180	0.952
	2hr	0.17±0.02	0.29±0.20	0.31±0.23	0.20±0.18	0.734 (f 3, 8= 0.44)			
	4hr	0.33±0.52	0.11±0.08	0.14±0.15	0.15±0.02	0.762 (f 3, 8= 0.39)			
	8hr	0.07±0.05	0.10±0.02	0.02±0.01	0.06±0.02	0.067 (f 3, 8= 3.55)			
	24hr	0.41±0.54	0.12±0.02	0.09±0.01	0.07±0.02	0.424 (f 3, 8= 1.04)			
	P-value	0.809 (f 4, 9= 0.39)	0.599 (f 4, 10= 0.72)	0.364 (f 4, 10= 1.21)	0.421 (f 4, 10= 1.07)				
Tyrosine	-2hr	0.08±0.01 ^{a}	0.06±0.00	0.07±0.01	0.07±0.01	0.135 (f 3, 8 = 2.48)	0.891	**0.000**	0.294
	2hr	0.06±0.01 ^{b}	0.07±0.01	0.06±0.00	0.06±0.01	0.620 (f 3, 8= 0.62)			
	4hr	0.04±0.01 ^{d}	0.05±0.00	0.06±0.02	0.05±0.02	0.538 (f 3, 8= 0.78)			
	8hr	0.04±0.01 ^{cd}	0.05±0.00	0.05±0.00	0.05±0.01	0.489 (f 3, 8= 0.89)			
	24hr	0.05±0.00 ^{bc}	0.05±0.01	0.05±0.00	0.06±0.00	0.342 (f 3, 8= 1.29)			
	P-value	**0.000 (f 4, 10= 14.02)**	0.080 (f 4, 10= 2.88)	0.081 (f 4, 10= 2.86)	0.295 (f 4, 10= 1.42)				

CD= Control diet, NA=Negative BCAAs, NL= Negative Leucine, PL= Positive Leucine. Analysis was performed using one-way ANOVA and GLMs, with Fisher's LSD method used for *post-hoc* examination. Values represent means of three samples at three sampling points (Total *n*=9). Glut. Acid= glutamate.

In the NL, the 4 hr peak was than all other times (p=0.010) and similarly in PL, the 4 hr peak was significantly higher than -2 hr and 2 hr which were higher than 8 hr (p=0.010).

Methionine had differences in all diets apart from the PL. In the CD, -2, 2 and 4 hr times were significantly higher than 8 hr and 24 hr (p=0.001). In NL, the highest different peak concentration was at 4 hr while in NA, the highest different peak was at 4 hr compared to -2, 2 and 24 hr (p=0.011). Phenylalanine had differences over time in the CD with the highest different concentrations at -2 hr and 2 hr followed by 4 hr and 24 hr which were higher than 8 hr (p=0.001).

Threonine had differences in the CD and PL diets. In the CD, 2 hr and 4 hr were significantly higher than -2 hr which was higher than 8 hr (p=0.001). While in PL, all concentrations were similar, but the 8 hr concentration was significantly lower than the other times (p=0.007). GLMs had differences in diet means for lysine, while a difference in time for all the muscle fEAAs (p=<0.05). An interaction between diet and time was seen for histidine and methionine (p=0.030, p=0.045).

3.3.3.4.3 The fNEAAs muscle tissue at week-7

Differences across diets at each time for the fNEAAs had differences in b-alanine and proline (Table 3.16, Figure 3.7, 3.8). The 2 hr time for b-alanine had differences in concentration across diets, with the CD higher than NL and PL (p=0.010). At the 8 hr point, NA had the highest concentration across all diets (p=0.001).

Proline at 4 hr had differences in concentration, with NL and NA significantly higher than CD and PL (p=0.011). Near significance (p≤ 0.10) was observed in alanine at 8 hr, b-alanine at -2 hr and 4 hr, glutamate at 8 hr, proline at 8 hr and 24 hr, taurine at 8 hr and tyrosine at -2 hr.

Within each diet over time had differences in the CD for alanine, with 2 hr having a higher concentration than -2 hr and 8 hr (p=0.004). b-Alanine at the 2 hr peak was different to -2, 8 and 24 hr, while glycine had the highest peak concentrations at 2 and 24 hr compared to -2 and 8 hr (p=0.001). Peak high concentrations of glutamate were at 4 hr, compared to -2 and 4 hr (p=0.023).

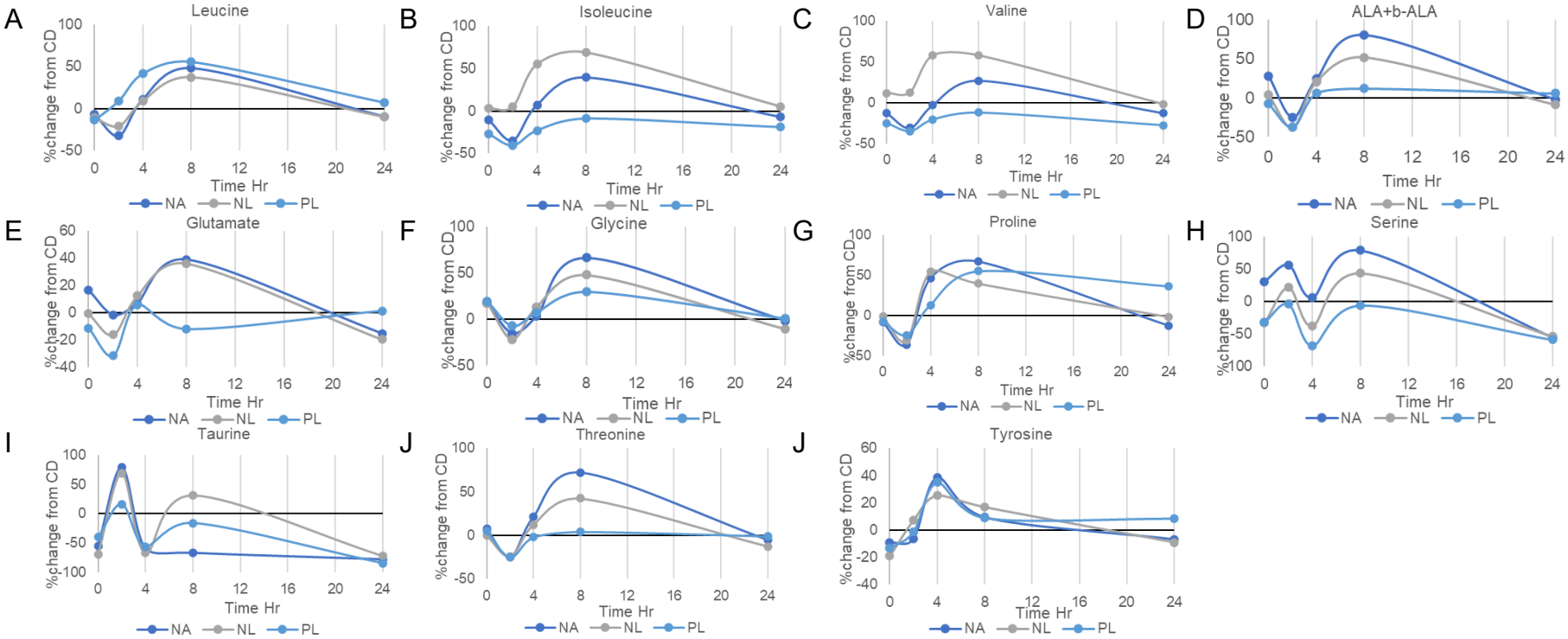


Figure 3.7 Muscle fNEAAs compared to CD (change%) A) leucine B) isoleucine C) valine D) arginine E) histidine F) lysine G) methionine H) phenylalanine I) threonine between diets at week-7. CD= Control diet, NA=Negative BCAAs, NL= Negative Leucine, PL= Positive Leucine

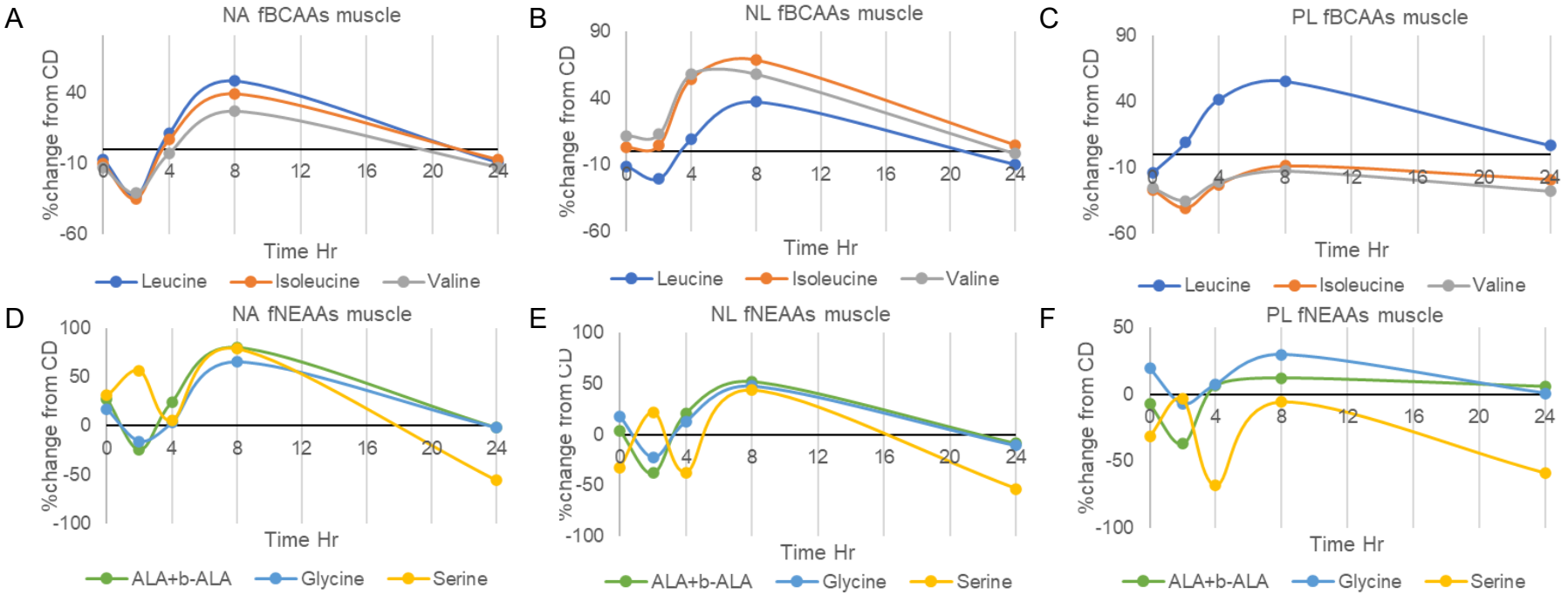


Figure 3.8 Within diet fAAs in muscle tissue compared to CD (change (%) over 24 hr) at week-7 A) NA fBCAAs B) NL fBCAAs C) PL fBCAAs D) NA fNEAAs E) NL fNEAAs F) PL fNEAAs. CD= Control diet, NA=Negative BCAAs, NL= Negative Leucine, PL= Positive Leucine

Interestingly in tyrosine, highest peak concentration was at -2 hr compared to all the other times (*p=0*). NL diet had a difference over time in proline, with the 4 hr time being different to the other timepoints (*p*=0.001). Similarly in NA, peak concentrations were at 4 hr (*p*=0.007).

In PL, alanine peak concentrations at 4 hr, were different to -2, 2 and 8 hr while in glutamate high peak concentrations were at 4 hr (*p=0*). Near significance (p≤ 0.10) was seen for *b*-alanine, glutamate and tyrosine in the NL and NA diets. Proline had near significance for the CD and PL diets, while for serine near significance was seen in NL. GLMs identified differences in diet means for *b*-alanine, while a difference in means over time was seen in alanine, glycine, glutamate, serine and tyrosine.

3.3.4 Blood chemistry

Blood chemistry results obtained from pooled plasma samples for red blood cell count (RBCC), haemoglobin (Hb), packed cell volume (PCV) and white blood cell count (WBCC) indicated no differences between the diets at week-3 nor week-7 (Table 3.17).

Although no statistical differences were seen between diets at each week or between the weeks, variability was high between individual pools and week (*p*=>0.05). RBCC (erythrocytes) trends between the weeks were alike, with higher counts in the CD and PL compared to the NL and NA. Week-3 ranged from 1.2 ±0.3 $x10^{12}$/L for CD to 1.0 ±0.2 $x10^{12}$/L in NL, while in week-7 RBCC ranged from 1.5 ±0.2 $x10^{12}$/L in the PL to 1.1 ±0.4 $x10^{12}$/L in NL. Counts in both weeks for NL and NA were similar, week-7 had increased RBCC in CD and PL. SRUC did attach comments noting that polychromatophilic cells (immature RBCs) were visible in the analyses at week-7. Polychromatophilic erythrocytes synthesise haemoglobin but in humans may be caused by hormonal responses to anaemia. In week-7, additional further in-depth analyses were conducted on heterophil, lymphocyte, monocyte and alkaline phosphatase (ALP), aspartate transaminase (AST), Creatine kinase (CK), and Albumin (ALB). Hb at week-3 ranged from 203.3 ±22.2g/L in the CD to 161.0 ±39.9g/L in the NA.

Table 3.17 Blood chemistry analysis between diets and weeks.

					One-way ANOVA	Two-way ANOVA P-value		
Time	CD	NL	NA	PL	P-value	Diet	Week	D*W
Week 3								
RBCC (x10^12/l)	1.2±0.3	1.0±0.2	1.1±0.2	1.2±0.1	0.362 (f 3, 8= 1.22)	0.083 (f 3, 16= 2.67)	0.063 (f 1, 16= 4.00)	0.720 (f 3, 16= 0.45)
Hb (g/l)	203.3±22.2	199.3±1.5	161.0±39.9	199.0±34.4	0.300 (f 3, 8= 1.45)	0.226 (f 3, 16= 1.61)	**0.000 (f 1, 16= 25.66)**	0.611(f 3, 16= 0.62)
PCV (l/l)	0.4±0.0	0.4±0.0	0.4±0.0	0.4±0.0	0.251 (f 3, 7= 1.71)	0.920 (f 3, 15= 0.16)	**0.048 (f 1, 15= 4.65)**	0.232 (f 3, 15= 1.59)
WBCC (x10^9/l)	16.0±4.5	9.1±3.5	10.8±4.8	14.2±7.1	0.395 (f 3, 8= 1.13)	0.499 (f 3, 16= 0.82)	**0.007 (f 1, 16= 9.37)**	0.726 (f 3, 16= 0.44)
Week 7								
RBCC (x10^12/l)	1.4±0.3	1.1±0.4	1.2±0.1	1.5±0.2	0.239 (f 3, 8= 1.72)			
Hb (g/l)	137.3±3.5	142.3±14.6	132.0±3.5	148.7±35.7	0.756 (f 3, 8= 0.40)			
PCV (l/l)	0.5±0.0	0.5±0.0	0.5±0.0	0.4±0.1	0.709 (f 3, 8= 0.47)			
WBCC (x10^9/l)	18.7±6.5	17.5±1.2	20.6±4.8	22.0±9.6	0.822 (f 3, 8= 0.30)			
Heterophil (x10^9/l)	5.7±1.2	4.3±1.0	5.4±1.0	5.8±2.9	0.710 (f 3, 8= 0.47)			
Lymphocyte (x10^9/l)	11.0±4.9	12.0±1.6	13.9±4.0	14.8±9.1	0.834 (f 3, 8= 0.29)			
Monocyte (x10^9/l)	1.9±0.5	1.2±0.3	1.2±0.6	1.5±0.6	0.323 (f 3, 8= 1.36)			
ALP (iu/l)	606.0±52.4	619.7±59.1	581.7±107.7	614.3±70.1	0.928 (f 3, 8= 0.15)			
AST (iu/l)	470.0±65.5	543.0±98.5	569.7±107.3	521.5±132.5	0.666 (f 3, 7= 0.55)			
CK (iu/l)	101267±84230	108200±74251	133600±53818	134967±99393	0.932 (f 3, 8= 0.14)			
ALB (g/l)	17.0±1.0	16.3±1.5	17.0±2.0	16.7±0.6	0.921 (f 3, 8= 0.16)			

Values represent means of three pooled plasma samples at the 4 hr sampling point in week-3 and week-7 (Total *n*=12). All values are means (*n*=12) ±standard deviation. Different superscripts indicate significant differences (p=<0.05). CD= Control diet, NA=Negative BCAAs, NL= Negative Leucine, PL= Positive Leucine. Red blood cell count (RBCC), Haemoglobin (Hb), Packed cell volume (PCV), White blood cell count (WBCC), alkaline phosphatase (ALP), aspartate transaminase (AST), Creatine kinase (CK), and Albumin (ALB). Analysis was performed using one-way ANOVA, with Fisher's LSD method used for *post-hoc* examination. A GLM was used to determine significance in diet, time and the interaction between diet and time (D*T).

NL and PL had similar values to the CD. Week-7 had similar values across the diets ranging from 148.7 ±35.7g/L in the PL to 132.0 ±3.5g/L in the NA. Hb values were lower in week-7 than in week-3 across all diets.

PCV (haematocrit) between the diets at each week and between the weeks were similar, with all diets at week-3 having 0.04 ±0.0l/L values and 0.5 ±0.0 at week-7, apart from PL which had no change between weeks.

WBCC was higher in week-7 than week-3. Week-3 values ranged from 16.0 ±4.5 $x10^9$/L in the CD to 9.1±3.5 $x10^9$/L in the NL and week-7 ranged from 22.0 ±9.6 $x10^9$/L for PL to 17.5 ±1.2 $x10^9$/L in NL. WBCC values for NL and NA had doubled between the weeks from 9.1 ±3.5 $x10^9$/L and 10.8 ±4.8 $x10^9$/L to 17.5 ±1.2 $x10^9$/L and 20.6 ±4.8 $x10^9$/L. Heterophil count ranged from 5.8 ±2.9 $x10^9$/L in PL to 4.3±1.0 $x10^9$/L in NL. Monocytes ranged from 1.9 ±0.5 $x10^9$/L in CD to 1.2±0.3 $x10^9$/L in both NL and NA diets. Lymphocyte count ranged from 14.8 ±9.1 $x10^9$/L in the PL to 11.0±4.9 $x10^9$/L in the CD. The CK levels in the current study ranged from 134967 ±99393 iu/L in the PL diet to 101267 ±84230 iu/L in the CD diet.

Further GLM analysis between the two sampling points displayed no differences in diets but differences in weeks for Hb (*p=0*), PCV (*p*=0.048) and WBCC (*p*=0.007). Near significance (p≤ 0.10) was observed for RBCC across diet and week. No interactions were observed between diet and week (D*W).

3.3.5 Plasma

3.3.5.1 Plasma fBCAAs week-3 and week-7 comparisons at 4 hr

Plasma analysis of the BCAAs in week three highlighted differences for isoleucine and valine (*p*=0.001, *p=0*). *Post-hoc* analysis displayed that the differences in isoleucine and valine were between the NL and the other diets (Table 3.18).

No differences were noted in leucine for week-3 but were seen in week-7, with the highest peak in PL compared the other three test diets (*p*=0.007). A similar trend was witnessed in isoleucine, with the PL diet being different to the other test diets, although this was due to PL having the lowest peak concentrations (*p*=0.017). The highest concentrations in week-7 for valine were in the NL diet, which post–hoc analysis distinguished the differences as being between NL and

the NA and PL diets (p=0.009). GLMs had differences in the means of all the BCAAs, with an additional difference in the means of the weeks for leucine. An interaction between diet and week (D*W) was seen in valine with a near significant interaction in isoleucine.

3.3.5.1.1 Plasma fEAAs week-3 and week-7 comparisons at 4 hr

Plasma EAAs had differences across the diets in week-3 for lysine, with the highest peak concentrations in NA compared to the other diets (p=0.015) (Table 3.18). A near significance was seen across week-7 for threonine (p≤ 0.10), all other plasma fEAAs had no differences across diets and between weeks.

Within each diet between weeks had a difference in lysine for the NL diet, with week-3 having a higher concentration than week-7 (p=0.022). This was trend was also seen in both NA and PL (p=0.014, p=0.006).

Threonine had an opposite trend in NA, with week-7 having higher concentration than week-3 (p=0.045). Near significance (p≤ 0.10) was seen for arginine in the NL, and threonine in the CD. GLMs showed differences in the means of the diets and weeks for lysine, with a significant interaction between the two (p=0.009, p=*0*, p=0.022).

3.3.5.1.2 Plasma fNEAAs week-3 and week-7 comparisons at 4 hr

fNEAAs across diets at week-3 had a difference in alanine, with NA concentrations higher than NL and CD (p=0.045) (Table 3.18). In week-3 and week-7 the differences across diets for serine were similar, with the lowest concentrations being in the PL diet (p=0.031, p=0.017). Within the diets between the weeks, had differences in alanine concentrations for NA and PL, with week-3 having significantly higher concentrations than week-7 (p=0.008, p=0.007). Whereas inversely, b-alanine had differences between the weeks for CD and PL, but week-7 had higher concentrations than week-3 (p=0.050, p=*0*). Glycine had higher week-7 concentrations than week-3 for CD, NA and PL (p=0.039, p=0.024, p=0.038). Similarly, taurine in the CD had higher week-7 concentrations than week-3 (p=0.037) while tyrosine in PL had higher week-3 concentrations than week-7 (p=0.004). Near significance was noted in NL for alanine and tyrosine, NA for serine and tyrosine and for *b*-alanine in PL diet.

Table 3.18 Total plasma fAAs of the test diets between week-3 and week-7. Data are expressed as mean ±standard deviation in µmol/ L and different superscripts indicate significant differences (p=<0.05) with *abc* displaying vertical and *zyx* horizontal differences.

					One-way ANOVA	Two-way ANOVA P-value		
Time 4hr	CD	NL	NA	PL	P-value	Diet	Week	D*W
Isoleucine								
Week 3	186.6±18.2 ^{y}	292.1±6.9 ^{z}	175.6±32.0 ^{y}	155.2±9.6 ^{y}	**0.001 (f 3, 7= 19.73)**	**0.000**	0.498	0.062
Week 7	239.62±52.53 ^{z}	252.2±33.0 ^{z}	210.30±29.90 ^{z}	141.06±4.18 ^{y}	**0.017 (f 3, 8 = 6.23)**			
P-value	0.174 (f1, 4= 2.72)	0.207 (f1, 3= 2.58)	0.242 (f1, 4= 1.88)	0.080 (f1, 4= 5.44)				
Leucine								
Week 3	294.19±37.07	302.96±45.54	290.55±48.18	369.11±64.56	0.254 (f 3, 8= 1.65)	**0.002**	**0.043**	0.194
Week 7	367.01±79.58 ^{y}	280.06±37.01 ^{y}	317.98±35.83 ^{y}	465.92±2.28 ^{z}	**0.007 (f 3, 8 = 8.63)**			
P-value	0.224 (f1, 4= 2.06)	0.536 (f1, 4= 0.46)	0.473 (f1, 4= 0.63)	0.060 (f1, 4= 6.74)				
Valine								
Week 3	402.86±56.55 ^{y}	672.79±51.30 ^{z}	317.72±51.44 ^{y}	319.12±27.21 ^{y}	**0.000 (f 3, 8= 36.71)**	**0.000**	0.188	**0.026**
Week 7	530.66±115.09 $^{z\,y}$	582.64±70.19 ^{z}	423.93±52.30 $^{y\,x}$	314.07±20.71 ^{x}	**0.009 (f 3, 8 = 7.99)**			
P-value	0.159 (f1, 4= 2.98)	0.147 (f1, 4= 3.23)	0.066 (f1, 4= 6.29)	0.811 (f1, 4= 0.07)				
Arginine								
Week 3	165.30±2.60	575.9±342.8	427.2±377.5	341.1±308.8	0.444 (f 3, 8= 0.99)	0.852	0.235	0.199
Week 7	436.0±443.7	182.7±26.4	209.84±25.55	150.89±8.64	0.434 (f 3, 8= 1.02)			
P-value	0.350 (f1, 4= 1.12)	0.119 (f1, 4= 3.92)	0.376 (f1, 4= 0.99)	0.346 (f1, 4= 1.14)				
Histidine								
Week 3	17.45±0.77	17.60±1.86	19.06±1.31	18.43±2.00	0.582 (f 3, 8= 0.69)	0.176	0.450	0.722
Week 7	16.78±2.98	16.45±3.04	19.94±1.80	16.71±2.12	0.344 (f 3, 7= 1.31)			
P-value	0.716 (f1, 3= 0.16)	0.605 (f1, 4= 0.31)	0.532 (f1, 4= 0.47)	0.364 (f1, 4= 1.05)				
Lysine								
Week 3	183.27±32.28 ^{y}	231.41±28.34 $^{y\,a}$	317.04±53.29 $^{a\,z}$	222.73±27.42 $^{a\,y}$	**0.015 (f 3, 8= 6.50)**	**0.009**	**0.000**	**0.022**
Week 7	182.00±45.53	142.70±31.27 ^{b}	176.13±22.93 ^{b}	126.50±14.53 ^{b}	0.160 (f 3, 8= 2.24)			
P-value	0.972 (f1, 4= 0.00)	**0.022 (f1, 4= 13.25)**	**0.014 (f1, 4= 17.70)**	**0.006 (f1, 4= 28.84)**				
Methionine								
Week 3	135.91±20.32	175.59±59.42	128.31±21.05	121.98±14.02	0.282 (f 3, 8= 1.52)	0.478	0.371	0.445
Week 7	164.11±55.20	150.29±57.89	183.48±61.88	128.58±4.95	0.618 (f 3, 8= 0.63)			
P-value	0.453 (f1, 4= 0.69)	0.625 (f1, 4= 0.28)	0.218 (f1, 4= 2.14)	0.485 (f1, 4= 0.59)				
Phenylalanine								
Week 3	100.41±17.65	113.83±19.02	122.18±25.59	111.81±8.85	0.585 (f 3, 8= 0.69)	0.485	0.685	0.489

	Week 7	116.08±22.21	101.30±16.84	118.41±12.29 z	100.80±7.18	0.410 (f 3, 8= 1.08)			
	P-value	0.393 (f1, 4= 0.92)	0.441 (f1, 4= 0.73)	0.829 (f1, 4= 0.05)	0.170 (f1, 4= 2.80)				
Threonine									
	Week 3	174.12±32.05	237.39±79.55	221.95±32.17 b	178.66±20.58	0.326 (f 3, 8= 1.35)	**0.035**	**0.017**	0.165
	Week 7	283.96±60.96	251.24±68.76	313.45±44.46 a	176.33±2.34	0.052 (f 3, 8= 4.01)			
	P-value	0.051 (f1, 4= 7.63)	0.831 (f1, 4= 0.05)	**0.045 (f1, 4= 8.34**)	0.855 (f1, 4= 0.04)				
Alanine									
	Week 3	699.49±85.43 y	691.12±95.01 y	934.62±115.24 a z	785.20±80.71 zy a	**0.045 (f 3, 8= 4.24)**	**0.035**	**0.000**	**0.020**
	Week 7	626.65±91.62	579.52±38.64	593.45±36.62 b	462.79±76.36 b	0.066 (f 3, 8= 3.58)			
	P-value	0.371 (f1, 4= 1.01)	0.133 (f1, 4= 3.55)	**0.008 (f1, 4= 23.88)**	**0.007 (f1, 4= 25.26)**				
***b*-Alanine**									
	Week 3	188.52±35.35 b	465.5±381.1	179.35±24.97 b	141.16±14.70	0.222 (f 3, 8= 1.82)	0.206	**0.001**	0.461
	Week 7	516.38±202.02 a	601.19±225.36	707.0±37.0 a	448.60±209.66	0.542 (f 3, 7= 0.78)			
	P-value	**0.050 (f1, 4= 7.67)**	0.371 (f1, 4= 1.01)	**0.000 (f1, 3= 383.37)**	0.064 (f1, 4= 6.42)				
Glycine									
	Week 3	668.77±48.16 b	852.7±358.8	749.68±26.49 b	705.49±68.65 b	0.658 (f 3, 8= 0.56)	0.492	**0.000**	0.462
	Week 7	1289.73±351.70 a	1157.01±310.64	1332.85±283.87 a	969.46±133.57 a	0.439 (f 3, 8= 1.00)			
	P-value	**0.039 (f1, 4= 9.18)**	0.329 (f1, 4= 1.23)	**0.024 (f1, 4= 12.55)**	**0.038 (f1, 4= 9.27)**				
Glut. acid									
	Week 3	103.59±2.09	135.84±28.19	112.21±13.55	110.51±10.12	0.168 (f 3, 8= 2.18)	0.107	0.723	0.189
	Week 7	115.85±14.68	119.75±20.16	136.35±22.50	100.37±13.18	0.191 (f 3, 8= 2.01)			
	P-value	0.225 (f1, 4= 2.05)	0.466 (f1, 4= 0.65)	0.187 (f1, 4= 2.53)	0.350 (f1, 4= 1.12)				
Proline									
	Week 3	62.52±12.48	78.72±28.34	72.30±22.38	64.60±15.98	0.766 (f 3, 8= 0.39)	0.393	0.098	0.385
	Week 7	91.23±30.19	74.50±18.57	104.90±25.76	68.72±3.18	0.248 (f 3, 8= 1.68)			
	P-value	0.202 (f1, 4= 2.32)	0.840 (f1, 4= 0.840)	0.173 (f1, 4= 2.74)	0.684 (f1, 4= 0.19)				
Serine									
	Week 3	325.56±15.47 z	301.01±74.06 z	325.00±40.98 z	179.40±66.55 y	**0.031 (f 3, 8= 4.95)**	**0.000**	**0.048**	0.744
	Week 7	391.83±73.41 z	382.76±89.76 z	380.26±33.95 z	188.95±45.21 y	**0.017 (f 3, 7= 6.96)**			
	P-value	0.199 (f1, 3= 2.69)	0.291 (f1, 4= 1.48)	0.146 (f1, 4= 3.24)	0.847 (f1, 4= 0.04)				
Taurine									
	Week 3	79.71±13.71 b	143.86±31.87	284.6±313.8	156.59±9.94	0.545 (f3, 7= 0.77)	**0.541**	**0.824**	**0.613**
	Week 7	181.83±50.55 a	175.47±29.40	187.31±57.60	168.36±18.03	0.946 (f3, 7= 0.12)			
	P-value	**0.037 (f1, 3= 12.81)**	0.275 (f1, 4= 1.59)	0.626 (f1, 4= 0.28)	0.474 (f1, 3= 0.67)				
Tyrosine									

Week 3	46.01±12.01	57.54±7.81	66.54±20.14	69.66±9.19 [a]	0.201 (f 3, 8= 1.94)	0.124	**0.000**	0.299
Week 7	35.49±8.31	38.82±9.65	44.75±3.72	35.18±4.39 [b]	0.366 (f 3, 8= 1.21)			
P-value	0.280 (f1, 4= 1.56)	0.059 (f1, 4= 6.83)	0.139 (f1, 4= 3.40)	**0.004 (f1, 4= 34.37)**				

Values represent means of three pooled samples for each test diet (Total *n*=12). All values are means (*n*=12) ± standard deviation. Different superscripts indicate significant differences (*p*=<0.05). CD= Control diet, NA=Negative BCAAs, NL= Negative Leucine and PL= Positive Leucine. Analysis was performed using one-way ANOVA, with Fisher LSD method used for *post-hoc* examination. A GLM was used to determine significance in diet, time and the interaction between diet and time. Glut. Acid= glutamate.

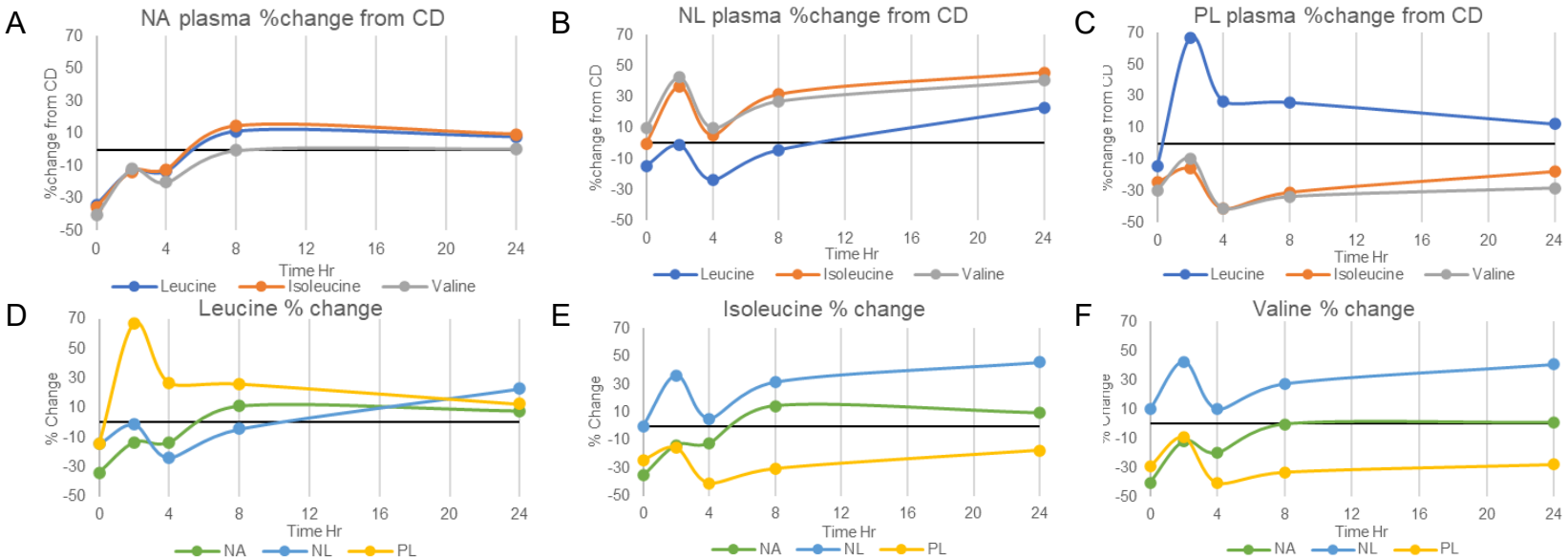


Figure 3.9 Individual plasma fBCAA and change (%) between the CD diet. A) NA B) NL C) PL D) leucine change (%) E) isoleucine change (%) F) valine change (%) from the CD diet. All values are means (*n*=9) ±standard deviation. Different superscripts indicate significant differences ($p<0.05$). CD= Control diet, NA=Negative BCAAs, NL= Negative Leucine, PL= Positive Leucine

3.3.5.1.3 Plasma fBCAAs over time and between times at week-7

Across each diet at each timepoint in week-7, for isoleucine and valine saw differences (p=<0.05) at each of the five timepoints, whereas differences in leucine were seen at 2, 4 and 8 hr (Table 3.19, Figure 3.9).

Leucine had significantly higher concentrations in PL than the other diets at 2 hr and 4 hr (p=*0*, p=0.007). While at 8 hr, PL concentrations were higher than NL and CD (p=0.033). In isoleucine, at -2 hr *post-hoc* analysis determined the differences in concentrations between the diets as CD and NL having the highest different concentrations to NA (p=0.031). At 2 hr, NL had the highest different concentration while at 4 hr, PL had the lowest significantly different concentration between the diets (p=0.001, p=0.017). NL at 8 hr and 24 hr had the highest different concentrations and CD and PL the lowest (p=0.004, p=0.032).

In valine, NL had the highest concentrations compared to the other diets at 2 hr and 24 hr (p=0.001, p=0.015). NL and CD had the highest different concentrations compared to the other diets at -2 hr (p=0.005). At 4 hr, NL had the highest concentration compared to NA and PL, while at 8 hr PL had the lowest different concentration (p=0.009, p=0.021). Within each diet over time, had differences in the CD diet for isoleucine and leucine, with *post-hoc* analysis displaying the differences as the 4 hr time having significantly higher concentrations than 8 and 24 hr (p=0.014, p=0.020). Interestingly, both isoleucine and leucine 24 hr concentrations were significantly lower than the -2 hr concentrations. NL isoleucine differences in concentration over time, had the 2 and 4 hr times significantly higher than the other three times, whereas for valine 2 and 4 hr were different to 8 and 24 hr (p=0.003, p=0.043).

PL had similar uptake differences for isoleucine and valine, whereby -2, 2 and 4 hr concentrations were higher than 8 and 24 hr (p=0.003, p=0.002). PL leucine concentration differences over time had higher different concentrations at 2 and 4 hr compared to the other three times (p=*0*). Both PL 2 hr concentrations of isoleucine and valine were significantly lower than the -2 hr point. GLMs looking at the differences in means for diet, time and the interaction (D*T) had differences

across all parameters for all BCAAs apart from there was no D*T interaction in valine.

The highest different plasma concentration mean across diets for isoleucine was NL, PL for leucine and NL for valine. In isoleucine and leucine, the highest different mean concentrations were at 2 and 4 hr, while in valine 4 hr was different to -2, 8 and 24 hr.

3.3.5.1.4 Plasma fEAAs over time and between times week-7

Differences in arginine concentrations were different between each diet at 2 hr, with the highest concentration in NA, followed by NL, followed by CD and PI having the lowest concentration across all diets (*p=0*) (Table 3.19, Figure 3.11). Lysine had differences across diets at 2, 8 and 24 hr (*p*=0.038, *p*=0.002, *p*=0.043). At 2 and 24 hr, Fisher's *post-hoc* analysis displayed differences in concentrations with NA higher than CD and PL, while at 8 hr NA was higher than NL and PL. Phenylalanine had differences across time at 8 hr with NA having higher concentrations than CD and NL (*p*=0.035).
Threonine had differences at 2 hr and 8 hr, with NA and NL the highest different concentrations at 2 hr while at 8 hr NA was the highest different concentration (*p*=0.011, *p*=0.015).

Differences within each diet over time for arginine had differences in NL, NA and PL (*p*=0.013, *p*=0.045, *p*=0.001). Surprisingly for NL and PL the highest different concentrations were at 24 hr, while for NA the highest was 24 hr, but it was similar to 8 hr. Although no differences were seen across diets at each time, differences in diets over time were seen in histidine, with differences in CD, NL and PL (*p*=0.002, *p=0*, *p=0*). Similarly to arginine, the 24 hr time in histidine was significantly higher than the other four timepoints.

Lysine had differences in time for CD and PL (*p*=0.016, *p*=0.011). The highest concentration of lysine in the CD was at -2 hr whereas in PL -2, 2 and 4 hr were similar but the 8 hr point was significantly lower than the rest. Methionine in the CD had a significantly high peak concentration at 4 hr (*p*=0.045). Phenylalanine had peak concentrations at 4 hr in the NA diet, with the 4 hr concentration higher than -2 and 24 hr (*p*=0.032).

Table 3.19 Week-7 total plasma fBCAAs of the test diets at five different time points. Data are expressed as mean ± standard deviation in µmol/ L and different superscripts indicate significant differences (p <0.05) with *abc* displaying vertical and *zyx* horizontal differences.

						One-way ANOVA	Two-way ANOVA P-value		
Time		CD	NL	NA	PL	P-value	Diet	Time	D*T
Isoleucine	-2hr	199.33±14.83 $^{ab\,z}$	199.16±8.55 $^{b\,z}$	128.60±51.84 ^{y}	150.66±9.89 $^{a\,zy}$	**0.031 (f 3, 8 = 4.95)**	**0.000**	**0.000**	**0.032**
	2hr	194.75±6.00 $^{ab\,y}$	265.81±8.10 $^{a\,z}$	168.26±33.41 ^{y}	164.10±13.41 $^{a\,y}$	**0.001 (f 3, 8 = 19.01)**			
	4hr	239.62±52.53 $^{a\,z}$	252.22±32.97 $^{a\,z}$	210.30±29.90 ^{z}	141.06±4.18 $^{a\,y}$	**0.017 (f 3, 8 = 6.23)**			
	8hr	155.70±17.39 $^{bc\,y}$	204.83±13.49 $^{b\,z}$	178.27±36.03 ^{zy}	108.00±11.30 $^{b\,x}$	**0.004 (f 3, 8 = 10.58)**			
	24hr	132.88±38.12 $^{c\,y}$	193.62±24.95 $^{b\,z}$	145.29±16.59 ^{zy}	109.79±26.79 $^{b\,y}$	**0.032 (f 3, 8 = 4.89)**			
	P-value	**0.014 (f 4, 10= 5.40)**	**0.003 (f 4, 10= 8.22)**	0.124 (f 4, 10= 2.36)	**0.003 (f 4, 10= 8.20)**				
Leucine									
	-2hr	322.03±28.81^{ab}	275.16±16.83	212.77±81.49	275.43±30.15 ^{bc}	0.103 (f 3, 8 = 2.87)	**0.000**	**0.000**	**0.000**
	2hr	306.29±8.10 $^{ab\,y}$	302.40±17.17 ^{y}	265.73±10.99 ^{x}	512.01±35.80 $^{a\,z}$	**0.000 (f 3, 8 = 87.53)**			
	4hr	367.01±79.58 $^{a\,y}$	280.06±37.01 ^{y}	317.98±35.83 ^{y}	465.92±2.28 $^{a\,z}$	**0.007 (f 3, 8 = 8.63)**			
	8hr	247.11±23.73 $^{bc\,y}$	236.33±4.74 ^{y}	275.38±38.11 ^{zy}	311.72±27.63 $^{b\,z}$	**0.033 (f 3, 8 = 4.86)**			
	24hr	213.84±64.24 ^{c}	263.00±26.57	230.97±15.38	240.51±59.92 ^{c}	0.643 (f 3, 8 = 0.58)			
	P-value	0**.020 (f 4, 10= 4.78)**	0.057 (f 4, 10= 3.29)	0.102 (f 4, 10= 2.58)	**0.000 (f 4, 10= 33.25)**				
Valine									
	-2hr	447.50±29.59 ^{z}	491.37±40.60 $^{ab\,z}$	267.1±105.0 ^{y}	316.04±26.45 $^{a\,y}$	**0.005 (f 3, 8 = 9.48)**	**0.000**	**0.000**	0.150
	2hr	404.07±34.44 ^{y}	575.92±23.84 $^{a\,z}$	355.23±66.48 ^{y}	366.27±29.91 $^{a\,y}$	**0.001 (f 3, 8 = 17.84)**			
	4hr	530.66±115.09 ^{zy}	582.64±70.19 $^{a\,z}$	423.93±52.30 ^{yx}	314.07±20.71 $^{a\,x}$	**0.009 (f 3, 8 = 7.99)**			
	8hr	366.20±86.40 ^{zy}	465.77±60.79 $^{b\,z}$	364.82±73.96 ^{zy}	244.04±19.40 $^{b\,y}$	**0.021 (f 3, 8 = 5.81)**			
	24hr	330.59±95.59 ^{y}	464.42±56.82 $^{b\,z}$	332.81±34.97 ^{y}	237.75±46.36 $^{b\,y}$	**0.015 (f 3, 8 = 6.63)**			
	P-value	0.083 (f 4, 10= 2.83)	**0.043 (f 4, 10= 3.68)**	0.180 (f 4, 10= 1.94)	**0.002 (f 4, 10= 9.69)**				
Arginine									
	-2hr	405.95±359.00	371.43±342.61 ^{b}	281.03±151.26 ^{b}	146.85±12.56 ^{c}	0.635 (f 3, 8 = 0.60)	0.214	**0.000**	0.816
	2hr	184.11±4.00 ^{x}	217.72±5.66 $^{b\,y}$	234.46±4.27 $^{b\,z}$	155.64±10.70 $^{c\,w}$	**0.000 (f 3, 8 = 82.00)**			
	4hr	436.00±443.69	182.74±26.44 ^{b}	209.84±25.55 ^{b}	150.89±9.64 ^{c}	0.434 (f 3, 8 = 1.02)			
	8hr	515.55±193.86	271.25±213.73 ^{b}	431.66±426.90 ^{ab}	336.80±175.94 ^{b}	0.719 (f 3, 8 = 0.46)			
	24hr	602.33±173.98	795.76±78.42 ^{a}	750.96±48.89 ^{a}	577.36±93.15 ^{a}	0.098 (f 3, 8 = 2.95)			
	P-value	0.484 (f4, 10= 0.93)	**0.013 (f4, 10= 5.50)**	**0.045 (f4, 10= 3.61)**	**0.001 (f4, 10= 13.25)**				
Histidine									
	-2hr	16.72±3.77 ^{b}	21.85±2.57 ^{b}	25.17±12.60	20.85±5.10 ^{b}	0.620 (f 3, 7 = 0.63)	0.455	**0.000**	0.553
	2hr	19.01±2.90 ^{b}	17.86±1.07 ^{bc}	20.37±1.64	16.96±3.77 ^{bc}	0.447 (f 3, 8 = 0.99)			

	4hr	16.78±2.98 [b]	16.45±3.04 [c]	19.94±1.80	16.71±2.12 [bc]	0.344 (f 3, 7 = 1.31)			
	8hr	15.03±3.36 [b]	16.04±2.09 [c]	19.61±5.56	13.73±1.10 [c]	0.408 (f 3, 6 = 1.13)			
	24hr	32.49±5.39 [a]	34.90±1.67 [a]	37.77±10.56	34.66±1.31 [a]	0.958 (f 3, 8 = 0.10)			
	P-value	**0.002 (f 4, 9= 9.96)**	**0.000 (f4, 8= 38.26)**	0.210 (f4, 10= 1.78)	**0.000 (f4, 9= 18.40)**				
Lysine									
	-2hr	259.32±42.60 [a]	220.06±61.24	217.05±112.86	159.13±13.46 [a]	0.402 (f 3, 8 = 1.11)	**0.000**	**0.001**	0.347
	2hr	178.53±6.82 [b y]	197.73±21.46 [zy]	245.33±45.32 [z]	153.16±37.60 [a y]	**0.038 (f 3, 8 = 4.58)**			
	4hr	182.00±45.53 [b]	142.70±31.27	176.13±22.93	126.50±14.53 [a]	0.160 (f 3, 8 = 2.24)			
	8hr	163.71±9.67 [b zy]	137.75±15.89 [y]	204.62±39.13 [z]	89.22±12.72 [b x]	**0.002 (f 3, 8 = 13.75)**			
	24hr	133.24±47.77 [b yx]	194.43±29.46 [zy]	208.70±42.28 [z]	125.08±2.27 [ab x]	**0.043 (f 3, 8 = 4.35)**			
	P-value	**0.016 (f 4, 10= 5.17)**	0.064 (f 4, 10= 3.15)	0.738 (f 4, 10= 0.50)	**0.011 (f 4, 10= 5.86)**				
Methionine									
	-2hr	109.53±19.85 [b]	108.96±37.42	67.05±29.71	97.16±15.16	0.258 (f 3, 8 = 1.63)	0.465	**0.000**	0.369
	2hr	109.36±1.54 [b]	149.14±51.04	147.11±44.49	113.27±10.83	0.383 (f 3, 8 = 1.16)			
	4hr	164.11±52.20 [a]	150.29±57.89	183.48±61.88	128.58±4.95	0.618 (f 3, 8 = 0.63)			
	8hr	109.01±39.80 [b]	90.34±1.09	105.80±9.88	160.66±79.22	0.309 (f 3, 8 = 1.41)			
	24hr	80.36±19.85 [b]	100.11±13.18	84.72±20.39	91.74±5.34	0.465 (f 3, 8 = 0.94)			
	P-value	**0.045** (f 4, 10= 3.63)	0.254 (f 4, 10= 1.58)	0.083 (f 4, 10= 2.83)	0.254 (f 4, 10= 1.58)				
Phenylalanine									
	-2hr	106.33±11.24	91.94±10.07	79.72±27.27 [c]	103.89±10.48	0.251 (f 3, 8 = 1.66)	0.796	**0.000**	0.091
	2hr	99.84±7.42	107.76±6.62	108.75±3.98 [ab]	100.73±8.02	0.302 (f 3, 8 = 1.44)			
	4hr	116.08±22.21	101.30±16.84	118.41±12.29 [a]	100.80±7.18	0.410 (f 3, 8 = 1.08)			
	8hr	89.70±9.36 [y]	89.28±4.17 [y]	109.85±10.29 [ab z]	95.53±4.72 [zy]	**0.035 (f 3, 8 = 4.75)**			
	24hr	74.53±19.67	89.16±13.19	85.29±5.55 [bc]	85.79±11.65	0.597 (f 3, 8 = 0.66)			
	P-value	0.056 (f 4, 10= 3.32)	0.234 (f 4, 10= 1.66)	**0.032** (f 4, 10= 4.08)	0.173 (f 4, 10= 1.98)				
Threonine									
	-2hr	188.80±11.18 [bc]	167.92±27.65 [c]	148.74±60.89 [c]	201.99±18.88 [a]	0.331 (f 3, 8 = 1.33)	**0.000**	**0.000**	**0.002**
	2hr	222.96±20.82 [ab y]	291.95±18.83 [a z]	304.75±38.20 [a z]	209.26±38.70 [a y]	**0.011 (f 3, 8 = 7.41)**			
	4hr	283.96±60.96 [a]	251.24±68.76 [ab]	313.45±44.46 [a]	176.33±2.34 [ab]	0.052 (f 3, 8 = 4.01)			
	8hr	175.05±7.47 [bc y]	174.33±4.26 [b y]	266.24±72.41 [ab z]	138.87±6.78 [b y]	**0.015 (f 3, 8 = 6.63)**			
	24hr	151.75±36.19 [c]	203.34±37.16 [bc]	196.31±18.20 [bc]	183.18±17.49 [a]	0.211 (f 3, 8 = 1.88)			
	P-value	**0.006** (f 4, 10= 7.02)	**0.011** (f 4, 10= 5.80)	**0.010** (f 4, 10= 6.00)	**0.016** (f 4, 10= 5.15)				
Alanine									
	-2hr	631.97±46.03	563.42±60.55 [b]	455.78±163.63 [c]	564.51±49.72	0.222 (f 3, 8 = 1.82)	**0.004**	**0.000**	**0.003**
	2hr	636.92±117.27 [yx]	778.26±44.23 [a zy]	846.13±63.27 [a z]	562.11±66.41 [x]	**0.008 (f 3, 8 = 8.35)**			

	4hr	626.65±91.62	579.52±38.64 ^{b}	593.45±36.62 ^{bc}	462.79±76.36	0.066 (f 3, 8 = 3.58)			
	8hr	454.65±51.09 ^{y}	409.64±27.37 $^{c\ y}$	692.85±123.10 $^{ab\ z}$	412.07±28.70 ^{y}	**0.003 (f 3, 8= 11.36)**			
	24hr	492.15±214.58	638.30±98.01 ^{b}	574.91±53.45 ^{bc}	529.62±110.73	0.593 (f 3, 8 = 0.67)			
	P-value	0.251 (f 4, 10= 1.59)	**0.000 (f 4, 10= 15.25)**	**0.008 (f 4, 10= 6.38)**	0.101 (f 4, 10= 2.59)				
b-Alanine									
	-2hr	194.47±57.62 ^{b}	362.96±186.81	245.84±87.06 ^{b}	378.22±65.38	0.204 (f 3, 8 = 1.92)	0.058	**0.000**	0.387
	2hr	582.07±72.83 ^{a}	547.42±19.76	783.98±294.60 ^{a}	487.03±142.56	0.232 (f 3, 8= 1.76)			
	4hr	516.38±202.02 ^{a}	601.19±225.36	894.17±325.30 ^{a}	448.60±209.66	0.206 (f 3, 8 = 1.91)			
	8hr	307.63±74.09 ^{b}	470.47±292.28	530.67±225.29 ^{ab}	231.23±58.05	0.263 (f 3, 8 = 1.60)			
	24hr	138.42±51.78 ^{b}	134.70±39.24	174.06±89.98 ^{b}	206.55±67.06	0.521 (f 3, 8 = 0.81)			
	P-value	**0.002** (f 4, 10= 9.91)	0.075 (f 4, 10= 2.95)	**0.011** (f 4, 10= 5.86)	0.065 (f 4, 10= 3.14)				
Glycine									
	-2hr	609.48±71.08 ^{c}	649.81±175.46 ^{c}	540.98±199.39 ^{c}	851.97±151.95 ^{b}	0.169 (f 3, 8 = 2.17)	0.078	**0.000**	0.145
	2hr	1050.36±208.95 ^{ab}	1318.84±215.73 ^{a}	1518.90±388.27 ^{a}	1075.15±45.15 ^{a}	0.141 (f 3, 8 = 2.42)			
	4hr	1289.73±351.70 ^{a}	1157.01±310.64 ^{ab}	1332.85±283.87 ^{a}	969.46±133.57 ^{ab}	0.439 (f 3, 8 = 1.00)			
	8hr	684.37±185.02 ^{bc}	827.64±293.80 ^{bc}	1096.53±337.81 ^{ab}	662.73±43.58 ^{c}	0.189 (f 3, 8 = 2.02)			
	24hr	572.23±169.39 ^{c}	611.65±51.15 ^{c}	636.95±57.49 ^{bc}	643.19±17.42 ^{c}	0.786 (f 3, 8 = 0.36)			
	P-value	**0.008** (f 4, 10= 6.30)	**0.013** (f 4, 10= 5.59)	**0.006** (f 4, 10= 7.03)	**0.001** (f 4, 10= 11.82)				
Glut. acid									
	-2hr	99.17±4.10 ^{ab}	111.88±12.09 ^{a}	85.00±33.84 ^{bc}	129.99±17.33 ^{a}	0.114 (f 3, 8 = 2.73)	0.067	**0.000**	**0.017**
	2hr	110.98±12.59 ^{ab}	116.38±9.55 ^{a}	125.31±9.98 ^{ab}	109.41±21.75 ^{ab}	0.551 (f 3, 8 = 0.75)			
	4hr	115.85±14.68 ^{a}	119.75±20.16 ^{a}	136.35±22.50 ^{a}	100.37±13.18 ^{bc}	0.191 (f 3, 8 = 2.01)			
	8hr	86.50±13.83 $^{bc\ y}$	88.11±7.79 $^{b\ y}$	124.56±27.26 $^{ab\ z}$	76.82±2.72 $^{c\ y}$	**0.027 (f 3, 8 = 5.27)**			
	24hr	58.08±25.42 ^{c}	71.96±10.13 ^{b}	82.76±10.93 ^{c}	76.83±2.72 ^{c}	0.344 (f 3, 8 = 1.29)			
	P-value	**0.008** (f 4, 10= 6.53)	**0.004** (f 4, 10= 7.96)	**0.046** (f 4, 10= 3.59)	**0.006** (f 4, 10= 6.88)				
Proline									
	-2hr	51.18±5.24 ^{bc}	46.09±6.70 ^{b}	35.10±12.39 ^{b}	53.33±17.78 ^{bc}	0.295 (f 3, 8 = 1.47)	**0.022**	**0.000**	0.051
	2hr	78.92±10.78 ^{ab}	93.24±11.72 ^{a}	92.17±13.86 ^{a}	71.93±9.05 ^{a}	0.138 (f 3, 8 = 2.45)			
	4hr	91.23±30.19 ^{a}	74.50±18.57 ^{a}	104.90±25.76 ^{a}	68.72±3.18 ^{ab}	0.248 (f 3, 8 = 1.68)			
	8hr	51.50±5.68 ^{bc}	53.17±0.14 ^{b}	94.05±40.89 ^{a}	45.26±3.74 ^{cd}	0.071 (f 3, 8 = 3.47)			
	24hr	32.99±8.90 ^{c}	36.61±3.67 ^{b}	37.44±4.86 ^{b}	32.18±9.29 ^{d}	0.756 (f 3, 8 = 0.40)			
	P-value	**0.006** (f 4, 10= 7.09)	**0.000** (f 4, 10= 14.57)	**0.009** (f 4, 10= 6.28)	**0.004** (f 4, 10= 8.04)				
Serine									
	-2hr	393.60±329.87	546.17±605.62	310.56±180.61 ^{b}	188.49±23.42	0.673 (f 3, 8 = 0.53)	0.138	**0.004**	0.846
	2hr	278.51±36.84 ^{y}	414.08±60.70 ^{z}	426.20±48.64 $^{b\ z}$	202.33±15.56 ^{y}	**0.001** (f 3, 8 = 18.44)			

	4hr	391.83 ± 73.41 ^{z}	382.76±89.79 ^{z}	380.26±33.95 $^{b\,z}$	188.95±45.21 ^{y}	**0.017** (f 3, 7 = 6.96)			
	8hr	491.85±576.17	223.82±20.22	294.12±76.42 ^{b}	324.43±300.97	0.815 (f 3, 7 = 0.31)			
	24hr	586.77±226.99	875.32±203.28	699.86±135.48 ^{a}	524.43±37.04	0.131 (f 3, 8 = 2.53)			
	P-value	0.828 (f 4, 9= 0.36)	0.150 (f 4, 10= 2.14)	**0.012** (f 4, 9= 5.99)	0.056 (f 4, 10= 3.33)				
Taurine									
	-2hr	305.35±375.48	338.25±426.20 ^{ab}	231.14±253.68	120.36±8.14 ^{b}	0.832 (f 3, 8= 0.29)	0.693	**0.000**	0.720
	2hr	164.57±25.74	183.24±35.94 ^{b}	201.69±33.64	194.55±39.85 ^{b}	0.592 (f 3, 8 = 0.67)			
	4hr	181.83±50.55	175.47±29.40 ^{b}	187.31±57.60	168.36±18.03 ^{b}	0.946 (f 3, 7 = 0.12)			
	8hr	68.05±25.00	68.99±18.95 ^{b}	410.31±505.25	294.79±393.81 ^{b}	0.505 (f 3, 8 = 0.85)			
	24hr	588.94±157.64	631.56±82.38 ^{a}	698.42±47	838.65±159.68 ^{a}	0.142 (f 3, 8 = 2.41)			
	P-value	0.068 (f 4, 9 = 3.21)	**0.040** (f 4, 10 = 3.77)	0.148 (f 4, 10= 2.16)	**0.005** (f 4, 10= 7.15)				
Tyrosine									
	-2hr	64.57±4.00 ^{a}	59.74±5.52 ^{a}	49.66±22.12	70.45±16.06 ^{a}	0.380 (f 3, 8 = 1.17)	0.914	**0.000**	0.387
	2hr	50.43±9.48 ^{b}	53.28±7.66 ^{a}	50.21±8.45	45.62±10.47 ^{bc}	0.780 (f 3, 8 = 0.37)			
	4hr	35.49±8.31 ^{c}	38.82±9.65 ^{b}	44.75±3.72	35.18±4.39 ^{c}	0.366 (f 3, 8 = 1.21)			
	8hr	43.93±3.63 ^{bc}	36.82±9.18 ^{b}	40.74±1.21	40.38±8.00 ^{c}	0.621 (f 3, 8 = 0.62)			
	24hr	50.12±10.30 ^{b}	57.87±6.39 ^{a}	52.84±8.86	58.51±5.13 ^{ab}	0.538 (f 3, 8 = 0.78)			
	P-value	**0.011** (f 4, 10= 5.78)	**0.012** (f 4, 10= 5.66)	0.712 (f 4, 10= 0.54)	**0.008** (f 4, 10= 6.46)				

Values represent means of three pooled samples for each test diet (Total n=12).All values are means (n=12) ± standard deviation. Different superscripts indicate significant differences ($p < 0.05$). CD= Control diet, NA=Negative BCAAs, NL= Negative Leucine and PL= Positive Leucine. Analysis was performed using one-way ANOVA, with Fisher LSD method used for *post-hoc* examination. A GLM was used to determine significance in diet, time and the interaction between diet and time.

Threonine had differences in all diets over time, with the CD diet having high different peak concentrations at 4 hr compared to -2, 8 and 24 hr, and a similar trend was seen in PL, although the peak concentration was at 2 hr (p=0.006, p=0.011). NA had high different peak concentrations at 2 and 4 hr compared to -2 and 24 hr (p=0.010). An opposing trend was seen in PL, whereby all times were similar apart from the lowest different concentration was seen at 8 hr (p=0.016).

3.3.5.1.5 Plasma fNEAAs over time and between diets

In the fNEAAs, differences between the diets were observed for alanine at the 2 and 8 hr timepoints (p=0.008), with differences between the NA diet versus the CD and PL diets (Table 3.19, Figure 3.10). Similarly, at 8 hr, the highest different peak concentration was in NA (p=0.003). In serine, differences at the 2 hr point were between NL and NA, and CD and PL (p=0.001) while at the 4 hr time, PL had the lowest value of the four diets (p=0.017). Glutamate had differences in concentrations between the diets at 8 hr, with NA having significantly higher values than the other diets (p=0.027).

Within each diet over time, the CD diet had differences in b-alanine, glycine, glutamate, proline, and tyrosine (p=0.002, p=0.008, p=0.008, p=0.006, p=0.011). *Post-hoc* analysis determined that the highest values in b-alanine, glycine, proline were higher at the 4 and 2 hr points in comparison to the others. Glutamate had the highest different concentrations at 4 hr compared to 8 and 24 hr. Tyrosine had an opposing trend, with the highest different concentration at -2 hr, and the lowest different concentration at 4 hr post-feeding.

NL had differences in alanine, (p=*0*), glycine (p=0.031), glutamate (p=0.004), proline (p=*0*), taurine (p=0.040) and tyrosine (p=0.012). *Post-hoc* analysis determined that the highest different concentrations in alanine were at the 2 hr point. In glutamate the highest different concentrations were at -2, 2 and 4 hr, similarly, proline and glycine had the highest different peaks at 2 and 4 hr post-prandial. Interestingly taurine had the highest concentration at 24 hr compared to 2, 4 and 8 hr, whereas tyrosine had its lowest concentrations at 4 and 8 hr.

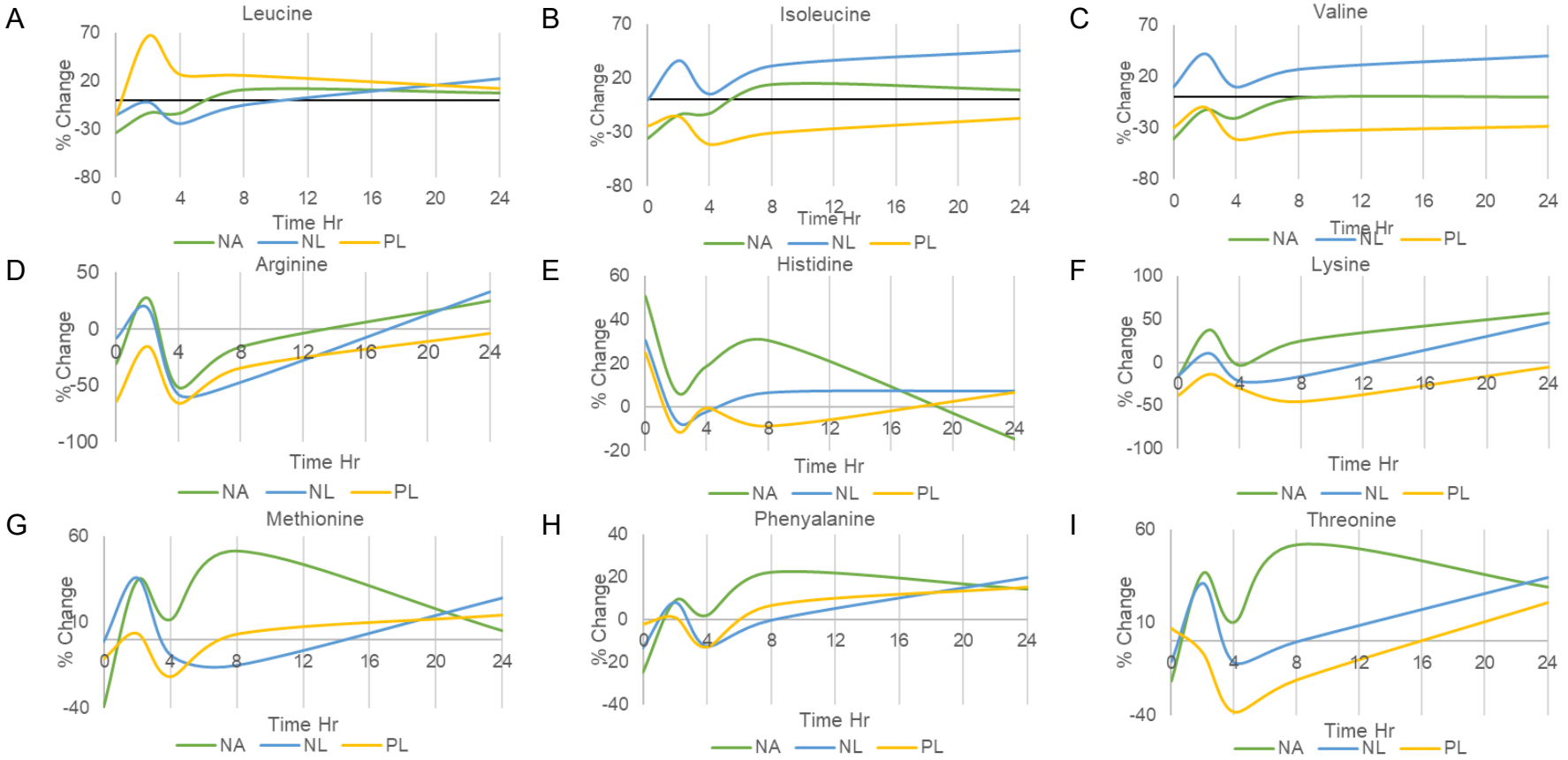


Figure 3.10 Individual plasma fEAAs change (%) compared to CD (control diet change (%) over time) A) leucine B) isoleucine C) valine D) arginine E) histidine F) lysine G) methionine H) phenylalanine I) threonine. CD= Control diet, NA=Negative BCAAs, NL= Negative Leucine and PL= Positive Leucine

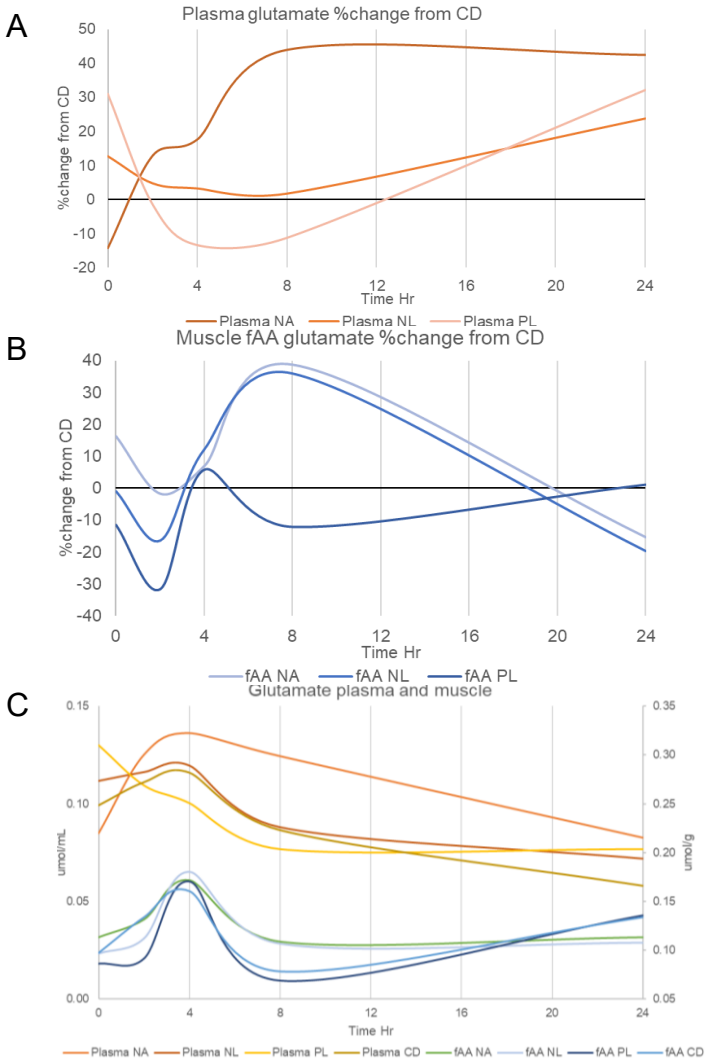


Figure 3.11 Glutamate in plasma and muscle tissue over 24 hr A) plasma glutamate change (%) compared to CD B) free glutamate change (%) from CD C) glutamate in plasma and muscle across all tissues over time.

In the NA diet, differences were detected over time for alanine, *b*-alanine, glycine, glutamate, proline, and serine (p=0.008, p=0.011, p=0.006, p=0.046, p=0.009, p=0.012). *b*-Alanine and glycine had the highest different peaks at 2 and 4 hr compared to -2 and 24 hr and similarly, proline had the lowest different peaks at -2 and 24 hr. Alanine had the highest peak at 2 hr which was different to -2, 4 and 24 hr while glutamate had a similar trend, but with the highest peak at 4 hr compared to -2 and 24 hr. Unusually serine had the highest different peak concentration at 24 hr compared to the other times.

PL had differences over time for glycine, glutamate, proline, taurine and tyrosine (p=0.001, p=0.006, p=0.004, p=0.005, p=0.008). Glycine and proline had high

peak concentrations at 2 hr compared to -2, 8 and 24 hr and glutamate peak concentration was at -2 hr which was different to 4, 8 and 24 hr. Taurine had the highest different concentration at 24 hr while tyrosine had the highest different peak at -2 hr compared to 2, 4 and 8 hr.

Plasma fNEAA GLMs had differences in diet for alanine and proline, whereas differences in time were seen across all NEAAs. Differences in the means for alanine were similar for NA and NL but different to PL, with PL having the lowest significant mean. NA proline means were higher than NL and PL. Differences in time for alanine showed peak means at 2 hr, *b*-alanine had similar mean concentrations for 2 and 4 hr, similar means for 8 and -2 hr, and the lowest different mean at 24 hr. Glycine and proline means at each time were similar to b-alanine although -2 hr was not different to 24 hr.

Glutamate mean concentrations at each time had 4 and 2 hr significantly higher than 8 and 24 hr. Taurine and serine 24 hr means were significantly higher than the other times. Tyrosine means were significantly higher at -2 and 24 hr compared to 8 hr. Interaction between diet and time (D*T) were seen for alanine and glutamate. Glutamate was examined change (%) from the CD diet in both plasma and as a fAA in muscle (Figure 3.11).

In plasma, PL diet had 31% higher glutamate levels than the CD at -2 hr, followed by NL with 13% higher concentrations while inversely, the NA diet had 14% less glutamate than the CD pre-prandial. At the 2 hr point, both PL and NL plasma dropped to nearly baseline levels while inversely, NA rose nearly 15% higher than the CD levels, continued at 4 hr, and by 8 hr was 44% higher than CD levels and 42% higher at 24 hr postprandial. NL gradually dropped at 4 hr, by 8 hr was 2% higher than the CD levels before increasing 24% higher than CD concentrations at 24 hr. PL followed a similar course as NL, with 4 and 8 hr dropping to 13% and 11% lower than the CD concentrations before a rise to 32% at 24 hr. In the muscle tissue, free glutamate levels were in opposition to plasma trends, with NA levels 16% higher than CD while PL was 11% less than CD levels (Figure 3.10, 3.12).

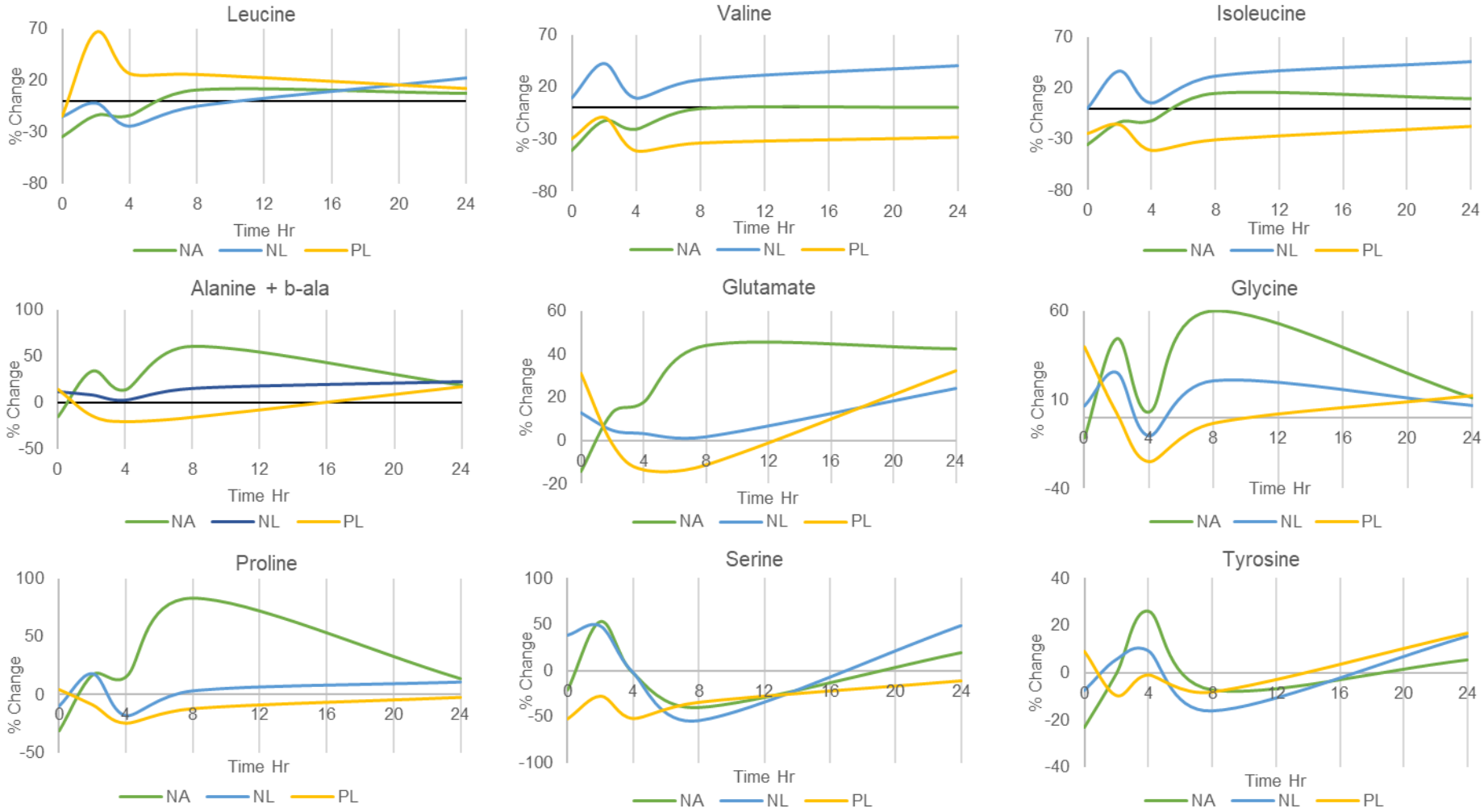


Figure 3.12 Individual plasma fNEAAs change (%) from CD. CD= Control diet, NA=Negative BCAAs, NL= Negative Leucine, PL= Positive Leucine

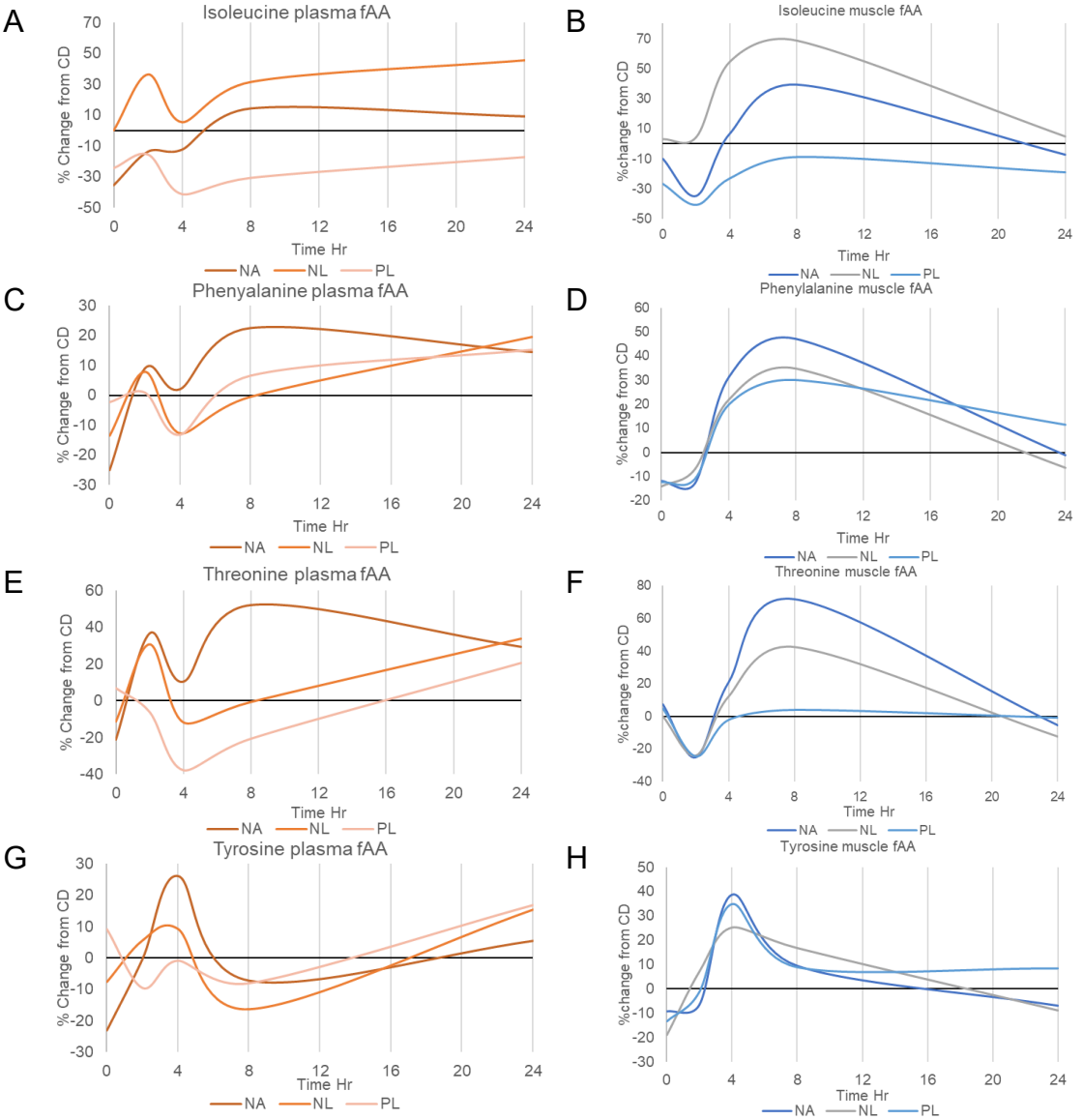


Figure 3.13 Keto- and glucogenic fAAs in plasma and muscle change (%) from CD A) isoleucine plasma B) isoleucine muscle C) phenylalanine plasma D) phenylalanine muscle E) threonine plasma F) threonine muscle G) tyrosine plasma H) tyrosine muscle. CD= Control diet, NA=Negative BCAAs, NL= Negative Leucine, PL= Positive Leucine.

NL was comparable to CD baseline levels. All diets fell below CD levels at 2 hr, with the largest decrease seen in PL followed by NL and finally NA (-32%, -16% and -2%). All diets increased in concentrations above CD at 4 hr, with the largest increase seen in NL while NA and PL had similar %changes (12%, 7% and 6%). NA and NL had the highest divergence from CD levels at 8 hr (39% and 36%) while inversely PL dropped 12% lower than CD levels. By the 24 hr point, NL and NA diets had dropped by up to 20% below CD levels while PL was comparable to CD levels.

3.3.6 Stable isotope analysis

3.3.6.1 Tissue comparisons and ratios of δ¹⁵N leucine

Stable nitrogen isotope ($\delta^{15}N$) is the resulting ratio between ^{15}N and ^{14}N, expressed as per mille/ parts per thousand (‰) deviation from the standard (Sabadel et al., 2025). $\delta^{15}N$ leucine concentrations in feed for week-3 were 1193 ±109‰ and week-7 was 7 ±3‰. The overall digestibility of $\delta^{15}N$ Leucine was 93%. Total $\delta^{15}N$ leucine concentration comparisons between tissue means at weeks 3 and 7 were significantly different (*p=0*, *p*=0.005) (Table 3.20). Within each tissue between weeks were significantly different (*p=0*) and GLMs displayed additional differences between the tissue means, weekly means and an interaction between the 2 (*p=0*).

Week-3 liver tissue had a mean of 741 ±139‰ and week-7 a mean of 243 ±39‰ (dry matter). Muscle tissue in week-3 had a mean of 332 ±33‰ and in week-7 184 ±48‰ (dry matter). WB analysis for week-3 had a mean of 301 ±52‰, week-7 233 ±35 ‰ and there were no differences between the weeks (*p*=0.156). The change (%) of $\delta^{15}N$ leucine concentration between the weeks was -205% in liver (-498‰), -80% in muscle (-135‰) and -29% in WB (-69‰). $\delta^{15}N$ leucine retention ratios between weeks 3 and 7 in liver were 0.34, muscle 0.56 and WB 0.78. $\delta^{15}N$ leucine reduction ratios expressed as a % in liver was 66%, muscle 44% and WB 22% over a 21 day period (Figure 3.14).

Table 3.20 Stable isotope analyses of $\delta^{15}N$ leucine in liver, muscle and whole bodies.

			* 2-sample T-Test	Two-way ANOVA P-value		
	Liver	Muscle	P-value	Tissue	Time	T*T
Week 3	741±139	332±33	**0.000**	**0.000**	**0.000**	**0.000**
Week 7	243±39	184±48	**0.005**			
P-value	**0.000**	**0.000**				
	Whole bodies					
Week 3	301±52					
Week 7	233±35					
P-value	0.156 *					

Values represent means of individual fish in the CD diet (Total *n*=12) with whole body values representing 3 pools of 8 fish/ tank. All values are means (*n*=12) ±standard deviation and reported in dry matter basis. To determine significant differences between the means, analysis was performed using a 2-sample t test for each parameter *p*=<0.05). GLM with Fisher's LSD method was used for *post-hoc* examination to determine significance in tissue, time and the interaction between tissue and time and to identify trends amongst the means (*p*=<0.05).

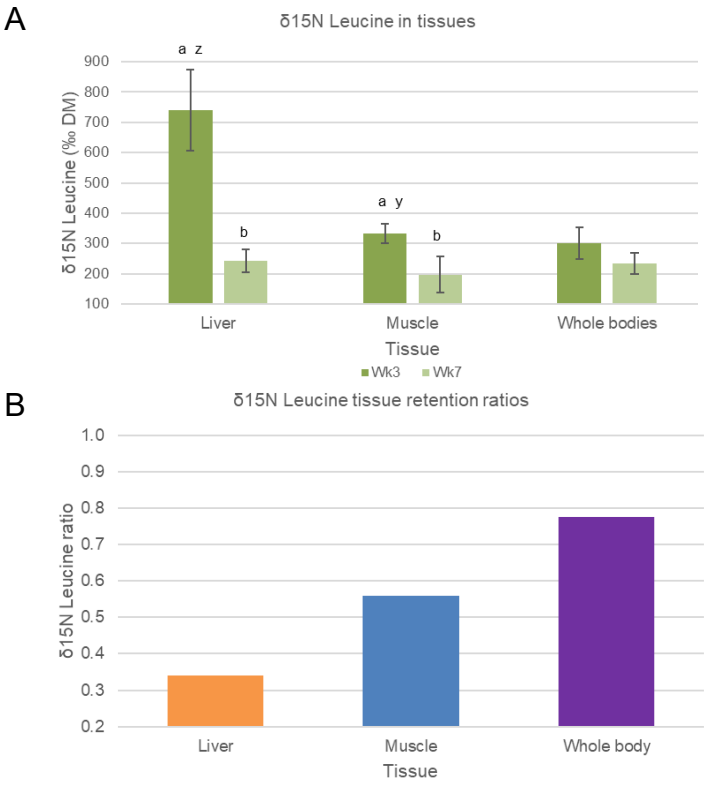


Figure 3.14 Labelled leucine (δ15N) A) δ15N leucine concentrations between tissues and weeks B) δ15N leucine retention ratios between tissues from week-3 and week-7. To determine significant differences between the tissue means, analysis was performed using a 2-sample t test for each parameter with significance determined at p=<0.05, error bars as standard deviation and reported in dry matter basis.

3.3.7 mRNA abundance

3.3.7.1 Absolute qPCR (copy numbers LOG_{10})

A GLM with Fisher's LSD *post-hoc* analysis was used to determine if there were differences in muscle tissue for the four test diets across the 3 timepoints and whether there was an interaction between time and diet (T*D). GLM differences were visible across time (p=*0*) with the -2 hr diet higher than 24 hr and the 4 hr sampling point the lowest value of the 3 (Figure 3.15 A). Overall, there were apparent differences in test diet means (p=0.049) with NL and PL diets significantly different to NA diet. An apparent interaction between time and diet (p=0.047) was determined.

One-way ANOVA differences within each diet over the 3 timepoints, showed muscle transcript differences in all diets apart from the CD.

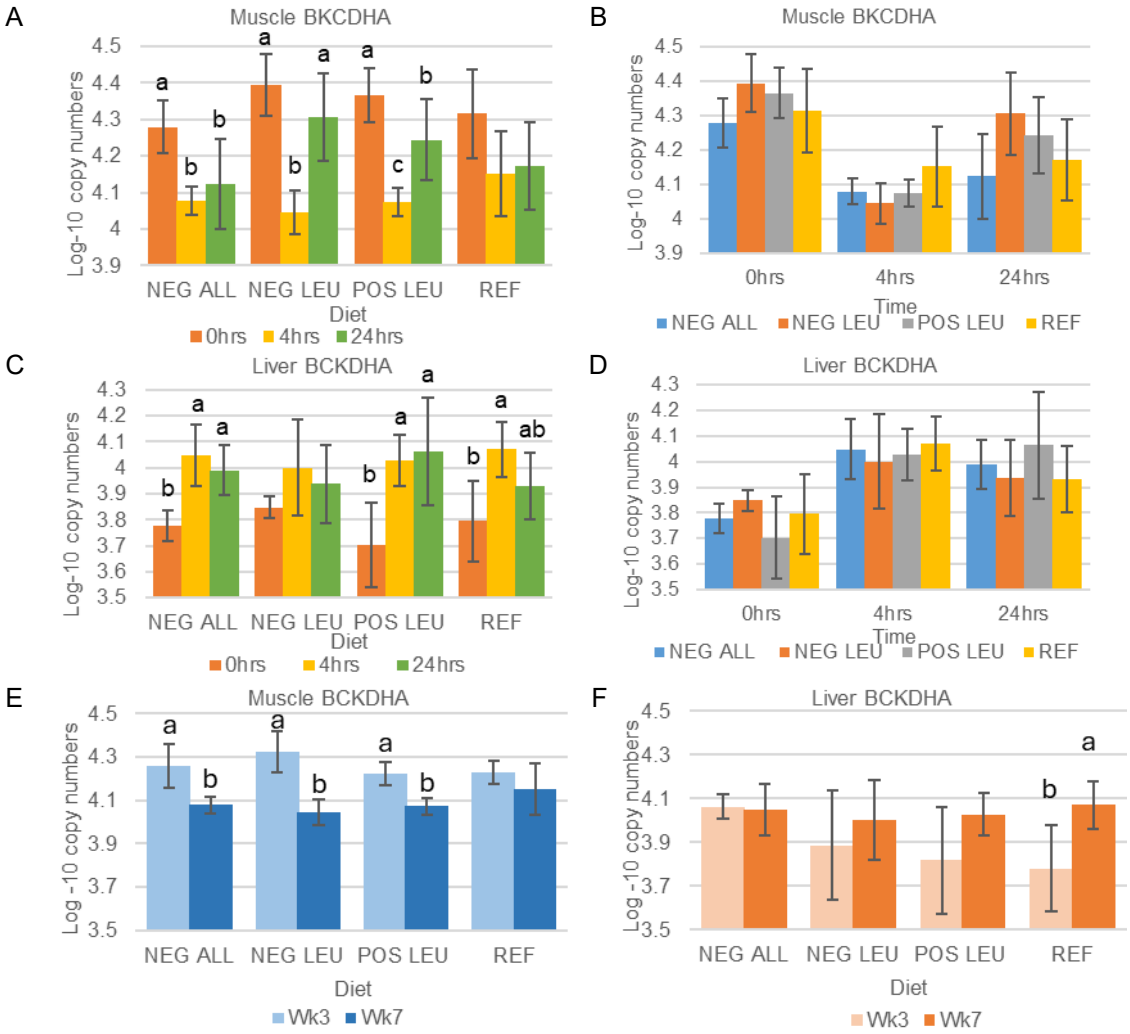


Figure 3.15 BCKDHA mRNA abundance in muscle (A,B,E) and liver (C,D,F) tissue A) within each diet over time B) between diets at each time C) within each diet over time D) between diets at each time E) within each diet between weeks F) within each diet between weeks. All values are means ±standard deviation. Analysis was performed using one-way ANOVA, with Fisher's LSD method used for *post-hoc* examination. REF= Control diet, NEG ALL= Negative BCAAs, NEG LEU= Negative Leucine, POS LEU= Positive Leucine.

Fisher's LSD *post-hoc* analysis had statistically higher mRNA abundance (p=<0.05) at the -2 hr time for the NA and PL diets compared to the 4 and 24 hr times. NL -2 and 24 hr were significantly higher than 4 hr (p=*0*) while PL had significant differences at each timepoint, with the 4 hr timepoint the lowest different time (p=*0*). CD had near significance over time (p=0.062). At each time between diets had no differences but near significance ($p\leq$ 0.10) was seen at 4 and 24 hr (p=0.092, p=0.070).

In liver tissue, a GLM with Fishers LSD *post-hoc* analysis was used to determine differences in mRNA transcripts between the diets, time and the interaction (D*T). Differences were highlighted in time, with the overall diet means at 4 and 24 hr higher than the means at -2 hr (*p=0*). One-way ANOVA with Fisher's *post-hoc* analysis was used to identify the differences over time within each diet (Figure 3.15 B). Differences were seen in the CD, NA and PL diets (*p*=0.020, *p=0*, *p*=0.003). NA and PL displayed similar trends, whereby -2 hr was significantly lower than the other two times. CD diet was similar, but the 4 hr time was different to the -2 hr but not the 24 hr timepoint. Similarly to the muscle tissue, no differences were seen across the diets at each time.

3.3.7.2 Week-3 and week-7 comparisons

GLMs with Fisher's *post-hoc* analysis was used to determine differences in transcript abundance (copy numbers (Log_{10})) between diets in week-3 and week-7 at 4 hr (Figure 3.15 C). Differences were examined between diet, week and the interaction (D*W).

In muscle tissue, differences were seen between the means of the weeks and an interaction between diet and week was noted (*p=0*, *p*=0.022). One-way ANOVA was used with Fisher's *post-hoc* analysis to identify where the location of the differences were. Differences within each diet between the weeks were seen in NL, NA and PL (*p=0*, *p*=0.002, *p=0*). The 3 diets followed similar trends, with week-3 mRNA abundance significantly higher than week-7 (*p*=<0.05). No differences were seen across the diets at each week, although near significance was observed in week-7 (*p*=0.092).

Similarly for liver tissue (copy numbers (Log_{10})) GLMs displayed differences between weeks but not diets (*p*=0.004). This was explored further with one-way ANOVAs and Fisher's *post-hoc* analysis. Within each diet between the weeks displayed differences in the CD diet, with week-7 significantly higher than week-3 (*p*=0.010) and near significance (*p*≤ 0.10) was seen in the PL (*p*=0.081). No differences were seen across the diets at each week (*p*=>0.05).

Exploration of the muscle BCKDH absolute copy numbers /µL in week-7 ranged from a high at -2 hr of 25144 ±4804/µL to a low of 11172 ±1493/µL at 4 hr, both extremes seen in the NL diet. The liver tissue absolute copy numbers ranged from a high of 12054 ±2896/µL at 4 hr in the CD diet to a low of 5336 ±1870/µL at -2 hr in the PL diet. Absolute copy numbers of BCKDH in muscle at 4 hr between week-3 and week-7 ranged from a high in week-3 of 21473 ±4927/µL to a low in week-7 of 11172 ±1493/µL, both seen in the NL diet. The absolute copy number /µL ranged in liver tissue from a high of 12054 ±2896/µL in week-7 to a low of 6520 ± 2626/µL at week-3, both were in the CD diet.

3.4 Discussion

The hypothesis for the first section of this trial was that the inclusion of BCAAs, especially leucine, at varying levels would affect the growth performance (growth, feed intake, health) of Atlantic salmon parr. The second hypothesis was whether the inclusion of BCAAs, especially leucine, at varying levels would affect the temporal AA variation and mRNA abundance. This trial has indicated the importance of BCAAs in growth and physiological responses in juvenile salmon. Studies have shown that the BCAAs, especially leucine, are involved in protein synthesis, muscle development and overall growth.

3.4.1 Feed and performance

3.4.1.1 Feed formulation, manufacture and digestibility

A common approach in aquaculture nutritional research is manipulation of varying levels of the test ingredient. This is done with optimisation in mind, with future effects on improving feed efficiency, health, performance, and growth. Feeds were formulated with the hypothesis that varying inclusion levels of BCAAs, notably leucine, would impact Atlantic salmon parr performance.

A key component of formulated feeds is the availability of the nutrients, and in this study a 21% inclusion rate of cAAs was added to a basal mix, with the deviations between the diets being in the BCAAs and the 3 NEAAs, glycine, serine, and alanine. The formulated feeds aimed to maintain isoproteic and

isolipidic features by adjusting NEAA levels to compensate for variations in BCAA content. This was done to maintain nutrient balance by providing all AAs required for protein synthesis and other metabolic processes, while exploring leucine and the BCAAs effect on growth and performance.

Gu et al. (2013) suggested that cAAs are differentially absorbed compared to intact proteins, with quicker absorption rates for the cAAs. In addition, Li et al. (2021) suggested that these differences in digestion and absorption rates may lead to poor performance such as lower growth, feed utilisation and poor health and welfare of aquatic animals.

Ahmad et al. (2021) suggested that there are different fish species specific BCAA requirements at all the different life stages. Choo et al. (1991) investigating the effects of leucine supplementation via the expense of glutamic acid on rainbow trout, included leucine in feed at 6.5% and saw no effect on feed intake or growth. They investigated further and found that at an inclusion level of 13.4%, 20% of fish suffered with gross lesions, concluding that this could be due to the toxicity of leucine at elevated levels. Due to this apparent toxicity, formulated leucine levels were kept at 5% inclusion in this study.

The BCAAs in the current study were supplemented by glycine, serine and alanine as these NEAAs may be biologically synthesised. Li et al. (2009) suggested that selected NEAAs have been used in previous studies with the understanding that their nutritional or physiological contributions are minimal may be incorrect. Some NEAAs are functional and may affect osmoregulation (glycine, β-alanine) antioxidative defence (glycine), appetite stimulation (alanine, serine) gluconeogenesis (glycine, serine), and sulphur AA metabolism (glycine, serine) (Li et al., 2021). These additional functions of the NEAAs may have contributed to the minimal differences in growth seen between the experimental diets.

Sun et al. (2016) examined the effects of glycine on Akt/mTOR/AMPK using mouse myoblast cell lines found that glycine enhanced protein synthesis. Cell growth over 24 hours was enhanced by up to 15% by administering 0.25 to 1.0 mmol glycine/L. DNA replication increased by 70 to 80%, protein synthesis by 20 to 80% and reduced protein degradation by 15 to 30%. Glycine plasma peak

concentration at 4 hr in the current trial had dietary ranges in week-3 from 668.77 ±48.16 to 852.7 ±358.8 μmol/L and in week-7 from 969.46 ±133.57 to 1332.85 ±283.87 μmol/L. These ranges were within and above the ranges used by Sun et al. (2016), which may suggest a possible effect of glycine on the experiment.

Meijer et al. (2015) exploring regulation of autophagy by AAs on cell studies (rat hepatocytes) found that a combination of alanine and leucine simulated a mixture of all AAs and had an inhibitory effect on autophagy/ proteolysis whereas alanine or leucine alone had no effect. This study demonstrated the importance of balanced AAs in a synchronised manner, whilst highlighting the possible contradicting effects of individual AAs and other possible unknown interactive effects.

Meng et al. (2020) to determine AA mTOR1 activation, used immunoblotting on mouse and human cell lines to determine phosphorylation of S6K1 at threonine 389 (pS6K1). Their results showed of the 20 standard AAs, the 10 that activated mTOR1 were alanine, arginine, asparagine, glutamine, histidine, leucine, methionine, threonine, valine and serine. Using concentrations ranging from 100 nM to 1 mM, mTOR activation ranged from 15 min to 1 hr. Their results additionally suggested that of the 10 AAs listed, all used the Rag GTPase pathway apart from asparagine and glutamine which used ARF1 independently of Rag GTPase pathway. Interestingly, although mTOR1 sensors for leucine, arginine and methionine have been identified, sensors for the other 5 AAs have not, suggesting an area for more research.

In addition to AA stimulation, Meng et al. (2020) also did AA withdrawal experiments, with varied results, concluding that due to a multitude of mTOR1 sensors, the withdrawal of 1 single AA may not affect mTOR1 activity, but the combined withdrawal of alanine, methionine, arginine, leucine, asparagine, glutamine and serine did appear to regulate mTOR1.

These studies suggest that there are indeed effects caused by different AA groups and individual AAs. Mammalian cell culture studies have demonstrated regulation by AAs, suggesting an impact of different AAs, however in this study whole animals were used. Although these may possibly be conserved across

vertebrates, further studies using specific Atlantic salmon cell lines are required to confirm these observations.

In animal feeds, digestibility is a measure of digestion and absorption of an ingredient through an animal's system. All AAs were included in the diets equally apart from the BCAAs, glycine, serine and alanine. The diets were formulated to contain varying levels of BCAAs, this theoretically, should not necessarily impact the digestibility results, as this is taken into consideration in the formula. In the current study DADC data, low digest data was not observed amongst the 6 AAs that were added at sub- or supra optimal levels. Leucine supplementation in the PL diet was double compared to NL and NA diets but had highest digest value (98%) compared to 95 and 94%, suggesting the potential for preferential uptake of dietary leucine up to 5%.

The varying differences in digestibility may imply alterative factors at play. Studies have suggested that the use of cAAs may overwhelm digestion and absorption capabilities within the gut, potentially leading to uptake conflicts with other AAs, wastage through gut evacuations resulting in poor digestibility. Additional studies have suggested that the absorbed cAAs may flood the system, leading to increased levels of cAAs in flux for longer periods of time before they are utilised or excreted.

In mammalian studies, antagonistic effects between AAs are known to occur between lysine and arginine, cystine and methionine, and the BCAAs. Lysine is one of the first limiting AAs and supplementation of synthetic lysine may affect arginine uptake with studies showing that arginine and lysine share carriers and compete at the brush border membrane (Wang et al., 2021). Although arginine and lysine were included at the same levels in the feed, no DADC differences were observed between diets for arginine, but differences were seen for lysine, with the lowest significant digestibility in the CD diet. Similarly, CD methionine had the lowest digestibility.

The BCAAs had differences in DADCs between the diets, although it seemed that the trends followed the formulations. In the PL, the BCAAs were consistently the highest across the diets suggesting that either leucine did not supress isoleucine

and valine absorption, or if it did, it may have delayed absorption without affecting the digestibility. Or, although the BCAA concentrations were elevated, the ratios were proportionate enabling optimal digestion/absorption and usage.

In summary, the diets were formulated to manipulate the levels of BCAAs, especially leucine in the diets, without jeopardising the isocalorific and isoproteic properties of the diets. The analysis of the feeds corresponded to the formulations, with PL substantially higher in leucine than the other diets, while the NA and NL had considerably lower levels of leucine. Only 1-2% variability between DADCs results occurred, suggesting fine margins and the possibility of minor errors occurring such as moisture absorption or weighing errors, which may have resulted in compounded errors and exaggerated statistical differences.

3.4.1.2 System and experimental design

Fish from the Salmonbreed strain were stocked at 120 fish per tank, with an average start weight of 19.4 g±0.39, with no statistical differences in biomass between the tanks. The average starting density was 3.2 ±0.07 kg /m^3 with a final average stocking density of 4.1 ±0.21 kg/m^3. Cañon Jones et al. (2011) in a study on stocking density effects Atlantic salmon parr suggested that although fish grew better at 30 kg/m^3, there was noticeably more aggression than fish stocked at 8 kg/m^3. This suggested a trade-off between growth and welfare, depending on the welfare indicator used as an assessment.

Interestingly, their study suggested although frequency of aggression was higher in the lower stocked fish, the intensity was worse in the higher stocked fish. Perhaps this frequency contributed to the reduced growth observed in the lower density fish as energy was spent avoiding the aggression and possibly a reduction in feed intake. From the author's personal experience, social dominance within RAS tanks develop, and may contribute to reduced feed intake resulting in large variation in population size/weight. Martins et al. (2012) in a review on behavioural indicators in aquaculture, suggested that this may be an individual response to stress, and fish with a low cortisol response tended to be socially dominant.

Individual lengths and weights were taken from a sub-set of the population at start-up (week-0), week-3 and week-7. Industry standard variation in weight for feed trials was 10%, while in this trial, starting weights had a variation of 15.8% and by week-7 had a 16.1% variation in end weight. To eliminate or minimise variation, experimental fish would normally be graded before the start of a trial. Noble et al. (2018) stated that grading was an essential tool for welfare and health, additionally offering health inspection opportunities without additional stress. If working with large numbers of fish, this may not always be possible and may lead to unfavourable conditions resulting in large variations in weight and inaccurate results**.** Although Noble et al. (2018) suggested grading is an important welfare tool and reduces variation, Kousoulaki et al. (2021) in their study on parr-smolts, reported that during smoltification in the freshwater stage, there were no differences in average weight between their experimental diets. Large individual variation had occurred across all experimental diets, an increase in body mass occurred in approximately 30% of fish, with some individuals increasing by 50% after 28 days, whilst 10% of the remaining parr-smolts had lost weight. This suggested that in addition to possible stressors such as routine weighing, the variability witnessed in the current trial may additionally been a factor of smoltification.

An additional effect of automatic feeders was discussed in Johansen & Jobling (1998) who investigated feeding regimes on cage-reared Atlantic salmon. They found that size variation was highest in fish fed by automatic feeders and suggested this may have been due to food competition. Although nowadays, modern technology has developed with sensors and cameras observing feeding in offshore cages, with operators controlling the feed rates. Fish in this trial were fed with point source feeders, which may have contributed to the size variability within each tank/ diet with dominant fish higher in the water column and possibly maintaining prime feed location in the tanks.

Variation between the bulk weight means and the individual means highlighted the differences between the 2 methods. The means of the individual fish /treatment (n=8) at week-3 resulted in the highest individual means in the NL and lowest in PL whereas the bulk weight means suggested higher means in the NA.

Similarly for week-7, individual means (*n*=24) implied the highest weight in CD and the lowest in PL, whereas bulk weights had the largest means weights in the NA.

The observed individual variation in the current study may have been due to a combination of ungraded parr, automatic feeders, the effects of silvering/ smoltification and exposure to stressors such as handling or repeated disturbance, which have been shown to affect feed intake and appetite (Noble et al., 2018).

Poor water quality may have affected feed intake and growth (S 3.1). Although water quality parameters were within chemically safe levels for Atlantic salmon, the water was cloudy (turbidity), with visible organics (suspended solids) within the water column. Instability of the cold-pressed feed led to pellets breaking up in the system which resulted in high suspended solids (SS) and organic load. The biofilter was mature and had been running for months with the same load of fish in the system but had continuously elevated nitrite (although within safe levels) over a 25 day period, from the 13NOV19- 7DEC19 (0.2-0.5 mg/L N). The 2-step nitrification process initially oxidises TAN, consumes bicarbonate and subsequently produces nitrite as a byproduct (Browdy et al., 2012) and the results may be indicative of variability within the nitrification cycle.

Tolerance of ammonia-nitrogen depends on species, physiology and life stage, with juveniles more susceptible to ammonia (Lindholm-Lehto, 2023). Un-ionised ammonia (NH_3) is toxic at high pH, temperature and low salinity (Randall & Tsui, 2002), with parameters <0.02 mg NH_3-N/ L safe for all life stages (Johnson et al., 2012). TAN (0.2-0.6 mg N/ L), NH_3 (0.3-0.8 mg NH_3/ L) and NH_4 (0.3-0.8 mg NH_4/ L) levels increased over a 13 day period (25NOV19 - 7DEC19) as well as CO_2 levels over the same period (5.0-7.0 mg/ L).

Indirect evidence of SS/ organic load may be inferred by elevated CO_2 levels, possibly indicative of organic breakdown and microbial respiration, while fluctuations in O_2 saturation may be suggestive of organic-rich systems with possible stress factors for the fish (Ebeling & Timmons, 2012). Variability in the alkalinity from 13NOV19 - 7DEC19 ranged from 30-300mg /L and this fluctuation

may suggest changes in organic inputs, nitrification and buffering capacity linked to decomposition. Although TAN was elevated, but still safe, over the 13 day period, it may have been due to the decomposition of the organics releasing ammonia. The process of efficient nitrification consumes O_2, alkalinity and increases CO_2 which can be seen in the overall water quality table (S 3.1).

Although the water chemistry parameters were within the safe ranges for Atlantic salmon, the effects of SS may still have impacted the performance of the fish (Korman et al., 2021). SS may cause physical abrasion of the gill lamellae, inflammation of the gill tissues, increased mucus production and reduced gaseous exchange even within chemically adequate water quality parameters. To produce excess mucous and respond to stress responses, an increase in energy expenditure is required (Canosa & Bertucci, 2023). This shift from growth to coping mechanisms may impede growth and feed utilisation.

In summary, the possibility of poor water quality, high individual variation at start, 24 hr automatic feeders, light regime, smoltification, diet formulation/ manufacture and gonadal development may have contributed to the overall lower than expected growth rates in this study. Real-time monitored RAS systems have been designed to optimise the control of many influential variables in order to reduce environmental factors that may influence any trial.

3.4.1.3 Morphometric and somatic indices

Morphometric and somatic indices were used in the current study as tools to review overall fish condition as a combination of both morphometric (non-invasive) and somatic indices (invasive) are required to provide an overall understanding of condition. Brown & Murphy (2004) suggested use of both morphometric and somatic indices as utilising just morphometric or visible changes, may overlook important physiological aspects such as gonadal development.

Morphometric and somatic indices were performed on a sub-set of the population at weeks-0, 3 and 7. Individual lengths and weights were taken on 30 fish at week-0, 96 fish at week-3 (8 fish /tank) and 288 fish at week-7 (24 fish /tank). Of

those fish, tissue weights were taken from 30 fish at week-0, 48 fish at week-3 and again 48 fish at week-7. Tissue samples were taken from a total of 48 fish (8/ tank) at week-3 and 288 fish at week-7.

Due to the complexity and temporal sensitivity of the sampling, at week-0 and week-3, six colleagues and staff were involved with the sampling, whereas at week-7, 14 colleagues and staff of varying capabilities and experience levels, were involved. Due to the temporal complexity as well as volume of the samples required, this may have introduced a multitude of errors.

Errors due to experimenter drift, haste, or training inadequacies, such as weighing the liver with the gallbladder included. The largest potential source for offset error (additive error) may have occurred with the weighing of the tissues and fish. The dissections on parr, to retrieve organs and tissue samples were complicated, time consuming and the resulting tissues were small. For example, the average of 48 hearts weighed at week-3 was 0.03 ±0.01 g. If balances were not dried, placed correctly, or tared this may have affected recorded results and subsequent analysis.

Somatic indices were used to determine growth differences of specific organs or tissues between the diets and the weeks. In week-3 there were differences in viscera weight between the diets and in turn, near significance in VSI% (p=>0.05 but p=<0.10), additionally, GLMs did display differences in the diet means as well as the week means for viscera (p=<0.05). With CD and NA means significantly larger than NL and PL. This could have been due to a few factors such as sampling inaccuracies, or the more likely possible inclusion of developmental gonads, as gonads were identified in some fish, ranging from 3.1-0.1 ±1.1 g and the misidentification of gonadal development and viscera fat cannot be excluded. Noble et al. (2018) suggested that male Atlantic salmon tended to be aggressive, and with the development of gonads observed in the current study, this may have contributed to variation in growth parameters from a behavioural perspective. Björnsson et al. (1994) in a study on factors influencing sexual maturity in Atlantic salmon parr, suggested that parr stopped feeding during sexual development and utilised somatic tissues for development of gonads. A combination of these

factors may have influenced feed intake and the variety of subsequent growth parameters.

Weight differences were identified by GLM between the means of the diets, with the CD and NA means larger than the PL. This trend was also witnessed for *K* and *Kn*-values. Differences in mean liver weights were seen with the NA diet means significantly higher than the NL and PL means. This difference in liver weight and near significance in HSI% ($p \leq 0.10$) may be indicative of energy storage differences between diets as suggested by Lai et al. (2023). In their study of leucine effects on Atlantic salmon, their high-level leucine diet had significantly lower HSI% values than the control. Blood chemistry analysis on enzymes and proteins indicative of hepatic damage, did not indicate any effect of liver size observed within the current study.

Brosnan & Brosnan (2006) suggested that as BCAAs shared the same enzymes in their first two steps of catabolism, their primary focus was not for glucose or ketone body synthesis, but rather, that the BCAA's primary role is for protein structure, and not their metabolic functions. In opposition to this, Zhu et al. (2023) suggested that although the BCAAs are nutritional signalling molecules, the BCAAs are catabolised in muscle as energy sources. If as Brosnan & Brosnan (2006) suggested, BCAAs primary focus was protein and most fish growth is driven naturally by protein synthesis, and this has not taken place, then increased lipid production with excess leucine makes sense. If leucine is ketogenic, valine glucogenic, and isoleucine both, then leucine and isoleucine intermediate products could contribute to the production of lipids or ketogenesis. Other AAs that are both keto- and glucogenic are phenylalanine, threonine, tryptophan, and tyrosine.

Between dietary phenylalanine, threonine, tyrosine, and isoleucine, only isoleucine was restricted in the NA diet and analysis of the feeds confirmed this difference between the diets. There were no differences between diets for phenylalanine (p=>0.05), but differences in threonine and tyrosine were noted (p=<0.05). Threonine ranged from 1.59 ±0.05% in NL to 1.39 ±0.07% in the PL, which equates to 0.09% or 0.009 g/kg difference between the highest and lowest

values in the feeds. Similarly for tyrosine, the range extended from 1.15 ±0.03% in NA to 1.08 ±0.01% in the CD, which equates to 0.03% or 0.003 g/kg difference. Although statistically the diets were different, the differences were so small it should not have made such a great difference/ impact.

Comesaña et al. (2022) studying the orexigenic effects of ICV (intracerebroventricularly) administered valine in rainbow trout concluded that increasing levels of valine increased feed uptake and mTOR activation. NA diet had significantly lower valine in the diet compared to the others, and yet, with the CD, had the largest growth suggesting that this effect may only be observed via ICV.

In summary, although precautions were taken to mitigate sources of error (random or systemic), it cannot be ruled out of any experimental trial with multiple factors involved. Choo et al. (1991) included leucine levels at 6.5% and found no inhibitory effect on growth or feed intake in rainbow trout whereas in the current study, growth was reduced. This may have been due to multiple factors. If the dietary BCAAs in the NA or NL diet were formulated at suboptimal levels, subsequent feed analysis confirmed this, then theoretically the AA differences between the fish could only come from endogenous processes. Suggesting a need for further exploration.

3.4.1.3.1 Morphometric

Length weight *b*-values had different growth between the weeks, with week-3 indicative of negative allometric growth, with the NA near to isometric growth (2.9). Week-7 NL diet had isometric growth (3.0), and the other diets had positive allometric. The *b*-value across species ranges from 2.5 to 4 (Le Cren, 1951).

Differences in the length weight values may be down to sex, season, species, habitat, and gonadal development (Connor et al., 2017). Froese (2006) suggested that different developmental stages may need to be estimated on separate length weight relationships as different life stages may influence body shape relationships with length, such as smoltification, where fish are slimmer as they increase with length. Although the *b*-value is a useful, informative tool, it is

not without bias such as less variability in smaller fish compared to larger fish (Connor et al., 2017). Berrill et al. (2003) suggested that gonadal development is preferentially initiated at the sacrifice of somatic growth and Ytrestøyl et al. (2023) in a study on photoperiod on Atlantic salmon seawater growth, suggested that reduced condition factor, decreased body lipids, and increased length may be due to smoltification.

Within the current trial, length weight *a*-values clearly demonstrated differential body shape between the weeks and between the diets at each week. Week-3 fish body shapes were all similarly short and deep (fusiform), with NA diet the lowest *a*-value and PL and NL the highest *a*-values. By week-7, body shapes had changed from short and deep (fusiform) to nearly elongated (0.009) across all diets apart from the NL which remained fusiform. Froese et al. (2014) stated that after a study on 1316 fish species *a*-values ranged from 0.0013 (eel-like), 0.0084 (elongated), 0.0137 (fusiform) and 0.0187 (short and deep) confirming *a*-values as indicative of body shape and form. NL body shape remained similar over the experimental period whereas WB lipid % were nearly statistically different between the weeks (p=0.052). This increased lipid store may have initiated and increased gonadal development.

Le Cren's (1951) *Kr*-factor displayed differences between the diets at each week, with NA and CD significantly higher than the other diets at week-3 while NA was significantly higher in week-7 than CD and PL. Le Cren (1951) described *Kn*-values as individual deviation from the average weight for length. *Kr*-values and *K*-values had similar results across the diets and between the weeks. Fulton's condition factor (*K*-factor) is useful to compare weight, whereas length-weight is useful to estimate weight from the length of fish within a species (Froese, 2006). Noble et al. (2018) suggested that the higher the *k*-value the rounder the fish shape, and it could be an indicator of total lipid content (Einen et al., 1998).

Johansen & Jobling (1998) stated that *K*-factor is reflective of lipid content, and this may contribute to the understanding of week-7 results but not week-3. The current trial had opposing results, with the lowest lipid levels in week-3 for the CD and NA diets whereas they had the highest *K*-values. Interestingly Hvas et al.

(2020) studying the effects of starvation on Atlantic salmon, found that no significant changes to weight or *K*-factor were found after 4-weeks of starvation. Their results would indicate that the *K*-factor differences in the current trial may not be indicative of starvation.

The differences in the *K*-factor values between the weeks suggested fluctuations in condition, with the differences between diets suggesting a possible dietary influence. Ytrestøyl et al. (2023) suggested an effect of smoltification by a reduction in the *K*-factor, increased length of the fish and reduced lipid values. This trend was seen in the current study.

In summary, length weight relationships were used to determine the body shape and growth patterns of the fish. Changes in the growth (*a*-values) between the weeks indicated a potential change in growth, from fusiform to more eel-like, while the *b*-values indicated differences in growth rates and proportions. Multiple factors may have contributed to the reduced growth rate observed in the current trial as well as the variability in morphometric and somatic indices.

3.4.1.4 *Weight gain and FCR*

Salmobreed fish were stocked with no statistical differences (p=>0.05) between biomass in each tank but did contain an initial individual variation of 16%. PL diet had the lowest start weights of 18.6g ±0.1 and the NL diet the highest at 19.2g ±0.1. Fish did not grow as expected over the 7-week trial, or to the industry standard of doubling their weight over a trial period. The NA diet had the highest increase in body weight of 77% whereas the PL had the lowest at 64%.

Feeds were formulated with an expected growth and performance outcome as follows; CD 100%> PL 90%>NL 70%>NA 50%. Total growth (bulk weight) compared to the CD weight between week-0 and week-3 were as follows PL -4.6%< NL -2.1% < CD < NA 2.5% and from week-4 to week-7 was similar PL -6.8%< CD < NL 0.4%< NA 2.9%. The main observable differences between the weeks were that by week-7 NL had exceeded the CD growth by 0.4% and the PL had dropped 6.8% further below the control.

Due to the sensitive nature of juvenile salmon, the experiment was designed with minimal intrusion/ disturbance, with fish weighed on sampling days (week-0, week-3, week-7). This was intended to minimise stress levels and the potential impact on feed intake and growth. A sample of fish (25%) from every tank were weighed on a weekly basis as a husbandry and welfare tool. Noble et al. (2018) suggested that weighing fish as a growth audit, could be time consuming and labour intensive and may disturb the fish and feeding. Metcalfe et al. (1987) examined behavioural response of juvenile Atlantic salmon exposed to a model predator and found that feeding response had recovered completely after 2 hr since the exposure.

A possibility of early maturation and smoltification may have been due to temperature effects. The mean temperature over the whole trial period was 13.0 °C ±0.72, with a range of 3.4 °C from a high of 14.2 °C to a low of 10.8 °C. Pino Martinez et al. (2023) studied the interactions of temperature and feed on post-smolt Atlantic salmon males concluded that water temperatures above 12.5 °C could increase early maturation and inversely affect smoltification. Maintaining temperatures at 18 °C resulted in nearly 100% maturation leading the authors to state temperature as the main driver of sexual maturation. Pino Martinez et al. (2023) reported that at 12.5 °C, effects of reduced feed intake (67% and 100%) was more of a driving factor than temperature on body weight.

Although their study did have high gonadal development in the 100% feed ration at 12.5 °C compared to the 67% ration by the end of their 7-month trial, observations of their body weight between the two rations did suggest that the 100% ration had higher weight gain but it was most likely due to gonadal development. This suggested that a lower feed rate may reduce gonadal development. Saunders et al. (1982) in their study on early maturation in Atlantic salmon, found that the fastest growing parr matured prematurely, this insight may contribute to unusual growth factors in the current trial.

The possibility of an effect of photoperiod on early maturation may have occurred due to the light regime of LD24:0. The trial was initially designed to have LD16:8, with feeding to satiation to occur during the light/ working hours. Unfortunately,

this was not facilitated, and fish were kept on a LD24:0 routine for the duration of the trial.

Berrill et al. (2003) studied the effects of photoperiod on early maturation and reported that fish exposed to LD24:0 from first feeding had <9% premature maturation and concluded that photoperiod was a trigger for early maturation. Guo et al. (2023) had similar results in their study on Atlantic salmon gonadal development, suggesting that the effect could be instantaneous. Although their study had predominantly higher gonadal maturity in the LD24:0 group, they suggested this was due to the elevated growth levels and subsequent early maturation. To overcome these shortcomings, they suggested photoperiod should be changed to LD18:6 or LD12:12 and thereby reducing sexual maturity from 40% to 20% in RAS systems. Interestingly Rodríguez et al. (2005) had similar results with exposure manipulation LD24:0 in European male sea bass (*Dicentrarchus labrax*) whereby photoperiod inhibited precocious maturation.

To accurately determine FCR, uneaten pellets are collected, dried, weighed and removed from the total feed. This requires well-equipped facilities to ensure pellet capture. With set feeding times, this can easily be done with a sieve on the outflow. Alternatively, a set feeding time range can allow for waste pellet collection throughout the time range. Biological FCR is the most common industry method used as it requires very little handling (total feed fed/ total biomass gain). However, this is not an accurate indicator and may cause welfare issues as well as financial losses.

In summary, although the results did show some variation in growth and condition factors between the diets, they were not consistently significant across timepoints or parameters. The use of AAs for energy rather than growth, may have contributed to the low growth across the treatments. Catabolism of AAs used for energy may have contributed to the poor water quality due to nitrogen excretion (ammonia) in the RAS system as previously discussed in (Browdy et al., 2012). The possible poor water quality and biofilter crash may have negatively impacted feed intake and subsequent growth rates.

Large individual variability within each diet/ population may suggest other factors may be involved in influencing growth in salmon juveniles, such as an effect of automatic feeders on size variation in post-smolt Atlantic salmon, potentially driving feed competition (Johansen & Jobling, 1998). Proteolysis of muscle tissue due to sexual development may have led to lower growth in addition to behavioural responses to maturation (Nemova et al., 2016). In agreement with this, Chabot et al. (2016) suggested that elevated metabolic rates may be exhibited during gonad maturation and spawning. In addition, the recorded whole weight of fish could not identify whether the weight was muscle growth or gonadal development.

Starting a feed trial with high individual variation is not ideal and may be a disadvantage to the experimental diet, although in this case, the hypothesis was partially supported. Leucine level did impact growth and condition, with the PL diet having the lowest growth and various other morphometric and somatic indices. How much of this effect can be contributed to a 5% leucine inclusion or a lower starting weight and all subsequent effects of that, cannot be identified/ quantified.

To summarise, the findings suggest that BCAAs in diets may influence growth and other physiological parameters in juvenile salmon. The complex interactions between dietary ingredients, genetics and environmental factors may need further in-depth research. Perhaps additional research looking at the long-term effects of varying BCAA supplementation on heath and performance under different environmental conditions may be more successful.

In conclusion to section 1 of this study, it has provided insights into the role of BCAAs and the physiological response in juvenile salmon. It has demonstrated the complexity of dietary composition, AA metabolism and the subsequent effect on fish performance.

3.4.2 Physiological analyses

3.4.2.1 Whole body analyses

Proximate analysis of the WB did not display significant trends between the diets at each week apart from a difference in protein in week-3. Protein levels were

significantly higher in all the diets compared to the NA diet. Within each diet between weeks had protein differences in the CD and PL diets. There were differences between the weeks for ash in the NA diet, moisture in NL and PL diets. Ash in generally made up of bone, and differences in ash content may be indicative of a change in the type of growth, as suggested in the morphometric data. No differences were seen for lipids within diets, although near significance ($p \leq 0.10$) was seen in the NL diet ($p=0.052$). GLMs with Fisher's *post-hoc* analyses displayed differences between the means of the weeks for moisture, with week-7 having higher overall means compared to week-3. Inversely to moisture, protein means were significantly different between the weeks, with week-3 means significantly higher than week-7 and an interaction between diet and week was identified in protein.

The differences in protein seen at week-3 indicated NA having the lowest significant value between the diets ($p=<0.05$) even though the fish were the largest between the diets (27.1 ±1.0 g). This may be contributed to either a higher fat content as seen in the morphometric and somatic indices, which may be substantiated by the significantly lower ash content of NA between week-3 and week-7. Additionally, low variability between protein samples may have enhanced a technical effect within the methodology.

No differences were observed between treatments for individual weights (weights of the individually sampled fish) or total weights (bulk tank weights as g /fish) at week-3, but differences were seen in *K*-values, *Kr*-values, and viscera fat ($p=<0.05$). Choo et al. (1991) in their study of varying levels of leucine in rainbow trout growth, found that increasing leucine influenced protein and lipids. As dietary leucine increased, total lipids increased, and body protein decreased. Similarly, in the current study, WB protein levels in week-3 were statistically lower in the NA diet compared to the other three diets ($p=<0.05$). Near significance was observed for total lipid (%) ($p=>0.05$ but $p=<0.10$), with the lowest total lipids in the NA diet, substantiating the results of Choo et al. (1991) whereby an effect of levels of leucine on lipid production was observed. Although in a mouse model, Yu et al. (2021) had opposing results, in that reducing isoleucine and valine, reduced adiposity but the reduction of leucine had increased adiposity.

The WB total lipid (%) did not show any differences between the diets at each week nor between the weeks, (p=>0.05). NA did have the lowest lipid (%) of all the diets at week-3, with a 1.5% difference between NA and the highest value in NL. This trend can be seen in the lipid digestibilities at week-3, with the lowest DADC for NA followed by NL. The lipids in the feeds were added to the basal mash, which was used as the base for the experimental feeds, and the variation in the total lipids of the WB do not reflect the feed lipid (%) results. NL had the highest total lipids in week-3 and may suggest a reliance on AAs that may be both keto- and glucogenic for lipid production. On further examination of the *a*-values in NL, body shape did not change but remained fusiform throughout the trial.

Week-7 total lipids were similar between the diets, and ranged from 9.0 ±0.4% in NA to 9.2 ±0.7% in the PL. The largest variation within the diets between weeks was seen in the NL, with week-3 total lipid values at 10.2 ±0.7% compared to week-7 values of 9.1 ±0.1% (p=0.052). Ytrestøyl et al. (2023) suggested that smoltification reduced lipid reserves, and this may be a contributing factor in the WB lipid reduction seen in the NL diet. Smolt status of the fish were visually assessed based on the criteria of the smolt index, where evaluation was based on parr marks, silver colouration and the darkness of the fin margins (Zah et al., 2025). On start-up, fish displayed parr marks and dark colouration but by week-7, fish displayed silver colouration, dark fins and feint to no parr marks, suggesting that smoltification had started to occur.

WB bBCAAs showed a different trend, although not significant, between week-3 and week-7 in change (%) from the CD. Week-3 NA demonstrated a lower total bBCAAs than the CD, NL was surprisingly higher than the CD, and PL was very similar to CD although slightly higher.

Week-3 bEAAs and bNEAAs followed this trend, with most of the AAs comparable to the CD, with NA lower than the CD for the bEAAs and the bNEAAs (Figure 3.4).

The lower bBCAAs at week-3 in the NA diet, were also validated by the lower protein levels of the whole-body analyses. Surprisingly, the bNEAAs in the NA

diet were generally lower when compared to the other diets, suggesting less uptake into the bodies. NL had higher change (%) compared to the CD for all AAs apart from histidine at week-3, suggesting a possible effect of decreased leucine on deposition of these AAs.

In week-7, all diets had higher bBCAAs, bEAAs and bNEAAs than the CD including the NA. NL throughout the weeks had higher bBCAAs than the other diets including the CD. These results are also seen in the total protein levels with the same effect of there being no difference at week-7. When looking at the *a*-values of the morphometric data, NL was the only diet whereby body shape did not change between weeks (*a*-values 0.031, 0.011) whereas for the other three diets, the body shape of the fish changed from fusiform to more eel-like.

There did appear to be an interaction between the NA diet at week-3 and the WB bBCAAs, bEAAs and bNEAAs. In the NA diet, the bBCAAs were lower at week-3, with phenylalanine, lysine and arginine between 3-4% lower in the bEAAs. Interestingly, PL influenced arginine deposition, with values lower than the CD.

The lower levels of these AAs in the NA could potentially indicate less deposition of these AAs in the WB. Although proximate analysis of the WB at week-3 did show a significantly lower protein values in NA, lower bBCAAs, bEAAs and bNEAAs (p=<0.05), no differences in total weight was seen.

Although graphical differences were observed in the bBCAAs when compared to CD, the actual µmol/g differences between the diets were minimal, with no statistical differences between the diets at each time, nor within each diet over time (p=>0.05). In the study of Hvas et al. (2020) using long term starvation in Atlantic salmon, they found that if weight was lost, it was lipid loss and not protein deposition, whereas in the current trial, differences were noted in WB protein between the diets at week-3 and between the means of week-3 and week-7, with week-3 means significantly higher than week-7 (p=<0.05). Week-3 WB protein levels did determine an effect of the BCAAs on protein accumulation but at week-7 this was less evident.

Overall, the WB concentrations of isoleucine, leucine, and valine did not significantly differ among the diets at both week-3 and week-7. These AAs are

essential for various physiological processes in fish, including protein synthesis, energy metabolism and the consistency in their concentrations across the diets suggests that the dietary treatments did not markedly influence their WB levels. Further research may be needed to explore the specific metabolic responses of fish to different dietary compositions and the implications for aquaculture practices.

3.4.2.2 Muscle fAAs week-3 week-7

Differences in fBCAAs in muscle tissue occurred between diets at each week and within the NA diet between weeks for isoleucine and valine (p=<0.05). NL had higher isoleucine and valine fBCAA concentrations across the diets at each week in the muscle tissue and when comparing to plasma fBCAA concentrations, a similar trend was visible. Intracellular fAAs are involved in regulation of protein synthesis, and in human plasma, fAAs concentrations are not necessarily indicative of intracellular and extracellular fAA concentrations, but rather the circulating fAAs (Lindholm et al., 1989). Felig et al. (1973) added that human blood (presumably erythrocytes) substantially contributed to the movement from muscle to gut and then to liver (up to 30% for alanine).

Although AA analysis of the feeds verified the formulations, with the NA and NL diet significantly lower in leucine, and the NA significantly lower in isoleucine and valine to the other diets, differences in uptake were observed (p=<0.05). fBCAAs in muscle tissue and plasma, seemed affected by leucine, with the NL diet having higher concentrations of isoleucine and valine compared to the other diets. Ren et al. (2015) studying the effects of dietary leucine on blunt snout bream (*Megalobrama amblycephala*) found that increasing levels of dietary leucine reduced plasma levels of isoleucine and valine. This was comparable to the plasma PL results in this study although the fBCAA concentrations were not always significantly lower in the PL than the other diets.

Ren et al. (2015) hypothesised that reduced growth seen in elevated dietary leucine could have been due to the toxicity of leucine, and the indirect stressors this may have had on the fish. A possible additional factor for the reduced growth witnessed by Ren et al. (2015) may have been due to the appetite suppressant

ability of leucine established by Lai et al. (2023) in their study on Atlantic salmon. High dietary leucine levels increased mRNA abundance of POMCA1 (pro-opiomelanocortin) an anorexigenic neuropeptide as well as increased mRNA abundance of AA transporters, suggestive of regulation of feed intake.

The variations seen in fAAs may be contributed to various interactions or metabolism as discussed by Duan et al. (2016) who stated that glutamate and alanine are products of BCAA metabolism in various tissues including muscle. They suggested that movement of leucine into cells corresponds to an efflux of glutamine via AA transporters (solute carrier family 1 member 5 and solute carrier family 7 member 5/SLC3A2).

Dabrowski et al. (2010) discussed protein in fish nutrition and suggested a 50% efficiency in the conversion between proline and arginine (and *vice versa*) when delivered in the diet. They also mentioned the conversion of glutamate and proline into arginine. Some of the fAA variability and apparent interactional effects may be explained by these studies.

In summary, fBCAA 4 hr muscle tissue between the diets at each week were significantly different for all apart from week-3 leucine. Interestingly, the NL was significantly higher across all diets at each week for isoleucine and valine (p=<0.05) but had no differences in concentrations between week-3 and week-7. This trend may suggest a suppression effect of leucine on the other fBCAAs or the possible interchangeability of the BCAAs. Isoleucine is both gluco- and ketogenic, possibly suggesting a biological failsafe. NA was the only diet to have significant differences in concentrations of isoleucine and valine between the weeks. GLMs had differences in the diet means, which was a possible confirmation of the success of the dietary formulations and biological responses. No differences were identified in the means of the weeks for the BCAAs and may suggest similar trends occurred at each week.

3.4.2.3 Muscle week-7 fAAs over time

The muscle fAA data over the 5 timepoints, suggested possible interactions between the fBCAAs and the other AAs, demonstrating the complexity of AA

metabolism and utilisation in this study. fBCAA peak concentrations tended to be around 4 hr post-prandial. A stable concentration of lysine, methionine and phenylalanine occurred at 4 hr indicating a possible competition or regulatory effect on uptake, metabolism or even utilisation. The mechanisms behind this may be due to competition for transporters, enzyme regulation or metabolic pathways (Kimball & Jefferson, 2006), and these interactions seen in the muscle tissue may impact fish performance as suppression of AAs by BCAAs may impact protein turnover, muscle development and metabolic balance.

Leucine in the PL did appear to suppress the uptake of isoleucine and valine, while inversely the NL diet had the largest increase in uptake of isoleucine and valine compared to CD and the other diets (Figure 3.5). This uptake did appear at the 2 hr mark, whereas isoleucine and valine uptake in the other diets dropped below CD levels at 2 hr before increasing at 4 hr. This early uptake trend was similar to the leucine uptake in the PL. Calder (2006) suggested a preferential BCAA cellular uptake in human B cell lines as follows: leucine > isoleucine > valine and a similar order of uptake was seen in the current trial.

Leucine in the PL appeared to influence arginine uptake, with arginine levels suppressed in the PL diet, dropping below CD levels at 2 hr as the leucine levels rose at 2 hr (Figure 3.6). This effect of leucine on arginine was also seen in the week-3 bEAAs. Threonine concentrations remained relatively stable in the muscle tissue, with differences between NA diets and CD and PL at 8 hr. The elevated levels at 8 hr in the NA may suggest a possible different regulatory effect or involvement in biosynthetic pathways compared to the BCAAs, as threonine is both keto- and glucogenic.

Wang et al. (2022) exploring the effects of leucine supplementation on blunt snout bream (*Megalobrama amblycephala*) found that fish fed either 1.61% or 2.15% leucine had differential fAAs in muscle tissue. Although the data is reported as g/kg wet weight, the trends would still be comparable to the current trial. The study looked at the fAAs in muscle tissue of fish fasted for 24 hr, and when comparing to this current study, lysine at -2 hr did see differences between the diets, with PL having the lowest values. Although in the study of Wang et al.

(2022) the higher leucine diet had higher lysine, leucine, isoleucine, threonine, valine, tyrosine, phenylalanine, lysine, and glutamate than the lower leucine diet. In the current study, leucine levels most comparable to the study of Wang et al. (2022), were in the NA diet (2.3%), with the PL formulated at 5.5%, similarities in muscle fAA trends did occur. There did appear to be an effect of leucine interaction with the other fAAs just not at the baseline timepoint -2 hr and 24 hr post-prandial.

In summary, significant differences in dietary fBCAA temporal uptake in muscle at week-7 was observed within all diets, apart from NA. This same trend was observed in the NA plasma BCAA concentrations over time and may suggest that the uptake over time was minimal possibly reflecting the effects of the feed formulation. In addition to the temporal fBCAA uptake stability in the NA, muscle and plasma leucine uptake in the NL had no significant variations in uptake over the 24 hr. This may either suggest that either peak uptake occurred out with the sampling times, possible tissue-specific requirements, preferential uptake, or it validates the diet formulation and manufacture. Additionally these findings may verify the ability of the method used to track the fAAs over time.

Interestingly, no differences in muscle uptake concentrations were seen for isoleucine in the PL but there were differences in plasma isoleucine uptake concentrations (p=<0.05). This discrimination in trends between PL plasma and muscle isoleucine may suggest a divergence from protein synthesis to energy production. The liver plays a regulatory role in BCAA metabolism, with excess isoleucine possibly involved in gluconeogenesis or ketogenesis.

In Chapter 2 liver tissue in the LD had no significant temporal differences for the fBCAAs whereas muscle had differences in isoleucine and leucine (p=<0.05). Although the dietary parameters were different, a similar trend was observed in the current trial. This may allude to either uptake competition between muscle isoleucine and the other fBCAAs/ fAAs, a tissue-specific demand for plasma isoleucine, the preferential involvement in gluconeogenesis/ ketogenesis rather than protein synthesis or an unknown primary metabolic function in Atlantic salmon parr. A possible area for further research would be exploring the isoleucine demand in other tissues such as brain and adipose tissues. The

BCAAs are thought to be precursors for neurotransmitters and other molecules, with isoleucine possibly an energy source in brain tissue.

Valine muscle uptake differed for all diets apart from the NA, whereas plasma valine had no differential uptake concentrations in NA and CD. The uptake stability in CD plasma valine, may be due to large variability in the 4 hr sampling time rendering the temporal concentrations statistically insignificant (530.66 ±115.09 µmol/L).

An additional possibility of the observed effects may be due to the degradation pathways of the BCAAs. First pass metabolism is said to occur in muscle tissues, a reversable step producing a-keto acids (fuel for muscle and liver tissues), pyruvate and alanine. Second pass is through the non-reversible rate limiting BCKDH. Valine is glucogenic, leucine ketogenic and isoleucine is both. Most of the NEAAs are glucogenic, suggesting a reversable relationship to glucose in relation to the intermediates in the citric acid /Krebs cycle, valine produces succinyl-CoA (glucose), leucine acetyl-CoA (ketone bodies)/ acetoacetyl CoA and isoleucine both acetyl CoA and succinyl-CoA.

fEAAs variability was seen in muscle tissues over time. All diets were formulated similarly with the only differences in BCAAs, glycine, serine and alanine (b-alanine) and constructed using the same basal mix. This may suggest uptake competition or some fEAAs more in demand than others. Possibly a tissue specific requirement/ need?

Examination of the plasma fEAAs did not identify any trends, highlighting a possible differential muscle uptake amongst the fEAAs. In mammalian models, all AAs (excluding the BCAAs) are thought to be primarily metabolised in the liver. Plasma and muscle fEAAs with significantly different uptake concentrations in both analyses were NA arginine, PL histidine, CD+ PL lysine, CD methionine and CD+PL threonine. These trends may suggest an effect of supra-optimal leucine (PL) enhancing the muscular requirements for lysine, histidine and threonine, whereas sub-optimal leucine (NA) enhanced the requirement for arginine. Arginine, in addition to leucine, is thought to activate *de novo* protein synthesis through mTOR pathway signalling.

This alternative arginine mTOR activation may in part contribute to a broader understanding of the current growth results whereby NA growth far superseded the hypothesised expected growth outcomes.

Muscle fNEAA temporal uptake differences within each diet had the highest variation of fNEAA uptake in the CD, with 5 of the 8 (5/8) fNEAAs significantly different over time (p=<0.05). Considering all diets were manufactured from the same basal mash with the only formulated differences in the BCAAs, glycine, serine and alanine (79% mash, 21% cAAs), one can suggest that the muscle uptake across the other diets may be a result of either the BCAAs or the 3 NEAAs (Figure 3.8).

Interestingly, the only temporal differences in uptake concentration in NL and NA were for proline. This may imply that sub-optimal levels of dietary leucine drive the uptake of muscular proline. PL had differential uptake in alanine, b-alanine and glutamic acid, possibly due to the elevated levels of leucine increasing the demand for other AAs (Liebig-barrel concept).

Exploring the similarities in significant temporal uptake trends between plasma NEAAs and muscle fNEAAs, CD differences in muscle uptake mirrored plasma differences.CD uptake was significantly different for both plasma and muscle in 4/8 NEAAs, these were b-alanine, glycine, and tyrosine, with PL+CD both different in glutamic acid (Figure 3.7). Similarly to muscle fAAs, this significant variation in uptake may highlight a possible biological requirement, possibly tissue-specific, that may need further exploration.

In addition to dietary inclusion levels, the differential temporal concentrations of alanine and glutamine/ glutamic acid, may be a consequence of the degradation of the BCAAs (alanine ↔ pyruvate, a-ketoglutarate ↔ glutamate). Blanco & Blanco (2017) suggested that alanine and glutamine account for up to 50% of the AAs released by muscle tissues in humans and this may have contributed to the variation in muscle and plasma concentrations. In conclusion, differential AA uptake was observed in plasma and muscle tissues, with some muscle uptake replicating plasma trends.

3.4.2.4 Plasma week-7 over time

Aoki et al. (2001) examining the plasma AAs in yellowtail (*Seriola quinqueradiata*) with non-fishmeal diets supplemented with cAAs, found that uptake of the supplemented cAAs was much faster than the whole protein AAs. The first plasma samples were taken at 3 hr post-prandial and the cAAs peak uptake was between 3-6 hr post-prandial. In the current study, in some cases peak uptake occurred at 2 hr, and it would be interesting if their trial had done an earlier sampling point as they may have missed an earlier peak uptake.

Schuhmacher et al. (1997) studying the effects of force-fed intact protein and cAA diets on plasma AAs in rainbow trout, had elevated EAA peaks at 18 hr post-prandial and a return to baseline levels were seen at 40 hr post-prandial. Similarly for the NEAAs, peak uptake was at 18 hr and a return to baseline was seen at 48 hr post-prandial. In the cAA diet, EAA and NEAA peak uptake was at 9 hr with a return to baseline at 40 hr. Their results were dissimilar to the current study, whereby the majority of peak uptake was between 2-4 hr. Their study had differences between the diet formulations, with the intact protein control diet containing different ingredients to the cAA. cAAs were included into the cAA diet at 50.96% and did not stipulate whether the feeds were cold-pressed or extruded. Their study may have benefited from using a basal starting mix for both diets and then manipulating the cAAs and intact proteins additionally to the basal mix.

Choo et al. (1991) included 13.4% leucine in rainbow trout diets and did not experience lower plasma concentrations of isoleucine and valine. This result may have been due to their study potentially missing peak uptake times as their samples were taken 30 min after feeding. In the current study, peak uptake times for the BCAAs ranged from 2 to 4 hr post-prandial and the PL diet did have ±50% lower isoleucine and valine. Brosnan & Brosnan (2006) suggested that this effect of excess leucine suppressing valine and isoleucine concentrations may be due to α-KIC inhibiting BCKDK which in turn activate BCKDH and initiates the irreversible step in BCAA catabolism. Wolfe (2017), shared similar sentiments as Brosnan & Brosnan (2006) but went further in suggesting that leucine activation of the BCAA oxidation pathway, and subsequent reduced plasma valine and isoleucine concentrations, may lead them to become rate limiting for protein

synthesis. Neinast et al. (2019) investigated the metabolic fate of BCAAs in both mice and mice cell lines, to reveal that by inhibiting BCKDK, and thus increasing BCAA oxidation, endogenous release of isoleucine from protein was not affected.

Nicklin et al. (2009) using mammalian cell culture lines, explored the effect of glutamine on mTOR signalling. Their data suggested that intracellular glutamine regulated EAA uptake by responding as an efflux substrate for SLC7A5/SLC3A2. This was done by transporting leucine/EAAs into the cell and glutamine out of the cells. Interestingly their study found that when they depleted cellular levels of glutamine, leucine uptake stopped and mTOR was inactivated, suggesting that glutamine uptake was the rate-limiting step in the mTOR pathway. The BCAT enzyme found in muscle and not liver, through the reversible conversion of BCAAs in BCKAs play a role in glutamine and glutamate synthesis (Holeček, 2001). This is achieved by α-ketoglutarate (α-KG) receiving the amino group from the BCAA/BCKA and producing glutamate, which in conjunction with ammonia, then form glutamine (Li et al., 2020).

Nolles et al. (2008) in a study on rats fed with either fAAs or intact proteins, found that AA intestinal absorption rates were regulated when the rats were adapted to the feeds for as little as 5 days. The authors hypothesised that this adaption of transporters in the GIT (gastrointestinal tract) was involved in the postprandial loss of AAs. In mammals fAAs are absorbed quickly, with high AA concentrations observed in circulation which may lead to oxidative losses (Nolles et al., 2008).

3.4.3 Amino acid interactions, metabolism and pathways

Dietary leucine did appear to affect plasma BCAA uptake as observed by the contrasting effects in NL and PL (Figure 3.9). Supra-optimal leucine in PL appeared to suppress isoleucine and valine uptake compared to increased uptake in the NL diet. PL plasma leucine appeared to suppress lysine uptake, with lowest concentration at 8 hr. Plasma threonine uptake was higher in NL and NA at 2 hr compared to CD and PL, suggesting a possible uptake interaction with leucine. NA plasma threonine and phenylalanine concentrations were higher than the other diets at 8 hr, possibly an influence of metabolic processes. NA plasma arginine uptake was significantly higher than all other diets at 2 hr, with the lowest

uptake in PL, a possible leucine interaction or preferential uptake due to minimal dietary leucine.

NA 8 hr plasma glutamate concentration significantly higher than other diets (Figure 3.10), with NA proline concentrations also higher at 8 hr compared to other diets (near significant (p=>0.05 but p=<0.10). Glutamate and proline are connected via glutamate metabolism and proline synthesis in addition to ammonia detoxification (Palma et al., 2019). These trends may suggest an effect of leucine.

Feeds were formulated to contain higher levels of alanine and *b*-alanine in the NA, NL and less in the PL (12%, 4% and -18%) when compared to the CD diet formulation. When the feeds were hydrolysed, the change (%) from the CD was that NA and NL were slightly higher (5% and 1%) while the PL was 19% lower than the CD levels. This was taken into consideration and plasma and muscle alanine (+b-ala) fAAs change (%) was corrected, this did not lead to any significant changes in overall trends.

In the current trial, the PL and NL diets had higher circulating plasma glutamate levels than the CD (31% and 13%) whilst the NA had about 14% less than CD levels at the -2 hr sampling point (Figure 3.10 A). By 2 hr post-prandial the opposite development was seen in plasma, with NA increasing and both PL and NL decreasing to levels comparable to the CD. This decreasing trend was seen in both diets until the 8 hr timepoint, with the largest difference in concentration occurring in the PL compared to CD levels (-13% and -11%).

Li et al. (2020) stated that in fish skeletal muscle due its proportionate size in comparison to the whole body, is the main site for glutamate/ glutamine synthesis in fish. In the muscle tissue at -2 hr, an opposite trend was seen to plasma, with NA glutamate levels higher than CD, PL the lowest, and NA had similar levels to CD (Figure 3.10 B, C). At 2 hr all diets decreased below CD levels, although the NA diet was the most similar in concentration to the CD. By 4 hr, all diets had risen above the CD baseline levels, while NA and NL continued to rise with the largest divergence from CD baseline at 8 hr. PL at 8 hr had decreased below CD concentrations before rising to CD baseline levels at 24 hr. NA and NL had

dropped to their lowest levels below CD levels by 24 hr. This may be indicative of the glutamate/glutamine synthesis pathway as BCAA first step metabolism produces BCKAs and glutamate.

Neinast et al. (2019) injected mice with a ^{13}C labelled BCAA and collected blood samples at 30 s then every minute after, while tissues were collected at 3 min and 5 min. They discovered that the peak BCAA concentrations had halved after 4min, but most surprisingly was the speed of transamination, as 1 min after infusion,^{13}C BCKAs had risen to 50% of the BCAA levels and by 3 min 3-HIB (3-hydroxyisobutyrate), another metabolite of valine, was found to be circulating at 20%. Their findings demonstrated that uptake of valine into tissues and subsequent release of 3-HIB back into the circulatory system, took approximately 3min. This process involved six mitochondrial enzymic reactions and even though their study used injected BCAAs rather than experimental feeds, the process from uptake to release was incredibly quick, and was a good demonstration of BCAA metabolic activity.

In summary, if the catabolism of valine could occur as quickly as Neinast et al. (2019) suggested in warm-blooded species such as mice, then it is quite possible that the sampling times used in this trial may have been too widespread. Even though Atlantic salmon parr/ smolts are ectothermic, relying on external temperatures for metabolism (Kullgren et al., 2013), the current results indicated that peak uptake of fAAs occurred at 4 hr but perhaps a sampling time every 2 hr until the 12 hr point may have clarified the extent of the undulating trends. Due to the size of the trial, the temporal complexity, small fish and the physical demand, shorter sampling times were not possible for this trial. Perhaps in future if less tissue samples were collected, less complicated methods for tissue preservation, larger fish, and more colleagues available, this may be possible to do. Future studies may also include the analysis of the BCKAs and subsequent BCAA metabolites.

3.4.3.1 Ketogenic and glucogenic amino acids

From an evolutionary perspective, a certain amount of plasticity and adjustments are essential for survival. From an AA perspective, these would be the keto- and

glucogenic dual-role AAs, namely isoleucine, phenylalanine, threonine, tyrosine and tryptophan.

In the current study, no significance was noted in growth between the AA manipulated experimental treatments (p=>0.05). Although this could be contributed to a variety of factors previously discussed, an additional factor could be the dual-role keto- and glucogenic AAs. In Figure 3.13, the dual-role fAAs in plasma and muscle compared to the CD (change (%), does seem to indicate dietary influences on temporal trends. In mammalian models, muscle tissue is not gluconeogenic, suggesting that valine and isoleucine are possibly metabolised elsewhere in gluconeogenesis (Bifari & Nisoli, 2017).

During periods of stress such as starvation/ fasting, ketogenic pathways enabling energy production from ketone bodies are prioritised, while during smoltification, glucogenic pathways are prioritised due to the high energy demands (Py et al., 2022). These temporal variations may be indicative of undulating temporal requirements. An alternative theory regarding the similarities in growth between the experimental diets was the possibility of metabolic adjustments to the diets, with the dual-role AAs providing substrates for metabolic flexibility and homeostasis.

3.4.3.2 Alternative absorption and excretion of cAAs

A possible theory for the homogenous growth witnessed in the second stage of this trial (week-3 to -7) was that with the excess feed and faeces not removed via the drum filter, the disintegration of the cold-pressed feed and the subsequent biofilter crash may have released the cAAs into the system. In an enclosed tightly controlled system like RAS, the only feed available is the manufactured feed provided and an alternate theory to the fish going off their feed (sexual maturity, smoltification, poor water quality) is the absorption or ingestion of the circulating cAAs in the RAS system. This may have been possible through digestion (intestinal uptake from water) and absorption from the gills and skin.

Glover et al. (2013) reviewing fish skin as a transport system, suggested that teleosts have no demand for nutrient permeable skin as it is used for ion exchange. Currently only Pacific hagfish (*Eptatretus stoutii*) are thought to absorb

nutrients through gills, skin and GIT. Studies by Bucking et al. (2011) demonstrated the tissue accumulation of radio-labelled glycine added to the water. In addition to hagfish, Katayama et al. (2016) identified 5 N^{15} labelled AAs (lysine, threonine, serine, phenylalanine, and tyrosine) that were absorbed through the water by salamander larvae (*Hynobius retardatus*). Interesting that the ketogenic AAs lysine, phenylalanine, and tyrosine were among the 5 readily absorbed.

Closing the life cycle of marine species is time consuming and full of constraints, with feed being one of the biggest hurdles. If salamander larvae can absorb AAs from the water, then this may be an area for further research from an industry, ornamental and environmental perspective.

Although these are the only published examples of AA absorption in vertebrates, a realistic idea of whether this has been explored either academically or from an industry standpoint is unknown, as research is generally not published unless there are significant findings.

A recent article by Griffin et al. (2023) demonstrated the transport rate of 1000 µM environmental ^{14}C radiolabelled leucine through the gills of green crab (*Carcinus maenas*) at 53.7 ±6.24 nmol/g/h and at lower concentrations of 10 µM the Dungeness crab (*Metacarcinus magister*) gill transfer rate was 7.08 ±2.27 nmol/g/h. The authors suggested that little is known about invertebrate transporters but evidence in other studies suggested AA gill transport via SLC6 family Na+/AA cotransporters on the basolateral and apical membrane. The hypothesis they proposed was that increased mitochondria provided ATP to power the Na+/K+ATPase increasing the electrochemical gradient in the cell. This resulted in increased cellular capacity of Na+/AA co-transport and allowed the AA transport across gill epithelia.

Dabrowski et al. (2010) theorised that the inclusion of fAAs in fish feeds had faster absorption times than intact proteins but may lead to hyperaminoacidaemia and the subsequent excretion of AAs (via gill and urinary tract). Hyperaminoacidaemia increases protein synthesis and anabolism, but Murai et al. (1984) studied the excretion levels of fAAs from intact and fAA diets on carp (*Cyprinus carpio*),

concluding that the poor growth was due to the excretion of AAs through gills and kidneys, rather than catabolism of the AAs. If AAs can be excreted through the gills, then there is a possibility they can be absorbed through them.

Ivanova et al. (2021) studying the use of fAAs in skin and gill mucus as a non-invasive health tool on Atlantic salmon parr/smolts (70-80g), found 19 AAs in gill mucus of which glutamic acid and alanine were the highest. The authors suggested this may have been due to the osmoregulation and ammonia excretion/synthesis. Gill mucus had double the metabolite concentration compared to skin mucus. Ivanova et al. (2021) did not specify if the fish were obtained from flow-through or RAS, it would have been interesting to see if this may have affected the results of their study.

A study using kelp bass (*Paralabrax clathratus*) injected intra-arterial labelled ^{14}C alanine into the bloodstream and within 30 min it was identified in mucous (Bever et al., 1981). Kajimura et al. (2004) explored nitrogen excretion in rainbow trout and identified 4-10% of nitrogen was excreted as AAs via the gills and 3-11% as protein via mucous. These findings highlight alternative AA excretion, which may suggest possible environmental uptake routes.

3.4.4 Haematology and biochemistry

Pooled blood pellets and plasma were sent for analysis at SRUC veterinary services (Scotland's Rural College, Edinburgh) as haematology analyses are a useful diagnostic tool to determine fish health and welfare (Witeska et al., 2022). Blood chemistry results obtained from pooled plasma samples for red blood cell count (RBCC), haemoglobin (Hb), packed cell volume (PCV) and white blood cell count (WBCC) indicated no differences between the diets at week-3 nor week-7. GLM did expose differences between the means of week-3 and week-7 for Hb, PCV and WBCC.

Across the different diets, RBCC, Hb, and PCV levels exhibited variations at both week-3 and week-7. Specifically, at week-7, fish fed the PL diet showed the highest RBCC and PCV levels, suggesting a potential enhancement in erythropoietic activity and oxygen-carrying capacity compared to other diets. However, these differences were not statistically significant (p=> 0.05), indicating

similar physiological responses to dietary treatments. Acute or chronic stressors in addition to nutritional imbalances such as sexual maturation, smoltification, photoperiod manipulation, handling and water quality may cause haematological alterations (Fazio et al., 2015) and reduced growth (Karakach et al., 2009). Walker-Vergara et al. (2020) stated that handling salmonids for more than 20 s may cause haematological variations of up to 25% in haematocrit.

Salmonids are sensitive to poor water quality and with a study in a rainbow trout exposed to nitrite, it was revealed that 80% of Hb was oxidised into methaemoglobin by exposure to nitrite concentrations as low as 0.2 mg/ L (Kroupova et al., 2005). In the current study, week-3 Hb means were significantly higher than week-7 means (p=<0.000). This may have been due to the technical variation either from sampling or laboratory-specific procedures as discussed in Seibel et al. (2021). The sampling and SRUC veterinary service methodology used in the current study were similar to previous studies such as Glencross et al. (2024) which utilised the services of SRUC. Between the experimental diets, Hb at week-7 ranged from 132-148 g/L which is higher than the range stipulated in Walker-Vergara et al. (2020) for pre-smolt (41-108 g/L) and post-smolt (53-111 g/L) Atlantic salmon.

WBCC had variations between weeks, while heterophil, lymphocyte, and monocyte counts demonstrated fluctuations across the different diets at week-7. WBCCs (leukocytes) parameters are good health indicators in fish due to their innate immune system and increased WBC values may be indicative of an immune response (Witeska et al., 2023). While no significant differences were observed among diets (p=> 0.05) for WBCC, there were differences between the means of the weeks (p=<0.05). This may suggest a system wide effect either driven by environmental or biological influences.

At Week-7 additional haematology analysis was conducted on heterophil, lymphocyte, monocyte, ALP, AST, CK, and ALB. Although no differences were observed for any of the parameters (p=>0.05), ALP, AST, CK, and ALB remained relatively consistent across different diets.

The CK levels in the current study ranged from 134967 ±99393 iu/L in the PL diet to 101267 ±84230 iu/L in the CD diet. CK parameters listed in Walker-Vergara et al. (2020) ranged from <25524 iu/L in pre-smolts, <16915 iu/L in post-smolts to <26352 in Atlantic salmon broodstock. Although the variation in the current data is large *i.e.* ±99393 iu/L standard deviation, the overall values are higher than the expected range for salmon parr.

Glencross et al. (2024) in a study exploring the benefits of dietary omega-3 in Atlantic salmon under hypoxic conditions, had CK ranges from 18,630 to 37,187 iu/L, which were significantly lower than the current trial. Yousaf & Powell (2012) in their study determining the effects of heart and skeletal muscle inflammation (HSMI) on CK levels in Atlantic salmon adults, suggested that high levels of CK may be due to tissue damage in fish. Their CK levels ranged from 16479.25 ±1844.49 iu/L in diseased fish (HSMI) to 1581.71 ±425.33 iu/L in anaemic fish.

Initial thoughts surrounding the elevated CK concentrations in this study were possible human or technical error in either sampling and storage or downstream laboratory analysis. Sampling, processing and storage were all conducted in accordance with the current recommendations (Fazio et al., 2015; Keitel-Gröner et al., 2025; Witeska et al., 2023, 2022).

Veiseth-Kent et al. (2010) studying the effects of crowding on Atlantic salmon, stated that the CK enzyme in muscle tissue was linked to energy metabolism, by phosphorylation of creatine phosphate to ADP (adenosine diphosphate) producing both ATP and creatine. With the BCAAs linked to energy production, perhaps some of the elevated levels of CK may be due to varying levels of BCAAs affecting the energy production and glycolysis/gluconeogenesis pathways.

Sandnes et al. (1988) suggested ALP activity was used as an indicator in fish for liver health, and ALT for liver and kidney health. In their study on adult Atlantic salmon, they suggested that ALP and AST were found in plasma in low levels, but following cell damage their concentrations were increased in plasma. Current ranges of AST (470-569 iu/L) were within the ranges in Walker-Vergara et al. (2020) but ALP results (581-619 iu/L) were approximately 3 times higher than the acceptable range of 79-282 iu/L for pre- and post-smolts.

Braceland et al. (2017) examining the treatment of blood samples and their effects on the biochemistry results in Atlantic salmon, suggested that there were no established protocols for salmon. Their study indicated that storage of samples at room temperature affected the results of ALP, AST and CK only after 48 hr. The samples sent to SRUC for analysis were stored on dry ice when not refrigerated (travel) and elevated levels of CK in the current study are unlikely to be due to suboptimal storage conditions.

Alterations to haematological and biochemical parameters may be an indication of pathogenic influences such as Waagbø et al. (1988) studying haematology and biochemical analyses of Atlantic salmon infected with vibriosis (*Vibrio salmonicida*), had similar results in their healthy (control fish) as the current study. The RBC, Hb, albumin and AST levels were all slightly lower, but their ALP levels were higher than the juveniles of the current study. Their study only used 10 diseased fish and 10 healthy fish, compared to the current study of 48/week (n=96).

A possible area of consideration for future studies is discussed in Pailla et al. (2000) who suggested in determining reference values of a-keto acids in relation to albumin levels in mammalian models. Their theory was that circulating BCKAs are released from muscle tissue and bound to albumin and therefore measurable. They results supported their theory, with significant correlations between albumin and BCKA concentrations. If their model could be applied to fish studies, it may be a valuable tool in nutritional studies with the possibility of non-lethal applications.

In summary, nutrition, disease status, stress, environment have been identified as affecting blood parameters in various models. Sandnes et al. (1988) tried to identify the normal range for blood parameters in Atlantic salmon and identified additional effects of day length (photoperiod) and water temperature. In the current study, although not statistically different (p=>0.05), variability did occur within week-7 with 6/11 parameters the highest in PL and 5/11 the lowest in NL. This may suggest an influence of leucine on blood parameters. Further

investigation into the immunomodulatory effects of different diets is warranted to elucidate their impacts on fish health and disease resistance.

3.4.5 $\delta^{15}N$ labelled leucine stable isotope

Stable isotope analysis, especially the nitrogen isotope, is commonly used to determine protein metabolism (Dvergedal et al., 2019). In the current study, $\delta^{15}N$ labelled leucine was used as a tool to determine $\delta^{15}N$ leucine accumulation between tissues in the CD. Results indicated differences across the tissues at each week and within the tissues between weeks (p=<0.05) (Figure 3.14). GLMs indicated differences in the tissue means, and the means by week, with week-3 substantially higher than week-7 (p=<0.05). No differences were identified in WB between week-3 and week-7 (p=>0.05).

WB, liver and muscle tissues were examined as muscle tissue in fish compared to other tissues, accounts for 40-60% of body weight and thereby contributes to growth (Verri et al., 2011). McCarthy et al. (1997) expanded on growth, explaining that fish growth could be due to either reduced proteolysis or increased protein synthesis. The current retention results suggested that overall, WB had a 22% decrease of $\delta^{15}N$ leucine. This may be explained by the change (%) in CD growth between week-3 and week-7 (24%), which was similarly aligned to the 22% decrease in $\delta^{15}N$ leucine. Dvergedal et al. (2019) explained that growth is the difference between absorption of nutrients from feeds and the loss of nutrients via faeces, whereas efficiency is the ratio between them. Although no temporal differences were seen in the WB samples of the current study (p=>0.05). This may have been due to low turnover rates or potentially an effect of gonadic growth and basal metabolism as suggested by Perga & Gerdeaux (2005) in their isotopic study on whitefish (*Coregonus lavaretus*).

In summary, $\delta^{15}N$ leucine in this study identified temporal and tissue differences of $\delta^{15}N$ leucine in juvenile Atlantic salmon. Liver, a highly metabolic tissue, had lower protein accretion rates than muscle tissue, substantiating the results of Dvergedal et al. (2019). Verri et al. (2011) suggested that the low growth efficiency found in liver tissue is from similar levels of protein synthesis and

degradation. WB tissues had the lowest rate of $\delta^{15}N$ leucine degradation over time.

Perhaps rather than using the stable isotope on one diet for 3 weeks, doing all diets for one week may have produced a more informed understanding on the utilisation of $\delta^{15}N$. The obstacles faced were that the other diets had sub-optimal levels of leucine, and Dvergedal et al. (2019) suggested that tissue saturation of SI should be at least 50% that of the feed level (0.1-2% feed inclusion).

3.4.6 BCKDH mRNA abundance

An exploratory look at BCAA metabolism using BCKDH (branched-chain α-ketoacid dehydrogenase) was used to determine if we could identify an effect of the diets, especially leucine, on BCAA metabolism (Figure 3.15). In mammalian studies, BCKDH is an enzyme complex (E1, E2, and E3 sub-units) involved in the second step of BCAA catabolism and is known to be rate limiting and tightly regulated as it is irreversible (Yahşi & Gunaydin, 2022). Leucine metabolites consist of α-ketoisocaproate (α-KIC) and β-hydroxy-β-methylbutyrate (HMB) (Duan et al., 2016). Isoleucine and valine are converted into α-keto-β-methylvalerate (KMV) and α-ketoisovalerate (KIV) (Chuang et al., 2006). In mammals, these ketoacids are then irreversibly catabolised into isovaleryl-CoA from KIC, 2-methylbutyryl-CoA from KMV, and isobutyryl-CoA from KIV (Mann et al., 2021). In the current study, BCKDH1A (E1) mRNA transcripts were higher in muscle tissue at -2 hr and 24 hr compared to 4 hr post-prandial, with the NL diet significantly different to the NA diet mRNA abundance.

3.4.6.1 Muscle

Muscle tissue transcripts showed differences within each diet over time in NL, NA and PL diets, with the highest transcript numbers at the -2 hr time aside from NL, where -2 hr and 24 hr transcript numbers were not different. NL and PL seemed to follow similar trends, with 4 hr abundance lower than the other times, whereas in NA, no differences were seen between 4 hr and 24 hr timepoints. These temporal differences in abundance may be indicative of an effect of the BCAAs, especially leucine, as no significant temporal differences were seen in the CD diet, but near significance was observed.

Plasma levels of circulating fBCAAs at -2 hr had the lowest different values in the NA diet for isoleucine, leucine, and valine, whereas NL and CD had the highest levels of isoleucine and valine compared to the other experimental diets. Plasma BCAAs overall had peak concentrations of BCAAs at 2 to 4 hr post prandial. BCKDH mRNA transcripts in muscle were highest at -2 hr and lowest at 4 hr. Lu et al. (2009) stated that elevated BCAAs or BCKA (branched-chain-α-ketoacids) in mammals have shown to activate BCKDH. The opposite is seen in the current study, with less muscle BCKDH mRNA abundance seen at 4 hr when compared to baseline levels at -2 hr

Circulating fBCAAs in muscle tissue had no significant differences across the diets at -2 hr, although near significance ($p \leq 0.10$) was seen in isoleucine and valine. Similarly to plasma, isoleucine and valine concentrations were higher in the CD and NL diets, and muscle fBCAA peak concentrations were at 2 hr and 4 hr. With significant differences across diets at 2 hr and 4 hr for the three BCAAs, apart from near significance in leucine at 2 hr. BCKDH muscle absolute copy numbers ranged from a high at prefeeding levels to the lowest at 4 hr, with both extremes seen in the NL diet. This could be due valine and isoleucine driving the response in the NL diet as it contained sub-optimum levels of leucine. Valine is glucogenic, and isoleucine is both glucogenic and ketogenic (Bifari & Nisoli, 2017). Hormones (glucocorticoids such as glucagon, growth hormone, epinephrine, and cortisol) may stimulate gluconeogenesis in rats by activating BCKDH, and in so doing provide more substrate (Harris et al., 2001). Similarly, for the 4 hr week-3 and week-7 copy numbers (/µL), the highest and lowest values were seen in NL diet.

3.4.6.2 Liver

Liver tissue had significant differences (p=<0.05) over time in mRNA abundance in the CD, NA, and PL diets. NA and PL diets had a similar trend, with the lowest different transcript numbers seen at -2 hr compared to 4 and 24 hr. This suggested that mRNA abundance was still elevated at 24 hr and did not return to baseline levels. CD was slightly different, with the highest different values at 4 hr

and the -2 and 24 hr timepoints similar, suggesting a return to baseline levels at 24 hr.

As the current study did not have liver fBCAA data, no trends could be examined between the tissue and the mRNA abundance. Liver tissue mRNA abundance displayed an opposing trend to muscle tissue, with the highest abundance at the 4 hr point. In current literature, elevated BCAAs or BCKAs may activate BCKDH enzymatic activity such as in rats, increased leucine in the blood, resulted in higher α-KIC concentrations, which inhibited BDKDK (branched chain keto acid dehydrogenase kinase) activity, and in so doing increased BCKDH activity, leading to irreversible BCAA catabolism (Harris et al., 2001). This may explain the low liver mRNA abundance at –2 hr baseline levels as the plasma BCAAs concentrations were lower at -2 and 24 hr than the other times.

The absolute copy number (/µL) range in liver tissue had the highest in the CD diet and the lowest in the PL diet. Similarly for the 4 hr week-3 and week-7 copy numbers, the CD diet had the highest variability across the diets.

Muscle BCKDH mRNA abundance (copy numbers LOG_{10}) between week-3 and week-7 at 4 hr, identified significantly different means between week-3 and week-7 and highlighted a significant interaction between diet and week (D*W) (p=<0.05). Week-3 means were significantly higher than week-7 (p=<0.05) whereas in liver tissue, an opposing trend was detected, whereby week-7 means were significantly higher than week-3 (p=<0.05).

Exploration of the week-7 temporal muscle BCKDH mRNA abundances within each diet highlighted differences at prefeeding times (p=<0.05), with prefeeding significantly higher than the other times for NA and PL, with no differences in CD. NL was the exception, with 4 hr significantly lower than -2 hr and 24 hr, suggesting a return to baseline levels at 24 hr. Although there were no significant differences in week-7 across diets at each timepoint, tissue specific temporal trends were identified. In muscle, mRNA abundance across the diets were elevated at the prefeeding time, before dropping at 4 hr and then rising again at 24 hr. An opposing trend was seen in liver, with the lowest abundance at prefeeding, rising to peak levels at 4 hr and then dropping slightly at 24 hr but not returning to

prefeeding levels. Biswas et al. (2020) examining the BCKAs and insulin in mice, proposed that a reduction in insulin enhances fatty acid oxidation. Excess lipids downregulate BCAA enzymes involved in catabolism, and they suggested that perhaps the fatty acids compete with the BCAAs as muscle substrates by regulating enzyme expression and activity.

mRNA abundance does not equate to protein abundance but is often used as a proxy (Upadhya & Ryan, 2022). Due to complexities such as regulation, technology is unable to predict protein abundance from mRNA, with current studies opting for multi-omics approaches (Payne, 2015). Although BCKDH mRNA transcript numbers in the current trial were higher in muscle than liver tissue, indicating higher BCKDH enzyme activity in muscle, without further proteomic studies these results are suggestive and not conclusive. Webb et al. (2019) studying enzyme activity in dairy cows, found that the different subunits of BCKDH had varying levels of mRNA abundance. Their study showed lower levels of BCKDHA in liver while having elevated levels of BCKDHB in liver tissue. Further research in this field is required to determine enzymic activity between the tissues and perhaps exploration of the BCKDH subunits in various Atlantic salmon tissues. If there are tissue specific mRNA abundance rates, and within each tissue differential cellular mRNA transcript abundance, then perhaps this may explain some variation between the data and highlight the importance of targeting specific regions in tissues. Although in this study the apical tip of the liver was used, this cannot always be confirmed due to the volume of samples required, technical abilities and the temporal importance over the sampling days.

In summary, these opposing trends may accentuate a possible effect of the experimental feeds on transcript abundance in muscle and liver tissues. Alternatively, these trends may also be indicative of a species-specific BCKDH activity, cellular-specific activity or a 24 hr starvation effect prior to refeeding. Although caution should be applied to the interpretation of transcript abundance data, it is a useful exploratory tool when conducted with further downstream analysis such as proteomics. Wessels et al. (2016) examining the effects of elevated dietary leucine in a pig model, found a leucine stimulation of non-tissue specific BCKDH activity, with increased activity in brain, liver and heart tissues.

Additionally, reduced tissue concentrations of free valine, isoleucine, and reduced feed intake was attributed to dietary leucine levels.

3.5 Chapter summary

Studies have shown that the BCAAs, especially leucine, are involved in protein synthesis, muscle development and overall growth. cAA feed supplementation in feed formulations offers significant potential throughout the animal feed industry, especially with increased use of plant proteins. Hypothetically, cAAs may improve feed efficiency, nutrient utilisation, and nutrient discharge. Although in this case, feed was manufactured using a cold-pressed method with 21% cAAs included in powdered form. Unfortunately this led to pellet instability in the water, resulting in dissolving pellets and subsequent effects.

In week-3 somatic indices, CD and NA had significantly higher viscera weight than NL and PL. At week-7, no significant differences were found. GLMs identified differences in diet means for weight, liver, and viscera. Differences between weeks were significant for all parameters except heart weight. No diet-by-week (D*W) interactions were observed. Whole-fish (WB) bBCAAs showed increased deposition at week-7 compared to week-3, with greater changes (%) relative to the CD diet.

Muscle fBCAAs showed significant differences between diets at each week, except for leucine at week 3. Within diets, NA had higher isoleucine and valine concentrations at week 7 compared to week 3. fEAAs were stable, with differences between diets at week 3 for arginine, lysine, and methionine. Within diets, arginine was higher at week 3 in CD and NA, and lysine was higher in NL. For fNEAAs, differences between diets occurred at week 3 for alanine, β-alanine, and glutamic acid, and at week 7 for proline. Within diets, glutamic acid in NA and tyrosine in CD were higher at week 3 compared to week 7.

At week-7, muscle fBCAAs showed temporal differences between diets at 2, 4, and 8 hr for isoleucine and valine, and at 4 and 8 hr for leucine. Within diets, CD exhibited temporal changes in all fBCAAs, while NA showed no temporal differences. For fEAAs, the largest concentration differences between diets

occurred at 3/5 timepoints, with lysine and methionine showing the most significant uptake differences within diets over time (3/4 timepoints).

Plasma fBCAA concentrations between week-3 and week-7 mirrored muscle fBCAA trends, showing differences across all diets at each week, except for leucine at week-3. No differences were observed within diets between weeks. Plasma fEAAs showed no significant differences between weeks across diets or within diets, except for lysine at week-3 and within NL, NA, and PL. For fNEAAs, differences between diets occurred only for alanine at week 3 and serine at weeks-3 and 7. Within diets, no differences were observed in NL between weeks.

At week-7, plasma fBCAAs showed significant differences between diets for isoleucine and valine, while leucine concentrations differed at 2, 4, and 8 hr. Temporal differences in fBCAAs were observed within the PL diet but not in the NA diet. Plasma fEAAs remained stable between diets, with differences at 7/30 time points, notably in lysine (3/5). Threonine was the only fEAA showing temporal differences across all diets. Plasma fNEAAs differed at 5/40 time points between diets, with no differences in β-alanine, glycine, proline, taurine, or tyrosine. Temporal differences within diets were observed for proline, glutamic acid, and glycine.

Haematology and biochemistry analyses did not identify differences between treatments but differences in the means between the weeks were visible. Elevated levels of CK were observed although not significant between treatments.

$\delta^{15}N$ labelled leucine stable isotope analysis was used in the CD to identify leucine deposition in liver, muscle and whole bodies between week-3 and week-7. Significance between tissues at each week and within each tissue between the weeks were identified. No differences in WB $\delta^{15}N$ labelled leucine were observed between the weeks suggesting the tissue-specific leucine turnover differences did not occur at the whole organism level. This alluded to an understanding of the protein homeostasis mechanisms in Atlantic salmon.

mRNA abundance of BCKDHA in liver and muscle tissues had alternate trends over the timepoints at week-7. This may demonstrate the post-prandial activity in

relation to nutrients although further proteomic studies would be needed to confirm this effect. This undulating opposing trend seen between the tissue may additionally highlight natural cellular oscillation in response to protein homeostasis. Muscle had differences within each diet over time at week-7, apart from the CD and similarly between week-3 and week-7 analyses. Liver tissue time differences within the diets at week-7 had abundance differences in all diets apart from the NL. Between the weeks comparisons in liver had no differences between the diets apart from CD. No differences were identified between the diets in week-7 for both tissues.

This trial demonstrated the importance of BCAAs in growth and physiological responses in juvenile Atlantic salmon. The findings suggest an anorectic effect of supra-optimal leucine on Atlantic salmon parr growth, with morphometric and somatic differences observed between the diets. Different δ15N leucine deposition rates between different tissues were identified and a possible effect of 24 hr starvation and proteolysis on BCKDHA mRNA transcripts. The current study has contributed to the understanding of AAs activity, especially the BCAAs, in Atlantic salmon, and highlighted area where further research is required.

Chapter 4

TOR BE OR NOT TOR BE? REGULATION IS THE QUESTION.

Abstract

This study utilises RNA-Seq to characterise transcriptional responses in the liver, brain, and heart tissues of Atlantic salmon (*Salmo salar*) subjected to hypoxic (D1L) and normoxic (D1H) conditions. Hypoxia-induced inhibition of the mechanistic target of rapamycin (mTOR) has been implicated in metabolic reprogramming, energy conservation, autophagy, and attenuated growth and protein synthesis. A comprehensive analysis of existing literature on mTOR in Atlantic salmon exposed substantial annotation challenges across multiple genomic databases. Systematic inaccuracies, including taxonomic misidentifications and misattributions to unrelated molecules and biological systems, necessitated extensive manual curation and reanalysis to ensure data fidelity.

To mitigate annotation inconsistencies, next-generation sequencing (NGS) pipelines were refined using a dual-stage mapping strategy, optimising read alignment against both transcriptomic and genomic references. However, gene model discrepancies persisted, contributing to quantification inconsistencies and highlighting the intrinsic limitations of annotation accuracy. Variability introduced by polymerase fidelity, sample integrity, and technical constraints inherent to high-throughput sequencing methodologies may have compounded the high error rates (>0.1%) characteristic of RNA-Seq platforms.

Functional annotation was performed using an array of bioinformatics tools, including KEGG, DAVID, ShinyGO, g:Profiler, STRING, Ensembl, and NCBI, to enhance confidence in downstream analyses. Nevertheless, substantial obstacles in mRNA transcript identification remained, with a significant fraction of differentially expressed genes (DEGs) unannotated due to incomplete or outdated database references. Ensembl identifiers frequently lacked corresponding gene conversions, and DAVID analysis yielded an annotation success rate of only ~35%. The Atlantic salmon genome's complexity, exacerbated by a fourth whole-genome duplication (WGD), further restricted annotation precision and necessitated reliance on manually curated protein/mRNA sequences.

Distinguishing paralogous genes remains a major challenge due to the high sequence similarity among duplicated gene copies, particularly in species with whole-genome duplication events like Atlantic salmon. This complexity is further exacerbated by the frequent misclassification of pseudogenes, which can lead to erroneous inclusion or exclusion of mRNA transcripts in differential expression analyses. Additionally, alternative splicing events, which are highly prevalent in teleost genomes, complicate mRNA transcript quantification and functional annotation, as current reference databases often lack comprehensive isoform-level annotations.

Multi-mapping ambiguities introduce additional confounders, as short-read sequencing technologies struggle to uniquely assign reads to highly similar genomic regions, leading to potential over- or underestimation of gene expression. Furthermore, inconsistent gene nomenclature across different annotation platforms complicates cross-study comparisons and meta-analyses, reducing the reproducibility and interpretability of results.

Functional enrichment analyses are similarly constrained by database variability and the inherent limitations of statistical correction methodologies. Differences in gene ontology (GO) term assignments, pathway definitions, and enrichment algorithms across databases lead to divergent results, raising concerns regarding the robustness of pathway-level interpretations. Inconsistencies in false discovery rate (FDR) corrections and statistical thresholds further complicate the validation of differentially expressed gene sets, highlighting the need for standardisation in functional genomics analyses. These challenges collectively underscore the necessity for improved computational frameworks, refined annotation pipelines, and integrative multiomic approaches to enhance the accuracy and reliability of transcriptomic research in Atlantic salmon.

The study’s findings indicate that mTOR regulation in Atlantic salmon is predominantly governed at the post-translational level, rather than via transcriptional control, underscoring the necessity for complementary proteomic investigations. This aligns with previous research demonstrating that mTOR activity is often modulated through phosphorylation and protein-protein

interactions rather than through transcriptional changes alone. Hypoxia-associated signalling pathways, including WNT and TNF-α, exhibited differential activation under experimental conditions, consistent with studies in other vertebrates however, due to the intrinsic limitations of RNA-Seq in delineating direct mechanistic interactions, the precise functional roles of these pathways remain ambiguous.

Furthermore, biological variability in hypoxia responses were evident, with dynamic and oscillatory gene expression patterns further complicating differential expression analyses. These findings highlight the need for integrative multiomic approaches, including phosphoproteomics and metabolomics, to unravel the complexities of mTOR-mediated hypoxic adaptation in Atlantic salmon.

This study underscores the inherent challenges of transcriptomic research in Atlantic salmon, driven by both technical limitations and the species' genomic complexity. The necessity for improved annotation pipelines, standardised gene nomenclature, and integrative multiomic methodologies is emphasised to enhance the resolution and interpretability of future studies. Despite these constraints, the research provides valuable insights into Atlantic salmon’s transcriptional adaptation to hypoxia, with potential applications in aquaculture and metabolic regulation. However, industry engagement and funding limitations continue to impede the advancement of functional genomic research in this species, necessitating targeted investment in annotation infrastructure and analytical methodologies.

Keywords: Atlantic salmon, mTOR, hypoxia, regulation, transcriptomics

4.1 Introduction

Aquaculture has advanced significantly since the 1970s, contributing to food security, economic growth, and environmental sustainability (Martinez-Porchas & Martinez-Cordova, 2012). Anthropogenic impacts such as pollution (chemical and physical), eutrophication, physical environment modifications have been widely explored mainly freshwater systems, however, novel environmental stressors *i.e.* rising sea temperatures, wind, salinity fluctuations, and other global warming consequences have prompted extensive research into their impact on teleost fish (Makrinos & Bowden, 2016; Mu et al., 2020). In cage culture, salmonids experience stressors affecting oxygen levels, such as gill disease, high stocking densities, temperature fluctuations, algal blooms, and oxygen stratification (Burt et al., 2012; Martínez et al., 2020).

4.1.1 Hypoxia in aquaculture

Recent studies indicate variable oxygen levels in Atlantic salmon cages, ranging from 8.2 to 5.3 mg/L depending on cage position and tidal (Burke et al., 2021). Hypoxia in salmon is classified below 6 mg/L, with an industry-imposed feeding threshold at this level (Burt et al., 2012). Oxygen saturation is influenced by salinity and temperature; for instance, at 2, 6, 10, 14, and 18°C, saturation levels are 55%, 61%, 66%, 72%, and 78%, respectively. While wild Atlantic salmon naturally endure prolonged fasting, reduced feed intake in response to declining oxygen availability, has been observed in farmed fish (Waagbø et al., 2017). Research by Remen et al. (2016) demonstrated that oxygen saturation of 24-40% at temperatures between 7-19°C severely suppresses appetite.

4.1.2 The mTOR pathway and its regulation under hypoxia

The mTOR pathway is a crucial regulator of cell growth, metabolism, and survival, responding to environmental signals such as nutrients, growth factors, energy levels, and oxygen availability (Wang et al., 2024). Teleosts adapt to hypoxic conditions by modulating the mTOR pathway (Xiao, 2015). The mTOR complex 1 (mTORC1), comprising mTOR, Raptor, PRAS40, Deptor, and LST8, regulates protein translation (Laplante & Sabatini, 2009) while mTOR complex 2 (mTORC2)

includes mTOR, LST8, DEPTOR, RICTOR, and SIN1, primarily modulating cytoskeleton organisation and cell survival (Yin et al., 2021).

Under hypoxia, mTOR activity is inhibited through multiple interconnected signalling pathways and hypoxia-inducible factor (HIF) pathway is a key mediator of this response. HIF1a activation allows for cellular adaption to low oxygen by activating genes involved in glucose metabolism and angiogenesis (blood vessel growth) (Ziello et al., 2007). The cellular response towards glycolysis (anaerobic glucose catabolism) for survival does not rely on oxygen although it is less energy efficient (Yfantis et al., 2023).

When oxygen levels decline, HIF stabilises and promotes the transcription of REDD1, a crucial regulator that inhibits mTOR signalling by activating the TSC1/2 complex. This leads to the suppression of Rheb, a GTPase necessary for mTORC1 activation (Thiepold et al., 2017). Additionally, hypoxia-induced energy depletion activates AMP-activated protein kinase (AMPK), a central metabolic regulator that inhibits mTORC1 by phosphorylating Raptor and promoting TSC1/2 activity (DeYoung et al., 2008; Leprivier & Rotblat, 2020). Furthermore, cellular stress under hypoxic conditions also triggers pathways involving unfolded protein response (UPR) mechanisms and reactive oxygen species (ROS), both of which contribute to mTOR inhibition. These integrated responses ensure metabolic reprogramming, enhancing cell survival by prioritising catabolic processes such as autophagy over anabolic growth pathways.

Additionally, other regulatory pathways influence mTOR under hypoxia, such as the WNT signalling pathway, through PI3K-AKT, upregulates growth factors such as IGF-1, contributing to metabolic shifts (Yoshida & Delafontaine, 2020). Conversely, inflammatory signals, such as TNF-α via the TNFα/IKKβ axis, suppress mTOR activity under stress conditions, prioritising immune function over cellular growth (Lee et al., 2007).

4.1.3 Transcriptomics and mtor regulation under hypoxia

Gene expression is governed by transcriptional and post-translational modifications (PTMs), which influence protein abundance, stability and function (Landini et al., 2022).

Gene expression is orchestrated through a complex interplay between transcriptional regulation and post-translational modifications (PTMs), both of which critically influence protein abundance, stability, and function. PTMs such as phosphorylation, ubiquitination, acetylation, methylation, and glycosylation fine-tune mTOR signalling in response to diverse stressors, including hypoxia and nutrient deprivation (Yin et al., 2021). Phosphorylation, mediated by kinases and counteracted by phosphatases, plays a pivotal role in mTOR activation and inhibition. Ubiquitination regulates protein degradation via the proteasome, while acetylation and methylation contribute to epigenetic modifications that indirectly influence mTOR gene expression.

Transcriptional regulation of mTOR is driven by a network of transcription factors, including hypoxia-inducible factor-1α (HIF-1α), forkhead box O (FOXO), and nuclear factor kappa B (NF-κB), which respond dynamically to environmental fluctuations (Jiang et al., 2019; Nanduri et al., 2008; Palazon et al., 2014). Epigenetic modifications, and miRNAs, also modulates mTOR activity in teleosts, responding to environmental and hormonal stimuli (Benak et al., 2025; Cao et al., 2023). Under hypoxic conditions, HIF-1α is stabilised, initiating a cascade that promotes REDD1 expression, subsequently inhibiting mTORC1 activity (Brugarolas et al., 2004). Simultaneously, FOXO transcription factors mediate stress-responsive gene expression, favouring autophagy over cellular proliferation (Kaelin & Ratcliffe, 2008).

Under hypoxia, cellular adaptation involves mTOR inhibition, reducing protein synthesis, cell growth, lipid and glucose metabolism while increasing autophagy and stress resistance (Brugarolas et al., 2004). This energy conservation mechanism ensures survival by prioritising cellular maintenance over anabolic processes. Hypoxia induces profound metabolic reprogramming through mTOR suppression (Dengler et al., 2014). This adaptation results in a downregulation of protein synthesis via reduced phosphorylation of downstream effectors, such as ribosomal protein S6 kinase (S6K) and eukaryotic translation initiation factor 4E-binding protein 1 (4E-BP1) (Wu et al., 2022).

Additionally, lipid and glucose metabolism undergo shifts, favouring anaerobic glycolysis over oxidative phosphorylation to optimise ATP production under limited oxygen availability (Balakrishnan et al., 2019). Concurrently, autophagic pathways are upregulated, facilitating the degradation of damaged organelles and proteins, ensuring cellular homeostasis and stress resistance (Lahiri et al., 2019). These regulatory mechanisms collectively function as an energy conservation strategy, prioritising survival over anabolic processes to mitigate hypoxic stress and enhance cellular resilience.

Transcriptomics, the study of RNA transcripts, provides insights into gene expression under specific conditions and RNA sequencing (RNA-Seq) is a powerful tool for analysing mTOR-related transcriptomic responses to hypoxia in Atlantic salmon and other fish (Deshpande et al., 2023; Wu et al., 2023). By identifying differentially expressed genes (DEGs), this approach aids in understanding molecular pathways involved in stress adaptation, energy metabolism including tissue-specific responses to hypoxia further enhancing knowledge of physiological adaptations. While RNA levels may not always correlate with final protein expression, transcriptomic analysis remains a valuable method for assessing cellular activity (Koussounadis et al., 2015).

The regulation of the mTOR pathway under hypoxia is complex, involving multiple signalling pathways and transcriptional mechanisms that enable teleosts to adapt to oxygen deprivation (Zhu et al., 2013). Transcriptomic analysis provides a crucial tool for understanding these adaptive responses, offering insights into hypoxia-induced metabolic shifts in Atlantic salmon (Qin et al., 2023). This research contributes to a deeper comprehension of cellular responses to environmental stressors in aquaculture, ultimately supporting improved management and sustainability in fish farming.

The first section of this chapter examined transcriptomic data between hypoxia and normoxia treatments. Liver, brain and heart mRNA transcripts were explored initially as the overall transcriptomic landscape and then in relation to the mTOR pathway. mRNA transcripts were categorised as statistically differentially expressed mRNAs. The second section looked at recategorising mRNA

transcripts by their FC differences looking at >2FC and <-2FC in up- and downregulated mRNA transcripts. This substantial data set was used for exploration in regard to the mTOR pathway. The third section of this chapter looked at the transcript response of a 1FC change in up- and downregulated mRNA transcripts in the mTOR pathway (1 to 1.99FC and -1 to -1.99FC).

4.2 Materials and methods

4.2.1 Literature search

A literature search was conducted to identify and quantify the available published data on mTOR with a focus on mTOR and Atlantic salmon. Online searches were conducted using Nature, Web of Science, Google Scholar, Scopus and PubMed. Search terms consisted of mTOR, and then including specific terms such as human, mammal, vertebrate, fish, teleost, salmon and Atlantic salmon. Common misidentified terms occurred between sites, with the salmon search term including papers on Salmon (author), salmon calcitonin, salmon lice, Durie-Salmon ([D-S] Staging System) salmonella and so on (Table 4.1, Figure 4.1). PubMed® Advanced Search Builder, with MeSH terms (Medical Subject Headings) was used in the final analysis, as it allowed for more flexibility and control compared to the other databases (Sayers et al., 2024) (Table 4.2).

Table 4.1 Search terms and difficulties encountered using multiple online sources

Site	Search parameters	Search terms	Inaccuracies
Nature	'that contain these terms' and 'where the title contains'		Title- no search terms in the title
Web of Science	'TS' and 'TI'		Fish- fluorescence in situ hybridization
Google scholar	And 'allintitle'		Salmon- salmonella Salmon- Author
Scopus	'TITLE-ABS-KEY'	'mtor' OR 'mtor1' OR 'target AND of AND rapamycin'	Salmon- Durie-Salmon staging system
PubMed	[All Fields] [Mesh] [tiab]	"TOR Serine-Threonine Kinases"[Mesh] OR mtor*[tiab] OR tor*[tiab]	Salmon- Durie-Salmon staging system, *Antrodia salmonea* (AS), salmon calcitonin, Salmon lice salmonella. Fish- Fisher exact test, fluorescence in situ hybridization

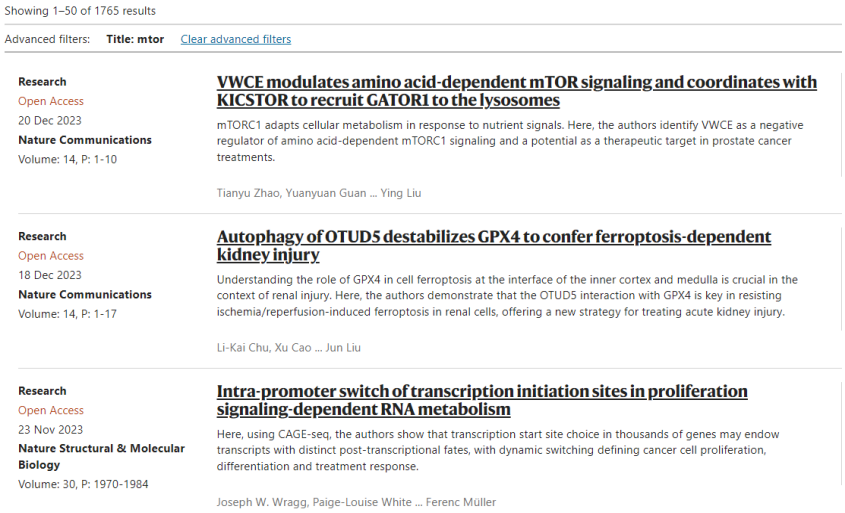


Figure 4.1 Example of search conducted in Nature with mTOR as a title but other papers come up and skew the result numbers.

4.2.2 PubMed Advanced Search Builder

The *[tiab] field code was used to restrict queries to title/ abstract, as well as to prevent 'automatic term mapping' *e.g. PubMed also finds "breast feeding" as a synonym for "nursing"*. The asterisk (*) was used as a way of searching multiple variants of a word (singular/plural/conjugations *etc*.), *e.g.* hypox*[tiab] resulted in searches including hypoxemia, hypoxic, hypoxia, hypoxia/reoxygenation *etc*. PubMed MeSH keywords/ terms may be lacking in some articles as they have not been assigned them, articles may not have been indexed in PubMed or in some cases terminology/concepts may be difficult to condense to a single keyword. To increase searchability of articles, both MeSH and tiab terms were used, and these were nested within brackets set within brackets for each query *e.g.*:

((("tor serine threonine kinases"[Mesh]) OR (mtor[tiab])) OR (tor1*[tiab])) AND ("(Humans"[Mesh]) OR (human*[tiab]) OR (people*[tiab]))*
(("TOR Serine-Threonine Kinases"[Mesh] OR mtor[tiab] OR tor1*[tiab]) AND ("Salmonidae"[Mesh] OR Salmonidae*[Tiab] OR salmonid*[Tiab]))*

Common errors in filtering occurred, in PubMed this was due to the *[tiab] code including everything starting with salmon. Initially this was avoided by using the 'NOT' function, which then proved to be too complex and the *[tiab] was amended to [tiab]. For example, in the 2019-2024 mTOR+ salmon category there were 8 results of which only 4 of those were linked to Atlantic salmon.

Table 4.2 mTOR PubMed MeSH search terms used in the PubMed Advanced Search Builder

Topic	MeSH terms	MeSH terms including Title or abstract(*[tiab])
mTOR	"TOR Serine-Threonine Kinases"[Mesh]	"TOR Serine-Threonine Kinases"[Mesh] OR mtor*[tiab] OR tor1*[tiab]
Human	"Humans"[Mesh]	"Humans"[Mesh] OR human*[tiab] OR people*[tiab]
Mammal	"Mammals"[Mesh]	"Mammals"[Mesh] OR mammal*[tiab] OR people*[tiab]
Vertebrate	"Vertebrates"[Mesh]	"Vertebrates"[Mesh] OR vertebrate*[tiab] OR chordata*[tiab]
Animal	"Animals"[Mesh]	"Animals"[Mesh] OR animal*[tiab] OR animal kingdom*[tiab]
Fish*	"Fishes"[Mesh]	"Fishes"[Mesh] OR fish[tiab]
Salmo salar	"*Salmo salar*"[Mesh]	"*Salmo salar*"[Mesh] OR salar*[tiab] OR salmo[tiab] NOT salmonella NOT salmonea
Salmon*	"Salmon"[Mesh]	"Salmon"[Mesh] OR salmon[tiab] NOT salmonella NOT salmonea
Salmonidae**	"Salmonidae"[Mesh]	"Salmonidae"[Mesh] OR Salmonidae*[tiab] OR salmonid*[tiab] NOT salmonella NOT salmonea

*Not included **Salmoniformes was included under the MeSH term Salmonidae

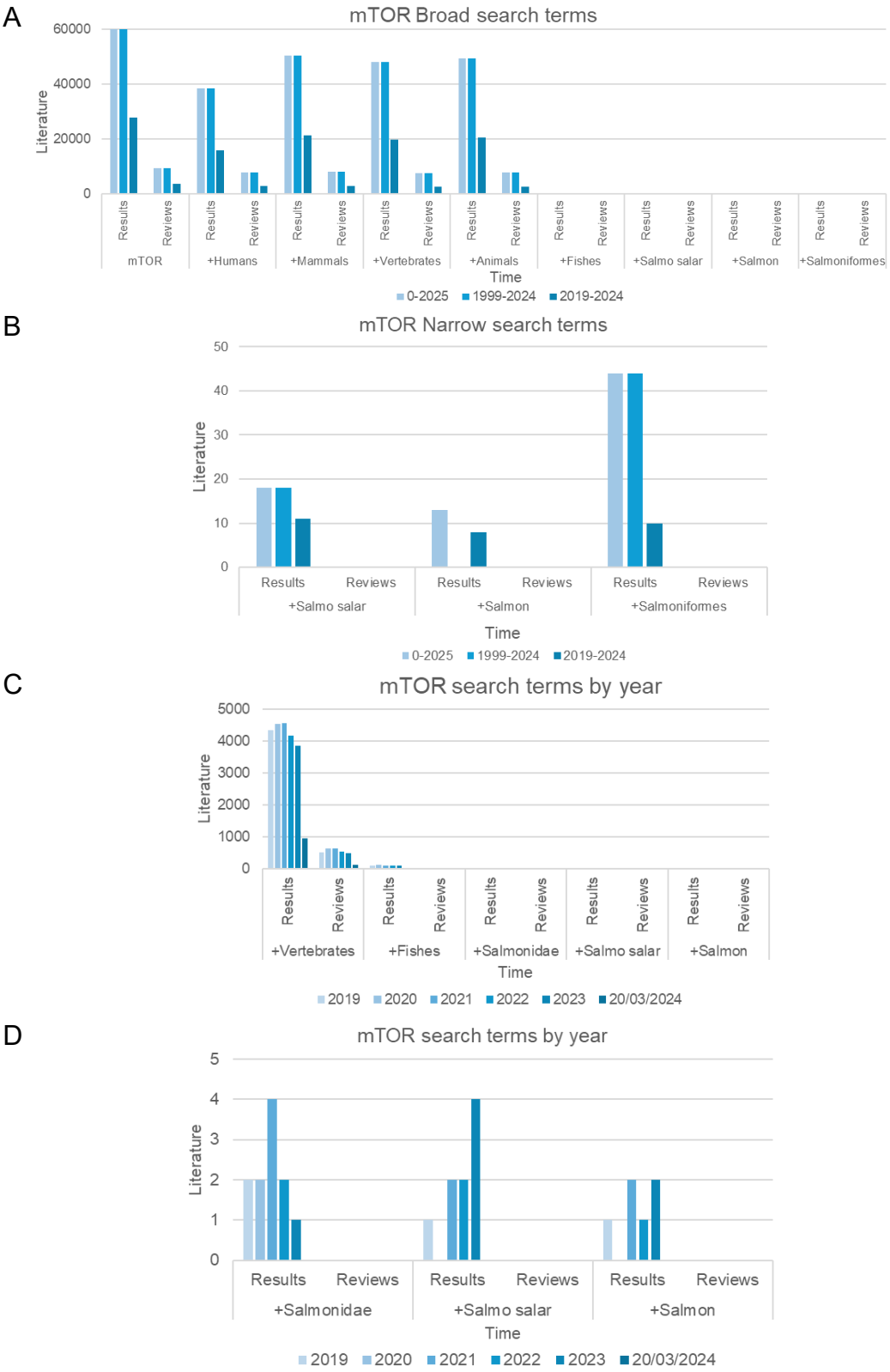


Figure 4.2 PubMed Advanced Search Builder results on mTOR literature A) mTOR broad range by period B) mTOR narrow range by period C) mTOR vertebrates by year D) mTOR salmonids by year. Period ranges were 0 to 2025, 1999 to 2024 and 2019 to 2024.

Results of each search were then categorised into 9 different groups: All time, 1999-2024, 2019-2024, 2019, 2020, 2021, 2022, 2023 and 2024 (Figure 4.2 A-D). This process was repeated for review articles. Figures were additionally included to display the lowest search terms in Figure 4.2 B-D.

4.2.3 Ethics

The following experiment was approved by the University of Stirling Animal Welfare and Ethical Review Body (reference AWERB-18/19–008) in accordance with the UK Home Office under the Animals Scientific Procedures Act 2013.

4.2.4 Experimental design

Post-smolt mixed sex Atlantic salmon (138.8 ± 0.65 g/fish; mean ± SD) tissue samples were collected from a 4-month seawater feeding trial studying the effects of hypoxia. The diet was formulated based on Atlantic salmon industry specifications to be isoenergetic and isoproteic, with 460 g/kg of protein, 240 g/kg of lipid (Table 4.3). The 4mm extruded feed was manufactured by SPAROS I&D (Olhão, Portugal) and stored at 4 °C.

The control diet (D1) was fed to the 2 treatments twice a day for 3 hr by an Arvotec automated feeding system (Arvo-tec Oy, Arvo-Tec T Drum 2000 Feeder, Huutokoski, Finland). To ensure satiation, fed was fed at an elevated recommended ration, with uneaten feed collected daily to estimate daily intake. Oxygenation levels were maintained by adjusting flow to the tanks (D1H >5 L/min, D1L <2 L/min) with D1L at 70% and D1H at 90% saturation levels. Water temperature averaged 10.7 ±2.0 ◦C. Oxygen levels and temperature were monitored using OxyGuard probe sensors (OxyGuard International A/S, Farum, Denmark) with oxygenation levels over the study period at 8.1 ±0.6 mg/L (89.6 ±2.7%) for normoxic and 6.8 ±0.5 mg/L (75.4 ±3.4%) for the hypoxic treatment. Although 70% saturation is sub-optimal for the purpose of this chapter it shall be called hypoxic (D1L) and 90% saturation normoxic (D1H).

At the end of the study fish were weighed, euthanised with MS-222 and cervical dislocation (Table 4.4). Liver, heart and brain tissues were collected from 2 fish/

tank (*n*=6/ tissue/ treatment), with each sample flash frozen on dry ice and stored at −80 °C for further analysis.

4.2.4.1 RNA extraction, sample preparation and RNA-sequencing

Brain, liver, and heart tissue samples were collected at the end of the 4-month trial, with each treatment having a total of 6 individual fish (*n*=2/ tank, totalling *n*=6/ treatment).

Total RNA was extracted in the university of Stirling's' Molecular laboratory (Stirling, Scotland) by Dr. Ahmed Elsheshtawy Ahmed. Briefly, 100 mg of tissue was homogenised, and total RNA was extracted using TRI Reagent (Merck KGaA, TRI Reagent® T9424, Darmstadt, Germany) according to the manufacturer's protocol.

Table 4.3 Diet formulation and composition used for both treatments.

Formulation:	D1
Fishmeal LT70	18.0%
Soy protein concentrate	16.0%
Wheat gluten	11.8%
Corn gluten	6.0%
Wheat meal	14.5%
Soy protein isolate	6.0%
Fish oil (Anchoveta)	1.6%
Rapeseed oil	3.0%
Linseed oil	5.0%
Olive oil	11.7%
Rape lecithin	1.0%
Vitamin and Mineral Premix (DSM OVN™)	0.5%
Choline chloride	0.1%
Natural antioxidant (Verdilox)	0.1%
Monocalcium phosphate	3.0%
Astaxanthin (Carophyll Pink 10%)	0.1%
L-Histidine	0.8%
L-Lysine	0.4%
L-Taurine	0.3%
DL-Methionine	0.1%
Yttrium oxide	0.1%
Composition (g/kg)	
Dry matter	954
Crude Protein	459
Lipid	243
Carbohydrates	180
Starch	92
Ash	72
Energy (MJ/kg)	23.3

All ingredients provided by SPAROS Lda from commercial suppliers.

Table 4.4 Performance after 4 months fed to satiation with oxygenation of D1L 70% and D1H 90%.

Performance	Diet	
	D1L	D1H
Initial (g/fish)	138.4	139.4
Final (g/fish)	594.9	686.4
Gain (g/fish)	456.5	547.0
Intake (g/fish)	404.8	476.2
FCR (feed/gain)	0.89	0.87
Survival (%)	100	100

Following extraction, RNA was eluted in 100 µL of nuclease-free DEPC-treated water (Thermo Fisher Scientific, diethylpyrocarbonate (DEPC) nuclease-free water R0601, Loughborough, UK) and RNA quality and quantity were assessed using a Nanodrop ND-1000 Spectrophotometer (Thermo Fisher Scientific, Nanodrop ND-1000 Spectrophotometer, Loughborough, UK).

RNA integrity was further evaluated by electrophoresis on a 1.5% (%v/v) agarose gel (Merck KGaA (Sigma-Aldrich), Agarose, Darmstadt, Germany) containing 0.1 µg/ mL ethidium bromide (Merck KGaA (Sigma-Aldrich), ethidium bromide E7637, Darmstadt, Germany) in Tris-acetate-EDTA (TAE) buffer (Merck KGaA (Sigma-Aldrich), Tris Acetate-EDTA (TAE) buffer T9650, Darmstadt, Germany).

RNA samples with a RIN (RNA Integrity Number) greater than or equal to 8.0 (RIN=>8.0), and RNA quality confirmed were selected for cDNA library construction by Dr. Benjamin Clokie using the Illumina Stranded Total RNA prep with Ribo-Zero library preparation kit (Illumina Inc., Illumina Stranded Total RNA prep with Ribo-Zero plus, San Diego, USA). The kit contained a ribodepletion step, which removed abundant rRNA molecules, with the intention of increasing abundance of RNA not purified by polyA+ selection such as mRNA transcripts. PolyA+ is primarily focused on protein-coding (PC) genes whereas ribodepletion captures a broader range of RNA species (Chen et al., 2020). Ribodepletion was used instead of polyA+ as the benefits included a more comprehensive transcriptomic landscape which included non-polyadenylated transcripts (ribosomal RNAs (rRNAs), enhancer RNAs, long non-coding RNAs (lncRNAs), non-canonical mRNAs), noncoding RNAs (tRNAs, siRNAs, snRNAs, microRNAs) (Kim et al., 2019). When using total RNA for sequencing, approximately 90% of

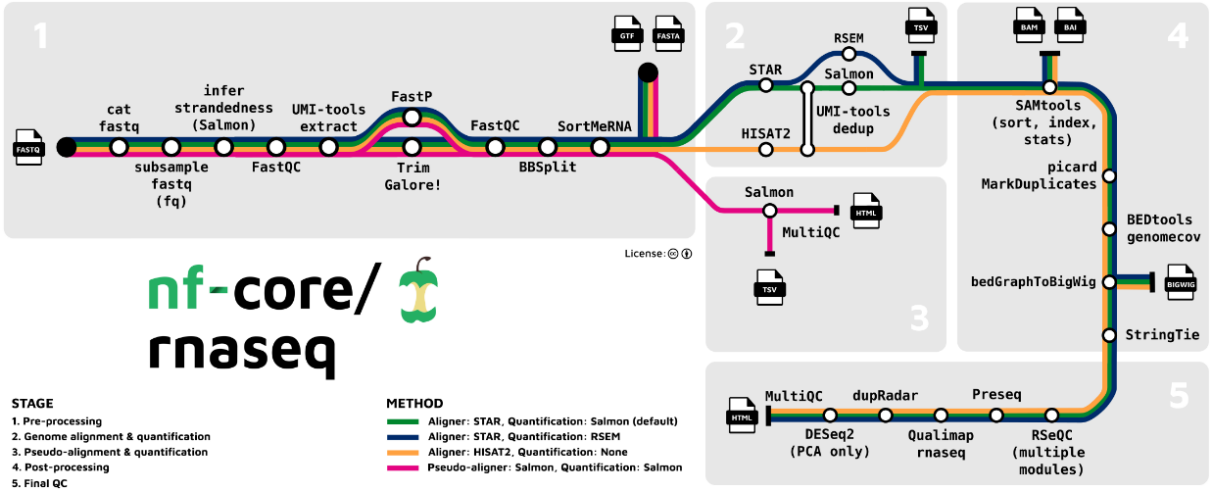


Figure 4.3 The nf-core/rnaseq pipeline used to process RNASeq data 1) Pre-processing 2) Genome alignment and quantification 3) Pseudo-alignment and quantification 4) Post-processing 5) Final QC. Green= Aligner: STAR, Quantification: Salmon (default), Dark blue= Aligner: STAR, Quantification: RSEM, Yellow= Aligner: HISAT2, Quantification: None, Red= Pseudo-aligner: Salmon, Quantification: Salmon. RSEM- quantification of gene and isoform expression, HISAT2- fast and sensitive alignment tool for mapping against a genome. nf-core/rnaseq (V.1.2.0).

reads may be rRNA whereas by using a ribodepletion step assuming a 97-99% rRNA removal, approximately 80-90% of reads would be of the transcriptome. Sequencing was performed on a Novaseq6000 (Illumina Inc., Novaseq6000, San Diego, USA) by the Earlham Institute (Norwich, UK) using a single lane on an SP4 v1.5 flow cell with 150 PE, with a target of 50 x10^6 reads/ sample.

4.2.5 Data analysis

4.2.5.1 Pipelines

The data returned from the sequencer was processed firstly though the core/RNAseq (v.3.10.1) pipeline in order to perform QC and alignment. The raw gene count data from this was then processed through the nf-core/differentialabundance (v.1.2.0) pipeline. The nf-core/rnaseq bioinformatics pipeline uses Nextflow, a task manager tool allowing tasks to be run across a multitude of computational infrastructure.

The RNAseq pipeline has been developed using current best practices for analysis of this data type. Briefly, raw RNASeq data FASTQ files were added to the pipeline (Figure 4.3), which performed quality control (QC), trimming and

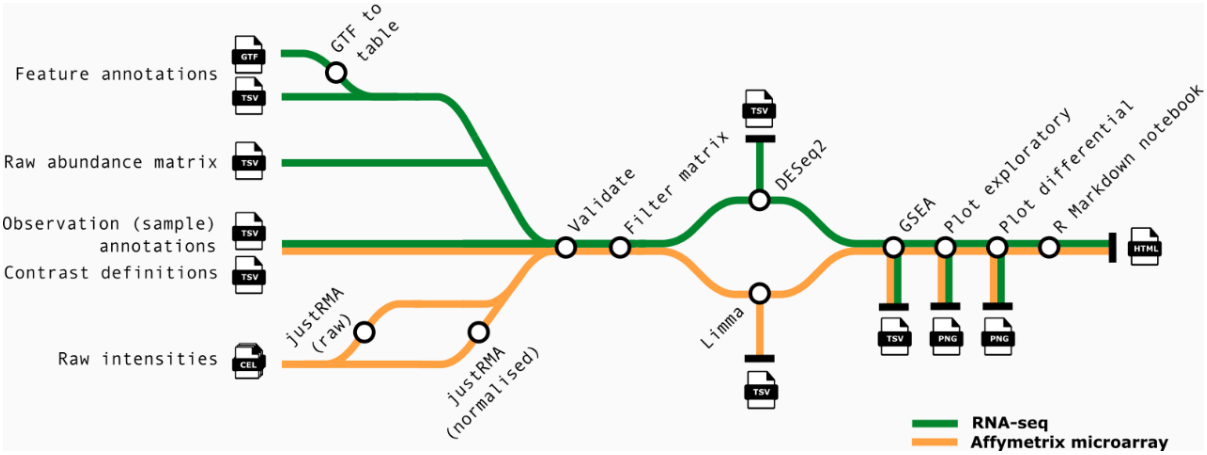


Figure 4.4 The nf-core/differentialabundance pipeline (v.1.2.0). The RNA-seq data produced in the nf-core/rnaseq pipeline

pseudo alignment, resulting in a gene expression matrix and a QC report. The aligner used was STAR (v2.7.9.a) (Spliced Transcripts Alignment to a Reference) and the quantification of transcript expression was performed using Salmon (v1.9.0.). The reference genome used was Salmo_salar. Ssal_v3.1 and the reference transcriptome Salmo_salar. Ssal_v3.1.109. The nf-core/differentialabundance pipeline (v.1.2.0) used the post-alignment expression data supplied by Salmon from the nf-core/rnaseq pipeline (Figure 4.4).

Raw count data was analysed in DESeq2. The default settings automatically fitted generalised linear models (GLMs) with negative binomial link function. The matrix consisting of raw counts of sequencing reads/fragments were additionally transformed to stabilise the variance across the mean. Count data was transformed into normalised, or variance stabilised in preparation for downstream analyses. Briefly, normalisation used the median of ratios method performed automatically in DESeq2, it calculated the geometric mean for each gene across the samples, divided by the counts for each gene in each sample by that mean. Variance stabilising transformations (VST) normalised data by the division of size factors (dispersion) corrected for library size and configuration, essentially distribution dependent on mean and variance. Further downstream analyses used ShinyNGS, a Shiny-based data mining app. ShinyNGS focused on the post-analysis exploration but allowed for adjustment of certain parameters, creation of plots such as heatmaps and volcano plots. Additionally, it was used for DEG identification as well as FC identification between treatments.

4.2.5.2 ShinyNGS

ShinyNGS, an R package, was used as a data mining online tool for downstream analysis of the RNA-seq data. ShinyNGS provided the tools for exploratory analysis such as heatmaps of the top 50 rows by variance for each tissue between the hypoxia and normoxia groups (D1L and D1H).

Heatmaps, displaying the intensity of a response between treatments, were additionally examined for visible clusters. Once identified, these were then further analysed to examine pathway level effects and potential biological responses.

Further identification of DEGs (differentially expressed genes) (between treatments and within tissues), were displayed on volcano plots, using variance stabilised data (VST). Parameters were set as p=<0.05 and q=<0.1 for both log2FC>2 and log2FC<-2. Additionally, to the DEGs identified and visualised in the volcano plots, the same parameters were used on normalised data, providing a larger data set for each tissue, from herein known as fold change data (FC). In addition to the initial FC, a further exploratory examination of mTOR mRNA transcripts (normalised data) between the ranges of 1 to 1.99 FC and -1 to -1.99 FC was conducted within each tissue.

4.2.5.3 Downstream analysis

All data sets recovered from ShinyNGS, heatmaps clusters, DEGs, FC and mTOR 1FC were further identified and analysed primarily using DAVID, with identification and classification using the web tools discussed below.

Ensembl IDs were submitted to DAVID gene enrichment and functional annotation analysis, which produced multiple statistical outputs after initially converting the Ensemble IDs input list to Entrez IDs. Fisher's Exact test was used to determine the *p*-value of gene enrichment terms, with p=< 0.05 suggesting an enriched association. Adjusted *p*-values were obtained using multiple testing; Benjamini (adjusted *p*-values (Benjamini & Hochberg, 1995)) and FDR (adjusted *p*-values for control of the false discovery rate (Huang et al., 2009, 2009). DAVID GO term associations used were direct biological process (GO:BP_D), direct molecular function (GO:MF_D), all biological process (GO:BP_A), all molecular function (GO:MF_A), and KEGG pathways. The GO_D terms were associated to

the GO terms from the original source (NCBI and UniProt). The GO_A used an expanded association to all ancestor terms (parents, grandparents, *etc*.). Both terms were used as GO_D terms were more specific while the GO_A results had specific and broad terms, allowing for a higher-level perspective.

DAVID parameters were set as EASE score p=<0.06, Bonferroni, Benjamini and FDR p=<0.05. Settings included a minimum of >=2 genes associated at p=<0.05. GO terms used were GO: _D = GO_DIRECT, GO: _A = GO_ALL.

DAVID was used as the primary tool for all GSEA and identification with additional assistance with pathway associations, identification and classifications from the publicly available web tools: ShinyGO (v0.80), DAVID (v. v2023q4), KEGG (v.112.0) and g:Profiler (v. e111_eg58_p18_f463989d) (Ge et al., 2020; Kanehisa et al., 2021; Kolberg et al., 2023; Sherman et al., 2022).

The identification of mRNA transcript IDs was low and additional transcript identification was required using Ensembl (v.112) and NCBI (Harrison et al., 2024; Sayers et al., 2022). In ShinyGO, mRNA transcript data sets were compared with the complete Atlantic salmon reference genome (Atlantic salmon genes Ssal_v3.1 (Ensembl)) for gene classification and information. All the web-based tools used various statistical methods in their analyses, or even the same statistical tests, with all yielding differing results. Therefore, it was decided to utilise DAVID for all GSEA.

ShinyGO ID and pathway mapping used Ensembl gene IDs or STRING protein IDs. g:Profiler enrichment analysis tool, g:GOSt, used multiple testing correction by default, with the choice of either their own algorithm (g:SCS), Bonferroni correction (BC), or Benjamini-Hochberg FDR (False Discovery Rate). The Benjamini-Hochberg method was used to calculate the False Discovery Rate (FDR). The FDR q-values adjust the p-values (aka adjusted p-values, adjP) for multiple testing to control error. The Enrichment FDR p-values indicated the significance of enrichment, with lower p-values suggesting less likelihood of a result by chance. The Fold Enrichment, used as a measurement of magnitude of enrichment with higher values indicating stronger enrichment, was defined as the ratio of genes (%) in data set to the corresponding background genes (%).

Table 4.5 mTOR MeSh results by year from 2019 to 2024**.** Search included "TOR Serine-Threonine Kinases"[Mesh] and "Salmonidae"[Mesh], or "*Salmo salar*"[Mesh] or "Salmon"[Mesh]. Comments listed the identified discrepancies within the search, which reduced the overall counts initially displayed within Figure 4.2 D. Highlighted cells indicate search duplications.

	PMID	Model	Misidentified terms	Comments
Salmonidae				
2019	31704904	Arctic char (*S. alpinus*)		mTOR x27, salmonid x11, Atlantic salmon x1
2019	30608904	Rainbow trout (*O. mykiss*)	No salmo, Coho salmon x2	mTOR x18
2020	32707879	Fish		mTOR x29, Salmonidae x1
2020	32092595	Rainbow trout	Chinook salmon x1	mTOR x8, salmonids x6,
2021	34863487	Rainbow trout		mTOR x6, salmonids x7
2021	34764336	Rainbow trout	No salmo	mTOR x1, TOR x30
2021	34114000	Rainbow trout	No salmo	mTOR x8
2022	35328356	Rainbow trout		mTOR x27, salmonids x1
2022	34933071	Atlantic salmon	*A. salmonicida* x34	mTOR x9, Atlantic salmon x34
2023	36704867	Rainbow trout		mTOR x3, salmonid x6, Atlantic salmon x4
2024	39611859	Rainbow trout	No salmo	mTOR x22
2024	38881412	Rainbow trout	No salmo, *Micropterus salmoides* x1	mTOR x11
Salmo salar				
2019	31704904	Arctic char		mTOR x27, salmonid x11, Atlantic salmon x1
2019	31687280	Human	NO salmon, Salmon module x37	mTOR x8
2020	31971825	Human	NO salmon, Durie-salmon [d-s] staging system	mTOR x4
2021	34681079	Atlantic salmon	*Lepeophtheirus salmonis*	mTOR x31, salmon x21, Atlantic salmon x16,
2022	35930149	Fish	no mtor or salmonids	Mahseer *Tor khudre*
2023	37533794	Coho Salmon (*O. kisutch*)	Coho salmon x37	mTOR x26, Atlantic salmon x4,
2023	37255176	Fish	no mtor or salmonids	*Tor putitora*
2023	37106872	Coho Salmon	Coho salmon x44	mTOR x19, Atlantic salmon x6,
2024	39555549	Coho Salmon	Coho Salmon x13	mTOR x14, Atlantic salmon x1
2024	39094498	Chicken	NO salmon, Salmon module x11	mTOR x2
2024	38481691	Human	NO salmon, Salmon calcitonin x2, hind cheek of salmon x2	mTOR x29
Salmon				
2019	31704904	Arctic char		mTOR x27, salmonid x11, Atlantic salmon x1
2019	31687280	Human	NO salmon, Salmon module x37	mTOR x8
2020	31971825	Human	NO salmon, Durie-salmon [d-s] staging system	mTOR x4
2021	34681079	Atlantic salmon	*L. salmonis*	mTOR x31, salmon x21, Atlantic salmon x16,
2023	37533794	Coho Salmon	Coho salmon x37	mTOR x26, Atlantic salmon x4,
2023	37106872	Coho Salmon	Coho salmon x44	mTOR x19, Atlantic salmon x6,
2024	39555549	Coho Salmon	Coho Salmon x13	mTOR x14, Atlantic salmon x1
2024	39094498	Chicken	NO salmon, Salmon module x11	mTOR x2
2024	38481691	Human	NO salmon, Salmon calcitonin x2, hind cheek of salmon x2	mTOR x29

4.3 Results and discussion

4.3.1 PubMed MeSH term searches

Within the mTOR PubMed MeSH search terms represented in Figure 4.2 D, an in-depth analysis of the content was conducted in relation to Atlantic salmon (Table 4.5). In the "TOR Serine-Threonine Kinases" [Mesh] AND "Salmonidae" [Mesh] term search, a total of 12 papers were returned, of which 9 studies were primarily conducted on rainbow trout, with 5 of the 9 not even mentioning 'salmo'. Only 1 of the 12 papers was focused on Atlantic salmon, this was a challenge trial using *Aeromonas salmonicida* but it only had 9 mentions of mTOR. In the 11 "*Salmo salar*"[Mesh] and 9 "Salmon"[Mesh] term searches, the resulting searches were identical apart from 2 papers in "*Salmo salar*"[Mesh]. These 2 papers did not include mTOR nor 'salmo' but did include Mahseer *Tor khudre* and *Tor putitora*. In addition, 4 papers were misidentified and included search terms such as Salmon module, Durie-salmon [d-s] staging system, Salmon calcitonin, and hind cheek of salmon including them into the MeSH terms. Overall, only 2 studies focused on Atlantic salmon, titled 'Immunostimulant Bathing Influences the Expression of Immune- and Metabolic-Related Genes in Atlantic Salmon Alevins' (PMID:34681079) and 'Genome-wide integrated analysis reveals functions of lncRNA-miRNA-mRNA interactions in Atlantic salmon challenged by *Aeromonas salmonicida'* (PMID:34933071). Although both studies mentioned mTOR (31, 9), it was not the primary focus.

Table 4.6 Summary of the RNA-seq data. Values represent the means of 3 tanks (*n*=6) /tissue /treatment.

	Tissue	P.E. Reads (10^6)	Total Seq. (10^6)	Trimmed (%BP)	Aligned reads (10^6)	Aligned (%)	Read Length (bp)
D1L	Brain	33±3	55±3	8±0%	20±2	60±0%	138±1
	Liver	38±6	68±11	10±0%	20±4	52±0%	135±1
	Heart	24±4	38±5	9±0%	13±2	56±0%	135±1
D1H	Brain	35±8	59±12	7±0%	20±5	58±0%	138±2
	Liver	35±3	64±6	10±0%	19±2	54±0%	135±1
	Heart	21±5	34±8	9±0%	12±3	56±0%	135±1

P.E reads= paired-end reads, Total Seq.= total sequences

4.3.2 Descriptive stats

The nf-core/rnaseq pipeline was used for the pre-processing of the FastQ files. The reads were aligned using STAR and HISAT2, quantified using Salmon, and RSEM. DESeq2 was used in the identification of differentially expressed genes (DEGs) through the nf-core/differentialabundance pipeline. The total reads per tissue were 1,173,848,315 (brain), 1,273,626,967 (liver) and 823,478,721 (heart). The total number of raw sequenced reads generated (total sequences 10^6) suggested a sequencing depth from 34 to 68 x10^6, with a lower number of sequences in heart tissue (34 to 38 x10^6) (Table 4.6).

The percentage of bases (BP%) that were trimmed from the raw reads during quality control ranged from 7 to 10%. The number of reads that successfully mapped (aligned) to Atlantic salmon ranged from 12 to 20 x10^6, with 52 to 60% of the total reads aligned to the reference genome Salmo_salar.Ssal_v3.1 and the reference transcriptome Salmo_salar.Ssal_v3.1.109 (S 4.1).

4.3.3 Magnitude and intensity transcriptome landscape comparisons

4.3.3.1 Differential expression: Magnitude

ShinyNGS was used to identify the DEGs under hypoxic conditions (D1L) compared to normoxic conditions (D1H). Parameters were set as >2 log2FC, and log2FC<-2, with p=<0.05 and q=<0.05. A total of 372 DEGs (199↑, 173↓) were identified across the tissues. The total liver DEG contribution was 127 (53↓, 74↑), brain 131 (49↓, 82↑) and heart 114 (71↓, 43↑). Amongst the upregulated mRNA transcripts, brain tissue had the largest contribution (82↑) whereas heart had the highest contribution within the downregulated DEGs (71↓) (Figure 4.6).

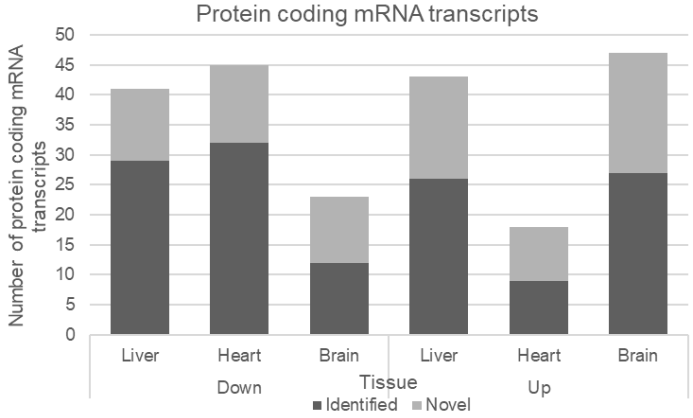


Figure 4.5 Identified and novel protein coding (PC) mRNA transcripts (VST) within each tissue.

Classification of DEGs were identified using DESeq2, ShinyNGS, ShinyGO, g:Profiler, DAVID and NCBI and highlighted differences across tissues for protein coding (PC) and non-coding RNA (ncRNA) mRNA transcripts. The largest overall contribution was from PC mRNA transcripts (217/372) followed by LncRNA (88/372). A similar trend was seen in both total up- and downregulated groups (108/199↑, 51/199↑, 109/173↓, 37/173↓) although LncRNA classification was higher in the upregulated group (51↑, 37↓). PC mRNA transcripts were similar in number for up- and downregulated groups (108/199↑ and 109/173↓) but the contribution (%) was higher for downregulated PC mRNA transcripts (63%↓ and 54%↑) (Figure 4.5).

Within each tissue, PC and LncRNA were the highest contributing classifications in brain and heart, apart from liver which had PC and rRNA. Liver classifications had similar PC contribution numbers for up- and downregulated liver mRNA transcripts (43↑, 41↓) but contribution (%) was higher for downregulated liver PC mRNA transcripts (77%↓, 58%↑). Upregulated liver rRNA had a higher contribution number than LncRNA (14↑, 10↑ or 19%, 14%). %↑) (Figure 4.7).

RNA polymerases (RNAPs) are enzyme complexes that transcribe DNA into various RNAs and are found in the nucleolus of eukaryotes. RNA polymerase I (Pol I) enzymic complex solely transcribes rRNA (28S, 18S, and 5.8S), Pol II mRNA (PC, some ncRNA such as miRNAs, snoRNAs) and Pol III transcribes the smallest of the RNAs (tRNA, 5s rRNA and some snRNAs) (Raha et al., 2010).

Although RNAPs are present in all cells, their activity may vary between tissues depending on cellular demands for specific RNAs. Pol I is more active in tissues with high protein synthesis rates, such as liver tissue, and this may explain the elevated levels of rRNA in the results. Pol I and Pol II are high in liver due to its involvement in metabolism (detoxification) and protein synthesis. The liver requires large quantities of ribosomes for protein synthesis, with ribosomal biogenesis energetically demanding, and requires all 3 RNAPs (Ni & Buszczak, 2023).

Pol II, which synthesises PC genes and most snRNAs (apart from U6 which is transcribed by Pol III), is active in all tissues. Tissues such as brain, a highly

metabolically active tissue, where regulation of neuron function and synaptic activity is high, may have elevated levels of all 3 RNAPs. Whereas heart tissue, requiring energy and protein synthesis, may have elevated levels of Pol I and Pol II.

In brain tissue, PC and LncRNA classifications were higher amongst upregulated mRNA transcripts compared to downregulated mRNA transcripts (47↑, 23↓ and 26↑, 11↓). The opposite trend was seen in heart tissue, with downregulated protein coding and LncRNA mRNA transcripts higher than upregulated (45↓, 18↑ and 21↓, 15↑). ncRNA profiling has identified roles and functions in mammalian models but remain largely under explored if fish (Xia et al., 2022). ncRNA have been shown to interact with RNA, DNA and proteins in gene regulation (Jacovetti et al., 2021).

Within the PC mRNA transcripts, 40% of upregulated liver PC were classed as novel (17/43↑) and 29% of downregulated PC mRNA transcripts (12/41↓). Similarly, 50% of heart and 43% of brain upregulated PC classifications were identified as novel (9/18↑, 20/47↑) whereas 29% of downregulated heart and 48% of brain were novel (13/45↓, 11/23↓).

Heart tissue transcript classification diversity included IgD gene (2↑, 2↓), pseudogene (1↑, 1↓) and processed pseudogene (1↑). Liver mRNA transcripts classifications included IgV gene (Variable chain immunoglobulin) (1↓), pseudogene (2↑,1↓) and processed pseudogene (1↑). Brain had the highest transcript diversity between the tissues, which included IgD gene (Diversity chain immunoglobulin) (2↑, 2↓), IgV gene (1↓), processed pseudogene (1↓), pseudogene (2↑,1↓) and miscRNA (2↑, 2↓) (Figure 4.6).

miscRNA (ncRNA that cannot be classified), was classified by ShinyGO as Metazoan signal recognition particle RNA (Metazoa_SRP). It is thought to be crucial for protein localisation and function, and was only found in brain, in both up- and downregulated mRNA transcripts (2↑, 2↓).

Non-coding small nucleolar RNAs (snoRNAs) are involved in rRNA modification and widely present in cell nucleoli. They are involved in the processing of

ribosomal RNA (rRNA) by introducing 2′-O-methylation and pseudouridylation modifications to rRNA molecules (Huang et al., 2022). Originally it was thought that their role was limited to rRNA modification, but recent studies has expanded their repertoire to including other RNA such as snRNAs and mRNAs (Mattick & Makunin, 2006).

Across the tissues, downregulated snoRNA were slightly higher than upregulated (4↑, 3↓), with heart the highest upregulated (2↑) and liver the highest in downregulated (2↓). Shen et al. (2024) suggested that snoRNAs are involved in regulation of oxidative stress response, DNA damage repair, regulation of cell cycle and cell death. The authors did acknowledge that there is no definitive theory to explain this. The current study did identify the upregulated hypoxia group as having the highest snoRNA and this may have been due to the emerging roles of snoRNA in DNA damage response.

snRNAs (spliceosomal RNAs) or processing RNAs, are involved in splicing, with the spliceosome made up of 5 nuclear ribonucleoprotein (snRNPs) U1, U2, U4, U5, and U6. Recently studies have shown that small Cajal body-specific RNAs (scaRNAs) modify snRNAs involved in spliceosome assembly and localisation (Bohnsack & Sloan, 2018). In the current study, up- and downregulated snRNAs across tissues were similar (7↓, 7↑) with liver having the highest upregulated number (4↑) and brain in the downregulated tissues (5↓).

Diversity chain immunoglobulins (IgD) were identified in heart and brain tissues, (heart 2↑ 2↓, brain 2↑ 2↓) and variable chain immunoglobulins (IgV) were found in liver (1↓) and brain (1↓). Immunoglobulins (Ig) are humoral immune responses (the body's defence against pathogens that are free in the blood, such as bacteria, parasites, and protozoa) key to the adaptive immune response. Mammalian immunoglobulins (Ig) are more diverse than in teleost fish, with teleosts having identified 3 classes: IgM, IgD and IgT/Z compared to 5 in mammals. Igs are either membrane-bound as a cell’s antigen receptor or secreted as an effect of adaptive immunity (Yu et al., 2020). In mammals, IgD and IgM are naïve B cell surface antigen receptors and each class of Ig anatomically and functionally distinctive, whilst in teleosts IgD has only been

identified in a transmembrane form (Hikima et al., 2011). The only exception to this so far has been in channel catfish and fugu, which displayed expression in membrane and secretory matrixes.

B cells in fish are found in the kidney, spleen, gut and blood and can be identified by their Ig expression, whilst Ig can be found in skin, gut, gill mucus, bile, as well as plasma (Mashoof & Criscitiello, 2016). Fillatreau et al. (2013), suggested that a low IgD response to Viral Haemorrhagic Septicaemia Virus (VHSV) infection in rainbow trout may have been due to a down regulation in activated B cells, concluding that B cell biology remains somewhat unknown in fish. Hikima et al. (2011) suggested that the function of IgD in teleosts is still largely unknown.

MRNA transcripts identified within multiple tissues were located in downregulated tissues, NOTUM1A (notum, palmitoleoyl-protein carboxylesterase a) was found in liver and heart, U5 spliceosomal RNA (ENSSSAG00000085703) in heart and brain, and U1 spliceosomal RNA (ENSSSAG00000092962) in liver and brain. In mammalian models, NOTUM1A is said to be a negative regulator of the WNT signalling pathway via post-translational modifications (Bayle et al., 2021). This may suggest that across all tissues, WNT signalling is being regulated by NOTUM1A.

4.3.3.1.1 Gene set enrichment analysis (GSEA)

Gene ontology analysis was conducted on all tissues up- and downregulated to identify GO term associations and pathways. Primary focus was to identify mTOR associated mRNA transcripts. Within the downregulated liver DEGs, E3 ubiquitin-protein ligase RNF152-like (106578589) was associated with the '*mTOR signaling pathway*' (sasa04150) (Figure 4.8). No other mTOR associated mRNA transcripts were identified within the 3 tissues (Electronic file: Tissue DEGs).

4.3.3.1.1.1 DEGs all tissues GSEA upregulated

Upregulated combined DEGs consisted of 199 mRNA transcripts, the largest contribution to the pool from brain (liver 74↑, brain 82↑, heart 43↑) (Figure 4.6 D). There were no duplicated/ common transcripts. DAVID successfully mapped 77 to Entrez gene IDs which were used in the analyses.

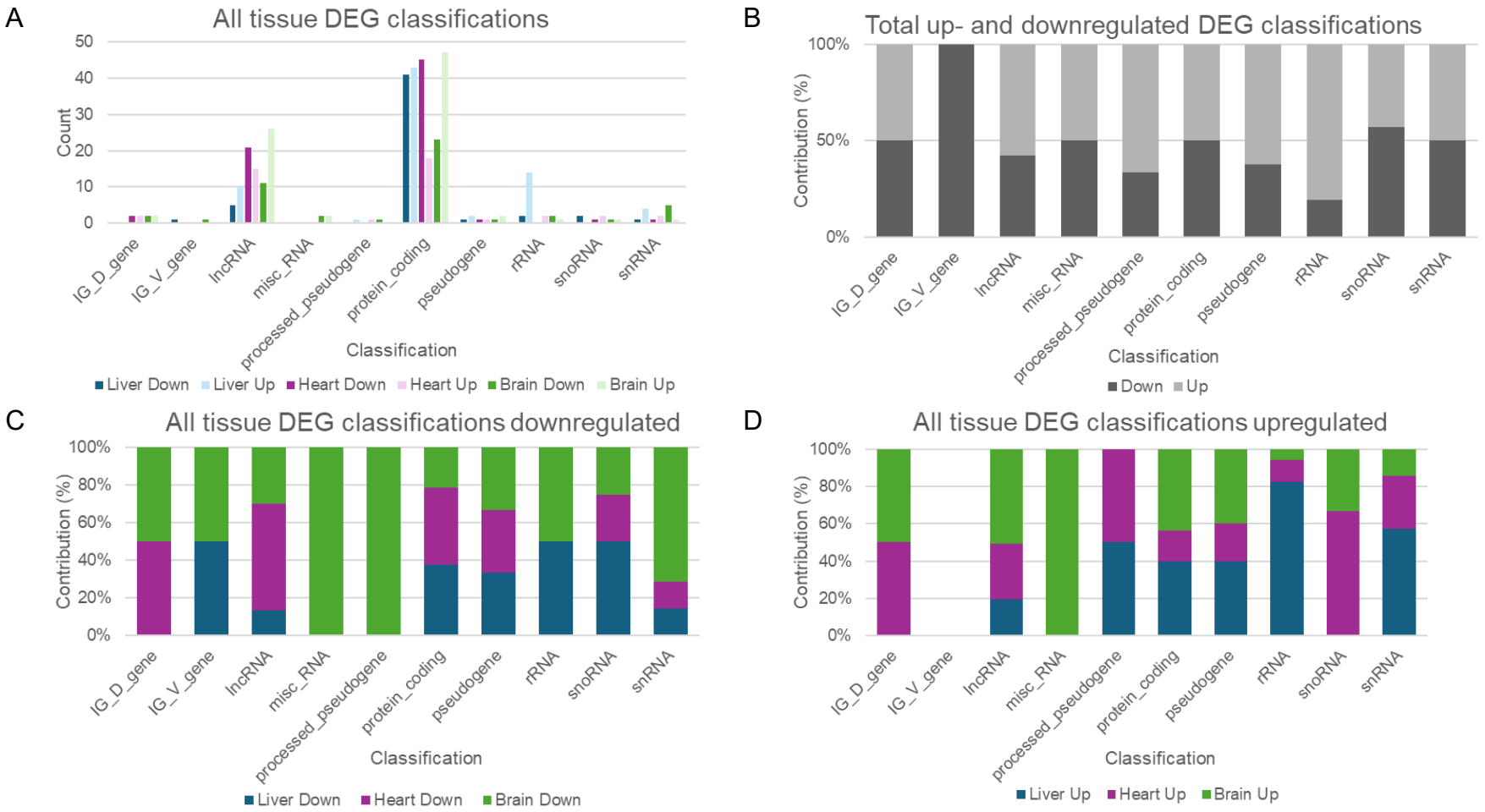


Figure 4.6 Classification of DEGs A) count comparison between up- and downregulated mRNA transcripts between liver, heart and brain tissues B) Contribution (%) between up- and downregulated transcript classifications C) Classification contribution (%) between individual tissues downregulated D). Classification contribution (%) between individual tissues upregulated. Classifications were identified using ShinyGO (v.0.80). Parameters to identify DEGs were set as log2FC >2, p-value<0.05 and q-value<0.05 for upregulated and log2FC<-2, p-value <0.05 and q-value <0.05 for downregulated DEGs.

Upregulated combined tissue mRNA transcripts identified GO:BP_D and GO:BP_A associations with '*anterior/posterior pattern specification*' (*p*=<0.05, *n*=5 GO:0009952). GO:BP terms were associated with homeobox proteins (100196597, 106579315, 100194490, 100196645, 100194467). GO:BP_A additionally associated the parent term '*regionalization*' (GO:0003002) with the above homeobox protein mRNA transcripts.

The biological processes associated with the upregulated DEGs were connected to pattern formation of cellular differentiation/ the perception of the environment. These are processes that involve cellular differentiation via the creation of defined regions through the subdivision of the anterior-posterior axis. Studies have suggested that hypoxia may influence the development of the body axis, which may impact the formation of organs and tissues (Li et al., 2024). In a study on tail regeneration of the western clawed frog (*Xenopus tropicalis)*, Patel et al. (2022) identified that HIF1A and WNT signalling are required for posterior specification/ differentiation, through posterior HOX genes.

GO:MF_D and GO:MF_A associations were all associated with '*transcription regulator activity*', suggesting that the upregulated mRNA transcripts were linked to transcription modulation, through non-enzymic activity with RNA polymerase II specificity. mRNA transcripts were additionally associated with binding to transcription regulatory regions possibly involved in initiation.

The term '*DNA-binding transcription factor activity*' was significantly associated with homeobox proteins, with the addition of motor neuron and pancreas homeobox protein 1-like, motor neuron and pancreas homeobox protein 1 and myelin transcription factor 1-like (123727885, 106578612, 106572224). Associated terms were '*DNA-binding transcription factor activity, RNA polymerase II-specific'*, and '*RNA polymerase II transcription regulatory region sequence-specific DNA binding*' (*p*=<0.05, *n*=14 GO:0000981, *n*=6 GO:0000977).

GO:MF_A associated the term '*sequence-specific double-stranded DNA binding'*, '*double-stranded DNA binding'* and '*DNA-binding transcription factor activity'* (*n*=15, GO:1990837, GO:0003690, GO:0003700) with the mRNA transcripts in

‘*DNA-binding transcription factor activity*’ with the inclusion of activating transcription factor 5a (ATF5A, 106602866) to the terms. No significant associated KEGG pathways were identified.

DAVID Gene Functional Classification tool was used to determine clusters with functional similarity by examining shared functional annotation terms. The DAVID enrichment score (ES) is the overall score for the enrichment group, determined by the DAVID EASE scores. The EASE score is a modified Fisher Exact P-value, although more conservative as it deducts 1 gene from the users’ pathway genes. Cluster 1 had the highest enrichment score ((ES) 5.01) of the 2 clusters and contained 12 mRNA transcripts consisting of 9 homeobox proteins, activating transcription factor 5a (ATF5A, 106602866), motor neuron and pancreas homeobox protein 1 (106578612) and myelin transcription factor 1-like (106572224). UniProt keywords (KW) suggested links to ‘*Transcription regulation’* (KW-0805, KW-0804).

Cluster 2 (ES 1.24) contained 6 mRNA transcripts functionally related to ‘*membrane*’ (GO:0016020) and consisted of sushi domain-containing protein 2 (106568204), transmembrane protein 130 (106609795), signalling lymphocytic activation molecule-like (106608914), retinol dehydrogenase 7-like (106566157), leptin a (LEPA) and CUB and sushi domain-containing protein 3-like (106570400). In addition to LEPA, pro-opiomelanocortin A2 (POMC*)* and solute carrier family 2, facilitated glucose transporter member 1-like were associated with the ‘*Adipocytokine signaling pathway*’ (sasa04920). POMC and LEPA*,* in addition to SMTLB (somatolactin beta), TSHBA (thyroid stimulating hormone subunit beta a) and P2Y purinoceptor 4-like were similarly associated with the ‘*Neuroactive ligand-receptor interaction’* (sasa04080) pathway.

Fish pituitary hormones (growth hormone (GH), prolactin*,* SMTLB) regulate the production and release of hormones, with prolactin having ties to osmoregulation, reproduction, immune responses, feeding and growth in fish (Zhu & Li, 2024). Somatolactin (SMTL) a fish specific hormone related to GH, exists in 2 forms, SMTLA (all fish) and SMTLB (freshwater species). It has been shown to play a role in plasma calcium and phosphate regulation, lipid metabolism, and possible

influencing reproductive processes such as gonadal development and spawning (Benedet et al., 2008). In a study examining SMTL and Corticotropin-releasing hormone (CRH) function in stress on grass carp pituitary cells, Du et al. (2023) indicated that SMTL may be involved in stress response through regulating energy metabolism.

Proopiomelanocortin A2 (POMC) produced by corticotropin-releasing hormone (CRH), has been shown in rodents to be affected by hypoxia. Kietzmann & Mäkelä (2021) suggested that POMC transcription was linked to glucose metabolism which was regulated by HIF-1α/ HIF-2α, with upstream mTOR and AMPK pathways regulating HIFs. Kietzmann & Mäkelä (2021) summarised in suggesting that levels of oxygen were important to POMC regulation and homeostasis. In teleosts, POMC is thought to be a species specific anorexigenic, with salmonids having conflicting data (Volkoff, 2016). Kalananthan et al. (2020) studying appetite control in Atlantic salmon, suggested that POMC mRNA levels were decreased after starvation but upregulated in short term feeding.

Leptin, an adipokine (cytokines and hormones from adipose tissue) and its cytokine receptor are said to be evolutionary conserved, regulating immune response at various life stages, nutritional status and energetic requirements (Londraville et al., 2014). In various fish studies leptin administered via IP or ICV has reduced feed intake, highlighting the role as an anorexigen. Additional qPCR studies on teleosts have reported increased mRNA abundance due to hypoxia, fasting and seasonal cycle.

In studies such as Fuentes et al. (2013) exploring the effects of nutritional status of fine flounder (*Paralichthys adspersus*) found that increased levels of circulating leptin during fasting lead to mTOR inactivation via AMPK in muscle tissue. The authors hypothesised that this may explain the effect of leptin on reduced growth rates in fish. Chu et al. (2010) explored the effects of hypoxia on zebrafish embryos and concluded that leptin was regulated by hypoxia possibly by HIF-1.

A small number of mRNA transcripts were individually linked to GO terms involving calcium ion transport these included voltage-dependent calcium channel gamma-3 subunit, GTP-binding protein RAD-like, short transient receptor potential channel 7 found in liver and calcium channel voltage-

dependent gamma subunit 7a (CACNG7A) in heart tissue (106602081, 106561976, 106568097, 106570002). Calcium ions are intracellular signalling molecules which in liver may regulate cellular processes such as glycolysis/gluconeogenesis, cellular regeneration and signalling pathways. In human heart tissue, CACNG7A may be involved in extracellular movement of calcium ions, signalling contraction. Myrka & Buck (2021) discussed how hypoxia may increase the release of calcium from inside the cell or increase the uptake depending on cell type.

In summary, upregulated mRNA transcripts showed strong associations with transcriptional regulation and developmental processes. GO terms related to '*anterior/posterior pattern specification*' (GO:0009952) were significantly enriched (p =<0.05), primarily due to the increased mRNA abundance of homeobox proteins (e.g., 100196597, 106579315, 100194490). Homeobox proteins play crucial roles in cellular differentiation and regionalisation during development (Pearson et al., 2005). The functionality of upregulated mRNA transcripts suggested involvement with regulation such as transcription regulation whereas mRNA transcripts linked to transport ('*localisation*' '*transmembrane transporter activity'*) were receptors (*e.g.* TRPC7A) involved in receptor-ligand interactions and hormones, a type of ligand, such as SMTLB.

Further analysis using the DAVID Gene Functional Classification tool identified two main clusters of functionally related transcripts. The first cluster (ES 5.01) comprised transcription factors such as activating transcription factor 5a (ATF5A, 106602866) and myelin transcription factor 1-like (106572224), suggesting a role in transcriptional regulation. The second cluster (ES 1.24) was enriched for membrane-associated proteins, including transmembrane proteins (106609795) and signalling molecules such as leptin (LEPA), implicating involvement in receptor-ligand interactions and metabolic adaptation (Ahima & Flier, 2000). The presence of calcium ion transport-related mRNA transcripts (CACNG7A, TRPC7A) suggests hypoxia-induced modulation of calcium signalling. Calcium ions regulate metabolic processes such as glycolysis, cellular regeneration, and muscle contraction (Myrka & Buck, 2021). The upregulation of CACNG7A in the heart tissue suggests its role in modulating cardiac contractions under hypoxia.

4.3.3.1.1.2 DEGs all tissues GSEA downregulated

Similarly to upregulated DEGs, 173↓ DEGS were subjected to GSEA utilising a variety of methods. The largest contribution to the pool was from heart (liver 53↓, brain 49↓, heart 71↓) (Figure 4.6 C). Of the 173↓, DAVID mapped 82 to entrez IDs for the GSEA analyses. Downregulated GO:BP_ D, GO:MF_D yielded no directly associated terms nor KEGG pathways (*p*=>0.05). There were 3 common/ duplicated transcripts between the tissues (173↓): ENSSSAG00000048313 (NOTUM1A, live and heart), ENSSSAG00000085703 (U5, heart and brain) and ENSSSAG00000092962 (U1, liver and brain).

The only associated terms amongst the downregulated DEGs were linked to cell communication, a biological process involved in interactions between a cell and the external environment (matrix, cells). The mRNA transcripts were associated with cell-cell signalling, more directly to synaptic signalling, suggesting cell-cell signalling within a synapse. Kleszka et al. (2020) stated that synaptic signalling/ transmission may be accountable for up to 50% of the brain's oxygen consumption, suggesting that it is highly oxygen dependent. The associations in the downregulated mRNA transcripts may imply an effect of hypoxia on brain signalling in the hypoxic group.

GO:BP_A significantly associated '*cell-cell signaling'* and '*synaptic signaling'* (*n*=8, GO:0007267, *n*=7 GO:0099536) with synaptosome associated protein 25a, glycine receptor subunit beta-like, neuronal acetylcholine receptor subunit alpha-2-like, beta-soluble NSF attachment protein-like, synaptotagmin-17 (SYT17*)*, synaptotagmin-1-like and ly6/PLAUR domain-containing protein 1 (106571603, 123733083, 106608318, 106599679, 106592101, 106584516, 106581664). Fibroblast growth factor-binding protein 2-like (106604540) was additionally associated with '*cell-cell signaling'*. A cluster of 9 mRNA transcripts with an enrichment score of 0.87 was identified using DAVID Gene Functional Classification tool. Significantly associated terms were UniProt key words *Membrane*', '*Transmembrane*' and GO:CC_D '*membrane*'(KW-0472, KW-0812, GO:0016020).

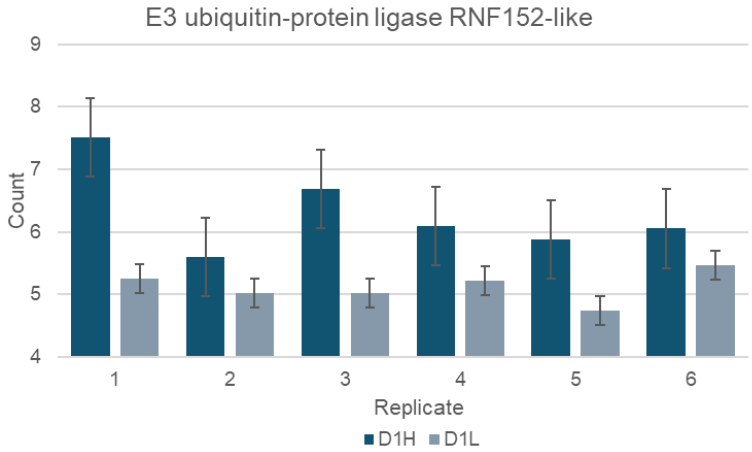


Figure 4.7 mTOR associated DEG E3 ubiquitin-protein ligase RNF152-like (106578589) transcript count (VST).

In summary, downregulated mRNA transcripts were predominantly associated with synaptic signalling and neurotransmission, indicated by enriched GO terms such as '*cell-cell signaling'* (GO:0007267) and '*synaptic signaling'* (GO:0099536). Key downregulated mRNA transcripts included synaptotagmin-17 (SYT17), neuronal acetylcholine receptor subunit alpha-2-like (CHRNA2B), and fibroblast growth factor-binding protein 2-like (106604540), suggesting reduced neurotransmission and synaptic activity under hypoxia. Downregulated mRNA transcripts were functionally grouped with *'transporter activity'* (*e.g.* SLC26A11, SLC4A10A, KCNG1, CHRNA2B) and '*localization*' (*e.g*. SYT17, SLC26A11, TMPRSS5, SLC4A10A, KCNG1, CHRNA2B, SYT8). Enrichment in transporter activity may indicate a reduction in transmembrane transport processes, which could contribute to cellular energy conservation under low-oxygen conditions. These functional processes are part of cellular homeostasis, such as enabling proteins or organelles to be transported or maintained.

4.3.3.1.1.3 Individual tissue DEGs

In liver, DAVID gene conversion tool successfully mapped 33/74 upregulated liver mRNA transcripts and 33/53 downregulated liver mRNA transcripts (Figure 4.8). No GO terms, KEGG pathways or gene functional classification associated results were identified in upregulated group. Downregulated liver DEGs identified E3 ubiquitin-protein ligase RNF152-like (106578589) as associated to the '*mTOR*

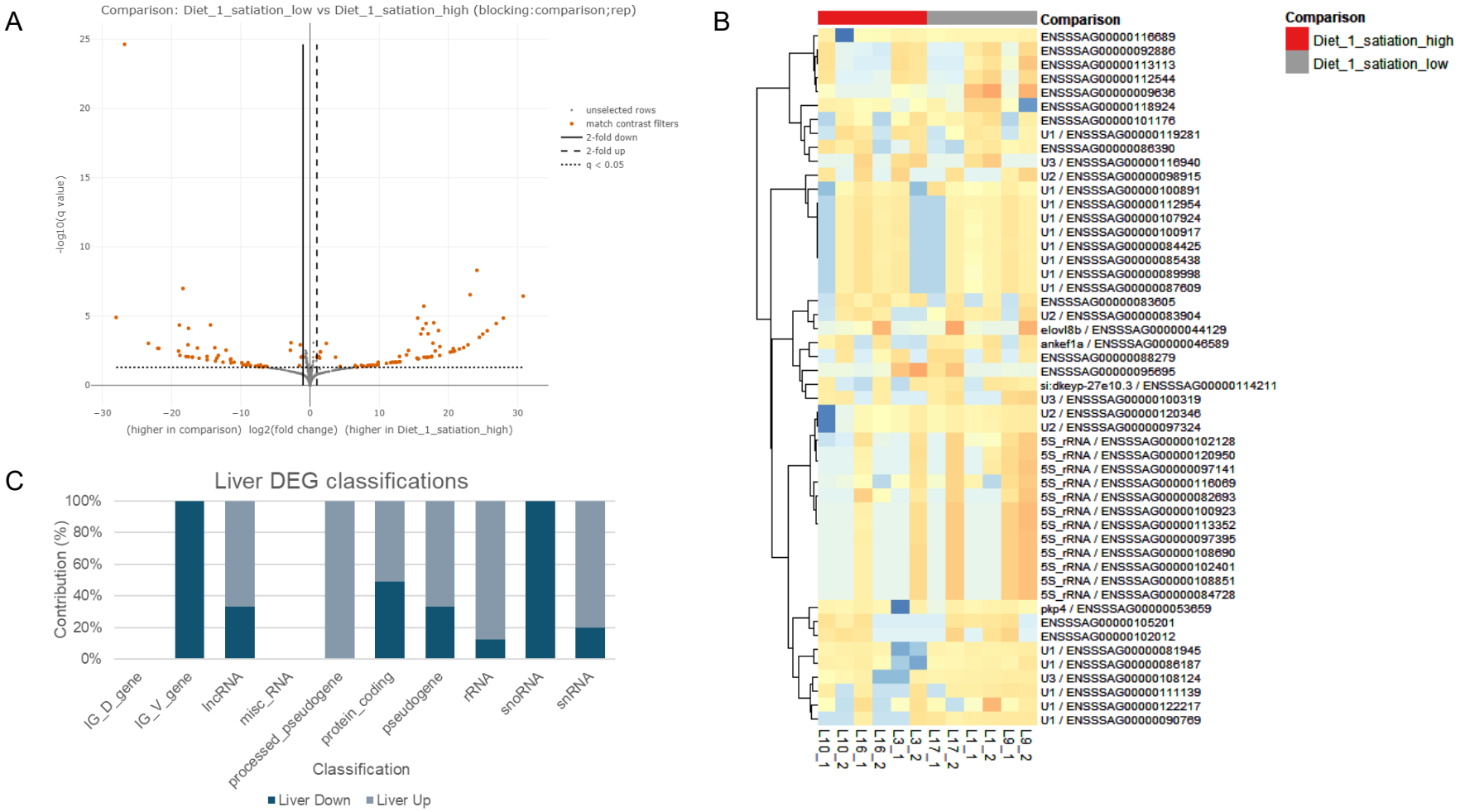


Figure 4.8 Liver tissue comparison between Diet 1 hypoxia (D1L) and D1 normoxia (D1H) treatments A.) volcano plot displaying DEGs with log2FC >2, p-value <0.05 and q-value <0.05 for upregulated and log2FC<-2, p-value <0.05 and q-value <0.05 for downregulated DEGs between the two treatments with p= 0.05 and q=0.05 B.) heatmap displaying the top 50 by variance up and down expressed mRNA transcripts in liver tissue. Clustered by row. Red indicated high expression and blue low expression C.) chart displaying variation in transcript identification. FC= fold change, DEGs= differentially expressed genes.

signaling pathway' (sasa04150) (Figure 4.7). Although no significant GO term associations were identified within upregulated liver mRNA transcripts, associations to high level groups such as *'localization'* and *'transporter activity'* were identified (NSMF, KCNMA1A, SLC2A3A, CT054, RRAD, TRPC7A). Downregulated liver mRNA transcripts were associated with the same higher groups as upregulated although less mRNA transcripts were identified, mRNA transcripts varied (SYT17, SLC4A10A, SYT8). Interestingly the 2 synaptotagmins in humans were associated with '*calcium ion binding activity'* and '*syntaxin binding'* with SYT17 additionally associated with '*phospholipid binding activity'*. The modulation of transporters and metabolic regulators suggests a possible shift in liver function toward energy conservation and metabolic homeostasis under hypoxia (Richards, 2009). As an organ, the liver is implicated in many vital functions and similar transcript associations in both up- and downregulated mRNA transcripts may enhance current understanding regarding metabolic activity in response to hypoxia in Atlantic salmon.

In mammalian models, SLC2A3 which codes for GLUT3, is highly expressed in brain tissue, and can be upregulated by Hif1a during hypoxia, enabling the transport of cellular glucose to satisfy the energy demands (Dai et al., 2020; Ziegler et al., 2020). In summary, the liver exhibited upregulation of mRNA transcripts involved in transport processes (SLC2A3A, TRPC7A), whereas downregulated mRNA transcripts (SYT17, SLC4A10A) were linked to calcium ion binding and phospholipid interactions.

In brain, DAVID converted 29/82 gene IDs amongst upregulated brain mRNA transcripts and 19/49 downregulated brain mRNA transcripts. No significant associations were found amongst downregulated mRNA transcripts (Figure 4.9 A). Upregulated brain mRNA transcripts were associated with GO:BP_D '*anterior/posterior pattern specification'* and '*regulation of transcription by RNA polymerase II'* (*n*=5 GO:0009952, *n*=11 GO:0006357). GO:BP_A additionally included the terms '*anterior/posterior pattern specification'*, '*regionalization*', '*pattern specification process*' and '*regulation of DNA-templated transcription*' (*n*=5 GO:0009952, GO:0003002, GO:0007389, *n*=13 GO:0006355).

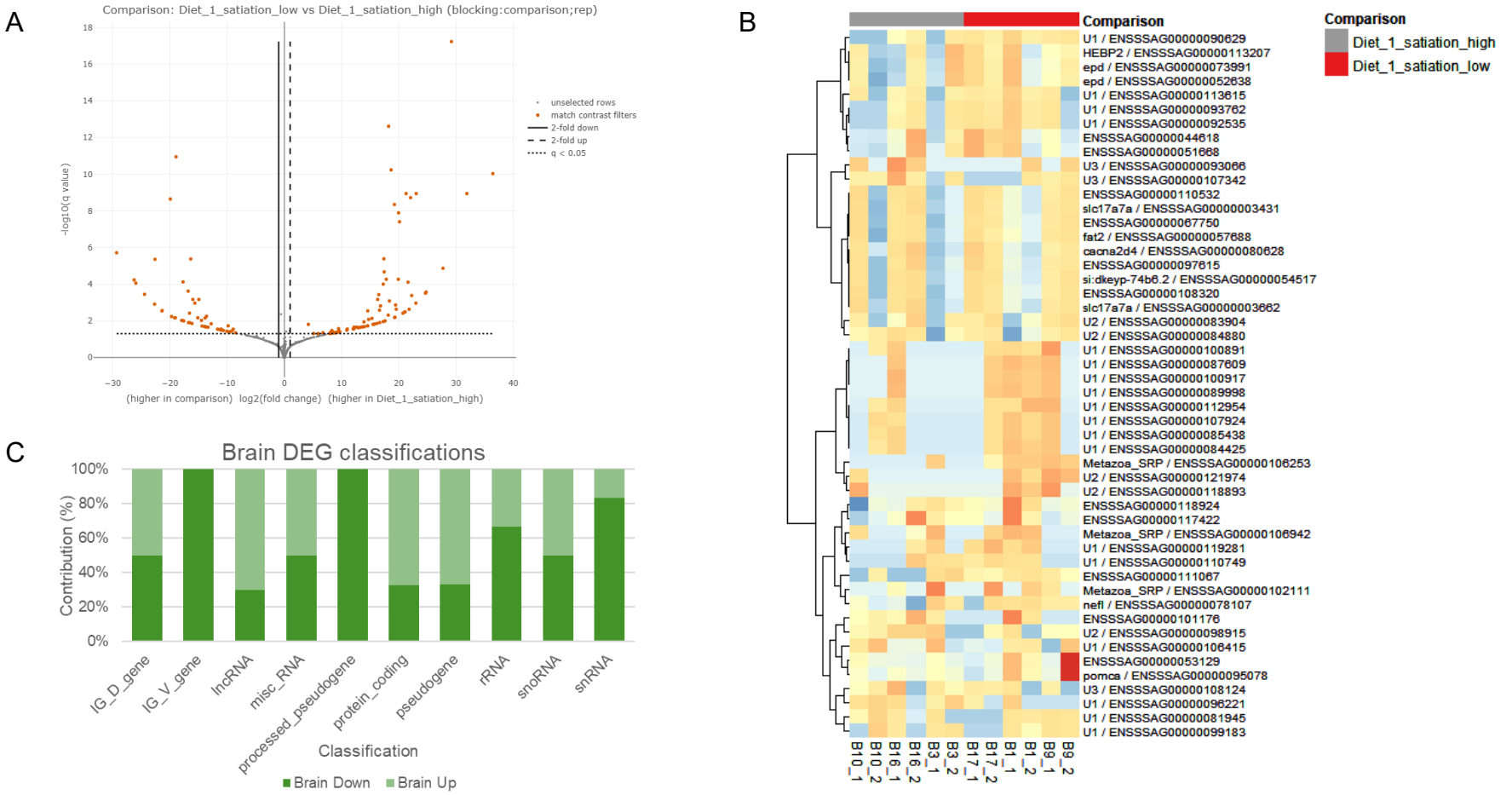


Figure 4.9 Brain tissue comparisons between Diet 1 hypoxia (D1L) and D1 normoxia (D1H) treatments A.) volcano plot displaying DEGs with log2FC >2, p-value <0.05 and q-value <0.05 for upregulated and log2FC<-2, p-value <0.05 and q-value <0.05 for downregulated DEGs between the two treatments with p= 0.05 and q=0.05 (variance stabilised) B.) heatmap displaying the top 50 up and down expressed mRNA transcripts in brain tissue. Red indicated high expression and blue low expression C.) chart displaying variation in transcript identification. FC= fold change, DEGs= differentially expressed genes.

GO:MF_D associated terms were '*DNA-binding transcription factor activity, RNA polymerase II-specific*' and '*RNA polymerase II transcription regulatory region sequence-specific DNA binding*' (*p*=<0.05, *n*=13 GO:0000981, *n*=5 GO:0000977). GO:MF_A included the terms '*DNA-binding transcription factor activity, RNA polymerase II-specific'*, '*sequence-specific double-stranded DNA binding*' and '*double-stranded DNA binding'* (*n*=13 GO:0000981, GO:1990837, GO:0003690). All the above terms were driven by 11 homeobox proteins as well as transcription factor 21(100195288) and doublesex- and mab-3-related transcription factor A1 (106608505). No associated KEGG pathways were identified. DAVID Gene Functional Classification tool identified 1 cluster (ES 7.91) which contained 10 homeobox proteins.

In brain tissue, downregulated mRNA transcripts had no associated terms while upregulated mRNA transcripts were associated with high level terms such as '*biosynthetic process'* and '*DNA-binding transcription factor activity'* driven by homeobox proteins. Afzal & Krumlauf (2022) suggested that HOX genes responded to major signalling pathways such as WNTs. Wang et al. (2024) suggested that human HOX genes in cancer studies, affect processes such as cellular proliferation, cell cycle, differentiation, apoptosis, angiogenesis (the formation of new blood vessels) and TGF-β signalling.

Mungpakdee et al. (2008) suggested that HOX genes encode transcription factors involved in pattern formation in vertebrates and identified 118 HOX genes in their study using Atlantic salmon. As a result, Singh & Krumlauf (2022) implied that multiple WGD events as observed by the Atlantic salmon HOX genes, could result in novel functions. Very few recent articles exploring HOX genes/ homeobox proteins specifically in Atlantic salmon exist, suggesting an area for further investigation is required.

In summary, brain showed upregulation of homeobox mRNA transcripts implying a potential neuroprotective response. GO terms related to '*anterior/posterior pattern specification*' (GO:0009952) and '*regulation of transcription by RNA polymerase II'* (GO:0006357) were enriched, suggesting adaptive transcriptional responses to hypoxia.

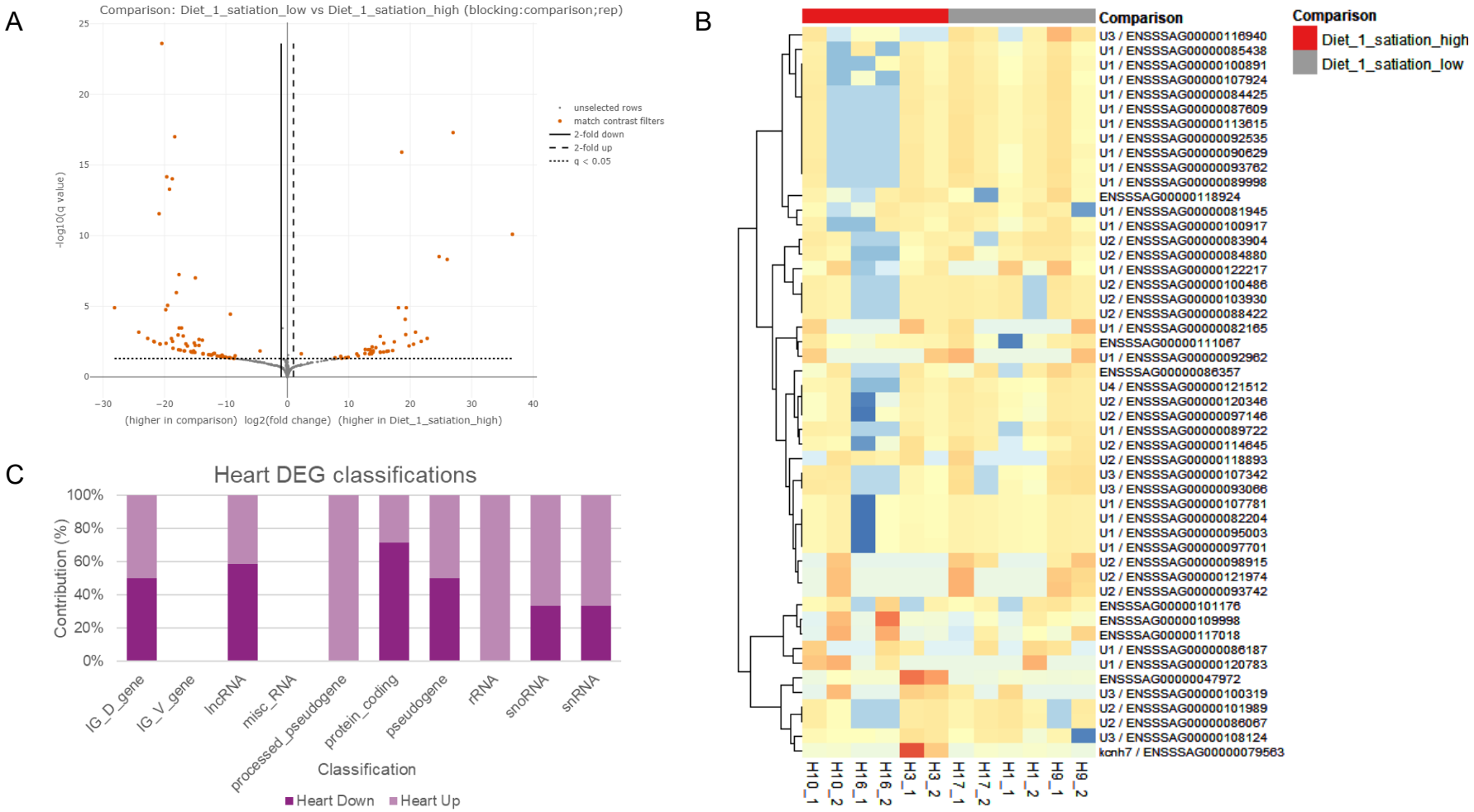


Figure 4.10 Heart tissue comparisons between Diet 1 hypoxia (D1L) and D1 normoxia (D1H) treatments A.) volcano plot displaying DEGs with log2FC >2, *p*=<0.05 and q-value <0.05 for upregulated and log2FC<-2, *p*=<0.05 and q-value <0.05 for downregulated DEGs between the two treatments with *p*=<0.05 and *q*=<0.05 (variance stabilised). B.) heatmap displaying Pearson's correlation coefficients for the top 50 up and down expressed mRNA transcripts in heart tissue. Red indicated high expression and blue low expression C.) chart displaying variation in transcript identification. FC= fold change, DEGs= differentially expressed genes. ShinyNGS

Heart tissue contained ↑43 mRNA transcripts of which DAVID successfully identified 15 (Figure 4.10). No significant associated GO terms or KEGG pathways were found, but 1 functional gene cluster was identified (ES 0.7) with UniProt keywords associated to the term '*Signal*' (KW-0732). The mRNA transcripts included transmembrane protein 121B-like, fibronectin type III domain-containing protein 10-like, transmembrane protein 240 and uncharacterized protein PB18E9.04c-like (106597677, 106583064, 106572021, 106561936).

There were ↓71 heart DEGs of which DAVID identified 33. No significant associations were identified for any GO Direct terms, GO all or KEGG pathways. ShinyGO classified 18 PC mRNA transcripts, of which 9 were determined to be novel PC mRNA transcripts and this may have contributed to the low GSEA associations. Functional groups were identified with higher level associations to '*biosynthetic process'* (GSC, B3GALT1) '*localisation*' (TMPRSS5, KCNG1, CHRNA2B) *'transporter activity'* (KCNG1, CHRNA2B) and '*transferase activity'* (B4GALNT1, B3GALT1) in downregulated mRNA transcripts.

In summary, no up- or downregulated heart mRNA transcripts were associated to GO terms or KEGG pathways, suggesting limited transcriptomic changes. Functional grouping of the downregulated mRNA transcripts may signify a possible mTOR inhibition with downregulation of '*biosynthetic process'.*

4.3.3.1.1.4 Summary DEGs

The number of mRNA transcripts varied between tissues, with 127 (53↓, 74↑) in liver, 131 in brain (49↓, 82↑) and 114 in heart (71↓, 43↑). Out of all tissues, brain had the largest response in upregulated mRNA transcripts, with ↑82/131 and heart the largest in downregulated mRNA transcripts 71↓/114.

As a metabolically active organ, the liver is highly productive in producing proteins (hormones, enzymes, plasma proteins *etc.)* and this may explain the subsequent elevated levels of overexpressed liver rRNA comparative to the other tissues. The rRNA results in the current study reinforce this role of the liver as a major protein synthesis organ compared to the brain and heart tissues. The liver, responsible

for metabolism and detoxification in response to hypoxia, conserves energy while producing essential proteins.

The brain requires protein synthesis, its largely linked to neural activity/ transmission, such as for neurotransmitters and synaptic proteins with hypoxic stress requiring adaptive responses such as minimising damage. All brain associated terms were linked to the homeobox mRNA transcripts, with potentially unknown roles in Atlantic salmon. Heart has less requirement for protein synthesis compared to liver, as its role is more tissue specific as a muscle organ, with protein synthesis linked to muscle contraction and repair.

The presence of calcium ion transport-related mRNA transcripts (CACNG7A, TRPC7A) suggests hypoxia-induced alteration in calcium signalling, possibly an adaptive response to ion homeostasis. Calcium ions regulate metabolic processes such as glycolysis, cellular regeneration, and muscle contraction (Myrka & Buck, 2021). The upregulation of CACNG7A in the heart tissue suggests its role in modulating cardiac contractions under hypoxia and calcium signalling may either promote cell survival or induce apoptosis highlighting the difficulties in identifying precise roles of the mRNA transcripts (Myrka & Buck, 2021). Nilsson & Randall (2010) suggested that acidosis is encountered under hypoxic conditions in hearts, and some fish mitigate the risk by increasing intracellular calcium

The synaptotagmin mRNA transcripts *(*SYT17, SYT8, SYT1-like*)* were all identified in downregulated liver tissue, suggesting a possible effect of hypoxia on the reduction of neural activity. This may possibly be a response in order to reduce energy usage in the brain and nervous system. The SYT1 mRNA transcripts in mice have been linked to fatty acid metabolism, bile acids, lipoprotein and vesicular transport, possibly suggesting roles in these processes may be reduced in the hypoxia group. In humans and mice, SYT17 is thought to be involved in membrane localisation (Wang et al., 2022) and is expressed everywhere although research is focused on synaptic communication (Ruhl et al., 2019) while more recently in mammals it has been called the master circadian oscillator (Fujioka et al., 2023). SYT8 in human pancreatic cell lines has been

demonstrated as promoting tumour growth (Fu et al., 2021). These recent studies have identified the variable roles of the synaptotagmins in well studied model species although underlying mechanisms in regulation and their roles are still unknown, emphasising the complexity involved in Atlantic salmon research.

4.3.3.2 Intensity by variance

Classifications of the top 50 mRNA transcripts by variance in liver tissue heatmaps (Figure 4.7 B), identified the highest contribution from snRNA, followed by rRNA and protein coding (18/50,14/50,14/50). Of the 14 PC mRNA transcripts, 6 were unidentified (novel). Identified mRNA transcripts were ladderlectin (106574391), ELOVL8B, ANKEF1A, PKP4, ladderlectin-like (106574392), ladderlectin (106574349), ladderlectin-like (106575496) and si:dkeyp-27e10.3 (UPF0606 protein KIAA1549-like (106576037)).

DAVID successfully mapped 42/50 liver mRNA transcripts (Figure 4.11). Enrichment analysis of the liver mRNA transcripts displayed no associated GO:BP terms. GO:MF_D and GO:MF_A both associated the term *'signaling receptor activity'* (*n*=4, GO:0038023) with GO:MF_A additionally identifying the higher term *'molecular transducer activity'* (*n*=4, GO:0060089) to ladderlectin (106574349, 106574391) and ladderlectin-like (106574392, 106575496). The Gene Functional Classification tool additionally clustered the ladderlectin mRNA transcripts together (ES 4.25).

In brain tissue, the largest classification contribution was snRNA followed by protein coding (23/50, 18/50) (Figure 4.11). Of the 18 PC mRNA transcripts, 3 were unidentified (novel). Identified mRNA transcripts were vesicular glutamate transporter 1 (106601845, 106606332), protein phosphatase methylesterase 1 (106578192), soluble guanylate cyclase 88E-like (106604839), ependymin (EPD), protocadherin Fat 2 (106612258), Ependymin-2 (EPD2), neurofilament light (NEFL), voltage-dependent calcium channel subunit alpha-2/delta-4 (CACNA2D4, 106561009), POMCA, neurogenic differentiation factor 2-like (106578342), cerebellin-1 (106608967), leucine-rich repeat-containing protein 3-like (106566167), and heme-binding protein 2 (106600932) (Figure 4.9 B).

Ependymin-2 *(*EPD2*)* was linked to '*calcium ion binding'* (GO:0005509) and is associated with fish nervous system plasticity and memory creation (McDougall et al., 2018). In a study observing the proteomic changes in *Carassius carassius* (crucian carp) due to anoxia, Smith et al. (2009) found that anoxic conditions increased the pre-proependymin protein (precursor to EPD) and suggested that EPD may reverse apoptosis. Garina (2021) discussed pain reception, migration, social dominance, oxygen, and disease on EPD expression, highlighting the role of EPD on physiological as well as behavioural responses. Garina (2021) offered a suggestion that the capacity of EPD to bind calcium ions (up to 66% of Ca2+ in cerebrospinal fluid) as well as its involvement in cell adhesion and migration may have reduced oxidative stress but the role of EPD in aggression/ social dominance, reproductive cycle and migration were unknown.

DAVID mapped 45/50 heart mRNA transcripts (Figure 4.11). GSEA analysis had GO:BP_*D 'regulation of synapse structure or activity'* and *'neurotransmitter loading into synaptic vesicle'* (*n*=2, GO:0050803, GO:0098700) terms associated with vesicular glutamate transporter 1 (106606332, 106601845). Heart tissue classifications had the largest contribution from snRNA (37/50) of which the largest contribution was U1 followed by U2 spliceosomal RNA (22/50, 14/50).

Pre-mRNA splicing is essential in the production of mRNA by removing introns and ligating exons (Singh & Singh, 2019).The spliceosome consists of 5 types of snRNA, U1, U2, U4, U5 and U6, which form 5 snRNPs and spliceosome assembling contains multiple steps with U1 the most abundant snRNA across various models (Morais et al., 2021). Silva et al. (2015) studied 5 fish species (*Astyanax, Characiformes, Characidae*) found a possible interaction between U1 snRNA and 5S rDNA due to the location of U1 and 5S rDNA sequence locations.

The 4 PC mRNA transcripts consisted of potassium voltage-gated channel subfamily H member 7-like (106575297), ENSSSAG00000047972 (novel), ENSSSAG00000111067 (novel), and ENSSSAG00000109998, which had conflicting results. NCBI identified it as 28S ribosomal RNA (123726919, pseudo) whereas Ensembl identified it as novel PC. No GSEA enrichment terms or pathways were identified (Figure 4.11 B).

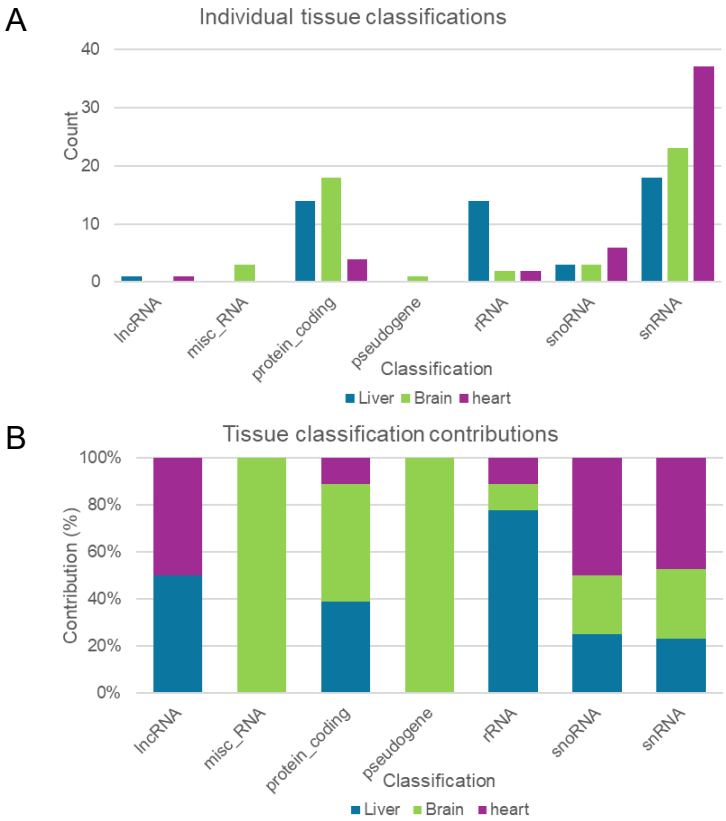


Figure 4.11 Top 50 mRNA transcripts by variance A) Individual tissue classification count B) Overall tissue classification contribution (%). VST heatmap data.

As an overview, an exploratory assessment was conducted on a combination of the top 50 mRNA transcripts by variance of all tissues. Higher level functions and processes such as '*cell adhesion'* (EPD, PKP4, FAT2, EPD), *'developmental process'* (FAT2, NEFL, neurogenic differentiation factor 2-like), and *'localisation'*/ '*'transporter activity'* (KCNH7, vesicular glutamate transporter 1 (106601845, 106606332)) were identified.

4.3.3.3 Summary magnitude and intensity

In summary, 199 DEGs were upregulated, and 173 mRNA transcripts downregulated across liver, brain and heart tissues. Brain had the highest overall contribution to upregulated DEGs (*n*=82/199) while downregulated heart tissue had the largest contribution to the downregulated DEGs (*n*=71/173).

Across the transcriptomic landscape, tissue specific response occurred, with liver having the largest response in rRNA (↑14/74) while brain had the largest response in PC (↑47/82). Upregulated brain had the largest LncRNA response

(↑26/82) while heart had the highest in the downregulated mRNA transcripts (↓21/71).

Amongst the combined tissue upregulated DEGs, all GO: BP terms were driven by 5 homeobox proteins (HOXD4AB, HOXB7AB, HOXB9AB, HOXB6AB, 106579315). In addition to these 5 drivers, GO:MF terms were driven by an additional 7 homeobox proteins and 4 transcription factors (HOXB8BA, HOXB8AB, HOXC8BA, HOXC8AB, ATF5A, transcription factor 21, motor neuron and pancreas homeobox protein 1-like, doublesex- and mab-3-related transcription factor A1, homeobox protein Hox-B5b, motor neuron and pancreas homeobox protein 1, myelin transcription factor 1-like).

Combined downregulated DEGs had GO:BP terms associated with '*cell-cell signalling'* and '*synaptic signalling'* driven by mRNA transcripts associated with '*regulation of neurotransmitters release'*, '*calcium ion binding'* and '*syntaxin binding'* (synaptosome associated protein 25a, fibroblast growth factor-binding protein 2-like, glycine receptor subunit beta-like, neuronal acetylcholine receptor subunit alpha-2-like, beta-soluble NSF attachment protein-like, SYT17, synaptotagmin-1-like, ly6/PLAUR domain-containing protein 1).

In summary, overall top 50 mRNA transcripts by variance, exhibited by heatmap across all tissues, expressed similar results with varying degrees of oscillation. Overall there was a limited response between treatments, suggesting that in this non-targeted primary assessment, significant transcriptomic changes were a result of oscillation of cellular processes rather than an effect of hypoxia. Primarily suggesting that mRNA regulation may not be the key regulatory response to hypoxia.

4.3.4 Gene ontology analysis (>2 <-2 fold change)

Further analyses were conducted on the normalised data sets for liver, brain and heart tissues to identify mTOR pathway mRNA transcripts between treatments conducted on fold change (FC) for up- and downregulated mRNA transcripts. mRNA transcripts were separated into bins, with upregulated FC categories set between >=2 to 4.99, >=5 to 9.99 and >=10 while downregulated were sectioned into bins ranging from <=-2 to -4.99, <=-5 to -9.99 and <=-10FC.

Data were subjected to analysis initially using DESeq2/ ShinyNGS, with additional use of DAVID, ShinyGO, NCBI, g:Profiler and Ensembl.

4.3.4.1 All tissues upregulated

DAVID converted 3112/8837 to gene ID with 536 further identified as duplicated mRNA transcripts between the tissues (Electronic file: Tissue Normalised 2FC). ShinyGO classifications identified the largest contributions from PC (5121/8026) and LncRNA (2556/8026).

Most significant GO:BP_D associated terms were *'visual perception'* (n=43, GO:0007601), *'G protein-coupled receptor signaling pathway'* (*n*=91, GO:0007186) and '*cell adhesion'* (*n*=51, GO:0007155). GO:BP_A terms included '*response to stimulus'*, '*multicellular organismal process'* and '*cell communication'* (*n*=624 GO:0050896, *n*=436 GO:0032501, *n*=534 GO:0007154). GO:MF_D terms were *'cytokine activity'* (*n*=46, GO:0005125), *'hormone activity'* (*n*=24, GO:0005179) and *'signaling receptor activity'* (*n*=38, GO:0038023). GO:MF_A included terms such as *'transporter activity'*, *'signaling receptor activity'* and *'hormone activity'* (*n*=255 GO:0005215, *n*=262 GO:0038023, *n*=35 GO:0005179). The most significantly enriched KEGG pathways were *'Cytokine-cytokine receptor interaction'* (*n*=75, sasa04060), *'Neuroactive ligand-receptor interaction'* (*n*=110, sasa04080) and *'Cytoskeleton in muscle cells'* (*n*=78, sasa04820).

Interestingly 43 upregulated mRNA transcripts were associated with *'visual perception'* which is a biological process (vision). Damsgaard et al. (2020) suggested that the vertebrate retina has a high metabolic rate, involving a high oxygen demand and that visual performance in teleosts can be severely reduced by limited oxygen supply.

There were 91 upregulated mRNA transcripts associated with *'G protein-coupled receptor signaling pathway*', which is cellular communication via signal transduction, ending in downstream regulation of cellular processes (*e.g.* transcription, metabolic processes). The plasma membrane G-protein-coupled receptors (GPCRs) respond to G proteins who bind guanosine triphosphate

(GTP) and guanosine diphosphate (GDP) depending on whether the protein is active (GTP) or inactive (GDP). G proteins can be inhibitory or can stimulate activity.

The higher level molecular function terms such as *'transporter activity'* suggested movement in and out of cells, *'signaling receptor activity'* suggested signalling associated with cellular activity in order to trigger a response, similar to *'hormone activity'* stimulating a biological response. Cytokines are intercellular regulators of cells in innate/adaptive and inflammatory responses, cell growth/death, cellular homeostasis and differentiation (Lazado et al., 2023). Martínez et al. (2020) suggested that genes associated with the innate immune system were transcriptionally activated in response to hypoxia.

'*Neuroactive ligand-receptor interaction'* is associated with neurotransmitter receptors and neuroreceptor genes and may regulate gene expression through the binding of ligands to receptors (Lazado et al., 2023). *'Cytoskeleton in muscle cells'* may be associated with muscle contraction in addition to muscle structure. Wulff et al. (2012) in a study examining the effects of hypoxia on rainbow trout muscle, found an effect of hypoxia on the regulation of cellular cytoskeleton, structure and cell volume. This may explain the transcript associations with this pathway in the upregulated group as a response to hypoxia.

In summary, functional enrichment analysis revealed significant associations with '*G protein-coupled receptor signaling'* (GO:0007186), '*visual perception*' (GO:0007601), and '*cell adhesion'* (GO:0007155). KEGG pathways highlighted were '*Cytokine-cytokine receptor interaction*' (sasa04060), '*Neuroactive ligand-receptor interaction*' (sasa04080), and '*Cytoskeleton in muscle cells*' (sasa04820), possibly suggesting increased broad regulatory roles across tissues in response to hypoxia.

4.3.4.2 <u>All tissues downregulated</u>

DAVID converted 3666/8742 gene ID with 701 duplicated mRNA transcripts between the tissues identified (<u>Electronic file: Tissue Normalised 2FC</u>). ShinyGO classifications identified 5514/8005 PC and 2297/8005 LncRNA.

GO:BP_D terms in all downregulated tissues included '*SMAD protein signal transduction'* '*negative regulation of endopeptidase activity*' and '*transmembrane transport*' (*n*=31 GO:0060395, *n*=20 GO:0010951, *n*=73 GO:0055085). GO:BP_A suggested broader terms such as '*multicellular organismal process'*, *'developmental process'* and '*cell communication'* (*n*=514 GO:0032501, *n*=515 GO:0032502, *n*=643 GO:0007154). GO:MF_D suggested associated terms such as *'cytokine activity'*, *'growth factor activity'* and *'serine-type endopeptidase activity'* (*n*=58 GO:0005125, *n*=54 GO:0008083, *n*=59 GO:0004252). GO:MF_A associated the terms *'transporter activity'*, *'molecular transducer activity'* and *'signaling receptor activity'* (*n*=337 GO:0005215, *n*=335 GO:0060089, *n*=335 GO:0038023). Associated KEGG pathways were *'Neuroactive ligand-receptor interaction'*, *'Cytokine-cytokine receptor interaction'* and *'Cell adhesion molecules'* (*n*=142 sasa04080, *n*=80 sasa04060, *n*=63 sasa04514).

GO terms such as '*SMAD protein signal transduction'* (GO:0060395) and '*negative regulation of endopeptidase activity'* (GO:0010951) were associated with downregulated mRNA transcripts. KEGG pathways included '*Neuroactive ligand-receptor interaction'* and '*Cell adhesion molecules'* (sasa04514), suggesting a possible reduced intercellular communication and neural activity. Both up- and downregulated mRNA transcripts were associated with *'Neuroactive ligand-receptor interaction'* and *'Cytokine-cytokine receptor interaction'.*

'Cell adhesion molecules' are located on the cell surface and may be involved in tissue formation, wound healing and immunity. Crossin (2012) suggested that in mammalian models, hypoxia activates HIF1α which affects WNT activity, which is a regulator of cell adhesion. In addition, the authors suggested that the WNT canonical pathway affected cell junctions, localisation and adhesion while the non-canonical WNT pathway affected cellular location and migration. The authors concluded with stating that these pathways significantly influenced cell adhesion and the cytoskeleton.

In the up- and downregulated groups, pathways associated with cell adhesion and cytoskeleton were identified in both groups. These pathways are essentially

linked, with the cytoskeleton providing cellular structure and the adhesion junctions anchoring the cell, thus aiding tissue formation. Jones et al. (2019) explained that changes in cellular shape, adhesion and cytoskeleton were part of the replication/ division phases in cell cycle. The transcript associations with these pathways in both groups may suggest possible natural cell cycle oscillations.

Downregulated pathways were additionally associated with '*Calcium signaling pathway'* and '*Adrenergic signaling in cardiomyocytes'* (*n*=89 sasa04020, *n*=64 sasa04261), while upregulated pathways were '*Steroid hormone biosynthesis'* and '*Calcium signaling pathway'* (*n*=15 sasa00140, *n*=66 sasa04020).

The upregulated '*Steroid hormone biosynthesis'* pathway had mRNA transcripts related to sex hormones such as HSD17B3 (hydroxysteroid (17-beta) dehydrogenase 3), oestradiol 17-beta-dehydrogenase 1-like, DHB3 (testosterone 17-beta-dehydrogenase 3). This may suggest an effect of hypoxia on reproduction and gonadal development.

Saha et al. (2022) stated that hypoxia affected gonadal development regardless of sex, endocrine disruption, and they concluded that due to the physiological/biochemical pathways affected by hypoxia, it was difficult to determine indirect/direct effects of hypoxia in teleosts. Some of these difficulties were conflicting results such as an interruption in the actual steroid biosynthesis, reduction due to gonadal impairments and even inverse effects on different species.

'*Adrenergic signaling in cardiomyocytes'* in mammalian modes is associated with the cardiac response to stress/ physical activity through neurotransmitters such as norepinephrine (noradrenaline). This results in the heart beating harder/ faster in order to fulfil the oxygen demand and could indicate an effect of hypoxia on this pathway. Alternatively, it may possibly be an effect of stressors (handling/ netting) which may suggest an effect of hypoxia in relation to other stressors. '*Calcium signaling pathway'* had a larger response in the downregulated group (↓89 ↑66), which may be connected to the stress response from the '*Adrenergic signaling in cardiomyocytes'.*

The downregulated pathways '*Adrenergic signaling in cardiomyocytes'* (sasa04261) and '*Calcium signaling pathway'* (sasa04020), may indicate impaired cardiac signalling under hypoxic conditions.

4.3.4.3 Liver GSEA

A total of 3685 upregulated liver mRNA transcripts (>2 FC) were subjected to GSEA. PC mRNA transcripts had the highest contribution followed by lncRNA (2241/3685, 1259/3685). Downregulated mRNA transcripts had a similar trend, with 1830 PC mRNA transcripts and 675 lncRNA from a total of 2564. The overall contribution of PC mRNA transcripts in the upregulated group was 61% whereas in downregulated PC mRNA transcripts it was 71%. Downregulated mRNA transcripts had higher diversity with 12/13 classifications compared to 11/13. Downregulated had no miscRNA and upregulated had no YRNA and IGV gene.

GO:BP_D terms associated with upregulated liver mRNA transcripts using DAVID were *'monoatomic ion transmembrane transport'* (*n*=15, GO:0034220). GO:BP_A terms were *'multicellular organismal process'*, '*cell communication'* and *'signaling'* (*n*=186 GO:0032501, *n*=235 GO:0007154, *n*=228 GO:0023052). GO:MF_A terms were *'gated channel activity'*, *'transmembrane transporter activity'* and *'transporter activity'* (*n*=55 GO:0022836, *n*=116 GO:0022857, *n*=118 GO:0005215). The top 3 enriched KEGG pathways (*p*=<0.05) using DAVID were *'Neuroactive ligand-receptor interaction'* (*n*=44, sasa04080), *'Calcium signaling pathway'* (*n*=34, sasa04020) and *'Cytokine-cytokine receptor interaction'* (*n*=26, sasa04060). DAVID Gene Functional Classification tool identified 45 clusters with the top 3 having enrichment scores (ES) of 4.51, 3.41 and 3.32.

The upregulated associated terms were biologically connected to ion transport, cell communication and signalling possibly indicating increased regulation of ion homeostasis, communication in response to hypoxia as well as systemic responses. The *'Neuroactive ligand-receptor interaction'* pathway associations may indicate increased communication in order to regulate metabolic and physiological responses to hypoxia. *'Calcium signaling pathway'* indicated signalling possibly as a response to hypoxia, suggesting increased energy

production and stress tolerance. *'Cytokine-cytokine receptor interaction'* may suggest ana response to stress or tissue damage.

Downregulated GO:BP_D terms were *'manganese ion transport', 'immune response'* and '*cell communication'* (*n*=6 GO:0006828 , *n*=25 GO:0006955, *n*=13 GO:0007154). GO:BP_A associated terms were '*cell-cell signaling'*, '*transmembrane transport*' and '*immune system process'* (*n*=46 GO:0007267, *n*=86 GO:0055085, *n*=54 GO:0002376). GO:MF_D *'signaling receptor activity'*, *'growth factor activity'* and *'cytokine activity'* (*n*=22 GO:0038023, *n*=20 GO:0008083, *n*=19 GO:0005125). GO:MF_A associated terms were *'transporter activity'*, *'signaling receptor regulator activity'* and *'receptor ligand activity'* (*n*=118 GO:0005215, *n*=49 GO:0030545, *n*=46 GO:0048018).

Downregulated pathways identified were *'Cytokine-cytokine receptor interaction'* (*n*=30, sasa04060), *'Cell adhesion molecules'* (*n*=24, sasa04514) and *'Intestinal immune network for IgA production'* (*n*=9, sasa04672). DAVID Gene Functional Classification tool identified 41 clusters with the top 3 having enrichment scores (ES) of 11.68, 5.57 and 4.86.

Biological processes and molecular functions associated with the downregulated mRNA transcripts may indicate a reduction in energy consuming processes. The KEGG pathways further demonstrated a possible energy saving strategy with downregulation of cell-cell interaction and signalling, although the downregulation of *'Intestinal immune network for IgA production'* may be a consequence of hypoxia, or possibly a reduction in immunity as energy saving adaption. This may be an area for further investigation.

Up- and downregulated liver mRNA transcripts, both had associations with *'Cytokine-cytokine receptor interaction'.* This may imply a hypoxia adaption with certain elements within the pathway upregulated for repair, protection whereas downregulated elements may suggest a reduction of non-essential process as a possible strategy. Upregulated associated pathways were *Neuroactive ligand-receptor interaction'* and *'Calcium signaling pathway'* whereas downregulated associated pathways were *'Cell adhesion molecules'* and *'Intestinal immune network for IgA production'.*

Zhang et al. (2024) suggested that IgA (immunoglobulin A) is important in protecting intestinal health and regulates the microbiome by releasing IgA into the intestinal cavity. Niklasson et al. (2011) examined the effects of hypoxia on Atlantic salmon, suggested that the hypoxic conditions in their study led to a suppression in the mucosal immunity, possibly through intestinal inflammation. The downregulation in the current study may be a consequence of sub-optimal oxygen as demonstrated by Niklasson et al. (2011).

4.3.4.3.1 Liver bins

In the liver tissue bin >10 FC, 90 mRNA transcripts were upregulated, of which only 29 Entrez gene IDs were identified by DAVID. No GO terms were associated within these mRNA transcripts.

Within the bin 5 to 9.99 FC, there were a total of 451 mRNA transcripts of which DAVID mapped 152 to gene IDs. GO:BP_D associated terms were *'multicellular organism development'* (GO:0007275) which included cadherin-20, cadherin-20, dickkopf-related protein 1, cadherin-22-like, eyes absent homolog 2-like, cadherin-24 and protein GREB1 (106578590, 106584214, 106577088, 106565306, 106565282, 106560237, 106610731). Additionally, GO:BP_D associated 4 cadherin mRNA transcripts with *'epithelium development'*, *'calcium-dependent cell-cell adhesion via plasma membrane cell adhesion molecules'* and *'Adherens junction organization'* (GO:0060429, GO:0016339, GO:0034332, 106565306, 106578590, 106584214, 106560237). No significant GO:MF_D associations were identified.

Within the 2 to 4.99 FC bin there were 3144 mRNA transcripts of which DAVID assigned gene IDs to 1159. Of these 1159, 10 mTOR pathway associated mRNA transcripts were detected. Significantly enriched KEGG pathways were '*Neuroactive ligand-receptor interaction'* (n=42, sasa04080) and *'Calcium signaling pathway'* (*n*=32, sasa04020). No significant GO:BP or GO:MF terms were associated with the mRNA transcripts.

Within the downregulated bin <-10 FC there were 40 mRNA transcripts of which DAVID identified 24. No significant KEGG pathways, GO:BP or GO:MF terms were associated with these mRNA transcripts. Within this range, eukaryotic

translation initiation factor 4E family member 2 (EIF4E2, 106600575) was associated with the mTOR pathway.

In the next bin category (-5 to -9.99 FC), DAVID successfully identified 141 of the 279 mRNA transcripts. No significant associations to KEGG pathways, GO:BP or GO:MF terms were identified. The -2 to -4.99 FC bin resulted in 2245 mRNA transcripts of which DAVID identified 1070. A total of 9 mTOR associated mRNA transcripts were identified within this range. The most significantly enriched KEGG pathway was *'Cytokine-cytokine receptor interaction'* (*n*=26, sasa04060). GO:BP associated terms were *'manganese ion transport'* (*n*=6 GO:0006828) and *'immune response'* (*n*=23 GO:0006955). Similarly, GO:MF terms were *'cytokine activity'* (*n*=18 GO:0005125), *'store-operated calcium channel activity'* (*n*=6 GO:0015279) and *'growth factor activity'* (*n*=17 GO:0008083).

Amongst the upregulated liver mRNA transcripts in the bin category 2 to 4.99FC, there were 2 associated pathways '*Neuroactive ligand-receptor interaction'* and *'Calcium signaling pathway'* whereas in the downregulated category -2 to -4.99 *'Cytokine-cytokine receptor interaction'* was the only pathway identified.

4.3.4.4 Brain GSEA

A total of ↑3076 and ↓2560 mRNA transcripts were mapped to Gene IDs by DAVID resulting in a total of ↑1188 and ↓836.

Brain upregulated GSEA GO:BP_D associated the terms 'visual perception', 'muscle contraction' and 'anterior/posterior pattern specification' (n= 26 GO:0007601, n= 18 GO:0006936, n= 15 GO:0009952) while GO:BP_A terms were *'multicellular organismal process', 'system process'* and *'sensory perception'* (*n*=192 GO:0032501, *n*=71 GO:0003008, *n*=34 GO:0007600). GO:MF_D terms were '*cytokine activity'*, *'hormone activity'* and *'growth factor activity'* (*n*=26 GO:0005125, *n*=15 GO:0005179, *n*=20 GO:0008083). GO:MF_A terms were *'signaling receptor activator activity'*, *'cytokine activity'* and *'hormone activity'* (*n*=63 GO:0030546, *n*=32 GO:0005125, *n*=24 GO:0005179).

Associated KEGG pathways were *'Cytoskeleton in muscle cells'*, *'Cytokine-cytokine receptor interaction'* and *'Motor proteins'* (*n*=54 sasa04820, *n*=38

sasa04060, *n*=28 sasa04814). Gene Functional Classification identified 48 clusters, with the top 3 having ES of 11.59, 7.26 and 7.16.

The upregulated biological terms suggested possible sensory and systemic responses to hypoxia, such as muscle contraction and visual perception although these may be a result of the sampling strategy. The upregulation of pattern specification may indicate changes in the structure or function in the brain. Increased signalling and communication through signalling molecules involved in immune responses, growth, and development may suggest an effect of hypoxia or other stressors. The upregulated pathway associations suggested a possible increase in muscle function/ structure, cellular transport/ motility and cytokine signalling. Motor proteins in mammalian models are linked to intracellular transport along the cytoskeleton, commonly through ATP hydrolysis and release which results in force and the direction of movement. The motor proteins are connected to cellular functions such as muscle contraction, cell migration, and membrane trafficking (Sweeney & Holzbaur, 2018).

Downregulated brain GO:BP_D GSEA terms were *'G protein-coupled receptor signaling pathway', 'chordate embryonic development'* and *'commitment of neuronal cell to specific neuron type in forebrain'* (*n*=37 GO:0007186, *n*=7 GO:0043009, *n*=4 GO:0021902). GO:BP_A terms highlighted *'G protein-coupled receptor signaling pathway', 'response to chemical'* and *'multicellular organismal process'* (*n*=66 GO:0007186, *n*=44 GO:0042221, *n*=113 GO:0032501).

GO:MF_D associated terms were *'peptide binding', 'structural molecule activity'* and *'hormone activity'* (*n*=9 GO:0042277, *n*=16 GO:0005198, *n*=12 GO:0005179). GO:MF_A terms were *'signaling receptor activity'*, *'transmembrane signaling receptor activity'* and *'hormone activity' (n*=93 GO:0038023, *n*=77 GO:0004888, *n*=15 GO:0005179).

Associated KEGG pathways were *'Neuroactive ligand-receptor interaction'* and *'Cytokine-cytokine receptor interaction'* (*n*=46 sasa04080, *n*=24 sasa04060). Gene Functional Classification identified 24 clusters with the top 3 highest ES of 7.03, 4.91 and 3.84. Upregulated brain mRNA transcripts were associated with '*Cytoskeleton in muscle cells'*, *'Cytokine-cytokine receptor interaction'* and *'Motor*

proteins' whereas downregulated associated pathways were *'Neuroactive ligand-receptor interaction'* and *'Cytokine-cytokine receptor interaction'.*

The downregulated biological process associated mRNA transcripts highlighted a possible shift to energy conservation by the downregulation of developmental processes possibly by reducing non-essential growth, signalling and differentiation processes. The molecular function associations additionally suggested possible mechanisms in the reduction of energy usage such as reducing hormone activity. Similarly, for the KEGG pathway associations, a reduction in neural signalling and cytokine signalling may concur with energy conservation strategies observed in downregulated tissues.

4.3.4.4.1 Brain Bins

Total mRNA transcripts in the>10FC bin were 115 of which DAVID mapped 67 to gene IDs. DAVID Gene Functional Classification tool identified 3 clusters (ES 10.1, 0.5, 0.16). All mRNA transcripts in cluster 1 were associated with transcription regulatory terms (GO:0006357, GO:0000981, GO:0000978).

GO:BP_D associated terms were *'embryonic skeletal system morphogenesis', 'anterior/posterior pattern specification', 'regulation of transcription by RNA polymerase II'* and *'response to nutrient levels'* (*n*=8 GO:0048704, *n*=10 GO:0009952, *n*=18 GO:0006357, *n*=3 GO:0031667). GO:BP_A terms were *'multicellular organismal process', 'biological regulation'* and *'regulation of metabolic process'* (*n*=22 GO:0032501, *n*=33 GO:0065007, *n*=21 GO:0019222).

The only GO:MF_D associated terms were *'RNA polymerase II cis-regulatory region sequence-specific DNA binding', 'DNA-binding transcription factor activity, RNA polymerase II-specific'* and *'hormone activity'* (*n*=18 GO:0000978, *n*=18 GO:0000981, *n*=4 GO:0005179). GO:MF_A terms were *'signaling receptor regulator activity', 'nucleic acid binding'* and *'hormone activity'* (*n*=6 GO:0030545, *n*=19 GO:0003676, *n*=5 GO:0005179). No KEGG pathways were identified.

Within the 5 to 9.99 FC bin, DAVID mapped 137/ 365 mRNA transcripts. DAVID Gene Functional Classification tool identified 5 clusters (ES 2.08, 1.42, 0.94). Cluster 1 was associated with *'calcium ion binding'* (*n*=6 GO:0005509) while

cluster 2 was associated with *'regulation of transcription by RNA polymerase II'* (*n=8* GO:00063570). The only GO term associated with this group was GO:BP_D *'visual perception'* (*n*=6 GO:0007601) and the associated KEGG pathway was *'Phototransduction'* (*n*=4 sasa04744).

A total of 984/2596 mRNA transcripts were converted by DAVID in the 2 to 4.99 FC group. DAVID Gene Functional Classification tool identified 37 clusters. Cluster 1 (ES 6.7) was associated with *'growth factor activity'* (*n*=14/16 GO:0008083) and UniProt keywords such as *'Signal'* (*n*=15/16 KW-0732). Cluster 2 (ES 5.4) was linked to terms such as *'collagen trimer'* (*n*=15/18 GO:0005581) and UniProt keywords such as *'Signal'* (*n*=16/18 KW-0732).

Associated KEGG pathways were *'Cytoskeleton in muscle cells', 'Cytokine-cytokine receptor interaction', 'Motor proteins', 'Glycolysis/ Gluconeogenesis', 'ECM-receptor interaction'* and 'Starch and sucrose metabolism' (*n*=48 sasa04820, *n*=34 sasa04060, *n*=23 sasa04814, *n*=11 sasa00010, *n*=13 sasa04512, *n*=7 sasa00500).

GO:BP_D associated terms were *'visual perception', 'muscle contraction'* and *'behavior'* (*n*=18 GO:0007601, *n*=13 GO:0006936, *n*=4 GO:0007610). GO:BP_A terms were *'developmental process'*, '*multicellular organismal process'* and *'response to external stimulus'* (*n*=149 GO:0032502, *n*=148 GO:0032501, *n*=40 GO:0009605).

GO:MF_D terms were *'cytokine activity'*, *'growth factor activity'* and *'melanin-concentrating hormone activity'* (*n*=24 GO:0005125, *n*=19 GO:0008083, *n*=4 GO:0030354, GO:0031777). GO:MF_A terms were *'signaling receptor regulator activity'*, *'cytokine activity'* and *'signaling receptor binding'* (*n*=53 GO:0030545, *n*=29 GO:0005125, *n*=67 GO:0005102).

Within the <-10 FC bin, DAVID successfully mapped 16/55 mRNA transcripts. No associated terms, or clusters were identified but *'Neuroactive ligand-receptor interaction'* pathway was significantly associated with these mRNA transcripts (*n*=4 sasa04080).

Within the -5 to -9.99 FC group, DAVID successfully mapped 89/294 mRNA transcripts to gene IDs. DAVID Gene Functional Classification tool identified 3

clusters, with forkhead box protein D1-like (106590051), forkhead box protein Q1 (106599739), interferon regulatory factor 1 (106589795) forkhead box G1a (foxg1a) mRNA transcripts in cluster 1 linked to transcription regulation (GO:0006357). Only 2 significant GO terms were identified in this group. GO:BP_D *'DNA catabolic process'* and GO:MF_D 'DNA nuclease activity' (*n*=3 GO:0006308, *n*= 3 GO:0004536). No KEGG pathways were identified.

In the -2 to -4.99 FC group, DAVID converted 731/2211 mRNA transcripts to gene IDs. DAVID Gene Functional Classification identified 22 clusters. Cluster 1 (ES 5.74) associated 62 mRNA transcripts with UniProt keywords such as *'Membrane'* (KW-0472) while cluster 2 (ES 4.51) consisting of 13 keratin mRNA transcripts and intermediate filament protein ON3 (106566665), uncharacterized 106561488 (106561488) was associated with UniProt terms such as *'Coiled coil'* (KW-0175).

GO:BP_D terms were *'G protein-coupled receptor signaling pathway', 'chordate embryonic development'* and *'embryonic morphogenesis'* (*n*=32 GO:0007186, *n*=7 GO:0043009, *n*=7 GO:0048598). GO:BP_A terms were *'multicellular organismal process'*, *'G protein-coupled receptor signaling pathway'*, '*cell communication'* and '*response to stimulus'* (*n*=59 G GO:0032501, *n*=100 GO:0007186, *n*=122 GO:0007154, *n*=144 GO:0050896).

GO:MF_D associated terms were *'structural molecule activity'*, *'neuropeptide hormone activity'* and *'hormone activity'* (*n*=14 GO:0005198, *n*=6 GO:0005184, *n*=10 GO:0005179). GO:MF_A terms were *'signaling receptor activity'*, *'molecular transducer activity'* and *'molecular function regulator activity'* (*n*= 83 GO:0038023, *n*=83 GO:0060089, *n*=64 GO:0098772). Associated KEGG pathways were *'Neuroactive ligand-receptor interaction'* and *'Cytokine-cytokine receptor interaction'* (*n*=38 sasa04080, *n*=21 sasa04060).

4.3.4.5 Heart GSEA

A total of ↑2076 and ↓3619 mRNA transcripts were mapped to Gene IDs by DAVID resulting in a total of ↑831 and ↓1897. Heart upregulated GO:BP_D associated terms were *'G protein-coupled receptor signaling pathway*' and

'cGMP biosynthetic process' (*n*=34 GO:0007186, *n*=7 GO:0006182) with GO:BP_A terms '*cell communication'*, '*response to stimulus'* and *'immune system process'* (*n*=160 GO:0007154, *n*=176 GO:0050896, GO:000237639). No GO:MF_D terms were associated but GO:MF_A terms were *'signaling receptor activity'*, *'molecular transducer activity'* and '*G protein-coupled receptor activity'* (*n*=89 GO:0038023, *n*=89 GO:0060089, *n*=43 GO:0004930). Associated KEGG pathways were *'Neuroactive ligand-receptor interaction'* and *'Cytokine-cytokine receptor interaction'* (*n*=31 sasa04080, *n*=21 sasa04060). Gene Functional Classification identified 32 clusters in the upregulated heart tissue with the top 3 highest ES of 5.57, 4.09 and 3.29.

GO term associations indicated an increase in cellular signalling pathways involving G protein-coupled receptors (GPCRs) and cyclic guanosine monophosphate (cGMP). GPCRs are involved in sensing environmental changes and initiating cellular responses. In fish, GPCR signalling may play a role in hypoxia-induced changes in blood flow, ion regulation, and metabolic adjustments as well as possible osmoregulation and stress responses. Nitric oxide (NO) is said to regulate cardiac performance, control the stress response from thermal and oxygen variation, additionally studies have demonstrated that it increases cGMP in fish exposed to hypoxia (Peter et al., 2022). Upregulation of mRNA transcripts associated with '*response to stimulus'* suggest sensing and adaption to hypoxia possibly through the increase in cell communication. The upregulation of neurotransmitters, hormones, and their receptors may indicate a regulation of the heart function. An increase in cytokine signalling may lead to possible mitigation of the hypoxia induced inflammation and oxidative stress.

Heart downregulated GO:BP_D terms were *'negative regulation of endopeptidase activity'*, *'blood coagulation'* and '*SMAD protein signal transduction'* (*n*=17 GO:0010951, *n*=17 GO:0007596, *n*=21 GO:0060395). GO:BP_A terms were *'monoatomic ion transport'*, '*multicellular organismal process'* and '*transmembrane transport*' (*n*=136 GO:0006811, *n*=276 GO:0032501, *n*=144 GO:0055085). GO:BP_A terms were *'transporter activity'*, *'channel activity'* and *'transmembrane transporter activity'* (*n*=199 GO:0005215, *n*=115 GO:0015267, *n*=184 GO:0022857).

Associated downregulated pathways were *'Adrenergic signaling in cardiomyocytes'*, '*Neuroactive ligand-receptor interaction'* and *'Calcium signaling pathway'* (*n*=41 sasa04261, *n*=69 sasa04080, *n*=53 sasa04020). Gene Functional Classification identified 87 clusters in the downregulated heart tissue with the top 3 highest ES of 27.75, 24.16 and 19.34.

Overall, the downregulated GO terms were associated with reduced ion transport, growth, repair and signalling activity, suggesting possible adaptions towards energy conservation and survival by downregulated non-essential processes. Downregulation of biological processes such as '*SMAD protein signal transduction'* may suggest signalling through TGF-*b* cytokines, which are involved in cell proliferation, differentiation, apoptosis, extracellular matrix (ECM), tissue homeostasis and tissue healing/regeneration. The downregulation of molecular processes such as transporters and channel activity may suggest a response to energy preservation.

Downregulated KEGG pathways suggested a possible decrease in heart rate and metabolic demand to minimize oxygen consumption as adrenergic signalling regulates heart rate and contractility. Downregulation of signalling between neurotransmitters, hormones, and their receptors as well as calcium signalling may suggest an adaptive strategy to reduce energy use and possible maintain energy homeostasis.

4.3.4.5.1 Heart bins

The only upregulated GO terms identified were in the 2 to 4.99FC category. GO:BP_D associated the mRNA transcripts with '*G protein-coupled receptor signaling pathway*' and '*cGMP biosynthetic process*' (GO:0007186, GO:0007186) with the higher terms '*biological regulation'*, '*cell communication*' and '*response to stimulus*' (GO:0065007, GO:0007154, GO:0050896). The only GO:MF_D term was '*guanylate cyclase activity'* (GO:0004383) while GO:MF_A associated terms were '*signaling receptor activity'*, '*transmembrane signaling receptor activity'* and *'molecular transducer activity'* (GO:0038023, GO:0004888, GO:0060089). The upregulated heart GO term associations in this category were similar to the combined upregulated heart GO terms previously discussed previously. These

signalling pathways suggest an adaption by enhanced cardiac function, cytokine signalling, metabolic shifts and signalling adaptation in relation to hypoxic conditions.

Amongst the downregulated mRNA transcripts, GO:BP_D terms in the <-10 FC category were '*potassium ion transmembrane transport'* (GO:0071805) with '*transmembrane transport'* '*potassium ion transport'* and '*monoatomic ion transport'* (GO:0055085, GO:0006813, GO:0006811) in the higher term GO:BP_A. GO:MF_D associated terms were '*transmembrane transporter activity'*, '*passive transmembrane transporter activity'* and *'transporter activity'* (GO:0022857, GO:0022803, GO:0005215).

The downregulation of the GO terms possibly indicates an energy conservation strategy by reducing ion regulatory processes. In mammalian studies, hypoxia may lead to the downregulation of Na+/K+-ATPase cellular activity in order to maintain cellular ATP levels (Gusarova et al., 2011). These associated GO terms may signify energy conservation.

The next category down, -5 to -9.99 FC, GO:BP_D terms were '*negative regulation of endopeptidase activity'*, '*blood coagulation'* and '*proteolysis*' (GO:0010951, GO:0007596, GO:0006508). Higher term GO:BP_A associations were '*regulation of body fluid levels', 'negative regulation of hydrolase activity'* and *'negative regulation of molecular function' (*GO:0050878, GO:0051346, GO:0044092).

GO:MF_D terms were '*serine-type endopeptidase inhibitor activity'*, *'serine-type endopeptidase activity'* and '*cysteine-type endopeptidase inhibitor activity*' (GO:0004867, GO:0004252, GO:0004869) with the higher molecular terms '*enzyme inhibitor activity'*, '*peptidase inhibitor activity*' and '*molecular function inhibitor activity*' (GO:0004857, GO:0030414, GO:0140678).

Within this category, biological processes appear to suggest a possible effect on the recycling of AAs, remodelling/ restructure of proteins while potentially shifting enzymic activity towards energy-saving.

Within the largest downregulated category, -2 to -4.99 FC, GO:BP_D associated terms were '*transmembrane transport'*, '*SMAD protein signal transduction'* and

'*hyaluronan biosynthetic process'* (GO:0055085, GO:0060395, GO:0030213) with the higher terms '*monoatomic ion transport'*, '*transport*' and '*multicellular organismal process*' (GO:0006811, GO:0006810, GO:0032501). Associated terms within GO:MF_D were *'cytokine activity', 'growth factor activity'* and *'signaling receptor activity'* (GO:0005125, GO:0008083, GO:0038023). The higher terms were '*transporter activity*' and '*signaling receptor binding*' (GO:0005215, GO:0005102).

Biological and molecular GO term associations indicate reduced cellular communication, transport, possible suppression of growth processes and reduced tissue growth/repair. Suggesting a broad downregulation of processes involved in function possibly indicative of energy conservation.

KEGG pathways associated with this category were '*Adrenergic signaling in cardiomyocytes*', *'Neuroactive ligand-receptor interaction'*, '*Cell adhesion molecules'*, *'Cytokine-cytokine receptor interaction'* and the '*Calcium signaling pathway*' (sasa04261, sasa04080, sasa04514, sasa04060, sasa04020).

KEGG pathway associations suggest possible energy saving strategies by reducing cardiac output/energy expenditure, neural signalling, cell-cell communication/ tissue remodelling, cytokine signalling and calcium signalling.

4.3.4.6 Summary of GSEA

In summary, differences in GO term associations between the up- and downregulated mRNA transcripts occurred. The trends identified in the upregulated mRNA transcripts were associated with communication, response to stimulus and multicellular organismal processes whereas the overall trend amongst downregulated transcripts appeared to suggest an adaptive response linked to energy conservation and a possible reduction in excessive immune responses.

The upregulated homeobox proteins and transcription factors suggested a compensatory response to hypoxia, potentially enhancing cell survival and regionalisation processes. Neurotransmission and synaptic activity in the downregulation of synaptic proteins and neurotransmitter receptors suggests a

possible suppression of neural activity, possibly an adaptive response in energy conservation. Calcium signalling and transport processes through the modulation of calcium channel mRNA transcripts suggests an important role for intracellular calcium homeostasis as a hypoxia response. Tissue-specific responses in liver and brain, exhibited pronounced metabolic and transcriptional shifts, while the heart showed relatively fewer transcriptomic changes.

Pathways such as the enrichment of '*Neuroactive ligand-receptor interaction*' and '*Cytokine-cytokine receptor interaction*' in both up- and downregulated datasets indicates complex regulatory mechanisms governing the hypoxic response in Atlantic salmon. This dual regulation may be a result of specific components of these pathways being up- or downregulated. Upregulation of the '*Neuroactive ligand-receptor interaction*' pathway may be involved in adaptive responses to hypoxia such as increased cardiac output and vasodilation while downregulation may conserve energy through the reduction of non-essential neural communication or possibly excessive hormone release. Upregulation of the '*Cytokine-cytokine receptor interaction*' pathway may suggest upregulation of pro-inflammatory cytokines like interleukin-6 (IL-6) or tumour necrosis factor-alpha (TNF-α) as a response to damage such as inflammation and oxidative stress due to hypoxia. Whereas downregulation may reduce non-essential cytokines, or harmful cytokines suggesting an energy saving strategy and a prevention of cytokine overactivation. In addition to this, the half-lives of cytokines range from minutes to hours, neurotransmitters last seconds, and neurotransmitter enzymes range from hours to days. This may suggest why excessive mRNA transcripts were identified. An alternative theory may be that these are the most studied genes from a pharmacological perspective, and therefore there have been more studies which may affect the annotation and ID of these mRNA transcripts.

4.3.5 mTOR pathway associations

Hypoxia has been demonstrated as inhibiting mTOR1; further analysis was used to identify mTOR pathway mRNA transcripts between treatments. In liver and brain tissue the largest quantity of mRNA transcripts were upregulated in D1L,

with the opposite occurring in heart tissue, with most mRNA transcripts downregulated in D1L. The largest number of mRNA transcripts associated with the mTOR pathway were in liver (*n*=20) and brain tissues (*n*=8) and the least in heart tissue (*n*=9) (Table 4.7).

4.3.5.1 Liver mTOR pathway mRNA transcripts of interest

A total of 20 (↑10, ↓10) mTOR associated mRNA transcripts were identified in liver tissue (Figure 4.12, Table 4.9).

All upregulated mRNA transcripts were identified within the 2 to 4.99 FC group and similarly 9 mRNA transcripts were identified between -2 to -4.99 and 1 in the <-10 FC group. mRNA transcripts identified between >2 to 4.99 FC were 4F2 cell-surface antigen heavy chain (↑2.30FC, 4F2/ SLC3A2) E3 ubiquitin-protein ligase RNF152-like (↑4.98FC, 106590060), S-phase kinase-associated protein 2-like (↑3.41FC, SKP2), STE20-related kinase adapter protein beta-like (↑2.26FC, STE20), cytosolic arginine sensor for mTORC1 subunit 1 (↑2.60FC, CASTOR1/ GATSL3?), large neutral amino acids transporter small subunit 1 (↑2.74FC, SLC7A5), proline-rich protein 5 (↑2.04FC, PRR5A), protein wnt-9b-like (↑2.19FC, WNT9B), proto-oncogene Wnt-3 (↑2.06FC, WNT3), tumour necrosis factor alpha (↑4.52FC, TNFA).

Table 4.7 Total mRNA transcripts by tissue associated to the mTOR pathway within the set bins and totals (%).

Tissue	Total (start)	INF/NA		Total	DAVID (ID)	mTOR pathway Bins			Total (%)	DAVID (%)
						2 to 5	5 to 10	>10		
Liver	6699	3014	↑	3685	1339	10			0.3	0.7
	4830	2266	↓	2564	1235	9		1	0.4	0.8
Brain	5066	1989	↑	3077	1188	3	1	1	0.2	0.4
	4736	2176	↓	2560	836	3			0.1	0.4
Heart	4661	2585	↑	2076	833	2	1		0.1	0.4
	6590	2972	↓	3618	1902	5		1	0.2	0.3

Total (start)= total mRNA transcripts, INF/NA= number of total mRNA transcripts not computable, Total= Total all subtracting the INF/NA, DAVID ID= Number of mRNA transcripts successfully identified by DAVID, Total (%)= Transcript (%) of Total, DAVID (%)= Transcript (%) of mapped DAVID IDs. ↑= upregulated in D1L, ↓= downregulated in D1L.

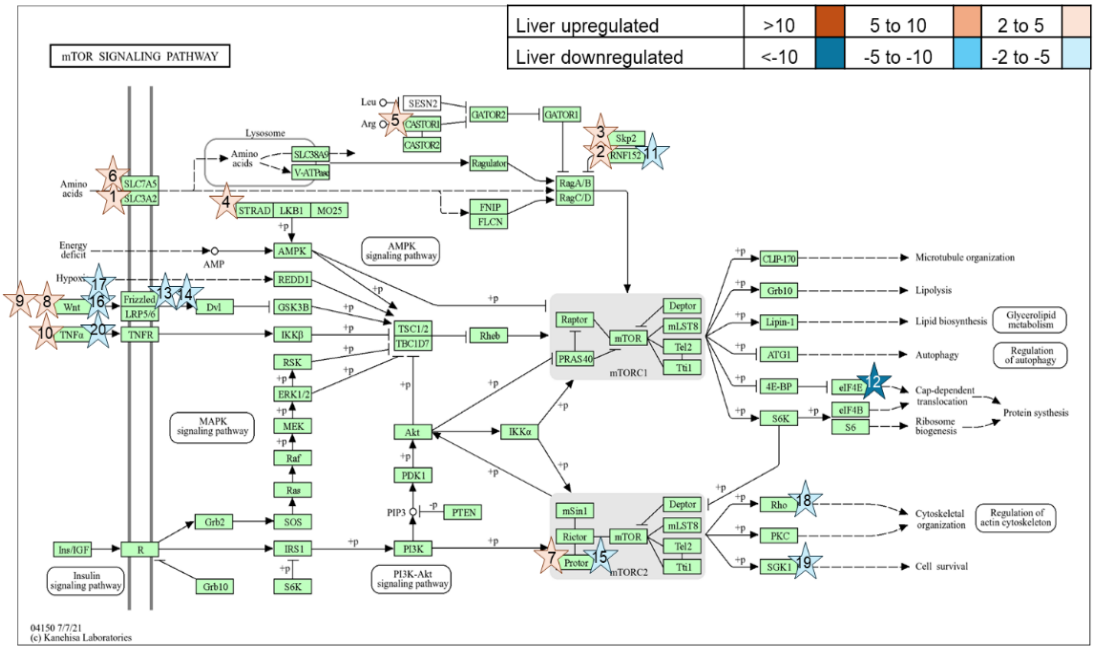


Figure 4.12 Liver mTOR pathway up- and downstream mRNA transcripts of interest. D1L upregulated in orange and downregulated in blue. Darkness of colours indicate higher fold number comparisons. (KEGG v.112.0). See Table 4.8 for identification and fold change.

The <-2 to -4.99 FC bin identified E3 ubiquitin-protein ligase RNF152-like (↓-3.87FC, 106578589), frizzled-7-A (↓-2.21FC, 106582548), frizzled-9 (↓-2.20, 106603626), proline-rich protein 5 (↓-2.52FC, PRR5), protein Wnt-10b-like (↓-4.67FC, WNT10B), protein Wnt-7b (↓-2.75FC, WNT7BB), rho-related GTP-binding protein rhoa-a (↓-2.05FC, RHOA), serine/threonine-protein kinase sgk1 (↓-3.24FC, 106589037), tumour necrosis factor a (TNF superfamily, member FA/ TNFA4).

Myrka & Buck (2021) suggested that RHOA may be triggered by hypoxia in various cells, and in mouse cell lines has been shown to disrupt the cell structure and intercellular adhesion in hepatocytes. In addition, the reduction in size of the hepatocytes may be indicative of a reduction in metabolic rate and inhibition of protein synthesis.

The only transcript identified in the <-10 FC bin was eukaryotic translation initiation factor 4E family member 2 (↓-11.06 FC, EIF4E2). With links to protein biosynthesis and associated with terms such as *'translation initiation'* (GO:0006413) and *'translation initiation factor activity'* (GO:0003743). Eukaryotic translation initiation factor 4E (ELF4E) is the mRNA cap binding protein and is

the master switch for eukaryotic translation, to activate it, ELF4A and ELF4G have to be bound to EIF4E, with 4E-BP (4E- binding proteins) located on the ELF4G binding site, subsequently downregulating translation of ELF4E (Matsuo et al., 1997).

In humans, translational initiation factors have been identified as a family consisting of EIF4E1, EIF4E2 and EIF4E3, with Mrvová et al. (2018) indicating that human EIF4E2 could have between 2 to 4 variants. Ho et al. (2016) in a study using human cell lines, implied a hypoxic translation initiation complex, $EIF4F^{H}$, (EIF4E2, EIF4A and EIF4G3/ EIF4G1) in addition to the normoxic EIF4F (EIF4E, EIF4A and EIF4G1). Brain mTOR pathway mRNA transcripts of interest

Of the 5636 mRNA transcripts, 2024 were converted by DAVID to gene IDs (1188/3076↑, 836/2560↓). Of these, only 8 mRNA transcripts were associated with the mTOR pathway. In upregulated brain mRNA transcripts, ↑5 mRNA transcripts were identified (*n*=3, *n*=1 in 5 to 10, *n*=1 in 10 up) and ↓3 in downregulated mRNA transcripts (*n*=3 in -2 to -5 FC) (Figure 4.13, Table 4.9).

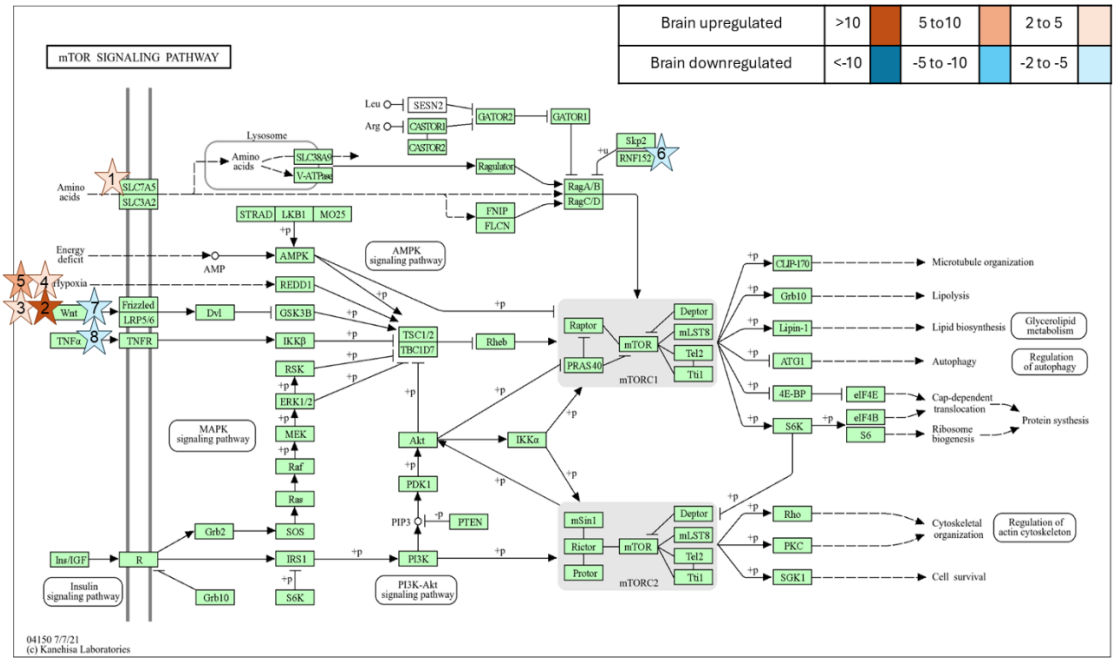


Figure 4.13 Brain mTOR pathway up-and downstream mRNA transcripts of interest. Diet 1 hypoxia (D1L) upregulated in orange and downregulated in blue. Darkness of colours indicate higher fold comparisons. (KEGG v.112.0) See Table 4.8 for identification and fold change.

In the 2 to 5 FC category the 3↑ mRNA transcripts were large neutral amino acids transporter small subunit 1-like (↑2.70 FC, 106587978), protein wnt-6-like (↑2.27 FC, WNT6B) and protein wnt-8a-like (↑2.33FC, WNT8A). There was 1↑ mTOR associated transcript in the 5 to 10 FC group, wingless-type MMTV integration site family, member 4b (↑5.47FC, WNT4B) and 1↑ in the >10 group identified as protein wnt-2-like (↑15.50FC, WNT2).

The 3↓ mTOR associated mRNA transcripts in the -2 to -5 FC group were E3 ubiquitin-protein ligase RNF152 (↓-2.28FC, RNF152), protein wnt-1 (↓-3.68FC, WNT1) and tumour necrosis factor a (TNF superfamily, member 2) (↓-3.81, TNFA/ TNFA4).

4.3.5.2 Heart mTOR pathway mRNA transcripts of interest

A total of ↑831/2076 and ↓1897/3619 mRNA transcripts were mapped to Gene IDs by DAVID. Heart had the least number of upregulated mRNA transcripts of all the tissues, with only ↑3 mRNA transcripts associated to the mTOR pathway. Downregulated mRNA transcripts identified 6 mTOR related mRNA transcripts, with 5/6 occurring between -2 to -4.99FC (Figure 4.14, Table 4.9).

Between 5 to 9.99 FC, 1 transcript was identified as dual specificity mitogen-activated protein kinase, kinase 2-like (↑5.71 FC, MAP2K2B) and between 2 to 4.99 FC an additional 2 mRNA transcripts were identified as frizzled-3-like (↑3.90 FC, 106610748), tumour necrosis factor alpha-2 precursor (↑4.52 FC, TNF-ALPHA-2).

In the bin category <-2 to -4.99, 5 mTOR related mRNA transcripts were identified as protein Wnt-16 (↓-2.06 FC, WNT16), protein Wnt-6 (↓-3.47 FC, WNT6B), protein wnt-9b-like (↓ -4.02 FC, WNT9B), tumour necrosis factor a (TNF superfamily, member 2) (↓-2.83 FC, TNFA/ TNFA4) and wingless-type MMTV integration site family, member 5a (↓-2.28 FC, WNT5A).

In the <-10 bin, only 1 transcript was associated with the mTOR pathway, large neutral amino acids transporter small subunit 1-like (106587978) which had the largest FC amongst all mTOR associated mRNA transcripts (↓-60.73 FC).

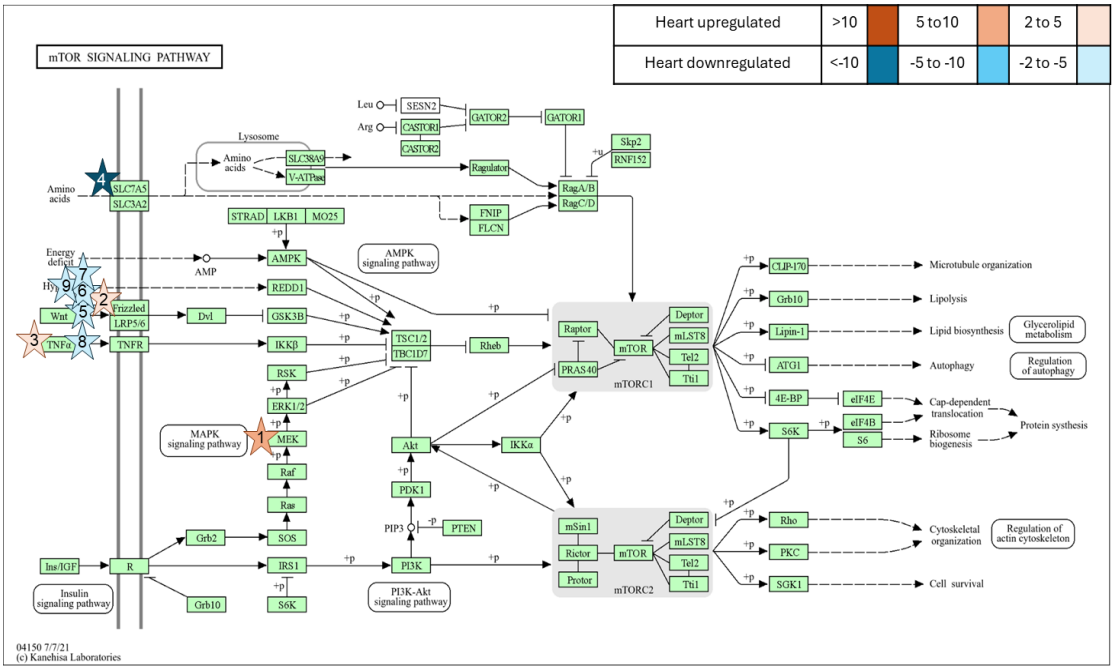


Figure 4.14 Heart mTOR pathway up- and downstream mRNA transcripts of interest. Diet 1 hypoxia (D1L) upregulated in orange and downregulated in blue. Darkness of colours indicate higher fold comparisons.(KEGG v.112.0). See Table 4.8 for identification and fold change.

Cassidy & Lamarre (2019) in a study examining tissue-specific effects of hypoxia on Arctic char (*Salvelinus alpinus*) mRNA transcripts and phosphorylation of proteins, suggested that heart tissue was less responsive than liver and muscle to hypoxia, proposing that salmonid hearts had access to oxygen via the coronary artery and therefore the last tissue to become hypoxic. This may explain response in downregulated heart tissue (831↑, 1897↓) compared to upregulated liver and brain tissues yielding the largest response**.**

4.3.5.2.1 Duplicated mTOR mRNA transcripts

Several duplicated mRNA transcripts were identified such as E3 ubiquitin-protein ligase RNF152-like was identified in both up- and downregulated liver as well as in downregulated brain tissues (↑4.98FC ssa19, ↓-3.87FC ssa29 and ↓-2.28FC ssa14) (Table 4.8).

Proteostasis is partly regulated by ubiquitin-mediated protein degradation. Zambrano-Carrasco et al. (2024) stated that the members may degrade up to 20% of cellular proteome. Ubiquitination of protein consists of 3 enzymes, E1, E2 and E3, with E3 mediating the linkage of E2 to a lysine residue in the final step.

Table 4.8 Duplicated mTOR associated mRNA transcripts identified in multiple tissues up- and downregulated.

Tissue		Gene ID	Location	Name
Liver	↓	106578589	ssa19	E3 ubiquitin-protein ligase RNF152-like (106578589) ENSSSAG00000092453
Brain	↓	106569247	ssa14	E3 ubiquitin-protein ligase RNF152 (106569247) ENSSSAG00000118842
Liver	↑	106590060	ssa29	E3 ubiquitin-protein ligase RNF152-like (106590060) ENSSSAG00000119062
Liver	↓	106589058	ssa27	tumour necrosis factor a (TNF superfamily, member 2) (106589058) ENSSSAG00000093995
Heart	↓	106589058	ssa27	tumour necrosis factor a (TNF superfamily, member 2) (106589058) ENSSSAG00000093995
Brain	↓	106589058	ssa27	tumour necrosis factor a (TNF superfamily, member 2) (106589058) ENSSSAG00000093995
Liver	↑	100136509	ssa14	tumour necrosis factor alpha (100136509) ENSSSAG00000044993
Heart	↑	100136458	ssa02	tumour necrosis factor alpha-2 precursor (100136458) ENSSSAG00000053783
Heart	↓	106587978	ssa26	large neutral amino acids transporter small subunit 1-like (106587978) ENSSSAG00000105539
Liver	↑	106573635	ssa16	large neutral amino acids transporter small subunit 1 (106573635) ENSSSAG00000051886
Brain	↑	106587978	ssa26	large neutral amino acids transporter small subunit 1-like (106587978) ENSSSAG00000105539
Liver	↓	100286559	ssa17	proline-rich protein 5 (100286559) ENSSSAG00000096966
Liver	↑	100286559	ssa17	proline-rich protein 5 (100286559) ENSSSAG00000072238
Heart	↓	106601131	ssa03	protein Wnt-9b-like (106601131) ENSSSAG00000022591
Liver	↑	106601131	ssa03	protein Wnt-9b-like (106601131) ENSSSAG00000022591

This variation in transcript abundance between tissues in the current study may be due to cellular oscillation involved in proteostasis.

Although chromosomal locations differed for all 3 mRNA transcripts, this occurrence was likely due to whole-genome duplication (WGD) as discussed by Lien et al. (2016), with chromosomes ssa29 and ssa19 demonstrating elevated levels of repetitive sequences. In addition to possible cellular homeostasis mechanisms and WGD, these mRNA transcripts may not even be E3 ubiquitin-protein ligases.

Tumour necrosis factor a (TNF superfamily, member 2) was found across all tissues downregulated and located on chromosome ssa27. Tumour necrosis factor alpha (100136509) was found on ssa14 (↑liver) and tumour necrosis factor alpha-2 precursor (100136458) on ssa02 (↑heart). Chromosomes ssa27 and ssa14 share homeologous regions but ssa02 does not.

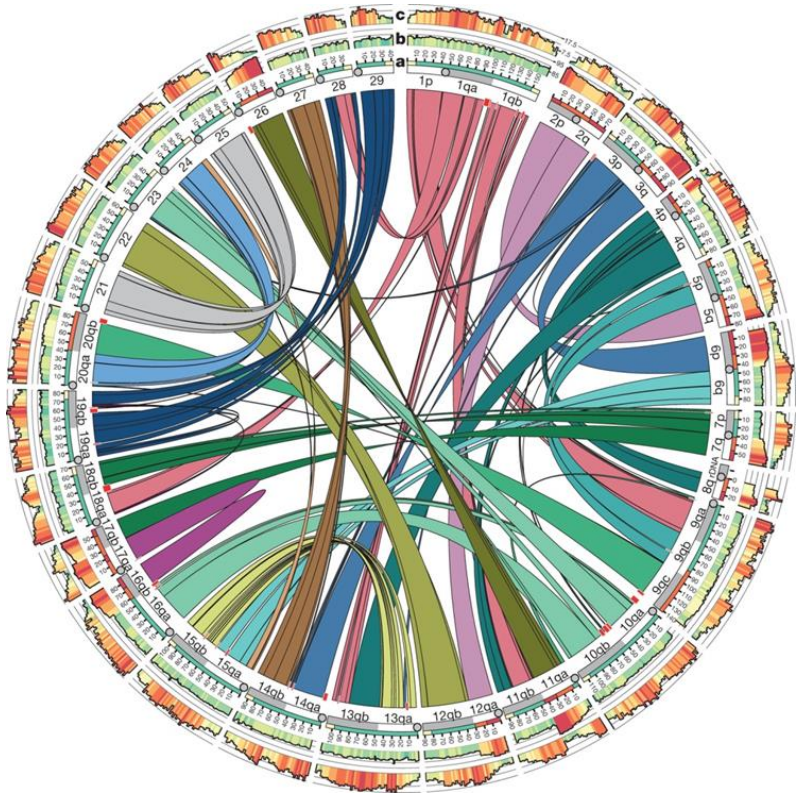


Figure 4.15 The duplicated Atlantic salmon genome from Lien et al. (2016).

Large neutral amino acids transporter small subunit 1-like was located on chromosome ssa26 and found downregulated in heart (↓-60.73FC) and upregulated in brain (↑2.70 FC) while large neutral amino acids transporter small subunit 1 was located on chromosome ssa16 in upregulated liver tissue (↑2.74FC). These chromosomes do not appear to share homeologous regions, but both have sequences not identified elsewhere (Figure 4.15).

Proline-rich protein 5 (PRRR5) was located on chromosome ssa17 and found in both up- and downregulated liver tissue (↑2.04FC, ↓-2.52FC). Similarly, protein WNT-9B-like was located on chromosome ssa03 and found in upregulated liver and downregulated heart tissue (↑2.19FC, ↓-4.02FC).

4.3.5.3 Heatmaps

Classifications of the top 50 mRNA transcripts by variance in liver tissue had the highest contribution from PC (43/50). A similar trend was seen in brain and heart tissues (35/50, 43/50).

Table 4.9 Identified mRNA transcripts of interest associated with the mTOR pathway from mRNA transcripts in liver, brain and heart tissue FC. Location of the GOIs in the mTOR pathway, FCs with both up- and downregulated mRNA transcripts for Diet 1 hypoxia (D1L) and the associated KEGG pathways. Normalised data analysed using DAVID. FC= fold change.

	Gene ID and ENSEMBL No.	Aliases	mTOR	Location	FC	Associated pathways in Atlantic salmon (KEGG sasa)
	Liver					
1	4F2 cell-surface antigen heavy chain (106563501) ENSSSAG00000111850	4F2, SLC3A2	↑mTOR	ssa11	↑2.30	sasa04150 mTOR Signalling pathway, sasa04216 Ferroptosis
2	E3 ubiquitin-protein ligase RNF152-like (106590060) ENSSSAG00000119062		↑mTOR	ssa29	↑4.98	sasa04150 mTOR signalling pathway GO:1904262: negative regulation of TORC1 signaling inhibition of TORC1 signaling
3	S-phase kinase-associated protein 2-like (106568170) ENSSSAG00000068716	SKP2	↑mTOR	ssa13	↑3.41	sasa04068 FoxO signaling pathway, sasa04110 Cell cycle, sasa04120 Ubiquitin mediated proteolysis, sasa04150 mTOR signaling pathway
4	STE20-related kinase adapter protein beta-like (106573852) ENSSSAG00000086478	STE20	↑mTOR	ssa16	↑2.26	sasa04150 mTOR signalling pathway
5	cytosolic arginine sensor for mTORC1 subunit 1 (106585238) ENSSSAG00000098539	CASTOR1, GATSL3??	↑mTOR	ssa24	↑2.60	sasa04150 mTOR signalling pathway
6	large neutral amino acids transporter small subunit 1 (106573635) ENSSSAG00000051886	SLC7A5	↑mTOR	ssa16	↑2.74	sasa04150 mTOR signalling pathway
7	proline-rich protein 5 (100286559) ENSSSAG00000072238	PRR5A	↑mTOR2	ssa17	↑2.04	sasa04150 mTOR signalling pathway
8	protein Wnt-9b-like (106601131) ENSSSAG00000022591	WNT9B	↑mTOR	ssa03	↑2.19	sasa04150 mTOR signaling pathway, sasa04310 Wnt signaling pathway, sasa04916 Melanogenesis
9	proto-oncogene Wnt-3 (106589299) ENSSSAG00000105288	WNT3	↑mTOR	ssa28	↑2.06	sasa04150 mTOR signaling pathway, sasa04310 Wnt signaling pathway, sasa04916 Melanogenesis
10	tumor necrosis factor alpha (100136509) ENSSSAG00000044993	TNFA	↑mTOR	ssa14	↑4.52	sasa04010 MAPK signaling pathway, sasa04060 Cytokine-cytokine receptor interaction, sasa04150 mTOR signaling pathway, sasa04210 Apoptosis, sasa04217 Necroptosis, sasa04350 TGF-beta signaling pathway, sasa04620 Toll-like receptor signaling pathway, sasa04621 NOD-like receptor signaling pathway, sasa04622 RIG-I-like receptor signaling pathway, sasa04625 C-type lectin receptor signaling pathway, sasa04920 Adipocytokine signaling pathway, sasa05132 Salmonella infection, sasa05168 Herpes simplex virus 1 infection

11	E3 ubiquitin-protein ligase RNF152-like (106578589) ENSSSAG00000092453		↑mTOR	ssa19	↓3.87	sasa04150 mTOR signalling pathway GO:1904262: negative regulation of TORC1 signaling, inhibition of TORC1 signaling
12	eukaryotic translation initiation factor 4E family member 2 (106600575) ENSSSAG00000066237	EIF4E2	mTOR↓	ssa03	↓11.06	sasa04150 mTOR signaling pathway, sasa04910 Insulin signaling pathway
13	frizzled-7-A (106582548) ENSSSAG00000050171		↑mTOR	ssa21	↓2.21	sasa04150 mTOR signaling pathway, sasa04310 Wnt signaling pathway, sasa04916 Melanogenesis
14	frizzled-9 (106603626) ENSSSAG00000086833		↑mTOR	ssa04	↓2.20	sasa04150 mTOR signaling pathway, sasa04310 Wnt signaling pathway, sasa04916 Melanogenesis
15	proline-rich protein 5 (100286559) ENSSSAG00000096966	PRR5	↑mTOR2	ssa17	↓2.52	sasa04150 mTOR signalling pathway GO:0038203: involved in TORC2 signaling, part of TORC2 complex
16	protein Wnt-10b-like (106572675) ENSSSAG00000067794	WNT10B	↑mTOR	ssa15	↓4.67	sasa04150 mTOR signaling pathway, sasa04310 Wnt signaling pathway, sasa04916 Melanogenesis
17	protein Wnt-7b (106584495) ENSSSAG00000086070	WNT7BB	↑mTOR	ssa23	↓2.75	sasa04150 mTOR signaling pathway, sasa04310 Wnt signaling pathway, sasa04916 Melanogenesis
18	rho-related GTP-binding protein rhoa-a (106592002) ENSSSAG00000116020	RHOA	mTOR2↓	ssa15	↓2.05	sasa04144 Endocytosis, sasa04150 mTOR signaling pathway, sasa04270 Vascular smooth muscle contraction, sasa04310 Wnt signaling pathway, sasa04350 TGF-beta signaling pathway, sasa04510 Focal adhesion, sasa04520 Adherens junction, sasa04530 Tight junction, sasa04621 NOD-like receptor signaling pathway, sasa04625 C-type lectin receptor signaling pathway, sasa04810 Regulation of actin cytoskeleton, sasa05100 Bacterial invasion of epithelial cells, sasa05132 Salmonella infection
19	serine/threonine-protein kinase Sgk1 (106589037) ENSSSAG00000070370	SI:CH211-195B13.1	mTOR2↓	ssa27	↓3.24	sasa04068 FoxO signaling pathway, sasa04148 Efferocytosis, sasa04150 mTOR signaling pathway
20	tumor necrosis factor a (TNF superfamily, member 2) (106589058) ENSSSAG00000093995	TNFA, TNFA4	↑mTOR	ssa27	↓3.10	sasa04010 MAPK signaling pathway, sasa04060 Cytokine-cytokine receptor interaction, sasa04150 mTOR signaling pathway, sasa04210 Apoptosis, sasa04217 Necroptosis, sasa04350 TGF-beta signaling pathway, sasa04620 Toll-like receptor signaling pathway, sasa04621 NOD-like receptor signaling pathway, sasa04622 RIG-I-like receptor signaling pathway, sasa04625 C-type lectin receptor signaling pathway, sasa04920 Adipocytokine signaling pathway, sasa05132 Salmonella infection, sasa05168 Herpes simplex virus 1 infection
	Brain					
1	large neutral amino acids transporter small subunit 1-like (106587978) ENSSSAG00000105539		↑mTOR	ssa26	↑2.70	sasa04150 mTOR signaling pathway
2	protein Wnt-2-like (106573123) ENSSSAG00000051639	WNT2	↑mTOR	ssa16	↑15.50	sasa04150 mTOR signaling pathway, sasa04310 Wnt signaling pathway, sasa04916 Melanogenesis

3	protein Wnt-6-like (106586152) ENSSSAG00000064418	WNT6B	↑mTOR	ssa25	↑2.27	sasa04150 mTOR signaling pathway, sasa04310 Wnt signaling pathway, sasa04916 Melanogenesis
4	protein Wnt-8a-like (106604410) ENSSSAG00000002345	WNT8A	↑mTOR	ssa05	↑2.33	sasa04150 mTOR signaling pathway, sasa04310 Wnt signaling pathway, sasa04916 Melanogenesis
5	wingless-type MMTV integration site family, member 4b (106605854) ENSSSAG00000061388	WNT4B	↑mTOR	ssa02	↑5.47	sasa04150 mTOR signaling pathway, sasa04310 Wnt signaling pathway, sasa04916 Melanogenesis
6	E3 ubiquitin-protein ligase RNF152 (106569247) ENSSSAG00000118842	RNF152	↑mTOR	ssa14	↓2.28	sasa04150 mTOR signaling pathway
7	protein Wnt-1 (106572674) ENSSSAG00000082480	WNT1	↑mTOR	ssa15	↓3.68	sasa04150 mTOR signaling pathway, sasa04310 Wnt signaling pathway, sasa04916 Melanogenesis
8	tumor necrosis factor a (TNF superfamily, member 2) (106589058) ENSSSAG00000093995	TNFA, TNFA4	↑mTOR	ssa27	↓3.81	sasa04010 MAPK signaling pathway, sasa04060 Cytokine-cytokine receptor interaction, sasa04150 mTOR signaling pathway, sasa04210 Apoptosis, sasa04217 Necroptosis, sasa04350 TGF-beta signaling pathway, sasa04620 Toll-like receptor signaling pathway, sasa04621 NOD-like receptor signaling pathway, sasa04622 RIG-I-like receptor signaling pathway, sasa04625 C-type lectin receptor signaling pathway, sasa04920 Adipocytokine signaling pathway, sasa05132 Salmonella infection, sasa05168 Herpes simplex virus 1 infection
	Heart					
1	dual specificity mitogen-activated protein kinase kinase 2-like (106600441) ENSSSAG00000081195	MAP2K2B	↑mTOR	ssa03	↑5.71	sasa04010 MAPK signaling pathway, sasa04012 ErbB signaling pathway, sasa04068 FoxO signaling pathway, sasa04140 Autophagy – animal, sasa04148 Efferocytosis, sasa04150 mTOR signaling pathway, sasa04210 Apoptosis, sasa04218 Cellular senescence, sasa04270 Vascular smooth muscle contraction, sasa04370 VEGF signaling pathway, sasa04371 Apelin signaling pathway, sasa04540 Gap junction, sasa04620 Toll-like receptor signaling pathway, sasa04810 Regulation of actin cytoskeleton, sasa04910 Insulin signaling pathway, sasa04912 GnRH signaling pathway, sasa04916 Melanogenesis, sasa05132 Salmonella infection
2	frizzled-3-like (106610748) ENSSSAG00000062930		↑mTOR	ssa09	↑3.90	sasa04150 mTOR signaling pathway, sasa04310 Wnt signaling pathway, sasa04916 Melanogenesis
3	tumor necrosis factor alpha-2 precursor (100136458) ENSSSAG00000053783	TNF-ALPHA-2	↑mTOR	ssa02	↑4.52	sasa04010 MAPK signaling pathway, sasa04060 Cytokine-cytokine receptor interaction, sasa04150 mTOR signaling pathway, sasa04210 Apoptosis, sasa04217 Necroptosis, sasa04350 TGF-beta signaling pathway, sasa04620 Toll-like receptor signaling pathway, sasa04621 NOD-like receptor signaling pathway, sasa04622 RIG-I-like receptor signaling pathway, sasa04625 C-type lectin receptor signaling pathway, sasa04920 Adipocytokine signaling

						pathway, sasa05132 Salmonella infection, sasa05168 Herpes simplex virus 1 infection
4	large neutral amino acids transporter small subunit 1-like (106587978) ENSSSAG00000105539		↑mTOR	ssa26	↓60.73	sasa04150 mTOR signaling pathway
5	protein Wnt-16 (106609305) ENSSSAG00000090697	WNT16	↑mTOR	ssa07	↓2.06	sasa04150 mTOR signaling pathway, sasa04310 Wnt signaling pathway, sasa04916 Melanogenesis
6	protein Wnt-6 (106581837) ENSSSAG00000057025	WNT6B	↑mTOR	ssa21	↓3.47	sasa04150 mTOR signaling pathway, sasa04310 Wnt signaling pathway, sasa04916 Melanogenesis
7	protein Wnt-9b-like (106601131) ENSSSAG00000022591	WNT9B	↑mTOR	ssa03	↓4.02	sasa04150 mTOR signaling pathway, sasa04310 Wnt signaling pathway, sasa04916 Melanogenesis
8	tumor necrosis factor a (TNF superfamily, member 2) (106589058) ENSSSAG00000093995	TNFA, TNFA4	↑mTOR	ssa27	↓2.83	sasa04010 MAPK signaling pathway, sasa04060 Cytokine-cytokine receptor interaction, sasa04150 mTOR signaling pathway, sasa04210 Apoptosis, sasa04217 Necroptosis, sasa04350 TGF-beta signaling pathway, sasa04620 Toll-like receptor signaling pathway, sasa04621 NOD-like receptor signaling pathway, sasa04622 RIG-I-like receptor signaling pathway, sasa04625 C-type lectin receptor signaling pathway, sasa04920 Adipocytokine signaling pathway, sasa05132 Salmonella infection, sasa05168 Herpes simplex virus 1 infection
9	wingless-type MMTV integration site family, member 5a (106566524) ENSSSAG00000106504	WNT5A	↑mTOR	ssa13	↓2.28	sasa04150 mTOR signaling pathway, sasa04310 Wnt signaling pathway, sasa04916 Melanogenesis

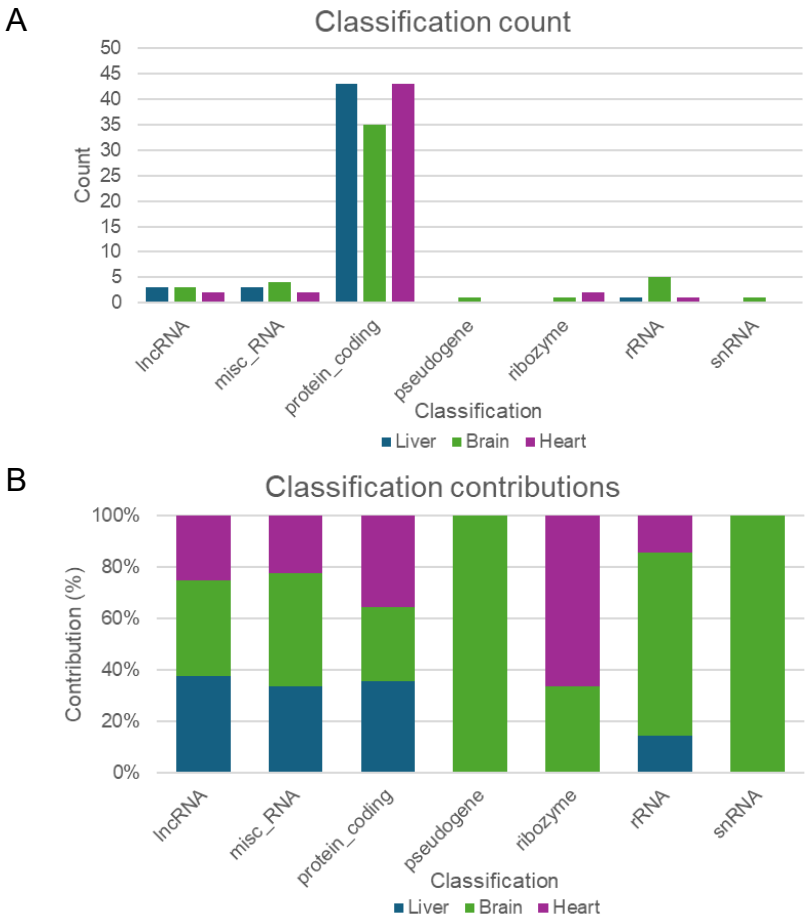


Figure 4.16 Classifications of the top 50 mRNA transcripts by variance of normalised data (FC) A) Tissue classification count B) Tissue classification contributions. Heatmaps normalised data.

Brain had the largest diversity between the 3 tissues, with mRNA transcripts classified into 7 categories, while liver had the lowest diversity (4/7). No mRNA transcripts were identified as mTOR associated (Figure 4.16 A, B, Figure 4.17 A).

GO:BP_D terms associated with liver mRNA transcripts were *'triglyceride mobilization'*, '*negative regulation of endopeptidase activity*' and 'heme transport' (*n*=3 GO:0006642, *n*=4 GO:0010951, *n*=2 GO:0015886). GO:BP_A were *'negative regulation of proteolysis', 'humoral immune response'* and *'transport'* (*n*=4 GO:0045861, *n*=4 GO:0006959, *n*=11 GO:0006810). Liver GO:MF_D associated terms were *'endopeptidase inhibitor activity', 'cholesterol transfer activity'* and *'low-density lipoprotein particle receptor binding'* (*n*=47 GO:0004866, *n*=3 GO:0120020, *n*=3 GO:0050750).

GO:MF_A terms were '*molecular function inhibitor activity'*, *'enzyme regulator activity'* and *'cysteine-type endopeptidase inhibitor activity'* (*n*=8 GO:0140678, *n*=8 GO:0030234, *n*=3 GO:0004869). The only KEGG pathway associated with the liver mRNA transcripts was *'Vitamin digestion and absorption'* (*n*=3 sasa04977) driven by apolipoprotein (100196111, 100136573, 106611125).

DAVID Gene Functional Classification tool identified 1 cluster (ES 2.67) associating hemopexin a (HPXA), transferrin-a (TFA), hemopexin b (HPXB) and serotransferrin-2-like (106599563) with UniProt keywords such as *'Iron transport'* and *'Iron'* (KW-0410, KW-0408).

Brain GO:BP_D terms were *'potassium ion import across plasma membrane', 'proton transmembrane transport'* and *'sodium ion export across plasma membrane'* (*n*=6 GO:1990573, *n*=5 GO:1902600, *n*=5 GO:0036376). Brain GO:BP_A terms were *'transport', 'import into cell'* and *'establishment of localization'* (n= 10 GO:0006810, *n*=8 GO:0098657, *n*=10 GO:0051234).

Brain GO:MF_D terms were *'P-type sodium: potassium-exchanging transporter activity', 'structural constituent of myelin sheath'* and *'ATP hydrolysis activity'* (*n*=5 GO:0005391, *n*=3 GO:0019911, *n*=5 GO:0016887). GO:MF_A associated terms were *'transmembrane transporter activity', 'metal ion binding'* and *'ATP-dependent activity'* (*n*=9 GO:0022857, *n*=10 GO:0046872, n=5 GO:0140657) (Figure 4.17 B).

Associated KEGG pathways were *'Cardiac muscle contraction', 'Adrenergic signaling in cardiomyocytes'* and *'Cytoskeleton in muscle cells'* (*n*=5 sasa04260, *n*=5 sasa04261, *n*=5 sasa04820). The pathways associated with brain mRNA transcripts were all associated with the 5 sodium/potassium-transporting ATPase subunits (100380633, 106605102, 106600489, 106583316, 106574724). DAVID Gene Functional Classification tool identified 1 cluster (ES 5.48) associating 5 sodium/potassium-transporting ATPase with UniProt keywords such as *'Transport'* and *'Sodium/potassium transport'* (KW-0813, KW-0740) (106605102, 106600489, 106583316, 106574724, 100380633).

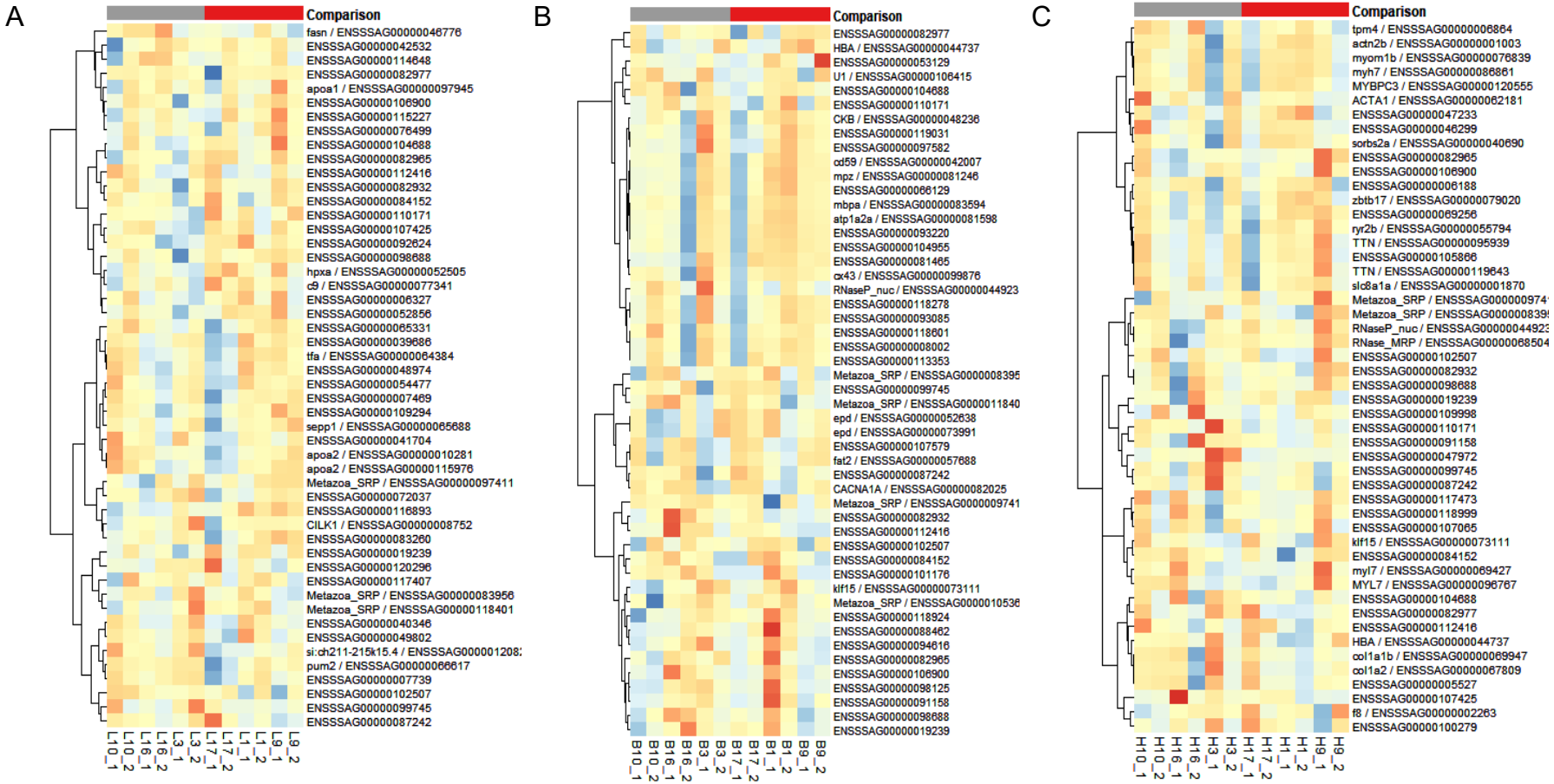


Figure 4.17 Heatmaps for the top 50 mRNA transcripts by variance for normalised data A) Liver B) Brain C) Heart. Clustered by row. Red indicated high expression and blue low expression. Grey = Normoxia , Red = Low normoxia. ShinyNGS

Heart GO:BP_D terms were *'system process', 'extracellular matrix organization'* and *'muscle contraction'* (*n*=6 GO:0003008, *n*=3 GO:0030198, *n*=3 GO:0006936).

Heart GO:BP_A were *'circulatory system process', 'muscle contraction'* and *'heart contraction'* (*n*=4 GO:0003013, *n*=4 GO:0006936, *n*=4 GO:0060047). Heart GO:MF_D associated terms were *'protein binding'* and '*extracellular matrix structural constituent'* (*n*=9 GO:0005515, *n*=3 GO:0005201). No GO:MF_A terms were associated with the mRNA transcripts. KEGG associated pathways were '*Cytoskeleton in muscle cells', 'Motor proteins'* and *'Cardiac muscle contraction'* (*n*=16 sasa04820, *n*=8 sasa04814, *n*=5 sasa04260) (Figure 4.17 C).

DAVID Gene Functional Classification tool identified 1 cluster (ES 1.89) amongst the heart mRNA transcripts associating titin (106586456, 106582275), myosin-binding protein C, cardiac-type-like (106587482) and myomesin 1b (*myom1b*) with UniProt keywords such as '*Immunoglobulin domain'* (KW-0393).

4.3.6 Hypoxia

The mTOR pathway is a key regulator of cellular metabolism, growth, and survival under hypoxia. mTOR functions in two distinct complexes: mTORC1, which promotes protein synthesis and cell growth, and mTORC2, which regulates cytoskeletal organization and cellular. Under normoxic conditions, mTORC1 is highly active, supporting anabolic processes such as protein and lipid synthesis.

However, under hypoxic conditions, mTORC1 activity is inhibited due to reduced ATP availability and activation of AMPK, an energy-sensing kinase that negatively regulates mTOR signalling (Chun & Kim, 2021).

4.3.6.1 mTOR 1 inhibition by HIF

Hypoxia triggers a complex cascade of cellular responses aimed at preserving energy and maintaining homeostasis. AMP-activated protein kinase (AMPK) and hypoxia-inducible factor (HIF-1α) levels increase under hypoxic conditions and inhibit mTOR complex in vertebrates (Olsvik et al., 2013). One of the primary regulators of the hypoxic response is hypoxia-inducible factor 1-alpha (HIF-1α), a transcription factor that activates genes involved in anaerobic metabolism,

angiogenesis, and erythropoiesis (Mandic et al., 2021). Under hypoxic conditions, HIF-1α stabilises and translocate to the nucleus, where it upregulates genes associated with glucose metabolism (Basheeruddin & Qausain, 2024) including SLC2A3 (solution carrier family 2) which encodes for GLUT3 (glucose transporter 3) linked to glycolysis.

4.3.6.2 AMPK Activation and Energy Sensing

AMPK (AMP-activated protein kinase) a conserved cellular energy sensor, activates due to low ATP levels (Richards, 2009). Increased cellular AMP:ATP ratio through processes such as glucose or reduced oxygen availability leading to metabolic stress or processes that increase ATP usage such as muscle contraction, activate AMPK.

Johansen et al. (2023) suggested that energetically costly processes such as protein synthesis may utilise 60-90% of cellular ATP. AMPK activation leads to phosphorylation of TSC1/TSC2, increasing GTPase-activating protein (GAP) activity towards Rheb and subsequent inactivation of the mTOR1 complex. AMPK can also directly phosphorylate raptor (part of the mTOR1 complex) and inhibit mTOR. Gwinn et al. (2008) suggested that AMPK was a metabolic mediator coordinating cell growth with energy status.

STE20-related kinase adapter protein beta-like (liver ↑2.26 FC) aka STRAD, MO25 and LKB1 complex were upstream from AMPK and phosphorylate AMPK under low nutrient conditions, thus inhibiting cell growth and protein synthesis by inactivating mTOR1. Initial identification through DESeq2 was unable to identify STE20 but subsequent data mining programs had conflicting results. NCBI although assigning a gene ID (106573852), categorised it as a pseudogene, Ensembl as a novel lncRNA, DAVID as STE20-related kinase adapter protein beta-like (106573852), g:Profiler as NA, ShinyGO as lncRNA and KEGG as STE20 (106573852). In addition, KEGG identified it on the mTOR pathway, additionally KEGG did list another STE20-related kinase adapter protein beta (106574923) and had both 106573852 and 106574923 listed on chromosome ssa16 whilst NCBI located 106574923 on chromosome ssa17 (ssa16 and ssa17 share homeologous regions). Although pseudogenes may produce lncRNAs and

have been demonstrated as regulators in human disorders at DNA, RNA and protein levels (Lou et al., 2020), it led to uncertainty as to the classification of STE20 (106573852) and highlighted another concern with classification, categorisation and annotation with mRNA transcripts and the complexity with downstream analysis.

4.3.6.3 Hypoxia and metabolic shifts

Under stressful conditions such as hypoxia, teleost are thought to shift from aerobic metabolism (oxidative phosphorylation) to anaerobic glycolysis reducing energy metabolism (Wu et al., 2023). When mTOR is inhibited, energy consumptive processes such as protein synthesis and lipid biosynthesis are reduced. The glycolysis pathway is upregulated by HIF-1α activation, and this metabolic shift may reduce growth. DAVID identified 16↑ and 19↓ mRNA transcripts across the tissues relating to the KEGG '*Glycolysis/ Gluconeogenesis pathway'* (sasa00010). Similarly for *'Glycerolipid metabolism'* (sasa00561) total number identified upregulated in D1L was 11↑ and 8↓. Teleosts under hypoxic conditions have adapted Glycerolipid metabolism, preferring lipolysis rather than synthesis. The catabolism of triglycerides is upregulated, producing free fatty acids and glycerol as alternate sources of energy. This is due to the oxygen and energy required for synthesis.

AA transporters, 4F2 (SLC3A2, ↑2.30 FC liver) and LAT1 (SLC7A5, ↑2.74 liver and ↑2.70 FC brain) are involved in AA sensing leading to activation of mTOR1 (Nachef et al., 2021). Investigating cancer in mammalian models, Hypoxia-inducible factor (HIF)-1 is thought to increase expression of nutrient transporters under hypoxic conditions (Wu et al., 2024). Under optimum conditions, the transporters will be upregulated and activate mTOR1, however in the current study, both transporters were upregulated in the hypoxic group, potentially indicating an acclimation to suboptimal oxygen conditions, a sub-optimal diet, or exerting a similar response as seen in cancerous mammalian cells. Most likely reason is that these regulatory mechanisms are just unknown and need further investigation e.g. use proteomics and transcriptomics. Raposo de Magalhães et al. (2022) studying the effects of stress on Gilthead Seabream, had similar

contradictory upregulated SLC3A2-SLC7A5 transporters results in net handled fish. This could mean that the upregulated SLC3A2-SLC7A5 mRNA transcripts may be due to handling stress rather than oxidative stress.

4.3.6.4 Hypoxia and autophagy

Autophagy is a catabolic process involved in degradation and protein turnover, essentially a recycling system (Laplante & Sabatini, 2009). Autophagosomes transfer cellular components such as proteins to the lysosome to be broken down by enzymes. In mammalian models, autophagy is inhibited by activation of mTOR by TSC-Ras /RHEB pathway or the PI3K-RHEB pathway (de Abreu et al., 2023). Autophagy downstream of mTOR1, is activated by ULK1 complex and is controlled by mTOR and AMPK (Zhou et al., 2022). Under stressful conditions such as hypoxia, autophagy is activated, thereby reducing metabolic demands and acting as an additional energy supply. It is thought that this is an adaptive response to survive fluctuating oxygen supply. High oxygen demanding fish, such as salmonids are less adapted to maintaining homeostasis, compared to low oxygen tolerant species such as carps, which may reduce their metabolic rate by 74% (Farhat et al., 2022). During normoxia, mTOR1 phosphorylates and thus represses ULK1, in turn inhibiting autophagy. Wang et al. (2024) suggested that ULK1 is phosphorylated by AMPK, subsequently negatively regulating AMPK, in addition, a possible feedback loop exists between AMPK, ULK1, and mTORC1, with AMPK directly phosphorylated and thereby inhibited by mTOR1.

In the current study, dual specificity mitogen-activated protein kinase kinase 2-like (MAP2K2B, ↑5.71 FC heart) located in the TSC-Ras /RHEB pathway (MAPK) and STE20-related kinase adapter protein beta-like (STE20, ↑2.26 FC liver) located upstream of AMPK were identified in upregulated tissues. No other mRNA transcripts linked to the classical MAPK or AMPK pathways were identified in downregulated mRNA transcripts.

E3 ubiquitin-protein ligase RNF152, located upstream of mTOR1, was associated with Ubiquitin mediated proteolysis, and associated with GO terms such as '*positive regulation of autophagy*' and '*negative regulation of TORC1 signaling*' (GO:0010508, GO:1904262). mRNA transcripts were identified in upregulated

liver tissue (↑4.98 FC) and in downregulated liver and brain tissues (↓-3.87 FC, ↓-2.28 FC) with each transcript located on different chromosomes.

The transforming growth factor-beta (TGF-*b*) family are cytokines involved in regulation of various cellular functions. '*TGF-beta signaling pathway'* (sasa:04350) had 42↓ mRNA transcripts associated with it. Tumour necrosis factor (TNFA) cytokines bind to tumour necrosis factor receptors (TNFR) upstream of mTOR1 along the TSC1/2 Rheb path. TSC1/2 are upstream negative mTOR1 regulators dependent on each other under hypoxic conditions to inhibit mTOR.

BCL2/adenovirus E1B 19 kDa protein-interacting protein 3-like (BNIP3, 106568353) was upregulated in tissues. Located downstream of HIF1a, in addition to REDD1, it was linked to hypoxia, bypassing TSC1/2 and inhibiting RHEB. Although not directly associated with the mTOR signalling pathway, it was linked to autophagy (sasa04140) and associated with GO terms such as '*positive regulation of apoptotic process*' (GO:0043065). In mammalian models, cross-talk between pathways such as mTOR and hypoxia inducible factor (HIF) may inhibit mTOR through BNIP3 and REDD1 (Cassidy & Lamarre, 2019).

4.3.6.5 Hypoxia and hormonal pathways

Hormones linked to regulation of growth and metabolic processes such as growth hormone (GH) and insulin-like growth factor (IGF) are linked to the mTOR pathway. In teleosts, AMPK, IGF/PI3K/Akt and MAPK (ERK) pathways are linked to hypoxia adaption, with pathways activated via hypoxia or redox status change (Zhu et al., 2013). MEK1/2 (MAP2K2B /MP2K2*?),* an activator of ERK 1/2 (extracellular signal-related kinases -1/2) was identified in upregulated heart mRNA transcripts (↑5.71 FC). ERK1/2 may be activated by growth factors or as an inflammatory response. MEK1/2 was associated with '*regulation of stress-activated MAPK cascade'* (GO:0032872). ERK was activated by hypoxia in a study on zebrafish by He et al. (2022). Additionally, hypoxia linked ERK signalling to pro-inflammatory cytokines and neutrophil migration in zebrafish (ERK regulated inflammation). This would suggest that elevated levels of MAP2K2B in the current trial (heart ↑5.71 FC) may be an effect of hypoxia via ERK1/2

signalling. Upregulated tissues identified 24↑ and 39↓ mRNA transcripts associated with *'hormone activity'* (GO:0005179).

4.3.6.6 Additional pathways

4.3.6.6.1 WNT, TNF-A and the mTOR pathway (WNT receptors Frizzled (FZD))

WNT (Wingless-related integration site) has been shown in human cell studies to stimulate mTOR signalling (Inoki et al., 2006) and In teleosts it is thought to have a role in cellular responses to stress. The WNT pathway consists of 2 pathways: the canonical pathway (WNT/B-CATENIN) and the non-canonical which is sub-divided into Planar Cell Polarity (WNT/PCP) and WNT/Ca2+ pathways (Komiya & Habas, 2008).

In humans, WNT proteins are classified into 2 classes: WNT1 (WNT2, WNT3, WNT3A, WNT8, WNT8A, WNT9A) and WNT5A *(*WNT4, WNT5A, WNT5B, WNT6, WNT7A, WNT11*),* with WNT1 involved in the WNT/B-CATENIN pathway and the WNT5A on the non-canonical WNT/PCP and WNT/Ca2+ pathways (Jamwal & Kumar, 2015). Mori et al. (2016) additionally suggested that WNTs activate numerous additional pathways, with Mazumdar et al. (2010) suggesting that HIF-1α activates WNT signalling in mammalian stem cells.

Madaro et al. (2023) studying the effects of acute stress on Atlantic salmon parr, found that 4 to 6 hr post-stress and restressed, the WNT pathway had the highest number of mRNA transcripts. This could indicate the elevated upregulated response of the WNT pathway mRNA transcripts may have been due to susceptibility to mechanical stressors (handling/ netting *etc*.) or biological stressors (hypoxia).

Other vertebrate studies have shown that hypoxia-induced modulation of these pathways (WNT and TNF-α) influences cell survival, proliferation, and metabolic adaptation (Bruick, 2003; Bruick & McKnight, 2001; Semenza, 2014).

The WNT and TNF-α signalling pathways are incredibly complex, with multiple multifunctional targets within the mTOR pathway identified within mammalian models. This is discussed further in the next section (Table 4.11). Very few

studies have explored Atlantic salmon WB physiological or cellular studies. With each of these in themselves providing additional areas of possible bias such as the inability to control multiple factors in WB studies or the potential of limitations in cellular studies due to the use of a single animal cell line.

4.3.7 mTOR 1FC

Out of the 7333 mapped mRNA transcripts across 3 tissues, within the ranges of >=2 or <=-2 (3360/8838↑, 3973/8742↓), a total of 37 mTOR mRNA transcripts were identified (18↑, 19↓). As a percentage, this equated to 0.5%↑ and 0.5%↓ of total mRNA transcripts as belonging to the mTOR pathway.

In pursuit of identifying further mTOR pathway mRNA transcripts, additional analysis was conducted on locating mRNA transcripts between >=1 to 1.99 FC and <=-1 to -1.99 FC within each tissue both up- and downregulated (Electronic file: Tissue Normalised 1FC).

The results indicated that a larger transcript abundance related to mTOR occurred between 1 to 1.99 FC up- and downregulated compared to the previous bins. With all the tissues combined a total of ↑400 ↓434 mTOR pathway associated mRNA transcripts were identified, of which ↑93 ↓175 were duplicated between the tissues. This suggested that the total mTOR pathway associated mRNA transcripts identified were ↑307 ↓259 or collectively, both up- and downregulated as 308.

Table 4.10 mTOR associated mRNA transcripts of interest in liver, brain and heart tissue. Identified using DAVID and parameters ranged from >=1.01 to 1.99 and <=-1.99 to -1.01 FC.

Tissue	Total (start)	INF/NA		Total	DAVID (ID)	mTOR pathway 1.01 to 1.99	Total (%)	DAVID (%)
Liver	23545	3014	↑	20531	13297	121	0.6	0.9
	20356	2266	↓	18090	13201	145	0.8	1.1
Brain	22006	1989	↑	20017	13641	137	0.7	1.0
	24760	2176	↓	22584	15805	158	0.7	1.0
Heart	19945	2585	↑	17360	12804	141	0.8	1.1
	21017	2972	↓	18045	12718	129	0.7	1.0

Total (start)= total mRNA transcripts, INF/NA= number of total mRNA transcripts not computable, Total= Total all subtracting the INF/NA, DAVID ID= Number of mRNA transcripts successfully mapped by DAVID,

Total (%)= Transcript (%) of Total, DAVID (%)= Transcript (%) of mapped DAVID IDs. ↑= upregulated in D1L, ↓= downregulated in D1L.

mTOR mRNA transcripts identified in liver tissue from the total mRNA transcripts were ↑121/20531 (0.6%), ↓145/18090 (0.8%). MRNA transcripts identified through DAVID were ↑121/13297 (0.9%), ↓145/13201 (1.1%).

In brain tissue total mTOR mRNA transcripts were ↑137/20017 (0.7%), ↓158/22584 (0.7%) while DAVID totals were ↑137/13641 (1.0%), ↓158/15805 (1.0%). Similarly for heart, total mRNA transcripts were ↑141/17360 (0.8%), ↓129/18045 (0.7%) with DAVID totals as ↑141/12804 (1.1%), ↓129/12718 (1.0%).

Similar mTOR identified totals (%) occurred across tissues, ranging from the highest totals in downregulated brain and liver (↓158, ↓145) and the lowest in upregulated liver (↑121). Amongst the upregulated group, heart had the highest mTOR associated mRNA transcripts (↑141). These trends were dissimilar to the ><2 bins (Tables 4.7, 4.10).

Although the total (%) of mRNA transcripts were considerably less, ranging from 0.4 to 0.1% and 0.8 to 0.3% of DAVID totals (%), liver tissue had the highest up- and downregulated mTOR associated mRNA transcripts (↑10, ↓10). Heart had the lowest in the upregulated group, while brain had the lowest amongst the downregulated tissues (↑3, ↓3).

Table 4.11 Additional pathways associated with 1FC mTOR mRNA transcripts.

KEGG Pathways	Upregulated (307)	Downregulated (260)	Pathway associations
Autophagy	100	87	MAPK, AMPK, Insulin
Insulin	99	87	MAPK, P13K-akt
FoxO	90	79	MAPK, P13K-akt, TGF-beta,
Melanogenesis	82	65	MAPK, Wnt
Wnt	74	58	MAPK, TGF-beta, Focal adhesion, Ubiquitin
Focal adhesion	71	64	MAPK, P13K-akt, Wnt
ErbB	68	59	MAPK, P13K-akt,
MAPK	64	54	TNF, Wnt
TGF-beta	20	17	MAPK, Ubiquitin proteolysis

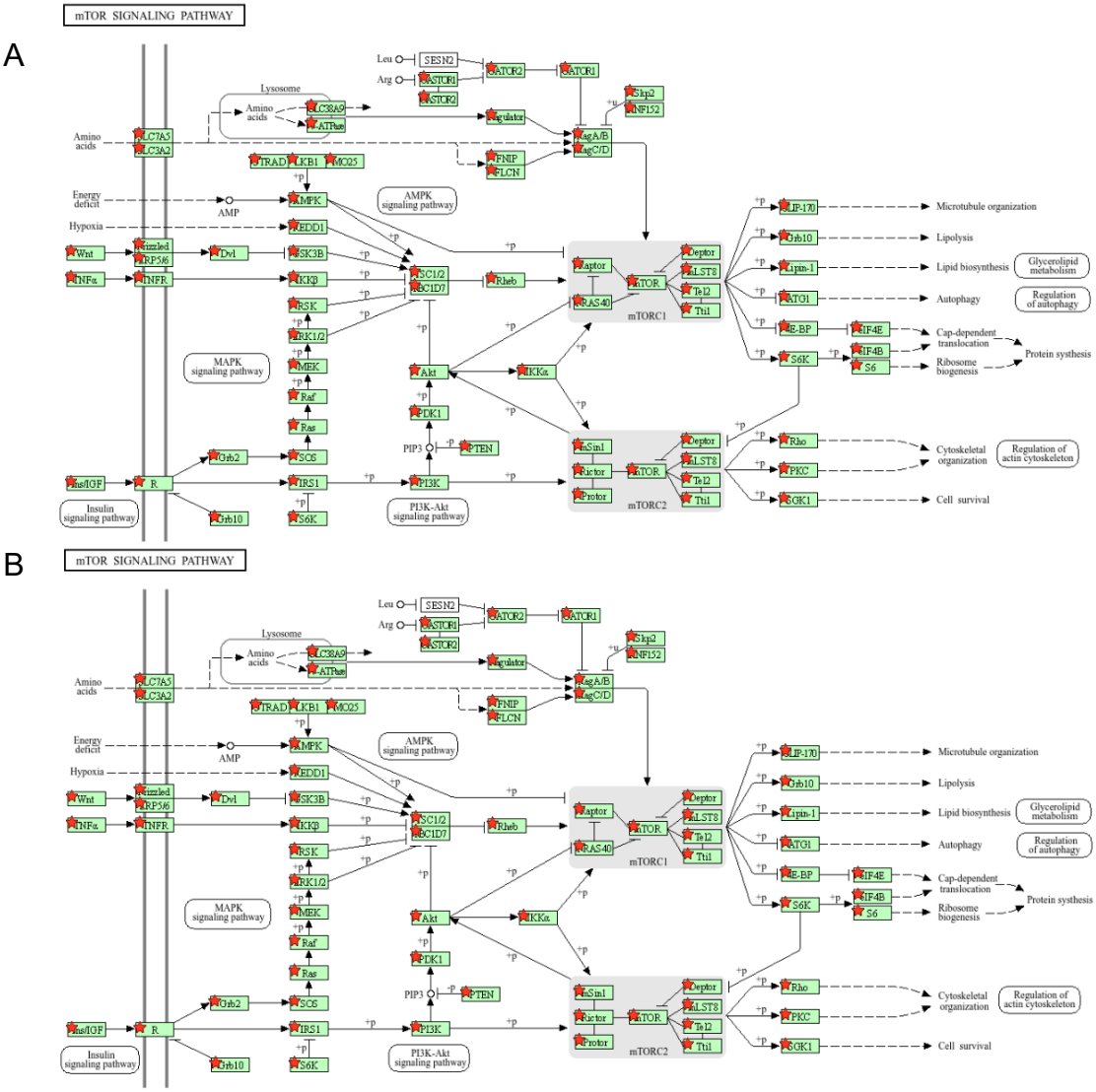


Figure 4.18 mTOR associated mRNA transcripts across all tissues A) upregulated B) downregulated.

These results may suggest a tissue-specific response at varying degrees of magnitude. All up- and downregulated mTOR associated mRNA transcripts were plotted onto KEGG mTOR pathways (Figure 4.18), offering a visual representation of mTOR regulation within the preset parameters. The upregulated mRNA transcripts (Figure 4.18 A) were similar to the downregulated mRNA transcripts (Figure 4.18 B), with mRNA transcripts highlighted in the mTOR pathway. Exploration of all up- and downregulated mRNA transcripts at an individual tissue level are displayed for liver Figure 4.19, brain Figure 4.20, and heart in Figure 4.21.

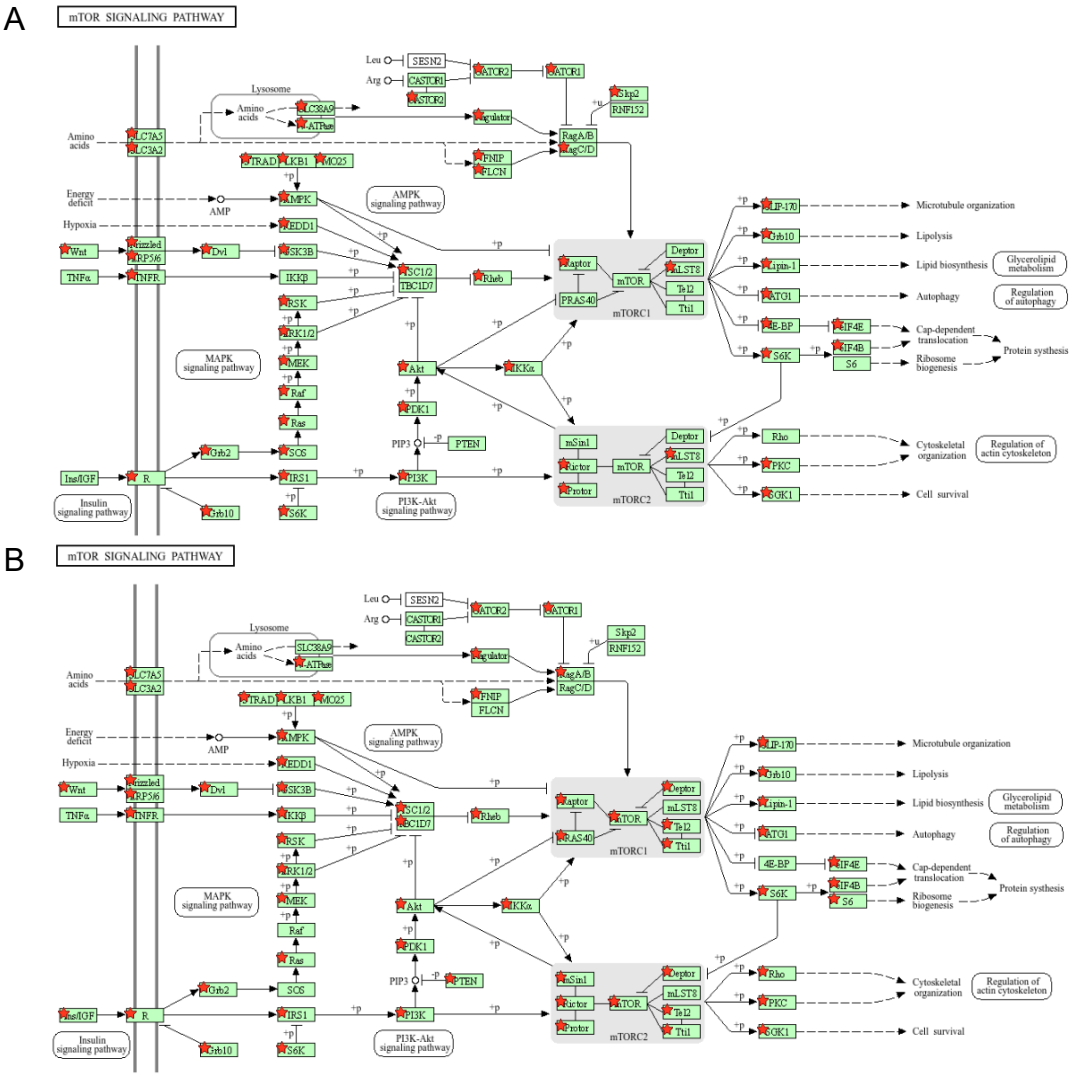


Figure 4.19 mTOR associated liver mRNA transcripts in A) upregulated B) downregulated mRNA transcripts.

The mTOR pathway associated mRNA transcripts were additionally submitted to DAVID to identify additional pathways associated with those specific mRNA transcripts. The compexity of transcriptomic analysis is demonstrated in Table 4.11, *e.g.*, of the 307 mTOR associated transcripts, a 100/307 were also associated with '*Autophagy – animal*' (sasa04140) of which that pathway is associated with MAPK, AMPK, and Insulin signalling pathways. This interconnectedness highlights the intricate relationships between the pathways which may complicated targeted qPCR studies focusing on targets within a specific pathway.This suggests a requirement for other approaches in understanding the model and mechanistic basis.The current transcriptomic data

indicate that it is unlikely to be transcriptionally affected by hypoxia, and thus dynamically operates naturally within the ranges >=1 to 1.99 FC and <=-1 to -1.99 FC. The results identify a change in state but did not identify any emergent properties. This may indicate that regulation of the mTOR pathway occurred at post-transcription/ post-translation.

4.4 Summary

In summary, RNA-Seq was performed on liver, brain and heart tissues between hypoxic (D1L) and normoxic treatments (D1H). Studies have suggested that adaptive responses to hypoxic conditions inhibit mTOR, enabling energy conservation, metabolic shifts, autophagy and a reduction in growth and protein synthesis.

4.4.1 Technical variation

In the initial exploratory searches for mTOR in literature, various online platforms were used to try and quantify the literature published on mTOR in Atlantic salmon. Scientific platforms such as Nature, Web of Science, Google Scholar, Scopus and PubMed were all explored. Each search tool had varying levels of user control, with some offering advanced searches. Common inaccuracies occurred with the salmon search term across all platforms.

Results included papers on Salmon (author), salmon calcitonin, salmon lice, Durie-Salmon [D-S] Staging System),Salmon sperm DNA, salmonella and so on.

With the search conducted using the parameters time range and keywords, the broader ranges which contained the largest volume of literature, could not identify these errors. When reaching the final stages of analysis, such as literature published in 2024, these falsely grouped papers were only then identified. This led to multiple reanalyses using various terms relevant to each online site (Tables 4.1, 4.2, 4.5). PubMed® Advanced Search Builder, with MeSH terms (Medical Subject Headings) allowed the most flexibility and control of the searches and was used in the final analysis.

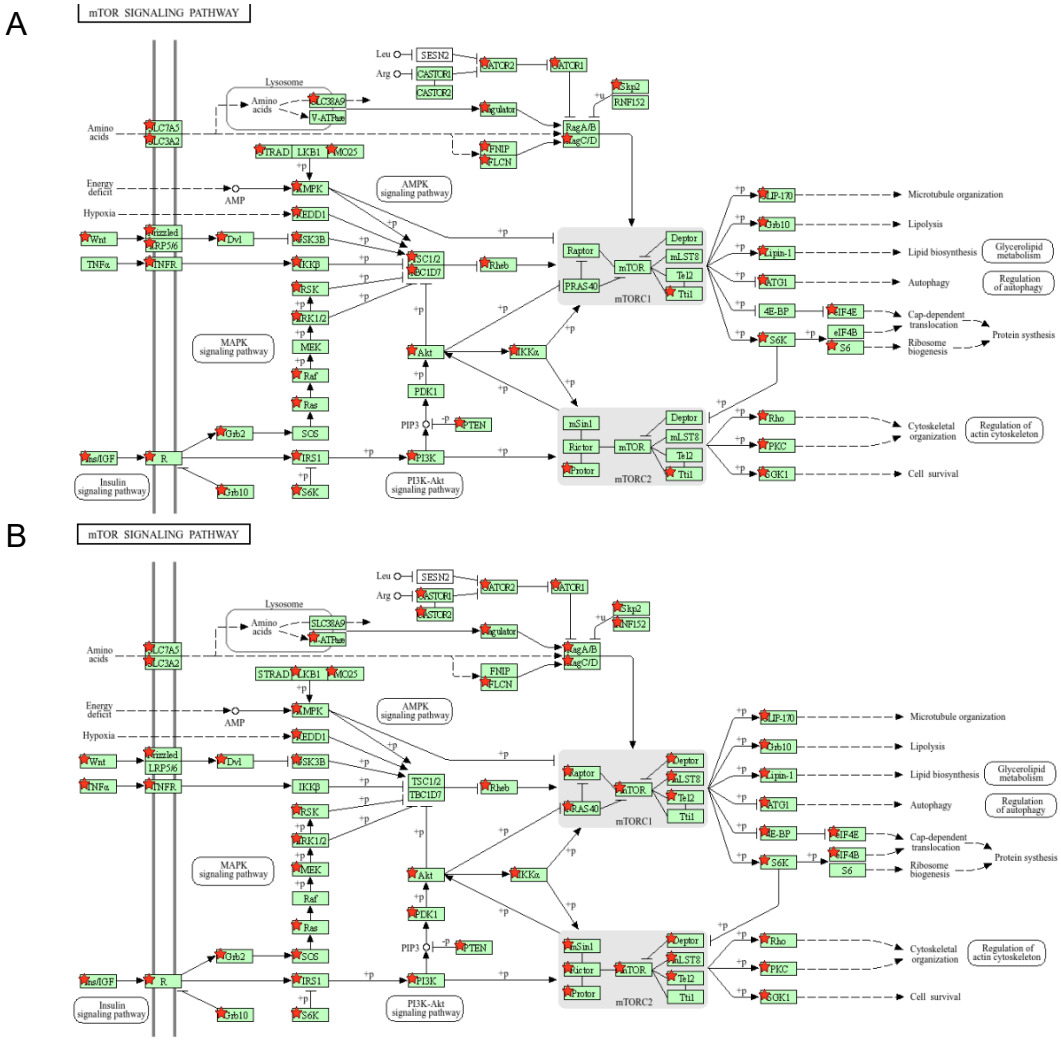


Figure 4.20 mTOR associated brain mRNA transcripts in A) upregulated B) downregulated mRNA transcripts.

Although PubMed MeSH searches still included terms such as Salmon (author) these were filtered out using terms such as 'NOT' or the adjustment of *[tiab] to [tiab] to try and obtain more accurate results. In some scenarios within the narrow search terms, these misidentified papers were filtered out manually. This was time consuming and potentially a source of inaccurate data for users unaware of these interfering/ false keyword terms.

Free web tools such as KEGG, DAVID, ShinyGO, g:Profiler, String, Ensembl, NCBI, GeneCards, etc. were used throughout this chapter. Towards the end of the analyses, established strengths of each program was identified and utilised, enhancing confidence in the results.

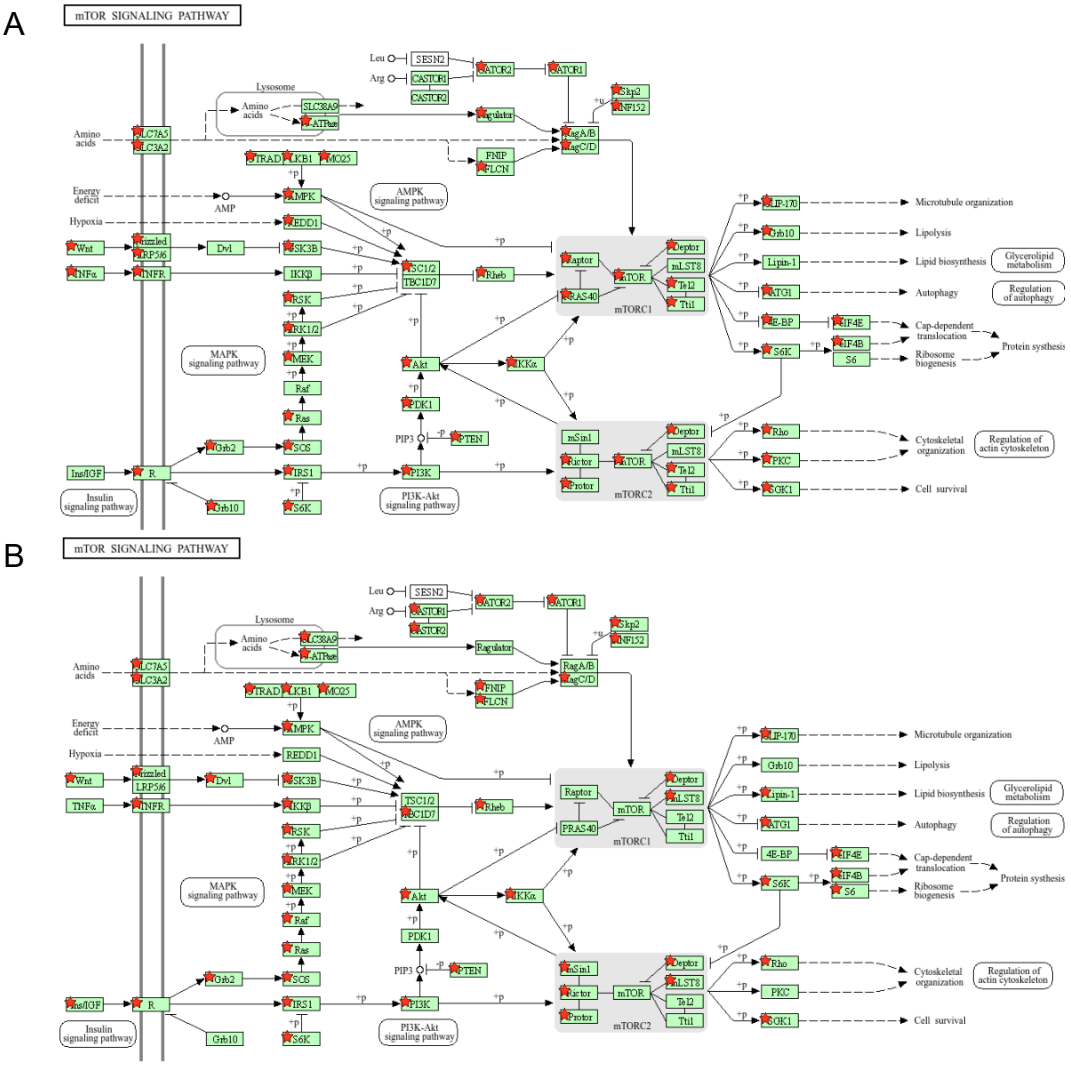


Figure 4.21 mTOR associated heart mRNA transcripts in A) upregulated B) downregulated mRNA transcripts.

Difficulties were experienced when conducting downstream analyses, resulting in time-consuming data reanalysis using multiple web tools discussed in detail below.

The primary and most significant hurdle experienced throughout this chapter was transcript identification/ annotation. Initial analysis using DESeq2 and ShinyNGS, resulted in multiple mRNA transcripts with Ensembl IDs only. For example, in ShinyNGS, downregulated DEGs in liver tissue identified a total of 53 GOIs of which 31 had no gene IDs and were labelled as NA. These were then submitted to DAVID gene conversion tool and 33/53 were allocated gene IDs (Entrez). The g:Profiler gene ID conversion tool (g:Convert) was additionally used for the same data set and managed to convert 27/53 Ensembl IDs to gene IDs.

DAVID and g:Profiler were more successful than any of the other web tools at assigning gene IDs, with DAVID achieving on average around a ±35% successful conversion rate. Although web tools such as g:Profiler use Ensembl BioMarts and DAVID utilises a knowledge base drawing from multiple sources (e.g. NCBI, UniProt, Ensembl, Gene Ontology, KEGG, Reactome, *etc*.) a 35% ID rate highlights the difficulties associated with these analyses and the caution required during interpretation of such data.

All analysis including GO terms were only conducted on mRNA transcripts converted to gene ID. This meant that approximately 2/3 of the data sets were eliminated and not utilised. This does not allow for full coverage of a transcriptome wide understanding, again highlighting the caveats one must take into account when interpreting such data. Multiple annotation bottlenecks occur within Atlantic salmon analysis.

Ensembl uses an automatic gene annotation system (annotation pipeline) which relies on protein/mRNA sequences from the scientific community to be submitted into public databases. (less salmon research = less sequences available) These are then annotated on genome assemblies from publicly available assemblies from INSDC (International Nucleotide Sequence Database Consortium consisting of NCBI GenBank, ENA, DDBJ).

Ensembl uses databases from The European Nucleotide Archive (ENA), UniProtKB (UniProtKB/Swiss-Prot- reviewed, manually annotated protein sequences and UniProtKB/TrEMBL- unreviewed proteins) and NCBI RefSeq to match genes/ mRNA transcripts. Ensemble classifies genes and mRNA transcripts into ‘known’ (matched to UniProtKB or NCBI RefSeq), ‘merged’ (manually annotated) or ‘novel’ if they do not match the genome in these databases. A bottleneck arises in this strategy as only the manually annotated proteins/ mRNAs from NCBI RefSeq are used in the Ensembl annotation process.

Companies such as NCBI have 7 RefSeq codes representing various levels/ states of review. Codes such as ‘PROVISIONAL’, a common status code in the current dataset, means ‘the record has not yet been subject to individual review’. This is a labour intensive, time consuming and costly process. Compared to

pharmaceutical studies using various models such as humans or mice, Atlantic salmon is not a high priority species with access to large volumes of resources/ funding. This is an additional bottleneck as funding is an important part of annotation, and in the words of Ensembl '*We select species to annotate on a case-by-case basis according to a number of factors such as: phylogenetic position, assembly quality, model organism, availability of species-specific sequence data (e.g. RNA-seq), additional funding*'.

Even the consensus coding sequence (CCDS) project, a collaboration of Ensembl, NCBI and HUGO Gene Nomenclature Committee (HGNC) to identify the PC regions of human and mouse genomes encounter obstacles such as getting the various independent collaborators to agree on areas where they had differing results. This relies on additional experimental validation but may improve as technology such as automatic annotation methods improve (NCBI The CCDS project, 2022).

All teleosts have undergone 3 whole-genome duplication (WGD) events, while Atlantic salmon have additionally undergone a 4th WGD event. This had led to a complex genome, with multiple annotation challenges such as pseudogenes (difficult to identify between functional and pseudo), duplicate genes/ paralogs (similar sequences but may have new functions (neofunctionalisation) or split/multiple functions (subfunctionalisation)), gene loss/ redundancy (difficulties identifying lost/ retained/ nonfunctional genes).

An example of this was E3 ubiquitin-protein ligase RNF152-like in liver (106578589, 106590060) and E3 ubiquitin-protein ligase RNF152 in brain (106569247) (liver ↑4.98FC ssa19, liver ↓-3.87FC ssa29, brain ↓-2.28FC ssa14). All had different gene IDs, different chromosomal locations, different regulation and are all classified as PC. In human studies ubiquitin mediated proteolysis is performed by 3 enzymes E1, E2 and E3, with 4 types of substrate-specific E3 enzymes encoded by more than 600 genes.

Without further studies, or regularly updated databases, it is only possible to speculate, with hesitation, as to the similarity of functionality and role of these mRNA transcripts in Atlantic salmon. Todd et al. (2016) suggested that proteomic

studies in addition to transcriptomics may improve and increase the context of functionality.

Alternative splicing/ exon skipping whereby multiple various mRNA transcripts (isoforms) are produced by the same gene may additionally have contributed to the annotation difficulties. Deshpande et al. (2023) suggested that in cases of multi-mapping, determining which transcript originated from which read may not be possible.

Issues arose with annotation that may may have been due to multi-mapping, where reads align to multiple locations on the genome. Examples such as ENSSSAG00000119778 (Liver ↑1.14 FC) which was mapped to 2 gene IDs (106590764 N-acylneuraminate cytidylyltransferase-like (Model), 100194895, NEUA, N-acylneuraminate cytidylyltransferase (Provisional)) with both listed by on chromosome 7 (ssa07) by NCBI, with different gene IDs but had similar names. Whereas an example such as ENSSSAG00000007858 (106563861, SUPT20, SPT20 homolog, SAGA complex component (Model), 106563858, ALG5, ALG5 dolichyl-phosphate beta-glucosyltransferase (Model) both on chromosome 11, different gene IDs, and completely different names. These 2 examples provided were found within the first 1619/20577 Ensembl IDs in upregulated liver tissue and highlight some difficulties experienced with Atlantic salmon annotation.

Difficulties in annotation classifications/ biotypes (PC, rRNA *etc*.) such as the classification of STE20 (106573852) previously discussed, where NCBI classified 106573852 as pseudo, Ensembl as novel lncRNA were noted during analyses. This may have been due to the possibility of paralogs misidentified as pseudogenes.

The use of non-standardised nomenclature with all the current online tools, resources, databases (both private and public), pipelines *etc*. is a significant limitation as is no universal scientific standard. GeneCards, the human gene database is testament to this. Using the example of ALG5 discussed previously, there are ±15 aliases. Similarly, for mTOR, the GeneCards tool ‘search aliases in other databases’ provided 24 mTOR aliases that it was able to search for.

Another example was ENSSSAG00000002846, which was ID as MYL11 (Myosin Light Chain 11, ShinyNGS, g:Profiler), MLC-2 (Myosin Light Chain 2, NCBI, DAVID), MYLPFA (Myosin Light Chain, Phosphorylatable, Fast Skeletal Muscle, Ensembl), and MYLPF (Myosin Light Chain, Phosphorylatable, Fast Skeletal Muscle, ShinyGO). All these terms were explored in GeneCards, and they are all correct, recognised aliases for MYL11. This increases the possibility of researchers potentially accessing a limited literature collection through incomplete search strategies either due to personally being unaware of the vast range of aliases or through search engine algorithms limitations. NCBI has tried to address this with their MeSH advanced search terms, and state that they collaborate with official nomenclature groups so that annotated genes are given their official names. But this is only a factor if the organism in question has official nomenclature groups.

Statistical testing to identify DEGs utilised a p-value of <0.05 or 5%. This would translate as out of 10000 genes tested, 500 would be differentially expressed in error (Type 1 error where a test rejects a true null hypothesis). To try and mitigate this, the FDR was used to control for the proportion of type 1 errors in the rejected null hypotheses.

A variety of free web-based tools were initially explored in the current functional enrichment analyses. The same datasets were analysed, with varying results between the platforms. This possibility of utilising a variety of platforms to perform

Table 4.12 Variation between webtools using FDR (BH).

Term	Web tool	FDR	Gene ID (#)	Pathway (#)
mTOR	DAVID	0	307	308
	g:Profiler	4.941×10^{-324}	242	252
	ShinyGO	$3.0\ x10^{-288}$	131	138
Autophagy	DAVID	7.6E-75	100	406
	g:Profiler	3.310×10-56	77	281
	ShinyGO	1.0E-61	43	121
Insulin	DAVID	2.2E-83	99	328
	g:Profiler	5.938×10-56	71	228
	ShinyGO	9.1E-58	41	122

FDR= Benjamini-Hochberg, Gene ID (#)= number of IDs in that pathway, Pathway (#)= number of IDs in that pathway.

analysis allows for the potential of manipulation or cherry picking of results. Each platform is widely available, easy to access, user friendly and peer reviewed. This may lead to the questionable credibility of published papers and the journals that have published them as discussed in depth by Wijesooriya et al. (2022).

If proven statistical methods such as a one-way ANOVA are computed the same across board whether its in MINITAB, SPSS, r *etc*. and the same results are obtained, then this concept should be transferrable to online webtools. If the Benjamini-Hochberg method (corrects for multiple testing and controls the false discovery rate (FDR)) is selected/ utilised, then similar results should occur depending on databases used by the individual tools as seen in Table 4.12.

If an adaption/improvement to the method is used, then this should be a separate statistical option such as the custom g:SCS (Set Counts and Sizes) in g:Profiler or the EASE score in DAVID (modified Fisher's Exact Test). Yet, the same set of data run through each online webtool, using the same method (BH FDR), yielded different results. This highlights the difficulties when using these tools, with different algorithms providing distinctly different outputs, with varying levels of user control.

DAVID was used for the statistical analyses of the enrichment analysis as it allowed for user interaction e.g. the adjustment of the count threshold and EASE, and the opportunity to display fold enrichment, Bonferroni, Benjamini, FDR and Fishers Exact at the same time. g:Profiler did offer the options of g:SCS, Bonferroni correction or Benjamini-Hochberg FDR but only 1 at a time, compared to DAVID that ran them all simultaneously and displayed them all in 1 file.

DAVID did not identify duplicated Ensemble IDs. This was an important feature when combining tissues to identify whether mRNA transcripts were tissue specific or not. G:Profiler did produce a list of duplicated mRNA transcripts, and this allowed for the tissue identification of those mRNA transcripts. Due to this, each dataset was additionally run through g:Profiler so that duplicated mRNA transcripts were identified and traced back to their respective tissues.

Todd et al. (2016) discussed the limitations of enrichment analysis on non-model species such as assigning functionality based on commonality of sequences in

model species, and the limitations with respect to little to no research to confirm the associations. Liu et al. (2015) further discussed the limitations with *de novo* annotation whereby <20% of bluehead wrasse (*Thalassoma bifasciatum*) contigs were successfully matched to proteins in BLASTX. Although they had to map to zebrafish gene IDs, they experienced similar difficulties to the current study, with only 30-50% of their data associated to GO terms and 20% mapped to KEGG pathways. This highlights the importance of annotation in transcriptomics as functional/ enrichment analysis relies on successful annotation to provide a more global understanding of the transcriptome.

DAVID had the most comprehensive list of contributing sources in its database, it still only successfully identified about ±35% of mRNA transcripts. The above-described technical issues highly the complexity of this area of bioinformatics. Although significant advances have been made in the past 20 years there are still many limitations and caveats that require attention.

4.4.2 Biological variation

Time-dependence: A caveat in an analysis such as transcriptomics is that it is a 'snapshot' overview of the system. It does not consider time dependence factors such as oscillations or even cell cycle stages. Homeostasis and oscillations are functions of a dynamic system, with homeostasis a product of negative feedback loops employed to maintain stable equilibrium points. Oscillatory systems are described as stable oscillations rather than set equilibrium points. An example of this includes transcription factors whereby negative feedback loops maybe be slowed down by phosphorylation or degradation and this delay causes oscillations. It has been suggested that oscillation is preferential as it reduces adaption/ desensitisation and avoids toxicity.

The cell cycle oscillations occur as processes cannot occur simultaneously, such as DNA synthesis during mitosis (DNA unavailable as chromatin condenses). This is an example of a negative feedback loop with time delays. Human cultured cells have been shown to divide every 24 hr, with mitosis (nuclear division) and cytokinesis (cell division) lasting approximately 1 hr. G1 phase follows the M

phase, and is metabolically active and lasts approximately 11 hr, S phase (Synthesis DNA replication) 8 hr and G2 (protein synthesis) approximately 4 hr (Cooper, 2000).

In this study mTOR was the main target for analysis. The analysis was carried out in tissue samples therefore without any discernible form of separating different cell states within the tissue. In human cell lines, mTOR1 activity has been shown to oscillate throughout the cell cycle. Joshi et al. (2024) demonstrated in their study using immunoblotting techniques in human cell lines, that mTOR1 activity was higher in S and G2 phases than in the mitosis and G1 phases. Although their study was conducted on human cell lines, more research would be required to determine if this occurred in Atlantic salmon cellular studies (*invitro*) and whole animal physiological studies (*in vivo*).

Sampling time: circadian rhythms regulate biological and behavioural processes such as cell cycle regulation, feed intake, energy, and brain activity over a 24 hr period in addition to regulating events such as smoltification and reproduction. Yúfera et al. (2017) exploring the circadian effects on gilthead sea bream (*Sparus aurata*) larvae, suggested that the molecular circadian and metabolic rhythms were highly synchronised and that at least 2 different waves of chromatin enzymes mediated circadian driven transcription.

Experimental hypoxia: Another possibility to consider was that the hypoxic treatment was not severe enough to cause downstream effects as oxygenation levels over the study were 8.1 ± 0.6 mg/L (90% saturation) for normoxic and 6.8 ± 0.5 mg/L (70% saturation) for the hypoxic treatment. Taking into consideration the standard deviation, this suggested a 0.2 mg/L difference between the treatments. Although a functional/ measurable change was observed for TNF-α and WNT on the mTOR pathway, as would be expected from hypoxia, suggesting that signalling was occurring but potentially not intense enough to produce a downstream effect as highlighted by the resulting data. In the aquaculture industry, low-normoxic conditions are more likely to occur in aquaculture than hypoxic conditions, but at the current level, this may not be significant enough to invoke a response observable at the transcriptome level.

An additional point to consider is the potential of adaption to moderate hypoxic conditions. Although fish species have adapted to moderate hypoxic conditions such as modifications in hyperventilation and cardiac efficiency, alterations in gills and haematological parameters which translates in the aquaculture industry as reduced feed rates and altered metabolism (Samaras et al., 2023). Kvamme et al. (2013) in a study exploring the effects of chronic hypoxia response in Atlantic salmon found elevated plasma cortisol at day 29 but not at day 58, with minimal differences in gene expression between the hypoxia and normoxia treatments. However, they did conclude that hypoxia may affects the immune system. More recently Zanuzzo et al. (2020) provided contrasting results in their study on temperature and oxygen stress on Atlantic salmon, where the immune system responded to a bacterial challenge similarly to control fish at optimum levels. In addition, Martínez et al. (2020) suggested a tissue specific immune response to hypoxia was observed in head kidney and spleen in their study on coho salmon (*Oncorhynchus kisutch)*.

Additional difficulties with current literature are that due to financial or technical reasons, molecular exploration is primarily conducted utilising qPCR techniques. With the challenges experienced with annotation, questions arise as to the validity of qPCR as a technique as qPCR may not be suitable for Atlantic salmon, or at least not yet. For example, in the current study the conflicting results of E3 ubiquitin-protein ligase or as previously mentioned the multimapped ENSSSAG00000007858 (106563861 SUPT20, or 106563858 ALG5) may mislead qPCR results unless they are confirmed as the correct targets.

E3 ubiquitin-protein ligase RNF152-like (106578589) was associated to the '*mTOR signaling pathway'* (sasa04150) with links to protein catabolism. Olsvik et al. (2013) evaluated the transcriptomic response of Atlantic salmon exposed to 4 months of oxygen and temperature stress, found that in liver tissue the protein ubiquitination pathway was affected by low oxygen. Pooley et al. (2013) exploring inflammatory stimulus in Atlantic salmon myocytes, identified E3 ligases suggesting an increase in protein degradation.

Wang et al. (2024) stated that RNF152 enzyme inhibits mTOR1 via RagA/ RRAGA when AAs are insufficient, and RHEB via TSC2 due to growth factor starvation. Meng et al. (2020) in a study using human cell lines and mice, suggested that RNF152 regulated autophagy, concluding that RNF152 is a mTOR1 regulator through both AAs and growth factors. Xiong et al. (2020) identified RNF152 as a positive regulator of TLR/IL-1R-mediated signalling in mice and Yoon et al. (2022) found that it was a negative regulator of WNT/β-CATENIN signalling in *Xenopus* embryos by the inhibition of Dishevelled.

These studies have demonstrated the varied mechanistic roles and the biological significance of RNF152 in various models, but the overarching questions are whether these mRNA transcripts are indeed RNF152 in Atlantic salmon? if they are, have they maintained similar functions/ new functions/ multiple functions? The current study has demonstrated that there is something of biological importance happening with RNF152, but whether these mRNA transcripts are annotation errors, or natural cellular oscillations (homeostasis) is unknown. Krasnov et al. (2021) reiterated that the difficulties with teleost transcriptomic studies are that many genes remain unexplored, and even though similarities may occur between model species, this does not imply preserved or similar functionality.

This may contribute to an understanding of the current data set but highlights the difficulties in finding explanations for the opposing results between the tissues, but further investigation and validation are required.

Deshpande et al. (2023) suggested that some alignment issues may be caused by technical variation (sequencing) or possibly by biological variations such as mutations. Individual variation may have played a role in the results as seen by the heatmaps with no clear distinct trends identified between the treatments. The individual variation observed in the heatmap results may have been the result of proactive and reactive stress coping styles observed in salmonids. Vaz-Serrano et al. (2011) described proactive behaviour as flight/fight responses, social dominance, bold behaviour and routine formation compared to reactive behaviour such as freeze/hide response, shy behaviour and social submissiveness.

Behavioural traits may affect aquaculture from both welfare and production perspectives (Laursen et al., 2011).

Physiologically these behaviours may result in variations in mortality, growth, condition factor and in response to handling, with stress identified through the hypothalamic-pituitary-inter-renal (HPI) axis (Ignatz et al., 2021). The importance of these behaviours, from an aquaculture industry perspective, is that proactive fish who avoid hypoxia, such as the Atlantic salmon in the study by Damsgård et al. (2019) may contribute to increased growth and developmental rate.

Todd et al. (2016) suggested that individual variation was the largest source of variation within a treatment with estimates of <0.2 CV for cell lines or inbred animals while variation between unrelated individuals may be higher than >0.3 CV (coefficient of variation).

4.4.2.1 mTOR 1 FC

In the exploration of the mTOR pathway between 1 FC and 1.99FC and -1 to -1.99 FC multiple mTOR pathway associated mRNA transcripts were identified. This suggested that this pathway is highly regulated as would be expected as the central cellular hub. The results additionally suggest that mTOR regulation is not observable using transcriptomics as it appears more likely to be post-transcriptionally regulated in response to hypoxia. Vilà et al. (2012) in a study between SLE (systemic lupus erythematosus) versus CT (control) mice, had a 0.56 FC in mRNA transcript abundance for FRAP1 *(*FK506 binding protein 12-rapamycin associated protein 1) in liver tissues, with the authors suggesting downregulation in SLE mice. Additional Western blot protein studies determined a significance between SLE and CT mice, with significantly higher mTOR protein levels in SLC mice. Marques-Ramos et al. (2017) examining the effects of hypoxia on human cell lines, found that although hypoxia slightly increased mTOR protein levels, the levels remained constant with no significance between the hypoxic and normoxic treated cell lines. These studies highlight the discrepancies as well as the unpredictability between mRNA transcript abundance and protein studies and further implicates that mTOR is possibly not transcriptionally regulated. Additionally protein studies have demonstrated the

stability of mTOR as a hub. Caution should be advised when exploring this pathway from a transcriptomic perspective as the identified transcript (%) is less than a 5% error rate. Confounding error either from technical or biological variation may additionally enhance the identification of false positive mRNA transcripts in this dataset even with additional statistical corrections (FDR).

This study highlights the regulation of mTOR in Atlantic salmon does not occur at the transcriptome level but rather at post-translation (PTM), suggesting transcription is not an accurate method of studying this pathway.

4.4.2.2 Summary

The transcriptomic data revealed oscillations within the pathways, but no distinct emergent properties were observed. Signalling occurred through the WNT/ TNF-α pathways, fortified by the multiple KEGG pathway associations with *'Cytokine-cytokine receptor interaction'* and other associated GO terms such as '*cell-cell signaling'* and *'signaling receptor activity'* through the WNT/ TNF-α pathways.

But signalling is complex, such as in the case of RHOA, and transcriptomics as a tool cannot differentiate or identify between pathways, or whether an effect is the result of one pathway or another. It is limited to identifying and quantifying the mRNA transcripts that are present at that time, it is unable to resolve mechanistic interactions.

In addition to the complexity of pathways, and the multifunctionality and interdependence of targets within them, they are modelled on mammalian studies, mostly human and mouse models, not Atlantic salmon. Add to that the uncertainty of whether these interacting pathways, modelled on mammalian species, are similar in structure and function to Atlantic salmon. Add to that the technical variations from WGD events, annotation issues, bioinformatics, neofunctionalisation and subfunctionalisation, classifications, protein complexes and so on, and it accumulates into a seemingly impossible task at hand.

Chapter 5

GENERAL DISCUSSION

5.1 Digestibility of intact proteins and cAAs

In Chapter 2, AA digestibilities were examined in Atlantic salmon post-smolts to identify if there were distinct digestibility differences between intact protein and cAA diets. Differences across the diets were noted for arginine, glutamate, isoleucine, leucine, proline and threonine (p=<0.05). Although differences were noted between individual AA digestibilities, they varied between diets and AAs, suggesting variability in ingredient and nutrient digestibility regardless of source.

In Chapter 3, all diets were prepared using the same basal mash and 21% cAAs were added to each diet. The only cAAs that varied between the diets were the BCAAs which were supplemented with the NEAAs serine, alanine (+b-ala) and glycine. In addition to the BCAAs, digestibility differences were noted for lysine, methionine and tyrosine (p=<0.05). This suggested a potential effect of the additional cAAs on the digestibility of the other cAAs/AAs. With regards to the BCAAs, PL even with the highest level of leucine across the diets, consistently had the overall highest digestibility.

Ingredient quality is key in feed manufacture for a multitude of reasons. If there are indeed no differences between the digestibility of intact proteins compared to cAA supplementation as seen in Chapter 2, but rather an interaction between nutrients driving the digestibility differences as seen in Chapter 3, then understanding these interactions may help develop a greater consideration in feed manufacture. This fine tuning of animal feed production may have considerable subsequent downstream effects, ranging from sustainability to health and welfare of farmed fish and surrounding environment not to mention the possible financial implications. Further studies are needed to explore these interactions.

Liebig's–barrel concept (based on Carl Sprengel's law of the minimum) suggests that growth is limited by the nutrient in the shortest supply. When formulating fish feeds, the most limiting AAs (lysine, methionine, arginine and threonine) are taken into consideration, with feeds formulated to contain sufficient levels of these limiting AAs. The 'ideal protein' concept, based on this barrel concept, estimates the dietary EAAs as proportions to total EAAs, thereby ensuring all EAAs are equally limiting. Ideal AAs are the ratio of the individual EAAs to lysine (100) and are commonly utilised in feed formulations.

Potentially elevated levels of compensatory AAs are suggested as having antagonistic effects, whereby an excess of one may limit another or may increase the requirement of other AAs, resulting in possible AA deficiencies. Known antagonistic relationships are thought to occur between the BCAAs, lysine and arginine as well as cystine and methionine. But as Xing et al. (2024) suggested, EAA requirements of fish and crustaceans, the known antagonistic effects of AAs on the requirements of fish are limited, suggesting further research required.

cAAs may currently be more expensive than intact protein sources but with more demand for plant proteins in carnivorous fish feeds, cAAs will continue being utilised in a supplementary manner to provide balanced AA feed profiles. Animals/ fish require nutrients, not ingredients, and with this in mind, it should be possible to formulate feeds purely based on artificial nutrients.

DADCs in this study suggested efficient and comparable nutrient absorption in the cAA and intact protein diets even though cAA absorption rates are generally considered faster than intact proteins.

In Chapter 3, PL overall had the highest DADCs but the lowest growth. PL WB analysis of protein identified week-3 as significantly higher in protein than week-7 (p=0.026). This suggested good absorption and utilisation of the cBCAAs, but protein accretion was not the end product. When formulating feeds, absorption rates of cAAs and possible subsequent interactions or antagonisms between nutrients need to be considered even though more research is required in this field.

If interactions/ antagonisms between nutrients within the nutrient pool supress growth, regardless of nutrient quantity/ quality, then there should be a possibility for enhanced growth/performance through exploration of these interactions. Manipulating the cAAs in collaboration with intact proteins and peptides may lead to a multitude of improvements in animal performance, welfare, environmental and financial implications. Further cell culture research is required initially using various Atlantic salmon cell lines to explore these interactions and gain a better understanding in Atlantic salmon in a species-specific manner.

Experimental research and feed formulations should additionally take into consideration the suggestions from Meng et al. (2020) whereby mTOR activity was not affected by the withdrawal of singular AAs but rather a multitude. Perhaps experimenting with formulating feeds with varying levels of a combination of alanine, methionine, arginine, leucine, asparagine, glutamine and serine is an avenue for further research.

The variation in the analysed dietary AAs between trial 1 and trial 2 were due to their formulation strategies and their intended responses. Trial 1 was formulated to identify and quantify the AA response, the transcript response. Trial 2 was formulated to identify/quantify growth and other parameters.

Trial 1 consisted of a basal diet with each cBCAA added at a 2% inclusion rate (20 g/kg) and thereby consisted of whole ingredients. The variability amongst the analysed dietary AAs was from 6.7% (LD) to 4.7% (CD, ID), with the basal mash alone accounting for 3.1% leucine.

In trial 2, the formulation was more controlled, with almost 20% of the diet consisting of bulkers and fillers (pregel/dextrose 10.8%, cellulose 8.3%), 21% cAAs, 37% of whole ingredients, 4% premix and 18.7% fish oil.

In summary, Chapter 2 demonstrated that the differences in digestibility between intact proteins and cAA diets were variable between the diets, suggesting potential digestibility differences of varying ingredients regardless of source. In Chapter 3, similar results were obtained, although the diets were similarly formulated, digestibility differences between nutrients were observed. This may

suggest that regardless of source, the variation may be down to individual nutrient digestibilities and their interactions with other nutrients.

5.2 BCAAs and AAs

In Chapter 2, plasma uptake across the BCAAs occurred at ±4 hr postprandial, suggesting that if nutrient availability was sufficient, BCAA catabolism and mTOR activation should occur after this. Due to the identification of plasma uptake times, this allowed for focused analysis of mRNA transcripts at 4 hr.

No temporal fBCAA differences were identified in liver tissue but differences did occur in muscle isoleucine and leucine uptake (p=<0.05) with the lowest uptake occurring at 24 hr postprandial. This tissue-specific uptake was explored further in Chapter 3.

Chapter 3 did identify temporal plasma and muscle uptake differences for the BCAAs, within each diet over time (apart from all BCAAs in NA, leucine in the NL and valine in the CD (high variation between samples)) and between the diets at each time. Plasma uptake in Chapter 3 had similar peak uptake times as Chapter 2, but the -2 and 24 hr trends varied between the diets and the BCAAs. This suggested differences in circulating fBCAAs and highlighted possible alternative mechanisms such as proteostasis and the reversible step in BCAA catabolism (BCAT) possibly connected to a-ketogluterate.

Although the trends in muscle were dissimilar to Chapter 2, with the 24 hr and prefeeding (-2 hr) timepoints similar, suggesting a return to baseline levels at 24 hr, which was unlike Chapter 2, with significantly lower 24 hr concentrations.

Studies to determine EAA requirements for fish are commonly estimated by analysing the WB or flesh of fish and using this as a baseline to then formulate feeds. This method may potentially be misguided/ misleading as the Chapter 3 WB bAAs were varied between experimental diets and weeks in the current study. Significant differences between diets were identified for histidine, methionine, phenylalanine, glutamate, taurine and tyrosine (p=<0.05). Significant differences within diets between weeks occurred for histidine, glutamate and taurine, possibly suggesting an effect of time on the deposition of these bAAs. A

possible suggestion for the differential deposition of these bAAs were that they were glucogenic or in the case of phenylalanine and tyrosine were dual-role AAs. Although no temporal or dietary trends were observed, the significant differences in bAAs may be an effect of cellular homeostasis and the metabolic fate of the bAAs at that specific time (4 hr postprandial) and that specific week.

In Chapter 2, muscle bAAs had no differences between the diets 4 hr postprandial, but liver tissue did for histidine and serine and near significance for threonine (p=<0.10). Similarly to Chapter 3, these were glucogenic AAs, although they occurred in the CD diet with significantly lower concentrations than the other diets.

A possible explanation for these differences may be down to technical error in the methods such as weighing errors or moisture absorption affecting the weights. Difficulties in using freeze dried material and static occurred when adding the samples to the Teflon tubes (CEM Microwave Technology Ltd., 907576) used in the Mars 6 microwave digester (CEM Microwave Technology Ltd., Mars 6), possible an additional source of error. The calculations to convert back to wet matter could possibly be a source of error. The significantly different concentrations of the bAAs were not isolated to dietary differences at week-3 or week-7 and neither were the within diet differences isolated to 1 specific diet.

5.2.1 AA interactions

AA interactions are said to occur in other models between the BCAAs, lysine and arginine and between glutamate and alanine. Rolland et al. (2016) examining the effects of methionine level and form on rainbow trout plasma profiles, stated that the addition of a cAA to the diets affected the plasma profiles of other AAs.

In Chapter 2 where the BCAAs were included at 2% to a basal diet (CD), differences in fBCAA uptake were observed. These BCAA uptake differences may have been due to the dietary 2% inclusion compared to the overall contribution.

In S 5.1, differences in Chapter 2 plasma uptake did seem to be related to the dietary inclusions of the BCAAs. Isoleucine in the ID, appeared to have increased uptake of all the fEAAs compared to the CD and other diets. The exceptions were

lysine and phenylalanine. At the 24 hr point, ID had higher concentrations than CD and the other diets for histidine, phenylalanine and tryptophan whereas the LD and VD diets had 24 hr concentrations lower than CD across all fEAAs. This highlighted a possible effect of valine and leucine on these fAAs.

Interestingly, at -2 hr, all the diets were lower than the CD for alanine, but higher than CD for glutamic acid (glutamate). Amongst the fNEAAs uptake was higher for tyrosine and serine in the ID. Proline at 24 hr had inverse change (%) compared to the ID, with peak concentrations at 24 hr compared to 8 hr in ID.

In S 5.2, differences in trial 2 plasma between the diets compared to the CD (change %) over 24 hr had elevated uptake of isoleucine and valine in the NL diet, whereas PL had lower uptake of the BCAAs apart from leucine. Amongst all the fAAs, similar trends did occur, with peak uptake at 2 hr and reduced uptake at 4 hr. This finding of increased isoleucine, possibly valine, uptake was similar to the results by Ren et al. (2015) who examined the effects of dietary leucine on blunt snout bream and found that in leucine deficient diets, the isoleucine plasma concentrations increased.

Dietary differences to these trends occurred in the PL diet for glutamate, alanine, proline, tyrosine, glycine and threonine, suggesting an effect of excess leucine on these AAs. In the NA, methionine, alanine, glutamate, glycine and proline were all elevated above all diets at 8 hr, suggesting possible uptake delays or release into plasma for further catabolism/ anabolism or the results or AA biosynthesis pathways. The current glutamate and alanine concentrations could potentially be indicative of BCAA metabolism. Glutamate may be a byproduct of BCAA catabolism into BCKA by BCAT, and alanine a byproduct of BCKA reverse synthesis of BCAAs as stated by Blasco et al. (1991) who examined the effects of starvation on plasma AAs in carp. Zhu et al. (2023) explored the effects of circadian rhythm on BCAA metabolism in Chinese perch (*Siniperca chuatsi*) suggested that fasting may increase BCAT expression in perch muscle, via circadian mechanisms, resulting in activation of the glutamate- alanine cycle. Biosynthesis of alanine could then be used by the liver via gluconeogenesis as energy.

Chapter 3 plasma arginine and lysine between the diets in at each time had significantly higher concentrations in the NA suggesting an increased uptake in the absence of leucine and/or the BCAAs.

In S 5.3, muscle fAAs from trial 2 were examined in relation to the fBCAAs and the fNEAAs that were used to top up dietary protein (N levels). Interestingly all diets when compared to the CD (change %) has similar fNEAA trends, with serine appearing to have an inhibitory effect on the uptake of glycine and alanine at 2 hr postprandial. All diets had higher -2 hr levels of alanine and glycine compared to the CD suggesting possible alternative mechanisms at work, while serine in the NA was elevated above the CD, suggesting elevated levels of circulating fNEAAs compared to the CD.

Very few studies have explored alternative fAAs intake in teleosts as discussed in Chapter 3 (3.4.3.2), but a handful of studies have explored environmental fAA uptake in teleost larvae (yolk-sack). This suggests that the mechanisms may biologically be in place and would be a beneficially unique area to explore further, through multi- omics approaches and through selective breeding programs.

The dual role glucogenic and ketogenic AAs discussed in Chapter 3 (Figure 3.13), namely isoleucine, phenylalanine, threonine, tyrosine and tryptophan (keto- and glucogenic) may be significant under periods of nutrient deficiency. The possibility of metabolic adjustments and adaptations to these dual-role AAs may be a field worth investigating especially from a nutritional perspective.

5.3 mRNA abundance

In Chapter 2, mRNA transcripts associated with BCAA metabolism were explored in the LD with absolute qPCR. BCAA metabolism is said to be initially catabolised in muscle tissue rather than liver tissue. To investigate this, temporal mRNA transcript abundance of BCAT1a, BCKDH1a, BCKDK was explored through absolute qPCR. Tissue transcript abundance for BCAT1a was higher in muscle tissue compared to liver tissue across all timepoints, with significant differences across time in liver. This first step is reversible which may explain the temporal stability seen in muscle tissue. The irreversible and rate limiting second step

catabolism by BCKDHA, displayed similar significantly different temporal trends across both tissues, with peak mRNA abundance at 4 and 8 hr postprandial. These trends mirrored the plasma leucine concentration levels, suggesting that leucine may elicit the mRNA transcript response seen in BCKDHA. BCKDK is thought to be the main regulator of BCKDH, with a high affinity for the leucine metabolite, KIC. BCKDH mRNA abundance was overall higher in muscle than liver tissue, with 24 hr levels higher than -2 hr baseline levels. This may have been due to the elevated levels of leucine and its metabolites driving its transcription.

Wiltafsky et al. (2010) examined the BCAAs effects on weaned pigs and identified tissue-specific mRNA abundances for the BCAA catabolism pathway. In their first experiment, increasing leucine and constant isoleucine, BCAT, BCKDH (E1a, E1b, E2) and BCKDK had the highest mRNA transcript response in heart tissue, followed by skeletal muscle (BCAT, BCKDK) and liver (BCKDH E1a, E1b, E2). In their second experiment, increasing leucine and constant valine, no differences in mRNA abundance occurred. The authors concluded that BCAA catabolism was posttranscriptionally regulated as no major differences occurred.

In Chapter 3, exploration of the effects of the varying amounts of dietary BCAAs, especially leucine, on BCKDHA mRNA transcripts were examined across diets, between week-3 and week-7, as well as over 3 timepoints at week-7. Muscle tissue did have higher mRNA abundance when compared to liver tissue, possibly oscillating between the tissues.

This trend identified as pre-feeding muscle mRNA transcripts were elevated compared to liver but dropped at 4 hr while liver mRNA transcripts increased and remained elevated at 24 hr. Similarly, muscle mRNA transcripts increased again at 24 hr. The higher muscle mRNA transcripts seen at pre-feeding, may be indicative of starvation, with BCKDHA prompting muscular BCAA catabolism, before a reduction is seen at 4 hr which may have been an effect of feeding. Overall, there did not appear to be any differences in mRNA abundance between the diets, leading to the deduction that the results were a natural physiological effect rather than a treatment effect.

Wessels et al. (2016) examining the effects of elevated dietary leucine in a pig model, found a leucine stimulation of non-tissue specific BCKDH activity, with increased activity in brain, liver and heart tissues. Additionally, reduced tissue concentrations of free valine, isoleucine, and reduced feed intake was attributed to dietary leucine levels.

In Chapter 3, dietary leucine did significantly increase the postprandial BCKDH mRNA abundance in liver tissue within the diets apart from the NL (p=<0.05). The lack of temporal mRNA abundance between the diets suggested dietary leucine did not affect BCKDH mRNA abundance in liver tissue.

In muscle tissue, NA and PL had similar trends where pre-feeding mRNA abundance was significantly higher than postprandial timepoints (p=<0.05), whereas NL had significantly lower 4 hr mRNA abundance compared to pre-feeding and 24 hr times. Although CD did follow a similar temporal trend, mRNA abundance was not significantly different (p=>0.05). The elevated pre-feeding abundance in NA and PL may be an indicator of maintenance such as proteostasis or cellular homeostasis. The unique trend in muscle NL may suggest that in leucine sub-optimal conditions, muscle may be the primary catabolic tissue in Atlantic salmon parr. The nonsignificant temporal liver mRNA abundance in the NL may further concur that under leucine deficit, the irreversible second step in BCAA catabolism occurs in muscle tissue. NL plasma and muscle had significantly higher free isoleucine and valine concentrations between the diets at 2, 4, and 8 hr post-prandial, suggesting optimal uptake. The elevated BCKDH liver mRNA transcripts at 4 and 24 hr may be in response to the circulating fAAs, although an adverse effect is seen in muscle tissues.

In Chapter 2, post-smolt BCKDH mRNA abundance in LD did not identify a tissue-specific trend, with pre-feeding and 24 hr abundance significantly lower than 4 and 8 hr postprandial suggesting a similar response in these tissues.

PL did appear to suppress the uptake of isoleucine and valine in plasma and muscle tissues. Pre-feeding plasma leucine was not significantly different across the diets, but a large range occurred between CD and NA. The elevated pre-feeding plasma leucine in the CD may be indicative of cellular mechanisms such

as proteolysis and the reversible 1st BCAA catabolism (BCAT) taking place in CD muscle tissue. Interestingly plasma arginine 2 hr post-prandial was significantly higher in the 2 diets with sub-optimal leucine and significantly lower in PL (NA>NL>CD>PL) with a similar trend occurring for lysine at 2, 8, and 24 hr post-prandial.

The supra-optimal dietary leucine in the PL did appear to affect valine and isoleucine concentrations in muscle and plasma tissues.

Langer et al. (2000) suggested the reduced concentration of plasma isoleucine and valine in response to elevated levels of leucine is not through absorption or transport conflicts, as studies with IV administration (of leucine or KIC) yielded similar trends. The authors suggested that excess leucine or KIC increased the transamination rates of isoleucine and valine into their respective BCKAs, resulting in reduced plasma concentrations. In mammalian models, elevated levels of KIC inhibit BCKDK (BCKDK enzyme responsible for phosphorylating and inactivating BCKDH) resulting in more BCKDH activity and greater oxidation of isoleucine and valine (Du et al., 2022).

An alternative leucine catabolic pathway is the conversion of KIC to β-hydroxy-β-methylbutyrate (HMB) by 4-hydroxyphenylpyruvate dioxygenase (4-HPPD or KIC dioxygenase). This enzyme is thought to be active in mammalian liver tissue but has also been located in muscle and kidney tissue. Wilkinson et al. (2013) in a study quantifying the human muscle protein synthesis rates between HMB and leucine, found the rapid availability in plasma and muscle tissue for both HMB and leucine. In addition, HMB did promote muscle anabolism, but just slightly less than leucine (HMB +70% vs. Leu +110%).

Inhibition at a tissue level would increase plasma concentrations, not reduce them. Further protein/enzyme studies are required to confirm these findings as mRNA abundance does not equate to protein production.

In summary, differences in mRNA abundance and temporal differences in Chapter 2 were seen for the BCAA catabolic pathway mRNA transcripts in LD. In Chapter 3, BCKDHA mRNA abundance was not affected by diet but more likely to have been affected by starvation, resulting in mRNA abundance oscillating

over time between muscle and liver tissues. Although mRNA abundance may not equate to protein levels, it is a useful tool in suggesting that similarly to mammalian studies, Atlantic salmon BCAA first step metabolism may occur in muscle tissue rather than liver. Additionally, the mRNA abundance of BCKDH in muscle and liver tissue may need further studies to clarify whether muscle tissue is BCKDH catabolically active tissue. Further studies are needed to confirm these findings.

5.4 mTOR

mTOR, a master cellular regulator, was examined in Chapter 2 by targeting up- and downstream mTOR pathway mRNA transcripts (SESN1, RRAG, MYO6 and MYOSTAT 1A). From an AA perspective, studies have shown that leucine activates mTOR and experimental diets were formulated to explore the effects of the BCAAs, in particular leucine, on mTOR. Overall RRAG A and MYOSTAT 1A had higher muscle mRNA abundance response than liver over time, whereas SESN1 had a larger response in liver than muscle tissue. Although a low copy number yield was seen, the overall trends suggested a tissue specific mRNA abundance response. mTOR, a regulator itself, is additionally strictly regulated up- and downstream, with feedback loops, crosstalk, *etc*. thereby ensuring overall stability. Additional studies will be required to determine whether these effects are treatment related or merely due to natural cellular oscillation.

Examining the effects of hypoxia on mTOR in Atlantic salmon in Chapter 4 was currently relevant to industry, as hypoxia or hypoxic events are set to intensify in aquaculture. These low oxygen events lead to poor growth and health and are linked to warming seawater, algae blooms, gill damage, overstocking and poor feed/waste management. By examining the transcriptomic response between treatments, this data may be used downstream, such as selective breeding for low oxygen resistance.

Statistically different DEGs in liver, brain and heart tissues contained no associated mTOR pathway mRNA transcripts apart from E3 ubiquitin-protein ligase RNF152-like (106578589) in downregulated liver DEGs. Upregulated DEGs (liver 74↑, brain 82↑, heart 43↑) were functionally associated with GO

terms such as '*RNA biosynthetic process*', '*DNA binding'* and '*regulation of metabolic processes'* which were driven by *hox* genes. Brain mRNA transcripts were the largest contributor amongst the upregulated mRNA transcripts, and this may have driven the GO terms towards tissue specific associations. Upregulated brain mRNA abundance was associated with higher level biological terms such as '*anterior/posterior pattern specification'*, '*regionalization*', '*pattern specification process*' and '*regulation of DNA-templated transcription*' which were all driven by the 11 homeobox proteins.

Downregulated DEGs (liver 53↓, brain 49↓, heart 71↓) had the highest contribution from heart tissue and were associated with higher terms such as '*cell-cell signaling'* and '*synaptic signaling'* and functionally grouped by with *'transporter activity'* and '*localization*'. Interestingly amongst the downregulated heart mRNA transcripts, no GO terms or KEGG pathway associations were identified. Amongst the heatmaps displaying the intensity of the DEGs, the largest contribution across all tissues was from snRNA followed by PC.

To locate mTOR mRNA transcripts, additional downstream analysis was conducted exploring FC differences in the RNA-seq data, with bins starting at >2FC and <-2FC. Within these parameters, identified mRNA transcripts linked to the mTOR pathway were minimal.

Gene ontology enrichment analysis revealed that across upregulated tissues, mRNA transcripts were associated with higher level GO terms such as *'transporter activity'*, *'signaling receptor activity'*, *'hormone activity'* and higher biological process terms such as '*response to stimulus'*, '*multicellular organismal process'* and '*cell communication'.* Similarly for downregulated FC mRNA transcripts, high level GO term association were '*multicellular organismal process'*, *'developmental process'*, '*cell communication'* with GO:MF terms such as *'transporter activity'*, *'molecular transducer activity'* and *'signaling receptor activity'.*

mTOR associated mRNA transcripts in liver tissue identified a total of 20 (↑10, ↓10). The ↑10 were all identified in the 2 to 4.99FC bin whereas ↓9 were identified between -2 to -4.99FC and ↓1 in the -<10FC bin. This suggested that mTOR

associated mRNA abundance operated at very low FC differences between the 2 treatments.

Upregulated mRNA transcripts were identified upstream of mTOR1 with PRR5A upstream of mTOR2 (Figure 4.12). Upregulated mRNA transcripts were located on the WNT, TNF-α, and AMPK pathways, as well as the AA sensors upstream from RAG (CASTOR, SLC7A5, SLC3A2) and 2 mRNA transcripts were associated with RNF152. The mRNA transcripts associated with nutrients and AAs may suggest an effect of hypoxia on these pathways. All upregulated mRNA transcripts were signalling upstream of mTOR with no downstream identified mRNA transcripts.

In the downregulated mTOR pathway associated mRNA transcripts, EIF4E was located downstream of mTOR1 and was associated with protein synthesis while RHOA and SGK1 were downstream of mTOR2 and associated with cytoskeleton dynamics, actin organisation and cell survival (regulation of actin cytoskeleton). Upstream of the 2 complexes, 4 mRNA transcripts were identified along WNT/frizzled pathway, 1 in TNF-α, PRRR5 and RNF152.

The differences in the liver mRNA transcripts between the up- and downregulated mRNA transcripts was that the upregulated mRNA transcripts were identified in the AMPK and the nutrients sensing pathways. This may indicate an effect of hypoxia on nutrient and energy levels.

Similarly for brain tissue, 8 (↑5, ↓3) mTOR associated mRNA transcripts were identified, with ↑3 in the 2 to 4.99FC bin and ↓3 in the -2 to -4.99FC bin. All mRNA transcripts identified in brain were located upstream of the mTOR complexes, with 4 upregulated mRNA transcripts associated with the WNT pathway and 1 transcript with SLC7A5 along the AA pathway. Of the 3 downregulated mRNA transcripts, they were identified in the WNT and TNFa pathways and 1 upstream of RRAG, RNF152. Similarly to upregulated liver mRNA transcripts, brain appeared to signal mTOR through the WNT and AA nutrient pathways.

A similar trend was seen in heart tissue, with a total of 9 mTOR associated mRNA transcripts, with ↑2 in the 2 to 4.99FC and ↓5 in the -2 to -4.99FC bins. All mRNA transcripts were located upstream of mTOR, with 4/6 downregulated mRNA

transcripts identified in the WNT pathway, 1 in TNF-α and SLC7A5. The 3 upregulated mRNA transcripts were identified along the WNT, TNFa and MEK pathways.

From approximately 17580 mRNA transcripts (liver 6249, brain 5637, heart 5694), a total of 20 mRNA transcripts were identified in liver (↑10, ↓10) 8 in brain (↑5, ↓3) and 9 in heart tissue (↑3, ↓6). These results indicated that the main pathway linked to mTOR under hypoxia was the WNT and TNF-α pathways and not the hypoxia (REDD1) pathway.

Due to this low mTOR mRNA transcript association, further investigation was conducted by exploring the mRNA transcripts between 1 to 1.99 FC and -1.99 to -1 FC. Of the 116627 mRNA transcripts across the 3 tissues, a total of 831 mTOR associated mRNA transcripts were identified (↑399 and ↓432).

These results indicated that regardless of the treatment, the majority of mTOR regulation occurred within a 1 FC distribution, highlighting the robustness of mTOR. This poses the question of the validity/ importance of research publishing mTOR associated results with anything less than a 2 FC as it may indicate natural oscillations within the pathway.

Transcriptomics and targeted qPCR are great investigative tools, telling a ‘snapshot’ story but may be misleading. With mRNA targets susceptible to physiological factors such as belonging to a complex, or natural oscillation potentially affecting results, the use of these tools, in conjunction with proteomics may provide a more effective and persuasive result/ argument.

mRNA abundance has been used as an estimation of protein production, but mammalian studies have shown this to differ between tissues, between cell types and even between bodily fluids (Wang et al., 2019). The proteome is highly variable and influenced by factors such as cell type, biochemical requirements and environment (Heywood et al., 2024). In addition to these various factors, cell state may influence mRNA levels. Liu et al. (2016) discussed how protein levels may be explained by mRNA levels, with up to 80% of protein variance explained by mRNA variance. In addition, cellular states may affect protein levels, with steady state cellular mRNA more likely to explain protein levels (when cells are

at steady state, *i.e.* mRNA levels remain stable for several hours). This highlights tissue-specific turnover rates possibly influencing mRNA abundance. DEGs of interest may be validated by further analyses using absolute qPCR, phosphoproteomics, and proteomic studies.

In summary, mTOR associated mRNA transcripts in the 2 to 4.99 and -2 to -4.99 had a larger volume of mTOR mRNA transcripts than the other bins. But the highest number of mRNA transcripts were identified in the 1 to 1.99FC and -1 to -1.99FC groups, with similar numbers for both up- and downregulated mRNA transcripts were identified suggesting mTOR regulation is not identifiable at the transcription level in Atlantic salmon.

Biological variability in response to hypoxia was potentially attributable to inter-individual genetic differences, stochastic gene expression variation, and compensatory physiological mechanisms, as noted in prior studies on hypoxia tolerance in teleosts (Rahman & Thomas, 2012; Regan & Richards, 2017). Additionally, dynamic and oscillatory gene expression patterns further complicated differential expression analyses, reflecting transient transcriptional regulation that RNA-Seq may fail to capture comprehensively (Leng et al., 2015; Li & Xiong, 2015).

Overall, identified differences in digestibility of nutrients regardless of source. Leucine did appear to affect the growth of Atlantic salmon parr with varied results. The identification of AA uptake was observed across all tissues with peak concentration times identified as well as possible interactions/ antagonisms. mRNA abundance did suggest and effect of leucine on the BCAA and mTOR mRNA transcripts although the biological effects of these are unknown. Transcriptomic analysis of the effects of hypoxia on mTOR signalling highlighted the role of mTOR as a master hub and suggested that mTOR regulation was not identified at the transcriptome level. Altogether, the present study presents descriptive data that provides valuable, novel, and interesting information on AA metabolism and growth in Atlantic salmon, a relatively unexplored field in this group of vertebrates, and leaves open interesting questions to be addressed in future studies.

REFERENCES

Abumrad, N. N., Abumrad, N. A., Sandler, M. P., & Lacy, W. W. (1985, January 2). The Metabolic Effects and Fate of Branched-Chain Amino and Keto Acids across Human Skeletal Muscle. (G. Kleinberger, P. Ferenci, P. Riederer, & H. Thaler, Eds), *Advances in Hepatic Encephalopathy and Urea Cycle Diseases: 5th International Symposium on Ammonia, Semmering, Austria, May 1984: Proceedings*. S.Karger AG. https://doi.org/10.1159/000410850

Abumrad, N. N., & Miller, B. (1983). The Physiologic and Nutritional Significance of Plasma-free Amino Acid Levels. *Journal of Parenteral and Enteral Nutrition*, *7*(2), 163–170. https://doi.org/10.1177/0148607183007002163

Adeva-Andany, M. M., López-Maside, L., Donapetry-García, C., Fernández-Fernández, C., & Sixto-Leal, C. (2017). Enzymes involved in branched-chain amino acid metabolism in humans. *Amino Acids*, *49*(6), 1005–1028. https://doi.org/10.1007/s00726-017-2412-7

Aftring, R. P., Block, K. P., & Buse, M. G. (1986). Leucine and isoleucine activate skeletal muscle branched-chain alpha-keto acid dehydrogenase in vivo. *American Journal of Physiology-Endocrinology and Metabolism*, *250*(5), E599–E604. https://doi.org/10.1152/ajpendo.1986.250.5.E599

Afzal, Z., & Krumlauf, R. (2022). Transcriptional Regulation and Implications for Controlling Hox Gene Expression. *Journal of Developmental Biology*, *10*(1), 4. https://doi.org/10.3390/jdb10010004

Ahima, R. S., & Flier, J. S. (2000). Adipose Tissue as an Endocrine Organ. *Trends in Endocrinology & Metabolism*, *11*(8), 327–332. https://doi.org/10.1016/S1043-2760(00)00301-5

Ahmad, I., Ahmed, I., & Dar, N. A. (2021). Effects of dietary leucine levels on growth performance, hematobiochemical parameters, liver profile, intestinal enzyme activities and target of rapamycin signalling pathway related gene expression in rainbow trout, *Oncorhynchus mykiss* fingerlings. *Aquaculture Nutrition*, *27*(6), 1837–1852. https://doi.org/10.1111/anu.13321

Ahmad, I., Ahmed, I., Fatma, S., & Peres, H. (2021). Role of branched-chain amino acids on growth, physiology and metabolism of different fish species: A review. *Aquaculture Nutrition*, *27*(5), 1270–1289. https://doi.org/10.1111/anu.13267

Ahmed, I., & Ahmad, I. (2020). Effect of dietary protein levels on growth performance, hematological profile and biochemical composition of fingerlings rainbow trout, *Oncorhynchus mykiss* reared in Indian Himalayan region. *Aquaculture Reports*, *16*, 100268. https://doi.org/10.1016/j.aqrep.2019.100268

Ainslie, G. R., Gibson, K. M., & Vogel, K. R. (2016). mTOR, Autophagy, Aminoacidopathies, and Human Genetic Disorders. In K. Maiese (Ed.), *Molecules to Medicine with mTOR* (pp. 143–166). Elsevier. https://doi.org/10.1016/B978-0-12-802733-2.00010-4

Ambardekar, A. A., Reigh, R. C., & Williams, M. B. (2009). Absorption of amino acids from intact dietary proteins and purified amino acid supplements follows different time-courses in channel catfish (*Ictalurus punctatus*). *Aquaculture*, *291*(3–4), 179–187. https://doi.org/10.1016/j.aquaculture.2009.02.044

Anthony, J. C., Yoshizawa, F., Anthony, T. G., Vary, T. C., Jefferson, L. S., & Kimball, S. R. (2000). Leucine Stimulates Translation Initiation in Skeletal Muscle of Postabsorptive Rats via a Rapamycin-Sensitive Pathway. *The Journal of Nutrition*, *130*(10), 2413–2419. https://doi.org/10.1093/jn/130.10.2413

Aoki, H., Akimoto, A., & Watanabe, T. (2001). Periodical changes of plasma free amino acid levels and feed digesta in yellowtail after feeding nonfishmeal diets with or without supplemental crystalline amino acids. *Fisheries Science*, *67*(4), 614–618. https://doi.org/10.1046/j.1444-2906.2001.00297.x

Aragão, C., Gonçalves, A. T., Costas, B., Azeredo, R., Xavier, M. J., & Engrola, S. (2022). Alternative Proteins for Fish Diets: Implications beyond Growth. *Animals*, *12*(9), 1211. https://doi.org/10.3390/ani12091211

Azevedo, P. A., Bureau, D. P., Leeson, S., & Cho, Y. (2002). Growth and efficiency of feed usage by Atlantic salmon (*Salmo salar*) fed diets with different dietary protein: Energy ratios at two feeding levels. *Fisheries Science*, *68*(4), 878–888. https://doi.org/10.1046/j.1444-2906.2002.00506.x

Babu, E., Kanai, Y., Chairoungdua, A., Kim, D. K., Iribe, Y., Tangtrongsup, S., Jutabha, P., Li, Y., Ahmed, N., Sakamoto, S., Anzai, N., Nagamori, S., & Endou, H. (2003). Identification of a Novel System L Amino Acid Transporter Structurally Distinct from Heterodimeric Amino Acid Transporters. *Journal of Biological Chemistry*, *278*(44), 43838–43845. https://doi.org/10.1074/jbc.M305221200

Balakrishnan, P., Liebe, T., Amro, E., Dhaka, L., Heinzel, T., & Heller, R. (2019). Metabolic Stress-Signaling and Metabolic Adaptation. In S. I. S. Rattan & M. Kyriazis (Eds.), *The Science of Hormesis in Health and Longevity* (pp. 139–148). Elsevier. https://doi.org/10.1016/B978-0-12-814253-0.00012-7

Barroso, J. B., Peragón, J., García-Salguero, L., de la Higuera, M., & Lupiáñez, J. A. (1999). Variations in the kinetic behaviour of the NADPH-production systems in different tissues of the trout when fed on an amino-acid-based diet at different frequencies. Publication No. 184 from the Drugs, Environmental Toxics and Cellular Metabolism Research. *The International Journal of Biochemistry & Cell Biology*, *31*(2), 277–290. https://doi.org/10.1016/S1357-2725(98)00114-9

Basheeruddin, M., & Qausain, S. (2024). Hypoxia-Inducible Factor 1-Alpha (HIF-1α): An Essential Regulator in Cellular Metabolic Control. *Cureus*, *16*(7), e63852. https://doi.org/10.7759/cureus.63852

Bayle, E. D., Svensson, F., Atkinson, B. N., Steadman, D., Willis, N. J., Woodward, H. L., Whiting, P., Vincent, J. P., & Fish, P. V. (2021). Carboxylesterase Notum Is a Druggable Target to Modulate Wnt Signaling. *Journal of Medicinal Chemistry*, *64*(8), 4289–4311. https://doi.org/10.1021/acs.jmedchem.0c01974

Belghit, I., Liland, N. S., Waagbø, R., Biancarosa, I., Pelusio, N., Li, Y., Krogdahl, Å., & Lock, E. J. (2018). Potential of insect-based diets for Atlantic salmon (*Salmo salar*). *Aquaculture*, *491*, 72–81. https://doi.org/10.1016/j.aquaculture.2018.03.016

Benak, D., Alanova, P., Holzerova, K., Chalupova, M., Opletalova, B., Kolar, F., Pavlinkova, G., & Hlavackova, M. (2025). Epitranscriptomic regulation of HIF-1: bidirectional regulatory pathways. *Molecular Medicine*, *31*(1), 105. https://doi.org/10.1186/s10020-025-01149-x

Benedet, S., Björnsson, B. T., Taranger, G. L., & Andersson, E. (2008). Cloning of somatolactin alpha, beta forms and the somatolactin receptor in Atlantic salmon: seasonal expression profile in pituitary and ovary of maturing female broodstock. *Reproductive Biology and Endocrinology : RB&E*, *6*, 42. https://doi.org/10.1186/1477-7827-6-42

Benjamini, Y., & Hochberg, Y. (1995). Controlling the False Discovery Rate: A Practical and Powerful Approach to Multiple Testing. *Journal of the Royal Statistical Society Series B: Statistical Methodology*, *57*(1), 289–300. https://doi.org/10.1111/j.2517-6161.1995.tb02031.x

Bera, P., Dhara, H., Mandal, S., Sau, S. K., & Das, S. (2025). Nutritional Strategies for Improving Reproductive Performance in Fishes. In I. Ahmed & I. Ahmad (Eds.), *Aquaculture: Enhancing Food Security and Nutrition* (pp. 409–430). Springer. https://doi.org/10.1007/978-3-031-92858-1_20

Berge, G. E., Bakke-McKellep, A. M., & Lied, E. (1999). In vitro uptake and interaction between arginine and lysine in the intestine of Atlantic salmon (*Salmo salar*). *Aquaculture*, *179*(1–4), 181–193. https://doi.org/10.1016/S0044-8486(99)00161-1

Berrill, I. K., Porter, M. J. R., Smart, A., Mitchell, D., & Bromage, N. R. (2003). Photoperiodic effects on precocious maturation, growth and smoltification in Atlantic salmon, *Salmo salar*. *Aquaculture*, *222*(1), 239–252. https://doi.org//10.1016/S0044-8486(03)00125-X

Besson, M., Komen, H., Rose, G., & Vandeputte, M. (2020). The genetic correlation between feed conversion ratio and growth rate affects the design of a breeding program for more sustainable fish production. *Genetics Selection Evolution*, *52*(1), 5. https://doi.org/10.1186/s12711-020-0524-0

Betz, C., & Hall, M. N. (2013). Where is mTOR and what is it doing there? *Journal of Cell Biology*, *203*(4), 563–574. https://doi.org/10.1083/jcb.201306041

Bever, K., Chenoweth, M., & Dunn, A. (1981). Amino acid gluconeogenesis and glucose turnover in kelp bass (*Paralabrax* sp.). *American Journal of Physiology-Regulatory, Integrative and Comparative Physiology*, *240*(3), R246–R252. https://doi.org/10.1152/ajpregu.1981.240.3.R246

Bifari, F., & Nisoli, E. (2017). Branched-chain amino acids differently modulate catabolic and anabolic states in mammals: a pharmacological point of view. *British Journal of Pharmacology*, *174*(11), 1366–1377. https://doi.org/10.1111/bph.13624

Biswas, D., Dao, K. T., Mercer, A., Cowie, A. M., Duffley, L., El Hiani, Y., Kienesberger, P. C., & Pulinilkunnil, T. (2020). Branched-chain ketoacid overload inhibits insulin action in the muscle. *Journal of Biological Chemistry*, *295*(46), 15597–15621. https://doi.org/10.1074/jbc.RA120.013121

Björnsson, B. Th., Taranger, G. L., Hansen, T., Stefansson, S. O., & Haux, C. (1994). The Interrelation between Photoperiod, Growth Hormone, and Sexual Maturation of Adult Atlantic Salmon (*Salmo salar*). *General and Comparative Endocrinology*, *93*(1), 70–81. https://doi.org/10.1006/gcen.1994.1009

Blanco, A., & Blanco, G. (2017). Amino Acid Metabolism. In A. Blanco & G. B. T. M. B. Blanco (Eds.), *Medical Biochemistry* (pp. 367–399). Elsevier. https://doi.org/10.1016/B978-0-12-803550-4.00016-1

Blasco, J., Fernández, J., & Gutiérrez, J. (1991). The effects of starvation and refeeding on plasma amino acid levels in carp, *Cyprinus carpio* L., 1758. *Journal of Fish Biology*, *38*(4), 587–598. https://doi.org/10.1111/j.1095-8649.1991.tb03145.x

Block, K. P., & Harper, A. E. (1991). High Levels of Dietary Amino and Branched-Chain α-Keto Acids Alter Plasma and Brain Amino Acid Concentrations in Rats. *The Journal of Nutrition*, *121*(5), 663–671. https://doi.org/10.1093/jn/121.5.663

Bo, T., & Fujii, J. (2024). Primary Roles of Branched Chain Amino Acids (BCAAs) and Their Metabolism in Physiology and Metabolic Disorders. *Molecules*, *30*(1), 56. https://doi.org/10.3390/molecules30010056

Bohnsack, M. T., & Sloan, K. E. (2018). Modifications in small nuclear RNAs and their roles in spliceosome assembly and function. *Biological Chemistry*, *399*(11), 1265–1276. https://doi.org/10.1515/hsz-2018-0205

Boyd, C. E., D'Abramo, L. R., Glencross, B. D., Huyben, D. C., Juarez, L. M., Lockwood, G. S., McNevin, A. A., Tacon, A. G. J., Teletchea, F., Tomasso, J. R., Tucker, C. S., & Valenti, W. C. (2020). Achieving sustainable aquaculture: Historical and current perspectives and future needs and challenges. *Journal of the World Aquaculture Society*, *51*(3), 578–633. https://doi.org/10.1111/jwas.12714

Braceland, M., Houston, K., Ashby, A., Matthews, C., Haining, H., Rodger, H., & Eckersall, P. D. (2017). Technical pre-analytical effects on the clinical biochemistry of Atlantic salmon (*Salmo salar* L.). *Journal of Fish Diseases*, *40*(1), 29–40. https://doi.org/10.1111/jfd.12476

Bröer, S., & Bröer, A. (2017). Amino acid homeostasis and signalling in mammalian cells and organisms. *The Biochemical Journal*, *474*(12), 1935–1963. https://doi.org/10.1042/BCJ20160822

Brosnan, J. T., & Brosnan, M. E. (2006). Branched-Chain Amino Acids: Enzyme and Substrate Regulation. *The Journal of Nutrition*, *136*(1), 207S-211S. https://doi.org/10.1093/jn/136.1.207S

Brosset, P., Lloret, J., Muñoz, M., Fauvel, C., Van Beveren, E., Marques, V., Fromentin, J. M., Ménard, F., & Saraux, C. (2016). Body reserves mediate trade-offs between life-history traits: new insights from small pelagic fish reproduction. *Royal Society Open Science*, *3*(10), 160202.

https://doi.org/10.1098/rsos.160202

Browdy, C. L., Ray, A. J., Leffler, J. W., & Avnimelech, Y. (2012). Biofloc-based Aquaculture Systems. In J. H. Tidwell (Ed.), *Aquaculture Production Systems* (1st Edi, pp. 278–307). Wiley. https://doi.org/10.1002/9781118250105.ch12

Brown, A. R., Wilson, R. W., & Tyler, C. R. (2025). Assessing the Benefits and Challenges of Recirculating Aquaculture Systems (RAS) for Atlantic Salmon Production. *Reviews in Fisheries Science & Aquaculture*, *33*(3), 380–401. https://doi.org/10.1080/23308249.2024.2433581

Brown, M. L., & Murphy, B. R. (2004). Seasonal dynamics of direct and indirect condition indices in relation to energy allocation in largemouth bass *Micropterus salmoides* (*Lacèpede*). *Ecology of Freshwater Fish*, *13*(1), 23–36. https://doi.org/10.1111/j.0906-6691.2004.00031.x

Brugarolas, J., Lei, K., Hurley, R. L., Manning, B. D., Reiling, J. H., Hafen, E., Witters, L. A., Ellisen, L. W., & Kaelin, W. G. (2004). Regulation of mTOR function in response to hypoxia by REDD1 and the TSC1/TSC2 tumor suppressor complex. *Genes & Development*, *18*(23), 2893–2904. https://doi.org/10.1101/gad.1256804

Bruick, R. K. (2003). Oxygen sensing in the hypoxic response pathway: regulation of the hypoxia-inducible transcription factor. *Genes & Development*, *17*(21), 2614–2623. https://doi.org/10.1101/gad.1145503

Bruick, R. K., & McKnight, S. L. (2001). A Conserved Family of Prolyl-4-Hydroxylases That Modify HIF. *Science*, *294*(5545), 1337–1340. https://doi.org/10.1126/science.1066373

Bucking, C., Glover, C. N., & Wood, C. M. (2011). Digestion under Duress: Nutrient Acquisition and Metabolism during Hypoxia in the Pacific Hagfish. *Physiological and Biochemical Zoology*, *84*(6), 607–617. https://doi.org/10.1086/662630

Burke, M., Grant, J., Filgueira, R., & Stone, T. (2021). Oceanographic processes control dissolved oxygen variability at a commercial Atlantic salmon farm:

Application of a real-time sensor network. *Aquaculture*, *533*, 736143. https://doi.org/10.1016/j.aquaculture.2020.736143

Burt, K., Hamoutene, D., Mabrouk, G., Lang, C., Puestow, T., Drover, D., Losier, R., & Page, F. (2012). Environmental conditions and occurrence of hypoxia within production cages of Atlantic salmon on the south coast of Newfoundland. *Aquaculture Research*, *43*(4), 607–620. https://doi.org/10.1111/j.1365-2109.2011.02867.x

Burton, D., & Burton, M. (2017). *Food procurement and processing*. (D. Burton & M. Burton, Eds.), *Essential Fish Biology: Diversity, structure, and function* (Vol. 1). Oxford University Press. https://doi.org/10.1093/oso/9780198785552.003.0004

Calder, P. C. (2006). Branched-Chain Amino Acids and Immunity. *The Journal of Nutrition*, *136*(1), 288S-293S. https://doi.org/10.1093/jn/136.1.288S

Cañon Jones, H. A., Noble, C., Damsgård, B., & Pearce, G. P. (2011). Social network analysis of the behavioural interactions that influence the development of fin damage in Atlantic salmon parr (*Salmo salar*) held at different stocking densities. *Applied Animal Behaviour Science*, *133*(1), 117–126. https://doi.org/10.1016/j.applanim.2011.05.005

Canosa, L. F., & Bertucci, J. I. (2023). The effect of environmental stressors on growth in fish and its endocrine control. *Frontiers in Endocrinology*, *14*, 1109461. https://doi.org/10.3389/fendo.2023.1109461

Cao, X., Cui, H., Ji, X., Li, B., Lu, R., Zhang, Y., & Chen, J. (2023). Determining the Potential Roles of Branched-Chain Amino Acids in the Regulation of Muscle Growth in Common Carp (*Cyprinus carpio*) Based on Transcriptome and MicroRNA Sequencing. *Aquaculture Nutrition*, 1–15. https://doi.org/10.1155/2023/7965735

Cao, Y., Liu, S., Liu, K., Abbasi, I. H. R., Cai, C., & Yao, J. (2019). Molecular mechanisms relating to amino acid regulation of protein synthesis. *Nutrition Research Reviews*, *32*(2), 183–191. https://doi.org/10.1017/S0954422419000052

Carrillo, M., Zanuy, S., & Herrera, E. (1980). Daily rhythms of amino acid levels in the plasma of goldfish (*Carassius auratus*). *Comparative Biochemistry and Physiology Part A: Physiology*, *67*(4), 581–586. https://doi.org/10.1016/0300-9629(80)90244-3

Carter, C. G., Houlihan, D. F., & He, Z. Y. (2000). Changes in tissue free amino acid concentrations in Atlantic salmon, *Salmo salar* L., after consumption of a low ration. *Fish Physiology and Biochemistry*, *23*(4), 295–306. https://doi.org/10.1023/A:1011187026997

Cassidy, A. A., & Lamarre, S. G. (2019). Activation of oxygen-responsive pathways is associated with altered protein metabolism in Arctic char exposed to hypoxia. *Journal of Experimental Biology*, *222*(22), jeb203901. https://doi.org/10.1242/jeb.203901

Castillo, S., & Gatlin, D. M. (2018). Dietary requirements for leucine, isoleucine and valine (branched-chain amino acids) by juvenile red drum *Sciaenops ocellatus*. *Aquaculture Nutrition*, *24*(3), 1056–1065. https://doi.org/10.1111/anu.12644

Cervantes, M., Arce, N., García, H., Cota, M., Htoo, J. K., & Morales, A. (2015). Expression of genes coding for selected amino acid transporters in small intestine , liver , and skeletal muscle of pigs fed excess branched-chain amino acids, *Genetics and Molecular Research*, *14*(3), 9779–9792. https://doi.org/10.4238/2015.August.19.11

Chabot, D., Steffensen, J. F., & Farrell, A. P. (2016). The determination of standard metabolic rate in fishes. *Journal of Fish Biology*, *88*(1), 81–121. https://doi.org/10.1111/jfb.12845

Chantranupong, L., Wolfson, R. L., Orozco, J. M., Saxton, R. A., Scaria, S. M., Bar-Peled, L., Spooner, E., Isasa, M., Gygi, S. P., & Sabatini, D. M. (2014). The Sestrins Interact with GATOR2 to Negatively Regulate the Amino-Acid-Sensing Pathway Upstream of mTORC1. *Cell Reports*, *9*(1), 1–8. https://doi.org/10.1016/j.celrep.2014.09.014

Chen, L., Yang, R., Kwan, T., Tang, C., Watt, S., Zhang, Y., Bourque, G., Ge, B., Downes, K., Frontini, M., Ouwehand, W. H., Lin, J. W., Soranzo, N., Pastinen, T., & Chen, L. (2020). Paired rRNA-depleted and polyA-selected RNA sequencing data and supporting multi-omics data from human T cells. *Scientific Data*, *7*(1), 376. https://doi.org/10.1038/s41597-020-00719-4

Chojnacka, K., Mikula, K., Izydorczyk, G., Skrzypczak, D., Witek-Krowiak, A., Gersz, A., Moustakas, K., Iwaniuk, J., Grzędzicki, M., & Korczyński, M. (2021). Innovative high digestibility protein feed materials reducing environmental impact through improved nitrogen-use efficiency in sustainable agriculture. *Journal of Environmental Management*, *291*, 112693. https://doi.org/10.1016/j.jenvman.2021.112693

Choo, P. S., Smith, T. K., Cho, C. Y., & Ferguson, H. W. (1991). Dietary Excesses of Leucine Influence Growth and Body Composition of Rainbow Trout. *The Journal of Nutrition*, *121*(12), 1932–1939. https://doi.org/10.1093/jn/121.12.1932

Chu, D. L. H., Li, V. W. T., & Yu, R. M. K. (2010). Leptin: Clue to poor appetite in oxygen-starved fish. *Molecular and Cellular Endocrinology*, *319*(1–2), 143–146. https://doi.org/10.1016/j.mce.2010.01.018

Chuang, D. T., Chuang, J. L., & Wynn, R. M. (2006). Lessons from Genetic Disorders of Branched-Chain Amino Acid Metabolism. *The Journal of Nutrition*, *136*(1), 243S-249S. https://doi.org/10.1093/jn/136.1.243S

Chun, Y., & Kim, J. (2021). AMPK–mTOR Signaling and Cellular Adaptations in Hypoxia. *International Journal of Molecular Sciences*, *22*(18), 9765. https://doi.org/10.3390/ijms22189765

Churova, M. V, Meshcheryakova, O. V, Veselov, A. E., Efremov, D. A., & Nemova, N. N. (2017). Activity of metabolic enzymes and muscle-specific gene expression in parr and smolts Atlantic salmon *Salmo salar* L. of different age groups. *Fish Physiology and Biochemistry*, *43*(4), 1117–1130. https://doi.org/10.1007/s10695-017-0357-0

Cleveland, B. M., & Radler, L. M. (2019). Essential amino acids exhibit variable effects on protein degradation in rainbow trout (*Oncorhynchus mykiss*) primary myocytes. *Comparative Biochemistry and Physiology Part A: Molecular & Integrative Physiology*, *229*, 33–39. https://doi.org/10.1016/j.cbpa.2018.11.019

Comesaña, S., Chivite, M., Blanco, A. M., Alborja-Valado, M., Calo, J., Conde-Sieira, M., & Soengas, J. L. (2022). Involvement of Mechanistic Target of Rapamycin (mTOR) in Valine Orexigenic Effects in Rainbow Trout. *Aquaculture Nutrition*, *2022*, 7509382. https://doi.org/10.1155/2022/7509382

Comesaña, S., Velasco, C., Conde-Sieira, M., Míguez, J. M., Soengas, J. L., & Morais, S. (2018). Feeding Stimulation Ability and Central Effects of Intraperitoneal Treatment of L-Leucine, L-Valine, and L-Proline on Amino Acid Sensing Systems in Rainbow Trout: Implication in Food Intake Control. *Frontiers in Physiology*, *9*. https://doi.org/10.3389/fphys.2018.01209

Comesaña, S., Velasco, C., & Soengas, J. L. (2021). Leucine sensing in rainbow trout hypothalamus is direct but separate from mTOR signalling in the regulation of food intake. *Aquaculture*, *543*, 737009. https://doi.org/10.1016/j.aquaculture.2021.737009

Conceição, L. E. C., Grasdalen, H., & Dinis, M. T. (2003). A new method to estimate the relative bioavailability of individual amino acids in fish larvae using 13C-NMR spectroscopy. *Comparative Biochemistry and Physiology Part B: Biochemistry and Molecular Biology*, *134*(1), 103–109. https://doi.org/10.1016/S1096-4959(02)00193-8

Conde-Sieira, M., & Soengas, J. L. (2017). Nutrient Sensing Systems in Fish: Impact on Food Intake Regulation and Energy Homeostasis. *Frontiers in Neuroscience*, *10*. https://doi.org/10.3389/fnins.2016.00603

Connor, L., Matson, R., & Kelly, F. L. (2017). Length-weight relationships for common freshwater fish species in Irish lakes and rivers. *Biology and Environment: Proceedings of the Royal Irish Academy*, *117B*(2), 65–75. https://doi.org/10.1353/bae.2017.0014

Conway, M. E., & Hutson, S. M. (2016). BCAA Metabolism and NH3 Homeostasis. In A. Schousboe & U. Sonnewald (Eds.), *The Glutamate/ GABA-Glutamine Cycle. Advances in Neurobiology* (13th ed., pp. 99–132). Cham: Springer International Publishing. https://doi.org/10.1007/978-3-319-45096-4_5

Cooney, R., Wan, A. H. L., O'Donncha, F., & Clifford, E. (2021). Designing environmentally efficient aquafeeds through the use of multicriteria decision support tools. *Current Opinion in Environmental Science & Health*, *23*, 100276. https://doi.org/10.1016/j.coesh.2021.100276

Cooper, G. M. (2000). The Eukaryotic Cell Cycle. In Sinauer Associates (Ed.), *The cell: a molecular approach* (2nd edition). Washington, D.C: ASM Press. https://www.ncbi.nlm.nih.gov/books/NBK9876/

Coppes Petricorena, Z. (2015). Chemical Composition of Fish and Fishery Products. In P. C. K. Cheung & B. M. Mehta (Eds.), *Handbook of Food Chemistry* (pp. 403–435). Springer. https://doi.org/10.1007/978-3-642-36605-5_12

Cota, D., Proulx, K., Smith, K. A. B., Kozma, S. C., Thomas, G., Woods, S. C., & Seeley, R. J. (2006). Hypothalamic mTOR Signaling Regulates Food Intake. *Science*, *312*(5775), 927–930. https://doi.org/10.1126/science.1124147

Cowey, C. B., & Walton, M. J. (1988). Studies on the uptake of 14 C amino acids derived from both dietary 14 C protein and dietary 14 C amino acids by rainbow trout, (*Salmo gairdneri*) Richardson. *Journal of Fish Biology*, *33*(2), 293–305. https://doi.org/10.1111/j.1095-8649.1988.tb05472.x

Craig, S., & Helfrich, L. A. (2009). Understanding Fish Nutrition, Feeds, and Feeding. *Virginia Cooperative Extension*, *420-256*. https://vtechworks.lib.vt.edu/server/api/core/bitstreams/d4934fad-224a-4e9d-a4c3-2b3f4fa9a9fe/content

Crossin, K. L. (2012). Oxygen levels and the regulation of cell adhesion in the nervous system: a control point for morphogenesis in development, disease and evolution? *Cell Adhesion & Migration*, *6*(1), 49–58.

https://doi.org/10.4161/cam.19582

Csapó, J., Varga-Visi, É., Lóki, K., Albert, C., & Salamon, S. (2008). The influence of extrusion on loss and racemization of amino acids. *Amino Acids*, *34*(2), 287–292. https://doi.org/10.1007/s00726-006-0484-x

Cynober, L. A. (2002). Plasma amino acid levels with a note on membrane transport: characteristics, regulation, and metabolic significance. *Nutrition*, *18*(9), 761–766. https://doi.org/10.1016/S0899-9007(02)00780-3

Dabrowski, K., Lee, K. J., & Rinchard, J. (2003). The Smallest Vertebrate, Teleost Fish, Can Utilize Synthetic Dipeptide-Based Diets. *The Journal of Nutrition*, *133*(12), 4225–4229. https://doi.org/10.1093/jn/133.12.4225

Dabrowski, K., Zhang, Y., Kwasek, K., Hliwa, P., & Ostaszewska, T. (2010). Effects of protein-, peptide- and free amino acid-based diets in fish nutrition. *Aquaculture Research*, *41*(5), 668–683. https://doi.org/10.1111/j.1365-2109.2010.02490.x

Dai, W., Xu, Y., Mo, S., Li, Q., Yu, J., Wang, R., Ma, Y., Ni, Y., Xiang, W., Han, L., Zhang, L., Cai, S., Qin, J., Chen, W. L., Jia, W., & Cai, G. (2020). GLUT3 induced by AMPK/CREB1 axis is key for withstanding energy stress and augments the efficacy of current colorectal cancer therapies. *Signal Transduction and Targeted Therapy*, *5*(1), 177. https://doi.org/10.1038/s41392-020-00220-9

Damsgaard, C., Lauridsen, H., Harter, T. S., Kwan, G. T., Thomsen, J. S., Funder, A. M., Supuran, C. T., Tresguerres, M., Matthews, P. G., & Brauner, C. J. (2020). A novel acidification mechanism for greatly enhanced oxygen supply to the fish retina. *ELife*, *9*. https://doi.org/10.7554/eLife.58995

Damsgård, B., Evensen, T. H., Øverli, Ø., Gorissen, M., Ebbesson, L. O. E., Rey, S., & Höglund, E. (2019). Proactive avoidance behaviour and pace-of-life syndrome in Atlantic salmon. *Royal Society Open Science*, *6*(3), 181859. https://doi.org/10.1098/rsos.181859

Dani, D. (2017). Status of aquaculture with respect to nutrition and feed. *International Journal of Fisheries and Aquatic Studies*, *5*, 333–345. https://www.researchgate.net/publication/314092033

de Abreu, M. S., Demin, K. A., Kotova, M. M., Mirzaei, F., Shariff, S., Kantawala, B., Zakharchenko, K. V, Kolesnikova, T. O., Dilbaryan, K., Grigoryan, A., Yenkoyan, K. B., & Kalueff, A. V. (2023). Developing Novel Experimental Models of m-TORopathic Epilepsy and Related Neuropathologies: Translational Insights from Zebrafish. *International Journal of Molecular Sciences*, *24*(2). https://doi.org/10.3390/ijms24021530

Dengler, V. L., Galbraith, M. D., & Espinosa, J. M. (2014). Transcriptional regulation by hypoxia inducible factors. *Critical Reviews in Biochemistry and Molecular Biology*, *49*(1), 1–15. https://doi.org/10.3109/10409238.2013.838205

Deshpande, D., Chhugani, K., Chang, Y., Karlsberg, A., Loeffler, C., Zhang, J., Muszyńska, A., Munteanu, V., Yang, H., Rotman, J., Tao, L., Balliu, B., Tseng, E., Eskin, E., Zhao, F., Mohammadi, P., P. Łabaj, P., & Mangul, S. (2023). RNA-seq data science: From raw data to effective interpretation. *Frontiers in Genetics*, *14*. https://doi.org/10.3389/fgene.2023.997383

Devic, E., Leschen, W., Murray, F., & Little, D. (2017). Growth performance, feed utilization and body composition of advanced nursing Nile tilapia (*Oreochromis niloticus*) fed diets containing Black Soldier Fly (*Hermetia illucens*) larvae meal. *Aquaculture Nutrition*, *24*. https://doi.org/10.1111/anu.12573

DeYoung, M. P., Horak, P., Sofer, A., Sgroi, D., & Ellisen, L. W. (2008). Hypoxia regulates TSC1/2–mTOR signaling and tumor suppression through REDD1-mediated 14–3–3 shuttling. *Genes & Development*, *22*(2), 239–251. https://doi.org/10.1101/gad.1617608

Dimou, A., Tsimihodimos, V., & Bairaktari, E. (2022). The Critical Role of the Branched Chain Amino Acids (BCAAs) Catabolism-Regulating Enzymes, Branched-Chain Aminotransferase (BCAT) and Branched-Chain α-Keto

Acid Dehydrogenase (BCKD), in Human Pathophysiology. *International Journal of Molecular Sciences*, *23*(7), 4022. https://doi.org/10.3390/ijms23074022

Dimou, A., Tsimihodimos, V., & Bairaktari, E. (2022). The Critical Role of the Branched Chain Amino Acids (BCAAs) Catabolism-Regulating Enzymes, Branched-Chain Aminotransferase (BCAT) and Branched-Chain α-Keto Acid Dehydrogenase (BCKD), in Human Pathophysiology. *International Journal of Molecular Sciences*, *23*(7), 4022. https://doi.org/10.3390/ijms23074022

Ding, C., Li, Y., Guo, F., Jiang, Y., Ying, W., Li, D., Yang, D., Xia, X., Liu, W., Zhao, Y., He, Y., Li, X., Sun, W., Liu, Q., Song, L., Zhen, B., Zhang, P., Qian, X., Qin, J., & He, F. (2016). A Cell-type-resolved Liver Proteome. *Molecular & Cellular Proteomics*, *15*(10), 3190–3202. https://doi.org/10.1074/mcp.M116.060145

Doering, C. B., Coursey, C., Spangler, W., & Danner, D. J. (1998). Murine branched chain α-ketoacid dehydrogenase kinase; cDNA cloning, tissue distribution, and temporal expression during embryonic development. *Gene*, *212*(2), 213–219. https://doi.org/10.1016/S0378-1119(98)00182-6

Drummond, M. J., & Rasmussen, B. B. (2008). Leucine-enriched nutrients and the regulation of mammalian target of rapamycin signalling and human skeletal muscle protein synthesis. *Current Opinion in Clinical Nutrition and Metabolic Care*, *11*(3), 222–226. https://doi.org/10.1097/MCO.0b013e3282fa17fb

Du, C., Liu, W. J., Yang, J., Zhao, S. S., & Liu, H. X. (2022). The Role of Branched-Chain Amino Acids and Branched-Chain α-Keto Acid Dehydrogenase Kinase in Metabolic Disorders. *Frontiers in Nutrition*, *9*, 932670. https://doi.org/10.3389/fnut.2022.932670

Du, R., Shi, X., Chen, F., Wang, L., Liang, H., & Hu, G. (2023). Corticotropin-Releasing Hormone: A Novel Stimulator of Somatolactin in Teleost Pituitary Cells. *Cells*. https://doi.org/10.3390/cells12242770

Duan, Y., Li, F., Li, Y., Tang, Y., Kong, X., Feng, Z., Anthony, T. G., Watford, M., Hou, Y., Wu, G., & Yin, Y. (2016). The role of leucine and its metabolites in protein and energy metabolism. *Amino Acids*, *48*(1), 41–51. https://doi.org/10.1007/s00726-015-2067-1

Duan, Y., Li, F., Li, Y., Tang, Y., Kong, X., Feng, Z., Anthony, T., Watford, M., Hou, Y., Wu, G., & Yin, Y. (2016). The role of leucine and its metabolites in protein and energy metabolism. *Amino Acids*, *4*, 41–51. https://doi.org/10.1007/s00726-015-2067-1

Duan, Y., Li, F., Li, Y., Tang, Y., Kong, X., Feng, Z., Anthony, T. G., Watford, M., Hou, Y., Wu, G., & Yin, Y. (2016). The role of leucine and its metabolites in protein and energy metabolism. *Amino Acids*, *48*(1), 41–51. https://doi.org/10.1007/s00726-015-2067-1

Dvergedal, H., Ødegård, J., Mydland, L. T., Øverland, M., Hansen, J. Ø., Ånestad, R. M., & Klemetsdal, G. (2019). Stable isotope profiling for large-scale evaluation of feed efficiency in Atlantic salmon (*Salmo salar*). *Aquaculture Research*, *50*(4), 1153–1161. https://doi.org/10.1111/are.13990

Ebeling, J. M., & Timmons, M. B. (2012). Recirculating Aquaculture Systems. In J. H. Tidwell (Ed.), *Aquaculture Production Systems* (1st edit, pp. 245–277). Wiley. https://doi.org/10.1002/9781118250105.ch11

Einarsson, M., Jokumsen, A., Baek, A., Jacobsen, C., Pedersen, S., Samuelsen, T., Palsson, J., Eliasen, O., & Triplenine, O. (2019). Nordic Centre of Excellence Network in Fishmeal and Fish oil. *Matis Zenodo*, 06–19, 62477. https://doi.org/10.5281/zenodo.3243334

Einen, O., Waagan, B., & Thomassen, M. S. (1998). Starvation prior to slaughter in Atlantic salmon (*Salmo salar*): I. Effects on weight loss, body shape, slaughter- and fillet-yield, proximate and fatty acid composition. *Aquaculture*, *166*(1), 85–104. https://doi.org/10.1016/S0044-8486(98)00279-8

England, B. K., Greiber, S., Mitch, W. E., Bowers, B. A., Herring, W. J., McKean, M., Ebb, R. G., Price, S. R., & Danner, D. J. (1995). Rat muscle branched-

chain ketoacid dehydrogenase activity and mRNAs increase with extracellular acidemia. *American Journal of Physiology-Cell Physiology*, *268*(6), C1395–C1400. https://doi.org/10.1152/ajpcell.1995.268.6.C1395

Espe, M. (2016). Functional amino acids in fish nutrition health and welfare. *Frontiers in Bioscience*, *8*(1), 757. https://doi.org/10.2741/757

Espe, M., Lai, F., Gomes, A. S., De Santis, C., Hartviksen, M. B., Holen, E., & Rønnestad, I. (2021). Leucine did not stimulate growth and accretion in either stressed or unstressed Atlantic salmon. *Aquaculture Nutrition*, *27*(6), 2459–2467. https://doi.org/10.1111/anu.13377

Espe, M., & Lied, E. (1994). Do Atlantic salmon (*Salmo salar*) utilize mixtures of free amino acids to the same extent as intact protein sources for muscle protein synthesis? *Comparative Biochemistry and Physiology Part A*, *107*(1), 249–254. https://doi.org/10.1016/0300-9629(94)90302-6

Espe, M., Veiseth-Kent, E., Zerrahn, J. E., Rønnestad, I., & Aksnes, A. (2016). Juvenile Atlantic salmon decrease white trunk muscle IGF-1 expression and reduce muscle and plasma free sulphur amino acids when methionine availability is low while liver sulphur metabolites mostly is unaffected by treatment. *Aquaculture Nutrition*, *22*(4), 801–812. https://doi.org/10.1111/anu.12294

Falco, F., Stincone, P., Cammarata, M., & Brandelli, A. (2020). Amino Acids as the Main Energy Source in Fish Tissues. *Aquaculture and Fisheries Studies*, *2*(2), 1–11. https://doi.org/10.31038/AFS.2020223

FAO. (2022). The State of World Fisheries and Aquaculture 2022. *Towards Blue Transformation*. *(SOFIA)*. Rome, FAO. https://doi.org/10.4060/cc0461en

Farhat, E., Talarico, G. G. M., Grégoire, M., Weber, J. M., & Mennigen, J. A. (2022). Epigenetic and post-transcriptional repression support metabolic suppression in chronically hypoxic goldfish. *Scientific Reports*, *12*(1), 5576. https://doi.org/10.1038/s41598-022-09374-8

Fazio, F., Ferrantelli, V., Fortino, G., Arfuso, F., Giangrosso, G., & Faggio, C. (2015). The influence of acute handling stress on some blood parameters in

cultured sea bream (*Sparus aurata* Linnaeus, 1758). *Italian Journal of Food Safety*, *4*(1), 4174. https://doi.org/10.4081/ijfs.2015.4174

Felig, P., Wahren, J., & Räf, L. (1973). Evidence of inter-organ amino-acid transport by blood cells in humans. *Proceedings of the National Academy of Sciences of the United States of America*, *70*(6), 1775–1779. https://doi.org/10.1073/pnas.70.6.1775

Fillatreau, S., Six, A., Magadan, S., Castro, R., Sunyer, J. O., & Boudinot, P. (2013). The Astonishing Diversity of Ig Classes and B Cell Repertoires in Teleost Fish. *Frontiers in Immunology*, *4*. https://doi.org/ 10.3389/fimmu.2013.00028

Folch, J., Lees, M., & Stanley, G. (1957). A simple method for the isolation and purification of total lipides from animal tissues. *Journal of Biological Chemistry*, *226*(1), 497–509. https://doi.org/10.1016/S0021-9258(18)64849-5

Froese, R. (2006). Cube law, condition factor and weight-length relationships: history, meta-analysis and recommendations. *Journal of Applied Ichthyology*, *22*(4), 241–253. https://doi.org/10.1111/j.1439-0426.2006.00805.x

Froese, R., Thorson, J. T., & Reyes, R. B. (2014). A Bayesian approach for estimating length-weight relationships in fishes. *Journal of Applied Ichthyology*, *30*(1), 78–85. https://doi.org/10.1111/jai.12299

Fu, Z., Liang, X., Shi, L., Tang, L., Chen, D., Liu, A., & Shao, C. (2021). SYT8 promotes pancreatic cancer progression via the TNNI2/ERRα/SIRT1 signaling pathway. *Cell Death Discovery*, *7*(1), 390. https://doi.org/10.1038/s41420-021-00779-4

Fuentes, E. N., Safian, D., Einarsdottir, I. E., Valdés, J. A., Elorza, A. A., Molina, A., & Björnsson, B. T. (2013). Nutritional status modulates plasma leptin, AMPK and TOR activation, and mitochondrial biogenesis: Implications for cell metabolism and growth in skeletal muscle of the fine flounder. *General and Comparative Endocrinology*, *186*, 172–180. https://doi.org/10.1016/j.ygcen.2013.02.009

Fujioka, A., Nagano, M., Ikegami, K., Masumoto, K-H., Yoshikawa, T., Koinuma, S., Nakahama, K-I., & Shigeyoshi, Y. (2023). Circadian expression and specific localization of synaptotagmin17 in the suprachiasmatic nucleus, the master circadian oscillator in mammals. *Brain Research*, *1798*, 148129. https://doi.org/10.1016/j.brainres.2022.148129

Gałęzowska, G., Ratajczyk, J., & Wolska, L. (2021). Determination of amino acids in human biological fluids by high-performance liquid chromatography: critical review. *Amino Acids*, *53*(7), 993–1009. https://doi.org/10.1007/s00726-021-03002-x

Gálvez, A. O., de Macêdo Dantas, D. M., de Moraes, L. B. S., & Mota, G. C. P. (2024). Aquaculture Diets: Live Feed and Sustainable Aquafeed. In N. M. Faudzi, M. D. Shah, N. Mazlan, S. Raehanah Muhamad Shaleh (Eds.), *Essentials of Aquaculture Practices* (pp. 21–40). Springer Nature. https://doi.org/10.1007/978-981-97-6699-4_2

Gan, L., Jiang, W. D., Wu, P., Liu, Y., Jiang, J., Li, S. H., Tang, L., Kuang, S. Y., Feng, L., & Zhou, X. Q. (2014). Flesh Quality Loss in Response to Dietary Isoleucine Deficiency and Excess in Fish: A Link to Impaired Nrf2-Dependent Antioxidant Defense in Muscle. *PLOS ONE*, *9*(12), e115129. https://doi.org/10.1371/journal.pone.0115129

Gao, Y., Dai, Z., Shi, C., Zhai, G., Jin, X., He, J., Lou, Q., & Yin, Z. (2016). Depletion of Myostatin b Promotes Somatic Growth and Lipid Metabolism in Zebrafish. *Frontiers in Endocrinology*, *7*. https://doi.org/10.3389/fendo.2016.00088

Garina, D. V. (2021). Ependymins: New Data on Participation in the Regulation of Physiological and Behavioral Responses in Teleosts (Review). *Inland Water Biology*, *14*(1), 78–86. https://doi.org/10.1134/S199508292101003X

Gatlin, D. M., Barrows, F. T., Brown, P., Dabrowski, K., Gaylord, T. G., Hardy, R. W., Herman, E., Hu, G., Krogdahl, Å., Nelson, R., Overturf, K., Rust, M., Sealey, W., Skonberg, D., J Souza, E., Stone, D., Wilson, R., & Wurtele, E. (2007). Expanding the utilization of sustainable plant products in aquafeeds: a review. *Aquaculture Research*, *38*(6), 551–579.

https://doi.org/10.1111/j.1365-2109.2007.01704.x

Ge, S. X., Jung, D., & Yao, R. (2020). ShinyGO: a graphical gene-set enrichment tool for animals and plants. *Bioinformatics*, *36*(8), 2628–2629. https://doi.org/10.1093/bioinformatics/btz931

Ginzinger, D. G. (2002). Gene quantification using real-time quantitative PCR: An emerging technology hits the mainstream. *Experimental Hematology*, *30*(6), 503–512. https://doi.org/10.1016/S0301-472X(02)00806-8

Glencross, B. D., Berry, A., Clokie, B., Hevroy, E., Huyben, D., Martinez-Rubio, L., Mathew, C. A., Munoz, P., MacKenzie, S., & Wilson, R. W. (2024). Isolation of intake mediated effects demonstrate that the phenomic benefits of dietary omega-3 are nominal to Atlantic salmon when reared in a challenging (hypoxic) environment. *Aquaculture*, *581*, 740461. https://doi.org/10.1016/j.aquaculture.2023.740461

Glencross, B. D., Booth, M., & Allan, G. L. (2007). A feed is only as good as its ingredients– a review of ingredient evaluation strategies for aquaculture feeds. *Aquaculture Nutrition*, *13*(1), 17–34. https://doi.org/10.1111/j.1365-2095.2007.00450.x

Glencross, B., Evans, D., Dods, K., McCafferty, P., Hawkins, W., Maas, R., & Sipsas, S. (2005). Evaluation of the digestible value of lupin and soybean protein concentrates and isolates when fed to rainbow trout, *Oncorhynchus mykiss*, using either stripping or settlement faecal collection methods. *Aquaculture*, *245*(1–4), 211–220. https://doi.org/10.1016/j.aquaculture.2004.11.033

Glencross, B., Grobler, T., & Huyben, D. (2021). Digestible nutrient and energy values of corn and wheat glutens fed to Atlantic salmon (*Salmo salar*) are affected by feed processing method. *Aquaculture*, *544*, 737133. https://doi.org/10.1016/j.aquaculture.2021.737133

Glover, C. N., Bucking, C., & Wood, C. M. (2013). The skin of fish as a transport epithelium: a review. *Journal of Comparative Physiology B*, *183*(7), 877–891. https://doi.org/10.1007/s00360-013-0761-4

Go, M., Shin, E., Jang, S. Y., Nam, M., Hwang, G. S., & Lee, S. Y. (2022). BCAT1 promotes osteoclast maturation by regulating branched-chain amino acid metabolism. *Experimental & Molecular Medicine*, *54*(6), 825–833. https://doi.org/10.1038/s12276-022-00775-3

Gollwitzer, P., Grützmacher, N., Wilhelm, S., Kümmel, D., & Demetriades, C. (2022). A Rag GTPase dimer code defines the regulation of mTORC1 by amino acids. *Nature Cell Biology*, *24*(9), 1394–1406. https://doi.org/10.1038/s41556-022-00976-y

Gómez, G. D., & Balcázar, J. L. (2008). A review on the interactions between gut microbiota and innate immunity of fish. *FEMS Immunology & Medical Microbiology*, *52*(2), 145–154. https://doi.org/10.1111/j.1574-695X.2007.00343.x

Gómez-Requeni, P., Mingarro, M., Calduch-Giner, J. A., Médale, F., Martin, S. A. M., Houlihan, D. F., Kaushik, S., & Pérez-Sánchez, J. (2004). Protein growth performance, amino acid utilisation and somatotropic axis responsiveness to fish meal replacement by plant protein sources in gilthead sea bream (*Sparus aurata*). *Aquaculture*, *232*(1), 493–510. https://doi.org/10.1016/S0044-8486(03)00532-5

Gray, N., Plumb, R. S., Wilson, I. D., & Nicholson, J. K. (2019). A validated UPLC-MS/MS assay for the quantification of amino acids and biogenic amines in rat urine. *Journal of Chromatography B*, *1106–1107*, 50–57. https://doi.org/10.1016/j.jchromb.2018.12.028

Gray, N., Zia, R., King, A., Patel, V. C., Wendon, J., McPhail, M. J. W., Coen, M., Plumb, R. S., Wilson, I. D., & Nicholson, J. K. (2017). High-Speed Quantitative UPLC-MS Analysis of Multiple Amines in Human Plasma and Serum via Precolumn Derivatization with 6-Aminoquinolyl-N-hydroxysuccinimidyl Carbamate: Application to Acetaminophen-Induced Liver Failure. *Analytical Chemistry*, *89*(4), 2478–2487. https://doi.org/10.1021/acs.analchem.6b04623

Green, T. J., Smullen, R., & Barnes, A. C. (2013). Dietary soybean protein concentrate-induced intestinal disorder in marine farmed Atlantic salmon,

Salmo salar is associated with alterations in gut microbiota. *Veterinary Microbiology*, *166*(1–2), 286–292. https://doi.org/10.1016/j.vetmic.2013.05.009

Griffin, R. A., Boyd, A., Weinrauch, A., & Blewett, T. A. (2023). Invasive investigation: uptake and transport of l-leucine in the gill epithelium of crustaceans. *Conservation Physiology*, *11*(1), coad015. https://doi.org/10.1093/conphys/coad015

Gu, M., Zhang, W. B., Bai, N., Mai, K. S., & Xu, W. (2013). Effects of dietary crystalline methionine or oligo-methionine on growth performance and feed utilization of white shrimp (*Litopenaeus vannamei*) fed plant protein-enriched diets. *Aquaculture Nutrition*, *19*(s1), 39–46. https://doi.org/10.1111/anu.12089

Guo, T., Wang, Y., Jiang, P., Li, J., Liu, Q., & Chi, L. (2023). miR-155 Regulates Photoperiod Induced Gonadal Development in Atlantic Salmon (*Salmo salar*) by Targeting Brain-Derived Neurotrophic Factor. *Fishes*. https://doi.org/10.3390/fishes8070345

Gusarova, G. A., Trejo, H. E., Dada, L. A., Briva, A., Welch, L. C., Hamanaka, R. B., Mutlu, G. M., Chandel, N. S., Prakriya, M., & Sznajder, J. I. (2011). Hypoxia leads to Na,K-ATPase downregulation via Ca(2+) release-activated Ca(2+) channels and AMPK activation. *Molecular and Cellular Biology*, *31*(17), 3546–3556. https://doi.org/10.1128/MCB.05114-11

Gwinn, D. M., Shackelford, D. B., Egan, D. F., Mihaylova, M. M., Mery, A., Vasquez, D. S., Turk, B. E., & Shaw, R. J. (2008). AMPK Phosphorylation of Raptor Mediates a Metabolic Checkpoint. *Molecular Cell*, *30*(2), 214–226. https://doi.org/10.1016/j.molcel.2008.03.003

Hall, T. R., Wallin, R., Reinhart, G. D., & Hutson, S. M. (1993). Branched chain aminotransferase isoenzymes. Purification and characterization of the rat brain isoenzyme. *Journal of Biological Chemistry*, *268*(5), 3092–3098. https://doi.org/10.1016/S0021-9258(18)53663-2

Hardy, R. W. (2010). Utilization of plant proteins in fish diets: effects of global demand and supplies of fishmeal. *Aquaculture Research*, *41*(5), 770–776. https://doi.org/10.1111/j.1365-2109.2009.02349.x

Hardy, R. W., & Kaushik, S. J. (2021). *Fish Nutrition*. Elsevier Science & Technology.http://ebookcentral.proquest.com/lib/stir/detail.action?docID=6785136

Harris, R. A., Kobayashi, R., Murakami, T., & Shimomura, Y. (2001). Regulation of Branched-Chain α-Keto Acid Dehydrogenase Kinase Expression in Rat Liver. *The Journal of Nutrition*, *131*(3), 841S-845S. https://doi.org/10.1093/jn/131.3.841S

Harrison, P. W., Amode, M. R., Austine-Orimoloye, O., Azov, A. G., Barba, M., Barnes, I., Becker, A., Bennett, R., Berry, A., Bhai, J., Bhurji, S. K., Boddu, S., Branco Lins, P. R., Brooks, L., Ramaraju, S. B., Campbell, L. I., Martinez, M. C., Charkhchi, M., Chougule, K., Cockburn, A., Davidson, C., De Silva, N. H., Dodiya, K., Donaldson, S., El Houdaigui, B., Naboulsi, T. E., Fatima, R., Giron, C. G., Genez, T., Grigoriadis, D., Ghattaoraya, G. S., Martinez, J. G., Gurbich, T. A., Hardy, M., Hollis, Z., Hourlier, T., Hunt, T., Kay, M., Kaykala, V., Le, T., Lemos, D., Lodha, D., Marques-Coelho, D., Maslen, G., Merino, G. A., Mirabueno, L. P., Mushtaq, A., Hossain, S. N., Ogeh, D. N., Sakthivel, M. P., Parker, A., Perry, M., Piližota, I., Poppleton, D., Prosovetskaia, I., Raj, S., Pérez-Silva, J. G., Salam, A. I. A., Saraf, S., Saraiva-Agostinho, N., Sheppard, D., Sinha, S., Sipos, B., Sitnik, V., Stark, W., Steed, E., Suner, M. M., Surapaneni, L., Sutinen, K., Tricomi, F. F., Urbina-Gómez, D., Veidenberg, A., Walsh, T. A., Ware, D., Wass, E., Willhoft, N. L., Allen, J., Alvarez-Jarreta, J., Chakiachvili, M., Flint, B., Giorgetti, S., Haggerty, L., Ilsley, G. R., Keatley, J., Loveland, J. E., Moore, B., Mudge, J. M., Naamati, G., Tate, J., Trevanion, S. J., Winterbottom, A., Frankish, A., Hunt, S. E., Cunningham, F., Dyer, S., Finn, R. D., Martin, F. J., & Yates, A. D. (2024). Ensembl 2024. *Nucleic Acids Research*, *52*(D1), D891–D899. https://doi.org/10.1093/nar/gkad1049

He, S.M., Sun, S., Chen, A.Q., Lv, S.J., Qiu, C.Z., Wei, M.L., Liu, W., Liu, H.R., Zhang, L., & Ren, D.L. (2022). Hypoxia regulates cytokines expression and neutrophils migration by ERK signaling in zebrafish. *Fish & Shellfish Immunology*, *125*, 212–219. https://doi.org/10.1016/j.fsi.2022.05.006

Heeley, N., Kirwan, P., Darwish, T., Arnaud, M., Evans, M. L., Merkle, F. T., Reimann, F., Gribble, F. M., & Blouet, C. (2018). Rapid sensing of l-leucine by human and murine hypothalamic neurons: Neurochemical and mechanistic insights. *Molecular Metabolism*, *10*, 14–27. https://doi.org/10.1016/j.molmet.2018.01.021

Heywood, W. E., Searle, J., Collis, R., Doykov, I., Ashworth, M., Sebire, N., Bamber, A., Gautel, M., Eaton, S., Coats, C. J., Elliott, P. M., & Mills, K. (2024). A proof of principle 2D spatial proteome mapping analysis reveals distinct regional differences in the cardiac proteome. *Life, 14*(8), 970. https://doi.org/10.3390/life14080970

Hikima, J-I, Jung, T. S., & Aoki, T. (2011). Immunoglobulin genes and their transcriptional control in teleosts. *Developmental & Comparative Immunology*, *35*(9), 924–936. https://doi.org/10.1016/j.dci.2010.10.011

Hinkle, J. S., Rivera, C. N., & Vaughan, R. A. (2022). Branched-Chain Amino Acids and Mitochondrial Biogenesis: An Overview and Mechanistic Summary. *Molecular Nutrition & Food Research*, *66*(20), 2200109. https://doi.org/10.1002/mnfr.202200109

Ho, J. J. D., Wang, M., Audas, T. E., Kwon, D., Carlsson, S. K., Timpano, S., Evagelou, S. L., Brothers, S., Gonzalgo, M. L., Krieger, J. R., Chen, S., Uniacke, J., & Lee, S. (2016). Systemic Reprogramming of Translation Efficiencies on Oxygen Stimulus. *Cell Reports*, *14*(6), 1293–1300. https://doi.org/10.1016/j.celrep.2016.01.036

Hoar, W. S. (2024). Chapter 2 - The physiology of smolting salmonids. In D. J. Randall, A. P. Farrell, C. J. Brauner, et al. (Eds.), *The 50th Anniversary Issue of Fish Physiology: Physiological Applications* (Vol. 40, pp. 9–70). Academic Press. https://doi.org/10.1016/bs.fp.2024.06.001

Holecek, M. (2001). Effect of starvation on branched-chain alpha-keto acid dehydrogenase activity in rat heart and skeletal muscle. *Physiological Research*, *50*(1), 19–24. https://doi.org/10.33549/physiolres.930000.50.19

Holecek, M. (2001). The BCAA–BCKA cycle: its relation to alanine and glutamine synthesis and protein balance. *Nutrition*, *17*(1), 70. https://doi.org/10.1016/S0899-9007(00)00483-4

Holecek, M. (2013). Branched-chain amino acids and ammonia metabolism in liver disease: Therapeutic implications. *Nutrition*, *29*(10), 1186–1191. https://doi.org/10.1016/j.nut.2013.01.022

Holecek, M. (2017). Beta-hydroxy-beta-methylbutyrate supplementation and skeletal muscle in healthy and muscle-wasting conditions. *Journal of Cachexia, Sarcopenia and Muscle*, *8*(4), 529–541. https://doi.org/10.1002/jcsm.12208

Holecek, M. (2018). Branched-chain amino acids in health and disease: Metabolism, alterations in blood plasma, and as supplements. *Nutrition & Metabolism*, *15*(1), 33. https://doi.org/10.1186/s12986-018-0271-1

Holecek, M. (2020). Why Are Branched-Chain Amino Acids Increased in Starvation and Diabetes? *Nutrients, 12*(10), 3087. https://doi.org/10.3390/nu12103087

Holecek, M., Sprongl, L., & Tilser, I. (2001). Metabolism of branched-chain amino acids in starved rats: the role of hepatic tissue. *Physiological Research*, *50*(1), 25–33.

Hoppe, A. (2012). What mRNA Abundances Can Tell us about Metabolism. *Metabolites*, *2*(3), 614–631. https://doi.org/10.3390/metabo2030614

Hou, Y., & Wu, G. (2018). Nutritionally Essential Amino Acids. *Advances in Nutrition*, *9*(6), 849–851. https://doi.org/10.1093/advances/nmy054

Hu, M., Wang, Y., Wang, Q., Zhao, M., Xiong, B., Qian, X., Zhao, Y., & Luo, Z. (2008). Replacement of fish meal by rendered animal protein ingredients with lysine and methionine supplementation to practical diets for gibel carp, *Carassius auratus gibelio*. *Aquaculture*, *275*(1), 260–265.

https://doi.org/10.1016/j.aquaculture.2008.01.005

Hua, K. (2013). Estimating maintenance amino acids requirements of fish through a nonlinear mixed modelling approach. *Aquaculture Research*, *44*(4), 542–553. https://doi.org/10.1111/j.1365-2109.2011.03057.x

Huang, D. W., Sherman, B. T., & Lempicki, R. A. (2009). Bioinformatics enrichment tools: paths toward the comprehensive functional analysis of large gene lists. *Nucleic Acids Research*, *37*(1), 1–13. https://doi.org/10.1093/nar/gkn923

Huang, D. W., Sherman, B. T., & Lempicki, R. A. (2009). Systematic and integrative analysis of large gene lists using DAVID bioinformatics resources. *Nature Protocols*, *4*(1), 44–57. https://doi.org/10.1038/nprot.2008.211

Huang, Z-H., Du, Y-P., Wen, J-T., Lu, B-F., & Zhao, Y. (2022). snoRNAs: functions and mechanisms in biological processes, and roles in tumor pathophysiology. *Cell Death Discovery*, *8*(1), 259. https://doi.org/10.1038/s41420-022-01056-8

Huang, Z., Tan, X_H., Zhou, C-P., Yang, Y-K., Qi, C-I., Zhao, S-Y., & Lin, H-Z. (2018). Effect of dietary valine levels on the growth performance, feed utilization and immune function of juvenile golden pompano, *Trachinotus ovatus*. *Aquaculture Nutrition*, *24*(1), 74–82. https://doi.org/10.1111/anu.12535

Hussain, S. M., Bano, A. A., Ali, S., Rizwan, M., Adrees, M., Zahoor, A. F., Sarker, P. K., Hussain, M., Arsalan, M. Z. ul H., Yong, J. W. H., & Naeem, A. (2024). Substitution of fishmeal: Highlights of potential plant protein sources for aquaculture sustainability. *Heliyon*, *10*(4), e26573. https://doi.org/10.1016/j.heliyon.2024.e26573

Huyben, D., Cronin, T., Bartie, K. L., Matthew, C., Sissener, N. H., Hundal, B. K., Homer, N. Z. M., Ruyter, B., & Glencross, B. (2023). Steroidogenic and innate immune responses in Atlantic salmon are influenced by dietary total

lipid, long chain polyunsaturated fatty acids and dissolved oxygen. *Aquaculture*, *564*. https://doi.org/10.1016/j.aquaculture.2022.739028

Huyben, D., Grobler, T., Matthew, C., Bou, M., Ruyter, B., & Glencross, B. (2021). Requirement for omega-3 long-chain polyunsaturated fatty acids by Atlantic salmon is relative to the dietary lipid level. *Aquaculture*, *531*, 735805. https://doi.org/10.1016/j.aquaculture.2020.735805

Huyben, D., Matthew, C., Muñoz-Lopez, P., Ruyter, B., & Glencross, B. (2021). Hypoxia does not change responses to dietary omega-3 long-chain polyunsaturated fatty acids, but rather reduces dietary energy demand by Atlantic salmon. *Aquaculture Nutrition*, *27*(5), 1396–1410. https://doi.org/10.1111/anu.13278

Hvas, M., Stien, L. H., & Oppedal, F. (2020). The metabolic rate response to feed withdrawal in Atlantic salmon post-smolts. *Aquaculture*, *529*, 735690. https://doi.org/10.1016/j.aquaculture.2020.735690

Ignatz, E. H., Zanuzzo, F. S., Sandrelli, R. M., Clow, K. A., Rise, M. L., & Gamperl, A. K. (2021). Phenotypic stress response does not influence the upper thermal tolerance of male Atlantic salmon (*Salmo salar*). *Journal of Thermal Biology*, *101*, 103102. https://doi.org/10.1016/j.jtherbio.2021.103102

Inoki, K., Ouyang, H., Zhu, T., Lindvall, C., Wang, Y., Zhang, X., Yang, Q., Bennett, C., Harada, Y., Stankunas, K., Wang, C-Y. He, X., MacDougald, O. A., You, M., Williams, B. O., & Guan, K. L. (2006). TSC2 Integrates Wnt and Energy Signals via a Coordinated Phosphorylation by AMPK and GSK3 to Regulate Cell Growth. *Cell*, *126*(5), 955–968. https://doi.org/10.1016/j.cell.2006.06.055

Ip, Y. K., & Chew, S. F. (2010). Ammonia production, excretion, toxicity, and defense in fish: a review. *Frontiers in Physiology*, *1*, 134. https://doi.org/10.3389/fphys.2010.00134

Isakov, A., Lorenz, H., Zolotarev, A., & Kotelnikova, E. (2020). Heteromolecular compounds in binary systems of amino acids with opposite and same chiralities. *CrystEngComm*, *22*. https://doi.org/10.1039/C9CE01333D

Ivanova, L., Rangel-Huerta, O. D., Tartor, H., Gjessing, M. C., Dahle, M. K., & Uhlig, S. (2021). Fish Skin and Gill Mucus: A Source of Metabolites for Non-Invasive Health Monitoring and Research. *Metabolites*, *12*(1). https://doi.org/10.3390/metabo12010028

Jacobsen, H. J., Samuelsen, T. A., Girons, A., & Kousoulaki, K. (2018). Different enzyme incorporation strategies in Atlantic salmon diet containing soybean meal: Effects on feed quality, fish performance, nutrient digestibility and distal intestinal morphology. *Aquaculture*, *491*, 302–309. https://doi.org/10.1016/j.aquaculture.2018.03.053

Jacovetti, C., Bayazit, M. B., & Regazzi, R. (2021). Emerging Classes of Small Non-Coding RNAs With Potential Implications in Diabetes and Associated Metabolic Disorders. *Frontiers in Endocrinology*, *12*. https://doi.org/10.3389/fendo.2021.670719

Jamwal, S., & Kumar, P. (2015). Antidepressants for neuroprotection in Huntington's disease: A review. *European Journal of Pharmacology*, *769*, 33–42. https://doi.org/10.1016/j.ejphar.2015.10.033

Jiang, Y., Yan, F., Feng, Z., Lazarovici, P., & Zheng, W. (2019). Signaling Network of Forkhead Family of Transcription Factors (FOXO) in Dietary Restriction. *Cells*, *9*(1). https://doi.org/10.3390/cells9010100

Jobling, M. (2012). National Research Council (NRC): Nutrient requirements of fish and shrimp. *Aquaculture International*, *20*(3), 601–602. https://doi.org/10.1007/s10499-011-9480-6

Johansen, A., Thiede, B., Anonsen, J. H., & Nilsson, G. E. (2023). Surviving without oxygen involves major tissue specific changes in the proteome of crucian carp (*Carassius carassius*). *PeerJ*, *11*, e14890. https://doi.org/10.7717/peerj.14890

Johansen, S. J., & Jobling, M. (1998). The influence of feeding regime on growth and slaughter traits of cage-reared Atlantic salmon. *Aquaculture International*, *6*, 1–17. https://doi.org/10.1023/A:1009250118318

Johnson, I., Sorokin, N., Atkinson, C., Rule, K., & Hope, S. J. (2012). Proposed EQS for Water Framework Directive Annex VIII substances : ammonia (un-ionised). *Water Framework Directive* (WFD52(ii)). UK: The Environment Agency. https://www.wfduk.org/sites/default/files/Media/ammonia.pdf

Jones, M. C., Zha, J., & Humphries, M. J. (2019). Connections between the cell cycle, cell adhesion and the cytoskeleton. *Philosophical Transactions of the Royal Society B: Biological Sciences*, *374*(1779). https://doi.org/10.1098/rstb.2018.0227

Joshi, J. N., Lerner, A. D., Scallo, F., Grumet, A. N., Matteson, P., Millonig, J. H., & Valvezan, A. J. (2024). mTORC1 activity oscillates throughout the cell cycle, promoting mitotic entry and differentially influencing autophagy induction. *Cell Reports*, *43*(8), 114543. https://doi.org/10.1016/j.celrep.2024.114543

Kaelin, W. G. J., & Ratcliffe, P. J. (2008). Oxygen sensing by metazoans: the central role of the HIF hydroxylase pathway. *Molecular Cell*, *30*(4), 393–402. https://doi.org/10.1016/j.molcel.2008.04.009

Kajimura, M., Croke, S. J., Glover, C. N., & Wood, C. M. (2004). Dogmas and controversies in the handling of nitrogenous wastes: The effect of feeding and fasting on the excretion of ammonia, urea and other nitrogenous waste products in rainbow trout. *Journal of Experimental Biology*, *207*(12), 1993–2002. https://doi.org/10.1242/jeb.00901

Kalananthan, T., Lai, F., Gomes, A. S., Murashita, K., Handeland, S., & Rønnestad, I. (2020). The Melanocortin System in Atlantic Salmon (*Salmo salar* L.) and Its Role in Appetite Control. *Frontiers in Neuroanatomy*, *14*. https://doi.org/10.3389/fnana.2020.00048

Kanehisa, M., Furumichi, M., Sato, Y., Ishiguro-Watanabe, M., & Tanabe, M. (2021). KEGG: integrating viruses and cellular organisms. *Nucleic Acids Research*, *49*(D1), D545–D551. https://doi.org/10.1093/nar/gkaa970

Karakach, T. K., Huenupi, E. C., Soo, E. C., Walter, J. A., & Afonso, L. O. B. (2009). 1H-NMR and mass spectrometric characterization of the metabolic

response of juvenile Atlantic salmon (*Salmo salar*) to long-term handling stress. *Metabolomics*, *5*(1), 123–137. https://doi.org/10.1007/s11306-008-0144-0

Katayama, N., Makoto, K., & Kishida, O. (2016). An aquatic vertebrate can use amino acids from environmental water. *Proceedings. Biological Sciences*, *283*(1839). https://doi.org/10.1098/rspb.2016.0996

Keitel-Gröner, F., Hoel, E., Husebø, C., Le, H. T. M. D., Bjerkestrand, K. M., Lagos, L., Sandstad, M., Knudsen, D. L., Rennemo, J., & Berge, K. (2024). Haematological and Biochemical Reference Intervals Towards a Proactive Health Monitoring Approach in Norwegian Atlantic Salmon Farming. *Journal of Fish Diseases, 48*(9), e14036. https://doi.org/10.1111/jfd.14036

Kietzmann, T., & Mäkelä, V. H. (2021). The hypoxia response and nutritional peptides. *Peptides*, *138*, 170507. https://doi.org/10.1016/j.peptides.2021.170507

Kim, M., Kowalsky, A. H., & Lee, J. H. (2021). Sestrins in Physiological Stress Responses. *Annual Review of Physiology*, *83*, 381–403. https://doi.org/10.1146/annurev-physiol-031620-092317

Kim, I. V, Ross, E. J., Dietrich, S., Döring, K., Sánchez Alvarado, A., & Kuhn, C. D. (2019). Efficient depletion of ribosomal RNA for RNA sequencing in planarians. *BMC Genomics*, *20*(1), 909. https://doi.org/10.1186/s12864-019-6292-y

Kimball, S. R., & Jefferson, L. S. (2006). Signaling Pathways and Molecular Mechanisms through which Branched-Chain Amino Acids Mediate Translational Control of Protein Synthesis. *The Journal of Nutrition*, *136*(1), 227S-231S. https://doi.org/10.1093/jn/136.1.227S

Kleszka, K., Leu, T., Quinting, T., Jastrow, H., Pechlivanis, S., Fandrey, J., & Schreiber, T. (2020). Hypoxia-inducible factor-2α is crucial for proper brain development. *Scientific Reports*, *10*(1), 19146. https://doi.org/10.1038/s41598-020-75838-4

Kok, B., Malcorps, W., Tlusty, M. F., Eltholth, M. M., Auchterlonie, N. A., Little, D. C., Harmsen, R., Newton, R. W., & Davies, S. J. (2020). Fish as feed: Using economic allocation to quantify the Fish In: Fish Out ratio of major fed aquaculture species. *Aquaculture*, *528*, 735474. https://doi.org/10.1016/j.aquaculture.2020.735474

Kolberg, L., Raudvere, U., Kuzmin, I., Adler, P., Vilo, J., & Peterson, H. (2023). g:Profiler- interoperable web service for functional enrichment analysis and gene identifier mapping (2023 update). *Nucleic Acids Research*, *51*(W1), W207–W212. https://doi.org/10.1093/nar/gkad347

Komiya, Y., & Habas, R. (2008). Wnt signal transduction pathways. *Organogenesis*, *4*(2), 68–75. https://doi.org/10.4161/org.4.2.5851

Korman, J., Yard, M. D., Dzul, M. C., Yackulic, C. B., Dodrill, M. J., Deemer, B. R., & Kennedy, T. A. (2021). Changes in prey, turbidity, and competition reduce somatic growth and cause the collapse of a fish population. *Ecological Monographs*, *91*(1), e01427. https://doi.org/10.1002/ecm.1427

Kousoulaki, K., Krasnov, A., Mørkøre, T., Sweetman, J., Torgersen, J. S., & Østbye, T. K. K. (2015). Metabolism, health and fillet nutritional quality in Atlantic salmon (*Salmo salar*) fed diets containing n-3-rich microalgae. *Journal of Nutritional Science*, *4*, e24. https://doi.org/10.1017/jns.2015.14

Kousoulaki, K., Krasnov, A., Ytteborg, E., Sweetman, J., Pedersen, M. E., Høst, V., & Murphy, R. (2021). A full factorial design to investigate interactions of variable essential amino acids, trace minerals and vitamins on Atlantic salmon smoltification and post transfer performance. *Aquaculture Reports*, *20*, 100704. https://doi.org/10.1016/j.aqrep.2021.100704

Koussounadis, A., Langdon, S. P., Um, I. H., Harrison, D. J., & Smith, V. A. (2015). Relationship between differentially expressed mRNA and mRNA-protein correlations in a xenograft model system. *Scientific Reports*, *5*(1), 10775. https://doi.org/10.1038/srep10775

Krasnov, A., Johansen, L. H., Karlsen, C., Sveen, L., Ytteborg, E., Timmerhaus, G., Lazado, C. C., & Afanasyev, S. (2021). Transcriptome Responses of

Atlantic Salmon (*Salmo salar* L.) to Viral and Bacterial Pathogens, Inflammation, and Stress. *Frontiers in Immunology*, *12*. https://doi.org/10.3389/fimmu.2021.705601

Krogdahl, Å., Penn, M., Thorsen, J., Refstie, S., & Bakke, A. M. (2010). Important antinutrients in plant feedstuffs for aquaculture: an update on recent findings regarding responses in salmonids. *Aquaculture Research*, *41*(3), 333–344. https://doi.org/10.1111/j.1365-2109.2009.02426.x

Krogdahl, Å., Sundby, A., & Holm, H. (2015). Characteristics of digestive processes in Atlantic salmon (*Salmo salar*). Enzyme pH optima, chyme pH, and enzyme activities. *Aquaculture*, *449*, 27–36. https://doi.org/10.1016/j.aquaculture.2015.02.032

Kroupova, H., Machova, J., & Svobodova, Z. (2005). Nitrite influence on fish: a review. *Veterinarni Medicina*, *50*(11), 461–471. http://dx.doi.org/10.17221/5650-VETMED

Kuhlmann, K., Cieselski, M., & Schumann, J. (2021). Relative versus absolute RNA quantification: a comparative analysis based on the example of endothelial expression of vasoactive receptors. *Biological Procedures Online*, *23*(1), 6. https://doi.org/10.1186/s12575-021-00144-w

Kullgren, A., Jutfelt, F., Fontanillas, R., Sundell, K., Samuelsson, L., Wiklander, K., Kling, P., Koppe, W., Larsson, D. G. J., Björnsson, B. T., & Jönsson, E. (2013). The impact of temperature on the metabolome and endocrine metabolic signals in Atlantic salmon (*Salmo salar*). *Comparative Biochemistry and Physiology Part A: Molecular & Integrative Physiology*, *164*(1), 44–53. https://doi.org/10.1016/j.cbpa.2012.10.005

Kvamme, B. O., Gadan, K., Finne-Fridell, F., Niklasson, L., Sundh, H., Sundell, K., Taranger, G. L., & Evensen, Ø. (2013). Modulation of innate immune responses in Atlantic salmon by chronic hypoxia-induced stress. *Fish & Shellfish Immunology*, *34*(1), 55–65. https://doi.org/10.1016/j.fsi.2012.10.006

Laager, R., Ninnis, R., & Keller, U. (1993). Comparison of the effects of recombinant human insulin-like growth factor-I and insulin on glucose and leucine kinetics in humans. *The Journal of Clinical Investigation*, *92*(4), 1903–1909. https://doi.org/10.1172/JCI116783

Lahiri, V., Hawkins, W. D., & Klionsky, D. J. (2019). Watch What You (Self-) Eat: Autophagic Mechanisms that Modulate Metabolism. *Cell Metabolism*, *29*(4), 803–826. https://doi.org/10.1016/j.cmet.2019.03.003

Lai, F., Comesaña, S., Gomes, A. S., Flatejord, D., Tolås, I., Espe, M., De Santis, C., Hartviksen, M. B., Verri, T., Soengas, J. L., & Rønnestad, I. (2023). Anorectic role of high dietary leucine in farmed Atlantic salmon (*Salmo salar* L.): Effects on feed intake, growth, amino acid transporters and appetite-control neuropeptides. *Aquaculture*, *566*, 739204. https://doi.org/10.1016/j.aquaculture.2022.739204

Lall, S. P., & Anderson, S. (2005). Amino acid nutrition of salmonids: Dietary requirements and bioavailability. In D. Montero, B. Basurco, I. Nengas, M. Alexis & M. Izquierdo (Eds.), *Cahiers Options Méditerranéennes (Mediterranean fish nutrition)* (Mediterran, Vol. 63). Zaragoza: CIHEAM. https://om.ciheam.org/ressources/om/pdf/c63/05600068.pdf

Lall, S. P., & Tibbetts, S. M. (2009). Nutrition, Feeding, and Behavior of Fish. *Veterinary Clinics of North America: Exotic Animal Practice*, *12*(2), 361–372. https://doi.org/10.1016/j.cvex.2009.01.005

Landini, A., Trbojević-Akmačić, I., Navarro, P., Tsepilov, Y. A., Sharapov, S. Z., Vučković, F., Polašek, O., Hayward, C., Petrović, T., Vilaj, M., Aulchenko, Y. S., Lauc, G., Wilson, J. F., & Klarić, L. (2022). Genetic regulation of post-translational modification of two distinct proteins. *Nature Communications*, *13*(1), 1586. https://doi.org/10.1038/s41467-022-29189-5

Langer, S., Scislowski, P. W. D., Brown, D. S., Dewey, P., & Fuller, M. F. (2000). Interactions among the branched-chain amino acids and their effects on methionine utilization in growing pigs: effects on plasma amino– and keto–acid concentrations and branched-chain keto-acid dehydrogenase activity. *British Journal of Nutrition*, *83*(1), 49–58.

https://doi.org/10.1017/S0007114500000088

Langi, S., Maulu, S., Hasimuna, O. J., Kaleinasho Kapula, V., & Tjipute, M. (2024). Nutritional requirements and effect of culture conditions on the performance of the African catfish (*Clarias gariepinus*): a review. *Cogent Food & Agriculture*, *10*(1), 2302642. https://doi.org/10.1080/23311932.2024.2302642

Lansard, M., Panserat, S., Plagnes-Juan, E., Seiliez, I., & Skiba-Cassy, S. (2010). Integration of insulin and amino acid signals that regulate hepatic metabolism-related gene expression in rainbow trout: role of TOR. *Amino Acids*, *39*(3), 801–810. https://doi.org/10.1007/s00726-010-0533-3

Laplante, M., & Sabatini, D. M. (2009). An Emerging Role of mTOR in Lipid Biosynthesis. *Current Biology*, *19*(22), R1046–R1052. https://doi.org/10.1016/j.cub.2009.09.058

Laplante, M., & Sabatini, D. M. (2009). mTOR signaling at a glance. *Journal of Cell Science*, *122*(Pt 20), 3589–3594. https://doi.org/10.1242/jcs.051011

Laplante, M., & Sabatini, D. M. (2009). mTOR signaling at a glance. *Journal of Cell Science*, *122*(Pt 20), 3589–3594. https://doi.org/10.1242/jcs.051011

Laursen, D. C., L. Olsén, H., Ruiz-Gomez, M. de L., Winberg, S., & Höglund, E. (2011). Behavioural responses to hypoxia provide a non-invasive method for distinguishing between stress coping styles in fish. *Applied Animal Behaviour Science*, *132*(3), 211–216. https://doi.org/10.1016/j.applanim.2011.03.011

Lazado, C. C., Iversen, M., & Sundaram, A. Y. M. (2023). Comparative basal transcriptome profiles of the olfactory rosette and gills of Atlantic salmon (*Salmo salar*) unveil shared and distinct immunological features. *Genomics*, *115*(3), 110632. https://doi.org/10.1016/j.ygeno.2023.110632

Le Cren, E. D. (1951). The Length-Weight Relationship and Seasonal Cycle in Gonad Weight and Condition in the Perch (*Perca fluviatilis*). *Journal of Animal Ecology*, *20*(2), 201–219. https://doi.org/10.2307/1540

Lee, A. J., Beno, D. W. A., Zhang, X., Shapiro, R., Mason, M., Mason-Bright, T., Surber, B., & Edens, N. K. (2015). A (14)C-leucine absorption, distribution,

metabolism and excretion (ADME) study in adult Sprague-Dawley rat reveals β-hydroxy-β-methylbutyrate as a metabolite. *Amino Acids*, *47*(5), 917–924. https://doi.org/10.1007/s00726-015-1920-6

Lee, D. F., Kuo, H. P., Chen, C. T., Hsu, J. M., Chou, C. K., Wei, Y., Sun, H. L., Li, L. Y., Ping, B., Huang, W. C., He, X., Hung, J. Y., Lai, C. C., Ding, Q., Su, J. L., Yang, J. Y., Sahin, A. A., Hortobagyi, G. N., Tsai, F. J., Tsai, C. H., & Hung, M. C. (2007). IKK beta suppression of TSC1 links inflammation and tumor angiogenesis via the mTOR pathway. *Cell*, *130*(3), 440–455. https://doi.org/10.1016/j.cell.2007.05.058

Lemos, D., & Weissman, D. (2021). Moulting in the grow-out of farmed shrimp: a review. *Reviews in Aquaculture*, *13*(1), 5–17. https://doi.org/10.1111/raq.12461

Leng, N., Chu, L. F., Barry, C., Li, Y., Choi, J., Li, X., Jiang, P., Stewart, R. M., Thomson, J. A., & Kendziorski, C. (2015). Oscope identifies oscillatory genes in unsynchronized single-cell RNA-seq experiments. *Nature Methods*, *12*(10), 947–950. https://doi.org/10.1038/nmeth.3549

Leprivier, G., & Rotblat, B. (2020). How does mTOR sense glucose starvation? AMPK is the usual suspect. *Cell Death Discovery*, *6*(1), 27. https://doi.org/10.1038/s41420-020-0260-9

Li, L., & Xiong, M. (2015). Dynamic Model for RNA-seq Data Analysis. *BioMed Research International*, *2015*(1), 1-13. https://doi.org/10.1155/2015/916352

Li, M., Jin, H., Zhao, Y., Zhu, G., Liu, Y., Long, H., & Shen, X. (2024). PHD2 safeguards modest mesendoderm development. *Communications Biology*, *7*(1), 1100. https://doi.org/10.1038/s42003-024-06824-z

Li, P., & Gatlin III, D. M. (2007). Evaluation of Dietary Supplementation of Graded Levels of β-Hydroxy-β-Methylbutyrate for Hybrid Striped Bass *Morone chrysops* × *M. saxatilis*. *Journal of Applied Aquaculture*, *19*(3), 77–88. https://doi.org/10.1300/J028v19n03_05

Li, P., Mai, K., Trushenski, J., & Wu, G. (2009). New developments in fish amino acid nutrition: towards functional and environmentally oriented aquafeeds. *Amino Acids*, *37*(1), 43–53. https://doi.org/10.1007/s00726-008-0171-1

Li, W., Ai, Q., Mai, K., Xu, W., Luo, Y., & Zhang, Y. (2013). Effects of dietary amino acid patterns on growth and protein metabolism of large yellow croaker (*Larimichthys crocea*) larvae. *Aquaculture*, *406–407*, 1–8. https://doi.org/10.1016/j.aquaculture.2013.04.029

Li, X., Zheng, S., & Wu, G. (2020). Nutrition and metabolism of glutamate and glutamine in fish. *Amino Acids*, *52*(5), 671–691. https://doi.org/10.1007/s00726-020-02851-2

Li, X., Zheng, S., & Wu, G. (2021). Nutrition and functions of amino acids in fish. In G. Wu (Ed.), *Amino acids in nutrition and health: Amino acids in the Nutrition of Companion, Zoo and Farm Animals* (pp. 133–168). Springer International Publishing. https://doi.org/10.1007/978-3-030-54462-1_8

Li, Y., Wei, H., Li, F., Duan, Y., Guo, Q., & Yin, Y. (2017). Effects of Low-Protein Diets Supplemented with Branched-Chain Amino Acid on Lipid Metabolism in White Adipose Tissue of Piglets. *Journal of Agricultural and Food Chemistry*, *65*(13), 2839–2848. https://doi.org/10.1021/acs.jafc.7b00488

Lien, S., Koop, B. F., Sandve, S. R., Miller, J. R., Kent, M. P., Nome, T., Hvidsten, T. R., Leong, J. S., Minkley, D. R., Zimin, A., Grammes, F., Grove, H., Gjuvsland, A., Walenz, B., Hermansen, R. A., von Schalburg, K., Rondeau, E. B., Di Genova, A., Samy, J. K. A., Olav Vik, J., Vigeland, M. D., Caler, L., Grimholt, U., Jentoft, S., Inge Våge, D., de Jong, P., Moen, T., Baranski, M., Palti, Y., Smith, D. R., Yorke, J. A., Nederbragt, A. J., Tooming-Klunderud, A., Jakobsen, K. S., Jiang, X., Fan, D., Hu, Y., Liberles, D. A., Vidal, R., Iturra, P., Jones, S. J. M., Jonassen, I., Maass, A., Omholt, S. W., & Davidson, W. S. (2016). The Atlantic salmon genome provides insights into rediploidization. *Nature*, *533*(7602), 200–205. https://doi.org/10.1038/nature17164

Lim, C. B., Chew, S. F., Anderson, P. M., & Ip, Y. K. (2001). Reduction in the Rates of Protein and Amino Acid Catabolism to Slow Down the Accumulation

of Endogenous Ammonia: A Strategy Potentially Adopted by Mudskippers (*Periophthalmodon schlosseri* and *Boleophthalmus boddaerti*) During Aerial Exposure in Constant Darkness. *Journal of Experimental Biology*, *204*(9), 1605–1614. https://doi.org/10.1242/jeb.204.9.1605

Lin, X., Du, Y., de Cruz, C., Zhao, J., Shao, X., & Xu, Q. (2024). Effects of supplementation with crystalline or coated methionine and lysine in low protein diet on growth performance, intestinal health and muscle quality of gibel carp, *Carassius auratus gibelio*. *Aquaculture Reports*, *36*, 102084. https://doi.org/10.1016/j.aqrep.2024.102084

Lindholm, B., Alvestrand, A., Fürst, P., & Bergström, J. (1989). Plasma and muscle free amino acids during continuous ambulatory peritoneal dialysis. *Kidney International*, *35*(5), 1219–1226. https://doi.org/10.1038/ki.1989.113

Lindholm-Lehto, P. (2023). Water quality monitoring in recirculating aquaculture systems. *Aquaculture, Fish and Fisheries*, *3*(2), 113–131. https://doi.org/10.1002/aff2.102

Ling, Z. N., Jiang, Y. F., Ru, J. N., Lu, J. H., Ding, B., & Wu, J. (2023). Amino acid metabolism in health and disease. *Signal Transduction and Targeted Therapy*, *8*(1), 345. https://doi.org/10.1038/s41392-023-01569-3

Liu, H., Lamm, M. S., Rutherford, K., Black, M. A., Godwin, J. R., & Gemmell, N. J. (2015). Large-scale transcriptome sequencing reveals novel expression patterns for key sex-related genes in a sex-changing fish. *Biology of Sex Differences*, *6*, 26. https://doi.org/10.1186/s13293-015-0044-8

Liu, J., Pan, M., Huang, D., Guo, Y., Yang, M., Zhang, W., & Mai, K. (2020). Myostatin-1 Inhibits Cell Proliferation by Inhibiting the mTOR Signal Pathway and MRFs, and Activating the Ubiquitin-Proteasomal System in Skeletal Muscle Cells of Japanese Flounder *Paralichthys olivaceus*. *Cells*, *9*(11), 2376. https://doi.org/10.3390/cells9112376

Liu, Y., Beyer, A., & Aebersold, R. (2016). On the dependency of cellular protein levels on mRNA abundance. *Cell*, *165*(3), 535–550. https://doi.org/10.1016/j.cell.2016.03.014

Londraville, R. L., Macotela, Y., Duff, R. J., Easterling, M. R., Liu, Q., & Crespi, E. J. (2014). Comparative endocrinology of leptin: Assessing function in a phylogenetic context. *General and Comparative Endocrinology*, *203*, 146–157. https://doi.org/10.1016/j.ygcen.2014.02.002

Lou, W., Ding, B., & Fu, P. (2020). Pseudogene-Derived lncRNAs and Their miRNA Sponging Mechanism in Human Cancer. *Frontiers in Cell and Developmental Biology*, *8*, 85. https://doi.org/10.3389/fcell.2020.00085

Lu, G., Sun, H., She, P., Youn, J. Y., Warburton, S., Ping, P., Vondriska, T. M., Cai, H., Lynch, C. J., & Wang, Y. (2009). Protein phosphatase 2Cm is a critical regulator of branched-chain amino acid catabolism in mice and cultured cells. *The Journal of Clinical Investigation*, *119*(6), 1678–1687. https://doi.org/10.1172/JCI38151

Ma, X. M., & Blenis, J. (2009). Molecular mechanisms of mTOR-mediated translational control. *Nature Reviews. Molecular Cell Biology*, *10*(5), 307–318. https://doi.org/10.1038/nrm2672

Madaro, A., Nilsson, J., Whatmore, P., Roh, H., Grove, S., Stien, L. H., & Olsen, R. E. (2023). Acute stress response on Atlantic salmon: a time-course study of the effects on plasma metabolites, mucus cortisol levels, and head kidney transcriptome profile. *Fish Physiology and Biochemistry*, *49*(1), 97–116. https://doi.org/10.1007/s10695-022-01163-4

Magistrati, E., & Polo, S. (2021). Myomics: myosin VI structural and functional plasticity. *Current Opinion in Structural Biology*, *67*, 33–40. https://doi.org/10.1016/j.sbi.2020.09.005

Mai, K., He, G., Xue, M., Xie, S. Q., & Kaushik, S. J. (2022). Protein and amino acids. In Ronald W. Hardy & S. J. Kaushik (Eds.), *Fish Nutrition* (4th Edi, pp. 181–302). Elsevier. https://doi.org/10.1016/B978-0-12-819587-1.00012-4

Majluf, P., Matthews, K., Pauly, D., Skerritt, D. J., & Palomares, M. L. D. (2024). A review of the global use of fishmeal and fish oil and the Fish In: Fish Out metric. *Science Advances*, *10*(42), eadn5650. https://doi.org/10.1126/sciadv.adn5650

Makrinos, D. L., & Bowden, T. J. (2016). Natural environmental impacts on teleost immune function. *Fish & Shellfish Immunology*, *53*, 50–57. https://doi.org/10.1016/j.fsi.2016.03.008

Mandic, M., Joyce, W., & Perry, S. F. (2021). The evolutionary and physiological significance of the Hif pathway in teleost fishes. *Journal of Experimental Biology*, *224*(18), jeb231936. https://doi.org/10.1242/jeb.231936

Mann, G., Mora, S., Madu, G., & Adegoke, O. (2021). Branched-chain Amino Acids: Catabolism in Skeletal Muscle and Implications for Muscle and Whole-body Metabolism. *Frontiers in Physiology*, *12*, 702826. https://doi.org/10.3389/fphys.2021.702826

Marandel, L., Seiliez, I., Véron, V., Skiba-Cassy, S., & Panserat, S. (2015). New insights into the nutritional regulation of gluconeogenesis in carnivorous rainbow trout (*Oncorhynchus mykiss*): a gene duplication trail. *Physiological Genomics*, *47*(7), 253–263. https://doi.org/10.1152/physiolgenomics.00026.2015

Marques-Ramos, A., Candeias, M. M., Menezes, J., Lacerda, R., Willcocks, M., Teixeira, A., Locker, N., & Romão, L. (2017). Cap-independent translation ensures mTOR expression and function upon protein synthesis inhibition. *RNA, 23*(11), 1712–1728. https://doi.org/10.1261/rna.063040.117

Martínez, D., De Lázaro, O., Cortés, P., Oyarzún-Salazar, R., Paschke, K., & Vargas-Chacoff, L. (2020). Hypoxia modulates the transcriptional immunological response in *Oncorhynchus kisutch*. *Fish & Shellfish Immunology*, *106*, 1042–1051. https://doi.org/10.1016/j.fsi.2020.09.025

Martinez-Porchas, M., & Martinez-Cordova, L. R. (2012). World aquaculture: environmental impacts and troubleshooting alternatives. *The Scientific World Journal*, *2012*, 389623. https://doi.org/10.1100/2012/389623

Martins, C. I. M., Galhardo, L., Noble, C., Damsgård, B., Spedicato, M. T., Zupa, W., Beauchaud, M., Kulczykowska, E., Massabuau, J. C., Carter, T., Planellas, S. R., & Kristiansen, T. (2012). Behavioural indicators of welfare

in farmed fish. *Fish Physiology and Biochemistry*, *38*(1), 17–41. https://doi.org/10.1007/s10695-011-9518-8

Mashoof, S., & Criscitiello, M. F. (2016). Fish Immunoglobulins. *Biology*, *5*(4). https://doi.org/10.3390/biology5040045

Matlock, B. (2015). Assessment of Nucleic Acid Purity. *Thermoscientific Technical Bulletin NanoDrop Spectrophotometers*, 1–2. https://assets.thermofisher.com/TFS-Assets/CAD/Product-Bulletins/TN52646-E-0215M-NucleicAcid.pdf

Matsuo, H., Li, H., McGuire, A. M., Fletcher, C. M., Gingras, A. C., Sonenberg, N., & Wagner, G. (1997). Structure of translation factor eIF4E bound to m7GDP and interaction with 4E-binding protein. *Nature Structural Biology*, *4*(9), 717–724. https://doi.org/10.1038/nsb0997-717

Mattick, J. S., & Makunin, I. V. (2006). Non-coding RNA. *Human Molecular Genetics*, *15*(suppl_1), R17–R29. https://doi.org/10.1093/hmg/ddl046

Mazumdar, J., O'Brien, W. T., Johnson, R. S., LaManna, J. C., Chavez, J. C., Klein, P. S., & Simon, M. C. (2010). O2 regulates stem cells through Wnt/β-catenin signalling. *Nature Cell Biology*, *12*(10), 1007–1013. https://doi.org/10.1038/ncb2102

McCarthy, I. D., Houlihan, D. F., & Carter, C. G. (1997). Individual variation in protein turnover and growth efficiency in rainbow trout, *Oncorhynchus mykiss* (Walbaum). *Proceedings of the Royal Society of London. Series B: Biological Sciences*, *257*(1349), 141–147. https://doi.org/10.1098/rspb.1994.0107

McDougall, C., Hammond, M. J., Dailey, S. C., Somorjai, I. M. L., Cummins, S. F., & Degnan, B. M. (2018). The evolution of ependymin-related proteins. *BMC Evolutionary Biology*, *18*(1), 182. https://doi.org/10.1186/s12862-018-1306-y

McPherron, A. C., Lawler, A. M., & Lee, S. J. (1997). Regulation of skeletal muscle mass in mice by a new TGF-p superfamily member. *Nature*, *387*(6628), 83–90. https://doi.org/10.1038/387083a0

Meijer, A. J., Lorin, S., Blommaart, E. F., & Codogno, P. (2015). Regulation of autophagy by amino acids and MTOR-dependent signal transduction. *Amino Acids*, *47*(10), 2037–2063. https://doi.org/10.1007/s00726-014-1765-4

Meng, D., Yang, Q., Wang, H., Melick, C. H., Navlani, R., Frank, A. R., & Jewell, J. L. (2020). Glutamine and asparagine activate mTORC1 independently of Rag GTPases. *Journal of Biological Chemistry*, *295*(10), 2890–2899. https://doi.org/10.1074/jbc.AC119.011578

Mente, E., Carter, C. G., Barnes, R. S. (Katersky), Vlahos, N., & Nengas, I. (2021). Post-Prandial Amino Acid Changes in Gilthead Sea Bream. *Animals*, *11*(7), 1889. https://doi.org/10.3390/ani11071889

Mente, E., Deguara, S., Santos, M. B., & Houlihan, D. (2003). White muscle free amino acid concentrations following feeding a maize gluten dietary protein in Atlantic salmon (*Salmo salar* L.). *Aquaculture*, *225*(1–4), 133–147. https://doi.org/10.1016/S0044-8486(03)00285-0

Metcalfe, N. B., Huntingford, F. A., & Thorpe, J. E. (1987). The influence of predation risk on the feeding motivation and foraging strategy of juvenile Atlantic salmon. *Animal Behaviour*, *35*(3), 901–911. https://doi.org/10.1016/S0003-3472(87)80125-2

Miles, R. D., & Chapman, F. (2006). The Benefits of Fish Meal in Aquaculture Diets. *University of Florida IFAS Extension*, (May 2006), 1–6. https://doi.org/10.32473/edis-fa122-2006

Milligan, C. L. (1997). The role of cortisol in amino acid mobilization and metabolism following exhaustive exercise in rainbow trout (*Oncorhynchus mykiss* Walbaum). *Fish Physiology and Biochemistry*, *16*(2), 119–128. https://doi.org/10.1007/BF00004669

Mobley, K. B., Aykanat, T., Czorlich, Y., House, A., Kurko, J., Miettinen, A., Moustakas-Verho, J., Salgado, A., Sinclair-Waters, M., Verta, J. P., & Primmer, C. R. (2021). Maturation in Atlantic salmon (*Salmo salar*, *Salmonidae*): a synthesis of ecological, genetic, and molecular processes. *Reviews in Fish Biology and Fisheries*, *31*(3), 523–571.

https://doi.org/10.1007/s11160-021-09656-w

Mokhtar, D. M., Zaccone, G., Alesci, A., Kuciel, M., Hussein, M. T., & Sayed, R. K. A. (2023). Main Components of Fish Immunity: An Overview of the Fish Immune System. *Fishes*. https://doi.org/10.3390/fishes8020093

Molina-Poveda, C. (2016 Nutrient requirements. In S. Nates (Ed.), *Aquafeed Formulation* (pp. 75–216). Elsevier. https://doi.org/10.1016/B978-0-12-800873-7.00004-X

Mommsen, T. P. (2004). Salmon spawning migration and muscle protein metabolism: the August Krogh principle at work. *Comparative Biochemistry and Physiology Part B: Biochemistry and Molecular Biology*, *139*(3), 383–400. https://doi.org/10.1016/j.cbpc.2004.09.018

Morais, P., Adachi, H., & Yu, Y. T. (2021). Spliceosomal snRNA Epitranscriptomics. *Frontiers in Genetics*, *12*. https://doi.org/10.3389/fgene.2021.652129

Morales, A., García, H., Araiza, A., Htoo, J. K., Cota, M., Arce, N., & Cervantes, M. (2012). Effect of L-valine supplementation to a wheat-based diet with leucine excess on performance, gene expression, and serum concentration of amino acids. *Journal of Animal Science*, *90*(suppl_4), 89–91. https://doi.org/10.2527/jas.51189

Mori, H., Yao, Y., Learman, B. S., Kurozumi, K., Ishida, J., Ramakrishnan, S. K., Overmyer, K. A., Xue, X., Cawthorn, W. P., Reid, M. A., Taylor, M., Ning, X., Shah, Y. M., & MacDougald, O. A. (2016). Induction of WNT11 by hypoxia and hypoxia-inducible factor-1α regulates cell proliferation, migration and invasion. *Scientific Reports*, *6*, 21520. https://doi.org/10.1038/srep21520

Morin, G., Pinel, K., Dias, K., Seiliez, I., & Beaumatin, F. (2020). RTH-149 Cell Line, a Useful Tool to Decipher Molecular Mechanisms Related to Fish Nutrition. *Cells*, *9*(8). https://doi.org/10.3390/cells9081754

Morrison, C. D., Xi, X., White, C. L., Ye, J., & Martin, R. J. (2007). Amino acids inhibit Agrp gene expression via an mTOR-dependent mechanism.

American Journal of Physiology-Endocrinology and Metabolism, *293*(1), E165–E171. https://doi.org/10.1152/ajpendo.00675.2006

Mrvová, S., Frydrýšková, K., Pospíšek, M., Vopálenský, V., & Mašek, T. (2018). Major splice variants and multiple polyadenylation site utilization in mRNAs encoding human translation initiation factors eIF4E1 and eIF4E3 regulate the translational regulators? *Molecular Genetics and Genomics*, *293*(1), 167–186. https://doi.org/10.1007/s00438-017-1375-4

Mu, Y., Li, W., Wei, Z., He, L., Zhang, W., & Chen, X. (2020). Transcriptome analysis reveals molecular strategies in gills and heart of large yellow croaker (*Larimichthys crocea*) under hypoxia stress. *Fish & Shellfish Immunology*, *104*, 304–313. https://doi.org/10.1016/j.fsi.2020.06.028

Munck, L. K., & Munck, B. G. (1992). Variation in amino acid transport along the rabbit small intestine. Mutual jejunal carriers of leucine and lysine. *Biochimica et Biophysica Acta- General Subjects*, *1116*(2), 83–90. https://doi.org/10.1016/0304-4165(92)90103-2

Mungpakdee, S., Seo, H. C., Angotzi, A., Dong, X., Akalin, A., & Chourrout, D. (2008). Differential Evolution of the Thirteen Atlantic Salmon Hox Clusters. *Molecular Biology and Evolution*, *25*, 1333–1343. https://doi.org/10.1093/molbev/msn097

Murai, T., Ogata, H., Takeuchi, T., Watanabe, T., & Nose, T. (1984). Composition of Free Amino Acid in Excretion of Carp Fed Amino Acid Diets and Casein-gelatin Diets. *Nippon Suisan Gakkaishi (Fisheries Science)*, *50*, 1957. https://doi.org/10.2331/suisan.50.1957

Myrka, A., & Buck, L. (2021). Cytoskeletal arrest: an anoxia tolerance mechanism. *Metabolites*, *11*(8). https://doi.org/10.3390/metabo11080561

Nachef, M., Ali, A. K., Almutairi, S. M., & Lee, S. H. (2021). Targeting SLC1A5 and SLC3A2/SLC7A5 as a Potential Strategy to Strengthen Anti-Tumor Immunity in the Tumor Microenvironment. *Frontiers in Immunology*, *12*. ttps://doi.org/10.3389/fimmu.2021.624324

Nanduri, J., Yuan, G., Kumar, G. K., Semenza, G. L., & Prabhakar, N. R. (2008). Transcriptional responses to intermittent hypoxia. *Respiratory Physiology & Neurobiology*, *164*(1–2), 277–281. https://doi.org/10.1016/j.resp.2008.07.006

Navarrete, P., Fuentes, P., De la Fuente, L., Barros, L., Magne, F., Opazo, R., Ibacache, C., Espejo, R., & Romero, J. (2013). Short-term effects of dietary soybean meal and lactic acid bacteria on the intestinal morphology and microbiota of Atlantic salmon (*Salmo salar*). *Aquaculture Nutrition*, *19*(5), 827–836. https://doi.org/10.1111/anu.12047

Navarrete, P., Fuentes, P., De la Fuente, L., Barros, L., Magne, F., Opazo, R., Ibacache, C., Espejo, R., & Romero, J. (2013). Short-term effects of dietary soybean meal and lactic acid bacteria on the intestinal morphology and microbiota of Atlantic salmon (*Salmo salar*). *Aquaculture Nutrition*, *19*(5), 827–836. https://doi.org/10.1111/anu.12047

Naylor, R., Goldburg, R., Primavera, J., Kautsky, N., Beveridge, M., Clay, J., Folke, C., Lubchenco, J., Mooney, H., & Troell, M. (2000). Effect of Aquaculture on World Fish Supplies. *Nature*, *405*, 1017–1024. https://doi.org/10.1038/35016500

NCBI The CCDS project. (2022). The CCDS project. Retrieved 15 February 2025, from https://www.ncbi.nlm.nih.gov/projects/CCDS/CcdsBrowse.cgi

Neinast, M. D., Jang, C., Hui, S., Murashige, D. S., Chu, Q., Morscher, R. J., Li, X., Zhan, L., White, E., Anthony, T. G., Rabinowitz, J. D., & Arany, Z. (2019). Quantitative Analysis of the Whole-Body Metabolic Fate of Branched-Chain Amino Acids. *Cell Metabolism*, *29*(2), 417-429.e4. https://doi.org/10.1016/j.cmet.2018.10.013

Neinast, M., Murashige, D., & Arany, Z. (2019). Branched chain amino acids. *Annual Review of Physiology*, *81*, 139–164. https://doi.org/10.1146/annurev-physiol-020518-114455

Nemova, N. N., Lysenko, L. A., & Kantserova, N. P. (2016). Degradation of skeletal muscle protein during growth and development of salmonid fish.

Russian Journal of Developmental Biology (Ontogenez), *47*(4), 197–208. https://doi.org/10.1134/S1062360416040068

Ni, C., & Buszczak, M. (2023). The homeostatic regulation of ribosome biogenesis. *Seminars in Cell & Developmental Biology*, *136*, 13–26. https://doi.org/10.1016/j.semcdb.2022.03.043

Nicklin, P., Bergman, P., Zhang, B., Triantafellow, E., Wang, H., Nyfeler, B., Yang, H., Hild, M., Kung, C., Wilson, C., Myer, V. E., MacKeigan, J. P., Porter, J. A., Wang, Y. K., Cantley, L. C., Finan, P. M., & Murphy, L. O. (2009). Bidirectional Transport of Amino Acids Regulates mTOR and Autophagy. *Cell*, *136*(3), 521–534. https://doi.org/10.1016/j.cell.2008.11.044

Nie, C., He, T., Zhang, W., Zhang, G., & Ma, X. (2018). Branched Chain Amino Acids : Beyond Nutrition Metabolism. *International Journal of Molecular Sciences*, *19*, 1–16. https://doi.org/10.3390/ijms19040954

Niklasson, L., Sundh, H., Fridell, F., Taranger, G. L., & Sundell, K. (2011). Disturbance of the intestinal mucosal immune system of farmed Atlantic salmon (*Salmo salar*), in response to long-term hypoxic conditions. *Fish & Shellfish Immunology*, *31*(6), 1072–1080. https://doi.org/10.1016/j.fsi.2011.09.011

Nilsson, G. E., & Randall, D. J. (2010). Adaptations to hypoxia in fishes. In G. E. Nilsson (Ed.), *Respiratory Physiology of Vertebrates: Life With and Without Oxygen* (pp. 131–173). Cambridge University Press. https://doi.org/10.1017/CBO9780511845178.006

Noble, C., Gismervik, S., Iversen, M., Kolarevic, J., Nilsson, J., Stien, L., & Turnbull, J. (2018). *Welfare Indicators for farmed Atlantic Salmon: tools for assessing fish welfare* (FISHWELL). Nofima. http://www.nofima.no/fishwell/english

Nolles, J. A., Peeters, I. G. S., Bremer, B. I., Moorman, R., Koopmanschap, R. E., Verstegen, M. W. A., & Schreurs, V. V. A. M. (2008). Dietary amino acids fed in free form or as protein do differently affect amino acid absorption in a

rat everted sac model. *Journal of Animal Physiology and Animal Nutrition*, *92*(5), 529–537. https://doi.org/10.1111/j.1439-0396.2007.00743.x

Nunes, A. J. P., Sá, M. V. C., Browdy, C. L., & Vazquez-Anon, M. (2014). Practical supplementation of shrimp and fish feeds with crystalline amino acids. *Aquaculture*, *431*, 20–27. https://doi.org/10.1016/j.aquaculture.2014.04.003

Nurdalila, A. A., Natnan, M. E., & Baharum, S. N. (2020). The effects of amino acids and fatty acids on the disease resistance of *Epinephelus fuscoguttatus* in response to *Vibrio vulnificus* infection. *3 Biotech*, *10*(12), 544. https://doi.org/10.1007/s13205-020-02543-4

Olsvik, P. A., Vikeså, V., Lie, K. K., & Hevrøy, E. M. (2013). Transcriptional responses to temperature and low oxygen stress in Atlantic salmon studied with next-generation sequencing technology. *BMC Genomics*, *14*(1), 817. https://doi.org/10.1186/1471-2164-14-817

Pailla, K., Blonde-Cynober, F., Aussel, C., De Bandt, J. P., & Cynober, L. (2000). Branched-chain keto-acids and pyruvate in blood: measurement by HPLC with fluorimetric detection and changes in older subjects. *Clinical Chemistry*, *46*(6), 848–853. https://doi.org/10.1093/clinchem/46.6.848

Palazon, A., Goldrath, A. W., Nizet, V., & Johnson, R. S. (2014). HIF transcription factors, inflammation, and immunity. *Immunity*, *41*(4), 518–528. https://doi.org/10.1016/j.immuni.2014.09.008

Palma, P. F. S., Bock, C., Silva, T. S., Guerreiro, P. M., Power, D. M., Pörtner, H. O., & Canário, A. V. M. (2019). STC1 and PTHrP modify carbohydrate and lipid metabolism in liver of a teleost fish. *Scientific Reports*, *9*(1), 723. https://doi.org/10.1038/s41598-018-36821-2

Patel, J. H., Schattinger, P. A., Takayoshi, E. E., & Wills, A. E. (2022). Hif1α and Wnt are required for posterior gene expression during *Xenopus tropicalis* tail regeneration. *Developmental Biology*, *483*, 157–168. https://doi.org/10.1016/j.ydbio.2022.01.007

Payne, S. H. (2015). The utility of protein and mRNA correlation. *Trends in Biochemical Sciences*, *40*(1), 1–3. https://doi.org/10.1016/j.tibs.2014.10.010

Pearson, J. C., Lemons, D., & McGinnis, W. (2005). Modulating Hox gene functions during animal body patterning. *Nature Reviews Genetics*, *6*(12), 893–904. https://doi.org/10.1038/nrg1726

Perga, M. E., & Gerdeaux, D. (2005). Are fish what they eat' all year round? Oecologia. *Oecologia*, *144*, 598–606. https://doi.org/10.1007/s00442-005-0069-5

Peter, M. C. S., Gayathry, R., & Peter, V. S. (2022). Inducible nitric oxide synthase/ nitric oxide system as a biomarker for stress and ease response in fish: implication on Na(+) homeostasis during hypoxia. *Frontiers in Physiology*, *13*, 821300. https://doi.org/10.3389/fphys.2022.821300

Pino Martinez, E., Balseiro, P., Stefansson, S. O., Kaneko, N., Norberg, B., Fleming, M. S., Imsland, A. K. D., & Handeland, S. O. (2023). Interaction of temperature and feed ration on male postsmolt maturation of Atlantic salmon (*Salmo salar* L.). *Aquaculture*, *562*, 738877. https://doi.org/10.1016/j.aquaculture.2022.738877

Pooley, N. J., Tacchi, L., Secombes, C. J., & Martin, S. A. M. (2013). Inflammatory responses in primary muscle cell cultures in Atlantic salmon (*Salmo salar*). *BMC Genomics*, *14*(1), 747. https://doi.org/10.1186/1471-2164-14-747

Py, C., Elizondo-González, R., & Peña-Rodríguez, A. (2022). Compensatory growth: Fitness cost in farmed fish and crustaceans. *Reviews in Aquaculture*, *14*(3), 1389–1417. https://doi.org/10.1111/raq.12656

Qin, H., Zhang, X., Xie, T., Gao, Y., Li, J., & Jia, Y. (2023). Hepatic transcriptomic analysis reveals that Hif1α/ ldha signal is involved in the regulation of hypoxia stress in black rockfish *Sebastes schlegelii*. *Comparative Biochemistry and Physiology Part D: Genomics and Proteomics*, *47*, 101098. https://doi.org/10.1016/j.cbd.2023.101098

Raha, D., Wang, Z., Moqtaderi, Z., Wu, L., Zhong, G., Gerstein, M., Struhl, K., & Snyder, M. (2010). Close association of RNA polymerase II and many transcription factors with Pol III genes. *Proceedings of the National Academy of Sciences*, *107*(8), 3639–3644. https://doi.org/10.1073/pnas.0911315106

Rahman, Md. S., & Thomas, P. (2012). Effects of Hypoxia Exposure on Hepatic Cytochrome P450 1A (CYP1A) Expression in Atlantic Croaker: Molecular Mechanisms of CYP1A Down-Regulation. *PLOS ONE*, *7*(7), e40825. https://doi.org/10.1371/journal.pone.0040825

Randall, D. J., & Tsui, T. K. N. (2002). Ammonia toxicity in fish. *Marine Pollution Bulletin*, *45*(1), 17–23. https://doi.org/10.1016/S0025-326X(02)00227-8

Raposo de Magalhães, C., Farinha, A. P., Blackburn, G., Whitfield, P. D., Carrilho, R., Schrama, D., Cerqueira, M., & Rodrigues, P. M. (2022). Gilthead Seabream Liver Integrative Proteomics and Metabolomics Analysis Reveals Regulation by Different Prosurvival Pathways in the Metabolic Adaptation to Stress. *International Journal of Molecular Sciences*, *23*(23). https://doi.org/10.3390/ijms232315395

Regan, M. D., & Richards, J. G. (2017). Rates of hypoxia induction alter mechanisms of O2 uptake and the critical O2 tension of goldfish. *Journal of Experimental Biology*, *220*(14), 2536–2544. https://doi.org/10.1242/jeb.154948

Rehman, S. U., Ali, R., Zhang, H., Zafar, M. H., & Wang, M. (2023). Research progress in the role and mechanism of Leucine in regulating animal growth and development. *Frontiers in Physiology*, *14*, 1252089. https://doi.org/10.3389/fphys.2023.1252089

Řehulka, J., & Minařík, B. (2016). Values of three branched plasma amino acids of farmed rainbow trout, *Oncorhynchus mykiss*. *Biologia*, *71*(10), 1184–1193. https://doi.org/10.1515/biolog-2016-0140

Reifenberg, P., & Zimmer, A. (2024). Branched-chain amino acids: physico-chemical properties, industrial synthesis and role in signaling, metabolism and energy production. *Amino Acids*, *56*(1), 51. https://doi.org/10.1007/s00726-024-03417-2

Remen, M., Sievers, M., Torgersen, T., & Oppedal, F. (2016). The oxygen threshold for maximal feed intake of Atlantic salmon post-smolts is highly temperature-dependent. *Aquaculture*, *464*, 582–592.

https://doi.org/10.1016/j.aquaculture.2016.07.037

Ren, M., Habte-Tsion, H. M., Liu, B., Miao, L., Ge, X., Xie, J., Liang, H., Zhou, Q., & Pan, L. (2015). Dietary leucine level affects growth performance, whole body composition, plasma parameters and relative expression of TOR and TNF-α in juvenile blunt snout bream, *Megalobrama amblycephala*. *Aquaculture*, *448*, 162–168. https://doi.org/10.1016/j.aquaculture.2015.06.008

Richards, J. G. (2009). Metabolic and Molecular Responses of Fish to Hypoxia. In J. Richards, A. Farrell, & C. Brauner (Eds.), *Hypoxia* (Vol. 27, pp. 443–485). Academic Press. https://doi.org/10.1016/S1546-5098(08)00010-1

Richter, H., Lückstädt, C., Focken, U., & Becker, K. (2000). An improved procedure to assess fish condition on the basis of length-weight relationships. *Archive of Fishery and Marine Research*, *48*(3), 226–235. https://www.researchgate.net/publication/268405378

Rodríguez, L., Begtashi, I., Zanuy, S., & Carrillo, M. (2005). Long-term exposure to continuous light inhibits precocity in European male sea bass (*Dicentrarchus labrax*, L.): hormonal aspects. *General and Comparative Endocrinology*, *140*(2), 116–125. https://doi.org/10.1016/j.ygcen.2004.10.011

Rolland, M., Feekings, J. P., Dalsgaard, J., Holm, J., & Skov, P. V. (2016). Modelling the effects of dietary methionine level and form on postprandial plasma essential amino acid profiles in rainbow trout (*Oncorhynchus mykiss*). *Aquaculture Nutrition*, *22*(6), 1185–1201. https://doi.org/10.1111/anu.12325

Rønnestad, I., Conceição, L. E. C., Aragão, C., & Dinis, M. T. (2000). Free Amino Acids Are Absorbed Faster and Assimilated More Efficiently than Protein in Postlarval Senegal Sole (*Solea senegalensis*). *The Journal of Nutrition*, *130*(11), 2809–2812. https://doi.org/10.1093/jn/130.11.2809

Rønnestad, I., Thorsen, A., & Finn, R. N. (1999). Fish larval nutrition: a review of recent advances in the roles of amino acids. *Aquaculture*, *177*(1), 201–216. https://doi.org/10.1016/S0044-8486(99)00082-4

Rozas-Serri, M., Correa, R., Walker-Vergara, R., Coñuecar, D., Barrientos, S., Leiva, C., Ildefonso, R., Senn, C., & Peña, A. (2022). Reference intervals for blood biomarkers in farmed Atlantic salmon, coho salmon and rainbow trout in Chile: promoting a preventive approach in Aquamedicine. *Biology*, *11*(7), 1066. https://doi.org/10.3390/biology11071066

Ruhl, D. A., Bomba-Warczak, E., Watson, E. T., Bradberry, M. M., Peterson, T. A., Basu, T., Frelka, A., Evans, C. S., Briguglio, J. S., Basta, T., Stowell, M. H. B., Savas, J. N., Roopra, A., Pearce, R. A., Piper, R. C., & Chapman, E. R. (2019). Synaptotagmin 17 controls neurite outgrowth and synaptic physiology via distinct cellular pathways. *Nature Communications*, *10*(1), 3532. https://doi.org/10.1038/s41467-019-11459-4

Sabadel, A. J. M., Riekenberg, P., Ayala-Diaz, M., Belk, M. C., Bennett, J., Bode, A., Bury, S. J., Dabouineau, L., Delgado, J., Finucci, B., García-Seoane, R., Giari, L., Henkens, J., IJsseldijk, L. L., Joling, T., Kerr-Hislop, O., MacLeod, C. D., Meyer, L., McGill, R. A. R., Negro, E., Quillfeldt, P., Reed, C., Roberts, C., Sayyaf Dezfuli, B., Schmidt, O., Sturbois, A., Suchomel, A. D., Thieltges, D. W., van der Lingen, C. D., van der Meer, M. T. J., Viana, I. G., Weston, M., Willis, T. J., & Filion, A. (2025). Establishing a comprehensive host-parasite stable isotope database to unravel trophic relationships. *Scientific Data*, *12*(1), 623. https://doi.org/10.1038/s41597-025-04970-5

Saha, N., Koner, D., & Sharma, R. (2022). Environmental hypoxia: A threat to the gonadal development and reproduction in bony fishes. *Aquaculture and Fisheries*, *7*(5), 572–582. https://doi.org/10.1016/j.aaf.2022.02.002

Samaras, A., Tsoukali, P., Katsika, L., Pavlidis, M., & Papadakis, I. E. (2023). Chronic impact of exposure to low dissolved oxygen on the physiology of *Dicentrarchus labrax* and *Sparus aurata* and its effects on the acute stress response. *Aquaculture*, *562*, 738830. https://doi.org/10.1016/j.aquaculture.2022.738830

Sancak, Y., Bar-Peled, L., Zoncu, R., Markhard, A. L., Nada, S., & Sabatini, D. M. (2010). Ragulator-Rag Complex Targets mTORC1 to the Lysosomal Surface and Is Necessary for Its Activation by Amino Acids. *Cell*, *141*(2), 290–303. https://doi.org/10.1016/j.cell.2010.02.024

Sancak, Y., Peterson, T. R., Shaul, Y. D., Lindquist, R. A., Thoreen, C. C., Bar-Peled, L., & Sabatini, D. M. (2008). The Rag GTPases Bind Raptor and Mediate Amino Acid Signaling to mTORC1. *Science*, *320*(5882), 1496–1501. https://doi.org/10.1126/science.1157535

Sandnes, K., Lie, Ø., & Waagbø, R. (1988). Normal ranges of some blood chemistry parameters in adult farmed Atlantic salmon, *Salmo salar*. *Journal of Fish Biology*, *32*(1), 129–136. https://doi.org/10.1111/j.1095-8649.1988.tb05341.x

Saunders, R. L., Henderson, E. B., & Glebe, B. D. (1982). Precocious sexual maturation and smoltification in male Atlantic salmon (*Salmo salar*). *Aquaculture*, *28*(1), 211–229. https://doi.org/10.1016/0044-8486(82)90024-2

Saxton, R. A., & Sabatini, D. M. (2017). mTOR Signaling in Growth, Metabolism, and Disease. *Cell*, *168*(6), 960–976. https://doi.org/10.1016/j.cell.2017.02.004

Sayers, E. W., Beck, J., Bolton, E. E., Brister, J. R., Chan, J., Comeau, D. C., Connor, R., DiCuccio, M., Farrell, C. M., Feldgarden, M., Fine, A. M., Funk, K., Hatcher, E., Hoeppner, M., Kane, M., Kannan, S., Katz, K. S., Kelly, C., Klimke, W., Kim, S., Kimchi, A., Landrum, M., Lathrop, S., Lu, Z., Malheiro, A., Marchler-Bauer, A., Murphy, T. D., Phan, L., Prasad, A. B., Pujar, S., Sawyer, A., Schmieder, E., Schneider, V. A., Schoch, C. L., Sharma, S., Thibaud-Nissen, F., Trawick, B. W., Venkatapathi, T., Wang, J., Pruitt, K. D., & Sherry, S. T. (2024). Database resources of the National Center for Biotechnology Information. *Nucleic Acids Research*, *52*(D1), D33–D43. https://doi.org/10.1093/nar/gkad1044

Sayers, E. W., Bolton, E. E., Brister, J. R., Canese, K., Chan, J., Comeau, D. C., Connor, R., Funk, K., Kelly, C., Kim, S., Madej, T., Marchler-Bauer, A.,

Lanczycki, C., Lathrop, S., Lu, Z., Thibaud-Nissen, F., Murphy, T., Phan, L., Skripchenko, Y., Tse, T., Wang, J., Williams, R., Trawick, B. W., Pruitt, K. D., & Sherry, S. T. (2022). Database resources of the national center for biotechnology information. *Nucleic Acids Research*, *50*(D1), D20–D26. https://doi.org/10.1093/nar/gkab1112

Schuhmacher, A., Wax, C., & Gropp, J. M. (1997). Plasma amino acids in rainbow trout (*Oncorhynchus mykiss*) fed intact protein or a crystalline amino acid diet. *Aquaculture*, *151*(1), 15–28. https://doi.org/10.1016/S0044-8486(96)01502-5

Seibel, H., Baßmann, B., & Rebl, A. (2021). Blood Will Tell: What Hematological Analyses Can Reveal About Fish Welfare. *Frontiers in Veterinary Science*, *8*, 616955. https://doi.org/10.3389/fvets.2021.616955

Seiliez, I., Taty Taty, G. C., Bugeon, J., Dias, K., Sabin, N., & Gabillard, J. C. (2013). Myostatin induces atrophy of trout myotubes through inhibiting the TORC1 signaling and promoting Ubiquitin–Proteasome and Autophagy-Lysosome degradative pathways. *General and Comparative Endocrinology*, *186*, 9–15. https://doi.org/10.1016/j.ygcen.2013.02.008

Semenza, G. L. (2014). Oxygen Sensing, Hypoxia-Inducible Factors, and Disease Pathophysiology. *Annual Review of Pathology: Mechanisms of Disease*, *9*(1), 47–71. https://doi.org/10.1146/annurev-pathol-012513-104720

Shen, L. P., Zhang, W. C., Deng, J. R., Qi, Z. H., Lin, Z. W., & Wang, Z. D. (2024). Advances in the mechanism of small nucleolar RNA and its role in DNA damage response. *Military Medical Research*, *11*(1), 53. https://doi.org/10.1186/s40779-024-00553-4

Sherman, B. T., Hao, M., Qiu, J., Jiao, X., Baseler, M. W., Lane, H. C., Imamichi, T., & Chang, W. (2022). DAVID: a web server for functional enrichment analysis and functional annotation of gene lists (2021 update). *Nucleic Acids Research*, *50*(W1), W216–W221. https://doi.org/10.1093/nar/gkac194

Shin, A. C., Fasshauer, M., Filatova, N., Grundell, L. A., Zielinski, E., Zhou, J. Y., Scherer, T., Lindtner, C., White, P. J., Lapworth, A. L., Ilkayeva, O., Knippschild, U., Wolf, A. M., Scheja, L., Grove, K. L., Smith, R. D., Qian, W. J., Lynch, C. J., Newgard, C. B., & Buettner, C. (2014). Brain insulin lowers circulating BCAA levels by inducing hepatic BCAA catabolism. *Cell Metabolism*, *20*(5), 898–909. https://doi.org/10.1016/j.cmet.2014.09.003

Sievers, F., & Higgins, D. G. (2021). The Clustal Omega Multiple Alignment Package BT- Multiple Sequence Alignment: Methods and Protocols. In K. Katoh (Ed.) (pp. 3–16). Springer. https://doi.org/10.1007/978-1-0716-1036-7_1

Silva, D. M. Z. A., Utsunomia, R., Pansonato-Alves, J. C., Oliveira, C., & Foresti, F. (2015). Chromosomal Mapping of Repetitive DNA Sequences in Five Species of *Astyanax* (*Characiformes, Characidae*) Reveals Independent Location of U1 and U2 snRNA Sites and Association of U1 snRNA and 5S rDNA. *Cytogenetic and Genome Research*, *146*(2), 144–152. https://doi.org/10.1159/000438813

Singh, N. P., & Krumlauf, R. (2022). Diversification and Functional Evolution of HOX Proteins. *Frontiers in Cell and Developmental Biology*, *10*. https://doi.org/10.3389/fcell.2022.798812

Singh, R. N., & Singh, N. N. (2019). A novel role of U1 snRNP: Splice site selection from a distance. *Biochimica et Biophysica Acta. Gene Regulatory Mechanisms*, *1862*(6), 634–642. https://doi.org/10.1016/j.bbagrm.2019.04.004

Sivanand, S., & Vander Heiden, M. G. (2020). Emerging Roles for Branched-Chain Amino Acid Metabolism in Cancer. *Cancer Cell*, *37*(2), 147–156. https://doi.org/10.1016/j.ccell.2019.12.011

Siwicki, A. K., Fuller, J. C., Nissen, S., Ostaszewski, P., & Studnicka, M. (2000). In vitro effects of β-hydroxy-β-methylbutyrate (HMB) on cell-mediated immunity in fish. *Veterinary Immunology and Immunopathology*, *76*(3), 191–197. https://doi.org/10.1016/S0165-2427(00)00211-7

Smith, R. W., Cash, P., Ellefsen, S., & Nilsson, G. E. (2009). Proteomic changes in the crucian carp brain during exposure to anoxia. *Proteomics*, *9*(8), 2217–2229. https://doi.org/10.1002/pmic.200800662

Sørensen, S. L., Park, Y., Gong, Y., Vasanth, G. K., Dahle, D., Korsnes, K., Phuong, T. H., Kiron, V., Øyen, S., Pittman, K., & Sørensen, M. (2021). Nutrient digestibility, growth, mucosal barrier status, and activity of leucocytes from head kidney of Atlantic salmon fed marine- or plant-derived protein and lipid sources. *Frontiers in Immunology*, *11*. https://doi.org/10.3389/fimmu.2020.623726

Sowers, S. (2009). A Primer On Branched Chain Amino Acids. *Smart Supplementation*, (5), 1–6. https://doi.org/10.1016/j.jaci.2007.09.010

Sprague, M., Fawcett, S., Betancor, M. B., Struthers, W., & Tocher, D. R. (2020). Variation in the nutritional composition of farmed Atlantic salmon (*Salmo salar* L.) fillets with emphasis on EPA and DHA contents. *Journal of Food Composition and Analysis*, *94*, 103618. https://doi.org/10.1016/j.jfca.2020.103618

Stothard, P. (2000). The sequence manipulation suite: JavaScript programs for analyzing and formatting protein and DNA sequences. *BioTechniques*, *28*(6), 1102,1104. https://doi.org/10.2144/00286ir01

Sugiura, S. H. (2025). Nutrient Requirements in Diets: Fundamental Issues in Sustainable Aquaculture Development. *Sustainability*, *17*(3), 1289. https://doi.org/10.3390/su17031289

Sugiura, S. H., Dong, F. M., Rathbone, C. K., & Hardy, R. W. (1998). Apparent protein digestibility and mineral availabilities in various feed ingredients for salmonid feeds. *Aquaculture*, *159*(3), 177–202. https://doi.org/10.1016/S0044-8486(97)00177-4

Sun, K., Wu, Z., Ji, Y., & Wu, G. (2016). Glycine regulates protein turnover by activating protein kinase B/Mammalian target of Rapamycin and by inhibiting MuRF1 and Atrogin-1 gene expression in C2C12 myoblasts. *The Journal of Nutrition*, *146*(12), 2461–2467. https://doi.org/10.3945/jn.116.231266a

Suryawan, A., Jeyapalan, A. S., Orellana, R. A., Wilson, F. A., Nguyen, H. V, & Davis, T. A. (2008). Leucine stimulates protein synthesis in skeletal muscle of neonatal pigs by enhancing mTORC1 activation. *American Journal of Physiology. Endocrinology and Metabolism*, *295*(4), E868-75. https://doi.org/10.1152/ajpendo.90314.2008

Sveier, H., Wathne, E., & Lied, E. (1999). Growth, feed and nutrient utilisation and gastrointestinal evacuation time in Atlantic salmon (*Salmo salar* L.): the effect of dietary fish meal particle size and protein concentration. *Aquaculture*, *180*(3–4), 265–282. https://doi.org/10.1016/S0044-8486(99)00196-9

Sweatt, A. J., Wood, M., Suryawan, A., Wallin, R., Willingham, M. C., & Hutson, S. M. (2004). Branched-chain amino acid catabolism: unique segregation of pathway enzymes in organ systems and peripheral nerves. *American Journal of Physiology. Endocrinology and Metabolism*, *286*(1), E64-76. https://doi.org/10.1152/ajpendo.00276.2003

Sweeney, H. L., & Holzbaur, E. L. F. (2018). Motor proteins. *Cold Spring Harbor Perspectives in Biology*, *10*(5). https://doi.org/10.1101/cshperspect.a021931

Szabo, E., Nagy, B., Czajlik, A., Komlodi, T., Ozohanics, O., Tretter, L., & Ambrus, A. (2024). Mitochondrial Alpha-Keto Acid Dehydrogenase Complexes: Recent Developments on Structure and Function in Health and Disease BT - Macromolecular Protein Complexes V: Structure and Function. In J. R. Harris & J. Marles-Wright (Eds.), *Macromolecular Protein Complexes V. Subcellular Biochemistry* (pp. 295–381). Springer International Publishing. https://doi.org/10.1007/978-3-031-58843-3_13

Taj, S., Han, Q., Wu, X., Yin, H., Tian, L., Yang, H., Liu, Y., & Huang, J. (2023). Effects of Dietary Protein-to-Energy Ratios on Growth, Immune Response, Antioxidative Capacity, Liver and Intestinal Histology, and Growth-Related Gene Expression in Hybrid Yellow Catfish (*Pelteobagrus fulvidraco* ♀ × *Pelteobagrus vachelli* ♂). *Aquaculture Nutrition*, *2023*, 9106332. https://doi.org/10.1155/2023/9106332

Tantikitti, C., & March, B. E. (1995). Dynamics of plasma free amino acids in rainbow trout (*Oncorhynchus mykiss*) under variety of dietary conditions. *Fish Physiology and Biochemistry*, *14*(3), 179–194. https://doi.org/10.1007/BF00004309

Teles, A. O., Couto, A., Enes, P., & Peres, H. (2020). Dietary protein requirements of fish– a meta-analysis. *Reviews in Aquaculture*, *12*(3), 1445–1477. https://doi.org/10.1111/raq.12391

Teo, M., Khoo, L. W., & Chew, W. (2024). A simplified small-scale workflow for determination of complete protein-bound amino acids using pre-column derivatization HPLC method. *Journal of Food Composition and Analysis*, *135*, 106571. https://doi.org/10.1016/j.jfca.2024.106571

Teodósio, R., Aragão, C., Conceição, L. E. C., Dias, J., & Engrola, S. (2022). Metabolic Fate Is Defined by Amino Acid Nature in Gilthead Seabream Fed Different Diet Formulations. *Animals : An Open Access Journal from MDPI*, *12*(13). https://doi.org/10.3390/ani12131713

Thiepold, A. L., Lorenz, N. I., Foltyn, M., Engel, A. L., Divé, I., Urban, H., Heller, S., Bruns, I., Hofmann, U., Dröse, S., Harter, P. N., Mittelbronn, M., Steinbach, J. P., & Ronellenfitsch, M. W. (2017). Mammalian target of rapamycin complex 1 activation sensitizes human glioma cells to hypoxia-induced cell death. *Brain*, *140*(10), 2623–2638. https://doi.org/10.1093/brain/awx196

Todd, E. V, Black, M. A., & Gemmell, N. J. (2016). The power and promise of RNA-seq in ecology and evolution. *Molecular Ecology*, *25*(6), 1224–1241. https://doi.org/10.1111/mec.13526

Tseng, Y. C., & Hwang, P. P. (2008). Some insights into energy metabolism for osmoregulation in fish. *Comparative Biochemistry and Physiology Part C: Toxicology & Pharmacology*, *148*(4), 419–429. https://doi.org/10.1016/j.cbpc.2008.04.009

Upadhya, S. R., & Ryan, C. J. (2022). Experimental reproducibility limits the correlation between mRNA and protein abundances in tumor proteomic profiles. *Cell Reports Methods*, *2*(9), 100288. https://doi.org/10.1016/j.crmeth.2022.100288

Valenzuela-Muñoz, V., Gallardo-Escárate, C., Valenzuela-Miranda, D., Nuñez-Acuña, G., Benavente, B. P., Alert, A., & Arevalo, M. (2023). Transcriptome Signatures of Atlantic Salmon—Resistant Phenotypes against Sea Lice Infestation Are Associated with Tissue Repair. *Genes*, *14*(5), 986. https://doi.org/10.3390/genes14050986

Van Der Boon, J., Van Den Thillart, G. E. E. J. M., & Addink, A. D. F. (1991). The effects of cortisol administration on intermediary metabolism in teleost fish. *Comparative Biochemistry and Physiology -- Part A: Physiology*, *100*(1), 47–53. https://doi.org/10.1016/0300-9629(91)90182-C

Van Koevering, M., & Nissen, S. (1992). Oxidation of leucine and alpha-ketoisocaproate to beta-hydroxy-beta-methylbutyrate in vivo. *American Journal of Physiology-Endocrinology and Metabolism*, *262*(1), E27–E31. https://doi.org/10.1152/ajpendo.1992.262.1.E27

Vaz-Serrano, J., Ruiz-Gomez, M. L., Gjøen, H. M., Skov, P. V, Huntingford, F. A., Øverli, Ø., & Höglund, E. (2011). Consistent boldness behaviour in early emerging fry of domesticated Atlantic salmon (*Salmo salar*): Decoupling of behavioural and physiological traits of the proactive stress coping style. *Physiology & Behavior*, *103*(3), 359–364. https://doi.org/10.1016/j.physbeh.2011.02.025

Veiseth-Kent, E., Grove, H., Færgestad, E. M., & Fjæra, S. O. (2010). Changes in muscle and blood plasma proteomes of Atlantic salmon (*Salmo salar*) induced by crowding. *Aquaculture*, *309*(1), 272–279. https://doi.org/10.1016/j.aquaculture.2010.09.028

Verri, T., Terova, G., Dabrowski, K., & Saroglia, M. (2011). Peptide transport and animal growth: the fish paradigm. *Biology Letters*, *7*(4), 597–600. https://doi.org/10.1098/rsbl.2010.1164

Vikeså, V., Nankervis, L., Remø, S. C., Waagbø, R., & Hevrøy, E. M. (2015). Pre and postprandial regulation of ghrelin, amino acids and IGF1 in Atlantic salmon (*Salmo salar* L.) at optimal and elevated seawater temperatures. *Aquaculture*, *438*, 159–169. https://doi.org/10.1016/j.aquaculture.2014.12.021

Vilà, L., Roglans, N., Baena, M., Barroso, E., Alegret, M., Merlos, M., & Laguna, J. C. (2012). Metabolic alterations and increased liver mTOR expression precede the development of autoimmune disease in a murine model of lupus erythematosus. *PlOS One*, *7*(12), e51118. https://doi.org/10.1371/journal.pone.0051118

Vogel, C., & Marcotte, E. M. (2012). Insights into the regulation of protein abundance from proteomic and transcriptomic analyses. *Nature Reviews. Genetics*, *13*(4), 227–232. https://doi.org/10.1038/nrg3185

Volkoff, H. (2016). The Neuroendocrine Regulation of Food Intake in Fish: A Review of Current Knowledge. *Frontiers in Neuroscience*, *10*. https://doi.org/10.3389/fnins.2016.00540

Waagbø, R., Jørgensen, S. M., Timmerhaus, G., Breck, O., & Olsvik, P. A. (2017). Short-term starvation at low temperature prior to harvest does not impact the health and acute stress response of adult Atlantic salmon. *PeerJ*, *5*, e3273. https://doi.org/10.7717/peerj.3273

Waagbø, R., Sandnes, K., Espelid, S., & Lie, Ø. (1988). Haematological and biochemical analyses of Atlantic salmon, *Salmo salar* L., suffering from coldwater *vibriosis* ('Hitra disease'). *Journal of Fish Diseases*, *11*(5), 417–423. https://doi.org/10.1111/j.1365-2761.1988.tb00737.x

Walker-Vergara, R., Arnés, Verónica. C., Müller, A., Ildefonso, R., & Rozas-Serri, M. A. (2020). Hematology in Salmonids. In M. A. Rozas-Serri (Eds.), *Manual of Clinical Pathology in Salmonids.* (2nd ed., pp. 20–36). ELANCO. https://doi.org/10.6084/m9.figshare.14703750.v1

Walton, M. J., & Cowey, C. B. (1982). Aspects of intermediary metabolism in salmonid fish. *Comparative Biochemistry and Physiology Part B: Comparative Biochemistry*, *73*(1), 59–79. https://doi.org/10.1016/0305-0491(82)90201-2

Walton, M. J., & Wilson, R. P. (1986). Postprandial changes in plasma and liver free amino acids of rainbow trout fed complete diets containing casein. *Aquaculture*, *51*(2), 105–115. https://doi.org/10.1016/0044-8486(86)90132-8

Wang, D., Eraslan, B., Wieland, T., Hallström, B., Hopf, T., Zolg, D. P., Zecha, J., Asplund, A., Li, L., Meng, C., Frejno, M., Schmidt, T., Schnatbaum, K., Wilhelm, M., Ponten, F., Uhlen, M., Gagneur, J., Hahne, H., & Kuster, B. (2019). A deep proteome and transcriptome abundance atlas of 29 healthy human tissues. *Molecular Systems Biology*, *15*(2), e8503. https://doi.org/10.15252/msb.20188503

Wang, J., Yan, X., Lu, R., Meng, X., & Nie, G. (2017). Peptide transporter 1 (PepT1) in fish: A review. *Aquaculture and Fisheries*, *2*(5), 193–206. https://doi.org/10.1016/j.aaf.2017.06.007

Wang, L., Liu, J., Li, Y., Ma, Q., Xu, H., Liang, M., & Wei, Y. (2023). Response of Turbot *Scophthalmus maximus* (Linnaeus, 1758) to Imbalanced Branched-Chain Amino Acids in Diets. *Fishes*, *8*(11), 534. https://doi.org/10.3390/fishes8110534

Wang, L., Sun, H., Cao, L., & Wang, J. (2024). Role of HOXA1-4 in the development of genetic and malignant diseases. *Biomarker Research*, *12*(1), 18. https://doi.org/10.1186/s40364-024-00569-x

Wang, M. M., Guo, H. X., Huang, Y. Y., Liu, W. B., Wang, X., Xiao, K., Xiong, W., Hua, H. K., Li, X. F., & Jiang, G. Z. (2022). Dietary Leucine Supplementation Improves Muscle Fiber Growth and Development by Activating AMPK/Sirt1 Pathway in Blunt Snout Bream (*Megalobrama amblycephala*). *Aquaculture Nutrition*, *2022*, 7285851. https://doi.org/10.1155/2022/7285851

Wang, Q., & Holst, J. (2015). L-type amino acid transport and cancer: targeting the mTORC1 pathway to inhibit neoplasia. *American Journal of Cancer Research*, *5*(4), 1281–1294.

Wang, Q., Xu, Z., & Ai, Q. (2021). Arginine metabolism and its functions in growth, nutrient utilization, and immunonutrition of fish. *Animal*, *7*(3), 716–727. https://doi.org/10.1016/j.aninu.2021.03.006

Wang, X., Yu, D., Wang, H., Lei, Z., Zhai, Y., Sun, M., Chen, S., & Yin, P. (2022). Rab3 and synaptotagmin proteins in the regulation of vesicle fusion and neurotransmitter release. *Life Sciences*, *309*, 120995. https://doi.org/10.1016/j.lfs.2022.120995

Wang, Y., Engel, T., & Teng, X. (2024). Post-translational regulation of the mTORC1 pathway: A switch that regulates metabolism-related gene expression. *Biochimica et Biophysica Acta- Gene Regulatory Mechanisms*, *1867*(1), 195005. https://doi.org/10.1016/j.bbagrm.2024.195005

Webb, L. A., Sadri, H., von Soosten, D., Dänicke, S., Egert, S., Stehle, P., & Sauerwein, H. (2019). Changes in tissue abundance and activity of enzymes related to branched-chain amino acid catabolism in dairy cows during early lactation. *Journal of Dairy Science*, *102*(4), 3556–3568. https://doi.org/10.3168/jds.2018-14463

Wecke, C., & Liebert, F. (2013). Improving the reliability of optimal in-feed amino acid ratios based on individual amino acid efficiency data from N balance studies in growing chicken. *Animals*, *3*(3), 558–573. https://doi.org/10.3390/ani3030558

Wei, Y., Sun, Z., Duan, M., Ma, Q., Xu, H., & Liang, M. (2022). Responses to graded levels of leucine and branched-chain amino acid imbalance in tiger puffer *Takifugu rubripes*. *Aquaculture*, *548*, 737699. https://doi.org/10.1016/j.aquaculture.2021.737699

Wessels, A. G., Kluge, H., Hirche, F., Kiowski, A., Schutkowski, A., Corrent, E., Bartelt, J., König, B., & Stangl, G. I. (2016). High leucine diets stimulate

cerebral branched-chain amino acid degradation and modify serotonin and ketone body concentrations in a pig model. *PLOS ONE*, *11*(3), 1–15. https://doi.org/10.1371/journal.pone.0150376

White, P. J., Lapworth, A. L., An, J., Wang, L., McGarrah, R. W., Stevens, R. D., Ilkayeva, O., George, T., Muehlbauer, M. J., Bain, J. R., Trimmer, J. K., Brosnan, M. J., Rolph, T. P., & Newgard, C. B. (2016). Branched-chain amino acid restriction in Zucker-fatty rats improves muscle insulin sensitivity by enhancing efficiency of fatty acid oxidation and acyl-glycine export. *Molecular Metabolism*, *5*(7), 538–551. https://doi.org/10.1016/j.molmet.2016.04.006

White, P. J., Lapworth, A. L., McGarrah, R. W., Kwee, L. C., Crown, S. B., Ilkayeva, O., An, J., Carson, M. W., Christopher, B. A., Ball, J. R., Davies, M. N., Kjalarsdottir, L., George, T., Muehlbauer, M. J., Bain, J. R., Stevens, R. D., Koves, T. R., Muoio, D. M., Brozinick, J. T., Gimeno, R. E., Brosnan, M. J., Rolph, T. P., Kraus, W. E., Shah, S. H., & Newgard, C. B. (2020). Muscle-Liver Trafficking of BCAA-Derived Nitrogen Underlies Obesity-Related Glycine Depletion. *Cell Reports*, *33*(6), 108375. https://doi.org/10.1016/j.celrep.2020.108375

Wijesooriya, K., Jadaan, S. A., Perera, K. L., Kaur, T., & Ziemann, M. (2022). Urgent need for consistent standards in functional enrichment analysis. *PLOS Computational Biology*, *18*(3), e1009935. https://doi.org/10.1371/journal.pcbi.1009935

Wilkinson, D. J., Hossain, T., Hill, D. S., Phillips, B. E., Crossland, H., Williams, J., Loughna, P., Churchward-Venne, T. A., Breen, L., Phillips, S. M., Etheridge, T., Rathmacher, J. A., Smith, K., Szewczyk, N. J., & Atherton, P. J. (2013). Effects of leucine and its metabolite β-hydroxy-β-methylbutyrate on human skeletal muscle protein metabolism. *The Journal of Physiology*, *591*(11), 2911–2923. https://doi.org/10.1113/jphysiol.2013.253203

Wilson, G. J., Layman, D. K., Moulton, C. J., Norton, L. E., Anthony, T. G., Proud, C. G., Rupassara, S. I., & Garlick, P. J. (2011). Leucine or carbohydrate supplementation reduces AMPK and eEF2 phosphorylation and extends

postprandial muscle protein synthesis in rats. *American Journal of Physiology-Endocrinology and Metabolism*, *301*(6), E1236–E1242. https://doi.org/10.1152/ajpendo.00242.2011

Wilson, R. P. (1986). Protein and amino acid requirements of fishes. *Annual Review of Nutrition*, *6*, 225–244. https://doi.org/10.1146/annurev.nu.06.070186.001301

Wiltafsky, M. K., Pfaffl, M. W., & Roth, F. X. (2010). The effects of branched-chain amino acid interactions on growth performance, blood metabolites, enzyme kinetics and transcriptomics in weaned pigs. *British Journal of Nutrition*, *103*(7), 964–976. https://doi.org/10.1017/S0007114509992212

Witeska, M., Kondera, E., & Bojarski, B. (2023). Hematological and Hematopoietic Analysis in Fish Toxicology- A Review. *Animals : An Open Access Journal from MDPI*, *13*(16). https://doi.org/10.3390/ani13162625

Witeska, M., Kondera, E., Ługowska, K., & Bojarski, B. (2022). Hematological methods in fish– Not only for beginners. *Aquaculture*, *547*, 737498. https://doi.org/10.1016/j.aquaculture.2021.737498

Wolfe, R. R. (2017). Branched-chain amino acids and muscle protein synthesis in humans: myth or reality? *Journal of the International Society of Sports Nutrition*, *14*(1), 30. https://doi.org/10.1186/s12970-017-0184-9

Wolfson, R. L., Chantranupong, L., Saxton, R. A., Shen, K., Scaria, S. M., Cantor, J. R., & Sabatini, D. M. (2016). Sestrin2 is a leucine sensor for the mTORC1 pathway. *Science*, *351*(6268), 43–48. https://doi.org/10.1126/science.aab2674

Wolfson, R. L., & Sabatini, D. M. (2017). The Dawn of the Age of Amino Acid Sensors for the mTORC1 Pathway. *Cell Metabolism*, *26*(2), 301–309. https://doi.org/10.1016/j.cmet.2017.07.001

Wu, D., Yan, R., Song, S., Swansiger, A. K., Li, Y., Prell, J. S., Zhou, Q., & Robinson, C. V. (2024). The complete assembly of human LAT1-4F2hc complex provides insights into its regulation, function and localisation.

Nature Communications, *15*(1), 3711. https://doi.org/10.1038/s41467-024-47948-4

Wu, X., Xie, W., Xie, W., Wei, W., & Guo, J. (2022). Beyond controlling cell size: functional analyses of S6K in tumorigenesis. *Cell Death & Disease*, *13*(7), 646. https://doi.org/10.1038/s41419-022-05081-4

Wu, Y., Lai, X., Lin, B., Lin, Y., Yang, Y., Zhang, M., Liu, S., Wu, J., Fu, X., & Shu, H. (2023). Transcriptome and hypoxia-responsive gene expression analyses reveal the physiological reaction to acute hypoxia and reoxygenation in *Epinephelus coioides*. *Aquaculture Reports*, *31*, 101655. https://doi.org/10.1016/j.aqrep.2023.101655

Wulff, T., Jokumsen, A., Højrup, P., & Jessen, F. (2012). Time-dependent changes in protein expression in rainbow trout muscle following hypoxia. *Journal of Proteomics*, *75*(8), 2342–2351. https://doi.org/10.1016/j.jprot.2012.02.010

Wullschleger, S., Loewith, R., & Hall, M. N. (2006). TOR Signaling in Growth and Metabolism. *Cell*, *124*(3), 471–484. https://doi.org/10.1016/j.cell.2006.01.016

Xia, Y-Q., Cheng, J-X., Liu, Y-F., Li, C-H., Liu, Y., & Liu, P-F. (2022). Genome-wide integrated analysis reveals functions of lncRNA-miRNA-mRNA interactions in Atlantic salmon challenged by *Aeromonas salmonicida*. *Genomics*, *114*(1), 328–339. https://doi.org/10.1016/j.ygeno.2021.12.013

Xiao, W. (2015). The hypoxia signaling pathway and hypoxic adaptation in fishes. *Science China. Life Sciences*, *58*(2), 148–155. https://doi.org/10.1007/s11427-015-4801-z

Xing, S., Liang, X., Zhang, X., Oliva-Teles, A., Peres, H., Li, M., Wang, H., Mai, K., Kaushik, S. J., & Xue, M. (2024). Essential amino acid requirements of fish and crustaceans, a meta-analysis. *Reviews in Aquaculture*, *16*(3), 1069–1086. https://doi.org/10.1111/raq.12886

Xiong, M. G., Xu, Z. S., Li, Y. H., Wang, S. Y., Wang, Y. Y., & Ran, Y. (2020). RNF152 positively regulates TLR/IL-1R signaling by enhancing MyD88 oligomerization. *EMBO Reports*, *21*(3), e48860. https://doi.org/10.15252/embr.201948860

Yadata, G. W., Ji, K., Liang, H., Ren, M., Ge, X., & Yang, Q. (2020). Effects of dietary protein levels with various stocking density on growth performance, whole body composition, plasma parameters, nitrogen emission and gene expression related to TOR signaling of juvenile blunt snout bream (*Megalobrama ambylcephala*). *Aquaculture*, *519*, 734730. https://doi.org/10.1016/j.aquaculture.2019.734730

Yahşi, B., & Gunaydin, G. (2022). Immunometabolism – The Role of Branched-Chain Amino Acids. *Frontiers in Immunology*, *13*, 886822. https://doi.org/10.3389/fimmu.2022.886822

Yamamoto, T., Matsunari, H., Furuita, H., Miura, M., Ozawa, R., Okazak, T., Oku, H., Murashita, K., & Yoshinaga, H. (2020). First feeding a plant-based diet to rainbow trout *Oncorhynchus mykiss* fry. *Aquaculture Science*, *68*(3), 211–220. https://doi.org/10.11233/aquaculturesci.68.211

Yang, J., Dolinger, M., Ritaccio, G., Mazurkiewicz, J., Conti, D., Zhu, X., & Huang, Y. (2012). Leucine stimulates insulin secretion via down-regulation of surface expression of adrenergic α2A receptor through the mTOR (mammalian target of rapamycin) pathway: implication in new-onset diabetes in renal transplantation. *The Journal of Biological Chemistry*, *287*(29), 24795–24806. https://doi.org/10.1074/jbc.M112.344259

Yfantis, A., Mylonis, I., Chachami, G., Nikolaidis, M., Amoutzias, G. D., Paraskeva, E., & Simos, G. (2023). Transcriptional Response to Hypoxia: The Role of HIF-1-Associated Co-Regulators. *Cells*, *12*(5). https://doi.org/10.3390/cells12050798

Yimam, M. A., Andreini, M., Carnevale, S., & Muscaritoli, M. (2025). Postprandial Aminoacidemia Following the Ingestion of Alternative and Sustainable Proteins in Humans: A Narrative Review. *Nutrients*, *17*(2). https://doi.org/10.3390/nu17020211

Yin, S., Liu, L., & Gan, W. (2021). The Roles of Post-Translational Modifications on mTOR Signaling. *International Journal of Molecular Sciences*, *22*(4). https://doi.org/10.3390/ijms22041784

Yoon, G. H., Kim, K., Park, D. S., & Choi, S. C. (2022, May). RNF152 negatively regulates Wnt/β-catenin signaling in Xenopus embryos. *BMB Reports*. Korea (South). https://doi.org/10.5483/BMBRep.2022.55.5.187

Yoshida, T., & Delafontaine, P. (2020). Mechanisms of IGF-1-Mediated Regulation of Skeletal Muscle Hypertrophy and Atrophy. *Cells*, *9*(9). https://doi.org/10.3390/cells9091970

Yousaf, M. N., & Powell, M. D. (2012). The Effects of Heart and Skeletal Muscle Inflammation and Cardiomyopathy Syndrome on Creatine Kinase and Lactate Dehydrogenase Levels in Atlantic Salmon (*Salmo salar* L.). *The Scientific World Journal*, *2012*, 741302. https://doi.org/10.1100/2012/741302

Ytrestøyl, T., Hjelle, E., Kolarevic, J., Takle, H., Rebl, A., Afanasyev, S., Krasnov, A., Brunsvik, P., & Terjesen, B. F. (2023). Photoperiod in recirculation aquaculture systems and timing of seawater transfer affect seawater growth performance of Atlantic salmon (*Salmo salar*). *Journal of the World Aquaculture Society*, *54*(1), 73–95. https://doi.org/10.1111/jwas.12880

Yu, D., Richardson, N. E., Green, C. L., Spicer, A. B., Murphy, M. E., Flores, V., Jang, C., Kasza, I., Nikodemova, M., Wakai, M. H., Tomasiewicz, J. L., Yang, S. E., Miller, B. R., Pak, H. H., Brinkman, J. A., Rojas, J. M., Quinn, W. J. 3rd, Cheng, E. P., Konon, E. N., Haider, L. R., Finke, M., Sonsalla, M., Alexander, C. M., Rabinowitz, J. D., Baur, J. A., Malecki, K. C., & Lamming, D. W. (2021). The adverse metabolic effects of branched-chain amino acids are mediated by isoleucine and valine. *Cell Metabolism*, *33*(5), 905-922.e6. https://doi.org/10.1016/j.cmet.2021.03.025

Yu, Y., Wang, Q., Huang, Z., Ding, L., & Xu, Z. (2020). Immunoglobulins, Mucosal Immunity and Vaccination in Teleost Fish. *Frontiers in Immunology*, *11*. https://doi.org/10.3389/fimmu.2020.567941

Yu, Y., Wang, Y., Jin, J., Han, D., Zhu, X., Liu, H., Zhang, Z., Yang, Y., & Xie, S. (2025). Interaction of dietary replacements of fishmeal by protein blend and feeding frequency on growth performance and protein utilization of gibel carp (*Carassius gibelio* var. CAS V). *Animal Nutrition*, *20*, 291–302. https://doi.org/10.1016/j.aninu.2024.11.007

Yúfera, M., Perera, E., Mata-Sotres, J. A., Calduch-Giner, J., Martínez-Rodríguez, G., & Pérez-Sánchez, J. (2017). The circadian transcriptome of marine fish (*Sparus aurata*) larvae reveals highly synchronized biological processes at the whole organism level. *Scientific Reports*, *7*(1), 12943. https://doi.org/10.1038/s41598-017-13514-w

Zah, S., Madsen, A., Bendiksen, E., Vatsos, I. N., & Korsnes, K. (2025). Leveraging blood biomarkers and machine learning to determine smoltification status of Atlantic salmon (*Salmo salar*). *Aquaculture International*, *33*(6), 480. https://doi.org/10.1007/s10499-025-02169-4

Zambrano-Carrasco, J., Zou, J., Wang, W., Sun, X., Li, J., & Su, H. (2024). Emerging roles of Cullin-RING ubiquitin ligases in cardiac development. *Cells*. https://doi.org/10.3390/cells13030235

Zanuzzo, F. S., Beemelmanns, A., Hall, J. R., Rise, M. L., & Gamperl, A. K. (2020). The innate immune response of Atlantic salmon (*Salmo salar*) is not negatively affected by high temperature and moderate hypoxia. *Frontiers in Immunology*, *11*, 1009. https://doi.org/10.3389/fimmu.2020.01009

Zarkasi, K. Z., Taylor, R. S., Abell, G. C. J., Tamplin, M. L., Glencross, B. D., & Bowman, J. P. (2016). Atlantic Salmon (Salmo salar L.) Gastrointestinal Microbial Community Dynamics in Relation to Digesta Properties and Diet. *Microbial Ecology*, *71*(3), 589–603. https://doi.org/10.1007/s00248-015-0728-y

Zehra, S., & Khan, M. A. (2017). Dietary thiamin and pyridoxine requirements of fingerling Indian major carp, *Cirrhinus mrigala* (Hamilton). *Aquaculture Research*, *48*(9), 4945–4957. https://doi.org/10.1111/are.13313

Zhang, B., Yang, H., Cai, G., Nie, Q., & Sun, Y. (2024). The interactions between the host immunity and intestinal microorganisms in fish. *Applied Microbiology and Biotechnology*, *108*(1), 30. https://doi.org/10.1007/s00253-023-12934-1

Zhang, G., Ye, Z., Jiang, Z., Wu, C., Ge, L., Wang, J., Xu, X., Wang, T., & Yang, J. (2024). Circadian patterns and photoperiodic modulation of clock gene expression and neuroendocrine hormone secretion in the marine teleost *Larimichthys crocea*. *Chronobiology International*, *41*(3), 329–346. https://doi.org/10.1080/07420528.2024.2315215

Zhang, S., Zeng, X., Ren, M., Mao, X., & Qiao, S. (2017). Novel metabolic and physiological functions of branched chain amino acids: a review. *Journal of Animal Science and Biotechnology*, *8*(1), 10. https://doi.org/10.1186/s40104-016-0139-z

Zhang, Y., Dabrowski, K., Hliwa, P., & Gomułka, P. (2006). Indispensable amino acid concentrations decrease in tissues of stomachless fish, common carp in response to free amino acid- or peptide-based diets. *Amino Acids*, *31*, 165–172. https://doi.org/10.1007/s00726-006-0345-7

Zhang, Y., Lu, R., Qin, C., & Nie, G. (2020). Precision nutritional regulation and aquaculture. *Aquaculture Reports*, *18*, 100496. https://doi.org/10.1016/j.aqrep.2020.100496

Zhang, Z., Li, D., Refaey, M. M., & Xu, W. (2017). High Spatial and Temporal Variations of Microbial Community along the Southern Catfish Gastrointestinal Tract: Insights into Dynamic Food Digestion. *Frontiers in Microbiology*. https://doi.org/10.3389/fmicb.2017.01531

Zheng, L., Wei, H., Cheng, C., Xiang, Q., Pang, J., & Peng, J. (2016). Supplementation of branched-chain amino acids to a reduced-protein diet improves growth performance in piglets: Involvement of increased feed intake and direct muscle growth-promoting effect. *British Journal of Nutrition*, *115*(12), 2236–2245. https://doi.org/10.1017/S0007114516000842

Zhou, M., Lu, G., Gao, C., Wang, Y., & Sun, H. (2012). Tissue-specific and nutrient regulation of the branched-chain α-keto acid dehydrogenase phosphatase, protein phosphatase 2Cm (PP2Cm). *The Journal of Biological Chemistry*, *287*(28), 23397–23406. https://doi.org/10.1074/jbc.M112.351031

Zhou, Z., He, Y., Wang, S., Wang, Y., Shan, P., & Li, P. (2022). Autophagy regulation in teleost fish: A double-edged sword. *Aquaculture*, *558*, 738369. https://doi.org/10.1016/j.aquaculture.2022.738369

Zhu, C. D., Wang, Z. H., & Yan, B. (2013). Strategies for hypoxia adaptation in fish species: A review. *Journal of Comparative Physiology B: Biochemical, Systemic, and Environmental Physiology*, *183*(8), 1005–1013. https://doi.org/10.1007/s00360-013-0762-3

Zhu, T., & Li, W. (2024). The regulation of prolactin secretion and its targeting function of teleost. *General and Comparative Endocrinology*, *354*, 114530. https://doi.org/10.1016/j.ygcen.2024.114530

Zhu, X., Liu, J., Cai, M., Bao, L., Chu, W., Pan, Y., Wu, P., & Zhang, J. (2023). The circadian rhythm regulates branched-chain amino acids metabolism in fast muscle of Chinese perch (*Siniperca chuatsi*) during short-term fasting by Clock-KLF15-Bcat2 pathway. *British Journal of Nutrition*, *130*(4), 604–615. https://doi.org/DOI: 10.1017/S0007114522003646

Ziegler, G. C., Almos, P., McNeill, R. V, Jansch, C., & Lesch, K. P. (2020). Cellular effects and clinical implications of SLC2A3 copy number variation. *Journal of Cellular Physiology*, *235*(12), 9021–9036. https://doi.org/10.1002/jcp.29753

Ziello, J. E., Jovin, I. S., & Huang, Y. (2007). Hypoxia-Inducible Factor (HIF)-1 regulatory pathway and its potential for therapeutic intervention in malignancy and ischemia. *The Yale Journal of Biology and Medicine*, *80*(2), 51–60.

Zlaugotne, B., Pubule, J., & Blumberga, D. (2022). Advantages and disadvantages of using more sustainable ingredients in fish feed. *Heliyon*, *8*(9), e10527. https://doi.org/10.1016/j.heliyon.2022.e10527

SUPPLEMENTARY DATA

S 2 Chapter 2

S 2.1 Proximate analysis of feeds, ingredients and faeces (MOPA)

	% Moisture	% Ash	% Protein	% Lipid	MJ/kg Energy	% NFE
Diet composition (dry matter basis)						
CD	9.7	6.5	53.1	13.9	22.7	19.3
LD	10.7	6.4	54.8	14.2	22.6	16.3
ID	11.5	6.4	54.6	14.2	22.5	16.0
VD	10.9	6.4	54.6	13.9	22.5	16.8
SPCD	7.1	6.7	56.9	9.1	21.8	22.3
WHE	9.7	5.2	60.4	12.8	22.9	13.6
CAS	6.3	6.8	61.5	9.4	22.3	17.5
Ingredient composition (dry matter basis)						
Basal	9.1	6.6	56.9	12.6	21.7	16.9
Leu	0.1	0.1	65.5	0.7	26.9	33.7
Ile	0.0	0.0	64.4	2.2	26.8	33.3
Val	0.0	0.0	72.6	0.9	24.7	26.4
Corn gluten (Biomar)	9.5	1.3	61.0	11.5	23.5	18.6
Wheat gluten (Biomar)	4.4	0.8	76.6	7.4	23.2	11.4
SPC	8.1	6.7	62.6	1.4	19.9	23.7
Whey	5.0	2.8	77.2	7.2	24.0	8.4
Casein	6.0	8.1	80.4	1.5	22.0	4.7
Faecal composition (dry matter basis)						
CD	84.7	21.5	19.5	4.0	84.7	
LD	89.2	21.5	19.6	5.2	89.2	
ID	87.8	21.5	18.9	5.9	87.8	
VD	87.6	21.7	19.7	5.3	87.6	
SPCD	86.4	19.8	21.0	3.5	86.4	
WHE	84.4	18.4	20.6	5.7	84.4	
CAS	84.6	22.6	17.5	5.2	84.6	

All values are percentages (%) unless otherwise stated. CD= Control diet, LD= Leucine diet, VD= Valine diet, ID= Isoleucine diet, WHE= Whey diet, CAS= Casein diet, SPCD= Soya Protein concentrate diet. *Carbohydrate content determined based on dry matter minus protein, ash and lipids.

S 2.2 Mineral content in ingredients

	Basal	Leu	Ile	Val	SPC	Whe	Cas	Cg	Wg
Dry matter basis g/kg (ppt)									
Na	4.26	0.03	0.001*	0.01	0.03	1.88	0.83	2.24	0.51
Mg	2.33	0.01	0.001*	0.001*	4.54	0.67	1.06	0.54	0.38
P	7.76	0.01	0.01	0.01	8.21	3.00	15.57	3.25	1.65
K	9.21	0.02	0.00	0.00	23.42	5.13	3.93	1.87	1.58
Ca	9.54	0.12	0.09	0.13	3.98	4.10	25.74	0.44	0.99
Y	1.67	*	*	*	*	*	*	*	*
Dry matter basis mg/kg (ppm)									
V	0.16	0.04	0.03	0.04	0.13	0.03	0.07	0.09	0.07
Cr	0.16	0.05	0.03	0.01	0.11	0.09	0.03	0.12	0.07
Mn	28.87	0.04	0.03	0.02	41.58	0.83	0.67	17.01	14.39
Fe	124.01	1.33	2.03	2.35	188.70	205.26	10.33	84.15	108.74
Co	0.12	0.00	0.00	0.002*	0.02	0.04	0.01	0.01	0.01
Ni	0.00	0.00	0.00	0.00	0.07	0.00	0.00	0.02	0.00
Cu	20.76	0.00	0.18	0.07	8.04	1.60	1.26	8.98	5.91
Zn	167.24	1.13	19.60	0.39	74.39	40.53	136.01	62.60	64.93

Basal= basal mash, Leu= Leucine, Ile= Isoleucine Val= Valine, Spc= Soya protein concentrate, Whe= Whey, Cas= Casein, Cg= Corn gluten, Wg= Wheat gluten. Na= Sodium, Mg= Magnesium, P=Phosphorous, K= Potassium, Ca= Calcium, V= Vanadium, Cr= Chromium, Mn= Manganese, Fe= Iron, Co= Cobalt, Ni= Nickel, Cu= Copper, Zn= Zinc.

S 2.3 Mineral content in feeds

	CD	LD	ID	VD	SPC	WHE	CAS
Dry matter basis g/kg (ppt)							
Na	4.1	4.3	4.0	4.1	2.8	3.5	3.1
Mg	2.2	2.1	2.1	2.2	2.8	1.7	1.8
P	8.4	8.6	8.3	8.8	8.3	6.8	10.4
K	9.8	9.3	9.3	9.5	13.4	8.2	7.9
Ca	10.3	10.2	9.7	10.6	8.7	8.5	14.5
Fe	0.2	0.1	0.1	0.1	0.2	0.1	0.1
Zn	0.1	0.1	0.1	0.1	0.1	0.1	0.1
Y	1.7	1.5	1.6	1.6	1.2	1.1	1.1
Dry matter basis mg/kg (ppm)							
V	0.2	0.2	0.3	0.2	0.2	0.2	0.2
Cr	1.0	0.9	2.3	0.8	1.0	0.8	0.8
Mn	44.0	39.8	46.1	41.8	43.4	28.8	29.6
Co	0.1	0.1	0.1	0.1	0.1	0.1	0.1
Ni	0.0	0.3	0.3	0.3	0.4	0.0	0.0
Cu	11.3	13.1	10.9	11.3	10.6	8.2	8.4

Na= Sodium, Mg= Magnesium, P=Phosphorous, K= Potassium, Ca= Calcium, V= Vanadium, Cr= Chromium, Mn= Manganese, Fe= Iron, Co= Cobalt, Ni= Nickel, Cu= Copper, Zn= Zinc. CD= Control diet, LD= Leucine diet, VD= Valine diet, ID= Isoleucine diet, WHE= Whey diet, CAS= Casein diet, SPCD= Soya Protein concentrate diet.

S 2.4 Minerals Faeces

	CD	LD	ID	VD	SPC	WHE	CAS
Dry matter basis g/kg (ppt)							
Na	24.7	28.7	27.4	26.8	25.7	19.5	24.7
Mg	28.0	26.3	26.4	27.3	27.6	24.8	28.0
P	13.5	14.9	13.5	12.6	8.5	7.8	13.5
K	1.6	1.8	1.7	1.7	1.7	1.2	1.6
Ca	43.0	39.9	41.4	40.8	32.0	34.3	43.0
Mn	0.1	0.1	0.1	0.1	0.1	0.1	0.1
Fe	0.4	0.4	0.6	0.4	0.3	0.3	0.4
Cu	0.0	0.0	0.0	0.0	0.0	0.0	0.0
Zn	0.3	0.3	0.3	0.2	0.2	0.1	0.2
Y	4.3	3.8	4.0	3.6	2.7	3.3	3.9
Dry matter basis mg/kg (ppm)							
V	0.4	0.5	0.8	0.5	0.4	0.4	0.4
Cr	1.9	3.4	2.4	2.3	4.7	2.0	2.9
Co	0.3	0.3	0.7	0.2	0.2	0.2	0.2
Ni	0.3	0.5	5.0	0.3	0.5	0.4	0.5

Na= Sodium, Mg= Magnesium, P=Phosphorous, K= Potassium, Ca= Calcium, V= Vanadium, Cr= Chromium, Mn= Manganese, Fe= Iron, Co= Cobalt, Ni= Nickel, Cu= Copper, Zn= Zinc. CD= Control diet, LD= Leucine diet, VD= Valine diet, ID= Isoleucine diet, WHE= Whey diet, CAS= Casein diet, SPCD= Soya Protein concentrate diet.

S 2.5 Amino acid analysis of test ingredients (g/100 g)

	Basal	Whe	Cas	Spc	Leu	Ile	Val	Cg	Wg
Dry matter %									
Crude protein	56.9	77.2	80.4	62.6	65.5	64.4	72.6	63.9	80.6
Lipid	12.6	7.2	1.5	1.4	0.7	2.2	0.9	9.5	7.3
Energy	21.7	24.0	22.0	20.0	26.9	26.8	24.7	22.8	23.1
Sum of AA	35.1	60.7	66.1	54.6	82.2	77.5	73.3	46.5	58.2
Alanine	1.7	2.9	1.8	2.5	0.0	0.0	0.0	3.7	1.4
Arginine	2.1	1.7	2.7	4.3	0.0	0.0	0.0	1.6	2.3
Asparagine	2.5	5.7	4.1	6.5	0.0	0.0	0.0	2.5	1.7
Cysteine	0.4	1.4	0.2	0.3	0.0	0.0	0.0	0.2	0.8
Glutamate	7.7	9.9	12.9	10.6	0.0	0.0	0.0	9.4	20.6
Glycine	1.7	1.5	1.4	2.4	0.0	0.0	0.0	1.4	2.2
Histidine	1.0	1.3	2.1	1.4	0.0	0.0	0.0	1.1	1.3
Isoleucine	1.2	3.2	3.3	2.8	0.3	77.5	0.0	2.0	2.0
Leucine	3.1	6.6	6.2	4.5	78.1	0.0	0.0	7.5	4.1
Lysine	1.4	4.5	4.3	3.6	0.0	0.0	0.0	0.7	0.8
Methionine	0.9	1.7	2.0	0.7	0.0	0.0	0.0	1.1	1.0
Phenylalanine	2.2	2.4	3.9	3.0	0.4	0.0	0.0	3.3	3.5
Proline	2.8	4.0	6.7	2.9	0.0	0.0	0.0	4.2	7.5
Serine	2.0	3.8	3.6	2.4	0.0	0.0	0.0	1.8	2.9
Threonine	1.4	4.8	2.9	2.0	0.0	0.0	0.0	1.4	1.5
Tyrosine	1.6	2.4	4.1	2.0	0.0	0.0	0.0	2.6	2.3
Valine	1.4	3.0	3.9	2.8	3.4	0.0	73.3	2.2	2.1
P	7.8	3.0	15.6	8.2	0.0	0.0	0.0	3.2	1.7
Y	1.7	0.0	0.0	0.0	0.0	0.0	0.0	0.0	0.0

Values are means ± standard deviation (week 1 n= 7, week 2 n= 6 and week 3 n=5). Different subscripts denote significant difference among diets ($p<0.05$). Basal, Whe= Whey Cas= Casein, Spc= Soya protein concentrate, Leu= Leucine, Val= Valine, Ile= Isoleucine, Cg= Corn gluten, Wg= Wheat gluten.

S 2.6 Amino acid analysis of test feeds (g/100 g)

	CD	LD	ID	VD	SPC	WHE	CAS
Dry matter %							
Crude protein	53.1	54.8	54.6	54.6	56.9	60.4	61.5
Lipid	13.9	14.2	14.2	13.9	9.1	12.8	9.4
Energy (MJ/kg)	22.6	22.8	22.8	22.7	21.7	23.0	22.1
Sum of AA	50.6	51.9	52.0	55.9	57.4	60.8	63.3
Alanine	2.7	2.7	2.6	2.8	2.9	3.1	2.7
Arginine	2.7	2.4	2.7	2.9	3.5	2.7	2.9
Asparagine	4.1	4.2	4.0	4.3	5.3	5.2	4.8
Cysteine	0.4	0.4	0.4	0.5	0.5	0.6	0.5
Glutamate	12.4	12.3	11.8	12.7	12.7	12.5	14.2
Glycine	2.3	2.2	2.2	2.4	2.6	2.2	2.2
Histidine	1.3	1.0	1.3	1.4	1.4	1.5	1.7
Isoleucine	2.4	2.1	**4.0**	2.5	2.3	3.1	2.7
Leucine	4.7	**6.7**	4.7	5.0	5.2	6.1	5.9
Lysine	2.5	2.5	2.4	2.6	2.9	3.8	3.6
Methionine	1.0	1.0	1.0	1.1	1.1	1.3	1.5
Phenylalanine	2.6	2.5	2.6	2.8	3.0	2.9	3.3
Proline	4.0	4.0	4.0	4.2	4.2	4.4	5.8
Serine	1.7	2.0	2.5	2.4	3.2	3.1	3.3
Threonine	1.5	1.8	1.8	1.8	2.2	3.0	2.5
Tyrosine	1.8	1.8	1.9	1.9	2.2	2.2	2.7
Valine	2.6	2.4	2.3	**4.7**	2.5	3.2	3.1
P	8.4	8.6	8.3	8.8	8.3	6.8	10.4
Y	1.7	1.5	1.6	1.6	1.2	1.1	1.1

All values are reported as dry matter (%) unless otherwise indicated. CD= Control diet, LD= Leucine diet, VD= Valine diet, ID= Isoleucine diet, WHE= Whey diet, CAS= Casein diet and SPCD= Soya Protein Concentrate diet. sAA= sum of all amino acids, Ala= Alanine, Arg= Arginine, Asp= Aspartic acid, Cys= Cysteine, Glu= Glutamine, Gly= Glycine, His= Histidine, Ile= Isoleucine, Leu= Leucine, Lys= Lysine, Met= Methionine, Phe= Phenylalanine, Pro= Proline, Ser= Serine, Thr= Threonine, Tyr= Tyrosine, and Val= Valine.

S 2.7 Faeces bAAs BCAAs and Intact protein diets (g/100 g)

Dry matter basis %	**CD**	**LD**	**ID**	**VD**	**SPC**	**WHE**	**CAS**
Sum of AA	10.7±1.2	12.3±0.6	11.6±0.9	12.1±1.6	12.4±1.1	13.4±0.2	11.5±1.1
Alanine	1.5±0.7	1.0±0.0	1.0±0.0	1.0±0.2	1.0±0.1	1.1±0.1	0.9±0.1
Arginine	0.3±0.1	0.4±0.0	0.4±0.0	0.4±0.0	0.3±0.0	0.3±0.0	0.3±0.0
Asparagine	0.7±0.1	0.9±0.1	0.7±0.1	0.8±0.1	1.0±0.1	1.0±0.1	0.8±0.1
Cysteine	0.3±0.1	0.4±0.3	0.5±0.2	0.4±0.1	0.4±0.1	0.3±0.1	0.3±0.1
Glutamate	1.1±0.1	1.2±0.9	1.1±0.2	1.2±0.2	1.3±0.2	1.4±0.1	1.1±0.2
Glycine	1.0±0.3	1.2±0.0	1.1±0.0	1.2±0.2	1.2±0.1	1.1±0.0	1.0±0.1
Histidine	0.2±0.0	0.2±0.0	0.2±0.0	0.2±0.1	0.2±0.1	0.1±0.0	0.1±0.0
Isoleucine	0.5±0.2	0.5±0.1	0.6±0.1	0.5±0.1	0.5±0.0	0.5±0.1	0.5±0.1
Leucine	1.4±0.7	1.8±0.2	1.7±0.0	1.8±0.3	1.7±0.2	1.8±0.2	1.4±0.3
Lysine	0.5±0.1	0.6±0.0	0.6±0.0	0.5±0.1	0.6±0.1	0.9±0.1	0.8±0.0
Methionine	0.4±0.1	0.4±0.1	0.4±0.1	0.3±0.0	0.4±0.1	0.4±0.1	0.4±0.1
Phenylalanine	0.3±0.2	0.4±0.1	0.4±0.1	0.3±0.1	0.3±0.0	0.3±0.0	0.3±0.0
Proline	0.7±0.3	1.0±0.0	0.9±0.0	1.0±0.2	1.0±0.1	1.1±0.0	1.0±0.2
Serine	0.4±0.1	0.6±0.1	0.5±0.2	0.5±0.2	0.6±0.2	0.7±0.1	0.6±0.2
Threonine	0.4±0.1	0.4±0.0	0.5±0.1	0.5±0.1	0.6±0.1	0.9±0.0	0.5±0.1
Tyrosine	0.3±0.2	0.4±0.0	0.3±0.1	0.6±0.4	0.4±0.1	0.4±0.0	0.4±0.0
Valine	0.7±0.2	0.7±0.3	0.7±0.3	0.7±0.4	1.0±0.0	0.9±0.3	0.9±0.1

S 2.8 bAA analysis of faeces from the BCAA diets (g/100 g)

Dry matter basis %	**CD**	**LD**	**ID**	**VD**	P value
Sum of AA	10.74±1.42	12.26±0.58	11.63±0.93	12.06±1.56	0.452
Alanine	1.46±0.89	1.01±0.04	0.97±0.04	1.04±0.18	0.868
Arginine	0.30±0.15	0.38±0.03	0.36±0.02	0.37±0.05	0.978
Asparagine	0.69±0.11	0.86±0.10	0.75±0.14	0.83±0.10	0.317
Cysteine	0.28±0.10	0.45±0.32	0.49±0.25	0.37±0.08	0.511
Glutamate	1.11±0.14	1.19±0.08	1.11±0.16	1.20±0.20	0.813
Glycine	1.00±0.33	1.19±0.03	1.14±0.05	1.20±0.25	0.641
Histidine	0.18±0.05	0.24±0.04	0.23±0.03	0.23±0.06	0.455
Isoleucine	0.52±0.19	0.55±0.13	0.57±0.09	0.55±0.15	0.982
Leucine	1.42±0.71	1.81±0.24	1.73±0.05	1.82±0.33	0.620
Lysine	0.55±0.14	0.62±0.05	0.56±0.04	0.52±0.08	0.585
Methionine	0.36±0.10	0.36±0.12	0.41±0.15	0.30±0.03	0.899
Phenylalanine	0.35±0.16	0.37±0.12	0.37±0.09	0.29±0.08	0.834
Proline	0.74±0.35	0.95±0.01	0.91±0.04	0.98±0.16	0.869
Serine	0.40±0.14	0.56±0.13	0.50±0.17	0.51±0.16	0.682
Threonine	0.42±0.13	0.55±0.05	0.51±0.07	0.52±0.07	0.346
Tyrosine	0.31±0.19	0.41±0.05	0.32±0.15	0.63±0.36	0.657
Valine	0.65±0.29	0.75±0.29	0.71±0.32	0.71±0.41	0.834

All values are means (n=3) ± standard deviation and documented as total percentages (%) unless otherwise stated. Different superscripts indicate significant differences ($p < 0.05$). CD= Control diet, LD= Leucine diet, VD= Valine diet, ID= Isoleucine diet.

S 2.9 AccQ-Tag method conditions

AccQ-Tag Profiling method	
Column flow rate	0.7 mL/min
Column temperature	55°C
Autosampler temperature	25°C
Injection volume	1 µL
Desolvation temperature	600°C
Desolvation gas flow rate	1,000 L/h,
Collision gas (argon) flow rate	0.15 mL/min,
Dwell time	0.01 s
Column	AccQTag Ultra Column 2.1 x 100 mm, 1.7µm (186003837)
UV detection	260 nm
Mobile Phase A	100% AccQ Tag Ultra eluent A concentrate
Mobile Phase B	90:10 Water: AccQ Tag Ultra eluent B
Mobile Phase C	100% HPLC-grade water (MilliQ)
Mobile Phase D	100% AccQ Tag Ultra eluent B

S 2.10 Primers

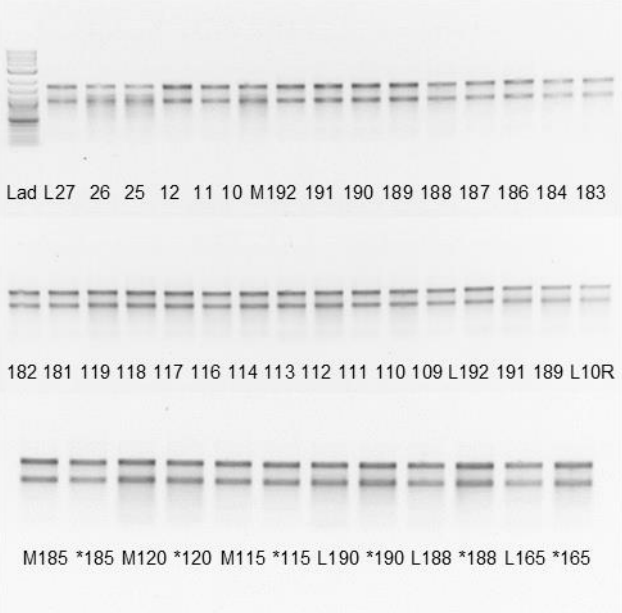
Oligo name	Oligo sequence
qSs4EBP_F	GCCTCCTGTGGAGAGAACTG
qSs4EBP_R	GCAACCATTGACGTTCTCCG
qSs4EBP1A_F	CGACTCCTACAGTCAGACGC
qSs4EBP1A_R	GGGTACGTGTGATCGGTGAA
qSsRRAG_F	AATGGGCAAGAGTGGGTCTG
qSsRRAG_R	ATCAGCACCTCCACATTCCG
qSsMYOSTAT1a_F	CACAACGCCTGTTGGACTTG
qSsMYOSTAT1a_R	TGGACGGAGCGTGTAACATT
qSsBACTIN_F	GGAAGATGAAATCGCCGCAC
qSSBACTIN_R	AACGTAGCTGTCCTTCTGGC
qSsEF1aM_F	ATGAGACAGACCGTTGCCG
qSsEF1aM_R	GCCTTAATGGCAGACTTGGTCA
qSsEF1aL_F	TGACACCGAAACTAAGCGACC
qSsEF1aL_R	ATGGTGATACCACGCTCACG
qSsMYO6_F	GTACGAGCTCAGCAAGTGGA
qSsMYO6_R	GGTGCGAGATCATAGTCGGT
qSsIGF1_F	TGTACTGTGCCCCTGTCAAG
qSsIGF1_R	CCCTGTCCGTTAGCTTCTGT
qSsSESN1_F	TTTGTGGTTGGGTGGTGGTT
qSsSESN1_R	ACAGTGCGATGATTGACTGGA
qSsBCKDK_F	CCCTCGCATGAACAACCTCT
qSsBCKDK_R	CAGGGCTAAGCAGCAAGTGA
qSsBCAT1a_F	CTGGCCAAGAGGTTCCACAAA
qSsBCAT1a_R	CCTATCAGAAGGAGTGCATTAAAGG
qSsBCAT1b_F	GTAATGCTGTGAAACAGCCGC
qSsBCAT1b_R	GCACGGACAACCCTATAGACG
qSsBCKDHA_F	CGTTCACTACGGCAGCAAAG
qSsBCKDHA_R	CGCCCTCTCCGAAGTAACAG
qSsBCKDH1b_F	CCATCTTGCCTTGGGACACT
qSsBCKDH1b_R	GGAAGCACTCCTCTTGCACT
qSs40SRPS11_HK_F	ATGAAGATGCAGAGGACCATCG
qSs40SRPS11_HK_R	ACTTCTGGAACTGCTTCTTGGC
qSs60SRPL13_HK_F	GCACCTGGTTCAACCAGC
qSs60SRPL13_HK_R	CATACGCAGGCTGGCGAA
qSs40SRPS5_F	AACTCCATGATGATGCACGG
qSs40SRPS5_R	GGTCTTGATGTTCCTGAAAGCA
qSs40SRPS7_F	CAGAAGCGTCCCAGGAGC
qSs40SRPS7_R	CCTGTGAGCTTCTTGTAGACACC
qSs60SRPL3_HK_F	GGCAAGAAGCAGCTGGAGAA
qSs60SRPL3_HK_R	TTACGCAGACCACGATGGGT
qSsPROGESTN_ab_F	ACCACATCCAAGGAAGGCAG
qSsPROGESTN_ab_R	CACCAGACTTGCCCTCCAAT

S 2.11 Primer co-efficient of determination (r^2), efficiency (%) and temperature plan. Oligonucleotide primers designed to assay mRNA abundance by rt-qPCR

Number	Oligo name	Oligo sequence	Size	DNA Tm °c	vol for 100pmol/ µl	Average time °c	Total av. °c	Efficiency (%)	R^2
Group 1									
39	qSs60SRPL3_HK_F	GGCAAGAAGCAGCTGGAGAA	20	59.4	304.0	59.4		125	0.9758
40	qSs60SRPL3_HK_R	TTACGCAGACCACGATGGGT	20	59.4	343.0				
41	qSsPROGESTN_ab_F	ACCACATCCAAGGAAGGCAG	20	59.4	373.0	59.4		157	0.9011
42	qSsPROGESTN_ab_R	CACCAGACTTGCCCTCCAAT	20	59.4	364.0		59.4		
29	qSsBCKDH1b_F	CCATCTTGCCTTGGGACACT	20	59.4	314.0	59.4		92	0.9945
30	qSsBCKDH1b_R	GGAAGCACTCCTCTTGCACT	20	59.4	364.0				
21	qSsBCKDK_F	CCCTCGCATGAACAACCTCT	20	59.4	342.0	59.4		90	0.9985
22	qSsBCKDK_R	CAGGGCTAAGCAGCAAGTGA	20	59.4	323.0				
15	qSsMYO6_F	GTACGAGCTCAGCAAGTGGA	20	59.4	264.0	59.4		99	0.9869
16	qSsMYO6_R	GGTGCGAGATCATAGTCGGT	20	59.4	316.0				
17	qSsIGF1_F	TGTACTGTGCCCCTGTCAAG	20	59.4	337.0	59.4		98	0.9940
18	qSsIGF1_R	CCCTGTCCGTTAGCTTCTGT	20	59.4	417.0				
Group 2									
5	qSsRRAG_F	AATGGGCAAGAGTGGGTCTG	20	59.4	342.0	59.4		97	0.9962
6	qSsRRAG_R	ATCAGCACCTCCACATTCCG	20	59.4	366.0				
9	qSsBACTIN_F	GGAAGATGAAATCGCCGCAC	20	59.4	303.0	59.4		99	0.9981
10	qSSBACTIN_R	AACGTAGCTGTCCTTCTGGC	20	59.4	357.0		59.5		
11	qSsEF1aM_F	ATGAGACAGACCGTTGCCG	19	58.8	332.0	59.6		102	0.9982
12	qSsEF1aM_R	GCCTTAATGGCAGACTTGGTCA	22	60.3	346.0				
13	qSsEF1aL_F	TGACACCGAAACTAAGCGACC	21	59.8	320.0	59.6		90	0.9991
14	qSsEF1aL_R	ATGGTGATACCACGCTCACG	20	59.4	357.0				
Group 3									
19	qSsSESN1_F	TTTGTGGTTGGGTGGTGGTT	20	57.3	379.0	57.6		81	0.9943
20	qSsSESN1_R	ACAGTGCGATGATTGACTGGA	21	57.9	359.0				
35	qSs40SRPS5_F	AACTCCATGATGATGCACGG	20	57.3	333.0	57.9		105	0.9987
36	qSs40SRPS5_R	GGTCTTGATGTTCCTGAAAGCA	22	58.4	335.0		57.7		
Group 4									
1	qSs4EBP_F	GCCTCCTGTGGAGAGAACTG	20	61.4	318.0	60.4		110	0.9881

2	qSs4EBP_R	GCAACCATTGACGTTCTCCG	20	59.4	322.0				
3	qSs4EBP1A_F	CGACTCCTACAGTCAGACGC	20	61.4	327.0	60.4		102	0.9971
4	qSs4EBP1A_R	GGGTACGTGTGATCGGTGAA	20	59.4	292.0		60.5		
23	qSsBCAT1a_F	CTGGCCAAGAGGTTCCACAAA	21	59.8	303.0	60.6		98	0.9938
24	qSsBCAT1a_R	CCTATCAGAAGGAGTGCATTAAAGG	25	61.3	265.0				
25	qSsBCAT1b_F	GTAATGCTGTGAAACAGCCGC	21	59.8	292.0	60.8		90	0.9895
26	qSsBCAT1b_R	GCACGGACAACCCTATAGACG	21	61.8	368.0				
27	qSsBCKDHA_F	CGTTCACTACGGCAGCAAAG	20	59.4	342.0	60.4		102	0.9980
28	qSsBCKDHA_R	CGCCCTCTCCGAAGTAACAG	20	61.4	346.0				
31	qSs40SRPS11_HK_F	ATGAAGATGCAGAGGACCATCG	22	60.3	303.0	60.3		106	0.9934
32	qSs40SRPS11_HK_R	ACTTCTGGAACTGCTTCTTGGC	22	60.3	361.0				
Group 5									
7	qSsMYOSTAT1a_F	CACAACGCCTGTTGGACTTG	20	59.4	384.0	58.4			
8	qSsMYOSTAT1a_R	TGGACGGAGCGTGTAACATT	20	57.3	334.0		58.3	93	0.9983
33	qSs60SRPL13_HK_F	GCACCTGGTTCAACCAGC	18	58.2	341.0	58.2			
34	qSs60SRPL13_HK_R	CATACGCAGGCTGGCGAA	18	58.2	335.0				
Group 6									
37	qSs40SRPS7_F	CAGAAGCGTCCCAGGAGC	18	60.5	322.0	61.5	61.5	93	0.9996
38	qSs40SRPS7_R	CCTGTGAGCTTCTTGTAGACACC	23	62.4	320.0				

S 2.12 RNA quality control gel with both muscle and liver tissue



S 2.13 High-capacity cDNA Reverse Transcription mastermix for cDNA synthesis

	Quantity (µL)
MM for 1x RNA sample	
10X RT BUFFER	2
25X dNTP Mix (100mM)	0.8
10X RT Random primer	1.5
Oligo dT primer	0.5
Multiscribe reverse transcriptase	1
Nuclease free water	4.2
Total RNA	10
MM for 1x RT-	
10X RT BUFFER	2
25X dNTP Mix (100mM)	0.8
10X RT Random primer	1.5
Oligo dT primer	0.5
Nuclease free water	5.2
Total RNA	10
MM for 1x NTC	
10X RT BUFFER	2
25X dNTP Mix (100mM)	0.8
10X RT Random primer	1.5
Oligo dT primer	0.5
Multiscribe reverse transcriptase	1
Nuclease free water	4.2
Nuclease free water	10

NTC non-template control, RT- reverse transcription negative

S 2.14 cDNA synthesis Thermocycler program (T Advanced, Biometra GmbH).

Step	Temperature (°C)	Time	
1	75	Preheat	
2	75	5 min	
3	12	Pause	(Add mastermix to samples)
4	25	Preheat	
5	25	10 min	
6	37	2 hr	
7	85	5 min	
8	12	5 min	

S 2.15 Mastermix preparation / reaction for MyTaq (PCR) and Luminaris HiGreen (qPCR).

Mastermix	Quantity per reaction (µL)
MyTaq PCR	
2X MyTaq	2.5
Primer F	0.15
Primer R	0.15
Nuclease free water	1.2
cDNA	1
Luminaris HiGreen qPCR	
Syber green	5
Primer F	0.5
Primer R	0.5
Nuclease free water	3*
cDNA	1*

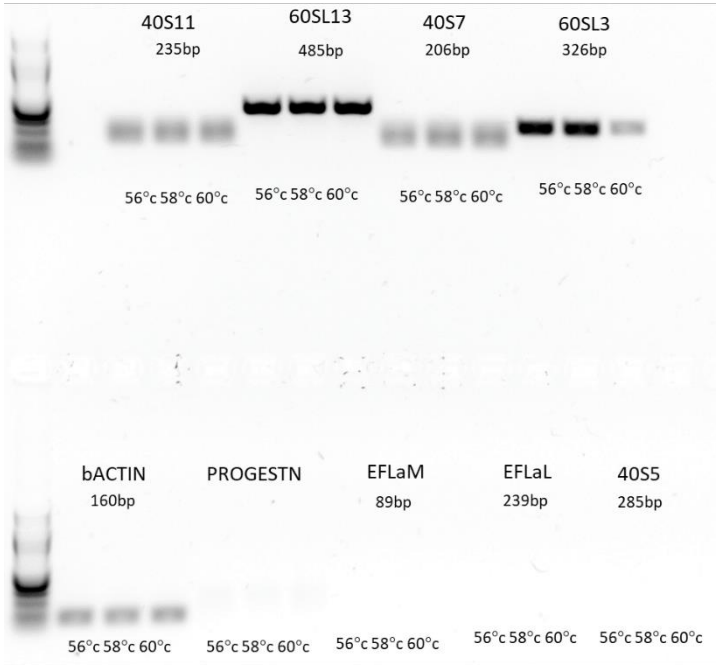
* For preparation of standards, 2.5 µL of pooled cDNA was used and 1.5 µL of Nuclease free water.

S 2.16 PCR conditions for primer efficiencies

Step	Temperature (°C)	Time	
1	95	1min	
2	95	15s	Step 2, 3, 4 x 30-34 cycles
3	**56-62**	15s	
4	72	2min	
5	20	30s	

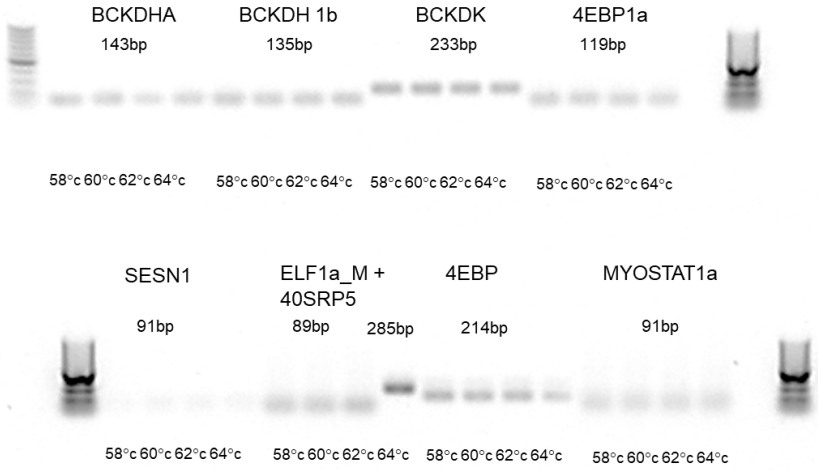
S 2.17 Primer optimisation

A



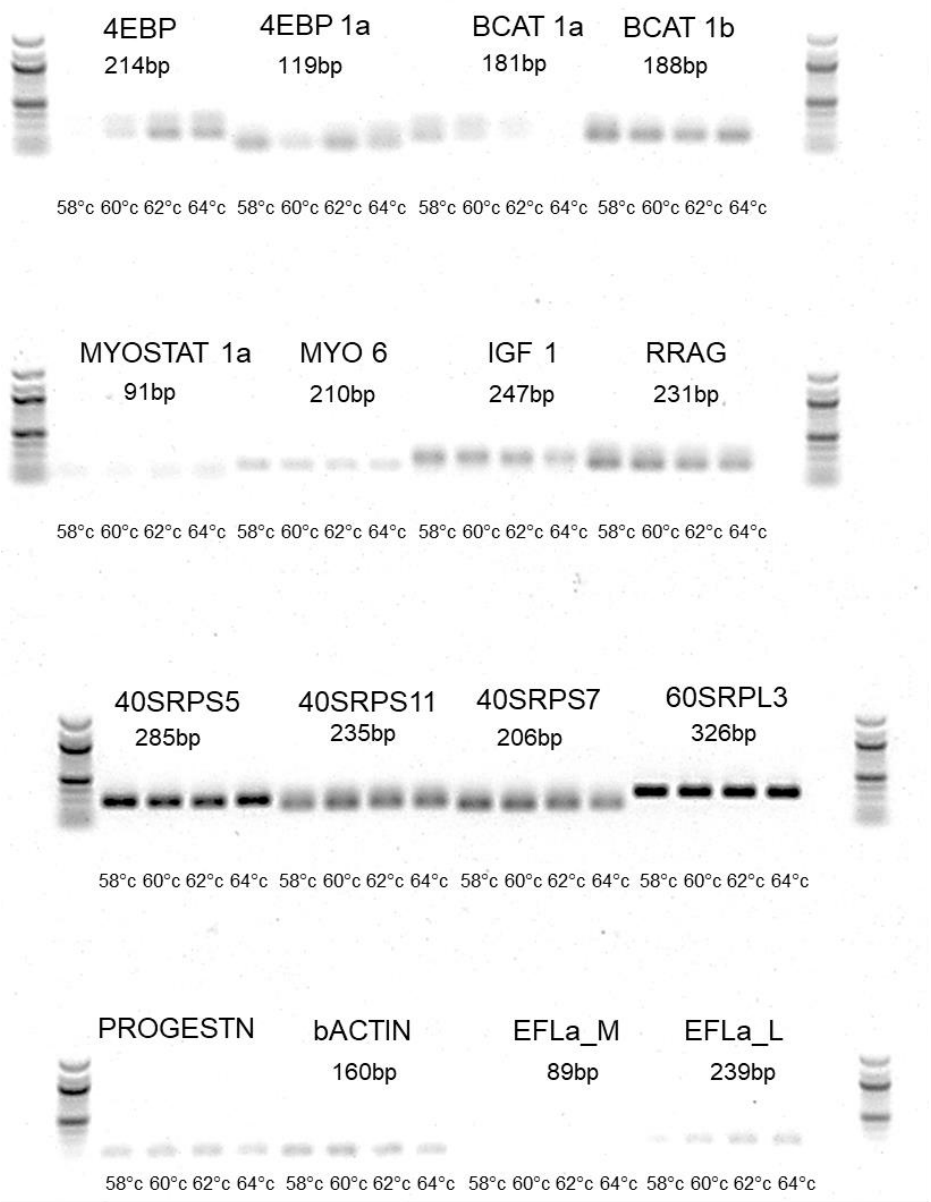
A) Housekeeping targets run at different temperatures using liver tissue.

B



B) Targets run at different temperatures using liver and muscle tissue.

Supplementary data



Targets run at different temperatures using liver and muscle tissue.

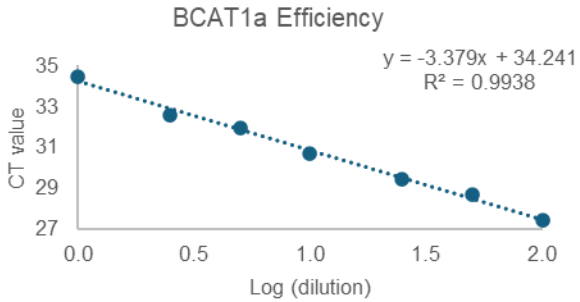
S 2.18 Serial dilutions of cDNA superpools (1:20) for 1 GOI loaded at 2.5 µL per well in duplicate.

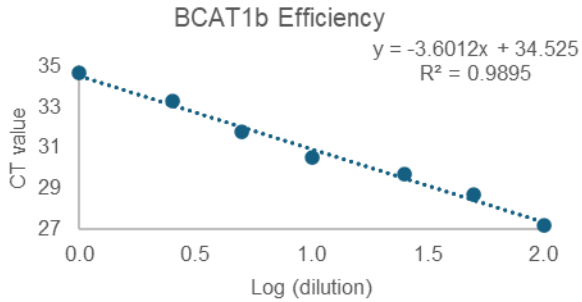
Dilution	cDNA (µL)	Water (µL)
1/5	2.4 (1:20)	9.6
1/10	6	6
1/20	6	6
1/50	4.8	7.2
1/100	6	6
1/200	6	6
1/500	4.8	7.2

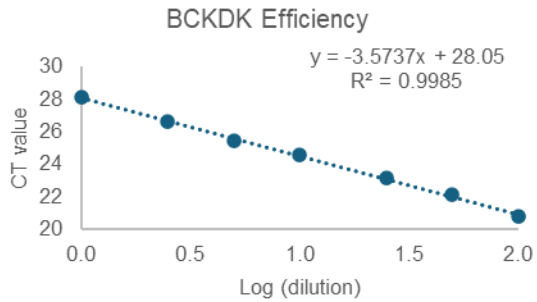
S 2.19 qPCR program (qTower3/G real-time PCR Thermal Cycler (Analytic Jena GmbH, Jena, Germany)

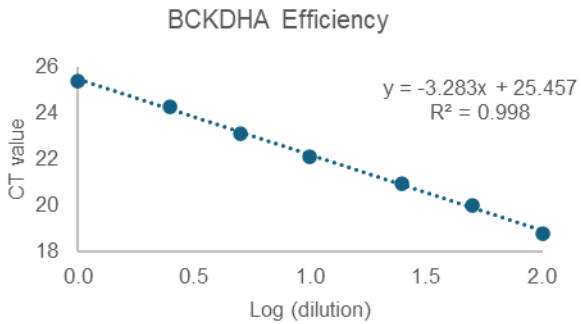
Step	Temperature (°C)	Time (m:s)	Go to	Loops
1	50	02:00	0	0
2	95	10:00	0	0
3	95	00:15	0	0
4	56-62	00:30	0	0
5	72	00:30	3	34
6	60	00:06	6	35

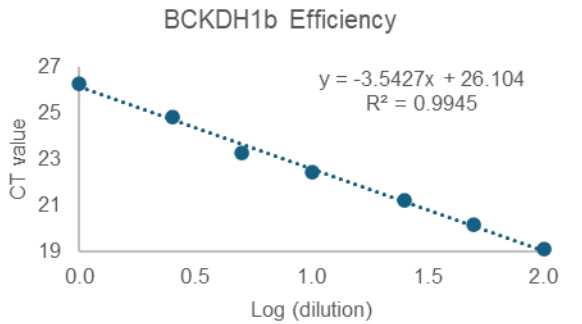
S 2.20 Primer efficiencies for BCAA catabolism



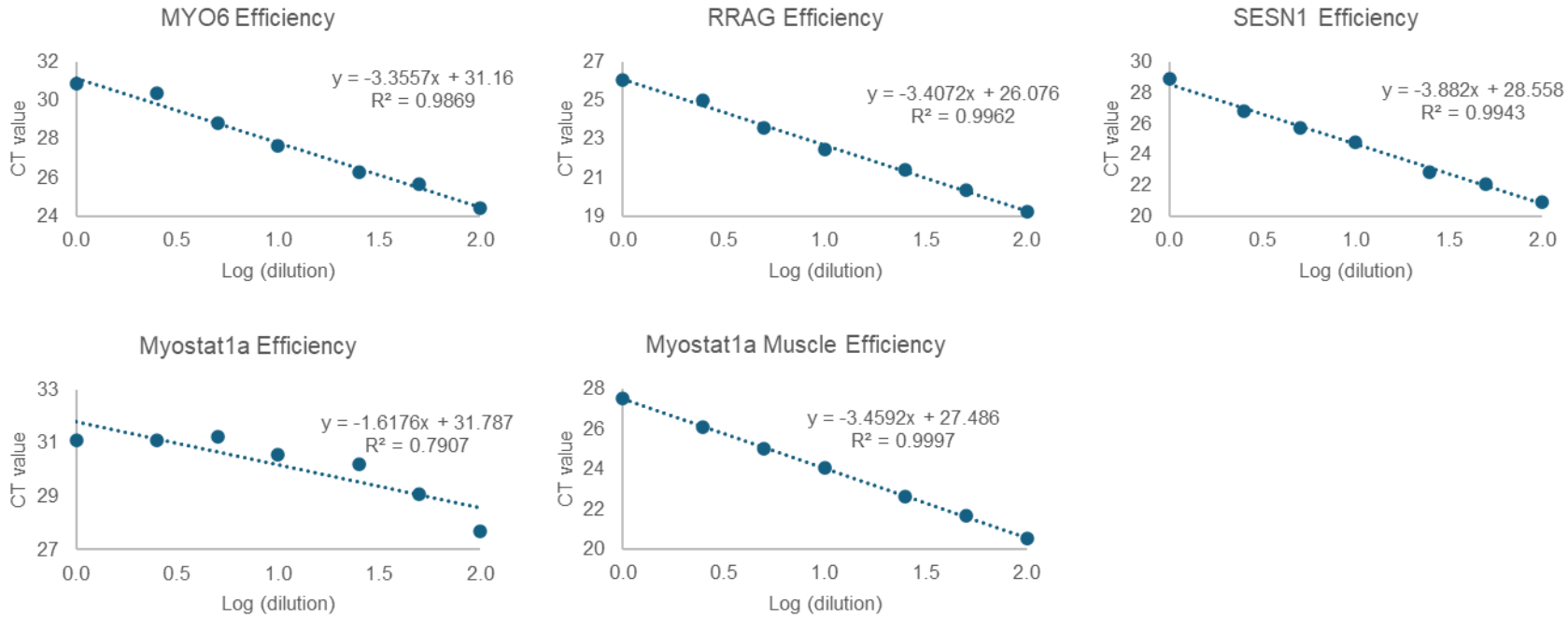




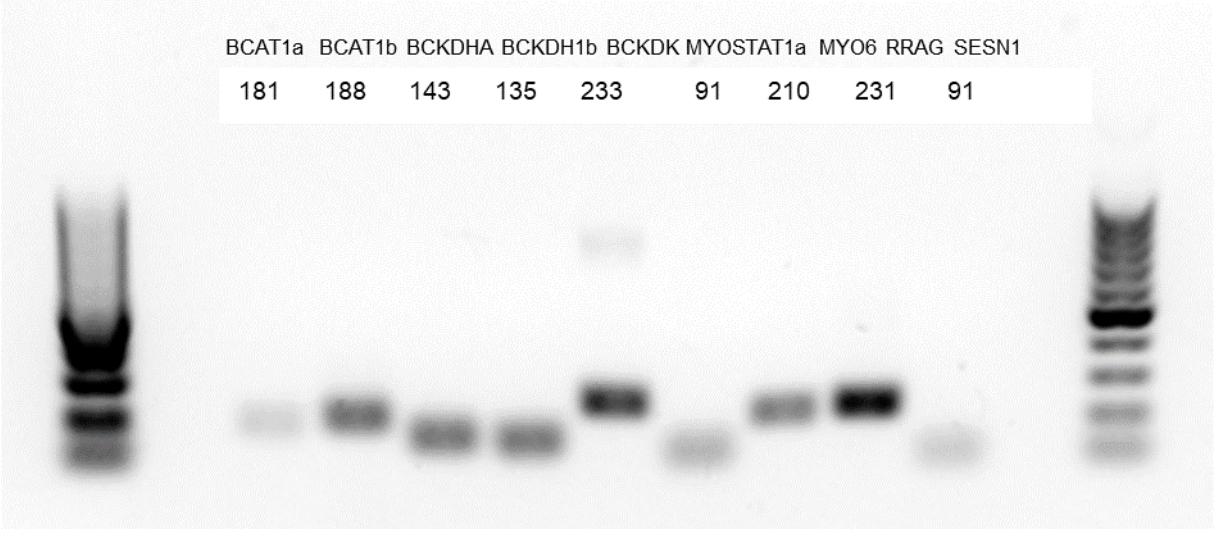




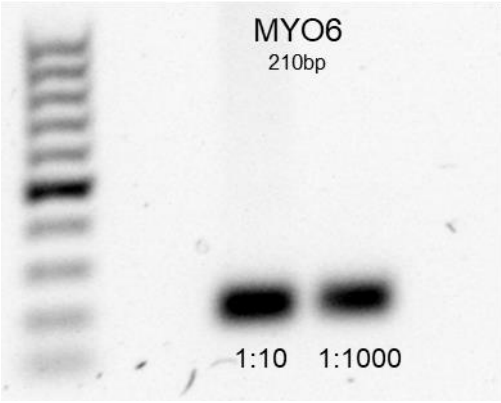
S 2.21 Primer efficiencies for mTOR pathway



S 2.22 PCR product gel preparation for cloning



S 2.23 MYO6 plasmid PCR dilutions



MYO6 plasmid PCR dilution gel run at 30 cycles at 62°c with a 100bp ladder.

S 2.24 Sequences: Myosin 6 (myo6) 210bp

>DZX235_27012353_27012353

GAGTCGCATGCTCCCGGCCGCATGGGCGGCCGCGGGAATTCGATTGTAC
GAGCTCAGCAAGTGGAAGTATGCCGAACTGAGGGATGCCATTAACACGTC
CTGTGACATTGAGTTGCTGGCTGCCTGCCGAGAGGAGTTCCACCGCCGG
CTGAAGGTCTATCACGCCTGGAAGTCAAAGAACAAGAAGCGTGGCAACGA
CACCGGCAATACTGAGCAGAGGGCCCCCAAATCAGTTACCGACTATGATC
TCGCACCAATCACTAGTGAATTCGCGGCCGCCTGCAGGTCGACCATATGG
GAGAGCTCCCAACGCGTTGGATGCATAGCTTGAGTATTCTATAGTGTCACC
TAAATAGCTTGGCGTAATCATGGTCATAGCTGTTTCCTGTGTGAAATTGTTA
TCCGCTCACAATTCCACACAACATACGAGCCGGAAGCATAAAGTGTAAAGC
CTGGGGTGCCTAATGAGTGAGCTAACTCACATTAATTGCGTTGCGCTCACT
GCCCGCTTTCCAGTCGGGAAACCTGTCGTGCCAGCTGCATTAATGAATCG
GCCAACGCGCGGGGAGAGGCGGTTTGCGTATTGGGCGCTCTTCCGCTTC
CTCGCTCACTGACTCGCTGCGCTCGGTCGTTCGGCTGCGGCGAGCGGTA
TCAGCTCACTCAAAGGCGGTAATACGGTTATCCACAGAATCAGGGGATAA
CGCAGGAAAGAACATGTGAGCAAAAGGCCAGCAAAAGGCCAGGAACCGT
AAAAAGGCCGCGTTGCTGGCGTTTTTCCATAGGCTCCGCCCCCCTGACGA
GCATCACAAAAATCGACGCTCAAGTCAGAGGTGGCGAAACCCGACAGGAC
TATAAAGATACCAGGCGTTTCCCCCTGGAAGCTCCCTCGTGCGCTCTCCT
GTTCCGACCCTGCCGCTTACCGGATACCTGTCCGCCTTTCTCCCTTCGGG
AAGCGTGGCGCTTTCTCATAGCTCACGCTGTAGGTATCTCAGTTCGGTGTA
GGTCGTTCGCTCCAAGCTGGGCTGTGTGCACGAACCCCCCGTTCAGCCC
GACCGCTGCGCCTTATCCGGTAACTATCGTCTTGAGTCCAACCCGGTAAG
ACACGACTTATCGCCACTGGCAGCAGCCACTGGTAACAGGATTAGCAGAA
CGAGGTATGTAGGCGGTGCTACAGAGT

F- GTACGAGCTCAGCAAGTGGA

R- ACCGACTATGATCTCGCACC

GTACGAGCTCAGCAAGTGGAAGTATGCCGAACTGAGGGATGCCATTAACA
CGTCCTGTGACATTGAGTTGCTGGCTGCCTGCCGAGAGGAGTTCCACCGC
CGGCTGAAGGTCTATCACGCCTGGAAGTCAAAGAACAAGAAGCGTGGCAA
CGACACCGGCAATACTGAGCAGAGGGCCCCCAAATCAGTTACCGACTATG
ATCTCGCACC

S 2.25 Sequences: RRAG A 231bp

>DZX236_27012360_27012360

AGTCCCTGCTCCGGCCGCCTGGGCGGCCGCGGGAATTCGATTAATGGGC
AAGAGTGGGTCTGGGAAGACGAGCATGAGATCGATCATCTTTGCCAATTA
CATAGCCCGAGACACACGGCGCCTTGGAGCCACGATTGATGTGGAGCACT
CCCATGTGCGATTCCTTGGCAATCTGGTTTTGAACTTGTGGGACTGTGGAG

GACAAGACACTTTCATGGAGAACTACTTCACCAGCCAGAGAGACAACATAT
TCCGGAATGTGGAGGTGCTGATATCCCCA

F- AATGGGCAAGAGTGGGTCTG

R- CGGAATGTGGAGGTGCTGAT

AATGGGCAAGAGTGGGTCTGGGAAGACGAGCATGAGATCGATCATCTTTG
CCAATTACATAGCCCGAGACACACGGCGCCTTGGAGCCACGATTGATGTG
GAGCACTCCCATGTGCGATTCCTTGGCAATCTGGTTTTGAACTTGTGGGAC
TGTGGAGGACAAGACACTTTCATGGAGAACTACTTCACCAGCCAGAGAGA
CAACATATTCCGGAATGTGGAGGTGCTGAT

S 2.26 Sequences: BCKDK 233bp

>DZX238_27012384_27012384

GAGTCGCATGCTCCGGCCGCCATGGGCGGCCGCGGGAATTCGATTCAGG
GCTAAGCAGCAAGTGATCTCAGACGCGGAAGCTCTCTCCCTTGCCGTCTA
TGTGGCGCAGGCGCAGGTAGACATCGGTGCCGATGCCCTGCATGGACTG
GATGGACAGGGAGCCACCCAGGTACTCGGCGTACGCCCGGGAGGTGGG
CAGCCCGAAGCCAAACCCGTGCATGGGGCCGGACTGAGGGCCGCTGTTG
GTCATGGTGTTGAAGAGGTTGTTCATGCGAGGGAATCACTAGTGAATTCG
CGGCCGCCTGCAGGTCGACCATATGGGAGAGCTCCCAACGCGTTGGATG
CATAGCTTGAGTATTCTATAGTGTCACCTAAATAGCTTGGCGTAATCATGGT
CATAGCTGTTTCCTGTGTGAAATTGTTATCCGCTCACAATTCCACACAACAT
ACGAGCCGGAAGCATAAAGTGTAAAGCCTGGGGTGCCTAATGAGTGAGCT
AACTCACATTAATTGCGTTGCGCTCACTGCCCGCTTTCCAGTCGGGAAACC
TGTCGTGCCAGCTGCATTAATGAATCGGCCAACGCGCGGGGAGAGGCGG
TTTGCGTATTGGGCGCTCTTCCGCTTCCTCGCTCACTGACTCGCTGCGCT
CGGTCGTTCGGCTGCGGCGAGCGGTATCAGCTCACTCAAAGGCGGTAATA
CGGTTATCCACAGAATCAGGGGATAACGCAGGAAAGAACATGTGAGCAAA
AGGCCAGCAAAAGGCCAGGAACCGTAAAAAGGCCGCGTTGCTGGCGTTTT
TCCATAGGCTCCGCCCCCCTGACGAGCATCACAAAAATCGACGCTCAAGT
CAGAGGTGGCGAAACCCGACAGGACTATAAAGATACCAGGCGTTTCCCCC
TGGAAGCTCCCTCGTGCGCTCTCCTGTTCCGACCCTGCCGCTTACCGGAT
ACCTGTCCGCCTTTCTCCCTTCGGGAAGCGTGGCGCTTTCTCATAGCTCA
CGCTGTAGGTATCTCAGTTCGGTGTAGGTCGTTCGCTCCAAGCTGGGCTG
TGTGCACGAACCCCCCGTTCAGCCCGACCGCTGCGCCTTATCCGGTAACT
ATCGTCTTGAGTCCAACCCGGTAAGACACGACTTATCGCCACTGGCAGCA
GCCACTGGTAACAGGATTAGCAGAACGAGGTATGTAGGCGGTGCTACAAA
AT

F- AGAGGTTGTTCATGCGAGGG

R- CAGGGCTAAGCAGCAAGTGA

CAGGGCTAAGCAGCAAGTGATCTCAGACGCGGAAGCTCTCTCCCTTGCCG
TCTATGTGGCGCAGGCGCAGGTAGACATCGGTGCCGATGCCCTGCATGG
ACTGGATGGACAGGGAGCCACCCAGGTACTCGGCGTACGCCCGGGAGGT
GGGCAGCCCGAAGCCAAACCCGTGCATGGGGCCGGACTGAGGGCCGCT
GTTGGTCATGGTGTTGAAGAGGTTGTTCATGCGAGGG

S 2.27 Sequences: BCKDHA E1 143bp

>DZX239_27012391_27012391

ACTCGCATGCTCCGGCCGCCATGGGCGGCCGCGGGAATTCGATTCGTTC
ACTACGGCAGCAAAGACCTCAACTTCGTCACCATCTCCTCTCCTCTGGCCA
CTCAGATCCCACAAGCTGCAGGGGCAGCGTACGCAGCCAAGAGAGAGAA
CACCAACCGTGCTGTGATCTGTTACTTCGGAGAGGGCGAATCACTAGTGA
ATTCGCGGCCGCCTGCAGGTCGACCATATGGGAGAGCTCCCAACGCGTT
GGATGCATAGCTTGAGTATTCTATAGTGTCACCTAAATAGCTTGGCGTAAT
CATGGTCATAGCTGTTTCCTGTGTGAAATTGTTATCCGCTCACAATTCCACA
CAACATACGAGCCGGAAGCATAAAGTGTAAAGCCTGGGGTGCCTAATGAG
TGAGCTAACTCACATTAATTGCGTTGCGCTCACTGCCCGCTTTCCAGTCGG
GAAACCTGTCGTGCCAGCTGCATTAATGAATCGGCCAACGCGCGGGGAGA
GGCGGTTTGCGTATTGGGCGCTCTTCCGCTTCCTCGCTCACTGACTCGCT
GCGCTCGGTCGTTCGGCTGCGGCGAGCGGTATCAGCTCACTCAAAGGCG
GTAATACGGTTATCCACAGAATCAGGGGATAACGCAGGAAAGAACATGTG
AGCAAAAGGCCAGCAAAAGGCCAGGAACCGTAAAAAGGCCGCGTTGCTG
GCGTTTTTCCATAGGCTCCGCCCCCCTGACGAGCATCACAAAAATCGACG
CTCAAGTCAGAGGTGGCGAAACCCGACAGGACTATAAAGATACCAGGCGT
TTCCCCCTGGAAGCTCCCTCGTGCGCTCTCCTGTTCCGACCCTGCCGCTT
ACCGGATACCTGTCCGCCTTTCTCCCTTCGGGAAGCGTGGCGCTTTCTCA
TAGCTCACGCTGTAGGTATCTCAGTTCGGTGTAGGTCGTTCGCTCCAAGCT
GGGCTGTGTGCACGAACCCCCCGTTCAGCCCGACCGCTGCGCCTTATCC
GGTAACTATCGTCTTGAGTCCAACCCGGTAAGACACGACTTATCGCCACTG
GCAGCAGCCACTGGTAACAGGATTAGCAGAGCGAGGTATGTAGGCGGTG
CTACAGAGTTCTTGAAGTGGTGGCCTAACTACGGCTACACTAGAAGAACA
GTATTTGGTATCTGCGCTCTGCTGAAGCCAGTTACCTTCGGAAAAAGAAT

TGGTA

F- CGTTCACTACGGCAGCAAAG

F- CTGTTACTTCGGAGAGGGCG

CGTTCACTACGGCAGCAAAGACCTCAACTTCGTCACCATCTCCTCTCCTCT
GGCCACTCAGATCCCACAAGCTGCAGGGGCAGCGTACGCAGCCAAGAGA
GAGAACACCAACCGTGCTGTGATCTGTTACTTCGGAGAGGGCG

S 2.28 Sequences: Sestrin 1 91bp

>DZX240_27012407_27012407

ATGGGCGGCCGCGGGTAATTCGATTAGTGCGAGTGATTGACTGGATCAAC
CTAACTCTATAATGTGTAGCAGGTTTGATTGCCCAAACACCACCCAACCAC
CACCCAACCACAAAAATCACTAGTGAATTCGCGGCCGCCTGCAGGTCGAC
CATATGGGAGAGCTCCCAACGCGTTGGATGCATAGCTTGAGTATTCTATAG
TGTCACCTAAATAGCTTGGCGTAATCATGGTCATAGCTGTTTCCTGTGTGA
AATTGTTATCCGCTCACAATTCCACACAACATACGAGCCGGAAGCATAAAG
TGTAAAGCCTGGGGTGCCTAATGAGTGAGCTAACTCACATTAATTGCGTTG
CGCTCACTGCCCGCTTTCCAGTCGGGAAACCTGTCGTGCCAGCTGCATTA
ATGAATCGGCCAACGCGCGGGGAGAGGCGGTTTGCGTATTGGGCGCTCT
TCCGCTTCCTCGCTCACTGACTCGCTGCGCTCGGTCGTTCGGCTGCGGCG
AGCGGTATCAGCTCACTCAAAGGCGGTAATACGGTTATCCACAGAATCAG
GGGATAACGCAGGAAAGAACATGTGAGCAAAAGGCCAGCAAAAGGCCAG
GAACCGTAAAAAGGCCGCGTTGCTGGCGTTTTTCCATAGGCTCCGCCCCC
CTGACGAGCATCACAAAAATCGACGCTCAAGTCAGAGGTGGCGAAACCCG
ACAGGACTATAAAGATACCAGGCGTTTCCCCCTGGAAGCTCCCTCGTGCG
CTCTCCTGTTCCGACCCTGCCGCTTACCGGATACCTGTCCGCCTTTCTCCC
TTCGGGAAGCGTGGCGCTTTCTCATAGCTCACGCTGTAGGTATCTCAGTTC
GGTGTAGGTCGTTCGCTCCAAGCTGGGCTGTGTGCACGAACCCCCCGTTC
AGCCCGACCGCTGCGCCTTATCCGGTAACTATCGTCTTGAGTCCAACCCG
GTAAGACACGACTTATCGCCACTGGCAGCAGCCACTGGTAACATGATT

F- AACCACCACCCAACCACAAA

R- ACAGTGCGATGATTGACTGGA

TAGTGCGAGTGATTGACTGGATCAACCTAACTCTATAATGTGTAGCAGGTT
TGATTGCCCAAACACCACCCAACCACCACCCAACCACAAA

S 2.29 Sequences: BCAT, cytosolic-like bp 181

>DZX242_27012421_27012421

AGTCGCATGCTCCGGCCGCCATGGGCGGCCGCGGGAATTCGATTTCAGAA
GGAGTGCATTAAAGGTTGTACTGAAGCTGCTGGTCTTGAAGATGGAGCGGG
GGACTGGTCGCGATATGATTGGCATGTGCAAACTGCCAATTAAACGACCAG
TGGTGCCCATTCACTCTGTTTCCGGCCATACTGCATGTCTGTCAGCTCTTTG
TGGAACCTCTTGGCCAGAATCACTAGTGAATTCGCGGCCGCCTGCAGGTCG
ACCATATGGGAGAGCTCCCAACGCGTTGGATGCATAGCTTGAGTATTCTATA
GTGTCACCTAAATAGCTTGGCGTAATCATGGTCATAGCTGTTTCCTGTGTGA
AATTGTTATCCGCTCACAATTCCACACAACATACGAGCCGGAAGCATAAAGT
GTAAAGCCTGGGGTGCCTAATGAGTGAGCTAACTCACATTAATTGCGTTGC
GCTCACTGCCCGCTTTCCAGTCGGGAAACCTGTCGTGCCAGCTGCATTAAT
GAATCGGCCAACGCGCGGGGAGAGGCGGTTTGCGTATTGGGCGCTCTTCC
GCTTCCTCGCTCACTGACTCGCTGCGCTCGGTCGTTCGGCTGCGGCGAGC
GGTATCAGCTCACTCAAAGGCGGTAATACGGTTATCCACAGAATCAGGGGA
TAACGCAGGAAAGAACATGTGAGCAGAAGGCCAGCAGAAGGCCAGGAACC
GTAGAAAGGCCGCGTTGCTGGCGTTTTTCCATAGGCTCCGCCGCCCTGACG
AGCATCACAAAAATCGACGCTCAAGTCAGAGGTGGCGAAACCCGACAGGAC
TATAAAGATACCAGGCGTTTCCTCCTGGAAGCTCCCTCGTGCGCTCTCCTGT
TCCGACGCTGCCGCTTACCGGATACCTGTCCGCCTTTCTCCCTTCGGGAAG
CGTGGCGCTGTCTCATAGCTCACGCTGTAGGTATCTCAGTTCGGTGTAGGT
CGTTCGCTCCAAGCTGGGCTGTGTGCACGAACCCCCCGTTCAGCCCGACC
GCTGCGCCTTATCAGGTAACTATCGTCTTGAGTCCAACCCGGTAAGACACG
ACTTATCGCCACTGGCAGCAGCCACTGGTAACAGGATTATCAGAAC

F-TTTGTGGAACCTCTTGGCCAG

R-CCTATCAGAAGGAGTGCATTAAAGG

bp181

GATTTCAGAAGGAGTGCATTAAAGGTTGTACTGAAGCTGCTGGTCTTGAAGA
TGGAGCGGGGGACTGGTCGCGATATGATTGGCATGTGCAAACTGCCAATTA
AACGACCAGTGGTGCCCATTCACTCTGTTTCCGGCCATACTGCATGTCTGTC
AGCTCTTTGTGGAACCTCTTGGCCAG

S 2.30 Sequences: BCAT 1b

>DZX243_27012438_27012438

TTCGCATGCTCCGGGCCGCCATGGCGGCCGCGGGAATTCGATTGCACGGA
CAACCCTATAGACGATCTCATTTAGTGTTTATTAAAAAGCTTGGAGGACGAC
TTCTTCTGTAACCTGTGCTACAGTATGATAAAGGACTGAATAGGAAAAAGAC
TGACTTTGTTCCTAATACAGAAATACAGACTAGAGTAGGTTGGTTGAACCGA
AGCTGCGGCTGTTTCACAGCATTACAATCACTAGTGAATTCGCGGCCGCCT

GCAGGTCGACCATATGGGAGAGCTCCCAACGCGTTGGATGCATAGCTTGAG
TATTCTATAGTGTCACCTAAATAGCTTGGCGTAATCATGGTCATAGCTGTTTC
CTGTGTGAAATTGTTATCCGCTCACAATTCCACACAACATACGAGCCGGAAG
CATAAAGTGTAAAGCCTGGGGTGCCTAATGAGTGAGCTAACTCACATTAATT
GCGTTGCGCTCACTGCCCGCTTTCCAGTCGGGAAACCTGTCGTGCCAGCTG
CATTAATGAATCGGCCAACGCGCGGGGAGAGGCGGTTTGCGTATTGGGCG
CTCTTCCGCTTCCTCGCTCACTGACTCGCTGCGCTCGGTCGTTCGGCTGCG
GCGAGCGGTATCAGCTCACTCAAAGGCGGTAATACGGTTATCCACAGAATC
AGGGGATAACGCAGGAAAGAACATGTGAGCAAAAGGCCAGCAAAAGGCCA
GGAACCGTAAAAAGGCCGCGTTGCTGGCGTTTTTCCATAGGCTCCGCCCCC
CTGACGAGCATCACAAAAATCGACGCTCAAGTCAGAGGTGGCGAAACCCGA
CAGGACTATAAAGATACCAGGCGTTTCCCCCTGGAAGCTCCCTCGTGCGCT
CTCCTGTTCCGACCCTGCCGCTTACCGGATACCTGTCCGCCTTTCTCCCTTC
GGGAAGCGTGGCGCTTTCTCATAGCTCACGCTGTAGGTATCTCAGTTCGGT
GTAGGTCGTTCGCTCCAAGCTGGGCTGTGTGCACGAACCCCCCGTTCAGC
CCGACCGCTGCGCCTTATCCGGTAACTATCGTCTTGAGTCCAACCCGGTAA
GACACGACTTATCGCCACTGGCAGCAGCCACTGGTAACAGGATTAGCAGAG
CGAGGTATGTAGGCGGTGCTACAGAGTTCTTGAAGTGGTGGCCTAACTACG
GCTACACTAGA

F- GCACGGACAACCCTATAGACG

R- GCGGCTGTTTCACAGCATTAC

Bp 188

GCACGGACAACCCTATAGACGATCTCATTTAGTGTTTATTAAAAAGCTTGGA
GGACGACTTCTTCTGTAACCTGTGCTACAGTATGATAAAGGACTGAATAGGA
AAAAGACTGACTTTGTTCCTAATACAGAAATACAGACTAGAGTAGGTTGGTT
GAACCGAAGCTGCGGCTGTTTCACAGCATTAC

S 2.31 Sequences: Myostat 1a

>DZX241_27012414_27012414

CCCTGGGGCGAGTTCGCATGCTCCGGGCCGCCATGGGCGGCCGCGGGAA
TTCGATTTGCGACGGAGTCGTTGTAACATGTAAGTGTTTTGAGGAAAAAAGT
GGCGTACTTATATTGTCTACTCACAGATCCACTCACCAAGTTCCAACAGGCC
GTTCGTGAATCACTAGTGAATTCGCGGCCGCCTGCAGGTCGACCATATGGG
AGAGCTCCCAACGCGTTGGATGCATAGCTTGAGTATTCTATAGTGTCACCTA
AATAGCTTGGCGTAATCATGGTCATAGCTGTTTCCTGTGTGAAATTGTTATC
CGCTCACAATTCCACACAACATACGAGCCGGAAGCATAAAGTGTAAAGCCT
GGGGTGCCTAATGAGTGAGCTAACTCACATTAATTGCGTTGCGCTCACTGC
CCGCTTTCCAGTCGGGAAACCTGTCGTGCCAGCTGCATTAATGAATCGGCC
AACGCGCGGGGAGAGGCGGTTTGCGTATTGGGCGCTCTTCCGCTTCCTCG
CTCACTGACTCGCTGCGCTCGGTCGTTCGGCTGCGGCGAGCGGTATCAGC
TCACTCAAAGGCGGTAATACGGTTATCCACAGAATCAGGGGATAACGCAGG
AAAGAACATGTGAGCAAAAGGCCAGCAAAAGGCCAGGAACCGTAAAAAGGC

CGCGTTGCTGGCGTTTTTCCATAGGCTCCGCCCCCCTGACGAGCATCACAA
AAATCGACGCTCAAGTCAGAGGTGGCGAAACCCGACAGGACTATAAAGATA
CCAGGCGTTTCCCCCTGGAAGCTCCCTCGTGCGCTCTCCTGTTCCGACCCT
GCCGCTTACCGGATACCTGTCCGCCTTTCTCCCTTCGGGAAGCGTGGCGCT
TTCTCATAGCTCACGCTGTAGGTATCTCAGTTCGGTGTAGGTCGTTCGCTCC
AAGCTGGGCTGTGTGCACGAACCCCCCGTTCAGCCCGACCGCTGCGCCTT
ATCCGGTAACTATCGTCTTGAGTCCAACCCGGTAAGACACGACTTATCGCCA
CTGGCAGCAGCCACTGGTAACAGGATTAGCAGAGCGAGGTATGTAGGCGG
TGCTACAGAGTTCTTGAAGTGGTGGCCTAACTACGGCTACACTAGAAGAAC
AGTATTTGGTATCTGCGCTCTGCTGAAGCCAGTTACCTTCGGAAAAAGAGTT
GGTAACTCTTGATCCGGCAAACAAACCACCGCTGGGAACGGTGGGTTTTTT
TGTTTTGCAAGCACCAGATTACGCCCAAAAAAAAAGGTTTCCAGAAAAATCT
TTGTTTTTTTTTTACGGGGGCGGAAACCCCCGGGGAAGAAAAACCCCCTTTA
GGGGTTTTTGGCGGGAAATTTAAAAAAGAGTTTTTCCCAAACCTCTTTTTATA
AAAAAAAGATTTTATAAAAACCCCAAAAAAAAAAAAAAAAAAACATAGGGGCG
GC

F- CACAACGCCTGTTGGACTTG

R- TGGACGGAGCGTGTAACATT

Vector F- GGAATTCGAT

vector R- ATCACTAGTG

99bp

TTGCGACGGAGTCGTGGAACTTTTAAGTGTTTTGTGGGAAAATGTGGCGTA

CTTTAGGCTACTCACGATCCACTCACCTAGTTCCAACAGGCGTTGTGA

S 2.32 bAAs Muscle 4hr post feeding (umol/ g)

	CD	LD	ID	VD	P-value (4hr)
Sum of AA					
Alanine	124.75±7.04	117.66±3.19	120.40±1.43	122.98±4.11	0.297 (f 3, 8= 1.46)
Arginine	65.74±3.78	62.26±2.17	63.92±0.69	64.30±3.03	0.503 (f 3, 8= 0.85)
Asparagine	140.85±7.68	129.09±5.22	133.41±3.10	136.82±5.47	0.145 (f 3, 8= 2.39)
Cysteine					
Glutamate	182.21±8.91	169.21±5.23	173.74±3.30	176.81±7.33	0.180 (f 3, 8= 2.09)
Glycine	112.74±0.69	111.39±5.14	113.16±2.74	113.15±2.85	0.922 (f 3, 6= 0.16)
Histidine	26.17±0.66	25.66±1.20	26.38±1.23	25.16±1.10	0.238 (f 3, 8= 1.73)
Isoleucine	73.22±6.88	66.61±2.94	69.16±1.76	70.52±7.25	0.520 (f 3, 8= 0.82)
Leucine	116.61±5.17	110.03±2.78	113.32±0.17	114.50±4.41	0.247 (f 3, 8= 1.68)
Lysine	121.49±6.23	112.26±2.88	115.86±1.80	118.37±7.33	0.232 (f 3, 8= 1.76)
Methionine	44.63±1.58	43.28±1.66	44.12±1.84	46.40±2.28	0.285 (f 3, 8= 1.51)
Phenylalanine	49.11±2.22	45.93±1.26	47.46±0.15	48.22±1.91	0.174 (f 3, 8= 2.13)
Proline	58.75±4.21	55.04±2.87	56.72±1.10	57.66±3.10	0.526 (f 3, 8= 0.80)
Serine	65.35±10.16	67.15±1.89	62.35±14.08	69.65±3.49	0.559 (f 3, 8= 0.66)
Taurine ****					
Threonine	67.19±5.74	68.91±1.31	71.06±1.43	70.63±3.29	0.532 (f 3, 8= 0.79)
Tyrosine	42.03±1.11	40.48±0.58	41.52±1.43	42.87±2.33	0.330 (f 3, 8= 1.33)
Valine	94.91±7.46	87.07±4.37	89.81±2.45	92.38±6.55	0.403 (f 3, 8= 1.10)

S 2.33 bAAs Liver 4hr post feeding (umol/ g)

	CD	LD	ID	VD	P-value (4hr)
Sum of AA					
Alanine	87.56±9.16	87.32±7.64	85.56±2.29	81.35±4.41	0.637 (f 3, 8= 0.59)
Arginine	53.26±5.13	52.48±4.41	51.89±1.27	49.64±2.86	0.677 (f 3, 8= 0.53)
Asparagine	100.39±9.07	99.47±10.68	96.76±2.73	92.88±4.98	0.634 (f 3, 8= 0.60)
Cysteine	4.43±***	7.68±1.57	7.08±0.97	4.36±2.18	0.194 (f 3, 5= 2.30)
Glutamate	135.54±10.85	132.95±11.80	132.48±3.36	124.47±6.71	0.492 (f 3, 8= 0.88)
Glycine	107.22±4.29	99.12±7.60	100.50±3.20	96.54±7.23	0.352 (f 3, 7= 1.28)
Histidine	20.30±0.91 [a]	16.66±0.72 [b]	16.65±1.52 [b]	16.53±1.85 [b]	**0.035 (f 3, 7= 5.11)**
Isoleucine	58.24±5.07	48.16±5.32	51.90±2.73	49.40±4.86	0.106 (f 3, 8= 2.84)
Leucine	93.60±8.53	91.74±7.85	91.56±2.76	87.22±5.13	0.680 (f 3, 8= 0.52)
Lysine	74.60±7.02	71.90±7.20	71.75±1.72	67.15±3.56	0.448 (f 3, 8= 0.98)
Methionine	27.92±2.52	29.43±3.42	29.58±2.80	26.73±1.62	0.542 (f 3, 8= 0.77)
Phenylalanine	44.08±4.06	42.45±3.97	42.86±1.06	40.71±2.42	0.635 (f 3, 8= 0.60)
Proline	55.09±4.93	53.65±5.35	53.24±1.27	49.92±2.80	0.474 (f 3, 8= 0.92)
Serine	38.79±5.04 [b]	62.79±6.81 [a]	57.43±5.48 [a]	54.08±4.99 [a]	**0.004 (f 3, 8= 10.05)**
Taurine	20.01±2.47	21.98±3.85	22.32±1.73	20.12±2.60	0.762 (f 3, 8= 0.39)
Threonine	44.69±3.61	55.08±5.79	52.66±3.09	50.29±2.82	0.061 (f 3, 8= 3.71)
Tyrosine	32.41±2.87	33.35±3.99	32.80±1.95	30.25±1.22	0.551 (f 3, 8= 0.75)
Valine	83.10±7.89	72.74±8.19	76.35±2.10	72.46±5.39	0.224 (f 3, 8= 1.81)

S 2.34 Total bAAs liver and muscle tissue LD g/100g

	0hrs	2hrs	4hrs	8hrs	24hrs	P-value
Liver						
Sum of AA	12.16±0.92	13.23±1.20	13.45±1.23	13.67±0.22	13.48±0.74	0.352 (f 4, 10= 1.25)
Tot. EAAs	6.11±0.37	6.68±0.60	6.67±0.63	6.86±0.12	6.95±0.14	0.220 (f 4, 10= 1.73)
EAAs ex. BCAAs	3.53±0.27	3.89±0.41	3.98±0.38	4.07±0.05	4.19±0.10	0.124 (f 4, 10= 2.35)
BCAAs	2.58±0.16	2.79±0.21	2.69±0.29	2.80±0.07	2.76±0.16	0.573 (f 4, 10= 0.76)
NEAAs	6.05±0.57	6.55±0.60	6.78±0.63	6.81±0.11	6.53±0.65	0.491 (f 4, 10= 0.92)
Muscle						
Sum of AA	16.90±0.42 [b]	17.49±0.24 [a]	16.92±0.37 [b]	17.60±0.13 [a]	17.20±0.19 [ab]	**0.045 (f 4, 10= 3.61)**
Tot. EAAs	8.60±0.33	9.01±0.22	8.69±0.23	9.08 ±0.14	8.85±0.27	0.154 (f 4, 10= 2.11)
EAAs ex. BCAAs	5.18±0.27	5.54±0.03	5.35±0.11	5.56±0.04	5.38±0.17	0.069 (f 4, 10= 3.07)
BCAAs	3.42±0.06	3.48±0.20	3.34±0.13	3.52±0.11	3.47±0.18	0.579 (f 4, 10= 0.75)
NEAAs	8.31±0.40	8.48±0.14	8.24±0.14	8.52±0.06	8.35±0.09	0.456 (f 4, 10= 0.99)

S 2.35 fAAs Muscle LD diet all timepoints umol/g

	0 hr	2 hr	4 hr	8 hr	24 hr	P-value
Sum of AA						
Alanine	3.01±0.25	3.18±0.39	3.43±0.70	3.26±0.33	3.17±0.37	0.828 (f 4, 10= 0.37)
b-Ala						
Arginine	0.32±0.35	0.56±0.37	0.59±0.74	0.54±0.70	0.40±0.53	0.970 (f 4, 10= 0.13)
Asparagine	0.04±0.02 [ab]	0.05±0.01 [a]	0.02±0.00 [c]	0.02±0.01 [bc]	0.02±0.01 [c]	0.009 (f 4, 10= 6.23)
Cysteine	0.02±0.01 [b]	0.04±0.01 [ab]	0.05±0.00 [a]	0.05±0.01 [a]	0.05±0.02 [a]	0.028 (f 4, 9= 4.54)
Glutamate	0.64±0.16 [ab]	0.70±0.10 [a]	0.40±0.04 [c]	0.47±0.12 [bc]	0.29±0.14 [c]	**0.011 (f 4, 10= 5.87)**
Glycine	2.15±0.59	2.18±0.52	2.45±0.75	2.49±0.89	2.46±0.72	0.951 (f 4, 10= 0.16)
Histidine	0.15±0.05	0.12±0.03	0.11±0.07	0.14±0.06	0.11±0.06	0.859 (f 4, 10= 0.32)
Isoleucine	0.18±0.02 [a]	0.16±0.01 [a]	0.18±0.02 [a]	0.17±0.01 [a]	0.13±0.02 [b]	**0.026 (f 4, 9= 4.67)**
Leucine	0.62±0.05 [a]	0.66±0.05 [a]	0.62±0.18 [a]	0.62±0.03 [a]	0.34±0.03 [b]	**0.008 (f 4, 10= 6.42)**
Lysine	0.08±0.02 [ab]	0.09±0.01 [a]	0.04±0.01 [c]	0.06±0.01 [bc]	0.06±0.02 [bc]	**0.033 (f 4, 10= 4.05)**
Methionine	0.12±0.02	0.12±0.01	0.11±0.02	0.12±0.02	0.09±0.01	0.145 (f 4, 10= 2.18)
Phenylalanine	0.19±0.04	0.18±0.02	0.20±0.07	0.19±0.02	0.13±0.01	0.265 (f 4, 10= 1.54)
Proline	1.40±0.44	1.38±0.42	1.67±0.10	1.57±0.33	0.91±0.47	0.202 (f 4, 10= 1.82)
Serine	0.09±0.04	0.13±0.05	0.13±0.06	0.18±0.12	0.09±0.09	0.603 (f 4, 10= 0.71)
Taurine	1.34±0.85	1.15±0.72	0.94±0.70	0.80±0.63	0.94±0.89	0.912 (f 4, 10= 0.23)
Threonine	0.67±0.15	0.55±0.09	0.59±0.11	0.60±0.07	0.46±0.10	0.269 (f 4, 10= 1.52)
Tyrosine	0.27±0.02	0.27±0.02	0.27±0.05	0.30±0.02	0.23±0.03	0.136 (f 4, 10= 2.25)
Tryptophan						
Valine	0.36±0.02	0.39±0.10	0.37±0.04	0.31±0.02	0.27±0.04	0.134 (f 4, 9= 2.33)

S 3 Chapter 3

S 3.1 Water quality parameters from the Recirculating aquaculture system (Biofilter, system water) at the Niall Brommage Freshwater Research Unit over the nutritional trial period.

Date	Temp	pH	O_2 Sat.	N (TAN)	NH_3	NH_4	Alk.	Nitrite (NO_2)	Nitrate (NO_3)	Cl.	Co_2
	°C		%	mg/l	mg/l	mg/l	mg/l	mg/l N	mg/l N	mg/l Cl	mg/l
05/11/19	14.1	7.5	120	0.0	0.1	0.1	190	0.3	4.4	175	4.0
06/11/19	14.2	7.3	107	0.1	0.1	0.1	125	0.3	7.0	160	4.4
07/11/19	14.1	7.1	121	0.2	0.3	0.3	160	0.2	6.4	155	4.7
08/11/19	14.2	7.1	120	0.3	0.3	0.4	195	0.3	8.3	160	5.3
09/11/19	14.1	7.3	118	0.2	0.3	0.3	180	0.4	4.5	145	4.7
10/11/19	14.1	7.3	120	0.2	0.3	0.3	120	0.4	8.3	160	4.6
11/11/19	14.1	7.3	119	0.1	0.1	0.1	135	0.3	5.7	155	4.4
12/11/19	14.1	7.3	120	0.1	0.1	0.1	135	0.3	5.8	160	4.8
13/11/19	14.1	7.3	120	0.2	0.2	0.2	130	0.4	7.8	170	5.0
14/11/19	13.9	7.2	107	0.2	0.2	0.2	30	0.5	8.1	220	5.0
15/11/19	13.0	7.2	109	0.3	0.3	0.4	160	0.5	6.7	160	5.6
16/11/19	13.1	7.2	110	0.2	0.2	0.2	165	0.5	5.8	160	4.9
17/11/19	13.1	7.2	108	0.1	0.1	0.1	160	0.4	6.1	160	5.1
18/11/19	13.1	7.1	110	0.2	0.2	0.2	170	0.4	5.1	190	5.3
19/11/19	13.1	7.1	110	0.2	0.2	0.2	180	0.5	6.4	130	5.5
20/11/19	13.1	7.4	110	0.2	0.2	0.2	135	0.3	7.2	150	5.3
21/11/19	13.1	7.3	105	0.3	0.3	0.3	155	0.4	6.1	185	5.7
22/11/19	13.1	7.2	118	0.1	0.2	0.2	135	0.4	8.3	140	4.8
23/11/19	12.8	7.4	110	0.2	0.2	0.2	250	0.4	6.8	145	5.0
24/11/19	12.8	7.2	112	0.3	0.3	0.3	175	0.2	7.3	175	5.5
25/11/19	12.8	6.8	110	0.6	0.8	0.8	300	0.4	6.8	175	5.5
26/11/19	12.8	7.2	113	0.3	0.4	0.4	130	0.4	8.7	130	5.5
27/11/19	12.8	7.3	107	0.2	0.3	0.3	150	0.3	5.3	145	6.1
28/11/19	12.7	7.3	109	0.3	0.4	0.4	130	0.4	6.5	140	6.5
29/11/19	12.7	7.3	109	0.6	0.8	0.8	185	0.3	5.8	180	6.1
30/11/19	12.7	7.3	102	0.3	0.3	0.3	55	0.4	7.4	160	7.0
01/12/19	12.7	7.3	104	0.6	0.7	0.7	125	0.3	7.8	135	6.0
02/12/19	12.7	7.3	111	0.4	0.5	0.5	75	0.4	7.2	160	6.0
03/12/19	12.7	7.3	99	0.4	0.5	0.5	175	0.4	7.2	145	6.4
04/12/19	12.7	7.3	101	0.3	0.4	0.4	95	0.4	5.9	145	6.6
05/12/19	12.7	7.3	102	0.4	0.4	0.5	160	0.4	5.6	140	7.0
06/12/19	12.7	7.3	106	0.4	0.5	0.6	165	0.4	6.4	130	6.1
07/12/19	12.7	7.4	110	0.4	0.5	0.5	160	0.4	4.7	150	6.8
08/12/19	12.7	7.5	112	0.2	0.3	0.3	170	0.1	5.1	160	5.2
09/12/19	12.7	7.5	110	0.2	0.2	0.2	140	0.2	6.2	140	4.2
10/12/19	12.6	7.3	101	0.3	0.4	0.4	95	0.2	9.9	160	5.7
11/12/19	12.6	7.3	111	0.2	0.2	0.3	160	0.2	6.5	140	5.0
12/12/19	12.6	7.3	106	0.1	0.1	0.1	145	0.1	6.6	140	5.0
13/12/19	12.5	7.3	107	0.2	0.3	0.3	170	0.2	4.9	155	5.3
14/12/19	12.5	7.6	109	0.1	0.2	0.2	265	0.2	5.1	145	4.7
15/12/19	12.4	7.4	104	0.1	0.1	0.1	185	0.2	4.7	145	4.9
16/12/19	10.8	7.2	105	0.2	0.2	0.3	200	0.2	4.7	125	5.1
17/12/19	12.5	7.4	103	0.1	0.1	0.1	85	0.1	4.7	155	4.2
18/12/19	11.4	7.4	104	0.0	0.0	0.0	175	0.1	5.0	165	4.3

Recirculating aquaculture system (Biofilter, system water) Niall Brommage Freshwater Research Unit. Alkalinity ($CaCO_3$) Nitrite (NO2) Nitrate (NO3) total ammonia nitrogen (TAN). Chl.= chloride, Alk.= alkalinity, sat.= saturation

S 3.2 Average water quality parameters

	Temp °c	pH	O_2 %	N (TAN) mg/L	NH_3 mg/L	NH_4 mg/L	Alkalinity mg/L	Nitrite mg/L N	Nitrate mg/L N	Chloride mg/L Cl	CO_2 mg/L
Av.	13.0	7.3	109.8	0.2	0.3	0.3	154.1	0.3	6.4	155.0	5.0
Std dev.	0.7	0.1	6.0	0.2	0.2	0.2	49.0	0.1	1.3	18.1	0.8

S 3.3 Mineral content in feeds and faeces

Mineral content in feed				
Dry matter basis g/kg (ppt)	**CD**	**NL**	**NA**	**PL**
Na	2.93	2.68	2.60	2.93
Mg	1.37	1.49	1.55	1.69
P	11.49	9.70	9.17	11.28
K	3.42	3.17	3.13	3.54
Ca	13.67	12.24	11.91	14.38
Mn	0.05	0.06	0.05	0.06
Fe	0.16	0.16	0.16	0.20
Cu	0.02	0.02	0.02	0.02
Zn	0.24	0.23	0.22	0.25
Y	0.78	0.69	0.66	0.82
Dry matter basis mg/kg (ppm)				
V	3.48	2.86	2.72	3.49
Cr	5.10	4.57	4.25	5.50
Co	0.23	0.19	0.18	0.20
Ni	1.43	1.58	1.27	1.45
Se	0.63	0.59	0.56	0.65
Mineral content in faeces				
Dry matter basis g/kg (ppt)				
Na	20.98	23.98	18.02	26.12
Mg	1.55	1.79	1.34	1.95
P	16.74	17.91	16.24	21.01
K	1.75	1.84	1.53	2.11
Ca	36.34	40.86	36.20	47.43
Mn	0.18	0.19	0.17	0.22
Fe	0.49	0.53	0.47	0.61
Cu	0.03	0.03	0.03	0.04
Zn	0.41	0.44	0.40	0.47
Y	3.27	3.35	2.90	4.17
Dry matter basis mg/kg (ppm)				
V	8.85	9.62	8.51	10.74
Cr	13.21	16.06	13.40	18.41
Co	0.57	0.45	0.49	0.54
Ni	2.37	3.13	2.49	3.14
Se	0.96	1.09	0.88	1.18

Feed analyses were conducted on homogenised pooled samples and faeces was conducted on pooled faeces /tank/treatment. CD= Control diet, NL= Negative leucine, NA= Negative All, PL= Positive leucine. Na= Sodium, Mg= Magnesium, P=Phosphorous, K= Potassium, Ca= Calcium, V= Vanadium, Cr= Chromium, Mn= Manganese, Fe= Iron, Co= Cobalt, Ni= Nickel, Cu= Copper, Se= Selenium, Zn= Zinc, Y= Yttrium.

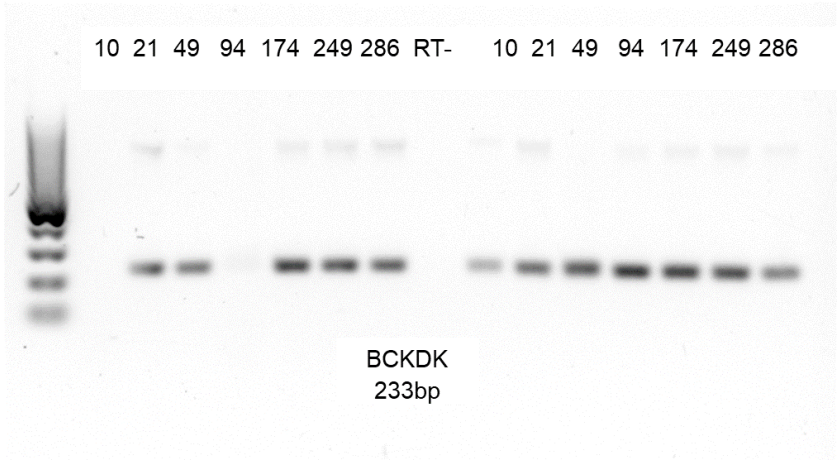
S 3.4 Faeces bAAs g/100g (week 3)

Dry matter %	CD	NL	NA	PL	P-value
Alanine	0.38±0.03	0.35±0.04	0.38±0.03	0.37±0.05	0.862 (f 3, 7= 0.25)
Arginine	0.41±0.07	0.37±0.03	0.36±0.02	0.30±0.04	0.102 (f 3, 8= 2.89)
Asparagine	0.83±0.16	0.72±0.08	0.78±0.07	0.71±0.11	0.507 (f 3, 8= 0.84)
b-Alanine	0.93±0.14 [a]	0.80±0.09 [a]	0.91±0.03 [a]	0.57±0.14 [b]	**0.027 (f 3, 7= 5.73)**
Cysteine	0.25±0.07	0.18±0.01	0.17±0.01	0.23±0.10	0.526 (f 3, 7= 0.81)
Glutamate	0.73±0.06	0.70±0.07	0.75±0.04	0.70±0.07	0.636 (f 3, 7= 0.60)
Glycine	1.09±0.12 [a]	1.07±0.04 [a]	1.01±0.03 [a]	0.85±0.07 [b]	**0.018 (f 3, 8= 6.20)**
Histidine	0.15±0.0	0.18±0.03	0.16±0.02	0.16±0.01	0.504 (f 3, 5= 0.90)
Isoleucine	0.48±0.08	0.48±0.03	0.44±0.00	0.41±0.02	0.197 (f 3, 8= 1.97)
Leucine	0.62±0.04	0.59±0.03	0.60±0.04	0.59±0.06	0.876 (f 3, 7= 0.22)
Lysine	0.75±0.01	0.64±0.08	0.70±0.07	0.69±0.11	0.566 (f 3, 7= 0.73)
Methionine	0.36±0.00	0.36±0.02	0.36±0.01	0.35±0.06	0.948 (f 3, 7= 0.12)
Phenylalanine	0.46±0.07	0.50±0.04	0.48±0.02	0.42±0.01	0.179 (f 3, 8= 2.10)
Proline	0.47±0.07	0.39±0.02	0.41±0.02	0.40±0.04	0.125 (f 3, 8= 2.59)
Serine	0.83±0.11	0.64±0.03	0.68±0.16	0.66±0.24	0.490 (f 3, 8= 0.88)
Threonine	0.49±0.01	0.46±0.01	0.43±0.06	0.45±0.07	0.657 (f 3, 7= 0.56)
Tyrosine	0.56±0.06	0.51±0.01	0.51±0.01	0.47±0.03	0.166 (f 3, 7= 2.28)
Valine	0.64±0.08	0.58±0.05	0.54±0.03	0.57±0.08	0.340 (f 3, 8= 1.30)

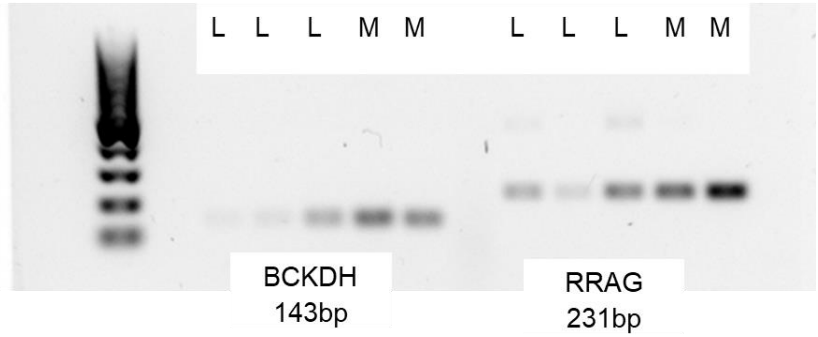
Statistical analysis was performed using one-way ANOVA, with Fisher LSD method used for post hoc examination. Values are reported as means (g/100g) and standard deviation of the mean. Different superscripts indicate significant differences ($p < 0.05$) with abc displaying horizontal differences. Analysis was conducted on pooled faeces / tank/ treatment/ (n=3) with analysis conducted in triplicate. CD= Control diet, NL= Negative leucine, NA= Negative All, PL= Positive leucine.

S 3.5 Thermo and Qiagen cDNA troubleshooting A) Troubleshooting Thermo PCR BCKDK product run using random liver cDNA, displaying double bands B) Troubleshooting Qiagen PCR BCKDH and RRAG product run using random liver and muscle cDNA, displaying double bands. A 100bp ladder was used.

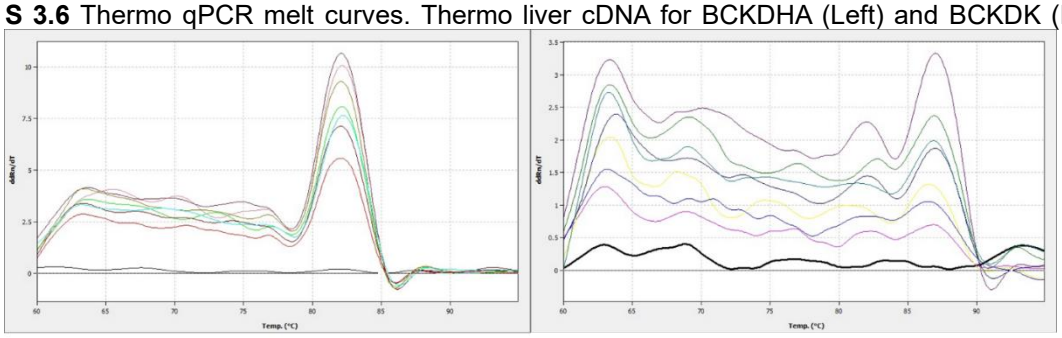
A



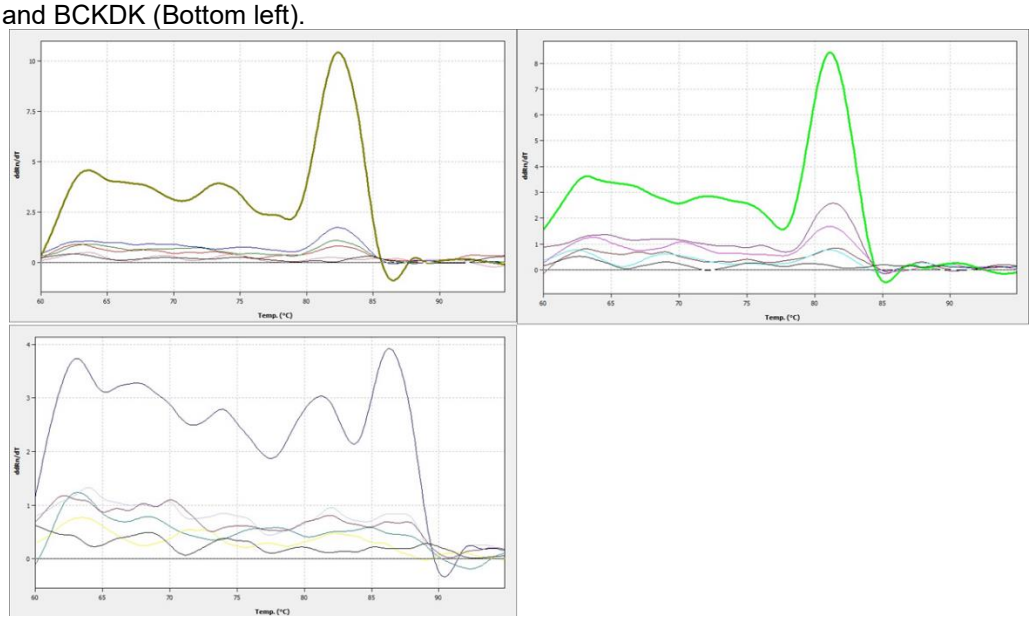
B



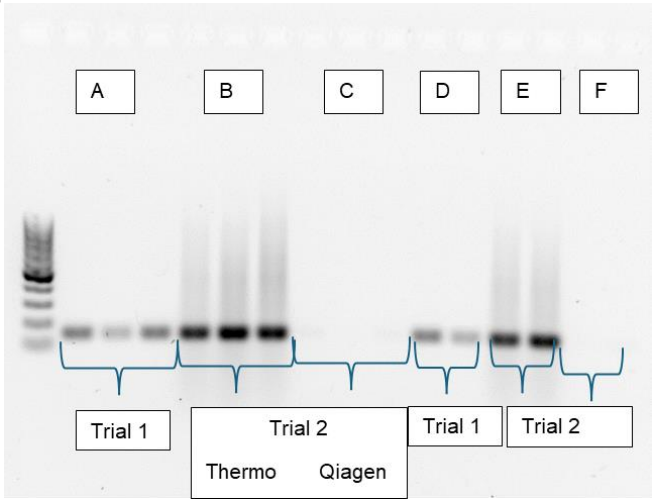
S 3.6 Thermo qPCR melt curves. Thermo liver cDNA for BCKDHA (Left) and BCKDK (Right).



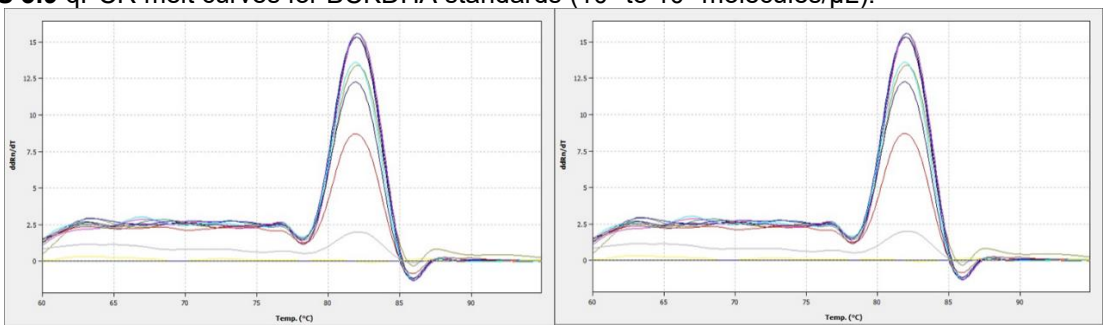
S 3.7 Qiagen qPCR melt curves. Qiagen liver and muscle cDNA BCKDHA (Left), RRAG (Right) and BCKDK (Bottom left).



S 3.8 PCR BCKDHA gel with Thermo and Qiagen liver samples. BCKDHA liver PCR gel. A) Trial 1 Thermo B) Trial 2 Thermo C) Trial 2 Qiagen D) Trial 1 Thermo E) Trial 2 Thermo F) Trial 2 Qiagen. A, B and C used freshly prepared primers whereas D, E and F used previously prepared primers.



S 3.9 qPCR melt curves for BCKDHA standards (10^9 to 10^1 molecules/µL).



S 4 Chapter 4

S 4.1 RNA-seq summary.

	Tissue	Sample ID	P.E. Reads (10^6)	Total Sequences (10^6)	Trimmed (%BP)	Aligned reads (10^6)	Aligned (%)
D1L	Brain						
		B1_1	31.0	53.0	9%	17.8	57%
		B1_2	29.7	50.1	8%	16.7	56%
		B9_1	30.5	52.3	7%	19.3	63%
		B9_2	33.2	57.0	7%	21.1	64%
		B17_1	38.6	63.6	8%	23.7	62%
		B17_2	33.0	52.8	9%	19.1	58%
	Liver						
		L1_1	30.8	56.0	10%	17.0	55%
		L1_2	46.0	82.7	10%	23.8	52%
		L9_1	32.9	59.9	10%	15.8	48%
		L9_2	34.6	63.0	9%	18.5	54%
		L17_1	37.7	66.1	11%	19.7	52%
		L17_2	45.5	81.9	10%	24.4	54%
	Heart						
		H1_1	20.3	33.4	8%	11.8	58%
		H1_2	28.3	45.2	9%	16.6	59%
		H9_1	25.4	41.3	9%	13.0	51%
		H9_2	19.7	32.8	9%	11.0	56%
		H17_1	21.4	35.6	9%	11.3	53%
		H17_2	26.1	41.9	10%	14.6	56%
D1H	Brain						
		B3_1	36.2	60.2	9%	19.5	54%
		B3_2	32.1	54.9	8%	19.7	62%
		B10_1	33.8	58.5	6%	21.5	64%
		B10_2	50.0	80.2	8%	29.0	58%
		B16_1	29.6	49.7	7%	15.7	53%
		B16_2	29.6	48.6	8%	17.3	59%
	Liver						
		L3_1	38.3	68.5	10%	22.3	58%
		L3_2	36.7	65.3	10%	19.2	52%
		L10_1	29.6	54.6	9%	16.7	56%
		L10_2	32.3	58.9	10%	16.4	51%
		L16_1	37.1	66.8	11%	19.7	53%
		L16_2	37.7	68.3	9%	21.3	56%
	Heart						
		H3_1	23.1	39.2	9%	12.6	55%
		H3_2	25.6	42.0	7%	14.8	58%
		H10_1	20.7	33.9	9%	11.3	55%
		H10_2	23.0	37.5	10%	12.6	55%
		H16_1	11.6	20.1	10%	7.0	61%
		H16_2	21.1	33.0	10%	11.3	54%

S 4.2 Statistically different transcripts using corrected p-value (p=0.05) and q-value (q=0.05) in liver (127), brain (131) and heart (114) tissues up or down regulated under hypoxic conditions (D1L). Variance stabilised DAVID, DESeq2 and ShinyNGS.

Ensembl ID	Gene name	Entrez ID	David name	p- value	q- value
Liver upregulated					
ENSSSAG00000081815	5_8S_rRNA	123728349	5.8S ribosomal RNA (123728349)	0.00	0.02
ENSSSAG00000082245	5S_rRNA			0.00	0.01
ENSSSAG00000083048	5S_rRNA			0.00	0.04
ENSSSAG00000087118	5S_rRNA			0.00	0.05
ENSSSAG00000087216	5S_rRNA			0.00	0.04
ENSSSAG00000100495	5S_rRNA			0.00	0.00
ENSSSAG00000102132	5S_rRNA			0.00	0.04
ENSSSAG00000102388	5S_rRNA			0.00	0.00
ENSSSAG00000102390	5S_rRNA			0.00	0.00
ENSSSAG00000103495	5S_rRNA			0.00	0.04
ENSSSAG00000113690	5S_rRNA	123731825	5S ribosomal RNA (123731825)	0.00	0.00
ENSSSAG00000113922	5S_rRNA			0.00	0.02
ENSSSAG00000117768	5S_rRNA			0.00	0.04
ENSSSAG00000118694	5S_rRNA			0.00	0.00
ENSSSAG00000054038	ATF5A	106602866	activating transcription factor 5a (atf5a)	0.00	0.00
ENSSSAG00000095070	CACNG3B	106602081	voltage-dependent calcium channel gamma-3 subunit (106602081)	0.00	0.02
ENSSSAG00000076975	CT054	100195454	CT054 protein (ct054)	0.00	0.01
ENSSSAG00000107977	HSP70	123743448	heat shock 70 kDa protein (123743448)	0.00	0.00
ENSSSAG00000111567	IGDCC3	106587238	immunoglobulin superfamily, DCC subclass, member 3 (igdcc3)	0.00	0.01
ENSSSAG00000056700	KCNMA1A	106613356	potassium large conductance calcium-activated channel, subfamily M, alpha member 1a (kcnma1a)	0.00	0.00
ENSSSAG00000077965	LDB3B	106589423	LIM domain-binding protein 3-like (106589423)	0.00	0.04
ENSSSAG00000095549	LEPA	106561227	leptin a (lepa)	0.00	0.04
ENSSSAG00000061677	MYL1	100194662	myosin, light chain 1, alkali; skeletal, fast (myl1)	0.00	0.00
ENSSSAG00000053560	NSMF	106580537	NMDA receptor synaptonuclear signaling and neuronal migration factor (106580537)	0.00	0.00
ENSSSAG00000058768	RDH5	106566157	retinol dehydrogenase 7-like (106566157)	0.00	0.01
ENSSSAG00000079826	RRAD	106561976	GTP-binding protein RAD-like (106561976)	0.00	0.03
ENSSSAG00000076641	SAXO2	106587795	stabilizer of axonemal microtubules 2 (106587795)	0.00	0.00
ENSSSAG00000079956	SI:CH73-127M5.1	106589430	neurotrypsin-like (106589430)	0.00	0.02
ENSSSAG00000067915	SLC2A3A	106569997	solute carrier family 2, facilitated glucose transporter member 1-like (106569997)	0.00	0.04

ENSSSAG00000101390	SPRED3	106613379	sprouty related EVH1 domain containing 3 (spred3)	0.00	0.00
ENSSSAG00000104905	TRPC7A	106568097	short transient receptor potential channel 7 (106568097)	0.00	0.02
ENSSSAG00000102748	U1	123730675	U1 spliceosomal RNA (123730675)	0.00	0.01
ENSSSAG00000103808	U1	123732146	U1 spliceosomal RNA (123732146)	0.00	0.00
ENSSSAG00000120783	U1	123730676	U1 spliceosomal RNA (123730676)	0.00	0.00
ENSSSAG00000118893	U2	123732494	U2 spliceosomal RNA (123732494)	0.00	0.04
ENSSSAG00000055648	NA	106611738	P2Y purinoceptor 4-like (106611738)	0.00	0.04
ENSSSAG00000055750	NA			0.00	0.02
ENSSSAG00000056368	NA	106565087	acidic mammalian chitinase-like (106565087)	0.00	0.03
ENSSSAG00000058326	NA			0.00	0.00
ENSSSAG00000058739	NA			0.00	0.01
ENSSSAG00000070458	NA	106567397	myotubularin-related protein 4 (106567397)	0.00	0.00
ENSSSAG00000074999	NA			0.00	0.00
ENSSSAG00000075895	NA			0.00	0.00
ENSSSAG00000076039	NA	106612817	calcium-binding protein 8 (106612817)	0.00	0.04
ENSSSAG00000078022	NA			0.00	0.01
ENSSSAG00000078584	NA	106567851	neuroligin-3-like (106567851)	0.00	0.00
ENSSSAG00000081578	NA	106586211	D-3-phosphoglycerate dehydrogenase (106586211)	0.00	0.00
ENSSSAG00000082708	NA			0.00	0.04
ENSSSAG00000083693	NA			0.00	0.00
ENSSSAG00000084203	NA	106561308	CD44 antigen-like (106561308)	0.00	0.01
ENSSSAG00000084605	NA			0.00	0.00
ENSSSAG00000086593	NA			0.00	0.01
ENSSSAG00000086932	NA			0.00	0.04
ENSSSAG00000090735	NA	106570400	CUB and sushi domain-containing protein 3-like (106570400)	0.00	0.01
ENSSSAG00000091460	NA			0.00	0.00
ENSSSAG00000094130	NA			0.00	0.04
ENSSSAG00000096913	NA			0.00	0.01
ENSSSAG00000097500	NA			0.00	0.01
ENSSSAG00000097899	NA	106584498	sodium- and chloride-dependent GABA transporter 2-like (106584498)	0.00	0.00
ENSSSAG00000101681	NA			0.00	0.00
ENSSSAG00000101871	NA			0.00	0.01
ENSSSAG00000102344	NA			0.00	0.01
ENSSSAG00000103335	NA			0.00	0.05
ENSSSAG00000103727	NA			0.00	0.01
ENSSSAG00000104711	NA			0.00	0.02
ENSSSAG00000105444	NA			0.00	0.03
ENSSSAG00000106417	NA			0.00	0.02
ENSSSAG00000108134	NA			0.00	0.00
ENSSSAG00000111546	NA			0.00	0.00
ENSSSAG00000118001	NA			0.00	0.00

ENSSSAG00000118130	NA			0.00	0.02
ENSSSAG00000118695	NA			0.00	0.00
ENSSSAG00000120317	NA	123733152	CD5 antigen-like (123733152)	0.00	0.01
ENSSSAG00000121970	NA			0.00	0.00

Liver down

ENSSSAG00000082283	5S_rRNA	123738099	5S ribosomal RNA (123738099)	0.00	0.05
ENSSSAG00000111532	5S_rRNA			0.00	0.00
ENSSSAG00000062181	ACTA1	106587486	actin, alpha skeletal muscle 2-like (106587486)	0.00	0.00
ENSSSAG00000042826	ANKS4B			0.00	0.04
ENSSSAG00000009881	APNL	106607311	DELTA-stichotoxin-Hcr4a (106607311)	0.00	0.04
ENSSSAG00000007788	CCNA1	106563854	cyclin A1 (ccna1)	0.00	0.00
ENSSSAG00000078949	COL17A1	106577015	collagen, type XVII, alpha 1b (col17a1b)	0.00	0.01
ENSSSAG00000090936	IGSF11	106580804	immunoglobulin superfamily member 11 (106580804)	0.00	0.02
ENSSSAG00000048424	KRT15	106587783	keratin, type I cytoskeletal 13-like (106587783)	0.00	0.02
ENSSSAG00000002846	MYL11	100137048	myosin regulatory light chain 2 (mlc-2)	0.00	0.04
ENSSSAG00000048313	NOTUM1A	106601896	palmitoleoyl-protein carboxylesterase notum1a (106601896)	0.00	0.01
ENSSSAG00000105285	PLPPR4B	106578508	phospholipid phosphatase-related protein type 4 (106578508)	0.00	0.00
ENSSSAG00000107382	PNPLA8	106596512	calcium-independent phospholipase A2-gamma (106596512)	0.00	0.04
ENSSSAG00000007031	PPP1R3CA	106607927	protein phosphatase 1 regulatory subunit 3C-B (106607927)	0.00	0.01
ENSSSAG00000071724	SLC4A10A	106574399	sodium-driven chloride bicarbonate exchanger (106574399)	0.00	0.02
ENSSSAG00000046503	SNAP25A	106571603	synaptosome associated protein 25a (snap25a)	0.00	0.01
ENSSSAG00000096988	SNORA79	123741918	small nucleolar RNA SNORA79 (123741918)	0.00	0.00
ENSSSAG00000114837	SNORD22	123728848	small nucleolar RNA SNORD22 (123728848)	0.00	0.00
ENSSSAG00000079501	SPEF1	100195749	sperm flagellar 1 (spef1)	0.00	0.04
ENSSSAG00000000429	SYT17	106592101	synaptotagmin-17 (106592101)	0.00	0.01
ENSSSAG00000119353	SYT8	106584516	synaptotagmin-1-like (106584516)	0.00	0.01
ENSSSAG00000092962	U1	123730671	U1 spliceosomal RNA (123730671)	0.00	0.00
ENSSSAG00000054140	VTG	100136426	Vitellogenin (100136426)	0.00	0.00
ENSSSAG00000000562	WFIKKN2A	106601671	WAP, Kazal, immunoglobulin, Kunitz and NTR domain-containing protein 2-like (106601671)	0.00	0.04
ENSSSAG00000007487	XPNPEP2	106611530	X-prolyl aminopeptidase (aminopeptidase P) 2, membrane-bound (xpnpep2)	0.00	0.01
ENSSSAG00000001726	NA			0.00	0.04
ENSSSAG00000041821	NA			0.00	0.04
ENSSSAG00000046967	NA			0.00	0.04
ENSSSAG00000049346	NA			0.00	0.01
ENSSSAG00000052032	NA			0.00	0.00
ENSSSAG00000053763	NA			0.00	0.00
ENSSSAG00000054620	NA	106565093	acidic mammalian chitinase-like (106565093)	0.00	0.00
ENSSSAG00000064688	NA	123729544	Fc receptor-like protein 5 (123729544)	0.00	0.04

ENSSSAG00000081104	NA	106583493	uncharacterized 106583493	0.00	0.01
ENSSSAG00000082866	NA	123733182	phosphoglucomutase-2-like (123733182)	0.00	0.00
ENSSSAG00000083949	NA			0.00	0.04
ENSSSAG00000085895	NA	106581664	ly6/PLAUR domain-containing protein 1 (106581664)	0.00	0.00
ENSSSAG00000086543	NA			0.00	0.01
ENSSSAG00000089740	NA			0.00	0.02
ENSSSAG00000092453	NA	106578589	E3 ubiquitin-protein ligase RNF152-like (106578589)	0.00	0.00
ENSSSAG00000096761	NA			0.00	0.01
ENSSSAG00000101965	NA			0.00	0.02
ENSSSAG00000109556	NA	123723709	deoxyribonuclease gamma-like (123723709)	0.00	0.00
ENSSSAG00000110269	NA			0.00	0.00
ENSSSAG00000111044	NA			0.00	0.01
ENSSSAG00000111067	NA			0.00	0.00
ENSSSAG00000111500	NA			0.00	0.02
ENSSSAG00000112436	NA	106577271	N-acetylaspartate synthetase-like (106577271)	0.00	0.03
ENSSSAG00000112724	NA			0.00	0.01
ENSSSAG00000118021	NA	106609948	uncharacterized 106609948	0.00	0.03
ENSSSAG00000119645	NA	123724367	butyrophilin subfamily 2 member A1-like (123724367)	0.00	0.04
ENSSSAG00000120360	NA			0.00	0.03
ENSSSAG00000121651	NA			0.00	0.01

Brain up

ENSSSAG00000082693	5S_rRNA	123730561	5S ribosomal RNA (123730561)	0.00	0.04
ENSSSAG00000002664	DMRTA1	106608505	doublesex- and mab-3-related transcription factor A1 (106608505)	0.00	0.00
ENSSSAG00000010021	EPDL2	106563665	ependymin-like 2 (epdl2)	0.00	0.02
ENSSSAG00000069650	GATM	106562859	glycine amidinotransferase (L-arginine:glycine amidinotransferase) (106562859)	0.00	0.00
ENSSSAG00000075744	GDNFB	106585911	glial cell derived neurotrophic factor b (gdnfb)	0.00	0.00
ENSSSAG00000112500	HOXB5BA	106579315	homeobox protein Hox-B5b (106579315)	0.00	0.00
ENSSSAG00000005990	HOXB6AB	100194490	homeobox protein HoxB6ab (hoxb6ab)	0.00	0.00
ENSSSAG00000005981	HOXB7AB	100196645	homeobox protein HoxB7ab (hoxb7ab)	0.00	0.00
ENSSSAG00000005971	HOXB8A	100194489	homeobox protein HoxB8ab (hoxb8ab)	0.00	0.00
ENSSSAG00000031831	HOXB8BA	100194494	homeobox protein HoxB8ba2 (hoxb8ba)	0.00	0.00
ENSSSAG00000004490	HOXB9AB	100196597	homeobox protein HoxB9ab (hoxb9ab)	0.00	0.00
ENSSSAG00000065782	HOXC8AB	100194442	homeobox protein HoxC8an (hoxc8ab)	0.00	0.01
ENSSSAG00000066778	HOXC8BA	100194449	homeobox protein HoxC8ba (hoxc8ba)	0.00	0.01
ENSSSAG00000072913	HOXD4AB	100194467	homeobox protein HoxD4ab (hoxd4ab)	0.00	0.00
ENSSSAG00000089423	METAZOA_SRP			0.00	0.00
ENSSSAG00000118294	METAZOA_SRP			0.00	0.02
ENSSSAG00000094921	MNX1	106578612	motor neuron and pancreas homeobox protein 1 (106578612)	0.00	0.00

ENSSSAG00000053828	NCA11	100195786	Neural cell adhesion molecule 1-A (nca11)	0.00	0.00
ENSSSAG00000070765	POMC A2	100510784	pro-opiomelanocortin A2 (100510784)	0.00	0.02
ENSSSAG00000078434	SETMAR			0.00	0.02
ENSSSAG00000063303	SI:CH211-263P13.7			0.00	0.04
ENSSSAG00000064165	SMTLB	100196589	somatolactin beta (smtlb)	0.00	0.03
ENSSSAG00000096772	TCF21	100195288	transcription factor 21 (100195288)	0.00	0.00
ENSSSAG00000050784	TSHBA	100136355	thyroid stimulating hormone subunit beta a (tshba)	0.00	0.01
ENSSSAG00000092000	U3	123742625	small nucleolar RNA U3 (123742625)	0.00	0.00
ENSSSAG00000108525	U5	123731493	U5 spliceosomal RNA (123731493)	0.00	0.00
ENSSSAG00000003797	NA			0.00	0.00
ENSSSAG00000013599	NA			0.00	0.04
ENSSSAG00000041979	NA			0.00	0.02
ENSSSAG00000047458	NA			0.00	0.04
ENSSSAG00000048909	NA	106608914	signaling lymphocytic activation molecule-like (106608914)	0.00	0.01
ENSSSAG00000051702	NA			0.00	0.02
ENSSSAG00000074962	NA			0.00	0.04
ENSSSAG00000075979	NA			0.00	0.05
ENSSSAG00000079440	NA			0.00	0.03
ENSSSAG00000079945	NA	106568204	sushi domain-containing protein 2 (106568204)	0.00	0.00
ENSSSAG00000082249	NA			0.00	0.03
ENSSSAG00000082626	NA			0.00	0.00
ENSSSAG00000082902	NA	123727885	motor neuron and pancreas homeobox protein 1-like (123727885)	0.00	0.00
ENSSSAG00000083792	NA			0.00	0.03
ENSSSAG00000084180	NA			0.00	0.05
ENSSSAG00000084757	NA			0.00	0.04
ENSSSAG00000086584	NA			0.00	0.01
ENSSSAG00000086832	NA			0.00	0.00
ENSSSAG00000087412	NA			0.00	0.05
ENSSSAG00000087891	NA	123739876	probable non-functional immunoglobulin kappa variable 6D-41 (123739876)	0.00	0.00
ENSSSAG00000088511	NA	123728641	uncharacterized 123728641	0.00	0.01
ENSSSAG00000088610	NA	106576650	cathepsin E-like (106576650)	0.00	0.01
ENSSSAG00000090016	NA			0.00	0.00
ENSSSAG00000090921	NA			0.00	0.02
ENSSSAG00000094275	NA			0.00	0.00
ENSSSAG00000094588	NA			0.00	0.02
ENSSSAG00000095228	NA			0.00	0.03
ENSSSAG00000096501	NA			0.00	0.02
ENSSSAG00000098045	NA			0.00	0.02
ENSSSAG00000102025	NA			0.00	0.00
ENSSSAG00000103652	NA			0.00	0.00

ENSSSAG00000104788	NA			0.00	0.05
ENSSSAG00000105017	NA			0.00	0.01
ENSSSAG00000105072	NA			0.00	0.04
ENSSSAG00000105273	NA			0.00	0.04
ENSSSAG00000105634	NA			0.00	0.03
ENSSSAG00000106182	NA	106593408	myosin heavy chain, fast skeletal muscle (106593408)	0.00	0.00
ENSSSAG00000106412	NA			0.00	0.04
ENSSSAG00000107979	NA			0.00	0.00
ENSSSAG00000110777	NA			0.00	0.00
ENSSSAG00000111431	NA			0.00	0.02
ENSSSAG00000111810	NA			0.00	0.02
ENSSSAG00000112142	NA			0.00	0.01
ENSSSAG00000113047	NA			0.00	0.00
ENSSSAG00000114292	NA			0.00	0.00
ENSSSAG00000115930	NA			0.00	0.05
ENSSSAG00000117518	NA			0.00	0.00
ENSSSAG00000117807	NA			0.00	0.04
ENSSSAG00000118253	NA			0.00	0.03
ENSSSAG00000118578	NA			0.00	0.04
ENSSSAG00000119368	NA			0.00	0.02
ENSSSAG00000119821	NA			0.00	0.04
ENSSSAG00000119988	NA			0.00	0.04
ENSSSAG00000121691	NA			0.00	0.00
ENSSSAG00000121912	NA			0.00	0.00
ENSSSAG00000121929	NA			0.00	0.00

Brain down

ENSSSAG00000081815	5_8S_rRNA	123728349	5.8S ribosomal RNA (123728349)	0.00	0.01
ENSSSAG00000081987	5_8S_rRNA	123726923	5.8S ribosomal RNA (123726923)	0.00	0.03
ENSSSAG00000095938	CEP72	106595451	centrosomal protein of 72 kDa-like (106595451)	0.00	0.00
ENSSSAG00000105510	CLDY	100196248	claudin f (cldnf)	0.00	0.04
ENSSSAG00000113292	GRAPA	123732578	GRB2-related adapter protein-like (123732578)	0.00	0.03
ENSSSAG00000009571	LDLRAD4B			0.00	0.01
ENSSSAG00000087665	METAZOA_SRP			0.00	0.00
ENSSSAG00000113042	METAZOA_SRP			0.00	0.02
ENSSSAG00000000912	SLC26A11			0.00	0.00
ENSSSAG00000055913	STK31	106577404	serine/threonine-protein kinase 31 (106577404)	0.00	0.00
ENSSSAG00000092962	U1	123730671	U1 spliceosomal RNA (123730671)	0.00	0.00
ENSSSAG00000096796	U1	123730673	U1 spliceosomal RNA (123730673)	0.00	0.01
ENSSSAG00000100946	U1	123742611	U1 spliceosomal RNA (123742611)	0.00	0.00

ENSSSAG00000085703	U5	123731482	U5 spliceosomal RNA (123731482)	0.00	0.00
ENSSSAG00000101666	U6	123725759	U6 spliceosomal RNA (123725759)	0.00	0.00
ENSSSAG00000117376	UPP1			0.00	0.03
ENSSSAG00000000275	NA			0.00	0.03
ENSSSAG00000010511	NA	106605243	uncharacterized 106605243	0.00	0.01
ENSSSAG00000049840	NA	106602993	odorant receptor 131-2-like (106602993)	0.00	0.01
ENSSSAG00000076487	NA			0.00	0.01
ENSSSAG00000077155	NA	106565075	nuclear factor of activated T-cells, cytoplasmic 2-like (106565075)	0.00	0.00
ENSSSAG00000080695	NA	106569563	protein piccolo-like (106569563)	0.00	0.03
ENSSSAG00000081928	NA	106612644/5	putative uncharacterized protein DDB_G0292636 (106612644/5)	0.00	0.03
ENSSSAG00000082637	NA			0.00	0.00
ENSSSAG00000084064	NA			0.00	0.00
ENSSSAG00000086747	NA			0.00	0.04
ENSSSAG00000087141	NA			0.00	0.02
ENSSSAG00000089654	NA	123733083	glycine receptor subunit beta-like (123733083)	0.00	0.00
ENSSSAG00000092194	NA	123731683	monocyte to macrophage differentiation factor 2-like (123731683)	0.00	0.01
ENSSSAG00000093731	NA			0.00	0.02
ENSSSAG00000096287	NA			0.00	0.01
ENSSSAG00000096345	NA			0.00	0.01
ENSSSAG00000097071	NA			0.00	0.01
ENSSSAG00000098150	NA			0.00	0.02
ENSSSAG00000099007	NA			0.00	0.03
ENSSSAG00000100496	NA			0.00	0.00
ENSSSAG00000103749	NA			0.00	0.03
ENSSSAG00000103892	NA			0.00	0.01
ENSSSAG00000106559	NA			0.00	0.01
ENSSSAG00000108134	NA			0.00	0.02
ENSSSAG00000110940	NA			0.00	0.00
ENSSSAG00000111601	NA			0.00	0.04
ENSSSAG00000113355	NA			0.00	0.00
ENSSSAG00000118051	NA			0.00	0.04
ENSSSAG00000118764	NA			0.00	0.01
ENSSSAG00000119161	NA			0.00	0.00
ENSSSAG00000119227	NA	123725422	uncharacterized 123725422	0.00	0.02
ENSSSAG00000120202	NA			0.00	0.01
ENSSSAG00000122148	NA			0.00	0.00

Heart up

ENSSSAG00000086113	5_8S_rRNA	123742644	5.8S ribosomal RNA (123742644)	0.00	0.00
ENSSSAG00000102401	5S_rRNA	123730578	5S ribosomal RNA (123730578)	0.00	0.01

ENSSSAG00000102787	CACNG7A	106570002	calcium channel, voltage-dependent, gamma subunit 7a (cacng7a)	0.00	0.00
ENSSSAG00000075724	MYT1A	106572224	myelin transcription factor 1-like (106572224)	0.00	0.00
ENSSSAG00000119219	TMEM130	106609795	transmembrane protein 130 (106609795)	0.00	0.04
ENSSSAG00000096796	U1	123730673	U1 spliceosomal RNA (123730673)	0.00	0.00
ENSSSAG00000100946	U1	123742611	U1 spliceosomal RNA (123742611)	0.00	0.00
ENSSSAG00000003844	NA			0.00	0.05
ENSSSAG00000006734	NA			0.00	0.02
ENSSSAG00000051058	NA	106567868	connector enhancer of kinase suppressor of ras 2-like (106567868)	0.00	0.01
ENSSSAG00000081752	NA			0.00	0.00
ENSSSAG00000082637	NA			0.00	0.04
ENSSSAG00000082987	NA			0.00	0.02
ENSSSAG00000083614	NA			0.00	0.00
ENSSSAG00000089281	NA			0.00	0.03
ENSSSAG00000090153	NA	106569908	BCL2/adenovirus E1B 19 kDa protein-interacting protein 2-like (106569908)	0.00	0.02
ENSSSAG00000090211	NA	123728813	small nucleolar RNA SNORD10 (123728813)	0.00	0.00
ENSSSAG00000091005	NA			0.00	0.00
ENSSSAG00000093153	NA			0.00	0.02
ENSSSAG00000094486	NA			0.00	0.02
ENSSSAG00000094902	NA	123727945	small nucleolar RNA SNORA57 (123727945)	0.00	0.00
ENSSSAG00000097317	NA	123723656	trypsin-1-like (123723656)	0.00	0.01
ENSSSAG00000100165	NA			0.00	0.01
ENSSSAG00000101089	NA			0.00	0.01
ENSSSAG00000101469	NA			0.00	0.03
ENSSSAG00000103419	NA			0.00	0.00
ENSSSAG00000106711	NA			0.00	0.00
ENSSSAG00000107417	NA			0.00	0.01
ENSSSAG00000107753	NA			0.00	0.02
ENSSSAG00000107995	NA			0.00	0.02
ENSSSAG00000108360	NA			0.00	0.00
ENSSSAG00000108822	NA	123733218	paired box protein Pax-5-like (123733218)	0.00	0.01
ENSSSAG00000109439	NA			0.00	0.02
ENSSSAG00000109752	NA			0.00	0.00
ENSSSAG00000111294	NA			0.00	0.02
ENSSSAG00000112495	NA	123732553	Fc receptor-like protein 5 (123732553)	0.00	0.02
ENSSSAG00000112639	NA			0.00	0.01
ENSSSAG00000113267	NA			0.00	0.01
ENSSSAG00000114615	NA			0.00	0.00
ENSSSAG00000117521	NA			0.00	0.04
ENSSSAG00000119786	NA			0.00	0.02
ENSSSAG00000119922	NA	123732236	RNA-splicing ligase RtcB homolog (123732236)	0.00	0.00
ENSSSAG00000120358	NA			0.00	0.02

Heart down

ENSSSAG00000101044	B3GALT1	106581793	UDP-Gal:betaGlcNAc beta 1,3-galactosyltransferase, polypeptide 1b (b3galt1b)	0.00	0.02
ENSSSAG00000067095	B4GALNT1B	106565528	beta-1,4 N-acetylgalactosaminyltransferase 1-like (106565528)	0.00	0.04
ENSSSAG00000106211	CFAP70			0.00	0.01
ENSSSAG00000109866	CHRNA2B	106608318	neuronal acetylcholine receptor subunit alpha-2-like (106608318)	0.00	0.00
ENSSSAG00000046419	COL26A1	106613322	collagen alpha-1(XXVI) chain-like (106613322)	0.00	0.04
ENSSSAG00000088763	ELAVL3	106593504	ELAV-like protein 3 (106593504)	0.00	0.01
ENSSSAG00000004720	FGFBP2A	106604540	fibroblast growth factor-binding protein 2-like (106604540)	0.00	0.00
ENSSSAG00000080325	FNDC10	106583064	fibronectin type III domain-containing protein 10-like (106583064)	0.00	0.03
ENSSSAG00000046590	GSC	106602411	Goosecoid (gsc)	0.00	0.01
ENSSSAG00000099980	KCNG1	106567113	potassium voltage-gated channel subfamily G member 1 (106567113)	0.00	0.03
ENSSSAG00000092519	KCNIP4	106608614	Kv channel-interacting protein 4 (106608614)	0.00	0.02
ENSSSAG00000106318	LGR5	106609731	leucine-rich repeat-containing G-protein coupled receptor 5 (106609731)	0.00	0.02
ENSSSAG00000111242	LIM2.2	106574149	lens intrinsic membrane protein 2.2 (lim2.2)	0.00	0.00
ENSSSAG00000048313	NOTUM1A	106601896	palmitoleoyl-protein carboxylesterase notum1a (106601896)	0.00	0.00
ENSSSAG00000069253	PI15B	106569289	peptidase inhibitor 15b (pi15b)	0.00	0.00
ENSSSAG00000080698	SEMA6BA	106569517	semaphorin-6B (106569517)	0.00	0.04
ENSSSAG00000071017	SI:CH211-113G11.6	106605326	semaphorin-7A-like (106605326)	0.00	0.04
ENSSSAG00000077126	SI:CH211-98N17.5	106561936	uncharacterized protein PB18E9.04c-like (106561936)	0.00	0.00
ENSSSAG00000114832	TMEM121B	106597677	transmembrane protein 121B-like (106597677)	0.00	0.02
ENSSSAG00000107752	TMEM240A	106572021	transmembrane protein 240 (106572021)	0.00	0.00
ENSSSAG00000065601	TMPRSS5	106581154	transmembrane protease serine 5-like (106581154)	0.00	0.00
ENSSSAG00000085703	U5	123731482	U5 spliceosomal RNA (123731482)	0.00	0.00
ENSSSAG00000001053	NA			0.00	0.00
ENSSSAG00000012719	NA	106606170	hairy/enhancer-of-split related with YRPW motif protein 1-like (106606170)	0.00	0.00
ENSSSAG00000022087	NA			0.00	0.02
ENSSSAG00000042360	NA	106600149	phosphatidylinositol 4-phosphate 5-kinase type-1 gamma-like (106600149)	0.00	0.02
ENSSSAG00000046636	NA	106586306	transmembrane protein 163 (106586306)	0.00	0.00
ENSSSAG00000049874	NA	106565021	growth/differentiation factor 5-like (106565021)	0.00	0.00
ENSSSAG00000056748	NA	106588311	brevican core protein (106588311)	0.00	0.01
ENSSSAG00000058815	NA			0.00	0.00
ENSSSAG00000078770	NA			0.00	0.04
ENSSSAG00000079481	NA	106580109	forkhead box protein N4 (106580109)	0.00	0.00
ENSSSAG00000079889	NA	100136434	matrix Gla protein (100136434)	0.00	0.02
ENSSSAG00000083982	NA			0.00	0.04
ENSSSAG00000084487	NA			0.00	0.05
ENSSSAG00000084751	NA			0.00	0.00

ENSSSAG00000084762	NA			0.00	0.02
ENSSSAG00000085804	NA			0.00	0.01
ENSSSAG00000086058	NA			0.00	0.03
ENSSSAG00000086515	NA			0.00	0.03
ENSSSAG00000089394	NA			0.00	0.00
ENSSSAG00000090847	NA			0.00	0.03
ENSSSAG00000091854	NA			0.00	0.00
ENSSSAG00000092338	NA	106577904	transcription factor Sox-19b-like (106577904)	0.00	0.04
ENSSSAG00000092596	NA			0.00	0.00
ENSSSAG00000092792	NA			0.00	0.03
ENSSSAG00000095507	NA			0.00	0.01
ENSSSAG00000097802	NA			0.00	0.03
ENSSSAG00000098603	NA			0.00	0.00
ENSSSAG00000099344	NA			0.00	0.01
ENSSSAG00000101783	NA			0.00	0.03
ENSSSAG00000102889	NA			0.00	0.00
ENSSSAG00000102939	NA			0.00	0.01
ENSSSAG00000103298	NA			0.00	0.00
ENSSSAG00000103467	NA	106602641	uncharacterized 106602641	0.00	0.04
ENSSSAG00000103816	NA	123731499	small nucleolar RNA ACA64 (123731499)	0.00	0.00
ENSSSAG00000104902	NA			0.00	0.00
ENSSSAG00000107363	NA			0.00	0.02
ENSSSAG00000108745	NA			0.00	0.00
ENSSSAG00000109973	NA			0.00	0.03
ENSSSAG00000110104	NA			0.00	0.05
ENSSSAG00000110388	NA			0.00	0.03
ENSSSAG00000111656	NA			0.00	0.00
ENSSSAG00000113076	NA	106599679	beta-soluble NSF attachment protein-like (106599679)	0.00	0.00
ENSSSAG00000115355	NA			0.00	0.00
ENSSSAG00000116297	NA			0.00	0.04
ENSSSAG00000117312	NA			0.00	0.00
ENSSSAG00000118431	NA			0.00	0.02
ENSSSAG00000118844	NA			0.00	0.01
ENSSSAG00000120844	NA	106577273	CD209 antigen-like (106577273)	0.00	0.01
ENSSSAG00000120911	NA			0.00	0.00

S 4.3 Protein coding transcripts identified within heatmaps. Names additionally sourced from DAVID, DESeq2, ShinyGO, NCBI, Ensembl and ShinyNGS.

Ensembl ID	Entrez ID	Name	Description
Liver			
ENSSSAG00000009636	106574391	LADDERLECTIN (106574391)	
ENSSSAG00000044129	106574012	ELOVL8B	ELOVL fatty acid elongase 8b
ENSSSAG00000046589	106571587	ANKEF1A	ankyrin repeat and EF-hand domain containing 1a
ENSSSAG00000053659	106575158	PKP4	plakophilin 4
ENSSSAG00000083605			Novel gene
ENSSSAG00000086390			Novel gene
ENSSSAG00000088279			Novel gene
ENSSSAG00000092886	106574392	LADDERLECTIN-LIKE (106574392)	
ENSSSAG00000102012			Novel gene
ENSSSAG00000105201			Novel gene
ENSSSAG00000112544	106574349	LADDERLECTIN (106574349)	
ENSSSAG00000113113	106575496	LADDERLECTIN-LIKE (106575496)	
ENSSSAG00000114211	106576037	SI:DKEYP-27E10.3	
ENSSSAG00000116689			Novel gene
Brain			
ENSSSAG00000003431	106601845	VESICULAR GLUTAMATE TRANSPORTER 1 (106601845)	
ENSSSAG00000003662	106606332	VESICULAR GLUTAMATE TRANSPORTER 1 (106606332)	
ENSSSAG00000044618	106578192	PROTEIN PHOSPHATASE METHYLESTERASE 1 (106578192)	
ENSSSAG00000051668	106604839	SOLUBLE GUANYLATE CYCLASE 88E-LIKE (106604839)	
ENSSSAG00000052638	100195880	EPD	ependymin **(NCBI)**
ENSSSAG00000054517	106577930	SI:DKEYP-74B6.2 CEREBELLIN-1 (106577930)	
ENSSSAG00000057688	106612258	FAT2	FAT atypical cadherin 2
ENSSSAG00000067750			Novel gene
ENSSSAG00000073991	100195838	EPD	Ependymin **(NCBI)**
ENSSSAG00000078107	100286493	NEFL	neurofilament light
ENSSSAG00000080628	106561009	CACNA2D4	
ENSSSAG00000095078	Not found???	POMCA	proopiomelanocortin a **(ShinyGO)**
ENSSSAG00000097615	106578342	NEUROGENIC DIFFERENTIATION FACTOR 2-LIKE (106578342)	
ENSSSAG00000108320	106608967	CEREBELLIN-1 (106608967)	

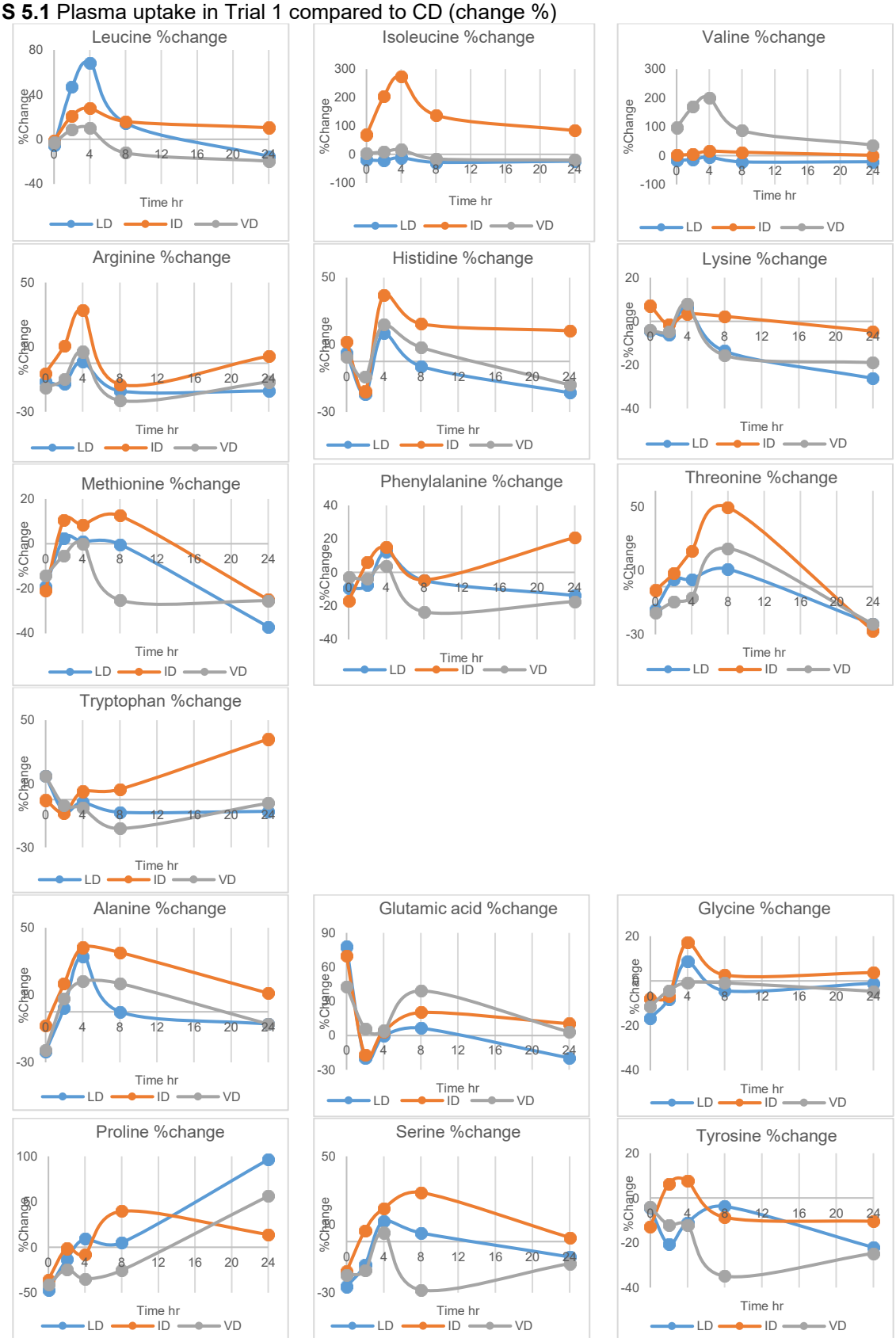
ENSSSAG00000110532	106566167	LEUCINE-RICH REPEAT-CONTAINING PROTEIN 3-LIKE (106566167)	
ENSSSAG00000111067			Novel gene
ENSSSAG00000113207	106600932	HEBP2	heme-binding protein soul5/ heme-binding protein 2????
ENSSSAG00000117422			Novel gene

Heart

ENSSSAG00000047972		MYOSIN, HEAVY CHAIN 6, CARDIAC MUSCLE, ALPHA (MYH6)?	Novel gene
ENSSSAG00000079563	106575297	POTASSIUM VOLTAGE-GATED CHANNEL SUBFAMILY H MEMBER 7-LIKE (106575297)	
ENSSSAG00000109998	123726919	28S RIBOSOMAL RNA (123726919)	pseudo
ENSSSAG00000111067			N/A

S 5 Chapter 5

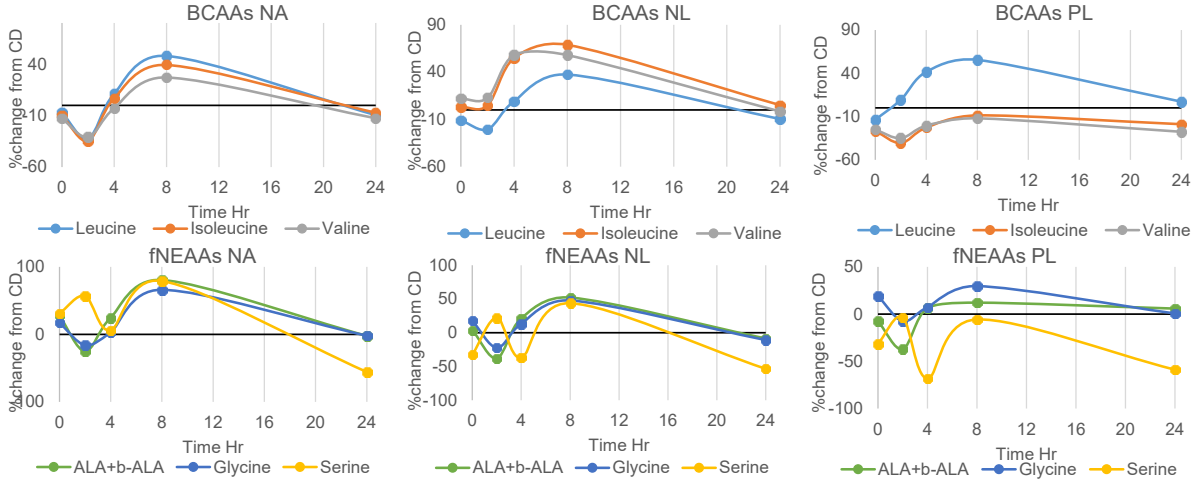
S 5.1 Plasma uptake in Trial 1 compared to CD (change %)



S 5.2 Plasma uptake in Trial 2 compared to the CD (change %)



S 5.3 Trial 2 fBCAAs and fNEAAs in muscle tissue compared to CD (change %)



‘Philosophy is empty if it isn't based on science. Science discovers, philosophy interprets.’

(Albert Einstein, Einstein and the Poet: Third conversation, 1948)